The influence of Asian monsoon variability on precipitation patterns over the Maldives

A thesis
submitted in fulfilment of the requirements for the Degree of
Doctor of Philosophy in Environmental Science
at the University of Canterbury

By

Zahid

University of Canterbury
Department of Geography
Christchurch, New Zealand

Declaration

I confirm that this is my own work and the use of all material from other sources has been properly and fully acknowledged.

Zahid

Abstract

Asian climate varies on various spatial and temporal scales and has a wide spectrum of climatic characteristics. Climate variability, especially decadal to inter-annual scale rainfall variability across Asia has gained considerable attention of climatologists over the last century due to the fact that rainfall variability is known to have caused considerable damage to southern Asian nations. Until recent, much of the existing literature on southern Asian climate focused on India and it is only recently that studies have focused on countries other than India. Although the Maldives is a nation within southern Asia (lying in the Indian Ocean southwest of India), literature on precipitation patterns over the Maldives and its connection to the Asian monsoon is lacking.

This thesis examines the variability of precipitation over the Maldives in relation to the Asian monsoon, since proper knowledge of the spatial and temporal variations of precipitation is essential for managing the water resources and agricultural sector of the Maldives. Yearly and monthly rainfall across the Maldives indicates that the rainfall varies temporally and spatially. Despite spatial variability of mean annual rainfall (January-December total) showing rainfall increasing from north to south, it was found that on average the northern and southern parts of the Maldives have received less rainfall during the monsoon season (May-November). This suggests that the mean annual rainfall maximum for the Maldives occurs between central and southern parts of the Maldives during the monsoon season. The Maldives monsoon rainfall is characterised by inter-decadal and inter-annual periodicities with a frequency of 12.9 and 2.5-4 years, and intra-seasonal periodicities (10-20 days and 30-60 day) in daily time series of monsoon rainfall for different regions of Asia. The fact that no objective criteria previously existed to identify monsoon onset and withdrawal dates in the Maldives, the criteria developed here for defining the monsoon season objectively for this region indicates that on average the rainy season or monsoon commences between 4 May and 13 May (mean onset dates based on outward longwave radiation (OLR) index and rain and wind criteria, respectively) and terminates in late November (21 and 23 November: mean withdrawal dates based on rain and wind, and OLR index criteria, respectively) for the Maldives. The mean length of the rainy season (LRS) based on the OLR index is 204 days, the mean LRS based on rain and wind is 11 days shorter (193 days). Results also demonstrate that the earliest monsoon onset for the Asian region occurs in the south of the Maldives in April.

Correlation coefficient maps generated between Maldives monsoon rainfall and meteorological parameters suggest that the most significant parameters that influence the interannual variability of the Maldives monsoon rainfall (MMR) are mean sea level pressure, surface air temperature, OLR, sea surface temperature (SST), and the zonal wind and relative humidity at various levels. Temporal consistency checks carried out for these parameters with the MMR led to the elimination of some of these predictors (which have less influence in the variance of MMR). The predictors which explained a significant amount of variance in the MMR were retained, including surface relative humidity during April (SRHAPR), 850 hPa level relative humidity during May (850RHMAY) and 500 hPa relative humidity for May (500RHMAY). These parameters were then used to formulate a regression model (using backward regression) for the prediction of Maldives monsoon rainfall. The predictors included in the model account for a significant part of the variance (76.6%, with a correlation coefficient, CC = 0.9) in MMR, indicating the usefulness of the model for medium-range prediction of MMR before the core monsoon season commences.

Global scale processes such as the El Niño-Southern Oscillation (ENSO) phenomenon influence the weather and climate around the globe, with ENSO considered to be one of the strongest natural phenomena influencing the climate of Asia on inter-annual time-scales. The association between the Maldives monsoon rainfall and ENSO events demonstrates that deficient/excess monsoon rainfall over the Maldives and India region is linked to the strong/moderate El Niño and La Niña events, respectively. During strong/moderate El Niño events, about 71.4% of the time the Maldives/India region experiences deficiencies in monsoon rainfall, while the Maldives/India region experiences excessive monsoon rainfall about 75% of the time during strong/moderate La Niña events. One of the regional scale processes that influence the climate of Asia is Eurasian snow cover. No previous studies have directly examined possible relationships between Eurasian snow and Maldives monsoon rainfall. The possible relationship between Eurasian snow cover (ESC) and the Maldives monsoon rainfall, explored in this research for the first time, appears to be only very weak. The results also demonstrate that the inverse relationship between the ESC and the Indian monsoon has weakened over recent decades. The correlation coefficient (-0.34) between Indian monsoon rainfall and ESC obtained for the 1973-94 period dropped to -0.18 for the 1979-2007 period. The inter-annual variability of the Indian and Australian monsoon rainfall experiences a remarkable biennial oscillation, which has been referred to as the tropospheric biennial oscillation (TBO). It is believed that the land and ocean surface conditions in March-May (MAM) over the Indo-Pacific region

play an important role in monsoon transitions. The Maldives monsoon rainfall transition from relatively strong/weak to relatively weak/strong in consecutive years demonstrates a TBO connection (via a biennial tendency in Maldives monsoon rainfall). In relation to the Maldives monsoon rainfall, TBO strong years occur about 47.1% of the time, while weak TBO years occur about 52.9% of the time. Only some of the El Niño and La Niña onset years correspond to strong TBO years, with El Niño onset years (1982, 1987 and 2002) corresponding to weak TBO years, while La Niña onset years (1988 and 2000) corresponding to strong TBO years. Variability (spatial and temporal) in Maldives precipitation associated with global and regional scale processes results in flood and drought events that have downstream impacts, such as on water resources and the agricultural sector of the Maldives. Excess (wet) or deficient rainfall years identified for the period 1992-2008 indicate that the central region is most vulnerable to flooding (5 years with excess rainfall: 27.8% of the time), while the southern region is least vulnerable to both flooding (2 years with excess rainfall: 11.1% of the time) and drought (2 years with deficit rainfall: 11.1% of the time). The northern and central regions show an equal number of years with deficit rainfall (3 years: 16.7% of the time), indicating that they are equally prone to drought events. Furthermore, field survey results demonstrate that about 23, 31 and 37% households (respondents) from the northern, central and southern regions experienced flood events. About 79, 58 and 77% of the farmers from the northern, central and southern areas also experienced floods on their farms. On the other hand, field survey results also suggest that the 49-63% of the households in outer islands of the Maldives and 48-62% of farmers experience shortage of rainwater.

Acknowledgements

This thesis is the end result of a long journey that has encountered many twists and turns. Becoming a parent or entering parenthood towards the beginning of my PhD was a huge personal challenge. During the final year of my PhD studies, earthquakes occurred on 4 September 2010 and 22 February 2011 in Christchurch causing huge disruption to my PhD research. I would like to thank God for granting me the strength, determination, courage and wisdom to overcome many personal challenges and hardships faced during the course of my PhD journey and providing pathways to complete this thesis.

During my PhD journey, I have encountered many people, who have helped me one way or another, to achieve this fruitful goal (completion of the thesis). My first and foremost thanks go to my supervisors: Professor Andrew Sturman, Dr. Peyman Zawar-Reza and Dr. Deirdre Hart, for their constructive ideas, suggestions, criticism and timely encouragement during my PhD programme. I was privileged to have the best possible combination of supervision in the Department. Every step of the way, my supervisory team laid the path for me to move forward with my research and directly or indirectly facilitated pursuit of my own research path, letting the research develop. I was overwhelmed by their patience, full support and encouragement (whether personal or academic) during this long journey. Without their constant guidance and support, it would be impossible for me to come to this stage and present this thesis. I admire their experience, confidence and advice and I appreciate their valuable timely feedback. I know I could not thank them enough and it is beyond words for me to express, but I would like to take this opportunity to express my deepest gratitude and appreciation towards my supervisors. Gratefully and sincerely, I thank you Professor Andrew Sturman, Dr. Peyman Zawar-Reza and Dr Deirdre Hart, both individually and collectively.

The government of New Zealand opened the door for me to purse my PhD studies through New Zealand's International Aid Development Agency (NZAID) open category scholarship. I would like to express my sincere appreciation to the New Zealand government for providing the scholarship and financially supporting my family in accompanying me to New Zealand. I would also like to extend my appreciation to my current NZAID advisor, Stephen Harte, and former NZAID advisor Jonie Chen, as well as Sarah Beaven at International Student Support (ISS), University of Canterbury, for taking care of the administrative side of my scholarship and for their constant support throughout my stay in New Zealand.

This work would not have been completed without the assistance and support from the Department of Geography and its staff. My fieldwork in the Maldives would not have been possible without the research grant from the Department of Geography. Furthermore, the Department's conference grant provided me the opportunity to attend and present papers at both international and local conferences. In addition to this, the Department provided opportunity for me to make full use of computer facilities and other resources in for research purposes without any restriction, and facilitated a great research environment. Department of Geography administrators, Anna Petrie and Susannah Hawtin, provided very efficient administrative support throughout my PhD programme, whether related to research grants, conference attendance or teaching assistant issues, and hence thanks are due to them. Many thanks are also due for the Department of Geography technical staff, especially John Thyne, Graham Furniss, Steven Sykes, Paul Bealing, Marney Brosnan and Justin Harrison for their support in solving everyday computer related problems, software and programming issues, or other issues I faced during the course of my study in the Department. I would like to thank Garth Cant and Henry Connor for their moral support and enthusiasm towards my research. My special thanks also go to associate Professor Simon Kingham and Dr. Doug Johnston at the Geography Department for their valuable feedback on my field survey questionnaire. The expert knowledge and feedback received from other Maldivian students (Ali Shareef and Mizna Mohamed) in the Department greatly facilitated the design of the questionnaire in relation to the local context. I am therefore very grateful to the Department and appreciate the range of support provided by its staff. Thank you all.

Over the course of my PhD journey, I was based at the University of Canterbury Atmospheric Research Centre office and was surrounded by atmospheric research colleagues, namely Basit Khan, Shuhaidah Noor, Marwan Katurji, Arash Moghaddam, Colin Simpson, Stuart Powell, Mohammad Sohrabinia, Omid Alizadeh Choobari, Sandipan Mukherjee and Kirsty Holland. These colleagues were always in reach and were ready to lend a helping hand. I was privileged by this experience and I would like to thank you all for being ideal roommates and for creating a great research environment. I would like to extend my special thanks to Basit Khan and Marwan Katurji for their constructive ideas and many thoughtful suggestions. Your conversations greatly boosted my level of thinking and enhanced my PhD research experience. I must acknowledge all other PhD students at the Department of Geography for their kindness and support throughout my PhD journey and for making my the PhD experience unforgettable and enjoyable in many ways.

I would also like to acknowledge my employer, the Department of Meteorology/National Meteorological Centre, Maldives, for their enormous support. The Department allowed me to take paid study leave from my work. I am very grateful for the direct assistance received from the Department of Meteorology, especially for providing local meteorological data needed for the research. The Department also provided some staff to assist with my fieldwork and contributed financially towards fieldwork expenses in the Maldives. Furthermore, I would like to thank the island offices and many individuals who helped during my fieldwork phase. The field survey would have been incomplete without the support and cooperation from the participants in the survey. I appreciate your time and responses.

Many thanks are extended to Ali Shareef. I will always remember your kind assistance that I received in extracting and handling global data sets. Furthermore, you introduced me to MATLAB and taught me many lessons. Ali, you are not only a classmate, office mate, university room mate, but you are also an invaluable asset! Dr. Abdulla Firag is another valuable person I must acknowledge for helping me with many MATLAB programming problems I faced during my PhD studies. Abdulla was always willing to extend his helping hand. Thank you Abdulla.

Studying away from family members and friends was a big personal challenge for me, as well as for my wife Yumna. The long time we spent in New Zealand would not have been easy without the support and friendship offered by the small Maldivian community in Christchurch. I enjoyed every bit of our many social gatherings, potluck dinners and trips that I shared with you all over the past years and our bond has become so strong that I feel you all are part of my extended family. I am so delighted to meet you all and I would like to extend my appreciation and gratitude to you all for the support and encouragement over the years and making our stay in New Zealand memorable. I was overwhelmed by the generous help and moral support offered by the Maldivian community in Christchurch during the most difficult times. It would be inappropriate to finish the words of thanks without expressing my deepest thanks and appreciation to Aminath Laafira and Hassan Fayyaz for providing shelter for my family following 4 September 2010 earthquake. They also opened their welcoming arms again following the 22 February 2011 earthquake and provided accommodation indefinitely for me and my family until we are ready to go back to our home country, the Maldives. Their kindness is beyond words to express and I would not be able to thank them enough.

In relation to my studies (from secondary school through to PhD), a single person that I admire most is Ajwad Musthafa. You are not only my school mate or class mate who shared the same bench during secondary school years, but you are my best friend. Over the last two decades, our friendship has developed to such an extent that now I feel that you are like my own brother who has been so steadfastly supportive and has encouraged me all the way through my studies. I admire your patience, knowledge and intelligence. You are the best! During the years I spent overseas, Ibrahim Waheed and Mohamed Abdul Latheef (two friends who I met during my secondary school days) have taken care of all my responsibilities back home and fulfilled everything for me. Mates, I thank you both. Special thanks also go to other secondary school class mates, especially Ahmed Shiham, Hussain Siraj, Ali Azwar, Abdulla Salih, Aslam Mohamed, Ahmed Naseem, Moosa Manik, Mohamed Naseer, Giyas Haneef, Najumulla Shareef, Hassan Bushry, Hussain Rasheed, Ibrahim Rasheed, Hassan Fiyaz, Yoosuf Ahmed, Ibrahim Wajeed, Fathimath Mohamed, Aishath Naila, Hawwa Zareena, Jeeza Mohamed, Khaulath Mohamed, Abbasa Abdul Hamid and Hidhaya Naseer. I thank you all for the companionship and support over the years and you all were inspirational to my studies.

The list of thanks would be incomplete without acknowledging my family members, who mean to me more than I can express. I send my deepest gratitude to my family members for their constant support and strong belief in me, especially my mother, Saeedha Abdul Muhusin. Mum, your encouraging words were inspirational to my studies. Thank you mum! Dear dad, it is sad to acknowledge that you are no longer with us anymore, but the words you said during my childhood still echo in my ears “If you are not educated, you will be forced to work as labourer (as a digging person under the hot sun) and you will not be able to work in a nice environment (under the fan or air-condition)”. These words are so inspirational to my studies. I miss you dad! My deep thanks and gratitude are also extended to my wife, Yumna Waheed Mohamed for all her endless love, companionship and encouragement. Yumna took every effort in daily life to help me complete this thesis and stood by my side through the good and bad times during this long journey. I was overwhelmed by Yumna’s support and responsibility in bringing up my son, Azwad Zahid Hameed. My son has been a role-model for me. Son, you reminded me about my studies every day “Bye-bye Daddy, go uni and study - see you soon”. Thank you my son! I could not have fulfilled this long journey without you, Yumna and Azwad, by my side. You two are pillars of this success.

Last but not least, my special thanks, gratitude and appreciation are due for my father-in-law, Ahmed Waheed Mohamed, and mother-in-law, Jameela Ahmed, together with other members of my wife's family, for letting me take Yumna away from you all, the very next day after we got married. I saw the tears rolled down from all of your eyes, knowing that you will not be able to meet your loving daughter or sister in years to come. Not only have I kept Yumna miles away from you all, but I also kept your first-ever grandson, Azwad, away for years. I appreciate and admire my father and mother-in-law's patience and I would like to convey my deepest thanks to them for the patience and support I have received. You never missed to call us on every week and those calls reminded me how much you missed us. Thank you "dad" and "mum"!

It is not possible to enumerate everybody who supported and assisted me during this long journey. In this regard, I would like to express my sincere thanks and appreciation individually and collectively to all the people who have assisted me one way or another during this journey. I will keep everyone's guidance, support and kind assistance in my mind forever; without your guidance, support and kind assistance it could have been very difficult or even not possible to complete my PhD studies. So I thank you all from the bottom of my heart.

I would like to dedicate this thesis to:

My late father, **Abdull Hameed** for his inspirational words during my childhood:

> "If you are not educated, you will be forced to work as labourer (as a digging person under the hot sun) and you will not be able to work in a nice environment (under the fan or air-condition)".

My mother, **Saeedha Abdull Muhusin** for her patience and encouraging words during the years I spent abroad to seek higher education and ongoing support towards my PhD study.

My wife, **Yumna Waheed Mohamed** for her eternal support throughout my PhD study.

My son, **Azwad Zahid Hameed** for his everyday inspirational words:

> "Bye-bye Daddy, go University and study - see you soon"

List of Figures

List of Tables

1 Introduction

The Asian summer monsoon is one of the most energetic components of the Earth's climate system and significantly affects the lives of more than 60% of the world's population. The term ‘‘monsoon’’ originated from the Arabic "mausim" first used by Arab sailors when referring to the annual alternating winds of the Arabian Sea, but is now more generally applied to tropical and subtropical seasonal reversals in both the atmospheric circulation and associated precipitation (Trenberth et al. 2000). The dominant monsoon systems in the world are the Asian-Australian, the African, and the American monsoons. Apart from the American monsoon, all other monsoons satisfy both a wind reversal and seasonal precipitation. The American monsoon has not been clearly identified with regard to wind reversals, but qualifies as a monsoon region in terms of precipitation (Trenberth et al. 2000; Webster et al. 1998). The annual cycles of the monsoon systems has led to the inhabitants of these monsoon regions dividing their lives, customs and economies into two distinct phases; namely the wet and the dry periods.

The Asian Monsoon is an annual event caused by the northward advance of the Inter-Tropical Convergence Zone (ITCZ) and associated precipitation over the Asian landmass during the boreal summer. The Asian monsoon is composed of two subsystems, the Indian (or South Asian) monsoon and the East Asian monsoon, roughly divided at 105° E (Wang et al. 2005). The Asian monsoon system is characterized by the Asian continental thermal low encircled by monsoon southerlies over south Asia and southwesterlies in southeast and east Asia. The Asian monsoon is an extremely complex phenomenon that encompasses variability over a wide range of spatial and temporal scales (Lau et al. 2000), driven by range of mechanisms/factors depicted in Figure 1.1. As indicated in the figure, the Pacific Decadal Oscillation (PDO), El Niño-Southern Oscillation (ENSO), Tropospheric biennial oscillation (TBO) Quasi-Biennial Oscillation (QBO), Indian Ocean Dipole (IOD), Eurasian snow cover (ESC) and Madden-Julian Oscillation (MJO) influence variability of the monsoon on different time scales and control the supply of rainfall in the region. It should be noted that some of the drivers/factors identified in Figure 1.1 were not covered in this research and this will be discussed in Chapter 9.

Since the Maldives lie close to the Asian continent, the variability of the Asian monsoon is likely to influence rainfall patterns over the Maldives. Understanding the mechanisms and controlling factors of the Asian monsoon and its influence on precipitation

patterns over the Maldives is important in order to estimate future impacts and to save lives from flood and drought events. Variability of the Asian monsoon and its influence on precipitation patterns over the Maldives will be analysed in this study.

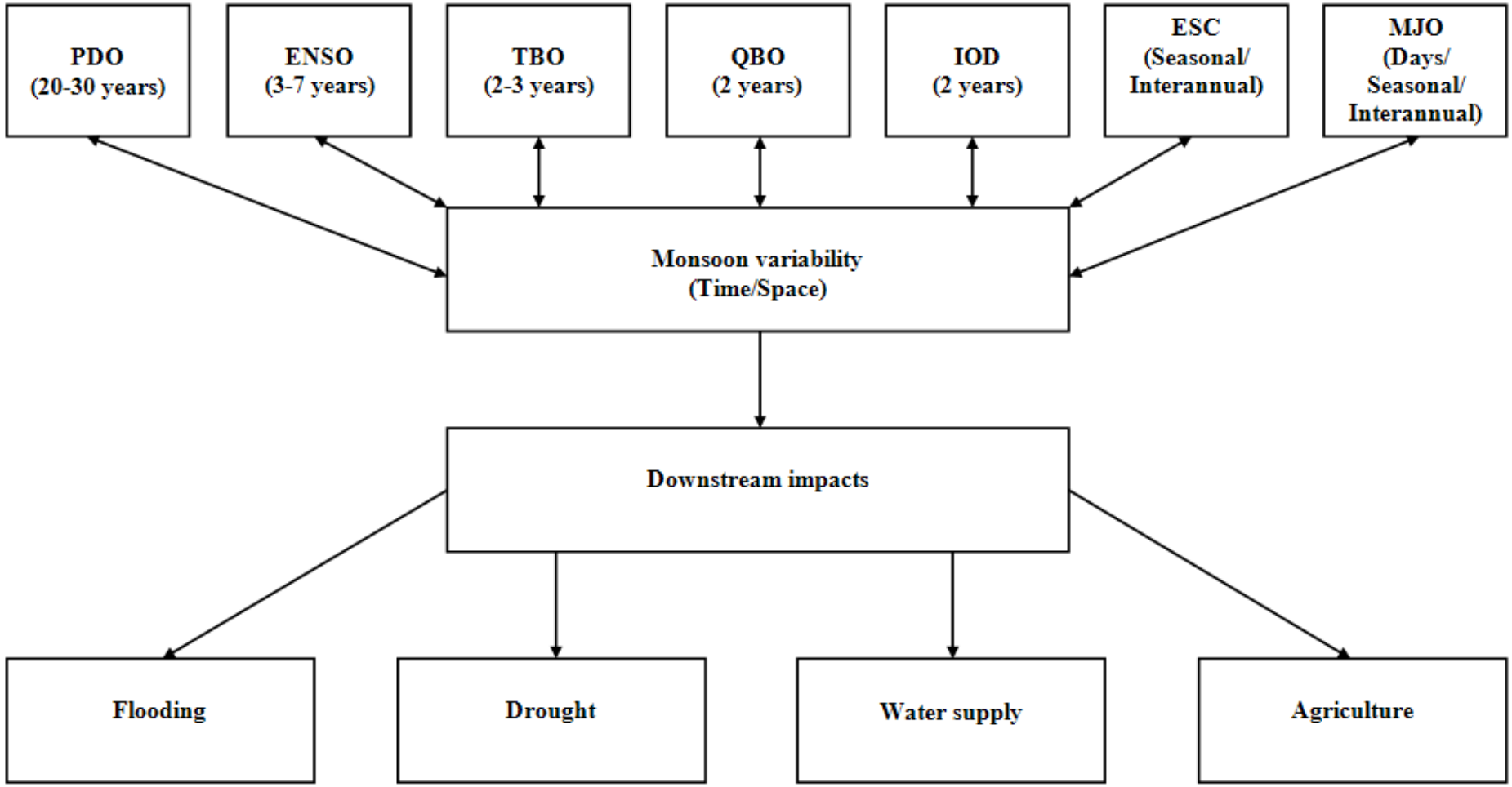

Figure 1.1: Conceptual model showing potential drivers of monsoon variability and associated downstream impacts.

1.1 Study location - the Maldives

The Maldives (or Maldive Islands), officially called the Republic of Maldives, is an island nation consisting of a group of coral atolls in the Indian Ocean (Figure 1.2), stretching 860 km from latitude 7° 6' 35" N, crossing the Equator to 0° 42' 24" S, and lying between 72° 32' 19" E and 73° 46' 13" E longitude (MEC 2004). Sri Lanka and India are the country's closest neighbours, lying 750 km and 600 km north and north-east of the Maldives, respectively. The Republic of Maldives consists of nearly 1,200 islands on 26 natural atolls (divided into 20 administrative atolls) encompassing an area of about 107,500 km^2. The width of the chain varies from 80 to 120 km from west to east (MHAHE 2001). The total land area is about 300 km^2, which makes the Maldives the smallest country in south Asia. The Maldives has been recognised as the flattest country on Earth, since none of the islands has en elevation more than 3 m above mean seal level and about 80% of the land area is less than 1 metre above mean sea level (Khan et al. 2002; MHAHE 1999). The population is spread over 199 inhabited islands with a total population of about 298,842 and the most populous island among 199 inhabited islands and the centre of commerce is the capital island, called Male' (MPND 2007b).

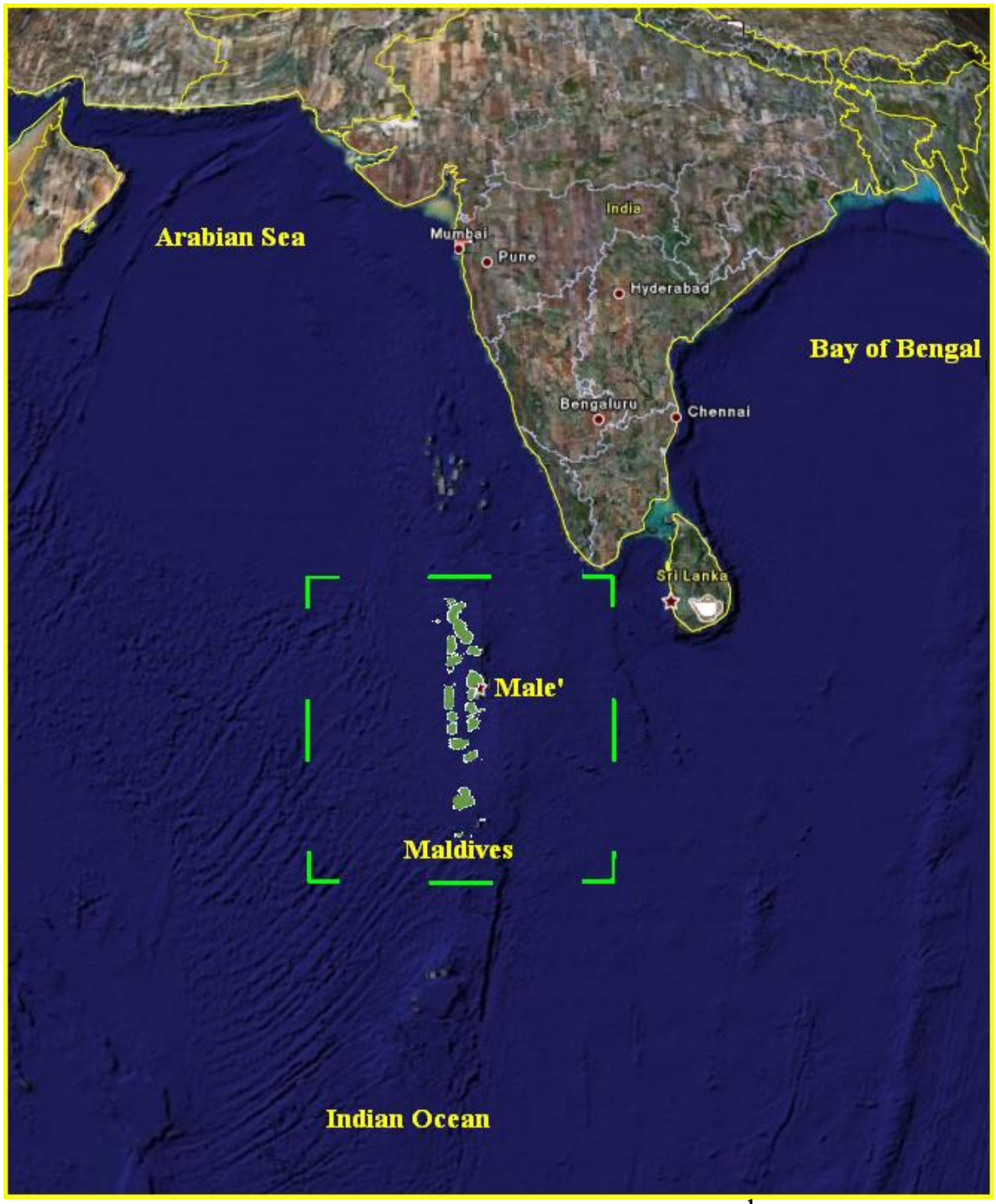

Figure 1.2: Location of the Maldives and neighbouring countries.[1]

1.2 Climate

The Maldives experiences a monsoonal climate. The two distinct seasons that the Maldives experiences are the dry season (northeast monsoon) and the wet season (southwest monsoon). Traditionally, the northeast monsoon extends from January to March

[1] Adapted from http://maps.google.com/

and the wet season or southwest monsoon runs from May to November (MEC 2004). During the southwest monsoon, the Maldives experiences torrential rain.

The Maldives, as an equatorial country, having only a small variation in mean monthly temperature. Hence, throughout the year, temperature remains almost the same and seasonally the temperature hardly varies. However, diurnally temperature ranges from around 31 degrees Celsius during daytime to 23 degrees Celsius at night. Since the Maldives consists of small islands that are surrounded by sea, hot days are often tempered by cooling sea breezes and balmy evening temperatures. The mean daily maximum temperature for central parts of the Maldives is 30.5 degrees Celsius and minimum temperature is 25.7 degrees Celsius. On the other hand, mean daily maximum and minimum temperatures for the south are 30.9 and 24.5 degrees Celsius, respectively. Furthermore, mean daily maximum and minimum temperatures for the north are 30.7 and 25.2 degrees Celsius, respectively. The highest temperature ever recorded in the Maldives was 36.8°C, recorded on 19 May 1991 at Kadhdhoo Meteorological Office. Likewise, the minimum temperature ever recorded in the Maldives was 17.2°C, recorded at the National Meteorological Centre on 11th April 1978.

The Maldives receive plenty of sunshine throughout the year, being located at the equator. On average, southern atolls of the Maldives receive 2704.07 hours of sunshine each year. Furthermore, central parts of the country receive 2784.51 hours of sunshine per year on average.

In the Maldives, ocean currents are driven by monsoonal winds. During the northeast monsoon, the westerly flowing currents tend to dominate. On the other hand, during the southwest monsoon easterly currents dominate (MHAHE 2002). The changes in current flow patterns occur in April and December. In April, the westward currents are weak and eastward currents will slowly develop. Similarly, in December eastward currents are weak and westward currents will develop slowly. These two months correspond to transition periods of the southwest and the northeast monsoons, respectively. The ocean currents flowing through channels between the atolls are driven by the monsoon winds (MEC 2004). In the Maldives, currents near the coastal shoreline are slightly different from the oceanic currents and are largely influenced by the location, orientation and morphology of the reefs.

Tides experienced in the Maldives are mixed semi-diurnal and diurnal with a strong diurnal inequality. Tide data from central and southern areas indicates maximum spring tide variation of about 1.1 m from central and southern atolls. Data from tide station in the central areas indicates a maximum tide of about 1 m. The highest astronomical tide level is

+0.64 m (MSL) and the lowest astronomical tide level is -0.56 m (MSL). Although there is a 0.2 m seasonal fluctuation in regional mean sea level, with an increase of about 0.1 m during February-April and a decrease of 0.1 m during September-November, seasonal variation in mean sea level in the Maldives is small (MHAHE 2002).

1.3 Economy

The Maldives' economy is driven by, and is dependent on, four economic sectors; namely tourism, fisheries, agriculture and the garment sector (MPND 2005). The tourism industry is the largest contributor to the Maldivian economy, significantly contributing to the national Gross Domestic Product (GDP). The tourism sector saw a rapid growth before the 2004 Asian tsunami. In 1995, tourism contributed about 34.5% to the national Gross Domestic Product (GDP) but after the tsunami (in 2005 and 2006), it contributed 22.7% and 27.1% to the GDP, respectively (MPND 2007b).

Being the biggest exporter and a major employment sector, the fisheries sector is the second largest economic sector in the Maldives and plays a significant role in the Maldivian economy and society at large. The fisheries sector is significantly important to all the regions of the country and is one of the highest generators of employment in the atolls. In the Maldives, the fisheries sector continues to be the most dominant in terms of employment, employing over 20% of labour force and contributing 6.3% to the GDP in 2006 (MPND 2005; 2007b).

The agricultural sector continues to play a minor role in the Maldives economy. In recent years the contribution from the agricultural sector to the economy decreased. In 1995, the agricultural sector contributed 3.6% to the national GDP, while in 2006 the contribution from the sector to the GDP was 2.2% (MPND 2005; 2007b). The extent of employment in the agricultural sector varies across the country. The northern islands, which are further away from the atoll capital where employment opportunities in the secondary and tertiary sectors are relatively limited compared to other islands, account for the highest employment from the agricultural sector (MEC 2004).

The production of clothing is the second most important export commodity for the Maldives, accounting for 39% of Maldives' exports in 1999 (MPND 2005). Those clothes produced for export are processed at garment factories set-up in four different locations (Seenu, Kaafu, Haa Dhaalu and Laamu atolls) with foreign investment. The economic contribution of the sector to government revenues is minimal (3% of export values). The sector employs only a small number of local Maldivians. Although, the garment sector has

employed about 2400 people, only 400 Maldivians are employed in the sector with the rest of the labour from foreign countries (MPND 2005).

1.4 Aims of the thesis

The majority of the population of the planet reside in the monsoon regions. The livelihood and well-being of these monsoon societies depends on the variations of the monsoon and the establishment of a symbiotic relationship between agricultural practices and climate. The Asian summer monsoon returns with remarkable regularity each year, and there are important interannual variations in the amount and distribution of rainfall. Variation of seasonal mean rainfall can have a substantial impact on crop yields and water resources of this region (Annamalai et al. 1999).

Modelling studies show that mean South Asian monsoon precipitation is likely to increase, with an accompanying enhancement of monsoon interannual variability, with increased CO_2 (Meehl and Arblaster 2003). Climate change related monsoon rainfall variability can have a severe impact for this region and for individual countries like the Maldives. Due to the smallness of the islands (the area of the largest island is about 5.16 km^2) (MPND 2000), the entire population and the infrastructure of the Maldives are very close to coastal areas. Its coastal setting and the low-lying nature of the islands make the Maldives one of the most vulnerable countries in the world to climate change and its associated natural disasters, such as floods and droughts. This may have strong negative impacts on the economy and the whole Maldivian society.

Although there has been considerable work done on the variability of the Asian monsoon by analyzing the extensive data sets of the Indian Meteorological Department (Lawrence and Webster 2001; Li and Zhang 2002), the nature of monsoon variability over other parts of the Asian monsoon region is not as well documented, especially for the Maldives. Hence the aims of the present study are:

1. To investigate the variability of the Asian Monsoon and its influence on precipitation patterns over the Maldives.
2. To examine possible downstream impacts of monsoon rainfall variability on the Maldives.

In order to address the two broad aims outlined above, a number of research questions were formulated as follows:

1. Does temporal and spatial variability of precipitation occur across the Maldives (between the northern, central and southern regions)? If so, what is the nature of this variability?
2. What factors control the interannual monsoon rainfall variability over the Maldives? Can the monsoon rainfall variability over the Maldives be due to variations in:
    a. sea surface temperature (SST)?
    b. atmospheric moisture?
    c. outgoing long wave radiation (OLR)?
    d. surface wind?
    e. surface temperature?
    f. mean sea level pressure (MSLP)?
3. Can the precipitation pattern over the Maldives be influenced by Eurasian snow cover?
4. To what extent are the variations in the precipitation pattern seen over the Maldives due to:
    a. global scale systems (El Niño-Southern Oscillation (ENSO)?
    b. regional scale systems (Tropospheric Biennial Oscillation (TBO) and Eurasian snow cover)?
5. What might be the possible impacts of monsoon rainfall variability in the case of the Maldives?

These research questions led to the following sub-aims:

1. Determination of temporal and spatial variability of precipitation patterns across the Maldives (between the northern, central and southern regions)
2. Investigation of controlling factors of the intra-seasonal and inter-annual monsoon rainfall variability over the Maldives
3. To examine the influence of Eurasian snow cover on the Maldives precipitation patterns
4. Investigation of different processes (global and regional scale) influencing the Maldives monsoon rainfall variability.

1.5 Motivation

In the past, the vulnerability of the Maldives to natural disasters was always thought to be moderate as it did not have a history of frequent and destructive events. Earthquakes and tsunamis are not linked to climate change, but pose a threat to the Maldives. For example, the tsunami that hit the shores of the Maldives and other Indian Ocean countries on the 26 December 2004 highlighted a real threat to the Maldives and changed the perception that the Maldives is "safe" from disasters.

Having the chance to work at one of the most important and relevant disaster related organisations (Department of Meteorology) in the Maldives, it was evident that not only do non-climatic disasters such as earthquakes or tsunamis impose a great threat to the Maldives, but also climate related events such as predicted sea level rise and the extreme events of floods and droughts pose a real threat to the Maldives. There is some level of confidence in model-projected changes in precipitation in the Indian Ocean region. The forecast increase in annual precipitation is restricted mainly to the northern Indian Ocean, where the model consensus is greatest, especially in the vicinity of the Maldives in June-July-August (JJA) (Christensen et al. 2007). In recent years, the Maldives has experienced climate related events such as flooding.

According to Lal et al. (2001), transient experiments performed with revised emission scenarios, including revised trends for all the principal anthropogenic forcing agents for the future, suggested an increase of about 7 to 10% in area-averaged annual mean precipitation over the Indian subcontinent by the 2080s. A decline of between 5 and 25% in area-averaged winter precipitation is likely, while during the monsoon season, an increase in area averaged summer precipitation of about 10 to 15% over the land regions is projected (Lal et al. 2001).

Its fragile ecological profile and low elevation, combined with its dependence on a limited number of economic sectors (tourism, fisheries and agriculture), makes the Maldives one of the most vulnerable countries to climate related events such as changes in flooding caused by monsoon precipitation. This is also due to its smallness, remoteness, geographic dispersion, lack of natural resources and low human resource base (MHAHE 2001). This has provided motivation to analyse the nature of the variability of the Asian monsoon and its influence on precipitation patterns over the Maldives and possible downstream impacts associated with this monsoon rainfall variability.

1.6 Thesis outline

The key components of the research strategy used to address the research questions outlined above and to achieve the main objectives of this research (to understand the nature of the variability of the Asian monsoon and its influence on precipitation patterns over the Maldives and associated impacts) are depicted in Figure 1.3. The analysis Chapters (3-8) are based on these components. Altogether the thesis consists of nine Chapters.

Chapter 1 deals with the introduction, covering the introduction of the topic, aims of the thesis, motivation, study location, climate and economy of the Maldives and the thesis outline. The data and research methodology are outlined in Chapter 2, which describes the data used for the study, including the different methods and techniques used to identify the nature of monsoon precipitation variability and its impacts. Some of the methods and techniques applied include correlation, regression, principal component analysis, composite analysis, power spectrum analysis and time-filtering techiniques. These methods and techniques have been widely used by other researchers to study monsoon variability (e.g. Guhathakura and Rajeevan (2008), DelSole and Shukla (2002), Singh (2006), Robock et al. (2003) and Munot and Kothawale (2000)).

The fact that no previous studies have looked at the rainfall over the Maldives, the thesis starts with a detailed descriptive analysis of rainfall variability in the Maldives (both in time and space) in Chapter 3.

The monsoon varies on different time scales: intra-seasonal, interannual and interdecadal. Characterisation of monsoon variability (decadal, interannual and intraseasonal monsoon variability) in the context of Maldives is presented for the first time in Chapter 4.

Chapter 5 investigates the factors influencing variability of monsoon precipitation. This chapter assesses whether the interannual monsoon rainfall variability over the Maldives is due to variations in sea surface temperature, mean sea level pressure, relative humidity, outgoing long-wave radiation, surface temperature and surface wind. This leads to the development of a model to predict Maldives monsoon rainfall, which is crucial for the agricultural and water resources sector of the Maldives.

A connection between El Niño-Southern Oscillation (ENSO) and the monsoon has been suggested by many researchers (e.g., Goswami 1998; Lau and Nath 2000; Pillai and Mohankumar 2009; Wang et al. 2001; Webster and Yang 1992) and one of the main factors that plays a major role in determining the variability of Indian summer monsoon rainfall (ISMR) on the interannual time-scale is the El Niño-Southern Oscillation (Pillai and

Mohankumar 2009). Chapter 6 therefore investigates the role of the El Niño-Southern Oscillation (ENSO) on the variability of Maldives monsoon rainfall (MMR).

The literature is lacking on the influence of regional scale processes on the Maldives monsoon rainfall, so that Chapter 7 assesses the influence of regional scale processes on monsoon rainfall, exploring in particular the connection between MMR and snow cover and the tropospheric biennial oscillation (TBO) (it comprises two parts – Part A: the snow cover connection and Part B: the role of the TBO).

Although monsoon rainfall has important effects on the Maldives, the implications of monsoon rainfall variability for the Maldives has not been addressed so far. Chapter 8 therefore describes the possible impacts on the Maldives associated with monsoon variability, including flooding and drought events, as well as agricultural and water resources impacts. Finally, Chapter 9 concludes the thesis by summarising the main findings of the study and directions for future work.

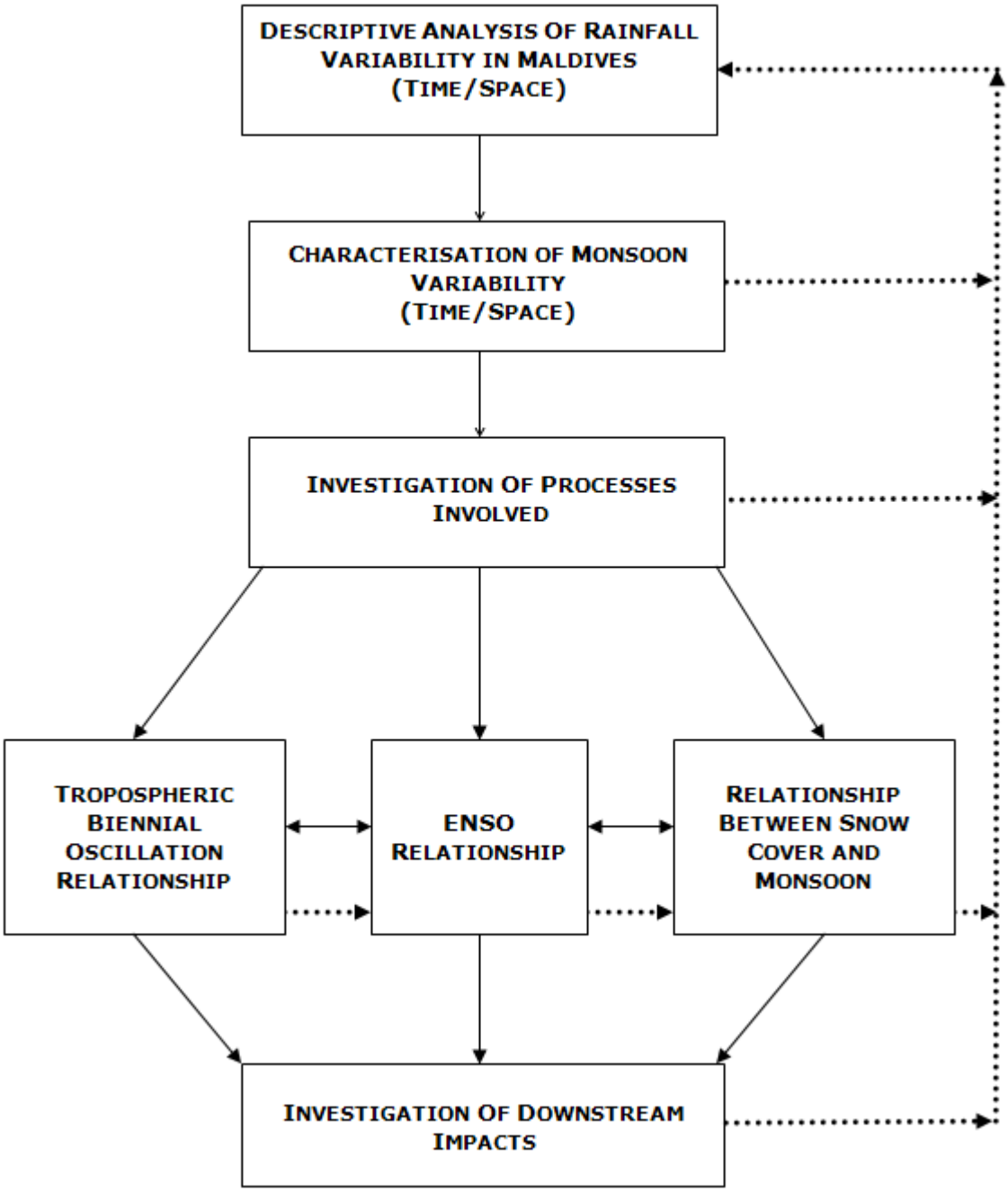

Figure 1.3: Conceptual diagram showing key components of the research.

2 Data and research methodology

Different datasets and methods were employed in this study to identify the nature of monsoon precipitation variability and its impacts. Datasets (ranging from global to regional to local and field survey data) and a wide range of analysis methods used in relation to the various research questions are summarised schematically in Figure 2.1 and described below. Details of data preparation and some statistical techniques are incorporated within the body of the thesis in conjunction with their use.

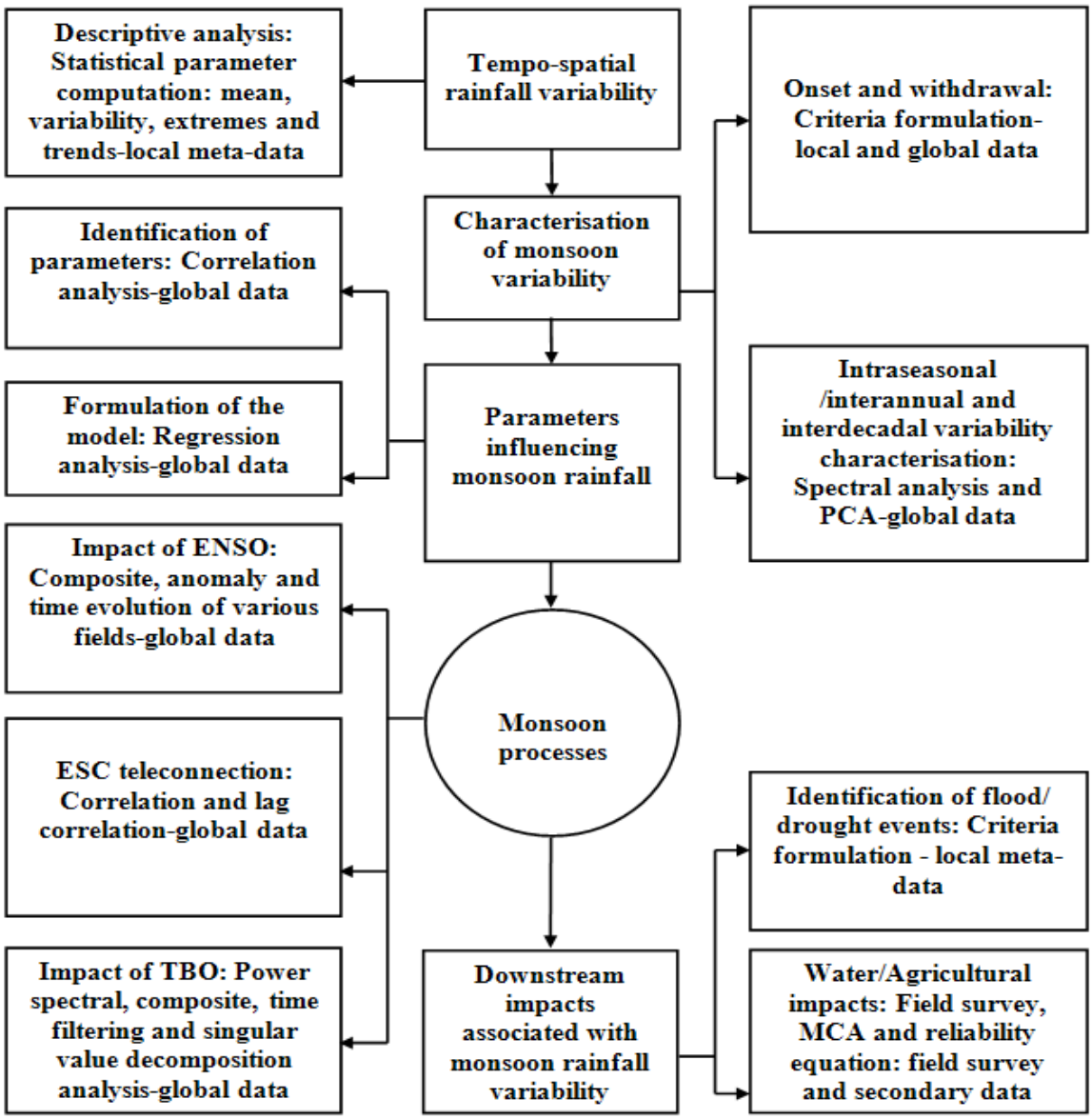

Figure 2.1: Schematic diagram showing different methods and data used for the analysis.

2.1 Global datasets

2.1.1 Daily precipitation data

Daily accumulated rainfall data were obtained from the TRMM 3B42 Version 6 (Tropical Rainfall Measuring Mission) which is a joint mission between NASA and the Japan Aerospace Exploration Agency, designed to monitor and study tropical rainfall. The data were acquired using the GES-DISC Interactive-online Visualization and Analysis Infrastructure (GIOVANNI) as part of NASA's Goddard Earth Sciences (GES) data and information services center (DISC) located at http://disc.gsfc.nasa.gov. The algorithm applied is the TRMM Multi-Satellite Precipitation Analysis (TMPA). Data were available for the period from 1998 to the present with a global spatial coverage of 50° S - 50° N and a spatial resolution of 0.25° x 0.25°.

During the rainfall data period (1998-2007) only two leap years (2000 and 2004) were contained in the data series. To standardize the calculation procedure, each year was considered to have 365 days (i.e. rainfall occurring on 29 February 2000 and 2004 were omitted from the analysis). Preliminary analysis suggests that omitting 29 February (2000 and 2004) rainfall for the calculation does not cause serious problems, because February is in the middle of the dry season for the Asian region (Yokoi 2007; pers. comm.) and very little precipitation was observed over nearly all of the sub-regions of Asia.

2.1.2 Monthly precipitation data

Enhanced mean monthly precipitation data from the Climate Prediction Center (CPC) merged analysis of precipitation (CMAP) was obtained for the Asian monsoon region (15°S-30°N, 30°E-120°E). Enhanced mean monthly precipitation values are derived by combining five kinds of satellite estimates (GPI, OPI, SSM/I scattering, SSM/I emission and MSU), while blended NCEP/NCAR reanalysis precipitation values are also included. Precipitation data were available for the period from 1979 to 2007 with a spatial coverage of 2.5 degree latitude x 2.5 degree longitude on the global grid.

2.1.3 Sea surface temperature (SST)

The extended reconstructed sea surface temperature (ERSST) was obtained from NOAA_ERSST_V3 data provided by NOAA/OAR/ESRL PSD at Boulder, Colorado, USA, from their web site at http://www.cdc.noaa.gov/. ERSST is constructed using the most recently available International Comprehensive Ocean-Atmosphere Data Set (ICOADS) for SST data and improved statistical methods that allow stable reconstruction using sparse

data. Monthly values of SST are available from January 1854 to the present with a spatial coverage of 2.0 degree latitude x 2.0 degree longitude global grid (89x180).

2.1.4 Mean sea level pressure (MSLP)

For mean sea level pressure (MSLP) data, NCEP/DOE 2 reanalysis data provided by the NOAA/OAR/ESRL PSD at Boulder, Colorado, USA, was obtained from their web site at http://www.cdc.noaa.gov/. The NCEP-DOE Reanalysis 2 project used a state-of-the-art analysis/forecast system to perform data assimilation using past data. NCEP-DOE Reanalysis 2 is an improved version of the NCEP Reanalysis 1 model that fixed errors and updated parameterizations of physical processes. The monthly data are available from 1979 to the present with a spatial resolution of 2.5-degree latitude x 2.5-degree longitude.

2.1.5 Air temperature (AT)

Monthly mean air temperature was obtained from Kalnay et al. (1996) NCEP/NCAR Reanalysis 1. The NCEP/NCAR Reanalysis 1 project used a state-of-the-art analysis/forecast system to perform data assimilation using past data from 1948 to the present. Monthly values are available for 1948 to the present with a spatial coverage of 2.5-degree latitude x 2.5-degree longitude.

2.1.6 Outgoing longwave radiation (OLR)

Daily and monthly National Oceanic and Atmospheric Administration (NOAA) interpolated Outgoing Longwave Radiation (OLR) was obtained from Liebmann and Smith (1996), at their web site (http://www.cdc.noaa.gov/data/gridded/data.interp_OLR.html). The National Environmental Satellite Data and Information Services (NESDIS) of NOAA archives the OLR data onto 2.5-degree latitude x 2.5-degree longitude grids with gaps filled with temporal and spatial interpolation. The interpolation technique is used to minimize the distance in space or time over which a value is interpolated. Details of the interpolation technique can be found in Liebmann and Smith (1996). Daily and monthly values of OLR are available from 1974 to the present. Monthly values are available for 1948 to the present with a spatial coverage of 2.5-degree latitude x 2.5-degree longitude. However, interpolated OLR for 17 March to 31 December of 1978 is unavailable due to satellite failure.

2.1.7 Eurasian snow cover (ESC)

Eurasian snow cover monthly data (time series) were obtained from the Rutgers University Global Snow Lab at http://climate.rutgers.edu/snowcover/, which has been

computed from the weekly NOAA visible satellite imagery and are described in Robinson et al. (1993) and Robinson and Frei (2000). The monthly data covers from November 1966 to present. From the monthly values, winter (December-February), spring (March-May) and snowmelt (snow cover in February minus snow cover in the following May) snow cover anomaly time series were generated for the period 1979-2007.

2.1.8 Zonal and meridional wind, relative and specific humidity and vertical velocity

Monthly data for these variables were obtained from the NCEP-DOE Reanalysis 2 dataset *(*NOAA/OAR/ESRL PSD, Boulder, Colorado, USA), from their web site at http://www.esrl.noaa.gov/psd/ for the period 1979 to 2007. Spatially, the data sets cover 2.5-degrees latitude (90º N-90º S) x 2.5-degree longitude (0º E-357.5º E) with 144x73 global grid points. For these data sets, the vertical levels used include 1000, 925, 850, 700, 500, 400, 300, 250, 200 and 100 hPa.

2.2 Local meteorological data

2.2.1 Precipitation data

Rainfall data (daily, monthly and yearly) from all the local meteorological rainfall stations (Figure 3.1) were obtained from the Maldives National Meteorological Centre (Department of Meteorology) for all the available years up to 2006. The most northern meteorological station (Hanimaadhoo station, Figure 3.1) has 15 years of rainfall data from 1992 to 2006. Thirty-two years of rainfall data are available from the Hulhule (central) station, from 1975 to 2006. Rainfall data from the Kadhdhoo meteorological station are available for the period 1990 to 2006. Rainfall data are available from the Kaadedhdhoo (Figure 3.1) station for 1994 to 2006. The southernmost meteorological station, Gan (Figure 3.1), has 29 years of rainfall data from 1978 to 2006. The rainfall data were updated from 2006 up to 2009 for the analysis in Chapter 8.

2.2.1.1 Use of multiple rainfall datasets

In this study two different types of rainfall datasets were used-ground observation and satellite rainfall data. Rain gauges are the only source of ground rainfall data used, while two sets of satellite rainfall data were used-namely TRMM and CMAP rainfall data. Satellite and ground measurements have their own advantages and limitations. Rain gauges are effective only if the rain occurs at and around the gauge site. Similarly, satellite based rainfall

measurements pick up good rain in localized cases if the satellite happens to pass over the event at the right time, and over the site or region of interest. Hence, the use of observational and satellite rainfall data by and large depends on the purpose, circumstances and availability of resources. Although observational rainfall data sets obtained from the Maldives provide useful information regarding the rainfall climatology of the Maldives, their use for the whole analysis is limited by their spatial (rainfall data is only from 5 meteorological stations across the Maldives, lying nearly on a straight line from north to south) and temporal coverage (some of the station rainfall data only goes back to 1994). Since ground measurements of rainfall are sparse and irregularly distributed, and the rainfall is spatially and temporally highly variable, alternative data sources such as satellite data represent an attractive alternative to ground measurements. Compared to ground measurements satellite data have the advantage of being collected spatially regularly and homogeneously.

In order to overcome limitations due to spatial coverage of observational rainfall data, gridded satellite data from CMAP were used. This approach provides a consistent series of climate data, enabling comparisons to be made in time and space. Although the CMAP rainfall dataset provides good spatial coverage (90° N-90° S, 0-360° E) with a horizontal resolution of 2.5° x 2.5° and temporal coverage of 1979 to present (Table 2.1)**,** their use is limited, since the data are only available on a monthly basis (monthly means) and hence cannot be used for studying intra-seasonal variability of rainfall (e.g. active and break periods within a season). The TRMM dataset is probably better for this purpose.

Although the TRMM rainfall dataset has short temporal coverage (from 1998 to present), rainfall data are available on a daily basis with a spatial resolution of 0.25° x 0.25° and the dataset is an ideal candidate for studying intra-seasonal variability of rainfall. However, it should be noted that TRMM rainfall data is based on area-averaged measurements and may have some bias due to averaging of localized high precipitation regions with nearby regions having lower precipitation rates. Due to the use of multiple rainfall data sets for different analysis in various sections of the thesis, the findings presented in the thesis may have some drawbacks.

Table 2.1: Summary of different rainfall indices used, together with their spatial resolution and data period.

Rainfall Indices	Region/locations	Spatial resolution	Data period	Data set
Monsoon season total rainfall (JJAS)	15 °S-30 °N/ 30°E-120 °E	2.5° x 2.5°	1979-2007	CMAP
All-Indian monsoon rainfall (AIMR)	68.75°-91.25 °E/ 6.25°-28.75 °N	2.5° x 2.5°	1979-2007	CMAP
Mean annual cycle (MAC)	70-75°E/12-20.25°N, 88-93°E/17.25-25.5°N, 103. 5-108.5 E°/6-14.25°N, 76-81E/20-28.25 N°, 70-75°E 0.5S-7.75°N	0.25° x 0.25°	1998-2007	TRMM
Maldives monsoon rainfall (JJAS)	68.75° E-76.25° E/ 8.75° N-1.25° S	2.5° x 2.5°	1979-2007	CMAP
Annual rainfall (AR)	6.75° N/73.17° E 4.19° N/73.53° E 1.86° N/72.10° E 0.49° N/72.10° E 0.69° S/73.16° E	-	1994-2006	Local observations
Extended monsoon rainfall (MJJASON)	6.75° N/73.17° E 4.19° N/73.53° E 0.69° S/73.16° E	-	1992-2006	Local observations

2.2.2 Other local data

The other local data used includes air temperature, relative humidity, mean sea level pressure, wind speed, cloud cover and sunshine and were obtained from the Maldives National Meteorological Centre (Department of Meteorology).

2.3 Field survey data

Details of the field survey carried out in the Maldives and data obtained during the field survey are described in Chapter 8 and methods used for the field survey data analysis are also described in Chapter 8.

2.4 Methods

2.4.1 Correlation analysis

Correlation analysis is a statistical procedure for determining the extent to which two or more variables are linearly related. The correlation coefficient (CC; r) is the numerical measure of the association and direction of a relationship between two variables. Throughout this research, correlation analysis has been widely used to assess relationship between rainfall and other variables. The practical importance of the rainfall time series trend was assessed by a simple measure, goodness of fit (r^2), which is the fraction of original variance of the rainfall series accounted for by the fitted trend line and is define as (Guhathakurta and Rajeevan 2008):

$$r^2 = 1 - \frac{Var\ (e_t)}{Var\ (x_t)}$$

where $Var\ (e_t)$ the variance of the rainfall is time series, and $Var\ (x_t)$ is the variance of the residuals from the trend line. r^2 can vary between 0 and 1. A value of 0 meas the trend line account for a small ahare of the rainfall variation, and 1 indicates that the rainfall series shows a simple linear trend (Guhathakurta and Rajeevan 2008).

2.4.2 Regression analysis

In this study, the stepwise backward selection method is adopted to assess the relationship between a dependent (predicted) variable and several independent (predictor) variables. Stepwise regression of independent variables is basically a combination of backward and forward procedures (Turalioglu et al. 2005). In backward selection, all the predictor variables are entered into the model. The weakest predictor variable is then removed and the regression re-calculated. If this significantly weakens the model then the predictor variable is re-entered, otherwise it is deleted. This procedure is then repeated until only useful predictor variables remain in the model.

Multiple regression enables assessment of the relationship between a dependent (predicted) variable and several independent (predictor) variables. It is valuable for quantifying the impact of various simultaneous influences upon a single dependent variable. Furthermore, because of bias associated with omitted variables when using simple regression, multiple regression is often essential even when the effect of only one of the independent variables is of interest. The end result of multiple regression is the

development of a regression model between the dependent variable and several independent variables. A general regression equation which has five independent variables can be expressed as (Turalioglu et al. 2005) :

$$Y = C_o + C_1X_1 + C_2X_2 + C_3X_3 + C_4X_4 + C_5X_5 + e$$

where C_0 is a constant of regression, $C_{1,2,3,4,5}$ are coefficients of regression and $X_{1,2,3,4,5}$ are independent variables. The values of the constant and the coefficients are determined using the least-squares method, which minimizes the error (e) in the above regression equation. The coefficient of determination (r^2) measures the proportion of the variability in the dependent variable that is explained by the regression model through the independent variables (Turalioglu et al. 2005) . It is the sum of all the deviations from the regression line squared and it measures the goodness of fit for the estimated regression model. r^2 tends to somewhat over-estimate the success of the model, so an Adjusted r^2 value is calculated which takes into account the number of variables in the model and the number of observations the model is based on. Hence, the adjusted r^2 value gives the most useful measure of the success of the model. In regression analysis, a value of adjusted r^2 = 1 indicates that the fitted equation accounts for all the variability of the values of the dependent variable in the sample data. At the other extreme, r^2 = 0 indicates that the regression equation explains none of the variability. It is assumed that a high r^2 assures a statistically significant regression equation and that a low r^2 indicates the opposite (Turalioglu et al. 2005). For regression analysis to work "correctly" (that is, to give unbiased and reliable results), a number of assumptions need to be met (Nayagam et al. 2008). This includes:

1. Linearity
2. Independence of residuals
3. Homoscedasticity and
4. Normality of residuals

The first assumption is related to the linearity between the dependent variable and the independent variables. The second assumption is related to the independence of the residuals. If the residuals are not independent the statistical viability tests are not valid. The third one (homoscedasticity) is related to the constant variance of the residuals (residuals must have constant variance). The fourth is the normal distribution of the errors. The

assumption of normality is that errors of prediction are normally distributed (no residuals should lie very far from the mean). According to Nayagam et al. (2008) , if all these assumptions were achieved for the data under consideration the multiple linear regression would provide good forecasts. The above assumptions will be discussed in more detail in Section 5.5.2.

2.4.3 Singular value decomposition

Singular value decomposition analysis described by Bretherton et al. (1992) and Wallace and Bretherton (1992) was employed to find the coupling patterns between Maldives region monsoon rainfall and transition conditions (500 hPa geopotential height, equatorial Indian Ocean and eastern equatorial Pacific SST) in March-April-May (MAM). The SVD technique is often used to determine the co-varying (coupling) patterns between two climate fields (Deser and Timlin 1997). The cross-covariance matrix of SVD identifies coupled spatial patterns between the two fields and explains as much as possible of the mean-squared temporal covariance (Bretherton et al. 1992). The cross-covariance matrix of SVD yields two spatially uncorrelated orthogonal sets of singular vectors and a set of singular values associated with each pair of vectors. Each pair of spatial patterns describes a fraction of the squared covariance between the two variables and the patterns are ordered according to the amount of squared covariance explained, with the first patterns describing the largest fraction of the squared covariance (Deser and Timlin 1997; Peng and Fyfe 1996). The expansion coefficients for each variable are computed by projecting the vectors onto the corresponding original data field and the correlation coefficient between two expansion coefficient time series indicates how strongly the coupled patterns are related (Peng and Fyfe 1996; Venegas et al. 1997). Details of application of the SVD method to meteorological data can be obtained from Bretherton et al. (1992), Wallace and Bretherton (1992) and Venegas et al. (1997). For the mentioned transition conditions and the precipitation data, anomalies are computed for all grid points and are used for the inputs of SVD method.

2.4.4 Principal component (empirical orthogonal function) analysis

Empirical orthogonal function (EOF), known as Principal component analysis (PCA) has been carried out to identify the most important patterns of the monsoon rainfall over Asia. PCA is a multivariate statistical method whose objective is to reduce the number

of predictive variables and transform them into new variables, called principal components (PC) (Sousa et al. 2007). The number of new variables or PCs are the same as the number of original variables (Field 2005; Sharma 1996; Tabachnick and Fidell 2007) and are independent linear combinations of the original data retaining the maximum possible variance of the original set (Sousa et al. 2007). The first new variable or PC accounts for the maximum variance in the data, followed by the second and the third PCs, which account for the variance that has not been accounted by the first PC. The first few PCs account for most of the variance in the original data (Sharma 1996). The number of principal components that should be retained is discussed within the body of the thesis (in Chapter 4).

2.4.5 Composite analysis

In order to examine the anomaly related to different fields, a composite procedure similar to that used by Palmer and Sun (1985) and Peng and Fyfe (1996) is adopted. In Chapter 6, for the case of ENSO composites, El Niño and La Niña years were identified and grouped together (all El Niño and La Niña years were averaged separately) to form a warm and cold SST anomaly composites. Similarly, a non-ENSO year composite was generated by averaging all the years, except non-El Niño and non-La Niña years. The difference between warm and cold composite anomalies is also generated. Similarly, composites were formed for different variables (OLR, vertical velocity, vertically integrated moisture transport (VIMT) and precipitation). In Chapter 7, years with high and low snow cover (for winter, spring and snowmelt) were identified to form composites of monsoon rainfall for the Maldives region to examine the influence of Eurasian snow cover on Maldives monsoon rainfall. Composites of strong minus weak ENSO-only TBO years and for non-ENSO-only TBO years were generated separately for SST, OLR, wind, moisture flux and local Hadley circulation to determine the formation and propagation of these fields before, during and after the monsoon onset, in relation to Maldives monsoon rainfall for ENSO-only TBO years and for non-ENSO years. Furthermore, SST anomaly composites using unfiltered data for wet, normal and dry years of Maldives monsoon rainfall (Table 7.9) for El Niño and La Niña events are formed to crosscheck whether some of the spatial composites and correlations are results of an artificial outcome of the band-pass filter used to separate the data into TBO and ENSO time scales. Details of identification of the El Niño, La Niña, strong and weak ENSO TBO and non-ENSO-only TBO, wet, normal and dry years are described in Chapter 7.

2.4.6 Time-filtering technique

In order to study the intraseasonal variability of five monsoon regions (Western Ghats, Bay of Bengal, East Asia, Central India and Maldive Islands: shown in Figure 4.28), precipitation data were extracted and the mean annual cycle (MAC) for each region was generated by averaging precipitation data for the 1998-2007 period. The obtained MAC time series were smoothed 300 times with a 1-2-1 filter to eliminate residual wiggles associated with imperfect sampling of the annual variation, without smearing the true annual variation (Hartmann and Michelsen 1989), thus helping to derive a smoothed mean annual cycle (SMAC) for each region (described in Chapter 4). To retrieve the 30-60 day and 10-20 day periodicity components, having cut-off periods of 25-70 days and 10-25 days, a Lanczos bandpass filter discussed by Hartmann and Michelsen (1989) and designed by Duchon (1979) was applied to the 154-day precipitation anomaly data.

Another filter that was applied in this study is Murakami's (1979) band-pass filter, which is used to separate the data into an approximately TBO time frame (2-3 year) and ENSO time frame (3-7 year), in order to differentiate the processes responsible for TBO and ENSO forcings. Two types of filters are designed for this purpose, one for seasonal rainfall means (June-September Maldives monsoon rainfall) and one for monthly data (e.g. SST and OLR). For both filters, the time frequencies of the peak-power point is represented by W_0 and the two lateral half-power points represented by W_1 and $W_2$and are related as follows (Li and Zhang 2002):

$$W_0^2 = W_1.W_2$$

Half power points of the response function for the TBO time scale window are located at 18 and 36 months, while for the ENSO time frame it is located at 42 and 86 months, with the spectral peak-power points of these two time scale windows located at 2 and 5 years, respectively (Li and Zhang 2002; Li et al. 2001; Pillai and Mohankumar 2009). Standardized anomaly data (precipitation and other variables) are used for the band-pass filter input. The words "times scale" are used interchangeably to mean time frame.

2.4.7 Power spectrum analysis

Identification of periodicities is important for the understanding of rainfall variability (Naidu et al. 1999). To examine the periodicity of the monsoon season rainfall over Asia, India and the Maldives, power spectrum analysis was carried out. Interannual time scale periodicities were determined following a similar method used by Munot and

Kothawale (2000). On the other hand, intraseasonal time scale periodicities of monsoon precipitation were determined following Yokoi et al. (2007). The power spectral density or the power spectrum estimates the periodicities based on procedures employing the fast Fourier transform (FFT) (Azad et al. 2008). The periodogram of a discrete-time series *x*(n) with unit time interval (so that the Nyquist frequency is 1/2) is given as (Azad et al. 2008):

$$\hat{x}(\omega_k) = \frac{2}{N}\left|\sum_{n=0}^{N-1} x(n)e^{-i\omega_k n}\right|^2,$$

where $\omega_k = \frac{2\pi k}{N}$, N is the sample size and $k = 0, 1, \ldots, N/2$ is the frequency index. The value of $\hat{x}(\omega_k)$ is a measure of the contribution to the "energy" of x by the frequency ω_k (Azad et al. 2008).

3 Rainfall variability – Descriptive analysis

In this chapter, a descriptive analysis of rainfall variability over the Maldives is provided by pooling all available precipitation data. In the past, no studies have looked at rainfall variability across the Maldives, so this is the first study of its kind. Due to the limited number of rainfall stations in Maldives (a total of five stations), temporal and spatial variability of precipitation across the country will be analysed by looking at the individual stations and by combining the rainfall data from all the stations (for the analysis of spatial variability). Figure 3.1 shows the locations of the five meteorological stations in the Maldives. The most northern station, Hanimaadhoo, is geographically located at 6.75° N and 73.17° E. Since the establishment of the Hanimaadhoo meteorological station in 1990, it has been considered that this station would represent the climate of the northern part of the Maldives. This is mainly due to the fact that there are no other meteorological stations in the north. The meteorological station at Hulhule (Figure 3.1) acts as the National Meteorological Centre, and is considered to represent the climate of the central part of the Maldives. The station is located at 4.19° N and 73.53° E. The Kadhdhoo meteorological station (Figure 3.1) is in the south and is the closest station to the National Meteorological Centre to the south. This station is located at 1.86° N and 72.10° E. The meteorological station at Kaadedhdhoo (Figure 3.1) is the second most southern meteorological station in the Maldives, located at 00.49° N 72.10° E. The most southern station, Gan, is located at 0.69° S and 73.16° E and is considered to represent the climate of the southern part of the Maldives.

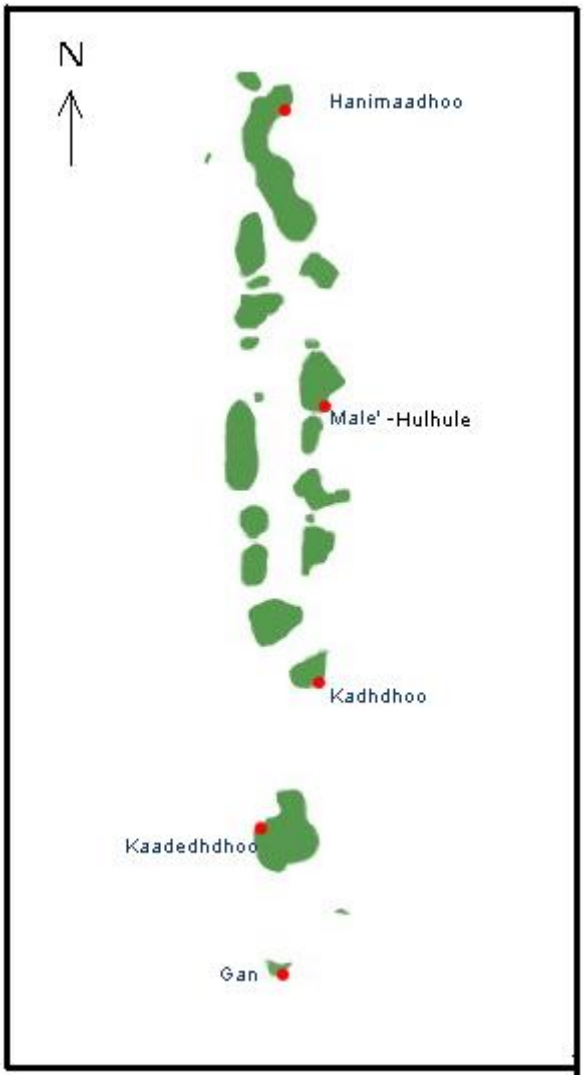

Figure 3.1: Location of the meteorological stations in the Maldives[2].

3.1 Temporal patterns of rainfall variability

3.1.1 Temporal pattern of annual rainfall variability

Temporal patterns of annual rainfall variability over the Maldives were examined using the rainfall data for the period 1975-2006 obtained from the five meteorological stations described above. It should be noted that the data period varies from location to location (Table 3.1). The annual rainfall at all stations shows considerable interannual variability (Figure 3.2). Some of the annual rainfall time series appear to fluctuate randomly, while some station shows a regular periodic pattern. For example, Hanimaadhoo total annual rainfall shows a periodic pattern. The Hulhule annual rainfall also shows an irregular pattern. The Kadhdhoo annual total rainfall also shows a periodic pattern, that was

[2] Taken from: www.met.gov.mv

disturbed due to the high rainfall observed in 2006. The time series of Kaadedhdhoo annual rainfall follow no regular pattern up to the year 1998, although after 1998 the annual rainfall time series shows a periodic pattern. Although the Gan annual time series shows interannual variability, there is no regular periodic pattern. Such rainfall periodicities will be examined in Chapter 4. Table 3.1 summarises the temporal coverage and statistical parameters for these stations. The precipitation varies considerably, with the minimum and maximum annual rainfall of 1346.5 mm (for the north: Hanimaadhoo) and 3185.7 mm (for the south: Gan), respectively. On average, the annual rainfall varied between 1785.4 (north) and 2295.3 mm (south) (Table 3.1).

Table 3.1: Annual rainfall statistics for the five meteorological stations.

Station name	Data period	Minimum (mm)	Mean (mm)	Maximum (mm)	Standard deviation
Hanimaadhoo	1992-2006	1346.5	1785.4	2240.5	289.6
Hulhule	1975-2006	1407.0	2003.3	2711.2	315.7
Kadhdhoo	1990-2006	1643.5	2290.6	3126.9	375.6
Kaadedhdhoo	1994-2006	1814.6	2285.1	3059.1	401.5
Gan	1978-2006	1548.8	2295.3	3185.7	351.9

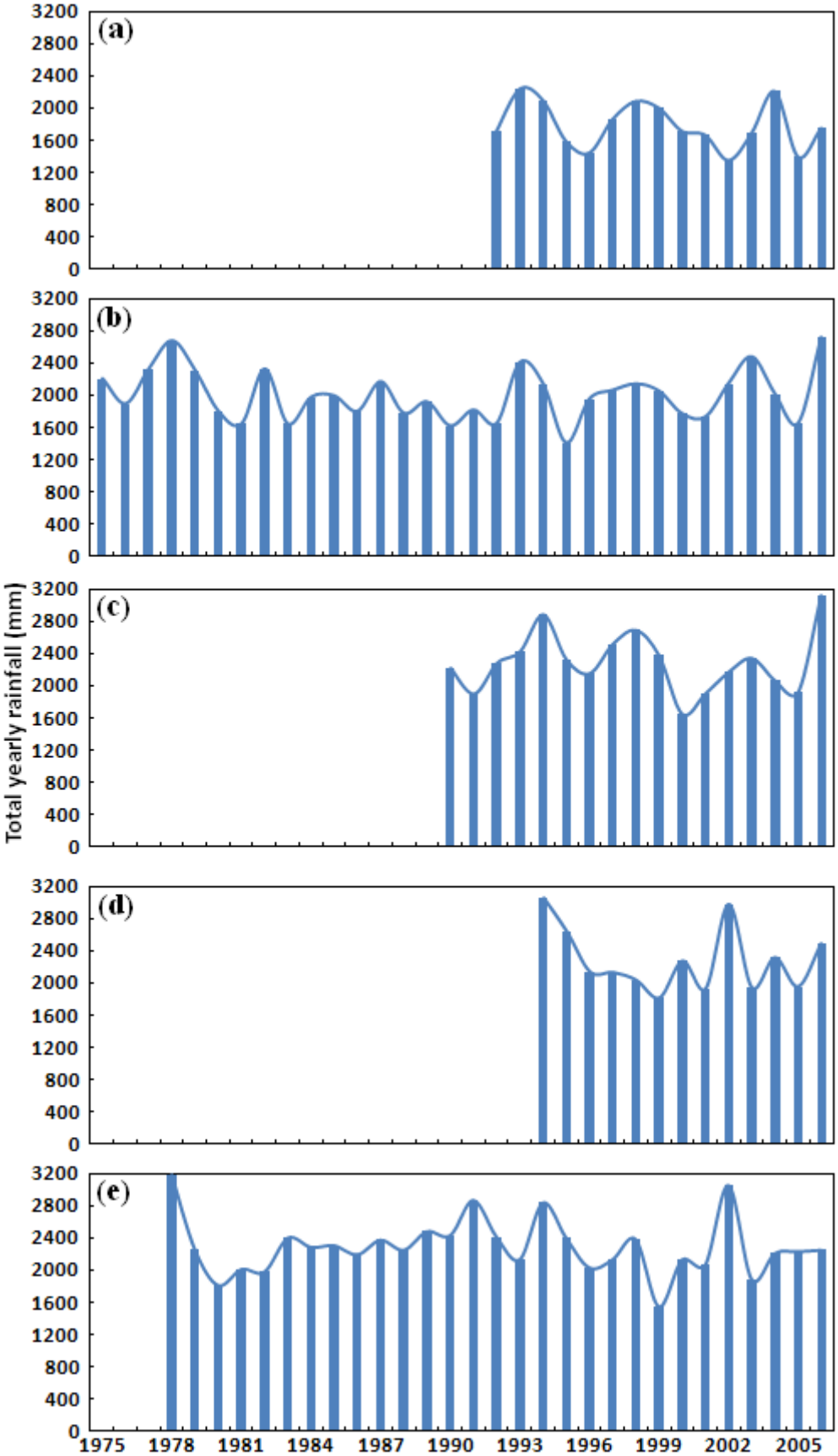

Figure 3.2: Yearly total rainfall for: (a) Hanimaadhoo, (b) Hulhule, (c) Kadhdhoo, (d) Kaadedhdhoo and (e) Gan. Note the difference in data period for each station.

Linear trend lines were fitted to the yearly total rainfall data series to investigate the general tendency of the series over the course of the observational data period as shown in Figure 3.3. The annual rainfall was also smoothed using a 3-year moving average (Figure 3.3) in order to damp time series fluctuations (Ho et al. 2003; Naidu et al. 1999). Except Kadhdhoo, all other locations show a general decreasing trend in annual rainfall (Table 3.2 and Figure 3.3). The maximum decreasing trend of 25.7 mm/year was obtained for the Kaadedhdhoo station (Table 3.2and Figure 3.3d). Visual determination of trends from the graphs (yearly rainfall and moving average) can be very subjective, depending on individual judgment. Hence, the rainfall time series trend for each location was assessed based on r^2, and is presented in Table 3.2. The calculated r^2 explains about 7.4, 0.1, 0.01, 6.2 and 1.4% of the total variance of annual rainfall for Hanimaadhoo, Hulhule, Kadhdhoo, Kaadedhdhoo and Gan, respectively. To determine whether there is a statistically significant trend in annual precipitation, a systematic trend analysis was performed using Spearman's non-parametric statistics (Ahmed et al. 2008; Antonopoulos et al. 2001; Dahmen and Hall 1990; De Luis et al. 2000; Grantz et al. 2007). Spearman rank correlation is similar to the Pearson's correlation coefficient, except that the data need not be normally distributed and it is robust against outliers (Grantz et al. 2007; Haylock et al. 2006). The Spearman rank correlation (R_s) was calculated following Ahmed et al.(2008), Antonopoulos et al. (2001) and Dahmen and Hall (1990) to detect significant trends at 95% significant level:

$$R_s = 1 - \frac{6\sum_{i=1}^{n} di^2}{n(n^2-1)}$$

where n is the number of years, di is the difference between X (years) and Y (rainfall) ranks: di = rank of Xi – rank of Yi. The null hypothesis, H_0: R_s = 0 (there is no trend) is checked against the alternative hypothesis, H_0: $R_s <> 0$ using the test statistic:

$$t_t = R_s\left(\sqrt{\frac{n-2}{1-R_s^2}}\right)$$

where t_t follows Student's t-distribution, with n-2 degrees of freedom (d.f.). According to Antonopoulos et al. (2001) and Dahmen and Hall (1990), at a 5% significance level, the annual rainfall time series has no significant trend if:

$$\mathbf{t}\,(\mathbf{d.f}, \mathbf{2.5}\%) < \boldsymbol{t_t} < \boldsymbol{t}(\mathbf{d.f}, \mathbf{97.5}\%)$$

and the null hypothesis is accepted if t_t is not contained in the critical region. Results of the Spearman's non-parametric test for all the locations are summarised in Table 3.2. None of the t statistics illustrate in the table satisfy the above inequality. Hence, the results presented in the table suggest that there exists no significant trend in Maldives annual rainfall (for any of the meteorological stations).

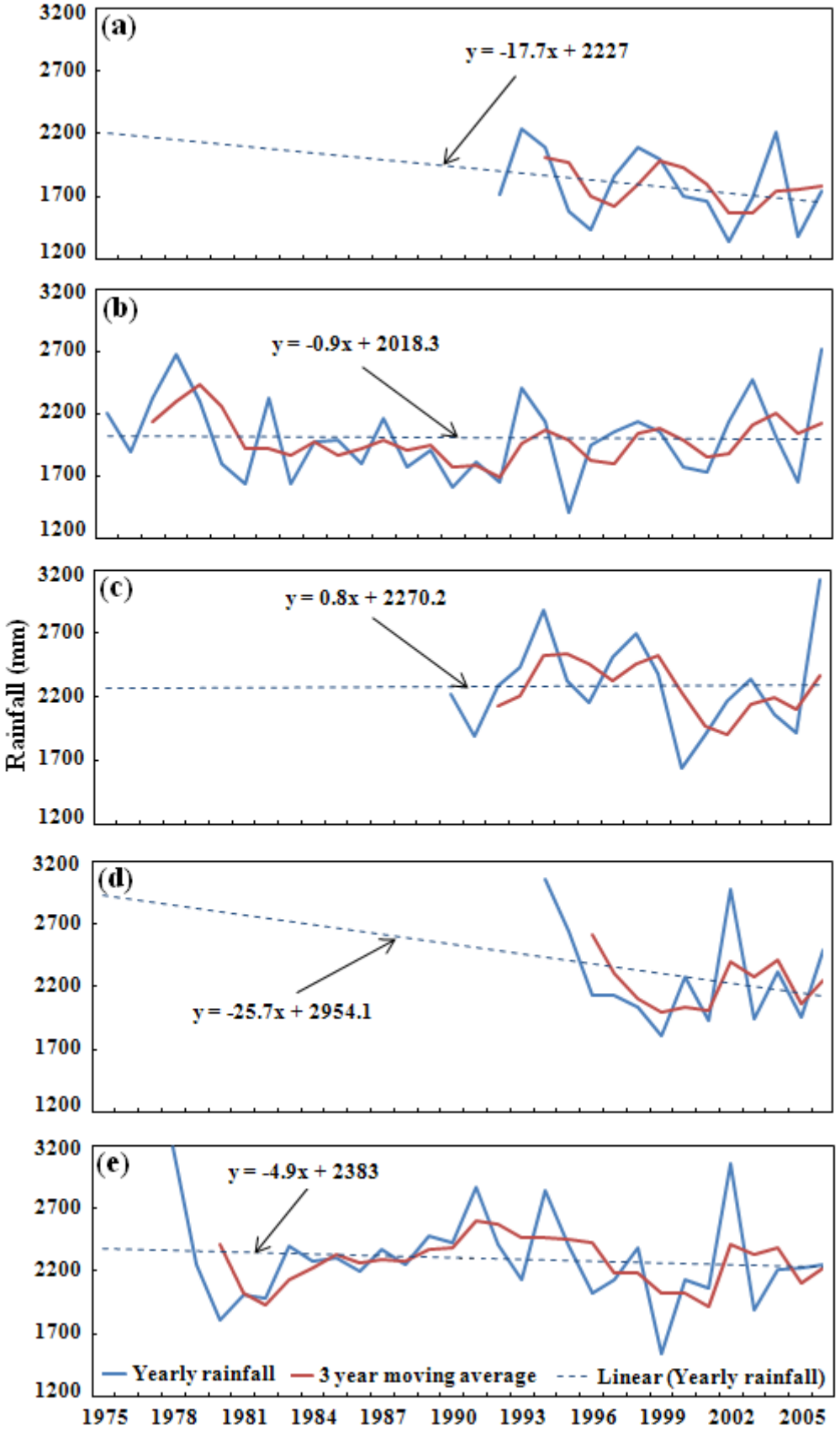

Figure 3.3: Yearly total rainfall and 3 year moving average together with yearly rainfall linear trend for: (a) Hanimaadhoo, (b) Hulhule, (c) Kadhdhoo, (d) Kaadedhdhoo and (e) Gan. Common legend is shown in bottom figure.

Table 3.2: Summary statistics of the annual rainfall for the five stations.

Station name	Rainfall trend (mm) (+/-)	r^2	d.f (n-2)	R_s	t_t
Hanimaadhoo	17.7 (-)	0.074	13	-0.282	-1.060
Hulhule	0.9 (-)	0.001	30	-0.045	-0.249
Kadhdhoo	0.8 (+)	0.0001	15	-0.042	-0.162
Kaadedhdhoo	25.7 (-)	0.062	11	-0.214	-0.728
Gan	2.9 (-)	0.014	27	-0.134	-0.705

Figure 3.4 shows the relationship between annual rainfall and rainy days for all the locations. The highest correlation coefficient (CC = 0.69) between total annual rainfall and yearly rainy days was obtained for Kaadedhdhoo (Figure 3.4d). On the other hand, the lowest CC (0.39) was obtained for Hulhule (Figure 3.4b). The correlation coefficient between annual rainfall and yearly rainy days (Figure 3.4) indicates there is positive relationship between the two variables for all the locations, which is significant at the 95% level. Analysis of daily rainfall reveals that the northern part of the Maldives (represented by Hanimaadhoo) experienced a minimum number of rainy days[3] (123 days in 1996: Table 3.3 and Figure 3.4a), with an average number of rainy days of 135 days/year and standard deviation of 8.5 days, while the southern part of the Maldives (represented by Gan) accounts for the highest number of rainy days (198 days occurred in 1989: Table 3.3 and Figure 3.4e), with an average number of rainy days of 164 days/year and a standard deviation of 17.6 days for the region. The lowest numbers of rainy days for the southern region was observed in 1982, accounting for a total of 124 rainy days (Table 3.3 and Figure 3.4e). The yearly total numbers of rainy days indicates that there is an increase in number of rainy days in the southern region (0.22 days/year). The maximum numbers of rainy days for the northern region was observed in 2004, accounting for a total of 154 rainy days (Table 3.3 and Figure 3.4a). The yearly total number of rainy days for this region indicates that there is a general increasing trend of the number of rainy days, with an increase of about 0.28 days/year. The lowest numbers of rainy days for central Maldives (represented by Hulhule) was observed in 1990, accounting for a total of 134 rainy days (Table 3.3 and

[3] In the Maldives, it is considered to be a rainy day if there is 0.3 mm or more of rain in a 24 hour period.

Figure 3.4b). The yearly total numbers of rainy days for central Maldives indicates that there is a general increasing trend of the number of rainy days with an increase of about 0.09 days/year. Analysis of Kadhdhoo daily rainfall reveals that on average this site receives rainfall on 156 days in a year. The highest and lowest numbers of rainy days were observed in 2006 and 1990, accounting for a total of 178 and 131 rainy days, respectively (Table 3.3 and Figure 3.4c). The yearly total numbers of rainy days indicates that there is a general increasing trend in the number of rainy days with an increase of about 1.26 days/year. Kaadedhdhoo daily rainfall reveals that on average this location of the Maldives receives rainfall on 162.5 days in a year. The highest and lowest numbers of rainy days were observed in 2006 and 1997, accounting for a total of 177 and 151 rainy days, respectively (Table 3.3 and Figure 3.4c). The yearly total numbers of rainy days indicates that there is no decreasing or increasing trend in number of rainy days.

Table 3.3: Annual total number of rainy days for the five meteorological stations.

Station name	Data period	Minimum (days)	Mean (days)	Maximum (days)	Standard deviation
Hanimaadhoo	**1992-2006**	**123**	**135**	**154**	**8.5**
Hulhule	**1975-2006**	**134**	**152**	**172**	**10.4**
Kadhdhoo	**1990-2006**	**131**	**156**	**178**	**13.1**
Kaadedhdhoo	**1994-2006**	**151**	**162**	**177**	**8.5**
Gan	**1981-2006**	**124**	**164**	**198**	**17.6**

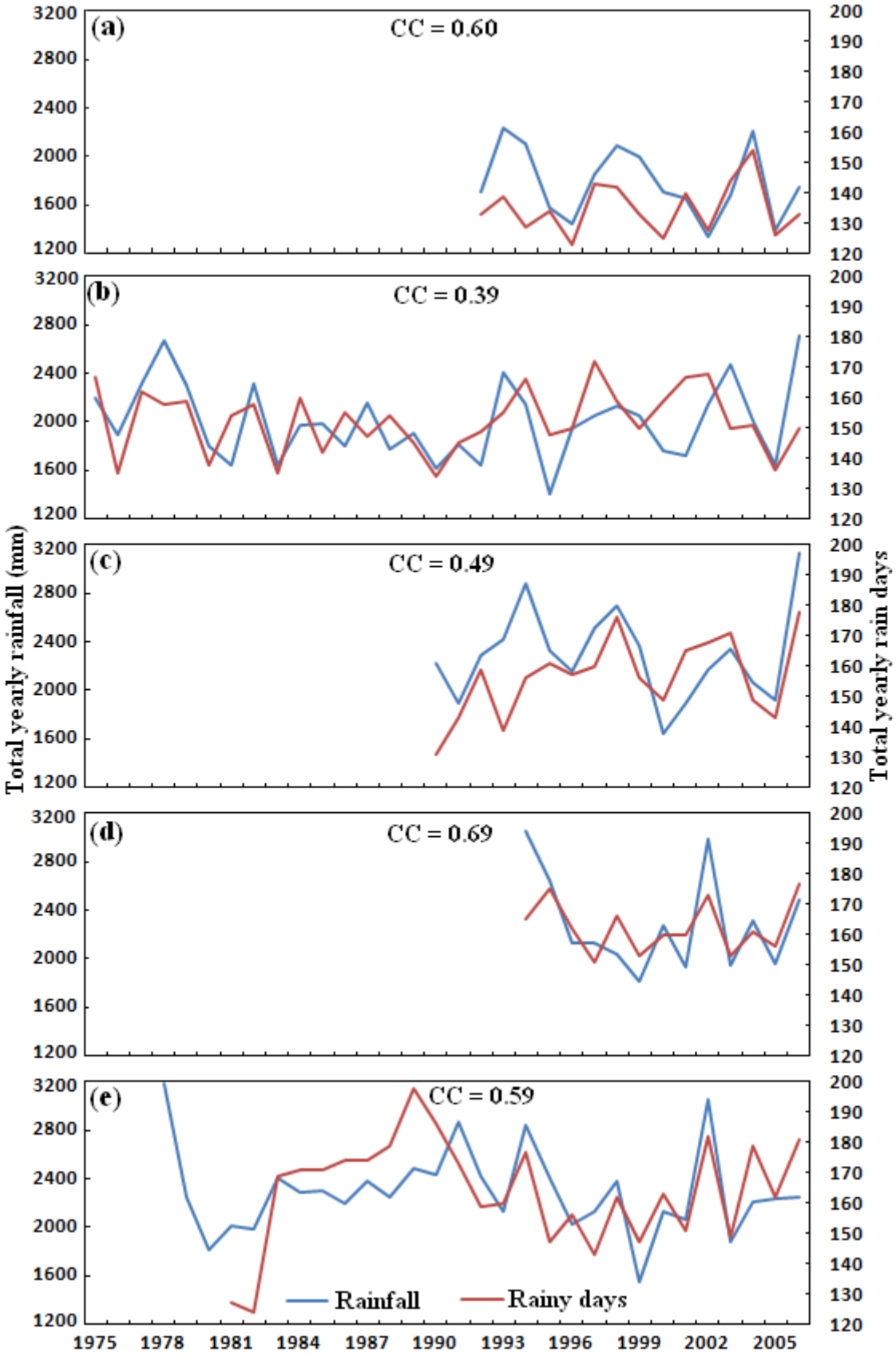

Figure 3.4: Yearly total rainfall and rainy days and their corresponding correlation coefficient (CC) for: (a) Hanimaadhoo, (b) Hulhule, (c) Kadhdhoo, (d) Kaadedhdhoo and (e) Gan. Common legend is shown in bottom figure.

3.1.2 Monthly rainfall comparison

Comparison of monthly average rainfall with average monthly rainy days shows a very similar pattern between the two variables for each station (Figure 3.5). As the figure illustrates, monthly rainfall and rainy days appears to be strongly related to each other, with the highest correlation coefficient (CC = 0.98) obtained for the northern region (Hanimaadhoo: Figure 3.5a). Slightly weaker correlations were found for other locations. However, the correlation coefficients obtained for all the stations were significant at 99% level, suggesting quite a strong positive relationship between rainfall and rainy days.

Average monthly rainfall varies from month to month, with most rain falling during the period May to November and relatively little falling outside this period, especially for the north (Hanimaadhoo: Figure 3.5a) and central (Hulhule: Figure 3.5b). A peak in monthly mean rainfall occurs in July for the north and amounts to 273.6 mm on average (Table 3.4). For the same region, a similar pattern also can be seen for the monthly rainy days, with the highest number of rainy days occurring in the months of June and July (Figure 3.5a), each month accounting for about 18.9 days of rain on average with the lowest number of rainy days in the month of March (2.1 days on average). There is a general decreasing trend of monthly average rainfall and rainy days from December to March with the lowest peak in March for the region (Hanimaadhoo: Figure 3.5a). During this month, average rainfall is 14.6 mm. The monthly mean rainfall and rainy days at Hanimaadhoo is 148.8 mm and 11.3 days, with a standard deviation of 89.2 mm and 6.1 days, respectively (Table 3.4). On average, the northern part of the Maldives receives about 4.9 mm of rain per day, with the heaviest rainfall within a twenty-four hour period for the station observed on 3 November, 1993 (135.6 mm).

For Hulhule and Kaadedhdhoo stations, a peak in monthly mean rainfall occurs in November, with 242.5 and 270.0 mm on average (Table 3.4 and Figure 3.5b and d), respectively. On the other hand, the highest number of rainy days for Hulhule and Kaadedhdhoo is observed for the month of September and October, respectively, each station accounting for about 17.4 and 19.2 days, respectively. The monthly mean rainfall and rainy days at Hulhule is 166.9 mm and 17.4 days, with a standard deviation of 68.8 mm and 4.7 days (Table 3.4), respectively. The lowest rainfall for Hulhule and Kaadedhdhoo occurred in the month of February and March, respectively, with an average rainfall of 40.9 and 71.8 mm, respectively. For the two stations, the lowest number of rainy days (4.3 and 7.1 days, respectively) occurred in the month of February (Figure 3.5b and d). On average, the central part of the Maldives (Hulhule) receives about 5.5 mm of rain per day, with the

heaviest rainfall within a twenty-four hour period for the central parts of the Maldives observed on 11 December, 1998 with 200.0 mm. Furthermore, on average Kaadedhdhoo receives about 6.3 mm of rain per day, with the heaviest rainfall within a twenty-four hour period for Kaadedhdhoo station observed on 9 July, 2002 with 219.8 mm.

The monthly mean rainfall and rainy days at Kadhdhoo is 190.9 mm (with a standard deviation of 75.1 mm) and 13.6 days (Table 3.4), respectively. The monthly average rainfall and rainy days for Kadhdhoo and Gan (Figure 3.5c and e, respectively) indicate a peak in rainfall and rainy days for these two stations occurring in the month of October. The average rainfall and rainy days for the month of October is 291.7 and 18.5 days, respectively, for Kadhdhoo, while for Gan it is 278.0 mm and 17.6 days, respectively. The lowest average rainfall and rainy days for Kadhdhoo and Gan occurred during the month of February (Figure 3.5). On average, the Kadhdhoo and Gan region receives about 6.3 mm of rain per day, with the heaviest rainfall within a twenty-four hour period for Kadhdhoo station observed on 7 October, 1990 with 178.2 mm, while for Gan the heaviest rainfall within a twenty-four hour period was observed on 27 June, 1997 (188.3 mm).

Table 3.4: Monthly rainfall and rainy day statistics for the five meteorological stations. Data periods are: 1992-2006, 1975-2006, 1990-2006, 1994-2006 and 1981-2006 for Hanimaadhoo, Hulhule, Kadhdhoo, Kaadedhdhoo and Gan, respectively.

Station name	Minimum	Mean	Maximum	Standard deviation
Monthly rainfall (mm)				
Hanimaadhoo	**14.6**	**148.8**	**273.6**	**89.2**
Hulhule	**40.9**	**166.9**	**242.5**	**68.8**
Kadhdhoo	**59.9**	**190.9**	**291.7**	**75.1**
Kaadedhdhoo	**71.8**	**190.4**	**270.0**	**64.0**
Gan	**102.8**	**191.3**	**278.0**	**49.9**
Monthly rainy days				
Hanimaadhoo	**2.1**	**11.3**	**18.9**	**6.1**
Hulhule	**4.3**	**12.7**	**17.4**	**4.7**
Kadhdhoo	**4.7**	**13.6**	**18.5**	**4.2**
Kaadedhdhoo	**7.1**	**13.6**	**19.2**	**3.5**
Gan	**7.5**	**13.7**	**17.6**	**2.9**

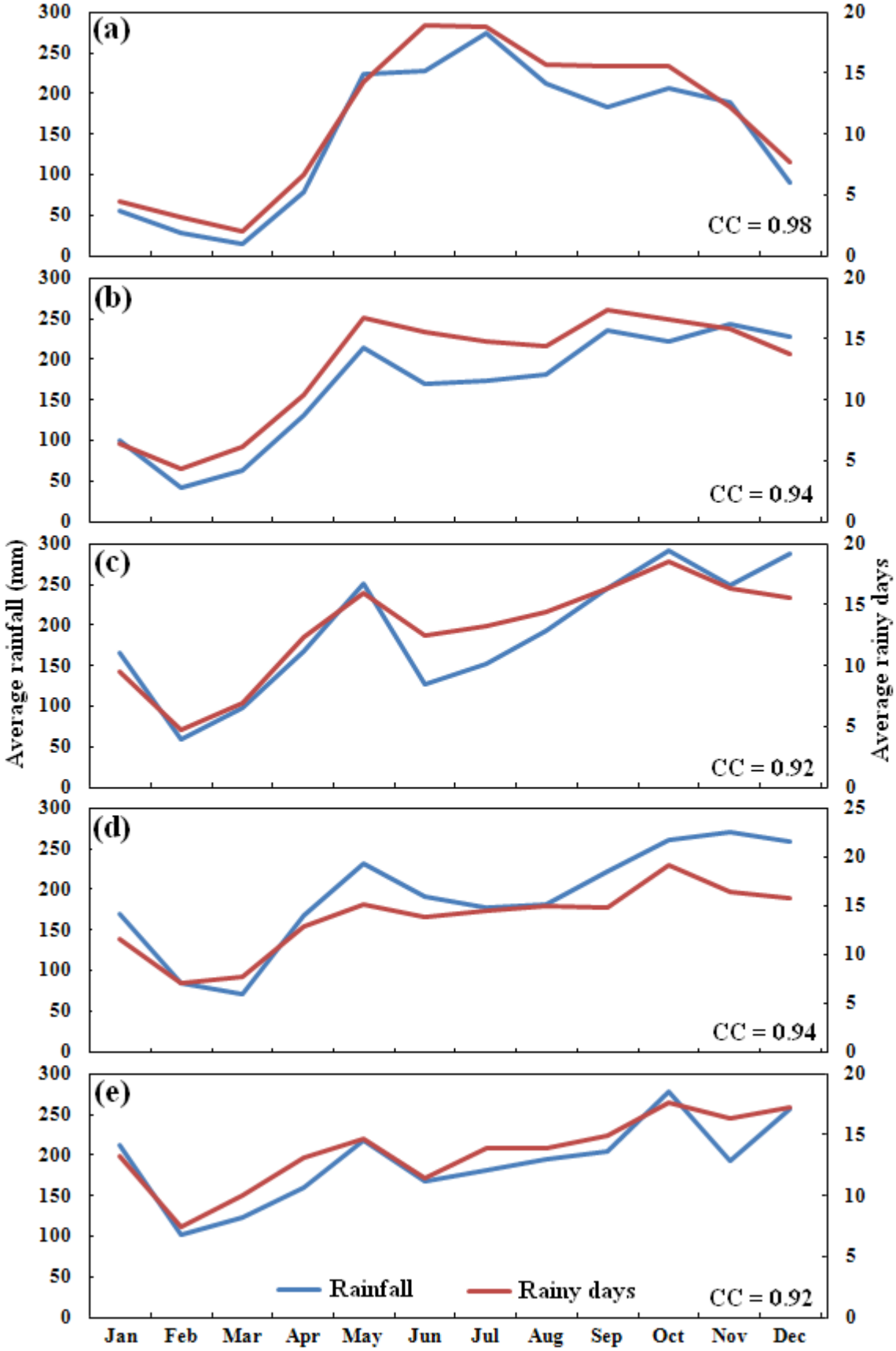

Figure 3.5: Monthly average rainfall and rainy days and their corresponding correlation coefficient (CC) for: (a) Hanimaadhoo, (b) Hulhule, (c) Kadhdhoo, (d) Kaadedhdhoo and (e) Gan. Common legend is shown in bottom figure.

Monthly rainfall from the Maldives was also compared with the monthly rainfall from the Lakshadweep Islands (Minicoy and Amini Island). The Lakshadweep islands are a group of islands that lies to the north of the Maldives in the Arabian Sea (Figure 3.6). Lakshadweep consists of an archipelago of 36 small sized coral islands scattered about 200-400 km from the western coast of southern India between latitude 8.25° N and 11.75° N and longitude 72.00° E and 74.00° E. The Minicoy and Amini Islands of Lakshadweep lie between 8.27º N and 73.05º E and 10.58º N and 72.73º N, respectively.

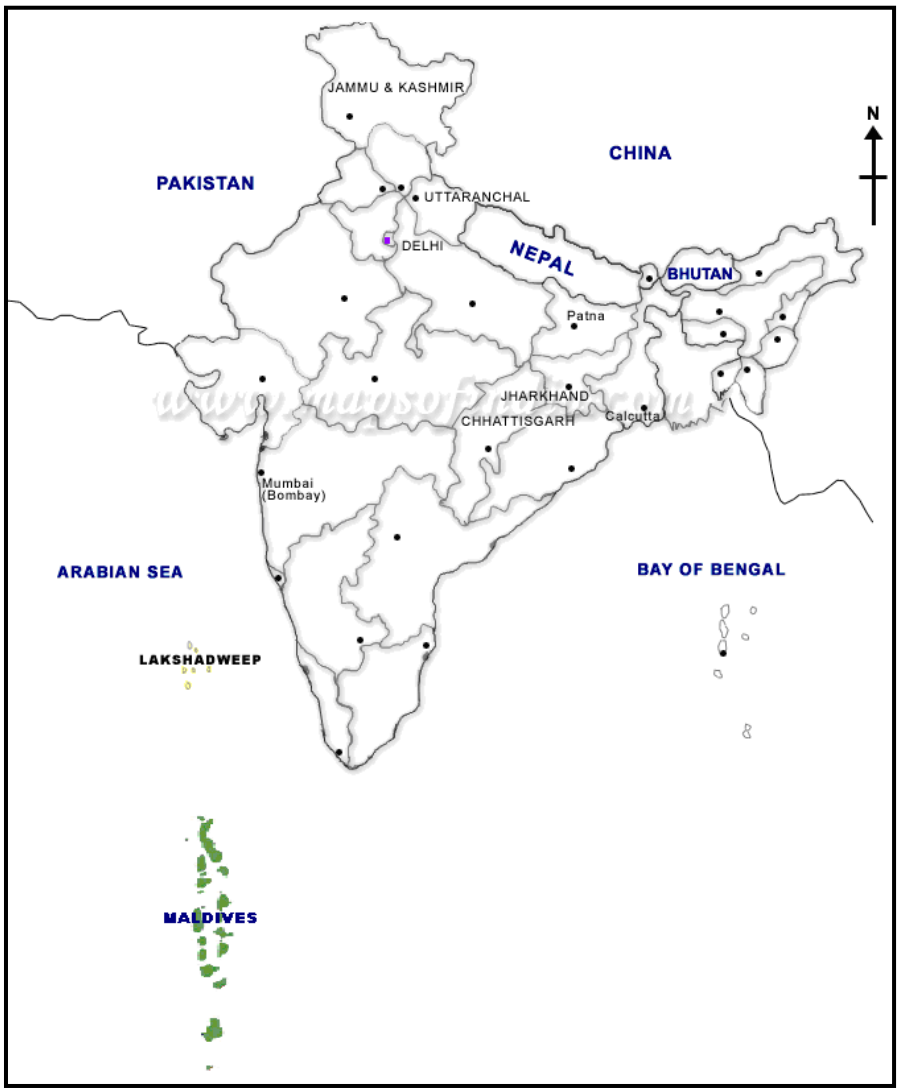

Figure 3.6: Lakshadweep islands in relation to the Maldives.

Figure 3.7 shows the comparison of Hanimaadhoo, Hulhule and Gan rainfall with Minicoy and Amini monthly rainfall. When mean monthly rainfall from the northern part (Hanimaadhoo) of the Maldives is compared with the mean monthly rainfalls from Minicoy and Amini, it shows very interesting patterns (Figure 3.7a). Between January and May, the

northern parts of the Maldives received more rainfall on average (except during March) compared to Minicoy and Amini. During March, Minicoy received more rainfall compared to Hanimaadhoo and Amini. During all the months between January and May, Amini received less rainfall on average compared to Minicoy and Hanimaadhoo (Figure 3.7a). Amini received more rainfall on average between June and August in comparison to the northern parts of the Maldives (Hanimaadhoo). However, in July Hanimaadhoo received more rainfall on average compared to Minicoy. In addition to this, Hanimaadhoo received more rainfall on average during the months of September to December, when compared with both Minicoy and Amini. During these months, Amini received less rainfall on average (Figure 3.7a). When mean monthly rainfall from central (Hulhule: Figure 3.7b) and southern (Gan: Figure 3.7c) parts of the Maldives is compared with the mean monthly rainfalls from Minicoy and Amini, it shows similar patterns as above. The correlation coefficients between Minicoy monthly rainfall and Hanimaadhoo, Hulhule and Gan monthly rainfall respectively (Table 3.5) show that there is a strong relationship between Minicoy monthly rainfall and northern Maldives rainfall. A much weaker relationship exists between Minicoy and central and southern Maldives rainfall. A very similar relationship also exists between Amini monthly rainfall and monthly rainfall at the Hanimaadhoo, Hulhule and Gan (Table 3.5). This suggests that the rainfall pattern over the northern Maldives resembles the regional rainfall patterns.

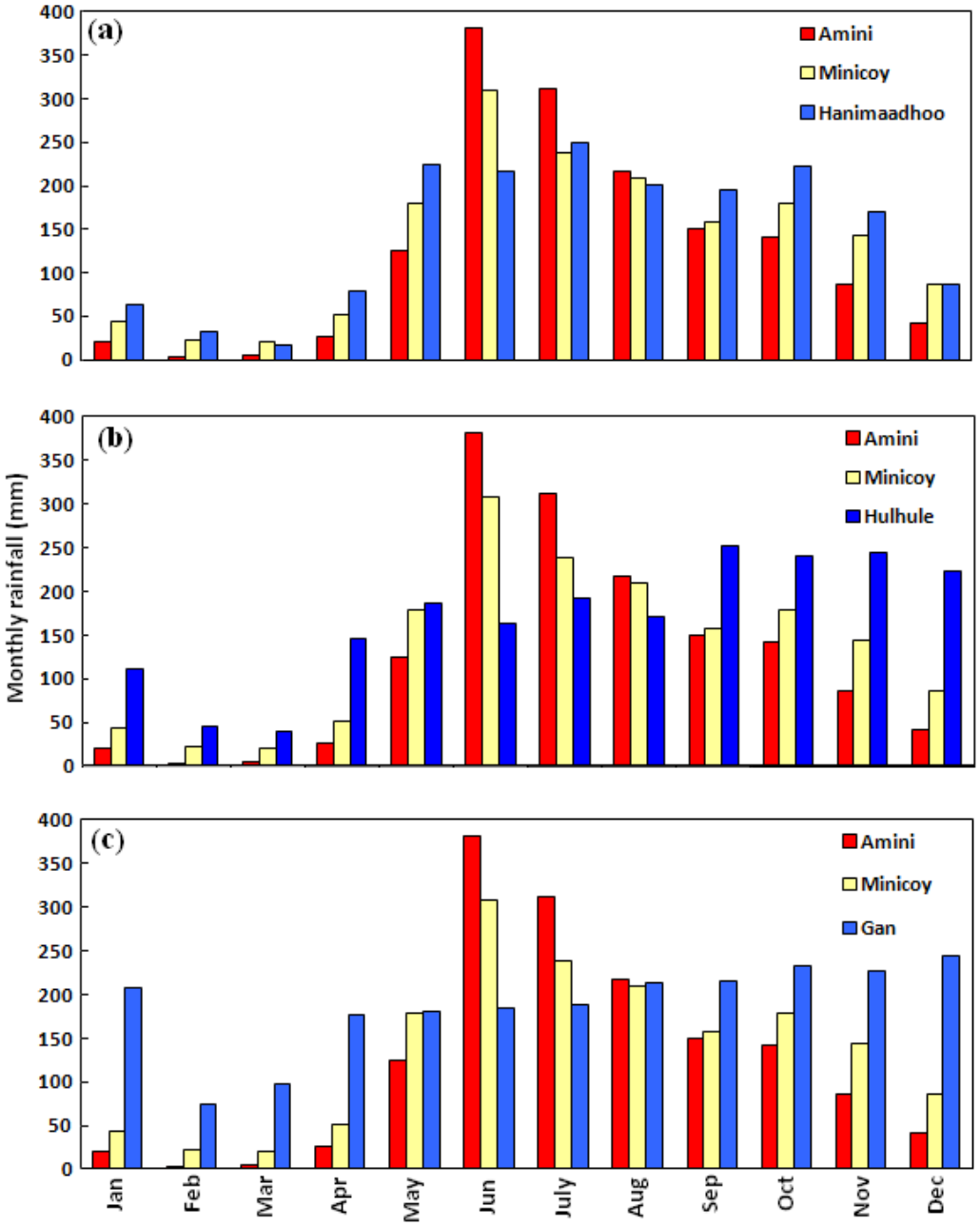

Figure 3.7: Monthly mean rainfall for: (a) Hanimaadhoo, (b) Hulhule and (c) Gan together with mean monthly rainfall for Amini and Minicoy.

Table 3.5: Correlations between Minicoy monthly rainfall and Hanimaadhoo, Hulhule and Gan monthly rainfall and also correlations between Amini monthly rainfall and Hanimaadhoo, Hulhule and Gan monthly rainfall.

	Minicoy	Amini
Hanimaadhoo	**0.92**	**0.82**
Hulhule	**0.56**	**0.39**
Gan	**0.44**	**0.29**

Figure 3.8 shows rainfall departure for the individual stations based on mean annual rainfall for the five stations using the common data period 1994-2006, while Table 3.6 shows annual rainfall statistics based on the same period. Hanimaadhoo shows 17.3 % below normal rainfall (Figure 3.8), compared to the Maldives mean annual rainfall (2123.7 mm: Table 3.6). Annual rainfall at the Hanimaadhoo station for the 1994-2006 period ranges from 1346.3 mm to 2209.3 mm with a mean of 1755.9 mm per year (Table 3.6). Annual rainfall at the Gan station varied from 1548.8 mm to 3048.8 mm, with a mean of 2243.9 mm pear year (Table 3.6). Compared to the mean annual rainfall for the Maldives, Gan station shows 5.7 % above average rainfall (Figure 3.8). The Gan station (to the south) has received more rainfall than the Hanimaadhoo station in all years, except in 1999. In most of the years, annual rainfall at the Hulhule is more than the annual rainfall at the Hanimaadhoo, but less than the Gan annual rainfall. Hulhule shows 5.0 % below normal rainfall (Figure 3.8), compared to the mean annual rainfall of the Maldives (2123.7 mm). Annual rainfall at the Hulhule station ranges from 1407.0 mm to 2711.2 mm with a mean of 2017.2 mm per year (Table 3.6). Kadhdhoo and Kaadedhdhoo show departures of 9.1 and 7.6 % from mean annual rainfall for the Maldives (Figure 3.8) which is consistent with the higher mean annual rainfall of 2316.4 and 2285.1 mm, respectively, compared with other stations (Table 3.6).

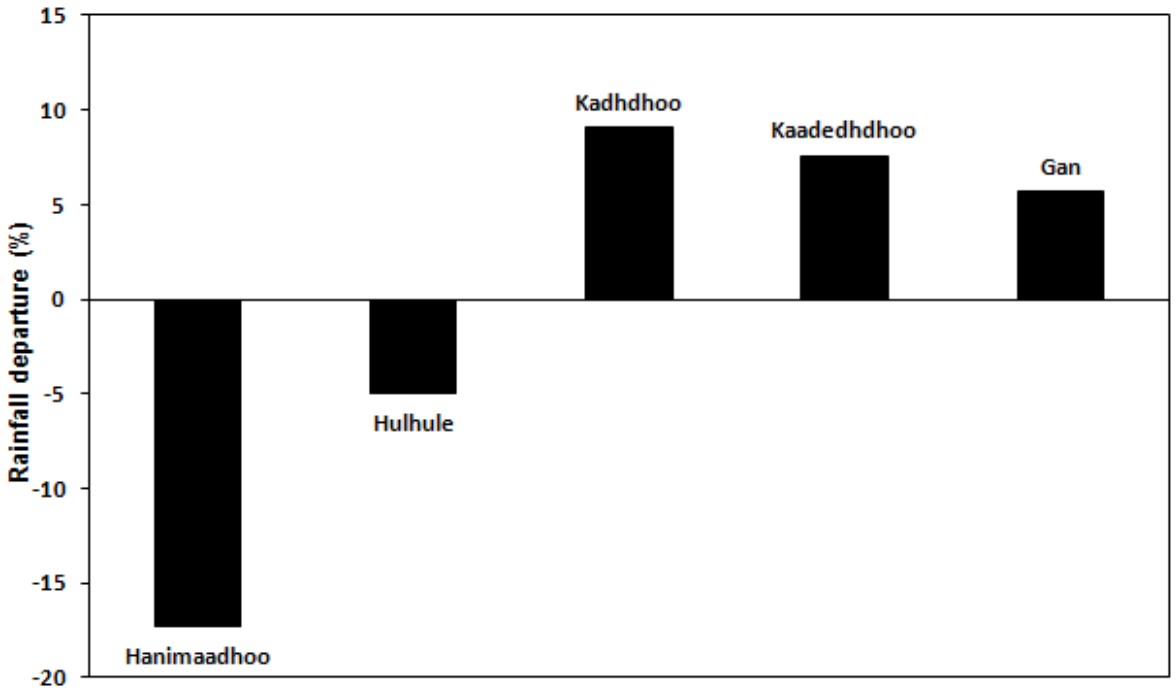

Figure 3.8: Rainfall departure from mean annual total rainfall for five stations based on the common data period (1994-2006).

Table 3.6: Statistics of the annual rainfall for the five stations for the common data period (from 1994 to 2006).

Station	Minimum	Mean	Maximum	Standard Deviation
Hanimaadhoo	1346.5	1755.9	2209.3	281.5
Hulhule	1407.0	2017.2	2711.2	341.0
Kadhdhoo	1643.5	2316.4	3126.9	415.2
Kaadedhdhoo	1814.6	2285.1	3059.1	401.5
Gan	1548.8	22243.9	3056.5	384.1
Mean	**1552.1**	**2123.7**	**2832.6**	**364.7**

3.2 Spatial rainfall variability

3.2.1 Spatial pattern of annual rainfall

To describe the spatial patterns of annual rainfall for the Maldives, data from the five meteorological stations were used for the period 1994 to 2006. This period corresponds to the years where the data are available for all the stations. The mean annual rainfall in the Maldives was 2123.7 mm, based on the five stations over the 13 years (from 1994 to 2006). Spatial distribution of mean annual rainfall shows that there is an increasing trend of rainfall from north to south (Figure 3.9a). Figure 3.9b-d depicts the spatial distribution of total annual rainfall for some selected years (1994, 2000 and 2006). These three years correspond to the beginning, middle and end of the data period, respectively. The spatial pattern of annual rainfall for the year 1994 (Figure 3.9b) also shows an increasing trend of rainfall from north to south and is very similar to the mean annual rainfall (Figure 3.9a). Although year 2000 annual rainfall shows higher rainfall for the southern part of the Maldives, the central region received the least rainfall in this year. On the other hand, in 2006, the central region received the highest rainfall, while the northern region received the least rainfall (Figure 3.9d).

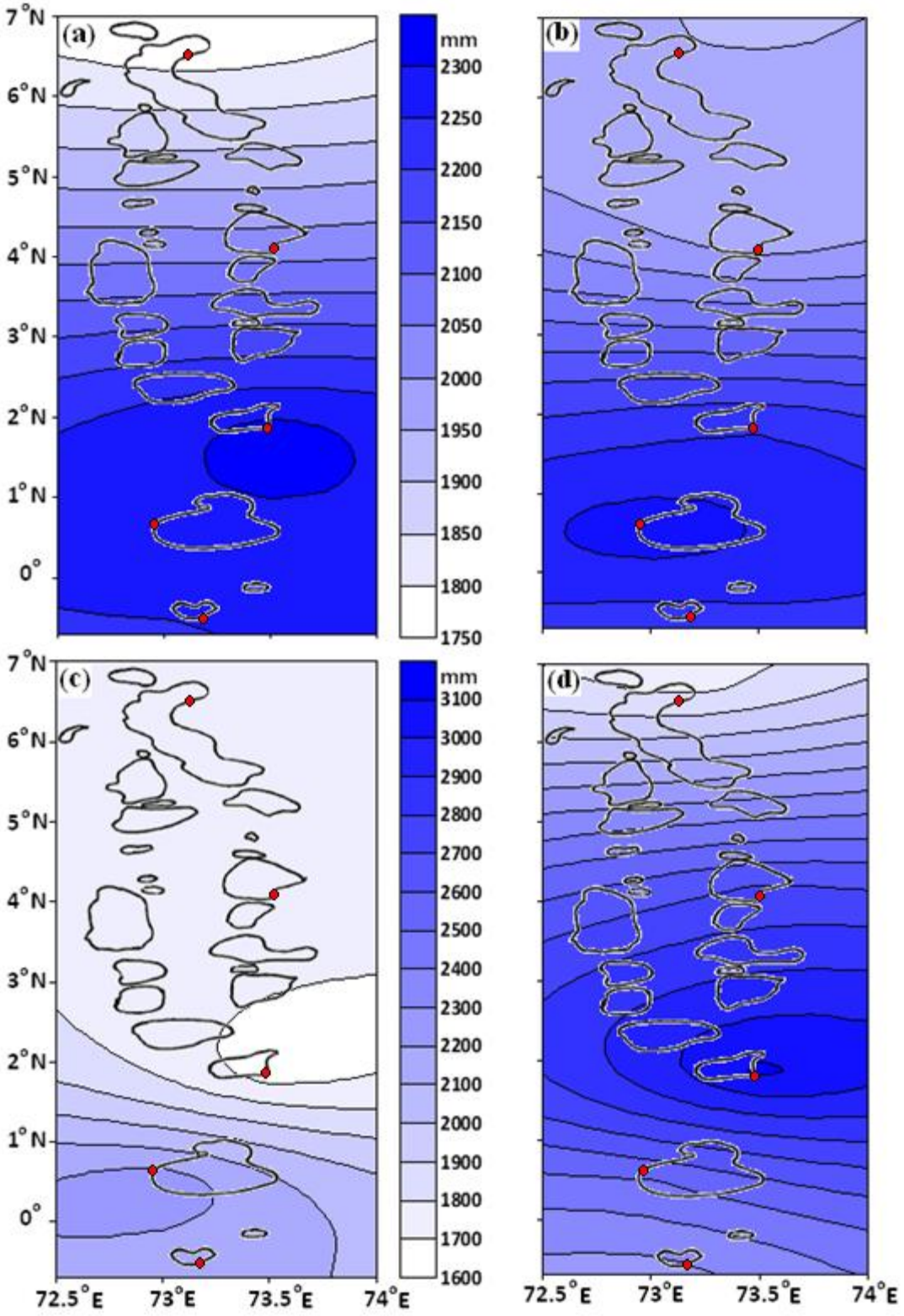

Figure 3.9: Spatial distribution of: (a) mean annual rainfall, (b) 1994 rainfall, (c) 2000 rainfall and (d) 2006 rainfall for the Maldives. Legend for (a) is shown beside it and a common legend for (b), (c) and (d) is shown in (c). The red dots indicate station locations.

3.2.2 Spatial pattern of monthly rainfall

The spatial distribution of monthly rainfall in the Maldives is illustrated Figure 3.10. In order to create monthly rainfall figures, only data for 1994 to 2006 were used from the five meteorological stations in the Maldives, since this period has data for all stations. Average rainfall for the month of January indicates that the rainfall in this month tends to increase from north to south (Figure 3.10a). In January, the average rainfall in the Maldives was of the order of 63.1 mm (for the north) to 208.5 mm (for the south). The same trend also occurs in February (not shown), but the lowest average rainfall for the northern region during February (32.4 mm) is about half of the January mean rainfall (63.1 mm). Furthermore, the highest average rainfall for February was observed for the southern region (Kaadedhdhoo: 84.3 mm), which is far less than the average January rainfall for the same region. Among the months shown in Figure 3.10, March shows quite a low average rainfall pattern for all regions, with an increasing trend from north to south (Figure 3.10b). During this month, the average rainfall varied between 15.7 mm (for north) and 97.5 mm (for south). During the month of April (not shown), the average rainfall varied between 78.2 mm and 176.6 mm for the north and south, respectively. As Figure 3.10c indicates, during the month of May, there is no evident increasing/decreasing trend from north to south or from south to north. During this month, the average rainfall ranges from 180.7 mm to 251.0 mm. The average lowest value for the month was observed in the south (Gan: 180.7 mm) and the highest average was observed near Kadhdhoo (251.0 mm). By the month of July, the trend reversed, with highest rainfall occurring over the north and a decreasing trend towards the south (Figure 3.10d). The average highest and lowest rainfall for the month of July was 249.4 mm and 160.3 mm, for north and south (Kadhdhoo), respectively. During the month of September, the highest average rainfall (253.0 mm) occurred over the central parts of the Maldives. By the month of November, the rainfall trend reversed again with an increasing trend from north to south, with minimum and maximum rainfall of 169.1 mm and 270.0 mm for the northern and southern regions, respectively (Figure 3.10f).

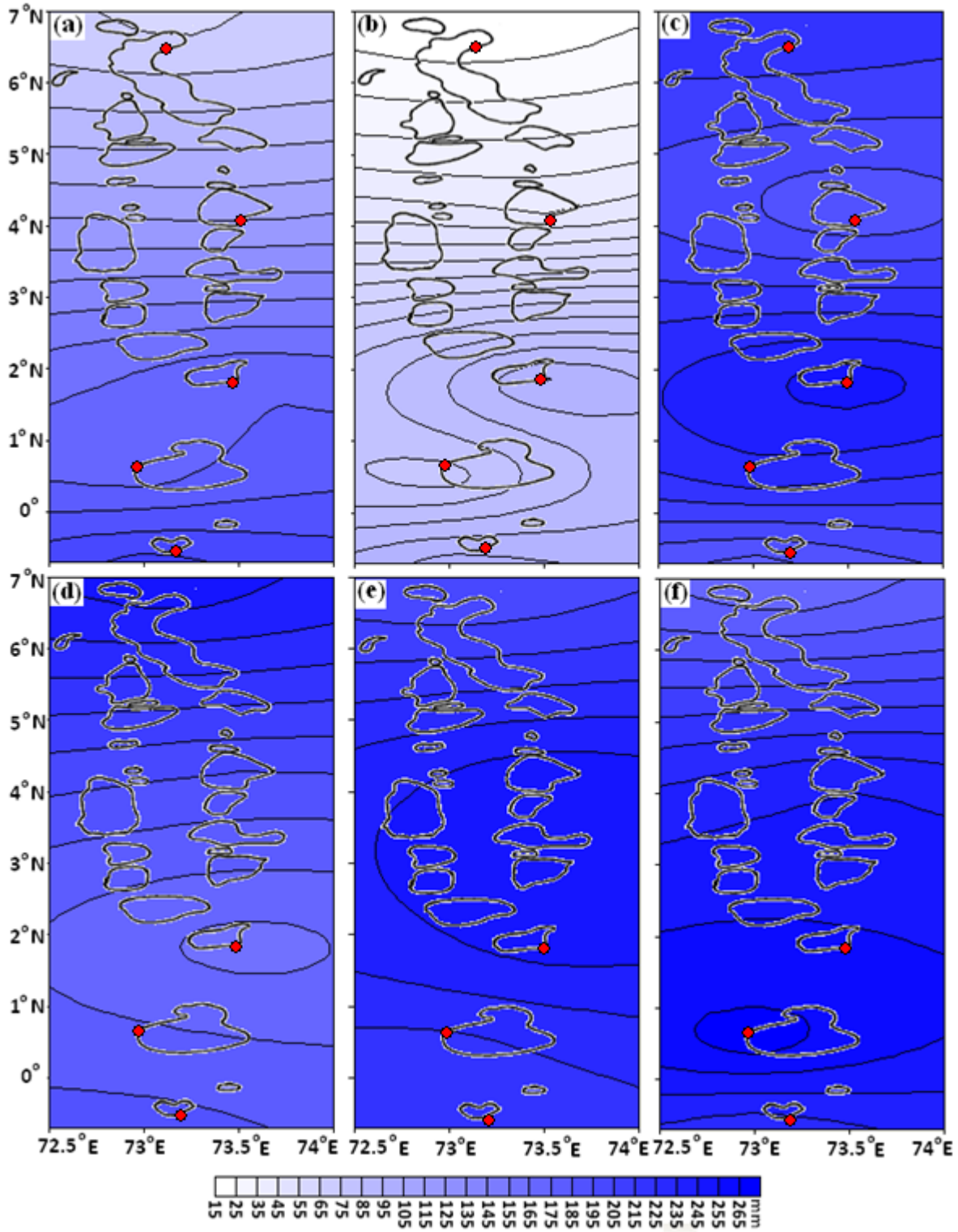

Figure 3.10: Spatial distribution of mean rainfall for: (a) January, (b) March, (c) May, (d) July, (e) September and (f) November. Common legend is shown at the bottom of the figure. The red dots indicate station locations.

3.3 Meteorological parameters and rainfall

An understanding of the characteristics of surface and upper air meteorological fields is essential for a complete understanding of the Indian monsoon and its variability (Mohapatra and Mohanty 2006). A significant correlation between different meteorological parameters and summer monsoon rainfall has been established (Cannon and McKendry 1999). This section will give a brief description of different meteorological parameters related to the annual rainfall over Hanimaadhoo (north), Hulhule (central) and Gan (south) of the Maldives. Meteorological parameters that will be presented in this section include annual average temperate, relative humidity, pressure, wind speed, cloud cover and sunshine for Hanimaadhoo, Hulhule and Gan. Relationship between monsoon rainfall and meteorological parameters will be discussed in Chapter 5 in more detail.

3.3.1 Air temperature

The diurnal temperature variation for the Maldives is small and is observed to reach maximum values of around 33°C during the day and minima of 23°C during the night. The highest and lowest temperature recorded for the northern parts of the Maldives are 34.4°C (27 April 1998) and 18.2°C (23 December 2002), respectively. On the other hand, the highest and lowest temperature recorded for the central parts are 34.1°C (16 & 28 April 1973) and 17.2°C (11 April 1978), respectively. The highest temperature ever recorded for the southern parts of the Maldives is 33.6°C, which was observed on 17 April 1998. The mean annual temperatures for the north, central and south are 28.6, 28.3 and 28.4 °C , respectively.

Figure 3.11 provides a comparison of total annual rainfall and mean annual temperature for Hanimaadhoo, Hulhule and Gan. When annual rainfall for different parts of the Maldives (the north, central and south) is compared with the annual mean temperature from the same areas, both the temperature and rainfall show interannual variability. The correlation coefficients between the two variables show a weak negative relationship, with the highest correlation obtained for Hulhule (Figure 3.11b). None of the correlations are significant at 95% level. The relationship between mean temperature and monsoon seasonal rainfall may have a stronger relationship, and this will be investigated in Chapter 4.

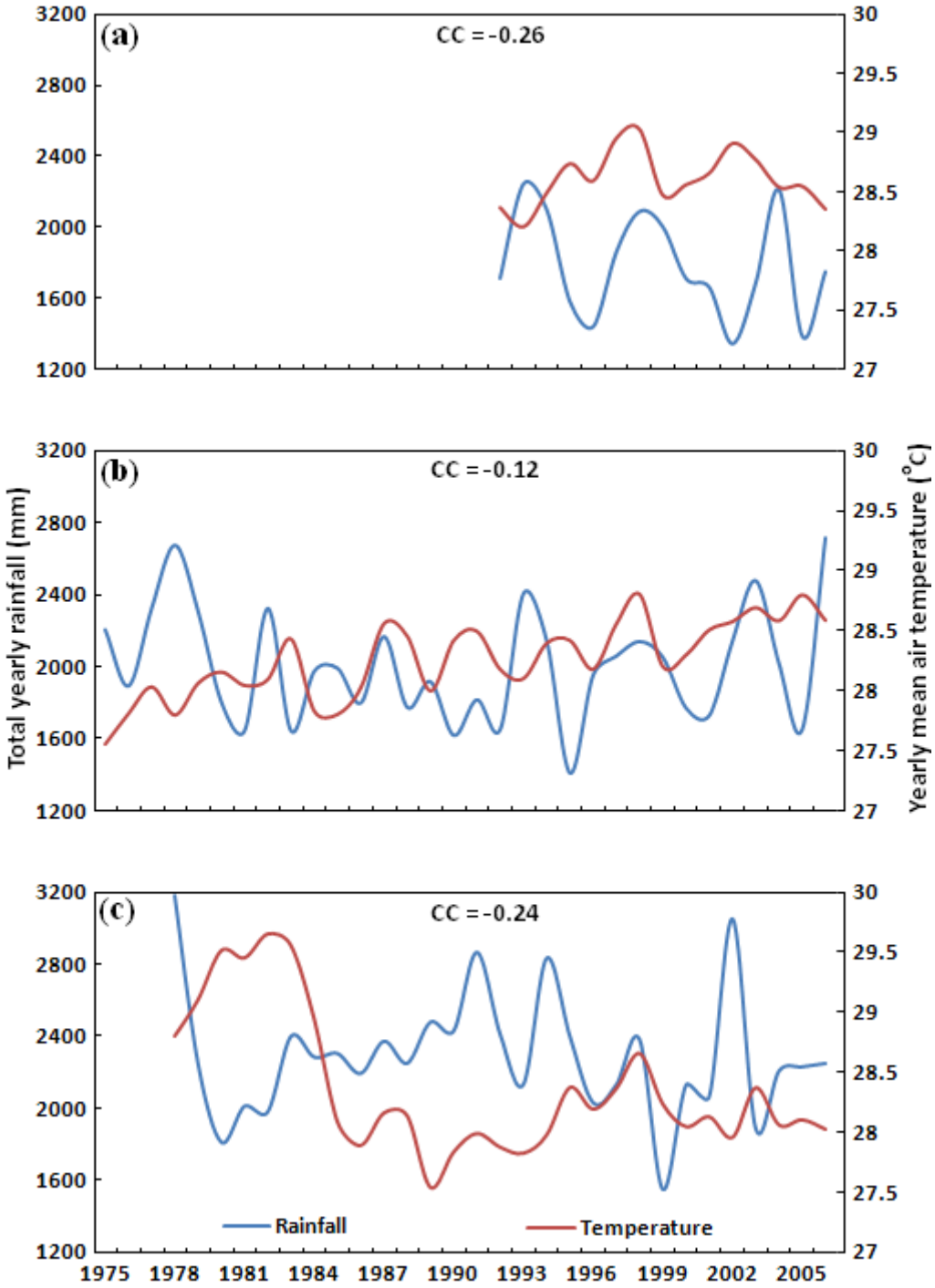

Figure 3.11: Annual total rainfall and mean air temperature and their corresponding correlation coefficient (CC) for: (a) Hanimaadhoo, (b) Hulhule and (c) Gan. Common legend is shown in bottom figure.

3.3.2 Relative humidity

The relative humidity is high all year round in the Maldives. The mean annual relative humidity is 79.6%. The minimum and maximum mean relative humidity for all sites in the Maldives is 72.2 and 88.1%, respectively. Figure 3.12 shows total annual rainfall and mean relative humidity for the Hanimaadhoo, Hulhule and Gan sites. The total

annual rainfall and mean relative humidity for the three locations shows interannual variability. The correlation between Hanimaadhoo (northern part of the Maldives) annual rainfall and relative humidity shows a negative correlation, with CC = -0.24, while the other two locations shows positive correlations. The CC = 0.39 found between rainfall and relative humidity for Hulhule is significant at 95% level, while the CCs found for the other two locations are not significant at 95% level.

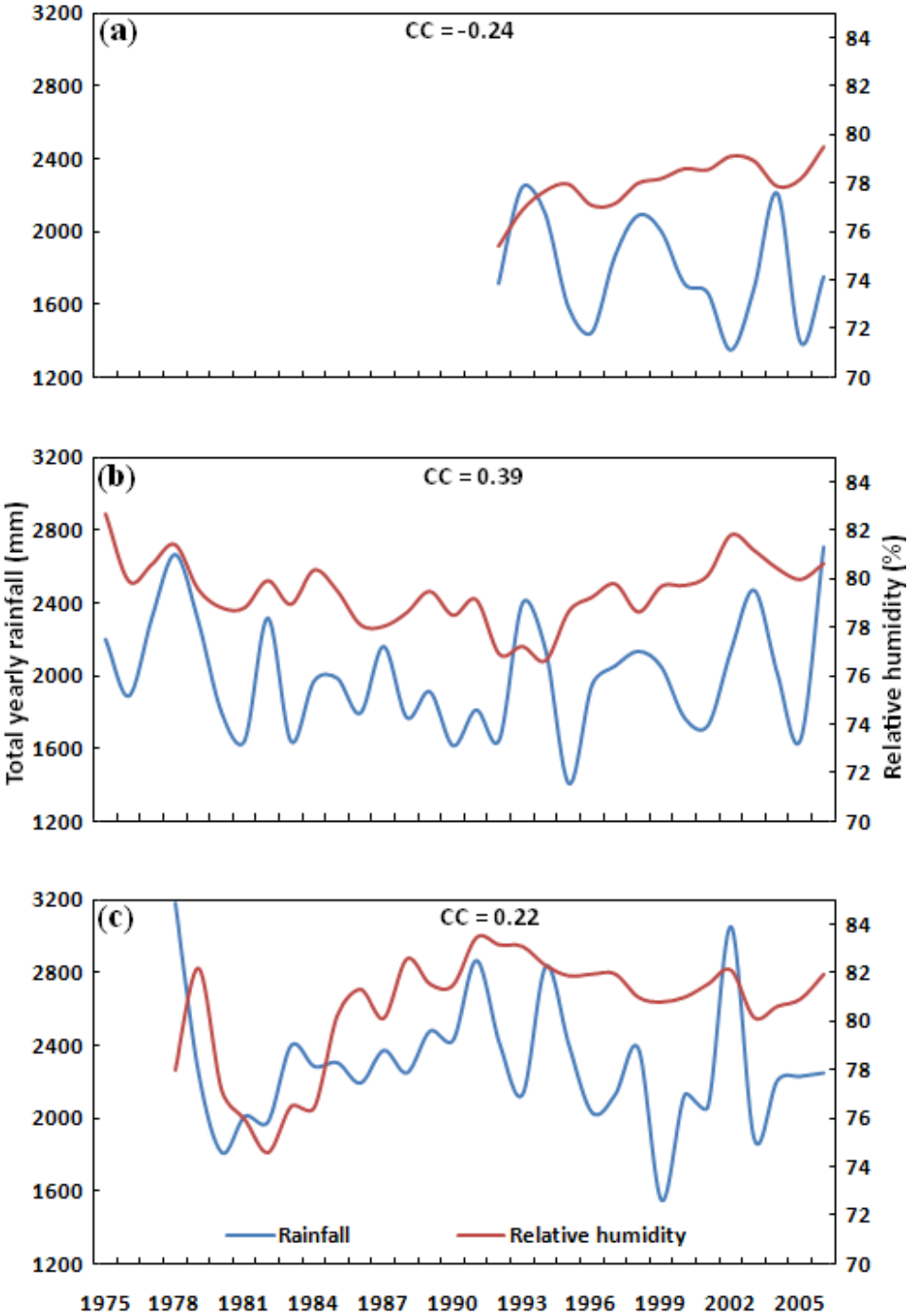

Figure 3.12: Annual total rainfall and mean relative humidity and their corresponding correlation coefficient (CC) for: (a) Hanimaadhoo, (b) Hulhule and (c) Gan. Common legend is shown in bottom figure.

3.3.3 Pressure

The annual mean sea level pressure for the Maldives is 1010.8 hPa, while the mean annual pressure for Hanimaadhoo, Hulhule and Gan is 1010.68, 1010.66 and 1010.99 hPa, respectively. The total annual rainfall and mean annual pressure show interannual variability for these three locations (Figure 3.13). For all locations, very weak correlations were found between annual rainfall and pressure. The highest correlation (CC = -0.29) found was for Hulhule (Figure 3.13b), which is insignificant at 95% level. Hence, there appears to be no connection between annual total rainfall and mean annual pressure for any of these locations.

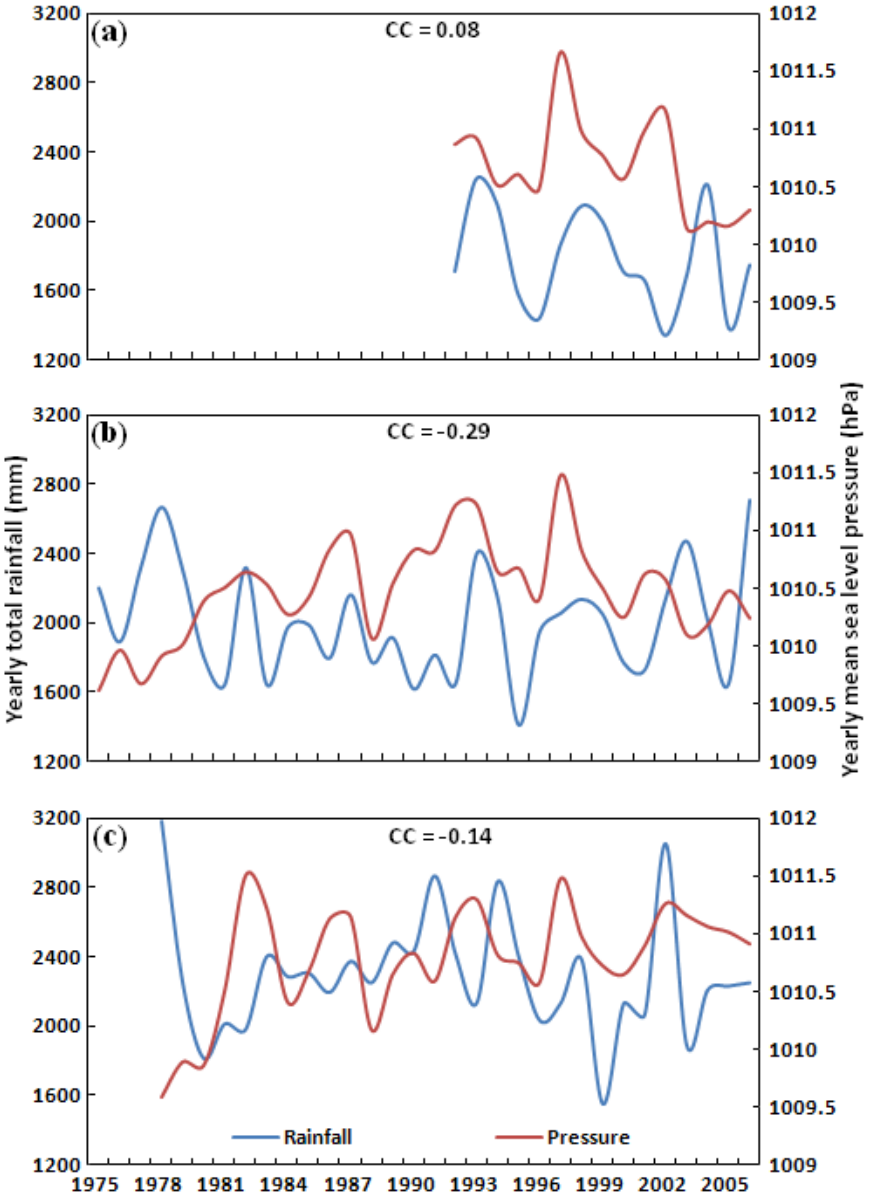

Figure 3.13: Annual total rainfall and mean sea level pressure (hPa) and their corresponding correlation coefficient (CC) for: (a) Hanimaadhoo, (b) Hulhule and (c) Gan. Common legend is shown in bottom figure.

3.3.4 Wind speed

The mean annual wind speed for the Maldives is 8.3 knots. The mean annual wind speeds for Hanimaadhoo, Hulhule and Gan are 8.0, 9.8 and 7.0 knots. The total annual rainfall and mean annual wind speed shows interannual variability for all three sites (Figure 3.14). The relationship between annual rainfall and wind speed for Hulhule shows a strong negative relationship (CC = -0.38: Figure 3.14b), significant at 95% level. Very weak CCs were found for the other two regions, indicating weak connection between annual rainfall and mean annual wind speed for the north and south (Figure 3.14a and c, respectively).

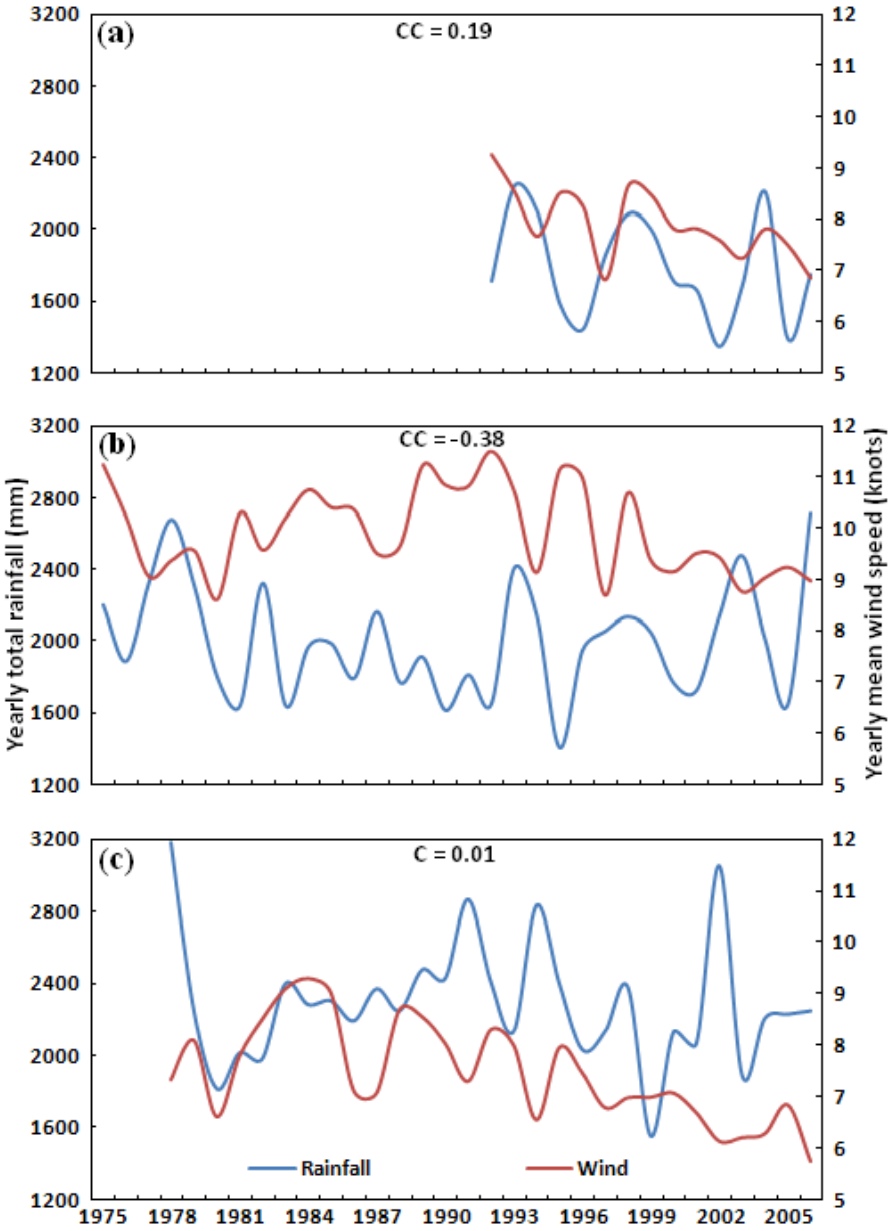

Figure 3.14: Annual total rainfall and mean wind speed (knots) and their corresponding correlation coefficient (CC) for: (a) Hanimaadhoo, (b) Hulhule and (c) Gan. Common legend is shown in bottom figure.

3.3.5 Cloud cover

The mean annual cloud cover for the Maldives is 62.2%, while that for Hanimaadhoo, Hulhule and Gan is 58.3, 64.1 and 64.2%, respectively. Figure 3.15 shows mean percentage cloud cover with the annual total rainfall for Hanimaadhoo, Hulhule and Gan. The total annual rainfall and mean percentage annual cloud cover shows interannual variability for these locations. Although all the locations show a positive relationship, the correlation coefficients indicate no significant relationship (CCs are insignificant at 95% level) between annual total rainfalls and mean percentage annual cloud cover for either of these locations. It is also worth noting that, during all years more than 50% of the sky is covered with cloud for all the locations.

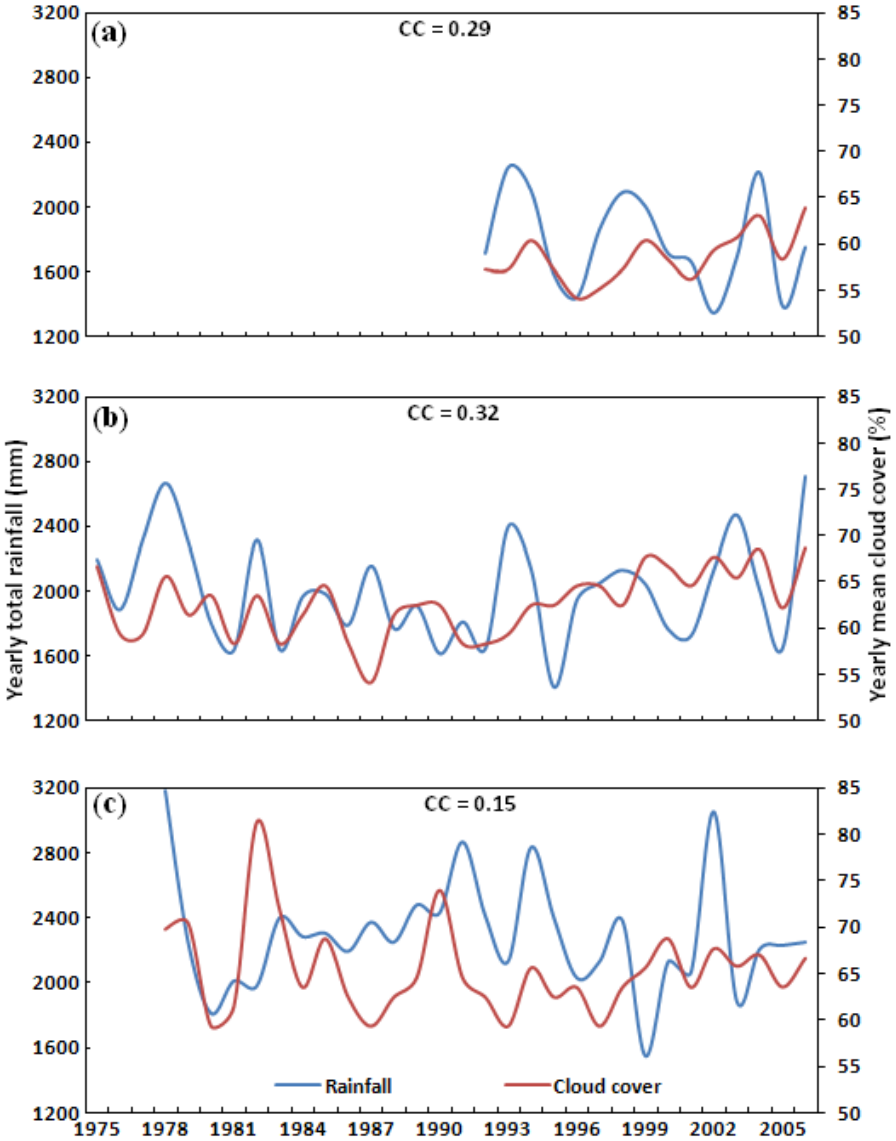

Figure 3.15: Annual total rainfall and mean cloud cover (%) and their corresponding correlation coefficient (CC) for: (a) Hanimaadhoo, (b) Hulhule and (c) Gan. Common legend is shown in bottom figure.

3.3.6 Sunshine

Figure 3.16 shows the total annual sunshine together with the annual total rainfall for Hanimaadhoo, Hulhule and Gan. Only four years (from 2003 to 2006) of sunshine data are available for Hanimaadhoo. The mean annual sunshine for the Maldives is 2733.96 hours, obtained from Hulhule and Gan data (1982 to 2006). The mean annual sunshine for Hanimaadhoo is 2781.73 hours (obtained from 2003 to 2006 data). The mean annual sunshine for Hulhule and Gan are 2775.21 and 2692.71 hours, respectively. The total annual rainfall and total annual sunshine shows interannual variability for the Hanimaadhoo, Hulhule and Gan (Figure 3.16). The correlation coefficient indicates that there is a negative relationship between annual rainfall and annual sunshine. The relationship is most strong for Hanimaadhoo (CC = -0.62). However, the relationship found for Hanimaadhoo should be used cautiously due to the short period of data. The CC found for Hulhule (CC = -0.47: Figure 3.16b) is significant at 95% level.

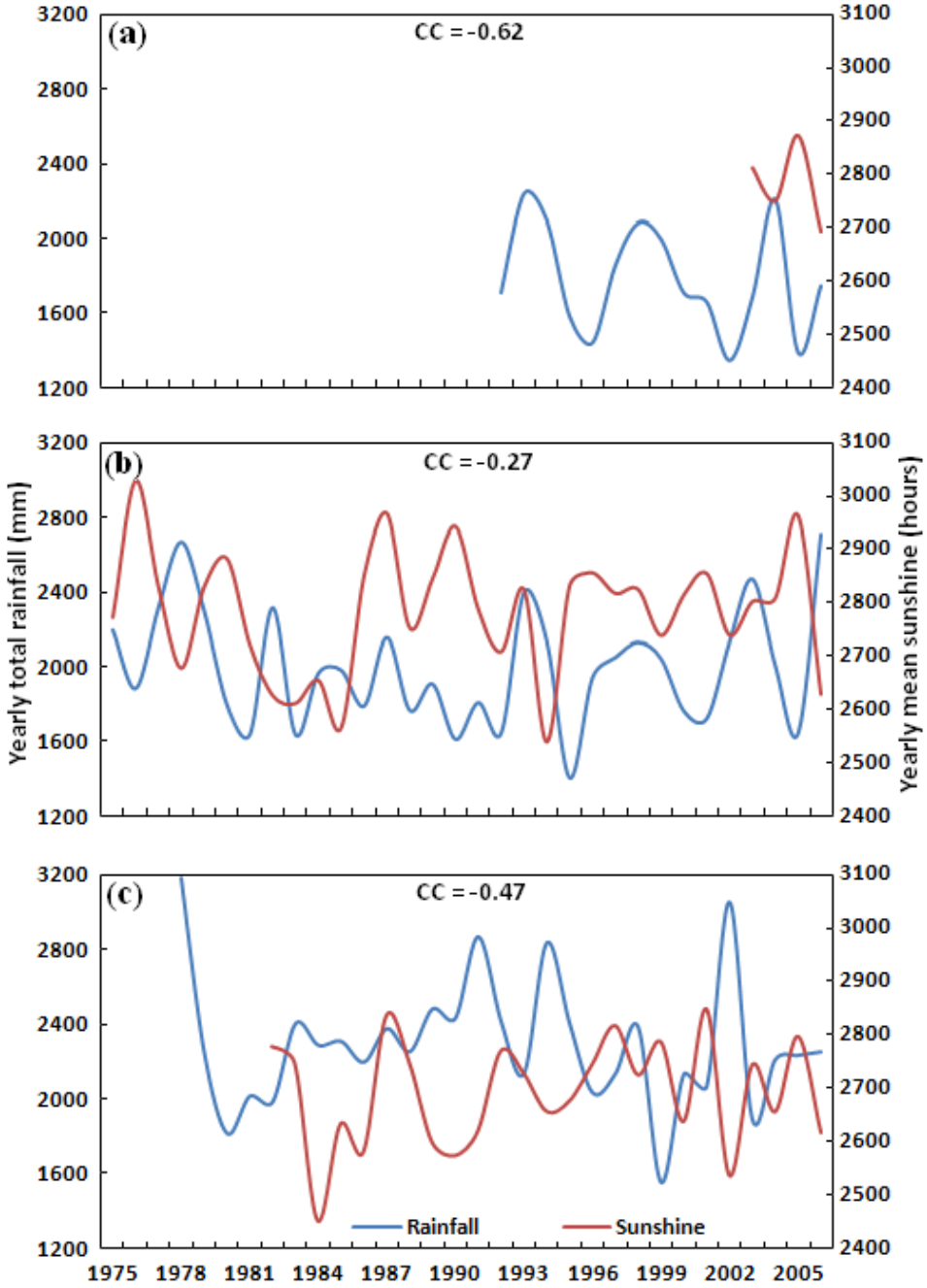

Figure 3.16: Annual total rainfall and mean sunshine (hours) and their corresponding correlation coefficient (CC) for: (a) Hanimaadhoo, (b) Hulhule and (c) Gan. Common legend is shown in bottom figure. Note the CC for Hanimaadhoo is based on 4 years of data.

4 Characterisation of monsoon variability

4.1 Monsoon systems

Ancient traders (Greek, Arab and medieval European adventurers) sailing the Indian Ocean and Arabian Sea used the term monsoon to describe steady seasonal winds of the tropical and sub-tropical oceans between the Persian Gulf, India and Zanzibar that blow persistently from the northeast during the winter and from the opposite direction (the southwest) during the summer. Monsoon is most often applied to the seasonal reversals of wind direction along the shores of the Indian Ocean, especially in the Arabian Sea. Among meteorologists today, the term monsoon refers to the seasonal change in the wind in the troposphere and its associated climatic effects, namely the high variability and unpredictability of rainfall. It is now more generally applied to tropical and subtropical seasonal reversals in both atmospheric circulation and associated precipitation (Trenberth et al. 2000).

The dominant monsoon systems in the world (the Asian–Australian, the African, and the American monsoons) are shown in Figure 4.1. The American monsoon has not been clearly identified with wind reversals (Webster et al. 1998). In these sectors of the tropics, the wet season migrates from one hemisphere to the other following the sun, and the large-scale overturning atmospheric circulation reverses (Trenberth et al. 2000). Monsoonal regions over the globe are generally identified by certain characteristics of the surface circulation in January and July, such as a shift in wind direction, the average frequency of prevailing wind directions, mean wind strength and number of cyclone-anticyclone alternations every two years in either month. Although these monsoon criteria do not include the rainfall explicitly, seasonality in rainfall is the most important manifestation of the monsoon circulation. The most satisfactory criteria for determining whether a region is monsoonal have been developed by Ramage (1971), who defined monsoon regions as areas where:

1. The prevailing wind direction shifts by at least 120° between January and July;
2. The average frequency of prevailing wind directions in both January and July exceeds 40%;
3. The mean resultant winds in at least one of the two months exceed 3 m/s; and

4. Fewer than one cyclone-anticyclone alternation occurs every two years in either January or July in a 5° latitude-longitude rectangle.

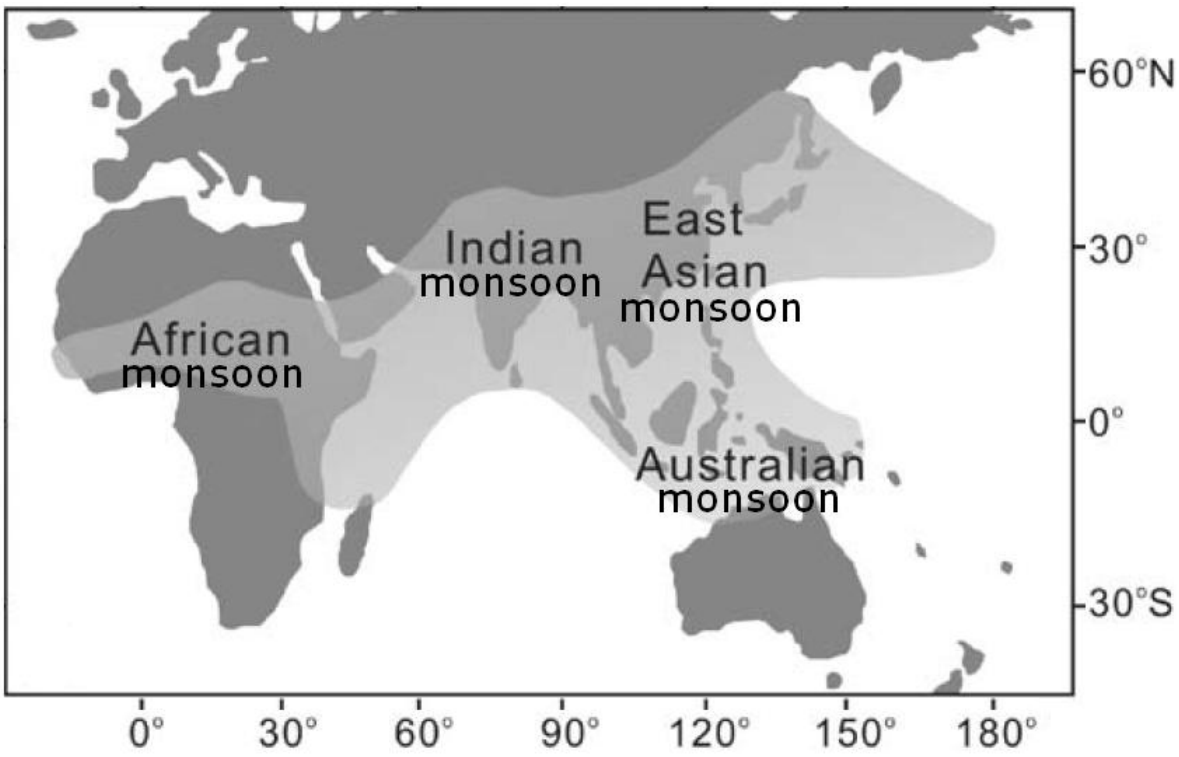

Figure 4.1: Monsoon systems in Asia, Africa and Australia. Adapted from Wang et al (2005).

Embedded within the broad monsoon region shown in Figure 4.1 are the more conventional regional monsoons. The term monsoon is customarily used in the southern Asian context to refer to the period of heavy rainfall between June-September, otherwise known as the 'Indian summer monsoon'. The common reference to a 'good' or 'bad' monsoon denotes whether the rainfall is in excess or deficit.

4.2 Asian monsoon and its variability

The Asian Monsoon (AM) varies on various time scales: intra-seasonal, interannual and interdecadal (Goswami and Mohan 2001; Webster and Yang 1992). The aim of this chapter is to characterise monsoon variability on different time scales (intra-seasonal, interannual and interdecadal). In the next chapter, the parameters influencing monsoon rainfall variability over the Maldives will be analysed.

Variations of the AM on different time scales are usually characterized by major features associated with different dominant modes, or spatial patterns, although these modes may be phase-locked, as is the case for interannual and intra-seasonal time scales

(Goswami and Mohan 2001). The factors responsible for monsoon variability on different time scales include internal dynamics, the influence of land and ocean variability, and teleconnections to climate variability in other regions (Krishnamurthy and Kinter 2003). Despite over a century of research, characterizing monsoon interannual variability still remains a problem to be solved. This is mainly because the Asian monsoon encompasses complex, multi-scale variability from days to decades, with spatial scales ranging from a few kilometres to thousands of kilometres. As a result, regional descriptions are not always compatible among themselves and with the larger scale picture. Notwithstanding this obvious difficulty, monsoon indices have been used commonly to provide a simple and quick characterization of the monsoon (Lau et al. 2004).

The Asian monsoon is characterized by a seasonal reversal of surface winds (Figure 4.2) and modification of precipitation. During the boreal summer, winds flow from the Southern Hemisphere. Associated with this is accumulation of moisture associated with generation of precipitation over the south Asian continent. On the other hand, in winter, dry winds flow from the cold land areas of Asia southwestward toward the warm ocean to the south. When these winds converge over the warm ocean south of the equator, Indonesia and the northern Australian continent the Australian monsoon results, producing monsoon precipitation over Australia (Clarke et al. 2000). It has been recognized for hundreds of years that the physics behind the annual monsoon cycle is the variation of incoming solar radiation (causing cross-equatorial pressure gradients) and the differential heating rate of the surface of land and ocean (Webster 1987), modified by the rotation of the Earth and the exchange of moisture between the ocean, atmosphere and land (Clarke et al. 2000). In addition to this, the Himalayas and the Tibetan Plateau provide additional strong thermal forcing that produces a distinct asymmetry to the summer monsoons of the Northern and Southern Hemispheres (Webster et al. 1998; Yanai and Li 1994). Not only are there seasonal changes in wind and precipitation in monsoonal regions, the monsoon regions also experience a high degree of variability on interdecadal, interannual and intra-seasonal time scales (Clarke et al. 2000).

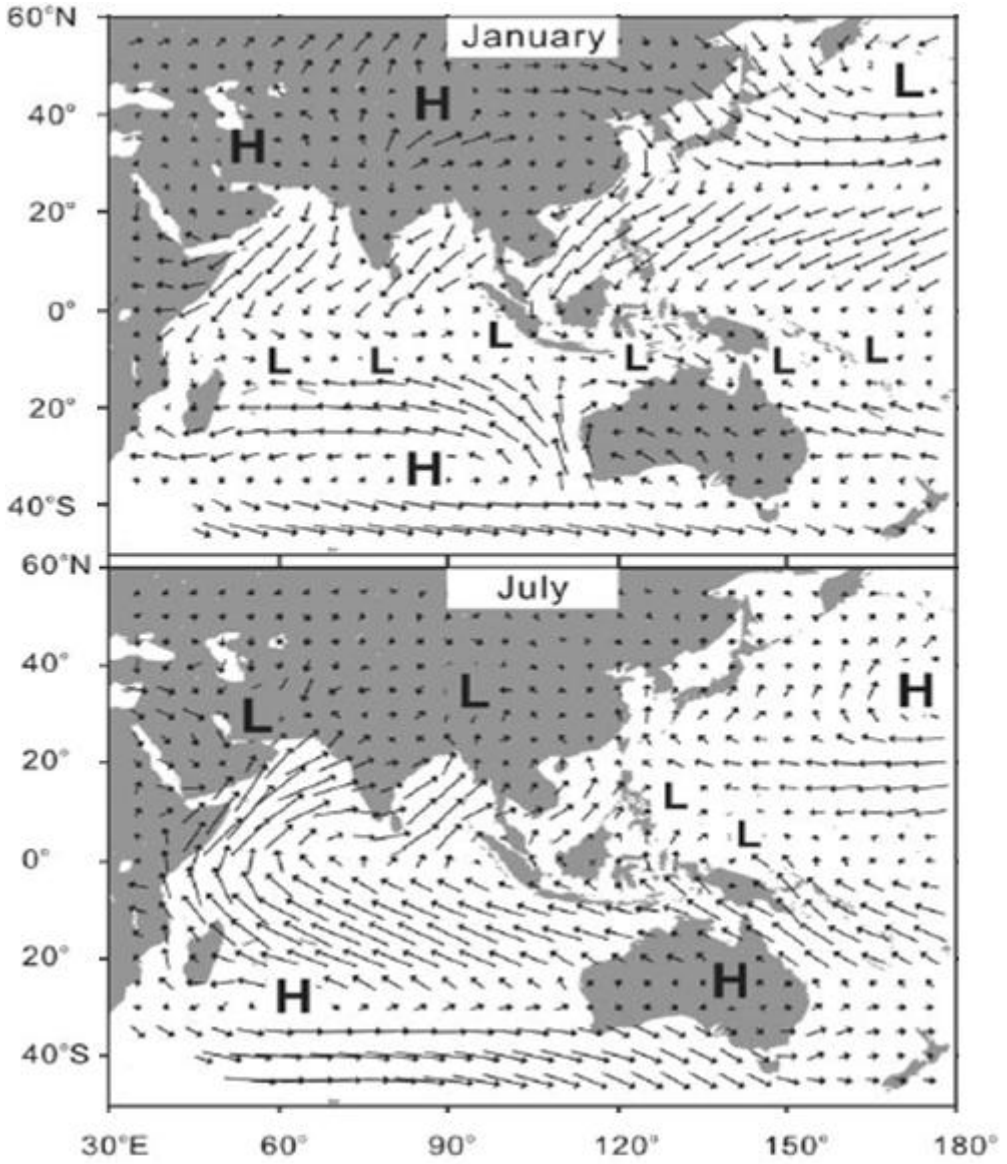

Figure 4.2: Surface pressure and wind patterns in January (top panel) and July (lower panel). Where L and H represents low and high pressure areas, respectively. Taken from Wang et al (2005).

4.2.1 Interdecadal variability

Various components of the Asian monsoon exhibit significant interdecadal variability (Goswami 2006). As ENSO is also known to exhibit interdecadal variability (Houghton et al. 2001), there have been studies to investigate whether the monsoon and the ENSO relationship observed in the interannual variability extends to the interdecadal time scale (Goswami 2006). Krishnamurthy and Kinter (2003) suggested that the interannual variability of the monsoon and ENSO appear to go through the same interdecadal modulation. The fact that the relationship between the Indian summer monsoon and ENSO has the same sign on interannual (over most of available historical data), as well as on interdecadal time scales, indicates that the mechanism through which the two interact may

be similar for both time scales (Goswami 2006). The inter-annually weak relationship between Indian Ocean sea surface temperature (SST) and Indian monsoon rainfall (IMR) anomalies becomes significantly stronger on the inter-decadal time scale (Krishnamurthy and Goswami 2000). A warm phase of the El Niño-Southern Oscillation (ENSO-SST related) influences the Indian monsoon by modifying the local Walker circulation close to the equator, which causes anomalous low-level convergence in the equatorial Indian Ocean, and thus drives an anomalous local Hadley circulation that decreases Indian monsoon rainfall. Alternatively, the cold phase of ENSO influences the Indian monsoon by modifying the local Walker circulation close to the equator, which causes anomalous low-level divergence in the equatorial Indian Ocean and thus drives an anomalous local Hadley circulation that increases Indian monsoon rainfall (Goswami 1998; Krishnamurthy and Goswami 2000). Kucharski et al (2006) showed that on the decadal time scale Indian Ocean equatorial warming causes a local low-level divergence that in turn reduces IMR, while cooling causes a local low-level divergence that in turn increases IMR. As can be seen from Figure **4.3**a, divergence is located at about 70° E and 5° S and convergence is located at about 90° E and 15° N (over India). This is also confirmed by the 925 hPa wind divergence pattern (Kucharski et al. 2006) (Figure 4.3).

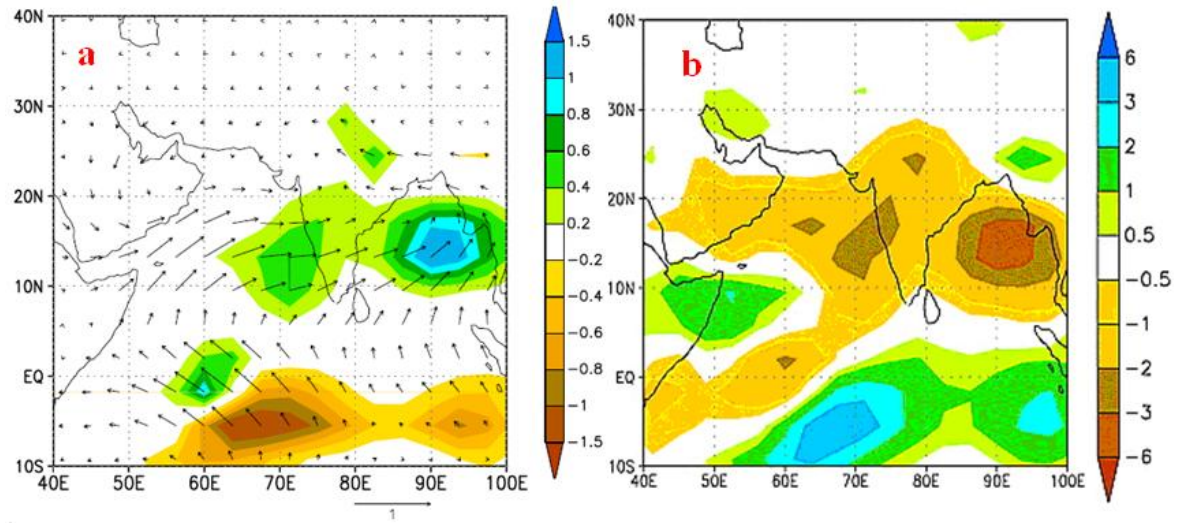

Figure 4.3: (a) Modelled rain (mm/day) and 925 hPa wind (m/s) and (b) 925 hPa wind divergence (10^{-7}/s). Taken from Kucharski et al (2006).

4.2.1.1 Interdecadal monsoon rainfall analysis

Enhanced mean monthly precipitation data from the Climate Prediction Center (CPC) merged analysis of precipitation (CMAP) was obtained for the Asian monsoon region (15°S-30°N, 30°E-120°E). Enhanced mean monthly precipitation values are derived by combining five kinds of satellite estimates (GPI, OPI, SSM/I scattering, SSM/I emission

and MSU), as well as blended NCEP/NCAR reanalysis precipitation values. Precipitation data were available for the period from 1979 to 2007 with a spatial coverage of 2.5 degree latitude x 2.5 degree longitude on the global grid.

The monsoon season precipitation (from June to September) for each grid point spanning 15 °S-30 °N and 30 °E-120 °E was filtered for each year. When the precipitation is averaged over the region for the period from 1979 to 2007, it shows spatial variability with two maxima located around 92 °E and 20 °N and 85 °E and 5 °S (Figure 4.4a). During the summer monsoon period (JJAS) these locations receive rainfall of about 16 mm/day on average. Another maximum is also located on the west coast of India (72°E and 14°N) with rainfall of about 15 mm/day. The lowest rainfall for JJAS months can be seen in the Arabian Sea and over the African continent, with rainfall less than 1 mm/day on average.

In order to gain insight into decadal variability of monsoon rainfall (JJAS), the rainfall anomalies for the same region are presented. Figure 4.4b-d shows spatial rainfall anomalies for different periods: 1979-1988, 1989-1998 and 1999-2007. It is clear from these figures that the rainfall anomaly patterns for the region for the different time periods show clear differences in spatial variability.

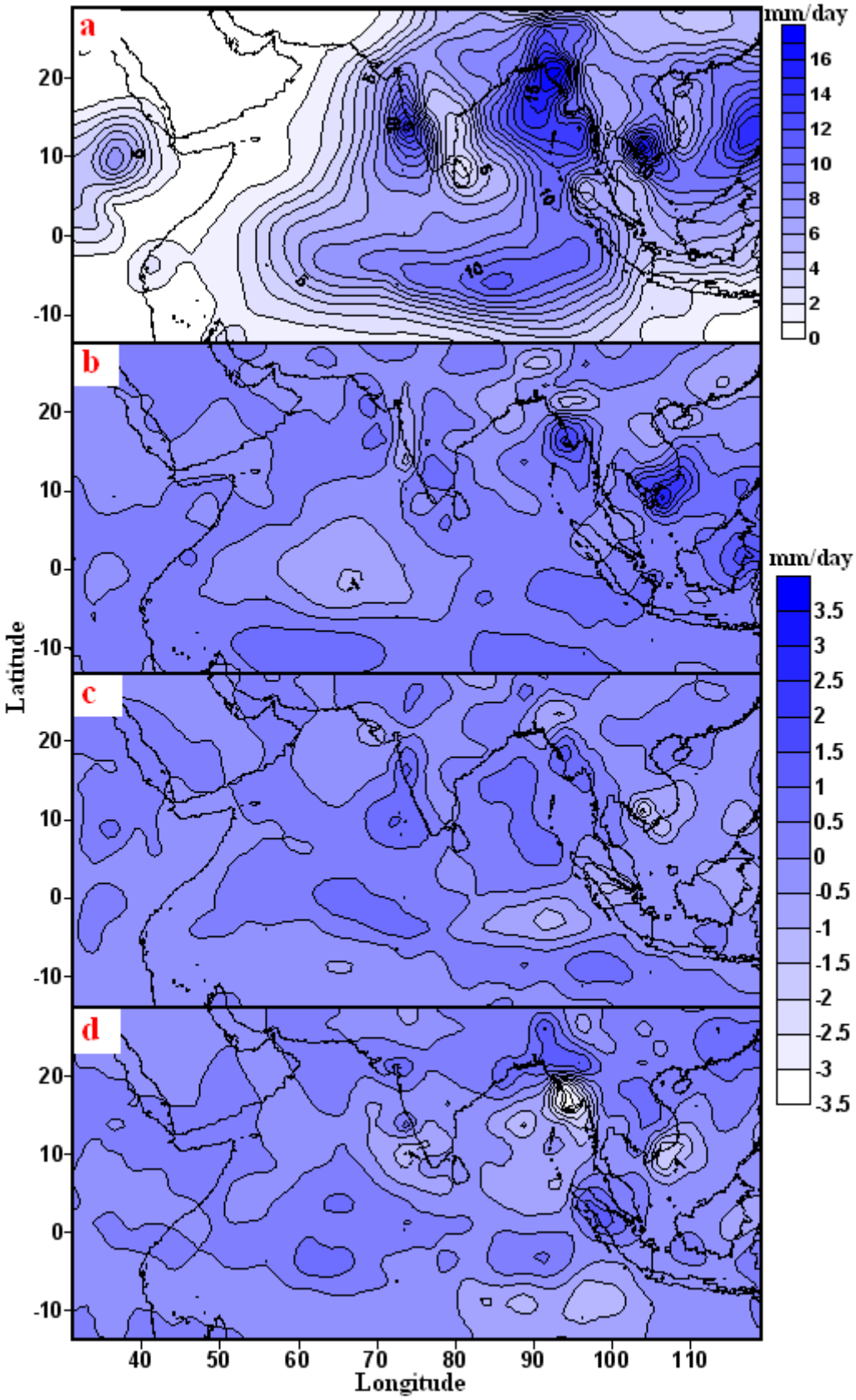

Figure 4.4: (a) June to September average rainfall (mm/day) for the Asian region from 1979 to 2007, with rainfall anomaly patterns for (b) 1979-88, (c) 1989-98 and (d) 1999-2007. All the anomalies are based on the 1979 to 2007 average (derived from CMAP data).

Figure 4.5 and Figure 4.6 show the time series of June to September (JJAS) total rainfall and percentage rainfall anomaly for the region from 1979 to 2007. As can see from Figure 4.5, the mean total rainfall is highest during the first decade (from 1979-1988) and lowest during 1999 to 2007, suggesting interdecadal variability of monsoon rainfall for the region. A similar pattern can be seen from the time series of June-September percentage rainfall anomaly (Figure 4.6). However, it should be noted that the mean for the last period (1999 to 2007) is only for 9 years. It is interesting to see that the large negative JJAS rainfall anomalies correspond to El Niño years. Not only do the time series of JJAS total rainfall and rainfall anomalies show interdecadal variability, but also subjection of the total rainfall for the region to Fourier analysis shows a 12.9 year periodicity (Figure 4.7).

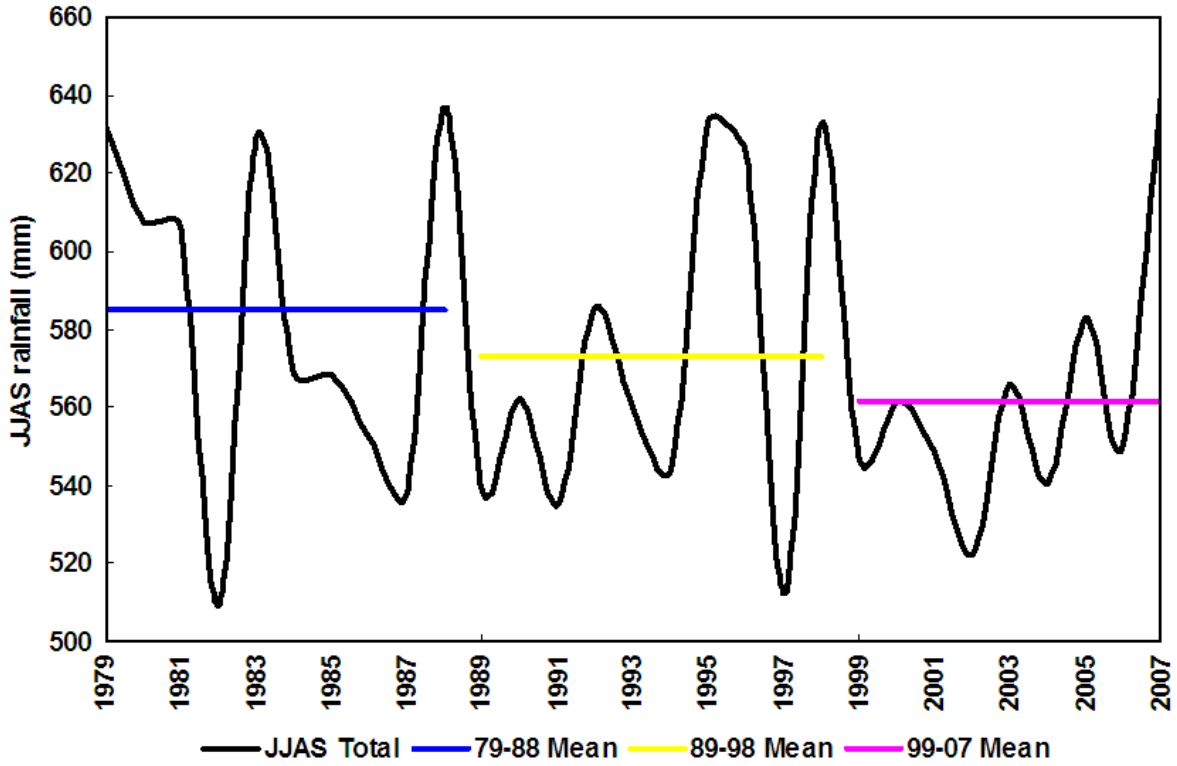

Figure 4.5: Time series of June-September (JJAS) total rainfall for the Asian monsoon region from 1979 to 2007 (based on CMAP data).

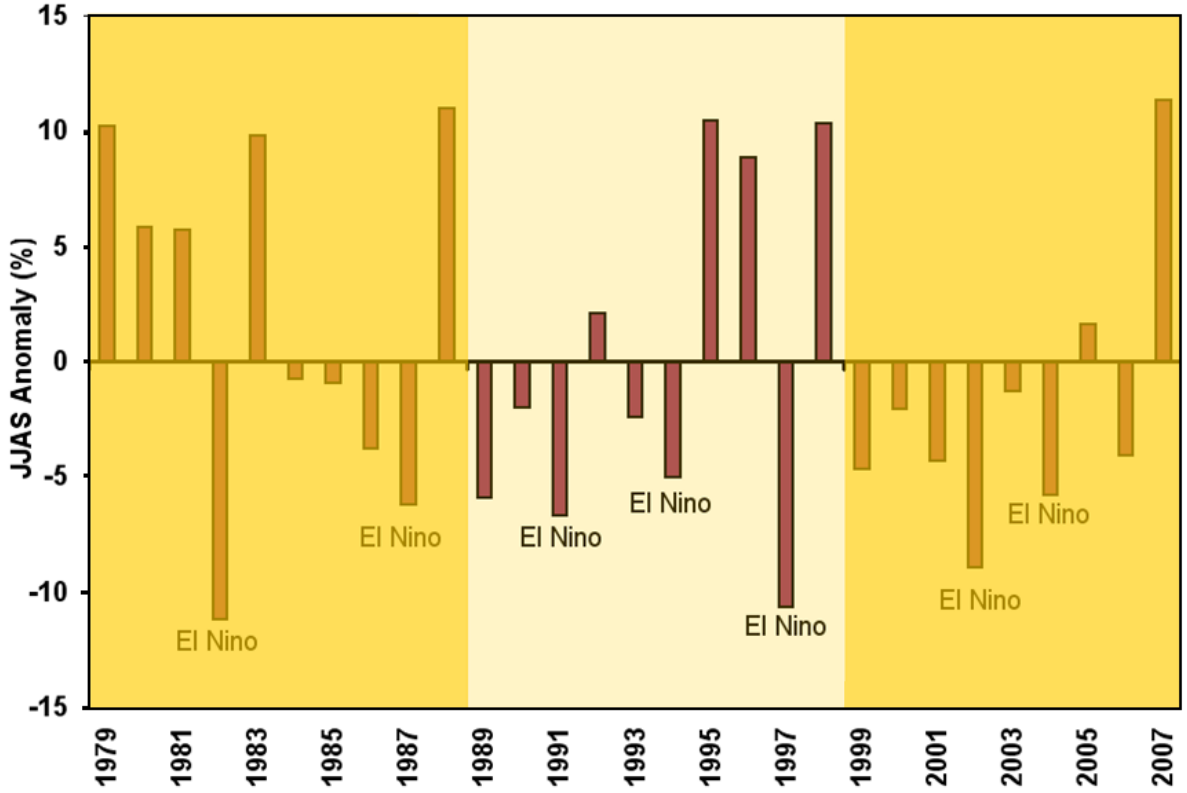

Figure 4.6: Time series of June-September (JJAS) percentage rainfall anomaly for the Asian monsoon region (based on CMAP data).

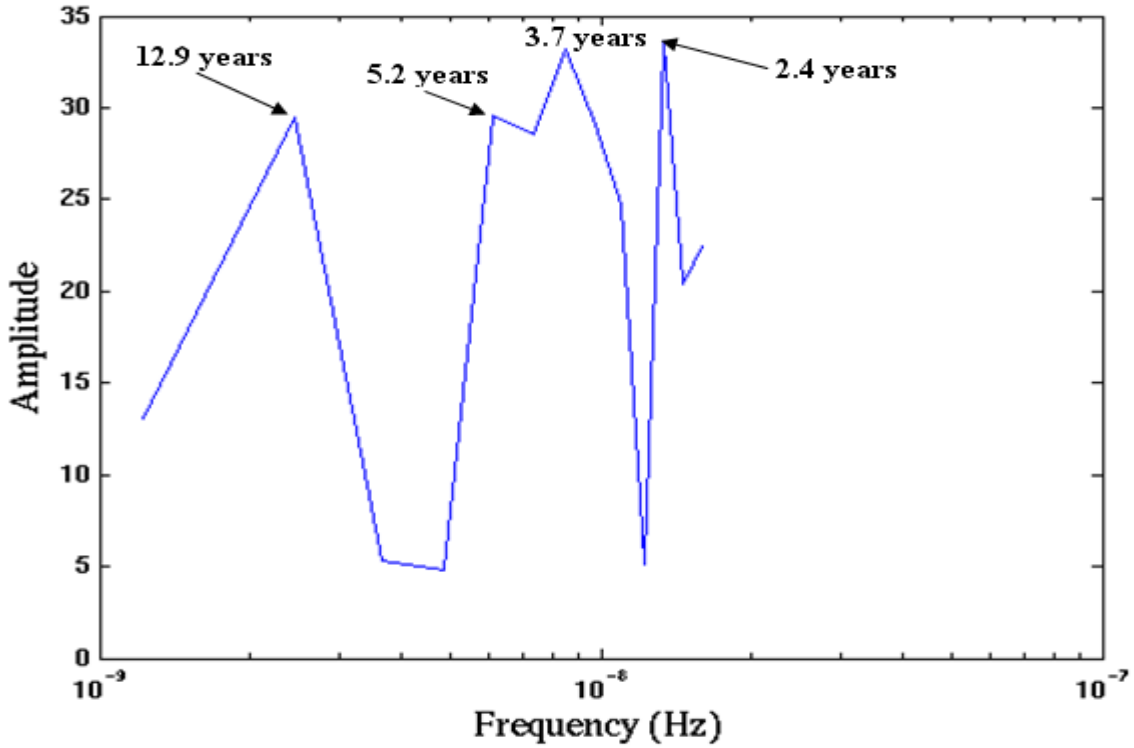

Figure 4.7: Fourier transform spectrum of yearly rainfall for the Asian monsoon region (based on CMAP data).

4.2.1.2 Relationship between decadal rainfall, SST, SLP and air temperature variability

Decadal variability of rainfall over the Asian monsoon region and its relationship with sea surface temperature (SST), sea level pressure (SLP), air temperature and outgoing longwave radiation (OLR) is examined in this section. Figure 4.8 shows spatial variability of JJAS (June-September) average rainfall, SST, SLP, air temperature and OLR. Time series of JJAS Asian region total rainfall, mean SST, SLP and air temperature are shown in Figure 4.9. During the first decade (1979-1988) the rainfall shows an above normal epoch. The last two decades (1989-1998 and 1999-2007) show rainfall below normal (1989-1998 is slightly below normal and 1999-2007 is significantly below normal). The Indian monsoon rainfall (IMR) also indicates above and below normal epochs on interdecadal scales (Figure 4.10). Two above normal epochs were found between 1878 and 1898, and between 1931 and 1960. The two below normal epochs for the IMR on decadal time scales were observed during 1898-1929 and 1961-1990 (Goswami 2006; Krishnamurthy and Goswami 2000).

The mean SLP Figure 4.9(c) shows an above normal epoch (during the first decade) and below normal epoch (during the last two decades). The mean SST and surface air temperature (Figure 4.9 b and d) show out of phase variability when compared with the rainfall (Figure 4.9a). That is, during the first two decades (1978 -1987 and 1988-1997) the mean SST and air temperature show a below normal epoch, while the last decade (1998-2007) shows an above normal epoch. Krishnamurthy and Goswami (2000) also suggested that there is an out of phase relationship between the interdecadal Indian monsoon and that of the Niño-3 sea surface temperature anomaly. Unlike the other variables, mean OLR (Figure 4.9e) shows an above normal epoch during the first and the third decadal period (1979-1988 and 1999-2007), while the 1989-1998 period shows a below normal epoch for mean OLR.

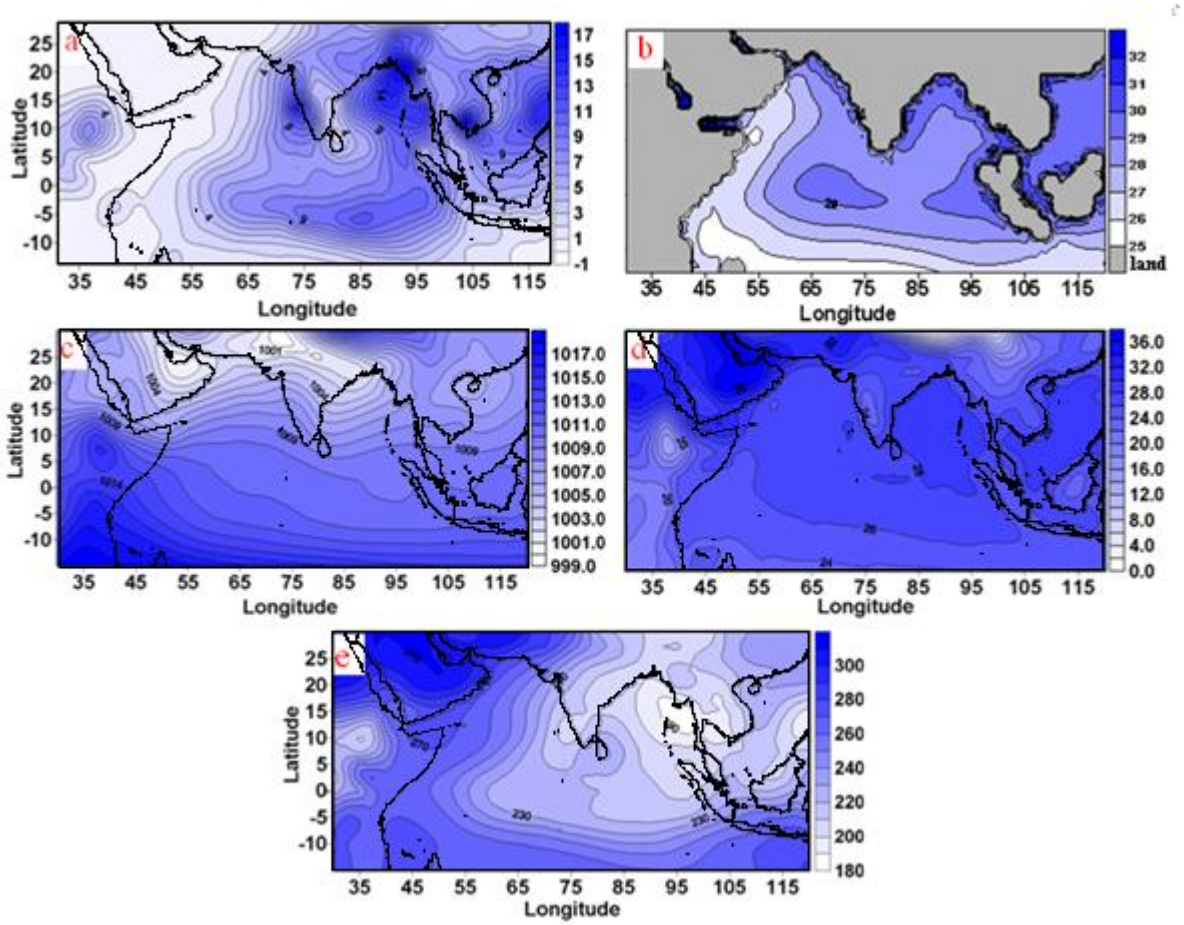

Figure 4.8: Spatial variability of June to September (JJAS): (a) average rainfall (mm/day) from 1979-2007, (b) average sea surface temperature (°C) from 1978-2007, (c) average sea level pressure (hPa) from 1979-2007, (d) average air temperature (°C) from 1978 to 2007 and (e) average outgoing longwave radiation (Wm^{-2}) from 1979 to 2007.

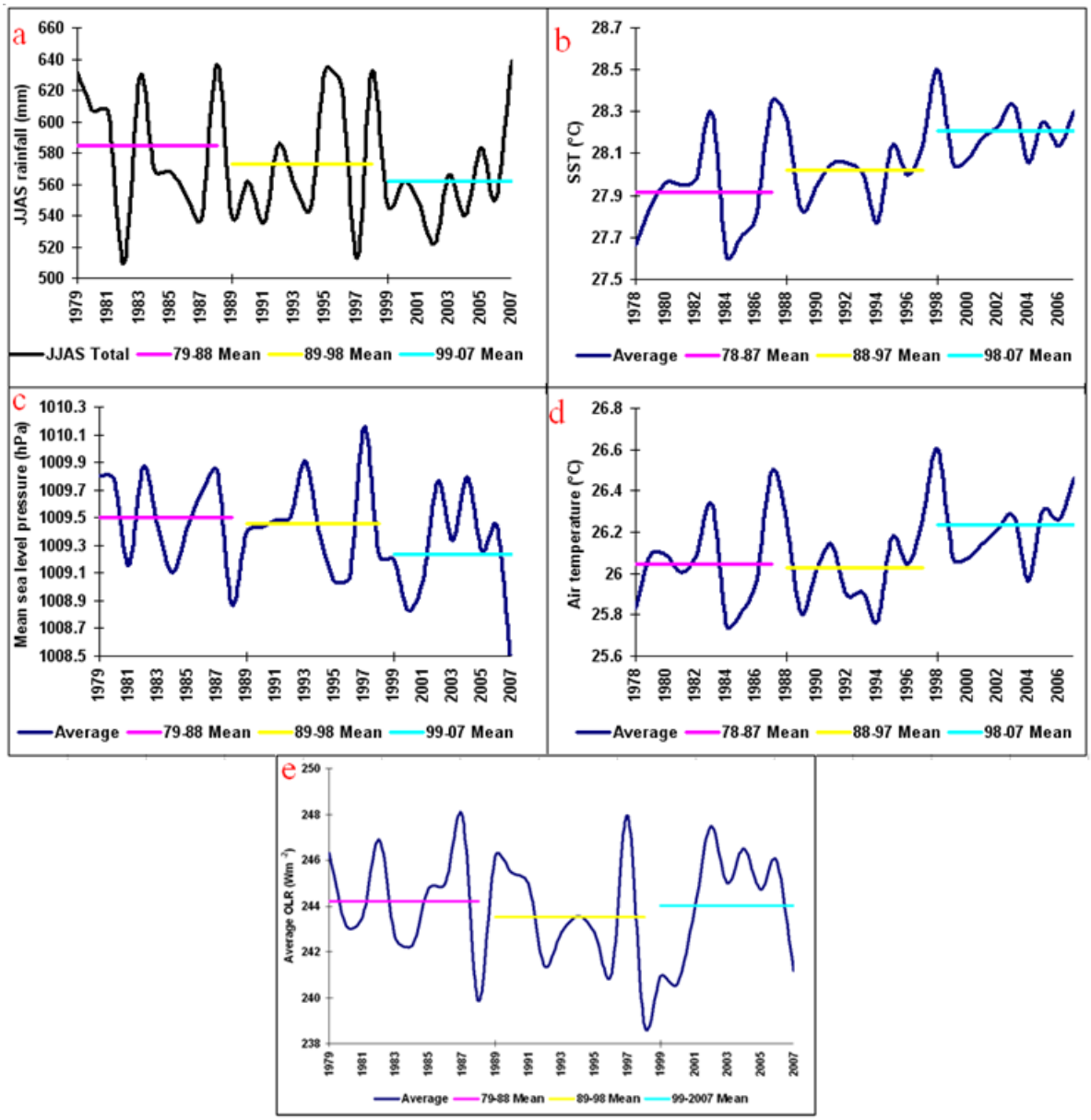

Figure 4.9: June - September (JJAS) interdecadal variability of: (a) total rainfall from 1979-2007, (b) average sea surface temperature from 1978-2007, (c) average sea level pressure from 1979-2007, (d) average air temperature from 1978 to 2007, and (e) average OLR from 1979-2007.

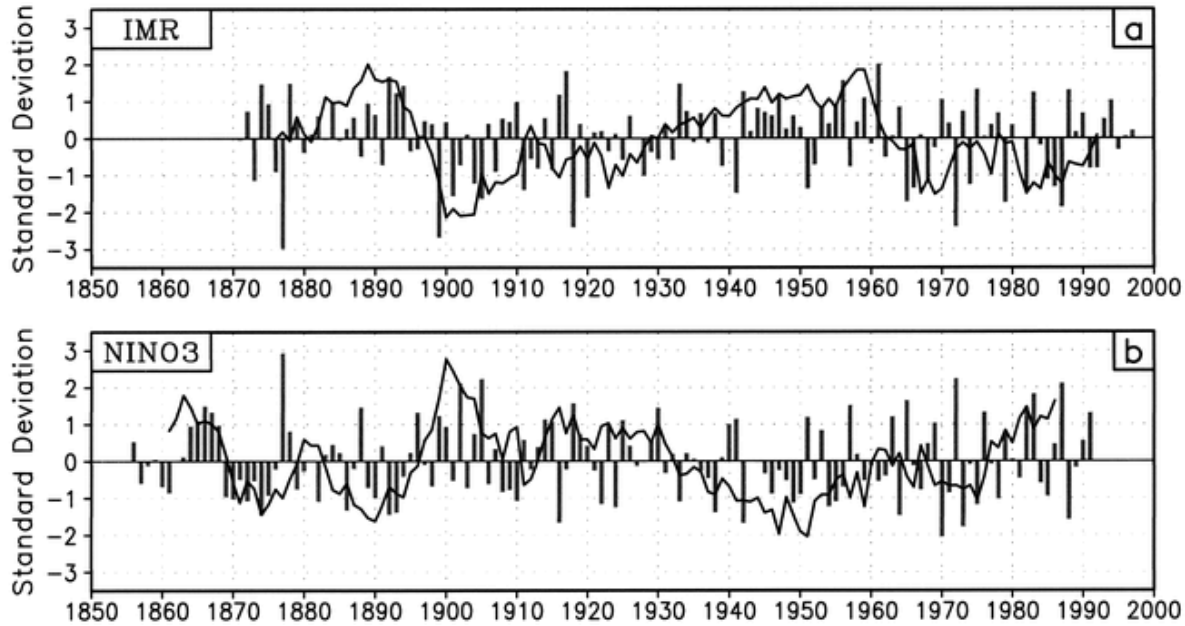

Figure 4.10: (a) Time series of JJAS seasonal anomaly of Indian monsoon rainfall (bar) and its 11-yr running mean (solid line). (b) Same as (a) but for JJAS seasonal anomaly of Niño-3 SST. Taken from Krishnamurthy and Goswami (2000).

4.2.2 Interannual variability

"The interannual variability of the Asian monsoon is defined as the yearly deviation of seasonal transition from the mean annual cycle" (Yang and Lau 2006). Year-to-year variation of the Asian monsoon is one of the strongest signals of the Earth's climate variability (Wang and Fan 1999). The interannual variability of the Asian monsoon is characterized by a set of seasonally and spatially varying characteristic features (Yang and Lau 2006). The most dominant mode of interannual variability of summer monsoon rainfall is associated with a dipole-like variation of precipitation between south Asia and south-east Asia. According to Krishnamurthy and Kinter (2003), the interannual variability of the seasonal monsoon is nonperiodic, and may result from inherent atmospheric dynamics that are nonlinear. The interannual variability of the monsoon can be further influenced by slowly varying forcings such as SST, soil moisture, sea ice and snow cover (Krishnamurthy and Kinter 2003).

4.2.2.1 Principal component analysis (PCA) of interannual monsoon rainfall analysis

In order to analyse the interannual rainfall variability during the monsoon season, principal component analysis (PCA) was performed on enhanced precipitation data for Jun-July-August-September total precipitation obtained from the Climate Prediction Center

(CPC) merged analysis of precipitation (CMAP) for the Asian monsoon region and the Indian region. Figure 4.11 indicates the geographical extent of the Asian region (30 °-120 °E and 15 °S-30 °N) and the Indian region (68.75°-91.25 ° E and 6.25°-28.75 °N) discussed in the text.

There is no single clear criterion that can be used to choose the number of principal components that are best retained in a given circumstance. By its nature, this is an arbitrary decision. However, there are two commonly used criteria, namely the Kaiser criterion and the scree test. Kaiser's criterion retains PCs with eigenvalues equal to or greater than 1 (Tabachnick and Fidell 2007). According to Field (2005), this method appears to be valid when the number of variables in the analysis is less than 30 or exceeds 250. The scree test is based on plotting a graph of each PC against its associated eigenvalue. It shows the relative importance of each PC (Field 2005). With this rule, a plot of the eigenvalues against the number of components is examined for an "elbow", with a sharp descent in the curve followed by a tailing off after the elbow or point of inflexion used as a rule to retain the number of important factors or PCs (Field 2005; Sharma 1996). However, the scree test is not exact, as it involves subjective judgment of where the discontinuity in eigenvalues occurs (Tabachnick and Fidell 2007). In this analysis, both criteria are taken into account when deciding the number of PCs to be retained. If there are discrepancies between these two criteria, the PCs which account for more than 5% of the total un-rotated data set variance will be considered.

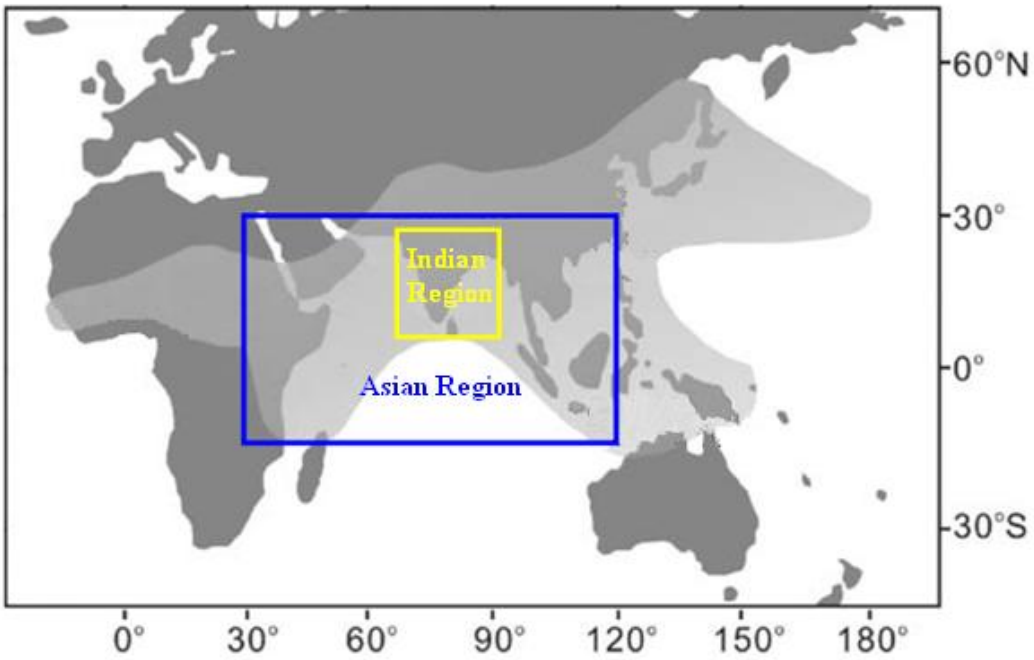

Figure 4.11: Extent of the Asian region (30-120° E and 15S-30° N) and the Indian region (68.75-91.25° E and 6.25 -28.75 ° N) mentioned in the text. Modified from (Wang et al. 2005).

Figure 4.12 shows the scree plot of eigenvalues against the number of principal components for the Asian and Indian region. The scree plot indicates that the number of PCs to be retained for the Asian and Indian region is 4. However, when Kaiser's criteria are considered, there are 28 and 19 PCs with eigenvalues equal to or greater than 1 for the Asian and Indian regions, respectively. The scree plot and Kaiser's criteria therefore indicate discrepancies for retaining the number of PCs. Hence the PCs that account for more than 5% of the variance are considered here. There are five PCs that explain more than 5% of the variance, as presented in Table 4.1. For the Asian region, the first five PCs account for about 49% of the interannual rainfall variability. On the other hand, the first five PCs account for about 65% of the interannual rainfall variability for the Indian region (Table 4.1).

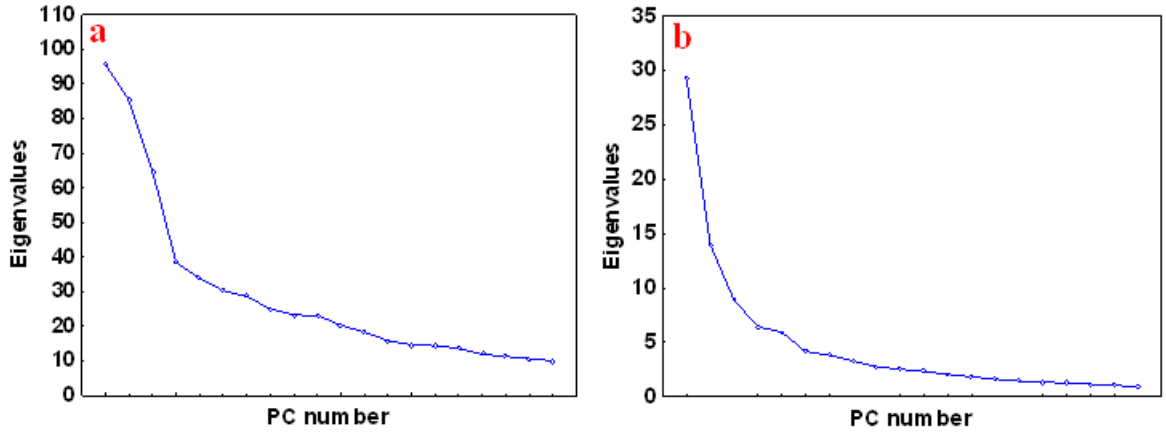

Figure 4.12: Scree plot of eigenvalues against principal component numbers (PCs) for the Asian region (a) and the Indian region (b).

Table 4.1: Percentage of variance explained by the first five un-rotated principal components (PCs) for the Asian and the Indian region.

	Asian Region	Indian Region
PCs	**Total variance (%)**	
1st	14.7	29.4
2nd	13.2	14.0
3rd	10.0	8.9
4th	5.9	6.4
5th	5.2	6.0
Total	**49.0**	**64.7**

In unrotated PCA, the first eigenvector or PC accounts for the largest amount of overall data set variance as shown above. When interpreting the PCs, it is useful to subject them to some form of rotation (Huth 1996). The advantage of rotation is to obtain more meaningful and interpretable dominant spatial modes of data fields than occurs in the unrotated solutions (Munoz and Rodrigo 2004; Sharma 1996). Varimax and quartimax are the most commonly used rotation methods. In the varimax rotation, the major objective is to have a PC structure in which each variable loads highly on one and only one PC. That is, a given variable should have a high loading on one PC and near zero loadings on other PCs, which results in each factor representing a distinct construct (Sharma 1996; Tabachnick and Fidell 2007). In this analysis, the first four principal components were subjected to varimax rotation.

Figure 4.13 below shows the spatial variability of the loadings for the first four principal components (PCs) or PC weights for the Asian and Indian region after subjecting them to varimax rotation. The first principal component (PC-1) (Figure 4.13a) explains about 14.7% of the spatial variability of June-September (JJAS) total rainfall for the Asian

region, while PC-1 (Figure 4.13e) explains 29.4% spatial variability for the Indian region. The spatial variability explained by PC-1 (Figure 4.13a) indicates higher rainfall values over the land areas. In addition to this, positive values can be seen around the Bay of Bengal (BoB) region and from the equator to the Arabian Sea region (Figure 4.13a). This could be due to the temperature contrast between land and the ocean. It is noticed from PC-1 (Figure 4.13e) for the Indian region that the positive values are mostly in the southern parts (east and west) of India and the surrounding ocean. As suggested by Singh (2006), the first principal component for the India region mostly represents the monsoon rainfall cycle. The amount of rainfall during the monsoon season (June-September) is due to the large scale spatial and temporal movement of the monsoon trough. In addition to this, the lows which form in this area contribute to the monsoon rainfall (Singh 2006).

The spatial patterns of the second principal component (PC-2) or PC weight shown in Figure 4.13 (b and f) explain about 13.2 and 14.0% of rainfall variability for the Asian and the Indian region, respectively. As can be seen from PC-2 (Figure 4.13b), the positive values are concentrated around the BoB, extending towards Indonesia and the surrounding sea. The spatial variability seen in Figure 4.13b might be related to the El Niño Southern Oscillation (ENSO index). This will be analysed in Chapter 6. The second principal component for the Indian region shows that positive values are in the east (over ocean) and the northwestern part of the country. The spatial variability seen for the Indian region might be related to the movement of monsoon lows/depression in quick succession through the northern Bay of Bengal (BoB), which also favours the development of mid-tropospheric lows over western India (Singh 2006).

The third principal component/PC weight (Figure 4.13 c and g) explains 10.0 and 8.9% of the total variance of monsoon season (JJAS) total rainfall for the Asian and Indian regions, respectively. From the spatial variability of PC-3 (Figure 4.13c), it is clear that there are no large positive areas, although there is a small positive area south of the equator between 50 and 80 °E. Spatial variability of PC-3 (Figure 4.13g) reveals that positive values are mostly concentrated in southern and northern (central) parts of the India. This may be related to the monsoon trough which is located near to the Himalayan foothills and oscillates north and south (Singh 2006).

The fourth principal component (PC-4) or PC weight explains 5.9 and 6.4% of the total variance of monsoon season (JJAS) total rainfall for the Asian and Indian regions, respectively. Spatial variability of PC-4 (Figure 4.13d) for the Asian region does not show any definite pattern, with a few pockets of positive and negative values seen across the

region. Spatial variability of PC-4 (Figure 4.13h) for the Indian region shows a positive area over the northeast of the India, which might be related to the break in the monsoon rainfall due to the movement of the monsoon trough to the north (Singh 2006).

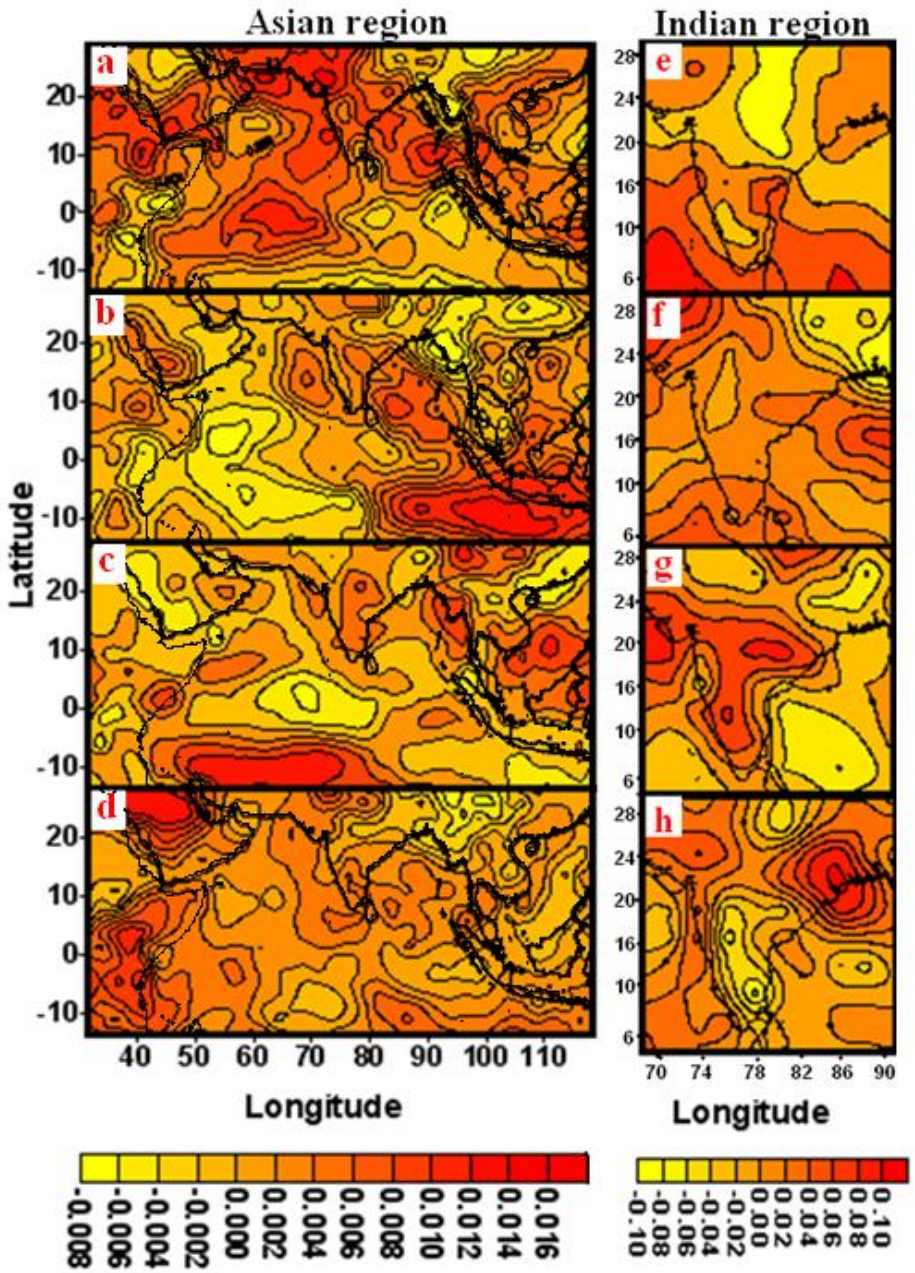

Figure 4.13: Spatial patterns of the first four principal components (PCs) : (a) PC-1, (b) PC-2, (c) PC-3 and (d) PC-4 of June-September (JJAS) total rainfall for the Asian region and (e) PC-1, (f) PC-2, (g) PC-3 and (h) PC-4 are the corresponding first four PCs for the Indian region. All the PCs were rotated using varimax rotation.

In addition to the principal components presented above, JJAS total rainfall for the top and bottom four scores for the first four PCs are presented in Figure 4.14 for the Asian region. JJAS total rainfall for the highest and lowest PC-1 scores allows assessment of the

influence of this PC on the magnitude of rainfall. The magnitude of JJAS total rainfall is higher for top scores (Figure 4.14; left panel) and lower for bottom scores (Figure 4.14; right panel). JJAS total rainfall for all the years shown in Figure 4.14 (left panel) corresponds to rainfall excess years (2007, 1996 and 1983: Figure 4.6), except year 1994, which is a dry year. On the other hand, JJAS total rainfall for the years shown in Figure 4.14 (right panel) corresponds to either dry (1987 and 2002: Figure 4.6) or normal (1990 and 1985: Figure 4.6) years. Rainfall for all the PCs shows that there is an east-west gradient between the Arabian Sea and the African continent. This area shows very low rainfall during the monsoon period.

Figure 4.15 shows the JJAS total rainfall corresponding to the highest (left panel) and lowest scores (right panel) of PC-2, with their corresponding years indicated in the figure. All the years (except 1998 and 1997) are normal in terms of JJAS total rainfall, while 1998 and 1997 are rainfall excess and dry years, respectively. JJAS total rainfall corresponding to highest scores of PC-2 (Figure 4.15, left panel) indicate that the rainfall is more concentrated in eastern parts of the Indian Ocean, while the lowest scores of PC-2 (Figure 4.15, right panel) indicate that the rainfall is shifted to the west. This indicates the influence of east-west movement of the Intertropical Convergence Zone (ITCZ) in the Indian Ocean region during the monsoon period (June-July-August-September).

JJAS total rainfalls for the first four highest and lowest scores of PC-3 are shown in Figure 4.16. The pattern of total rainfall for the highest (Figure 4.15, left panel) and lowest scores (Figure 4.15, right panel) indicates that rainfall is more concentrated in eastern parts of the Indian Ocean. When JJAS total rainfall corresponding to the highest and lowest scores of PC-3 are compared, there is some suggestion that the rainfall corresponding to the lowest scores is shifted more to the north. This might be related to the south-north movement of the ITCZ.

JJAS total rainfall for the first four highest and lowest scores of PC-4 (together with their corresponding years) for the Asian region are shown in Figure 4.17. JJAS total rainfall corresponding to the highest scores (Figure 4.17, left panel) is more widespread than the rainfall corresponding to the lowest scores (Figure 4.17, right panel) of PC-4.

It should be noted that the results of the above analysis (PCA) suggest that the patterns shown by PC-3 and PC-4 are significantly less clear than for PC-1 and PC-2. Hence, PC-3 and PC-4 do not provide much explanation about the interannual variability of precipitation over the Asian region.

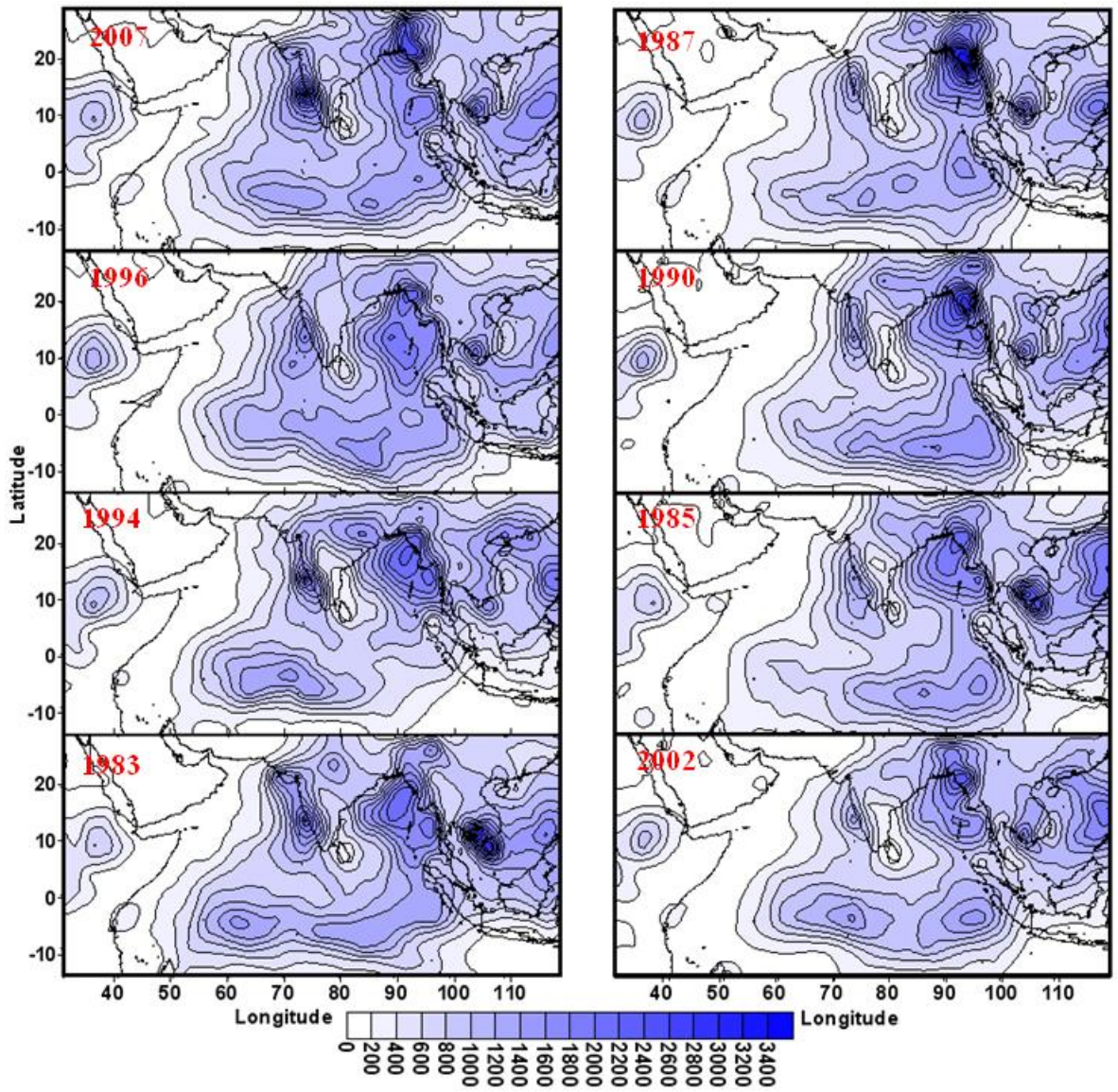

Figure 4.14: JJAS total rainfall for the first four highest (left panel) and lowest (right panel) scores of PC-1 for the Asian region, with their corresponding years indicated.

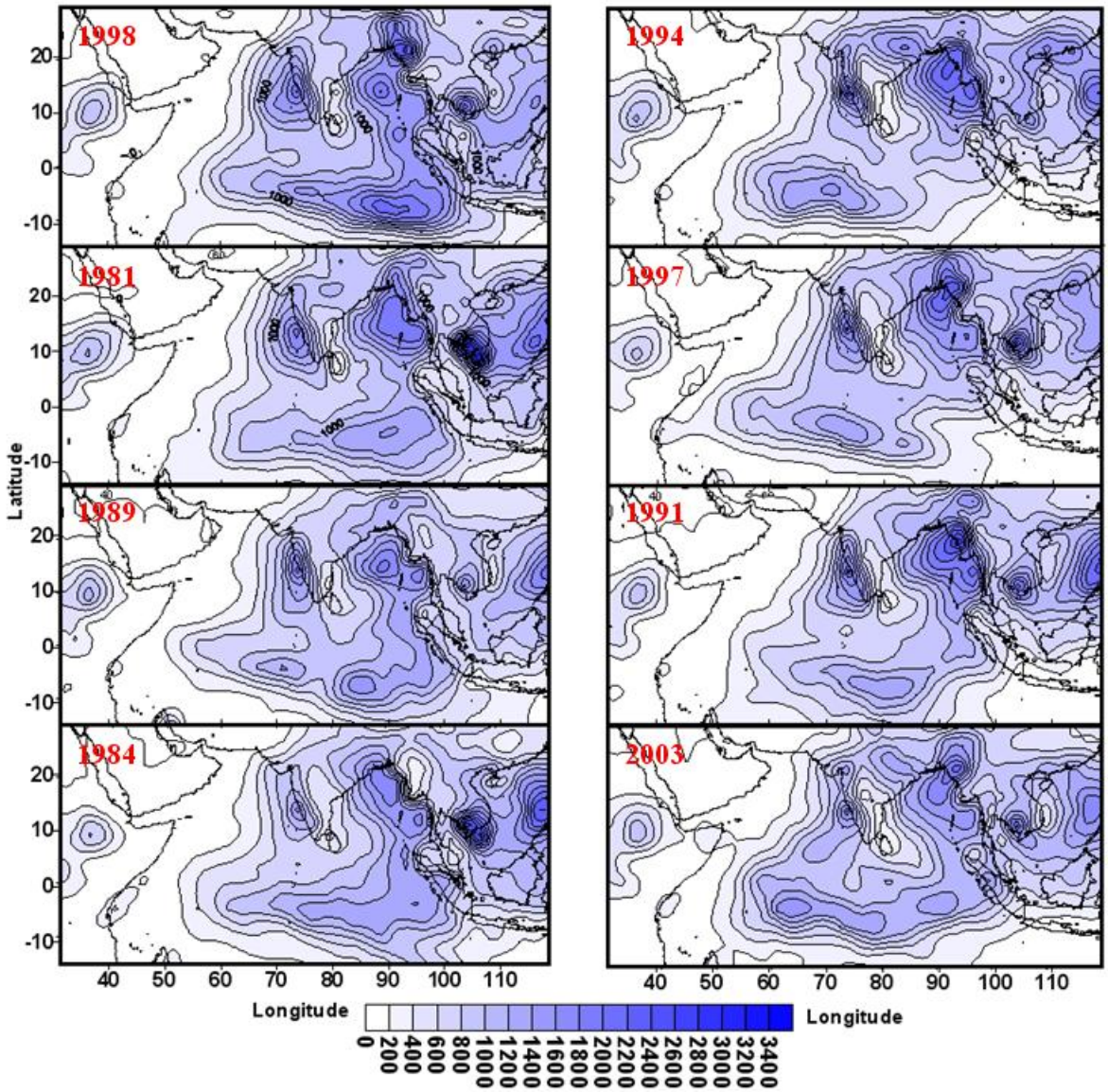

Figure 4.15: JJAS total rainfall for the first four highest (left panel) and lowest (right panel) scores of PC-2 for the Asian region, with their corresponding years indicated.

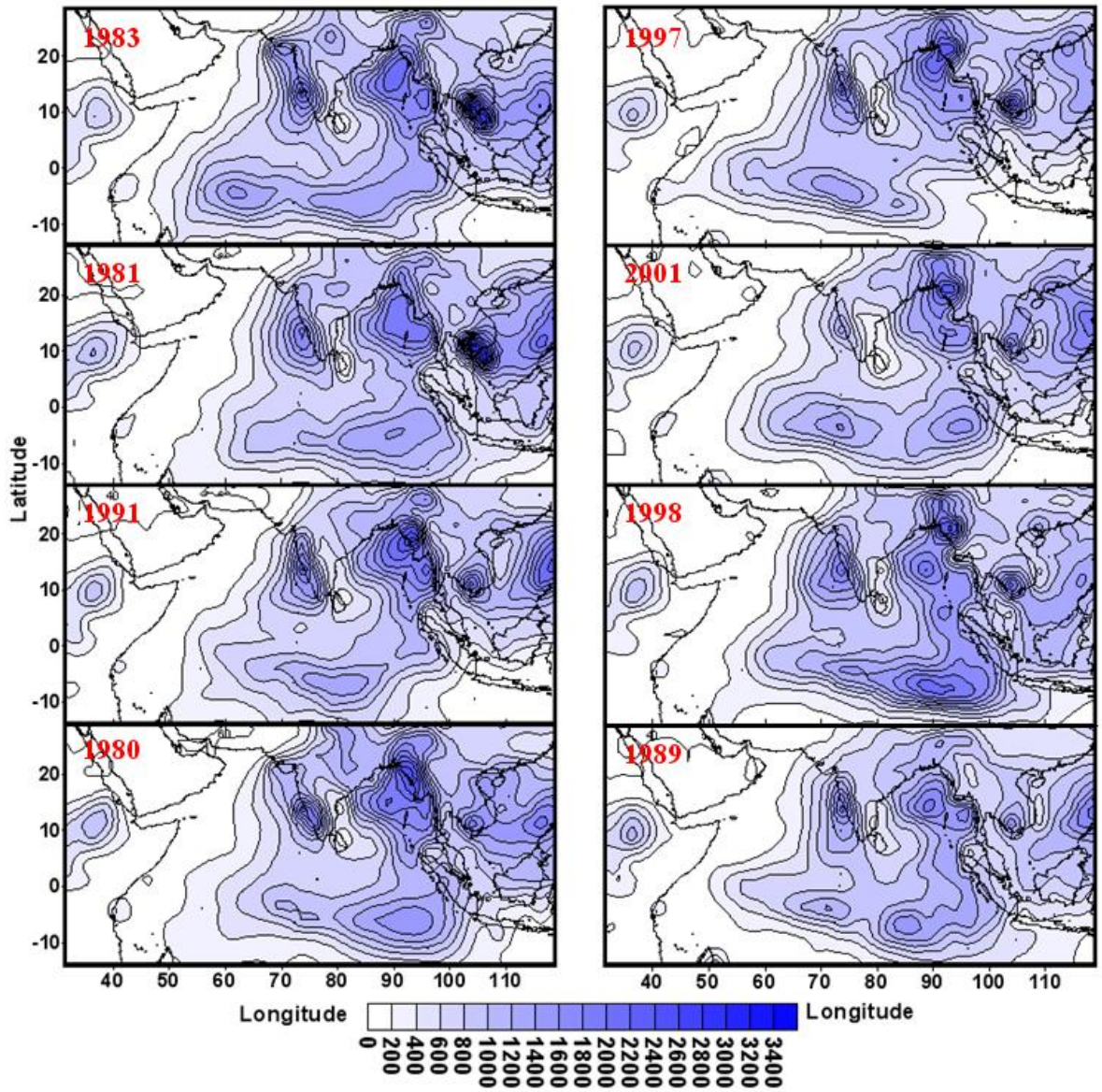

Figure 4.16: JJAS total rainfall for the first four highest (left panel) and lowest (right panel) scores of PC-3 for the Asian region, with their corresponding years indicated.

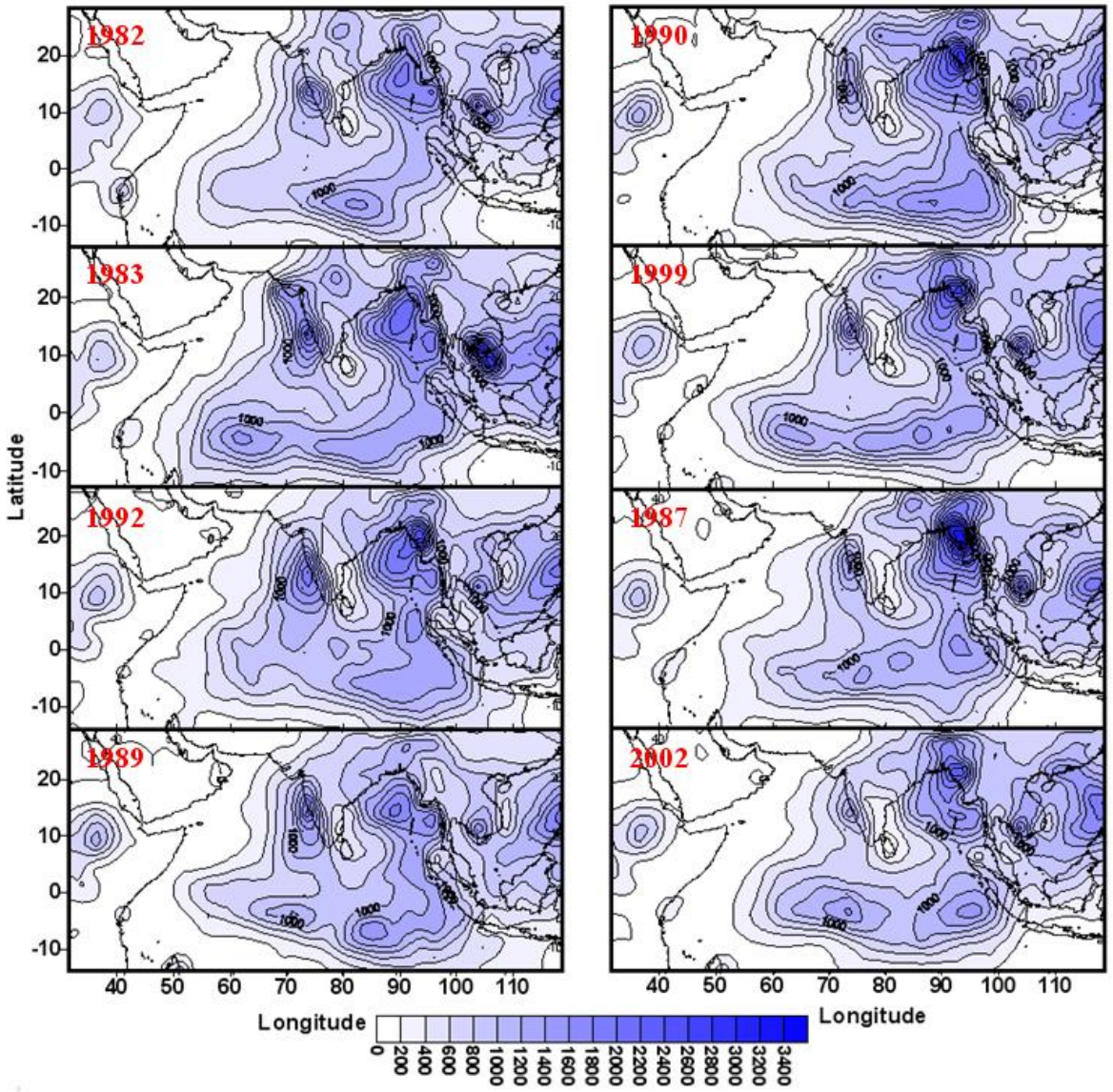

Figure 4.17: JJAS total rainfall for the first four highest (left panel) and lowest (right panel) scores of PC-4 for the Asian region, with their corresponding years indicated.

JJAS total rainfall for the top and bottom four scores for the first four PCs are also presented in Figure 4.18 to 4.21 for the Indian region. JJAS total rainfall for the highest and lowest PC-1 scores again reflects the magnitude of rainfall. The first four highest scores of PC-1 (Figure 4.18, left panel) correspond to the excess rainfall years for the Indian region. This indicates that the highest scores of PC-1 represent the magnitude of JJAS total rainfall. On the other hand, JJAS total rainfall for the lowest scores of PC-1 (Figure 4.18, left panel) for the Indian region correspond to dry (2002 and 1999), excess (1980) and normal (1990) rainfall years, so the relationship appears less clearcut.

JJAS total rainfall corresponding to the other PCs highest and lowest scores (PC-2, PC-3 and PC-4) for the Indian region is shown in Figure 4.19 to Figure 4.21. These figures

show very similar patterns of JJAS total rainfall, with the highest rainfall occurring in the Bay of Bengal (BoB) region and west coast of India. The rainfall pattern shown in these figures also suggests that there is an east-west gradient. This may be due to east-west propagation of the Inter-Tropical Convergence Zone (ITCZ) during the monsoon period. Other patterns appear too subtle to interpret.

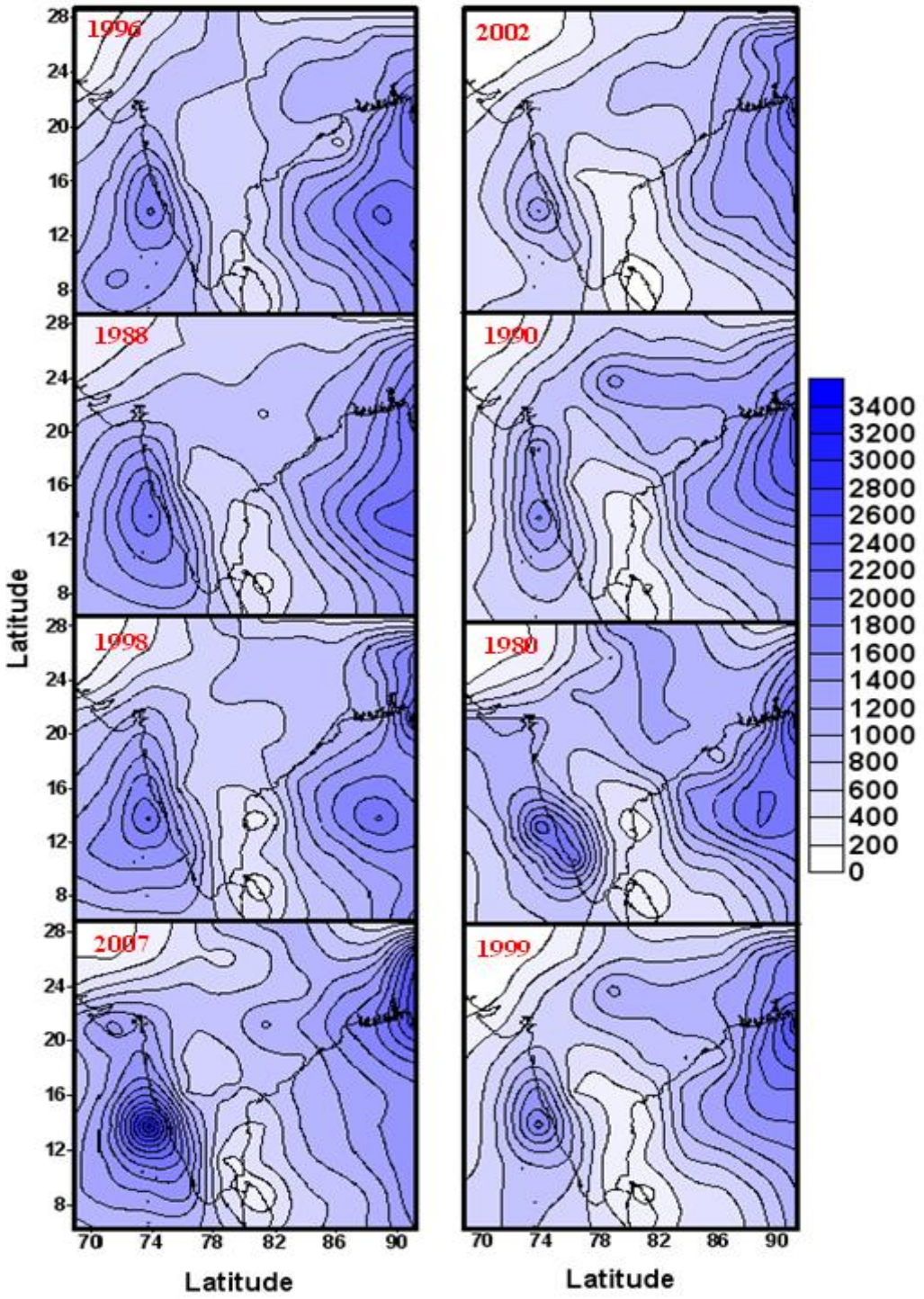

Figure 4.18: JJAS total rainfall for the first four highest (left panel) and lowest (right panel) scores of PC-1 for the Indian region, with their corresponding years indicated.

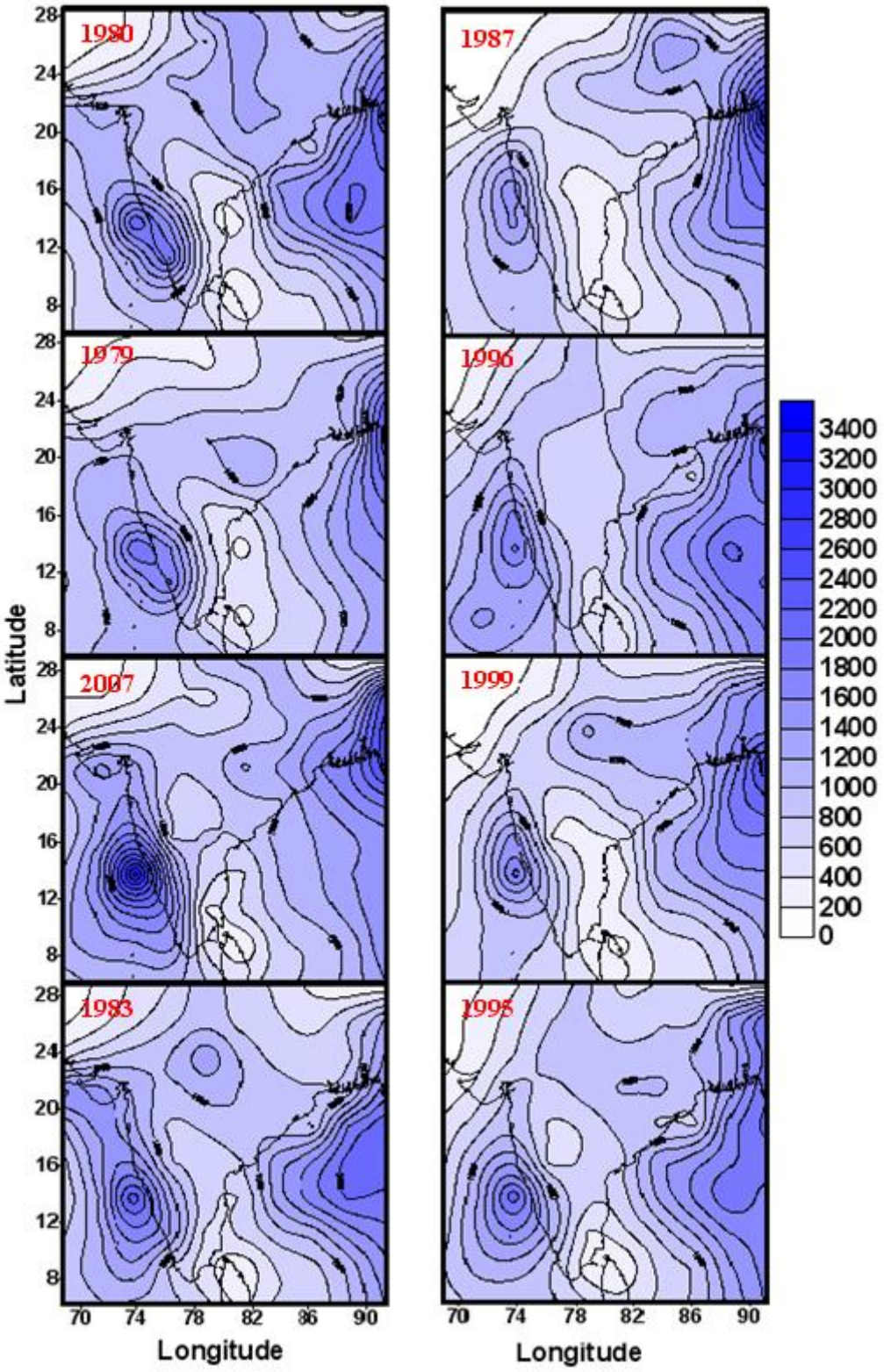

Figure 4.19: JJAS total rainfall for the first four highest (left panel) and lowest (right panel) scores of PC-2 for the Indian region, with their corresponding years indicated.

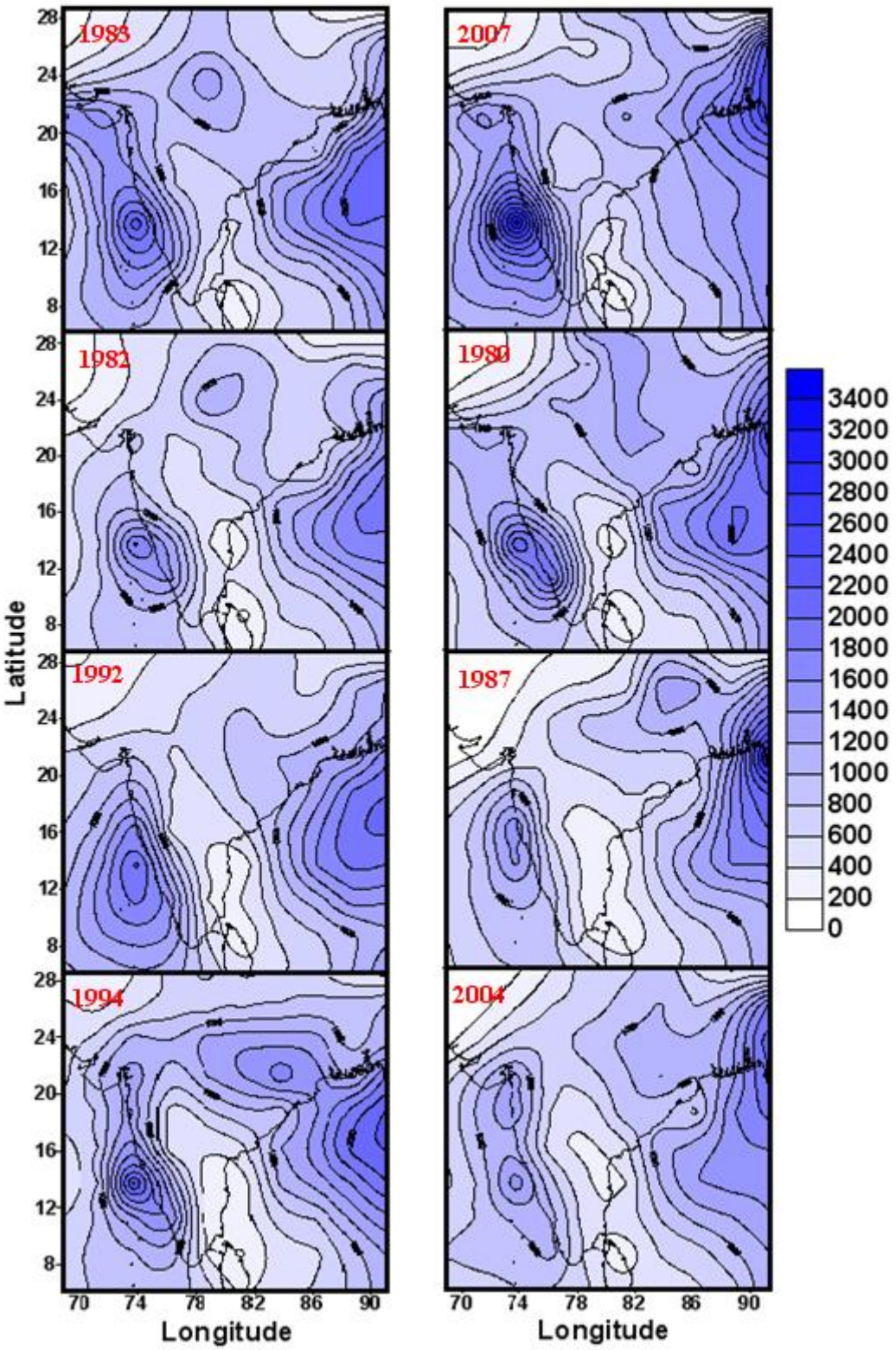

Figure 4.20: JJAS total rainfall for the first four highest (left panel) and lowest (right panel) scores of PC-3 for the Indian region, with their corresponding years indicated.

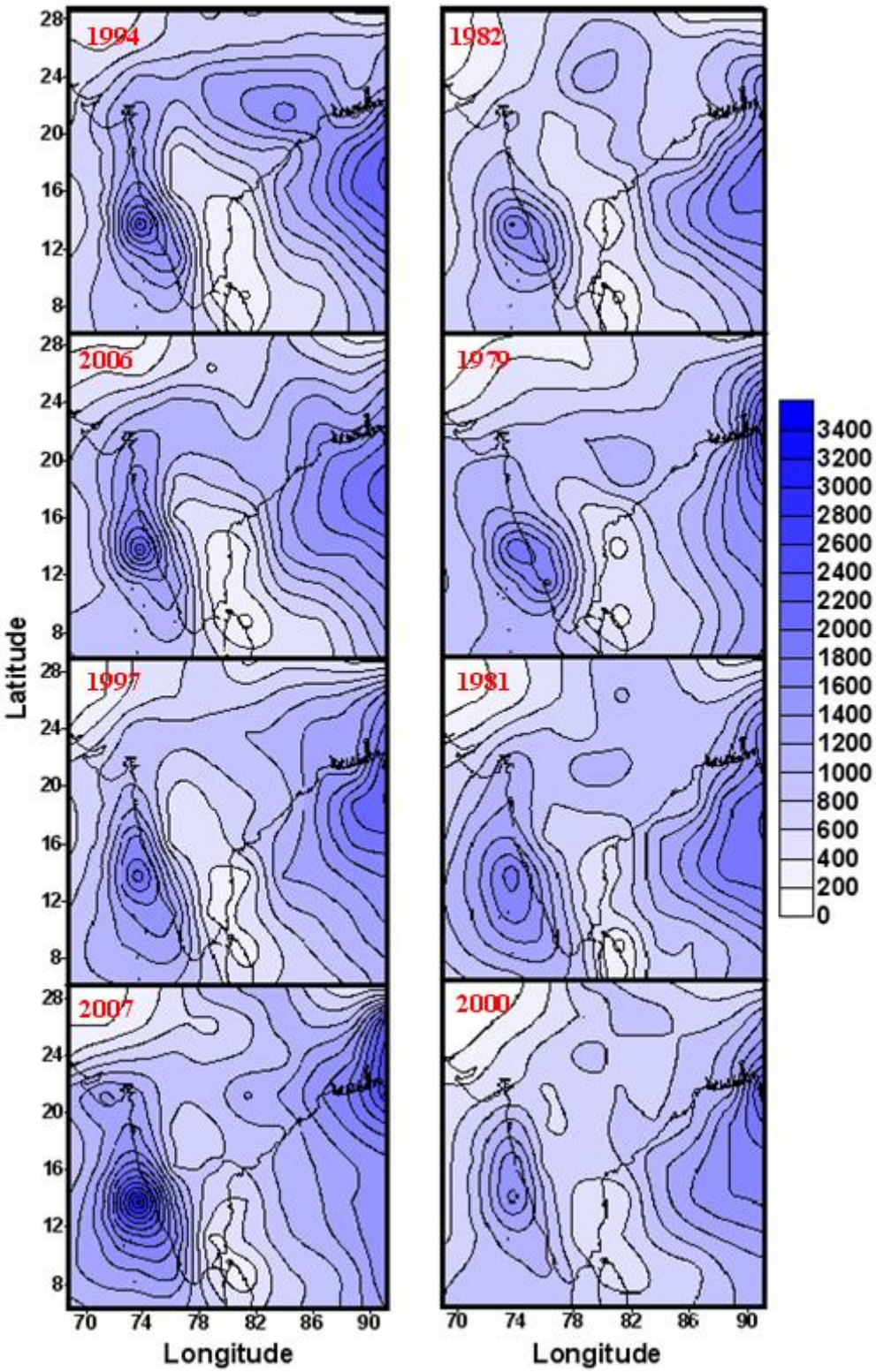

Figure 4.21: JJAS total rainfall for the first four highest (left panel) and lowest (right panel) scores of PC-4 for the Indian region, with their corresponding years indicated.

In order to gain insight into the interannual variability of JJAS total rainfall, time series of the first four principal components are analysed. The first four principal components or PC scores were subjected to varimax rotation and the results are presented

in Figure 4.22 for the Asian and Indian region, separately. These time series show significant interannual variability. Correlation analysis was carried out between time series derived from the spatial average of JJAS rainfall over each region and corresponding area principal components. Results show that the first two principal components or PC scores for the Asian region are moderately correlated (positive) with the mean JJAS rainfall for the whole region with a correlation coefficient (CC) = 0.59 for both components (Figure 4.23a and b). The third principal component/PC score is weakly correlated (positive) with mean JJAS rainfall with CC = 0.44, while PC-4 is very weakly correlated (negative) to mean JJAS rainfall with CC = -0.17 for the Asian region. The PC-1 and JJAS total rainfall for the Indian region is moderately correlated (positive, Figure 4.24a). The correlation coefficient between PC-1 for the Indian region and mean JJAS rainfall for the Indian region is higher (CC = 0.67, Figure 4.24a) compared to the first and second principal component for the Asian region (Figure 4.23a and b). The correlation between PC-2 and mean JJAS rainfall for the Indian region (Figure 4.24b) is the same as the first and second principal component for the Asian region (Figure 4.23a and b) (moderately correlated, with CC = 0.59). The second and the third principal components or PC scores for the Indian region are weakly correlated to mean JJAS rainfall with CC = -0.09 (negatively correlated) and 0.21 (positively correlated), respectively. Since the first two principal components for both regions are associated with mean JJAS rainfall with a correlation coefficient greater than 0.59, the first two principal components represent the dominant mode of interannual monsoon rainfall variability for these two regions. However, it should be noted that the two areas are different in size, which may have an effect on the strength of the PCs for each area. For example, the larger area is likely to be influenced by more factors (e.g. ENSO), hence weakening any relationships observed.

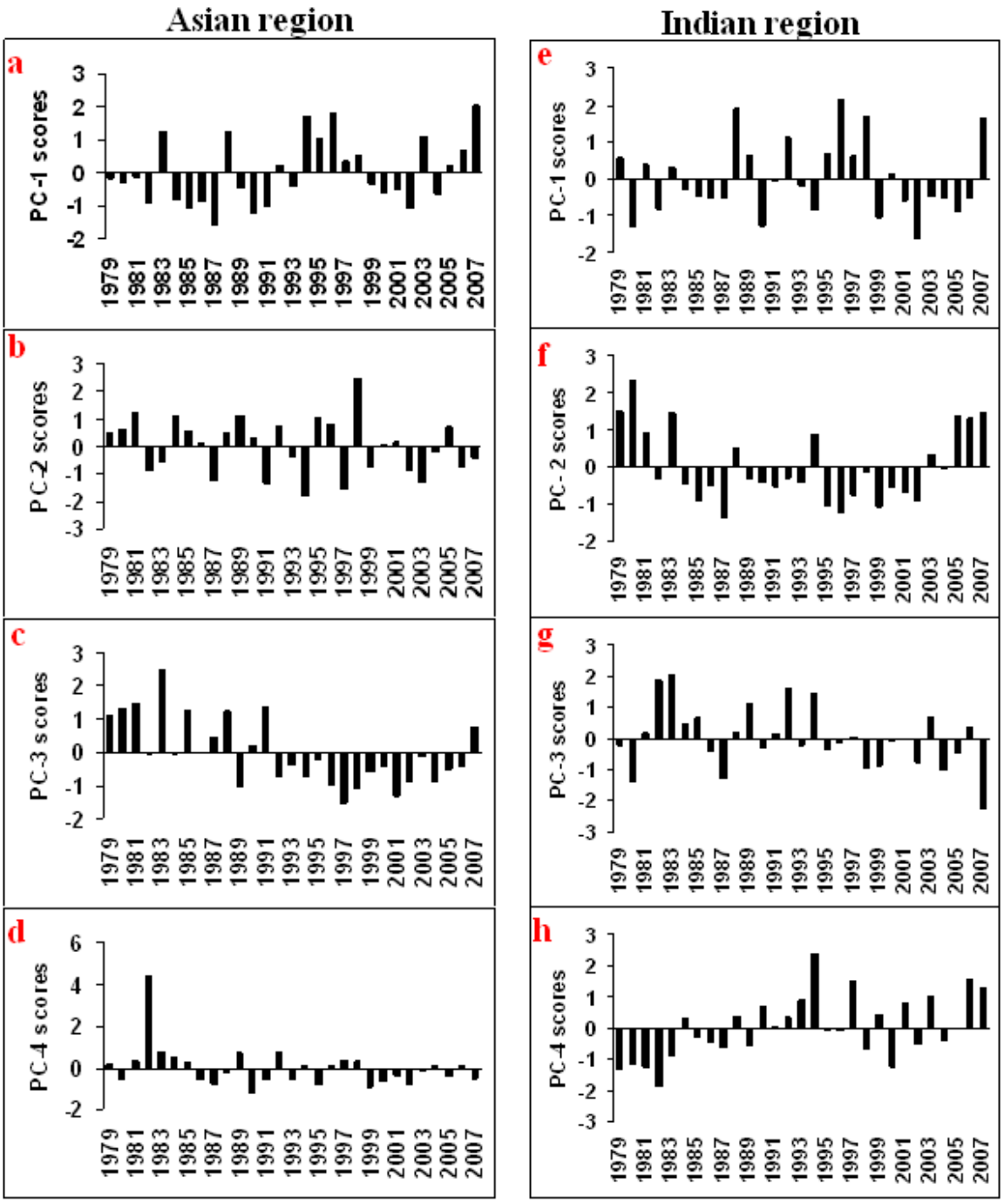

Figure 4.22: Time series of the first four principal components: (a) PC-1, (b) PC-2, (c) PC-3 and (d) PC-4 of June-September (JJAS) total rainfall for the Asian region, with (e) PC-1, (f) PC-2, (g) PC-3 and (h) PC-4 being the corresponding first four PCs for the Indian region. All the PCs were rotated using varimax rotation.

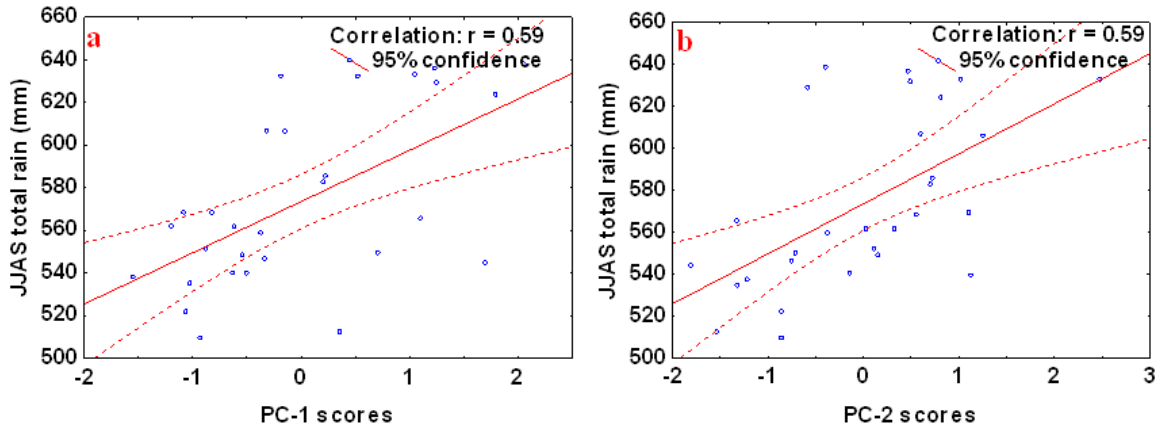

Figure 4.23: First two principal component scores: (a) PC-1and (b) PC-2 versus spatial mean June-September (JJAS) rainfall for the Asian region from 1979 to 2007. All the principal components were rotated using varimax rotation.

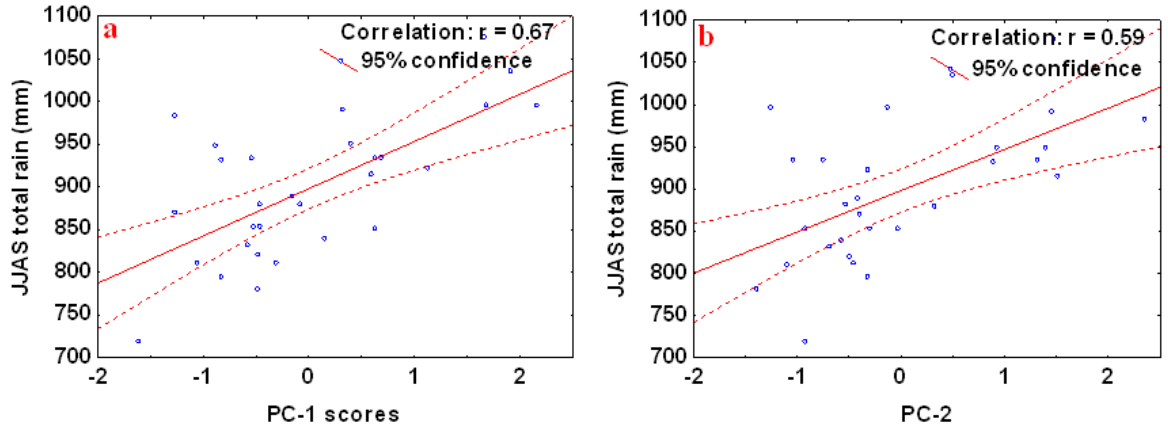

Figure 4.24: First two principal component scores: (a) PC-1 and (b) PC-2 versus spatial mean June-September (JJAS) rainfall for the Indian region from 1979 to 2007. All the principal components are rotated using varimax rotation.

4.2.2.2 Identification of excess and deficient years of monsoon rainfall

It has been suggested that extremes of monsoon rainfall can lead to devastating floods and droughts, resulting in enormous economic loss though agricultural loss and property damage (Clarke et al. 2000; Goswami 2004; Webster et al. 1998). According to Goswami (2004) there is a tendency for El Niño's to be associated with droughts and La Niña's to be associated with above normal rainfall conditions over India. It was shown in Section 4.2.1.1 that the large negative values in June to September (JJAS) total rainfall anomalies for the Asian region correspond to El Niño years (Figure 4.6). However, it should be noted that droughts and floods can occur in the absence of El Niño or La Niña, especially for the southern Asian region.

The statistical parameters of monsoon rainfall (JJAS total) (mean, standard deviation (S) and coefficient of variation (C.V.)) were computed for the Asian and Indian regions separately and are presented in Table 4.2. The maximum total rainfall for the Asian region during JJAS was observed in 2007 (638.5 mm) with a mean of 573.6 mm and a standard deviation of 40.6 for the whole area. The Indian region also experienced the maximum total rainfall in 2007 (1077.5 mm) with a standard deviation of 82.6 (Table 4.2). It can be seen from Table 4.2 that interannual variability in JJAS total rainfall over the Asian and Indian region, is reflected by a coefficient of variation of 7.1 and 9.2%, respectively.

In this section, an attempt has been made to identify excess and deficient years of monsoon rainfall (June to September: JJAS) for the Asian region as a whole and for the Indian region (see Figure 4.11) using 29 years of enhanced mean monthly precipitation data obtained from the Climate Prediction Center (CPC) merged analysis of precipitation (CMAP) for the Asian monsoon region and the Indian region. Following Parthasarathy et al (1994), an excess (wet) or flood year has been defined when monsoon rainfall (JJAS total rainfall) is $R_i \geq \overline{R} + S$ and a deficient (dry) or drought year is defined as when monsoon rainfall (JJAS total rainfall) is $R_i \leq \overline{R} + S$, where R_i is the monsoon rainfall of the ith year, $\overline{R}$ is the mean and S is the standard deviation of the data series. Following the above criteria, 7 and 6 years fall into the categories of excess or flood years for the Asian and Indian regions, respectively (Table 4.3, Figure 4.25). It is interesting to note that all the flood years for the Indian region (except 1980) coincide with the Asian season flood years (Table 4.3: highlighted in bold). For the Asian region, only 3 years fall into the category of deficient or drought years. On the other hand, for the Indian region there are 5 years that fall into the category of deficient or drought years (Table 4.3, Figure 4.25).

Table 4.2: Statistical details of monsoon rainfall for the Asian and the Indian regions.

Parameters	Asian Region	Indian Region
Mean	573.6	898.0
Standard deviation (S)	40.6	82.6
Minimum	509.2	718.3
Maximum	638.5	1077.5
Coefficient of variation (C.V.)	7.1	9.2

Table 4.3: Excess and deficient years of monsoon rainfall for the Asian and Indian regions based on rainfall data from 1979 to 2007. Common years are highlighted in bold.

Excess years		Deficient years	
Asian Region	**Indian Region**	**Asian Region**	**Indian Region**
1979	1980	**1982**	**1982**
1983	**1983**	1997	1984
1988	**1988**	**2002**	1987
1995	**1996**		1999
1996	**1998**		**2002**
1998	**2007**		
2007			
Total: 7	6	3	5

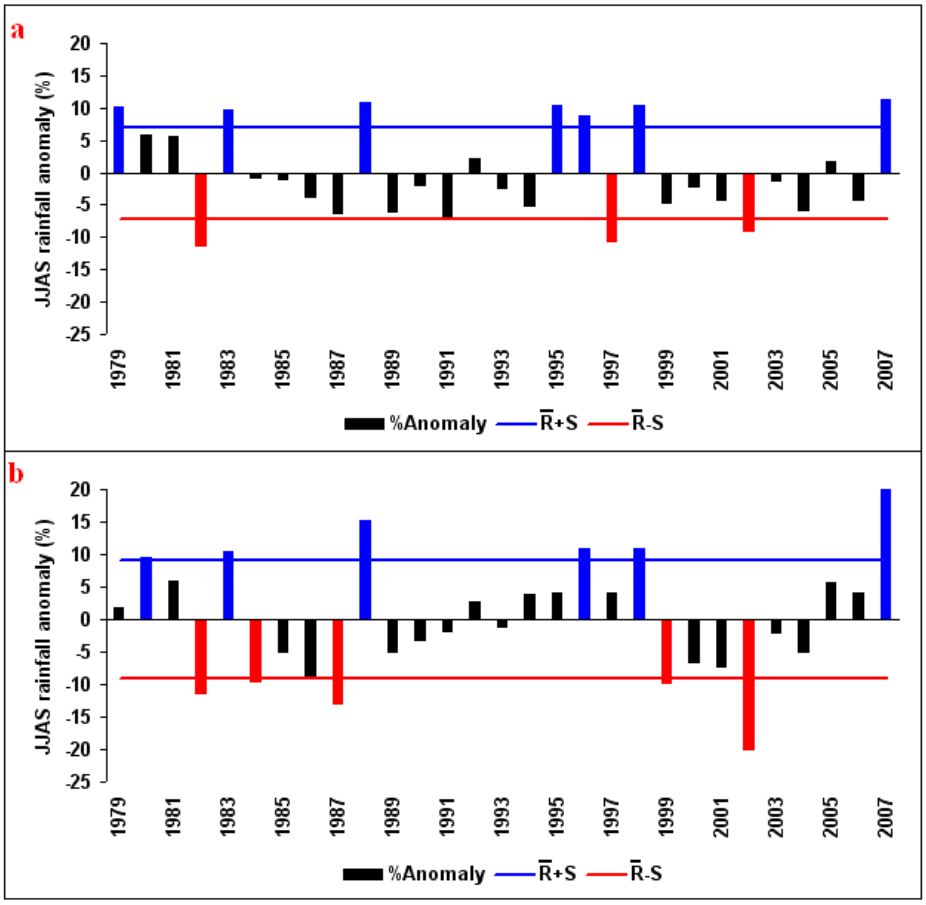

Figure 4.25: Time series of excess and deficient years of monsoon rainfall: (a) for the Asian and (b) for the Indian region based on rainfall data from 1979 to 2007. Blue and red bars indicate flood and drought years, respectively. Normal years are indicated by black bars, while $\overline{R}$ and S are defined in the text.

A major proportion of the annual rainfall over most of the Asian region occurs during the summer monsoon season (June to September) (Kripalani and Kulkarni 2001). Here an attempt has been made to compare the monsoon rainfall (June-September) and its

contribution to annual rainfall (January-December) for the Asian region as a whole, and for the Indian region separately (see Figure 4.11 for the definition of these two regions). Analysis of the all-India summer monsoon rainfall for the period 1871 to 1978 using 306 stations reveals that the Indian subcontinent receives about 78% of its rainfall during the summer monsoon season (Mooley and Parthasarathy 1984). Furthermore, Kumar and Prasad (1997) suggested that the meteorological subdivisions in the subcontinent receive about 60% to 90% of annual rainfall during the summer monsoon season. Percentage contributions to annual rainfall from monsoon rainfall (JJAS total) for the Asian and Indian regions (see Figure 4.11) using enhanced mean monthly precipitation data obtained from the Climate Prediction Center (CPC) merged analysis of precipitation (CMAP) for the period between 1979 to 2006 were calculated and are presented in Table 4.4 and Figure 4.26 for the Asian and Indian regions. It can be seen from Table 4.4 that there is not much difference in the coefficient of variation (4.3 and 5.8% for Asian and Indian regions, respectively) for the two regions. However, Figure 4.26 shows that the percentage contribution (red line) to yearly total rainfall from June-September (JJAS) total rainfall varies from year to year. It is also clear from Figure 4.26 that the percentage contribution (red line) to yearly total rainfall from June-September (JJAS) total rainfall for the Asian region is much lower in all years when compared with the Indian region. On average, the monsoon rainfall contributed about 38.6 and 62.6% (Table 4.4) to the yearly total rainfall for the Asian and Indian region, respectively. In the year 2002, the monsoon contributed the lowest proportion for both regions, while in the years 1979 and 1983 the monsoon contributed the highest proportion for the Asian and Indian regions, respectively. It is interesting to see that 2002 (lowest contribution from JJAS total rainfall to the yearly total rainfall for both regions) is a rainfall deficient year for both regions (Table 4.3, Figure 4.25). The years 1979 and 1983 (highest contribution from JJAS total rainfall to the yearly total rainfall for the Asian and Indian regions, respectively) correspond to excess rainfall years for both regions (Table 4.3, Figure 4.25).

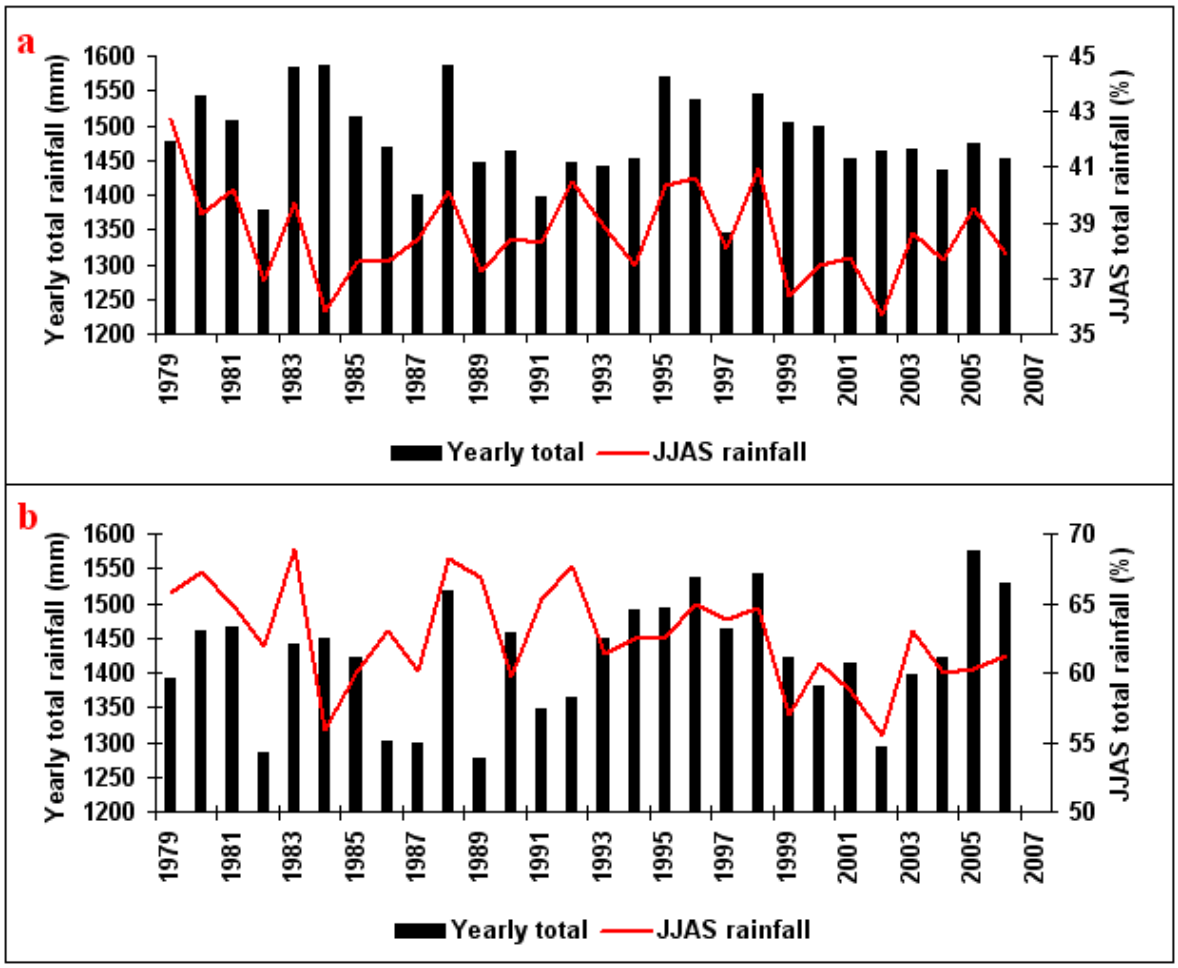

Figure 4.26: (a) Yearly total rainfall (bars) and percentage contribution (red line) to yearly total rainfall from June-September (JJAS) rainfall for the Asian region, and (b) same as (a) but for the Indian region.

Table 4.4: Percentage contribution from yearly total rainfall to June-September (JJAS) rainfall for the Asian and Indian regions.

Parameters	Asian Region	Indian Region
Mean	38.6	62.6
Standard Deviation	1.7	3.6
Minimum	35.7	55.5
Maximum	42.8	68.9
Coefficient of variation (C.V.)	4.3	5.8

4.2.2.3 Periodicities of monsoon rainfall

It was shown above that the rainfall for both regions (Asia and India) has varied significantly from year to year. On the interannual time scale the Asian monsoon exhibits a strong distinct bienniality with a strong monsoon tending to be followed by a weak monsoon and vice versa (Clarke et al. 2000; Lau and Wang 2005). For example, Indian

rainfall varies on an interannual time scale with a periodicity of 2-3 years (Clarke et al. 2000; Mooley and Parthasarathy 1984). Kumar (1997) have also discovered a quasi-biennial oscillation (QBO) and ENSO-type periodicities in the rainfall series over homogeneous regions of India.

In order to determine whether there is any periodicity at the interannual time scale in the rainfall for the regions considered here (Asia and India, see Figure 4.11), Fourier spectral analysis was carried out separately for the two regions. Figure 4.27 shows the results of Fourier analysis. It is clear from these figures that the rainfall shows peaks in the 2.4-3.7 year range. This quasi-biennial component may be related to the tropospheric biennial oscillation (TBO) and appears in other atmospheric variables, including surface pressure, wind and SST (Clarke et al. 2000). Although the amplitude for the next peak is not very dominant, both regions show a periodicity of 5.2 years (Figure 4.27). Munot and Kothawale (2000) carried out a similar power spectrum analysis using rainfall series for all-India and homogeneous regions of India, and found that significant cycles of a 2-3 year period exist for all-India as a whole and for the northwest, west-central and peninsula India. Furthermore, northeast India and peninsula India rainfall also shows 3-5 year cycles and it was suggested that the 3-5 year periodicity may be related to ENSO (Munot and Kothawale 2000). Li and Zhang (2002) pointed out that the physical processes that determine the monsoon rainfall variation on quasi-biennial (2-3 year) and lower-frequency (3-7 year) time scales are different and that the quasi-biennial variability of the monsoon is primarily determined by local processes in the Indian Ocean, while the lower-frequency variability of the monsoon is primarily attributed to remote forcing mechanisms.

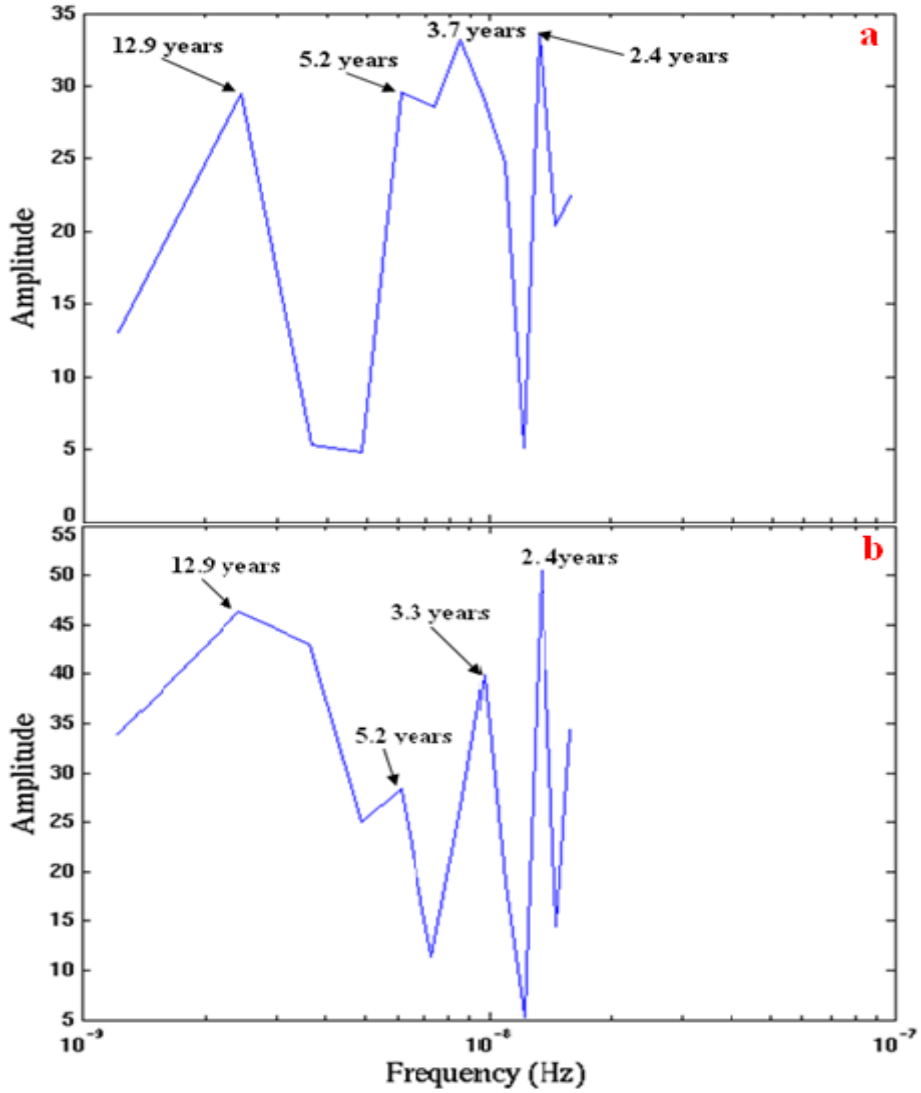

Figure 4.27: Fourier transform spectrum showing interannual variability of rainfall for the (a) Asian and (b) Indian regions (based on rainfall data from CMAP from 1979 to 2006).

4.2.3 Intraseasonal variability

The Asian Monsoon fluctuates or varies on an intraseasonal scale (Sumi et al. 2005). Initial recognition of the intraseasonal variability or oscillation occurred in the early 1970's with the suggestion of 30-60 day or 40-50 day oscillations in the tropics (Ding 2007). The intraseasonal oscillation (ISO) is one of the most dominant large-scale features of the monsoon (Hoyos and Webster 2007). Studies of the Asian summer monsoon have suggested that the intraseasonal oscillations (ISOs) of the Asian summer monsoon have periods between 10 and 90 days, with two preferred bands of periods – one between 10 and 20 days and the other between 30 and 60 days (Krishnamurti and Ardanuy 1980; Krishnamurti and Bhalme 1976);(Yasunari 1980). On the other hand, Sumi et al (2005)

suggested that the time-scale is relatively broad and its period extends from 20 days to 50 days and argued that the most dominant and interesting intraseasonal fluctuations are associated with the Madden- Julian Oscillation (MJO).

Intraseasonal variability of monsoon rainfall during a monsoon season is characterized by the occurrence of active-break cycles of wet or dry phases (Krishnamurthy and Shukla 2000; Sumi et al. 2005). The dry and wet spells of the active and break conditions represent intraseasonal variations of the monsoon with time scales longer than synoptic variability, but shorter than a season. Over the Indian subcontinent, the wet or dry spells are the manifestation of repeated northward propagation of the intertropical convergence zone (ITCZ) from the equatorial position to the continental position and results from superposition of 10-20 day and 30-60 day oscillations. According to Goswami (2004) both oscillations (the 10-20 and 30- 60 day) contribute roughly equally to the total intraseasonal variability (ISV) in the south Asian summer monsoon (SAM) region.

Roxy and Tanimoto (2007) examined the intraseasonal variability (10-60 days) of sea surface temperature (SST) over the northern Indian Ocean and its influence on regional precipitation variability over the Indian subcontinent and found that the intraseasonal precipitation anomalies over the Western Ghats (WG) in the southwest and Ganges-Mahanadi Basin (GB) in the northeast of the Indian subcontinent are not correlated to each other. They suggested that the WG is influenced by the ocean-atmosphere effect over the Arabian Sea and the GB influenced by both the Arabian Sea and BoB. Furthermore, it is suggested that the intraseasonal variability over the Indian subcontinent differs from that of Indochina Peninsula (Yokoi et al. 2007). This suggests that there are regional differences in intraseasonal variability within Asian monsoon regions. Hence, to study the intraseasonal variability of the Asian monsoon, five sub-regions (Figure 4.28) within the Asian monsoon region were chosen. The three sub-regions (WG: Western Ghats, BoB: Bay of Bengal and EA: East Asia) were selected based on average seasonal (JJAS) rainfall maxima (Figure 4.8a). Characteristics of intraseasonal variability of precipitation over land areas seem to be modulated by complex surface conditions and thus are expected to be different from those over the ocean (Yokoi et al. 2007). Hence two sub-regions (CI: Central India and MI: Maldive Islands) were selected to include a continental and oceanic region, respectively.

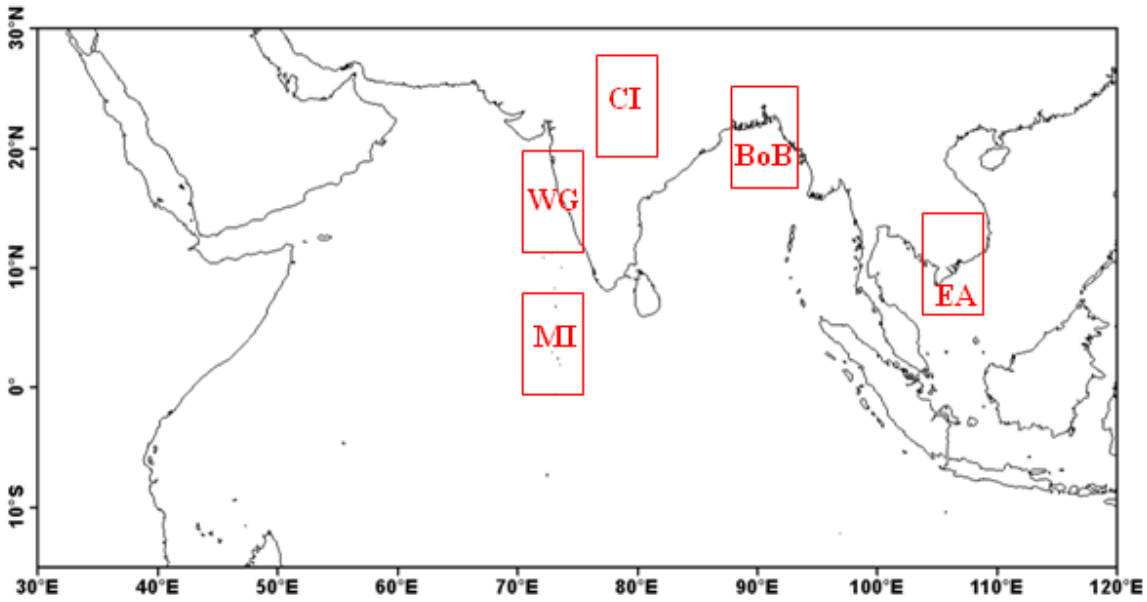

Figure 4.28: Geographical locations of the sub-regions selected to study interannual variability of the Asian monsoon. Where WG = Western Ghats, BoB = Bay of Bengal, EA = East Asia, CI = Central India and MI = Maldive Islands.

In order to study the intraseasonal variability of monsoon for the five regions outlined in Figure 4.28, precipitation data were obtained for the Asian region from the Tropical Rainfall Measuring Mission (TRMM) from 1998-2007 (details of TRMM precipitation data were provided in Section 2.1.1). From this dataset, precipitation data were extracted for the five regions (shown in Figure 4.28). Figure 4.29 shows the mean annual cycle, while Figure 4.30 shows the smoothed mean annual cycle for the five regions outlined in Figure 4.28. The mean annual cycle (MAC) for each region was created by averaging 10 years (1998-2007) of precipitation data obtained from the Tropical Rainfall Measuring Mission (TRMM) for each region separately, and averaging each calendar day over the 10 years (to get the mean annual cycle). The resulting MAC time series were smoothed 300 times with a 1-2-1 filter to obtain the smoothed mean annual cycle (SMAC) for each region. The rainfall occurring on 29 February (in leap years 2000 and 2004) was omitted from the above calculation (mean annual and smoothed mean annual cycle) and from the following analysis (see Section 2.1.1 for details about the leap year issue).

As Figure 4.29 and Figure 4.30 indicate, there are regional differences in the MAC and SMAC of precipitation within the Asian monsoon regions. Although the amplitude of the annual cycle are different for each region (with the highest amplitude for BoB), the Bay of Bengal (BoB) and Western Ghats (WG) regions show quite similar annual cycles (in both MAC and SMAC: Figure 4.29 and Figure 4.30) with a correlation coefficient (CC) of

0.78 and 0.97 (Table 4.5), respectively. The MAC and SMAC cycles between the BoB and Central India (CI) region also indicate high correlation (CC of 0.76 and 0.91, respectively) between the two regions. The highest correlation for the MAC and SMAC for the East Asia (EA) region is also with the BoB (CC of 0.67 and 0.86, respectively). It is clear from Figure 4.29 and Figure 4.30 that the amplitude of MAC and the SMAC is smallest and relatively constant throughout the year for the Maldive Islands (MI) region. The correlations between mean annual cycle for the MI region and that for the other regions are weak (Table 4.5). On the other hand, the smoothed mean annual cycle for the MI region shows high correlation (0.71) with the EA region smoothed mean annual cycle.

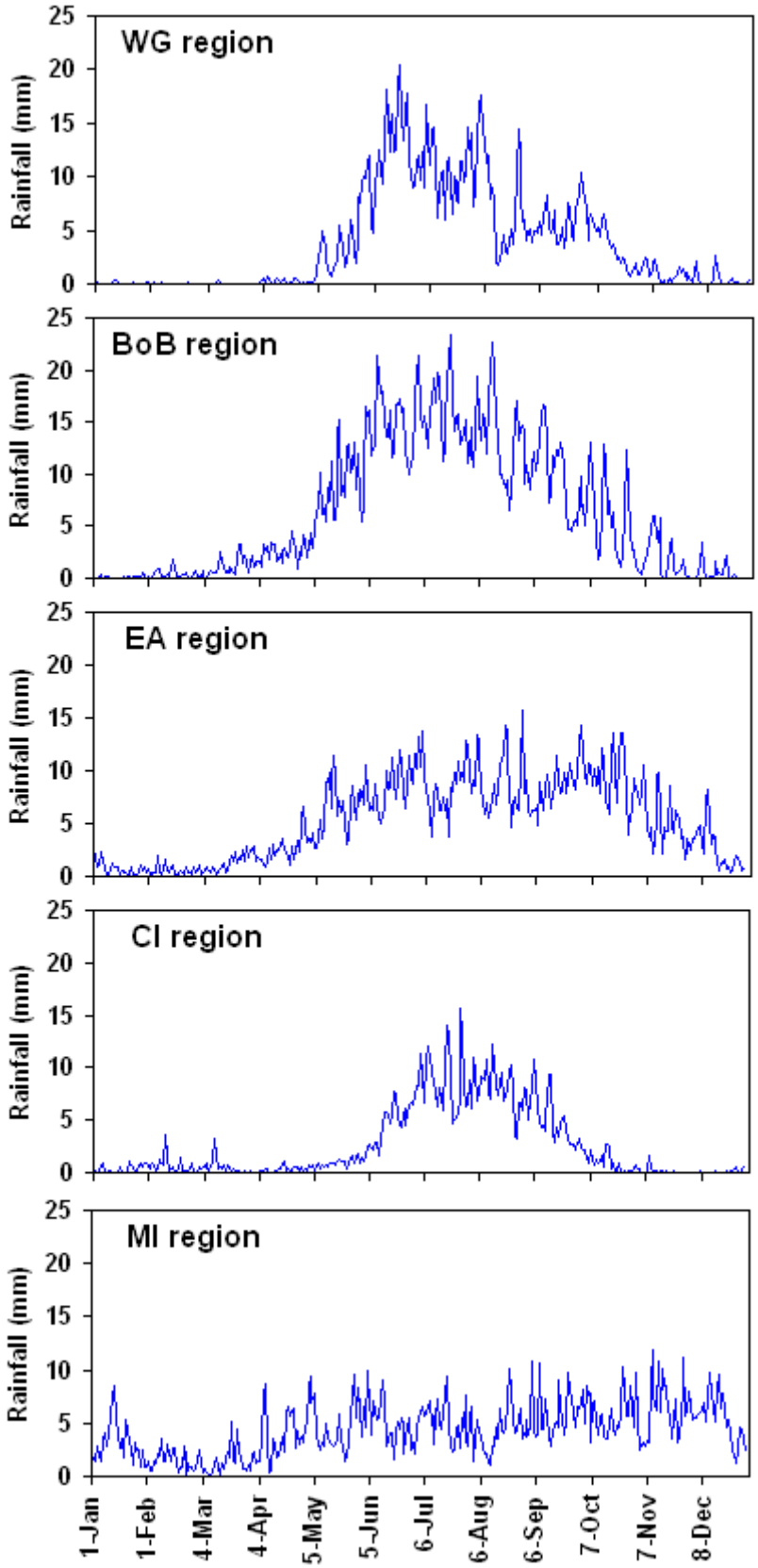

Figure 4.29: Mean annual cycle of precipitation (mm/day) over the WG (70-75E; 12-20.25N), BoB (88-93E and 17.25-25.5), EA (103. 5 – 108.5 E and 6-14.25N), CI (76-81E and 20-28.25 N) and MI (70-75E and 0.5S-7.75N) (see Figure 4.28 for locations) within the Asian monsoon domain.

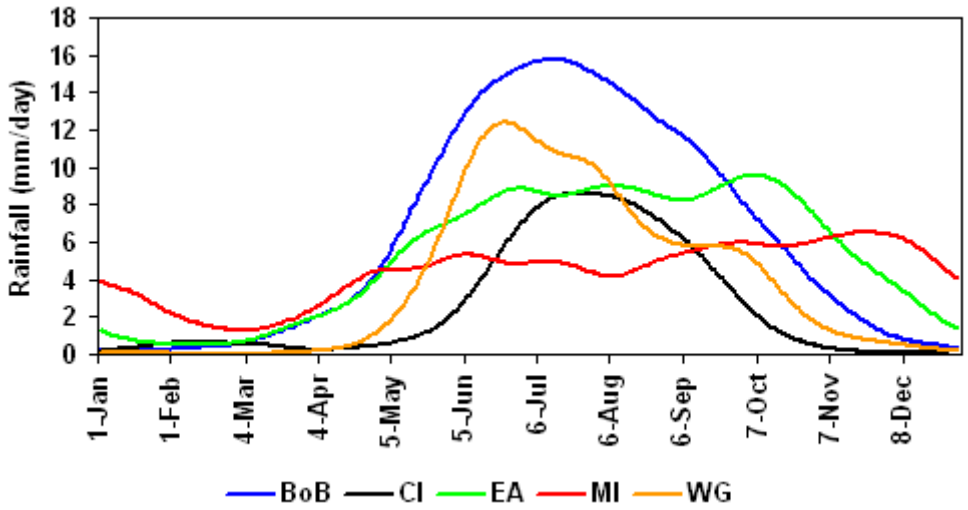

Figure 4.30: Same as Figure 4.29, but smoothed mean annual cycle of rainfall over the five regions.

Table 4.5: Mean annual and smoothed mean annual cycle correlations between regions. Where WG = Western Ghats, BoB = Bay of Bengal, EA = East Asia, CI = Central India and MI = Maldive Islands.

Mean annual cycle						Smoothed mean annual cycle					
	BoB	**CI**	**EA**	**MI**	**WG**		**BoB**	**CI**	**EA**	**MI**	**WG**
BoB	1					**BoB**	1				
CI	0.76	1				**CI**	0.91	1			
EA	0.67	0.54	1			**EA**	0.86	0.72	1		
MI	0.22	0.12	0.37	1		**MI**	0.40	0.23	0.71	1	
WG	0.78	0.71	0.64	0.21	1	**WG**	0.97	0.87	0.81	0.38	1

Year to year changes in the behaviour of intraseasonal oscillations or variability of monsoon rainfall can be demonstrated by displaying the time series of precipitation (Kripalani et al. 2004; Lawrence and Webster 2000). The years 2002 and 2003 were chosen because they have been identified as drought and normal years (Kripalani et al. 2004), respectively, for the Indian region. For the Asian region, the months June through to September (June-September) represent the monsoon core period, so that the rainfall for the June-September period was used to display the intraseasonal variability of monsoon rainfall for different regions of the Asia. Figure 4.31 displays the time series for the five regions (averaged over the Western Ghats, Bay of Bengal, East Asia, central India and Maldive Islands regions: see Figure 4.28) during the monsoon period (June-September), while Figure 4.32 shows time-latitude sections of precipitation for the same years for the same regions (averaged along longitudes 70-75E (for WG and MI), 88-93E (BoB), 76-81E (CI)

and 103. 5-108.5 E (EA)). The time-latitude section of precipitation for the MI region is not shown since it is the same as for the WG region.

For the WG region, the rainfall during 2002 was defined by two active periods (rainfall above normal), one at around 15 June and another one at 5 August (Figure 4.31 and Figure 4.32). On the other hand, the daily time series of rainfall (Figure 4.31) and the time-latitude section of rainfall (Figure 4.32) indicate that the year 2003 for the WG region was marked by three active periods of rainfall (15 June, early and middle July) during the early stage of the 2003 monsoon season. During the two seasons, existence of break periods (rainfall below average) is evident for the WG region. No well-defined active or break periods emerge from Figure 4.31 and Figure 4.32 for the BoB region during the two seasons. The time series of rainfall during the 2002 summer season for the CI region is marked by long breaks (Figure 4.31: middle panel, left), the first one between late June to middle July, the second one between 20-30 July and the third break starting from 15 September. Conversely, no well-defined break periods are discernible for the CI region during the 2003 summer monsoon season. The time series of 2003 summer rainfall (Figure 4.31: middle panel, right) is largely devoid of low rainfall days and is marked by relatively steady rainfall from one day to the next throughout the season. From the time-latitude section of rainfall for the CI region (Figure 4.32: middle panel,), no well-defined active or break periods are discernible during the 2002 and 2003 summer season. No well-defined active or break periods are evident from the time series and time-latitude section (Figure 4.31 and Figure 4.32) of precipitation for the EA region during both summer seasons. The time series of precipitation for the MI region (Figure 4.31: bottom panel, left) indicates the existence of active and break periods during the 2002 summer monsoon. The time series of 2003 summer rainfall (Figure 4.31: bottom panel, right) for the MI region is largely devoid of low rainfall days, and is marked by relatively steady rainfall from one day to the next through most of the season. No well-defined active periods are discernible for the MI region until later in the monsoon season, when a long break (between 10 August and the middle of September) is evident. Time-latitude sections of precipitation for the MI region (not shown) also indicate that there are no well-defined active or break periods for the two seasons, except for this long break.

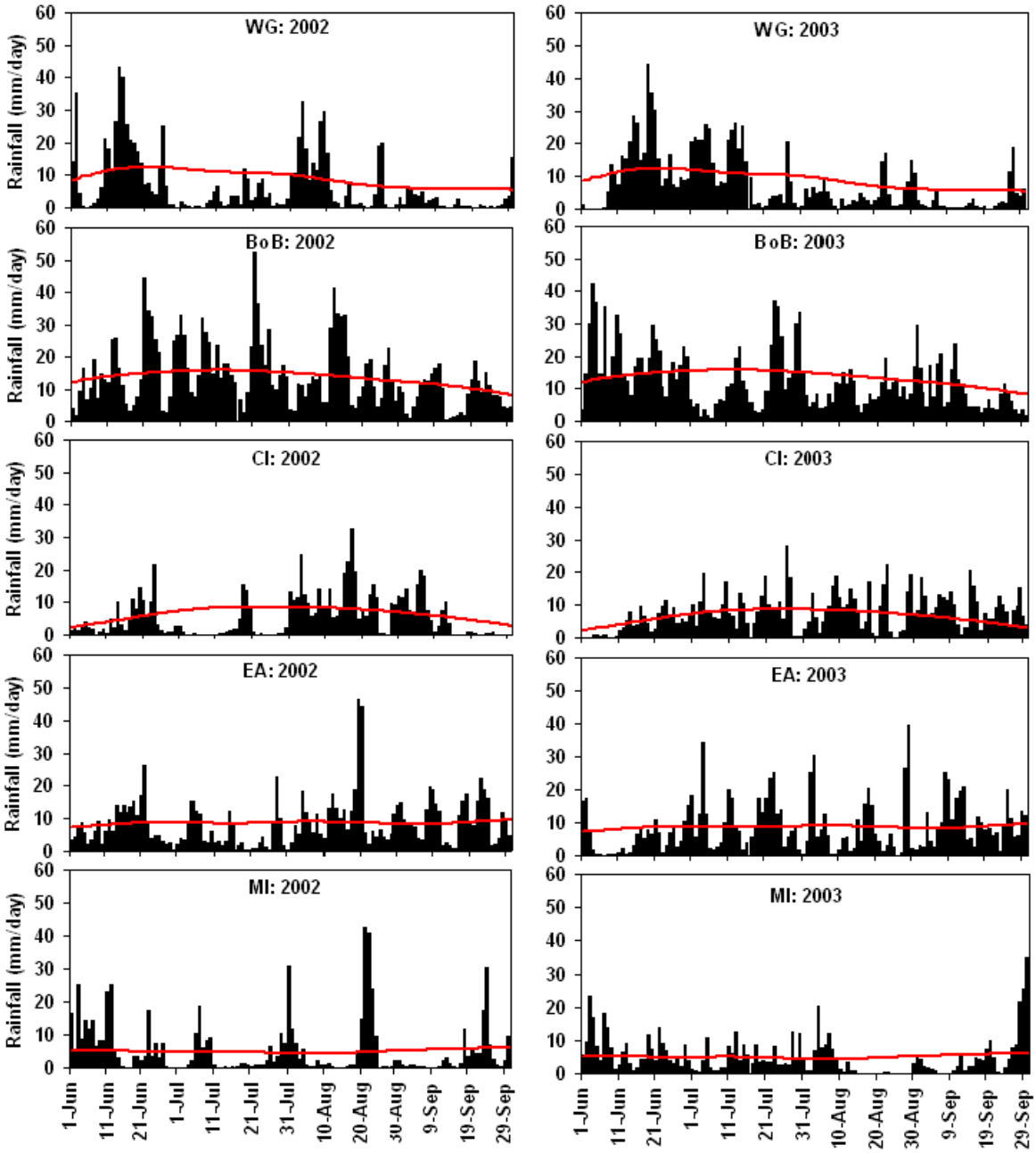

Figure 4.31: Time series of daily precipitation (mm/day) averaged over the WG (70-75E; 12-20.25N), BoB (88-93E and 17.25-25.5), CI (76-81E and 20-28.25 N), EA (103. 5-108.5 E and 6-14.25N) and MI (70-75E and 0.5S-7.75N) for Jun–Sep 2002 and 2003. Solid curve (red) in each plot represents 10-year mean smoothed values.

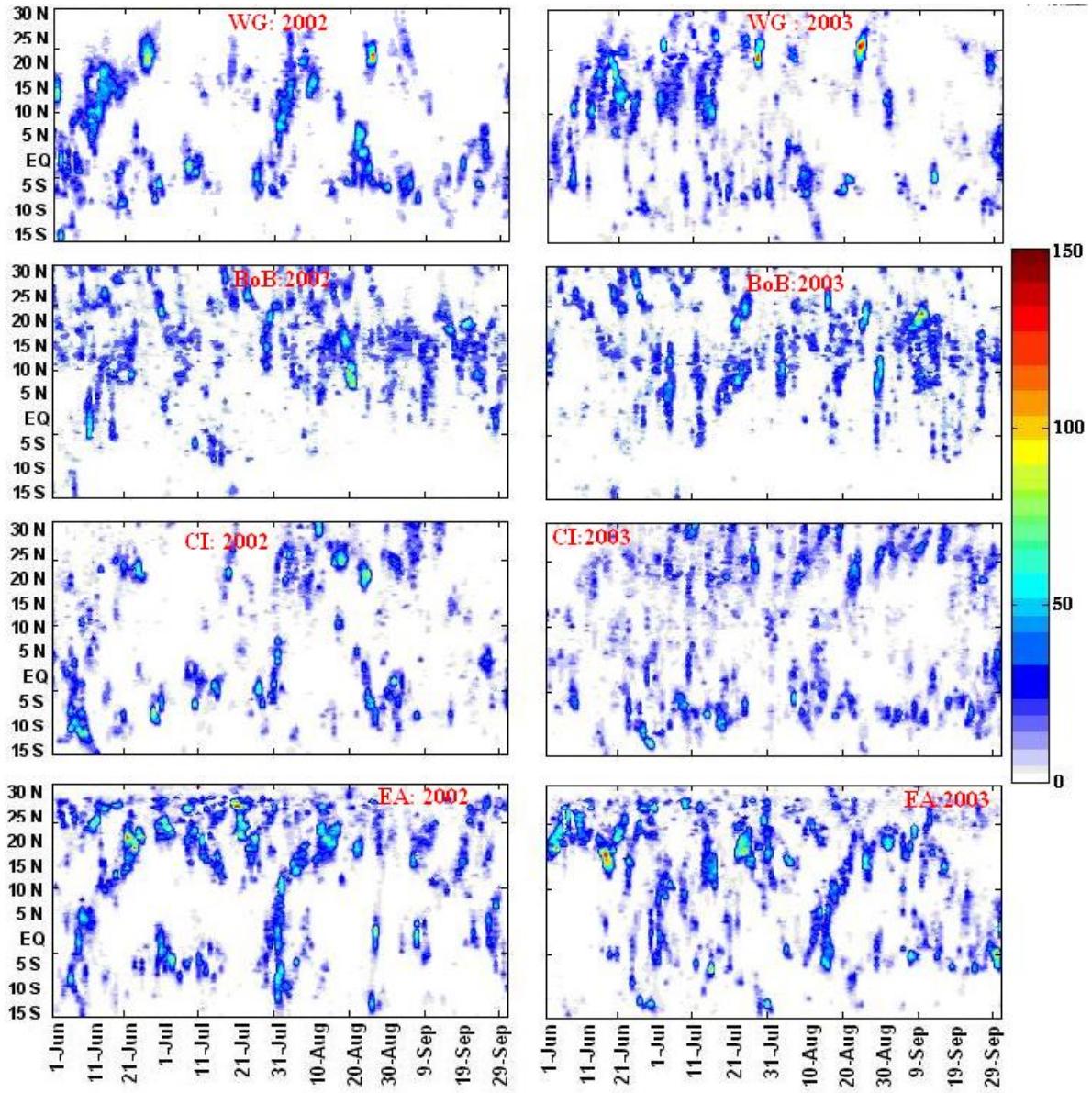

Figure 4.32: Time-latitude sections of daily precipitation averaged over 70-75E (WG), 88-93E (BoB), 76-81E (CI) and 103. 5 – 108.5 E (EA) for Jun–Sep 2002 and 2003. The time-latitude daily precipitation for the MI region (70-75E) is not shown since it is the same as for the WG region. Contour interval is 5 mm/day.

Following Yokoi et al. (2007), Fourier analysis was carried out to determine intraseasonal time scale periodicities of monsoon precipitation for each region discussed above. Stidd (1953) suggested that the frequency distribution of the cube roots of daily precipitation data was closer to the normal distribution than that of the original data. Hence, the cube roots of the gridded precipitation data were used here. Following Hartmann and Michelsen (1989) and Yokoi et al.(2007), the cube roots of the gridded precipitation data for each calendar day were averaged over the 10 years (1998-2007) to get the mean annual

cycle of precipitation. The resulting mean annual cycle was then smoothed 300 times with a 1-2-1 filter to obtain the smoothed mean annual cycle. According to Hartmann and Michelsen (1989), the 1-2-1 filter eliminates residual wiggles associated with imperfect sampling of the annual variation without smearing the true annual variation. From the smoothed mean annual cycle, precipitation anomalies were calculated for each year. Yokoi et al. (2007) pointed out that even if other definitions of smoothed mean annual cycle (such as the sum of the first three, four, or five harmonics) of the original mean annual cycles were used, the results do not change qualitatively. From the precipitation anomaly time series for each region, a 154-day period (from 15 May to 15 October) was extracted for each year. The 154-day period was chosen so that it includes 15 days before and after the core monsoon rainy season (1 June – 30 September) for most of the Asian regions. However, it should be noted that the climatological onset and withdrawal dates of the monsoon differ from place to place by more than one month (Yokoi et al. 2007) as discussed in Section 4.4. After elimination of linear trends, a Lanczos bandpass filter (Duchon 1979) with cutoff periods of 25-70 days and 10-25 days was applied to the 154-day precipitation anomaly data to retrieve the 30-60 day and 10-20 day periodicity components. The resulting data were used to calculate the Fourier spectrum for each year and then averaged over the 10 years to obtain an averaged spectrum for the 30-60 day and 10-20 day components separately. Averaged Fourier spectra for the five regions are depicted in Figure 4.33.

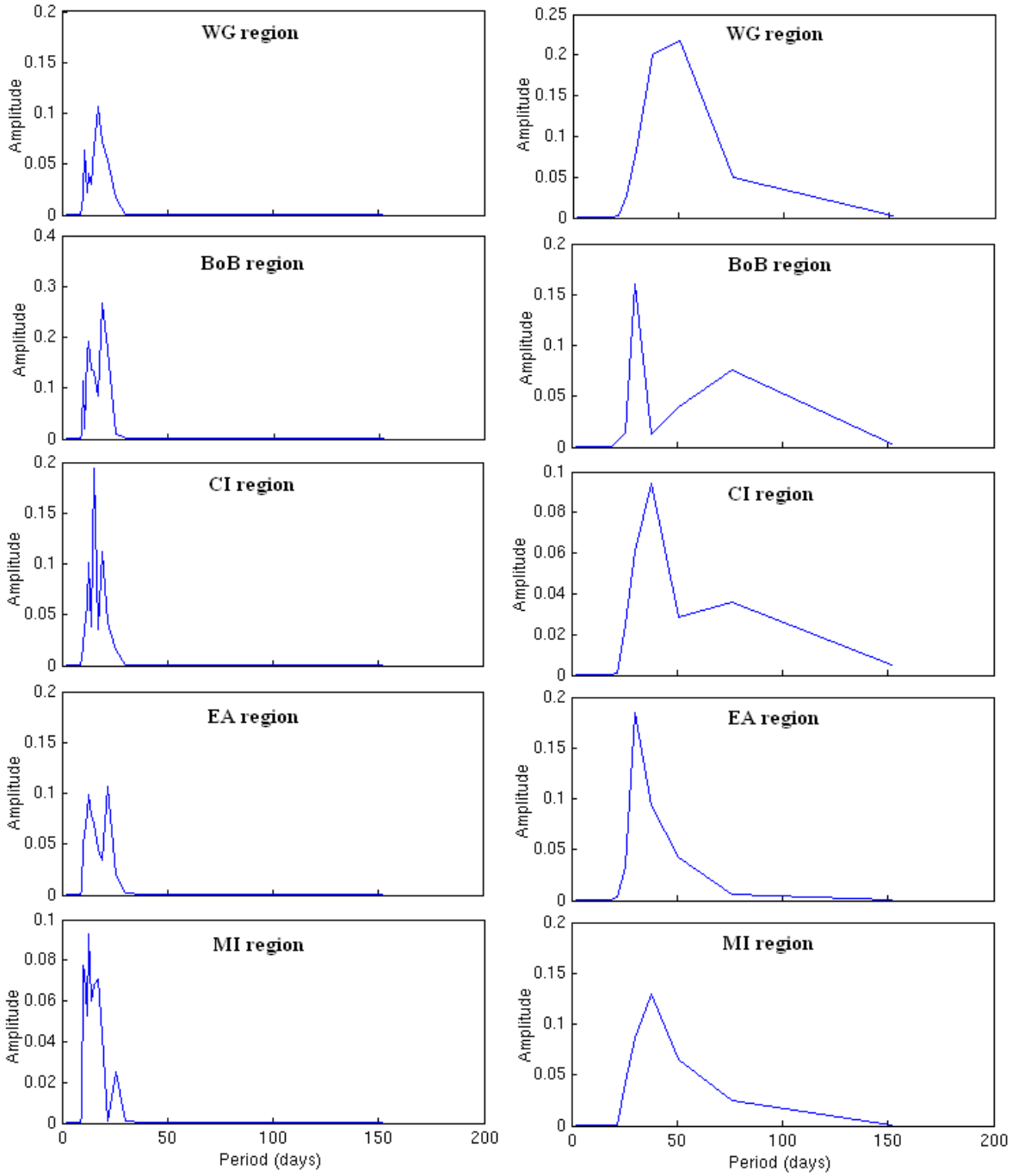

Figure 4.33: Mean Fourier spectra for Western Ghats, Bay of Bengal, Central India, East Asia and the Maldive Islands region based on 154 days (15 May to 15October) over the period 1998-2007. Left and right panel shows 10-20 day and 30-60 day periodicity components, respectively.

The Fourier spectra presented in Figure 4.33 reveal important intra-seasonal time scale periodicities (10-20 days and 30-60 day) in daily time series of monsoon rainfall for different regions of the Asia. For the WG, the average spectrum shows periodicities between 10-20 days and 30-60 days. Hoyos and Webster (2007) have also identified periodicities between 5-50 days for the same region. There is a spectral peak around 75

days, which is common to the BoB and CI region. Other periodicities for these two regions include 10-20 and 30-60 days. The EA region also indicates the existence of 10-20 day and 30-60 day periodicities. The average spectra shown in Figure 4.33 also clearly show periodicities in the range of 10-20 days and 30-60 days with the highest peaks around 13 and 38 days for the 10-20 and 30-60 period, respectively. The broad periods (10-20 and 30-60 day) that were depicted above have been related to the active and break cycles of monsoon rainfall over the Indian region (Kripalani et al. 2004). More specifically, the 10-20 day oscillation is a westward propagating mode closely related to the monsoon active and break conditions (Goswami 2005). The time series of rainfall shown in Figure 4.31 for 2002 and 2003 for different regions also clearly indicate existence of 10-20 day active and break periods in monsoon rainfall.

4.3 Maldives monsoon rainfall variability

As discussed above, the interannual variability of the Asian monsoon is one of the strongest signals of the Earth's climate variability (Wang and Fan 1999) and is due to the yearly deviation of seasonal transition from the mean annual cycle (Yang and Lau 2006). The most dominant mode of interannual variability of summer monsoon rainfall is associated with a dipole-like variation of precipitation between south Asia and southeast Asia. The interannual variability of the monsoon is influenced by slowly varying forcings such as SST, soil moisture, sea ice and snow cover (Krishnamurthy and Kinter 2003) and it can vary from location to location.

Past studies of the Asian summer monsoon mainly focused on the Indian region. In this section, interannual variability of the Maldives monsoon rainfall will be analysed using rainfall station data. This investigation is the first of its kind to look at monsoon rainfall variability across the Maldive islands, which stretch from about one degree south to seven degrees north (Figure 1.2). It was presented in Section 3.2.1 that annual rainfall varies spatially across the Maldive islands, with annual rainfall decreasing from south towards north. In order to analyse the monsoon rainfall for the Maldives, rainfall data were obtained from the five locations shown in Figure 3.1.

Past studies of interannual variability of the Asian summer monsoon mostly focused on the Northern Hemisphere summer period (June-July-August-September). According to Ding and Chan (2005) the durations of dry and wet seasons may be different for different parts of the Asian monsoon region, depending on their climate and the degree of influence of the Asian monsoon. McGregor and Nieuwolt (1998) also pointed out that, depending on

the location in the region, the rainy and dry seasons arrive at different times. Analysis of temporal rainfall variability for different parts of the Maldives indicates that during the months of May-November, the Maldives receives substantial amounts of rainfall (see Section 3.1.2 for monthly rainfall series), and it will be shown in Section 4.4.1 that the wet season extends from May to November for the Maldives region. Hence, to study interannual variability of the Maldives monsoon rainfall, only May-June-July-August-September-October-November (MJJASON) rainfall will be used for the following analysis. From the daily rainfall data, total monthly rainfall was computed for each month for each year and May-June-July-August-September-October-November (MJJASON) total rainfall was extracted for each year.

4.3.1 Interannual monsoon rainfall

The Maldives receives an average rainfall of 1492.2 mm during the monsoon season (May-November) and this varies largely in space and time. Spatial patterns of mean annual monsoon rainfall (May-November total) for the Maldives are shown in Figure 4.34. It can be seen that on average the northern and southern parts of the Maldives received less rainfall during the monsoon season (May-November), with two minima occurring at around 4.5° N and 0.7° S. Spatial distribution of mean annual monsoon rainfall indicates that rainfall maxima occur between central and southern parts of the Maldives during this season. On the other hand, spatial distribution of mean annual rainfall (January-December total) shows that rainfall increases from north to south (Figure 3.9a). The mean annual monsoon rainfall maxima located between central and southern Maldives (Figure 4.34) during this period may be related to the double crossing of Inter Tropical Convergence Zone (ITCZ) during the year.

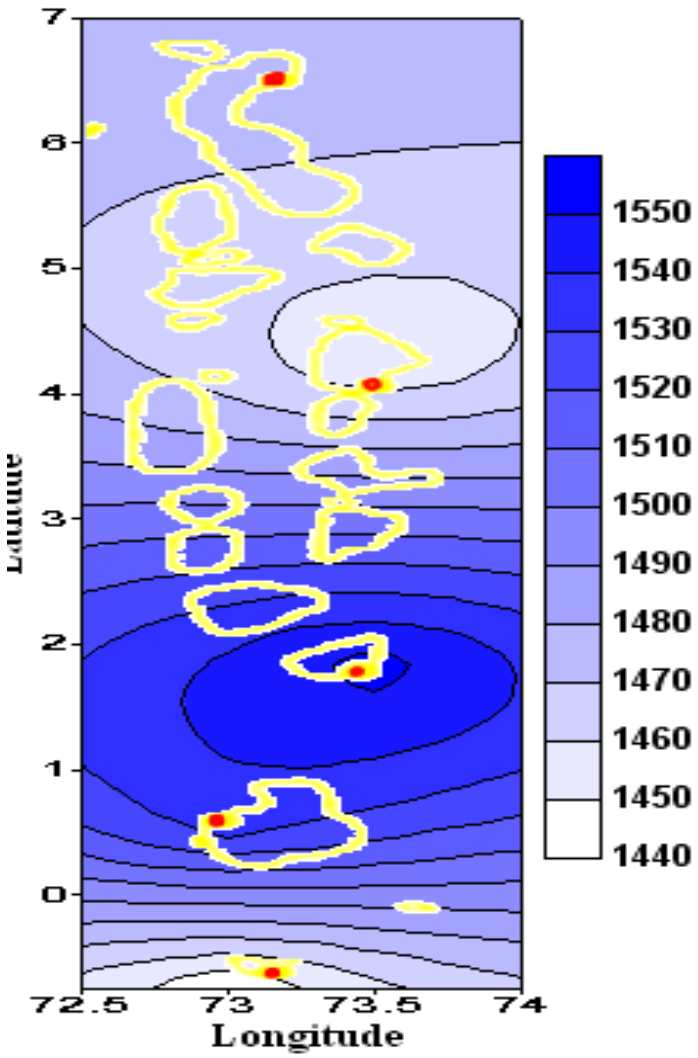

Figure 4.34: Spatial distribution of mean annual monsoon rainfall (May-November total) based on 1994-2006 data. The red dots indicate where the rainfall data were obtained.

The monsoon rainfall for the Maldives also varies from year to year. The Maldives monsoon rainfall varied from the lowest value of 1268.5 mm in 2001 to the highest value of 1838.8 mm in 1994, over the 13-year period (1994-2006). Figure 4.35 shows the interannual variability of monsoon rainfall, standardized by its own standard deviation (221.1). The normalized rainfall anomaly for the Maldives varied from -1.5 in 2001 to +1.8 in 1994. Spatial variability of total monsoon season rainfall for selected years (1994, 2000 and 2006) is presented in Figure 4.36 to show interannual variability of monsoon rainfall across the Maldives. The three years (1994, 2000 and 2006) presented in Figure 4.36 correspond to the beginning, middle and end of the data period, respectively. The three years show quite different spatial variability across the Maldives. In 1994, the annual monsoon rainfall is quite high throughout the Maldives, compared to the year 2000 and

2006. In 2000, central parts of the Maldives received less rainfall compared to other areas of the Maldives during the monsoon season. On the other hand, the year 2006 shows maximum rainfall in central parts of the Maldives during the monsoon period.

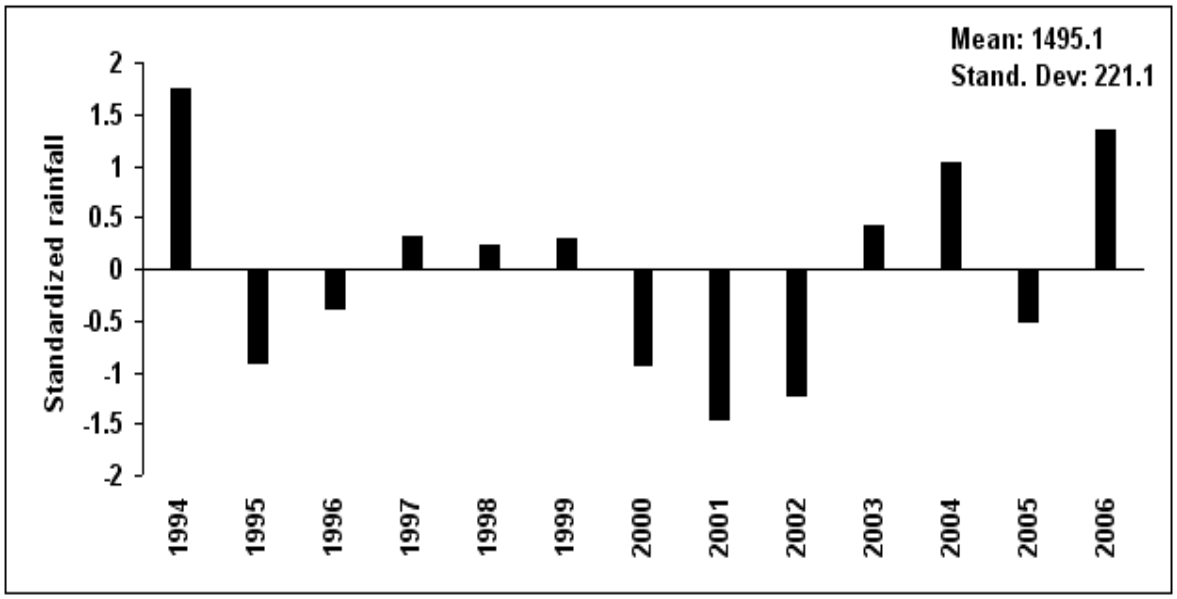

Figure 4.35: Interannual variations (standardized by the standard deviation) of the Maldives monsoon rainfall (May-November), based on 13 years (1992-2006) of rainfall data averaged over five stations.

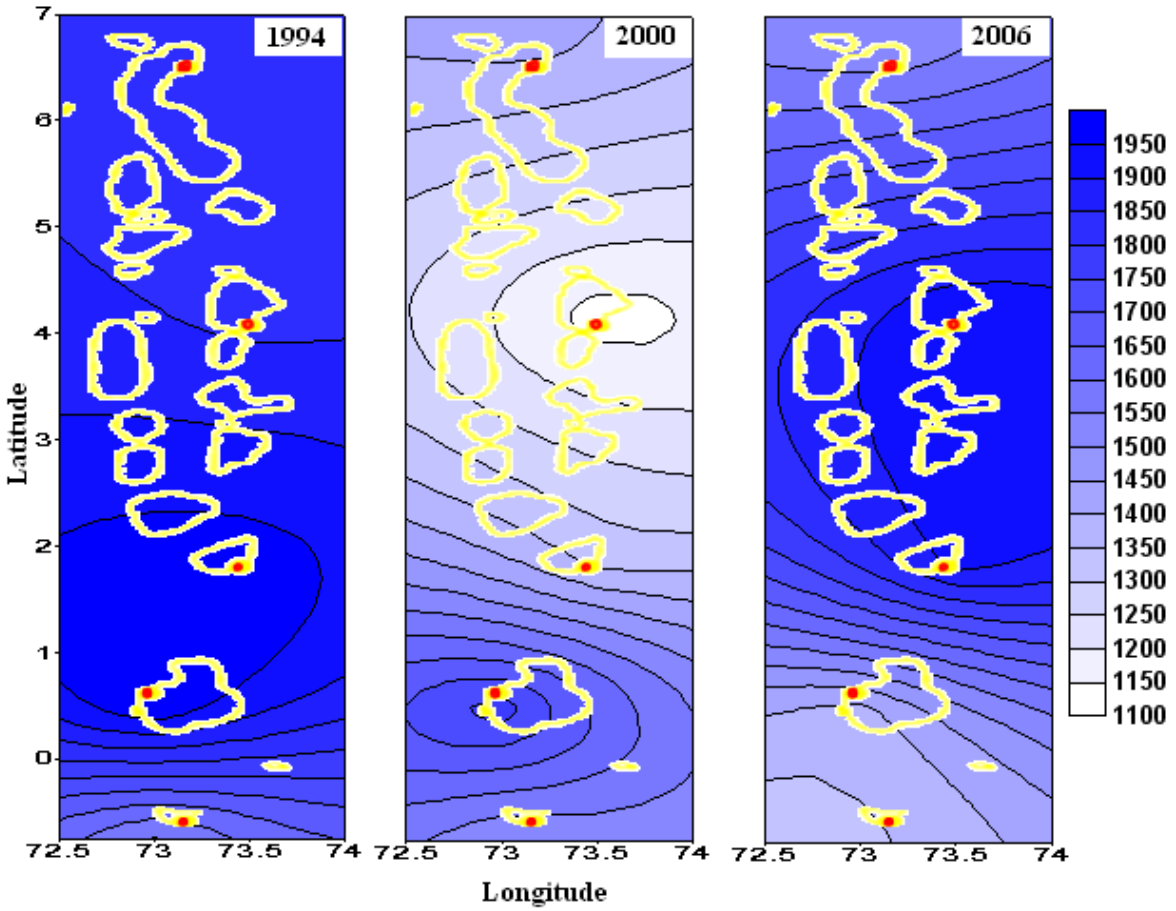

Figure 4.36: Spatial distribution of annual monsoon rainfall (May-November total) for 1994, 2000 and 2006. The red dots indicate where the rainfall data were obtained. The contours are in mm.

As mentioned before, a major proportion of the annual rainfall over most of the Asian region occurs during the summer monsoon season (June to September) (Kripalani and Kulkarni 2001) and significantly affects annual gross national product (Yang and Lau 2006). According to Mooley and Parthasarathy (1984) the Indian subcontinent receives about 78% of its rainfall during the summer monsoon season. In addition to this, Kumar and Prasad (1997) suggested that the meteorological subdivisions in the Indian subcontinent receive about 60% to 90% of annual rainfall during the summer monsoon season. As pointed out above, a major proportion of the annual rainfall over the Maldives occurs during the monsoon season (May-November). Here an attempt has been made to examine the contribution of the Maldives monsoon annual rainfall (May-November total) to the annual (January-December total) rainfall. Figure 4.37 shows the interannual variability of Maldives monsoon rainfall (together with linear trend: blue line) and percentage contributions to annual rainfall (red line) from monsoon rainfall (May-November) for the northern, central and southern parts of the Maldives.

It is clear from Figure 4.37 that monsoon rainfall varies from year to year and the percentage contribution (red line) to yearly total rainfall from May-November total rainfall also varies from year to year. On average, the northern part of the Maldives receives about 85.0 % of its annual rainfall from monsoon rainfall. The southern parts of the Maldives receive the least, with an average percentage contribution of 62.7% to yearly total rainfall derived from monsoon season rainfall. The central part of the Maldives receives about 71.9 % of its annual total rainfall from monsoon rainfall.

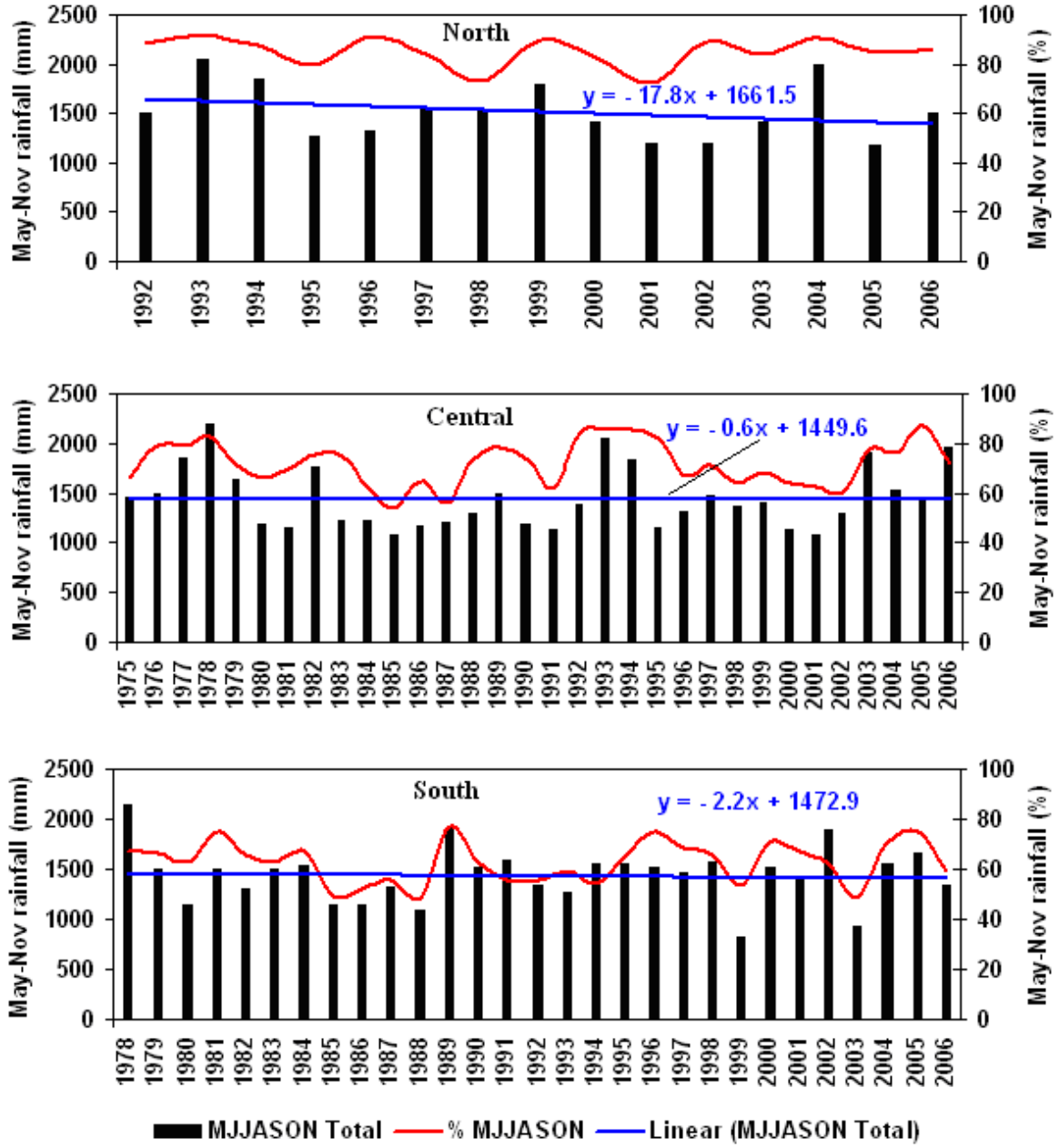

Figure 4.37: Interannual variability of monsoon rainfall (May-November: MJJASON) (bars) and percentage contribution (red line) to yearly total rainfall for northern, central and southern parts of the Maldives.

4.3.2 Interannual periodicities of Maldives monsoon rainfall

There has been a number of attempts to study rainfall periodicities in other parts of the Asian region, especially the Indian monsoon region. Mooley and Parthasarathy (1984) analysed all-India summer monsoon (June to September) rainfall for the period 1871 to 1978 to understand the interannual and long-term variability of the monsoon. On the other hand, Naidu et al. (1999) have analysed periodicities of annual rainfall for 29 sub-divisions of India and all-India (area-weighted average of the sub-divisions) by using the rainfall series for a period of 124 years (1871–1994), and identified periods in the range of 2–2.5 years, 3-8 years and 8-12 years. Preliminary analysis of annual (January-December) total rainfall for the northern, central and southern parts of the Maldives also indicates existence of 2.2-5.2 year cycles and a 13 year periodicity (south: Figure 4.38)

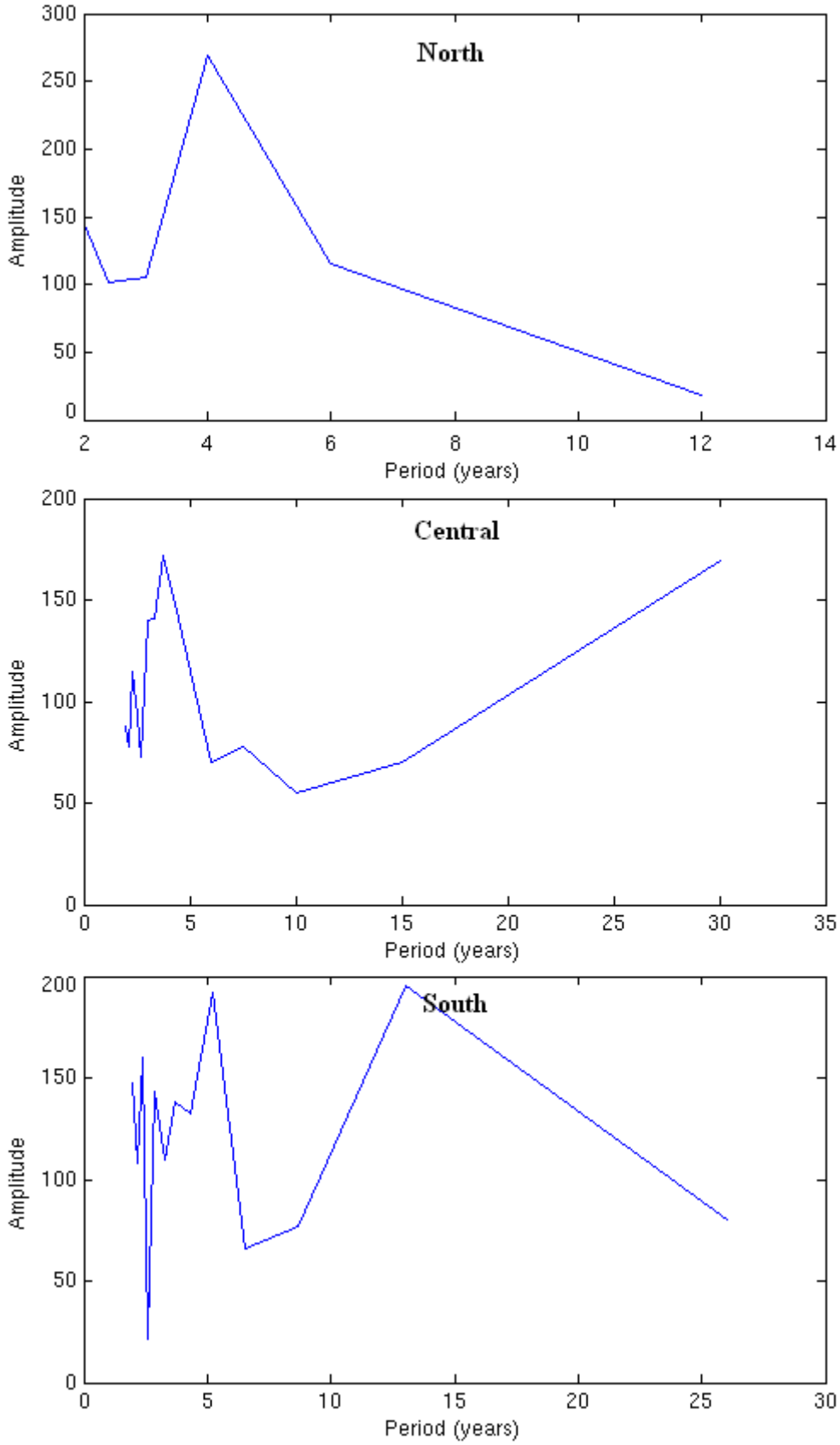

Figure 4.38: Fourier transform spectra of yearly total rainfall for northern, central and southern regions of the Maldives based on 15 years (1992-2006), 29 years (1978 to 2006) and 32 years (1975 to 2006), respectively.

To study interannual periodicities of monsoon rainfall (May-November) for different regions of the Maldives (northern, central and southern), spectral analysis was performed using a Fast Fourier Transform. May-November (214 days) daily rainfall totals for each year were extracted for each region to obtain monsoon season annual rainfall. The resulting time series for each region was subjected to de-trending in order to eliminate any trend that may exist in the rainfall data series. Periodicities of annual monsoon rainfall series were obtained by performing Fourier Transform spectral analysis on the de-trended annual monsoon rainfall series for the northern, central and southern regions separately. The results of the Fourier Transform spectral analysis are shown in Figure 4.39 and Figure 4.40. The periodicities shown in Figure 4.39 were based on 15 years (1992-2006) of rainfall data. The power spectra indicate that predominant periodicities exist in the Maldives annual monsoon rainfall with periods ranging from 2.5-4 years (Figure 4.39). The northern and southern parts of the Maldives show only one periodicity at around 4 and 3 years (Figure 4.39), respectively, while the central parts of the Maldives show two dominant periods – one at 2 years and a second at 4 years (Figure 4.39). Similar to the quasi-biennial oscillation (QBO) which was discovered by Kumar (1997) in the rainfall series over homogeneous regions of India, the 2-3 year periodicity in the Maldives annual monsoon rainfall may also be attributed to the QBO.

The periodicities shown in Figure 4.40 were based on 29 years (Figure 4.40a and b: from 1978-2006) and 32 years (Figure 4.40c: from 1975-2006) of rainfall data from the southern and central parts of the Maldives. When 29 years of data were used, the significant interannual periodicities emerging from power spectra are in the range of 2.2-5.2 years (Figure 4.40 a and b). On the other hand, 32 years of data indicate longer period variations, ranging from 3.7-7.5 years (Figure 4.40 c). The periodicity in the 3.7-7.5 year range may be attributed to the El Niño Southern Oscillation (ENSO) (Mooley and Parthasarathy 1984; Naidu et al. 1999)

The periodicities shown here for the Maldives annual monsoon rainfall are similar to those discovered for Indian summer monsoon rainfall. Mooley and Parthasarathy (1984) have identified a periodicity of 2.8 years in the all-India summer monsoon rainfall series. Furthermore, Munot and Kothawale (2000) showed 3-5 year cycles for northeast India and peninsula India and suggested that the 3-5 year periodicity may be related to ENSO.

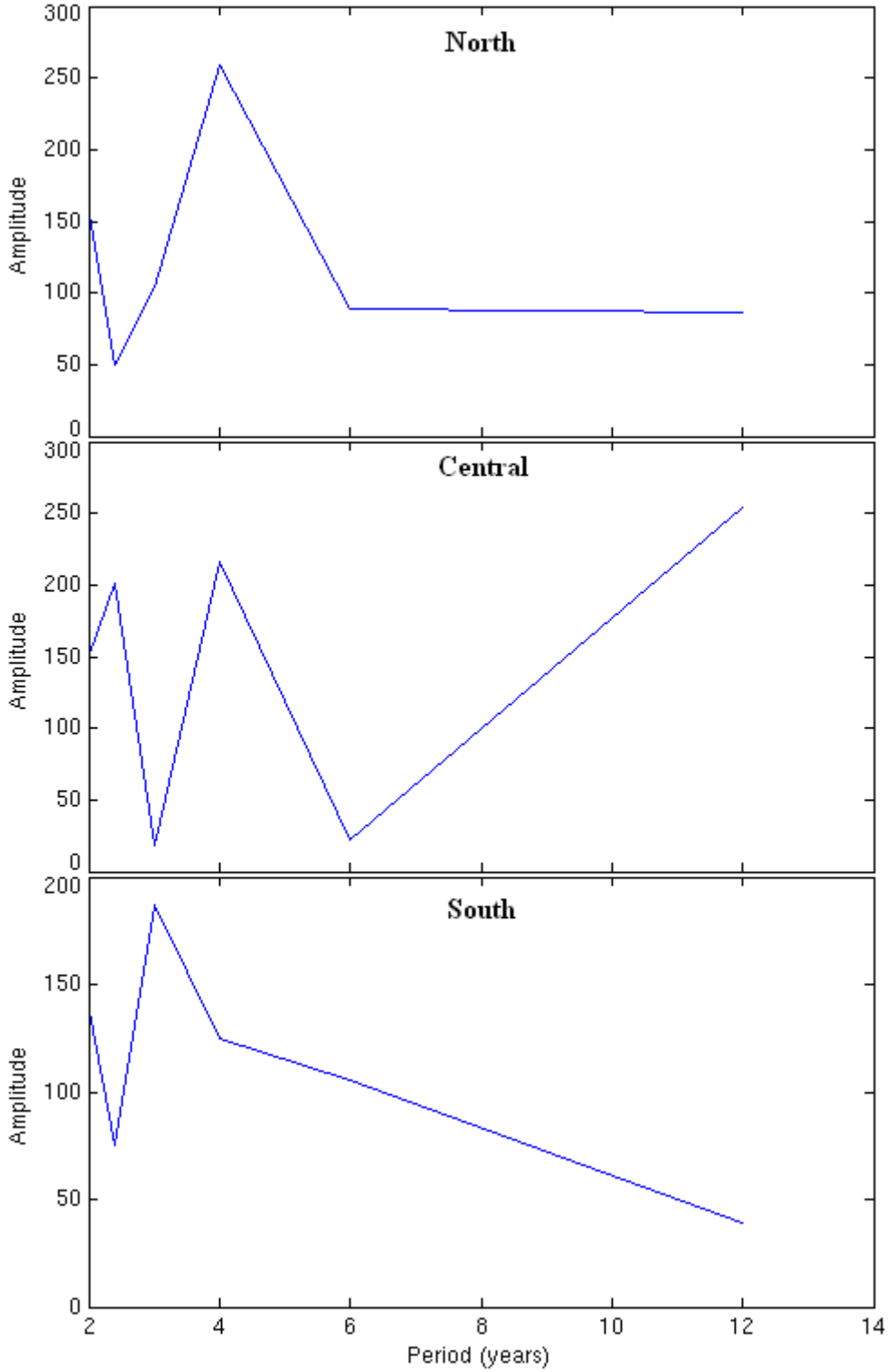

Figure 4.39: Fourier transform spectra of monsoon season (May to November) total rainfall for northern, central and southern parts of Maldives, based on 15 years (1992 to 2006) of data.

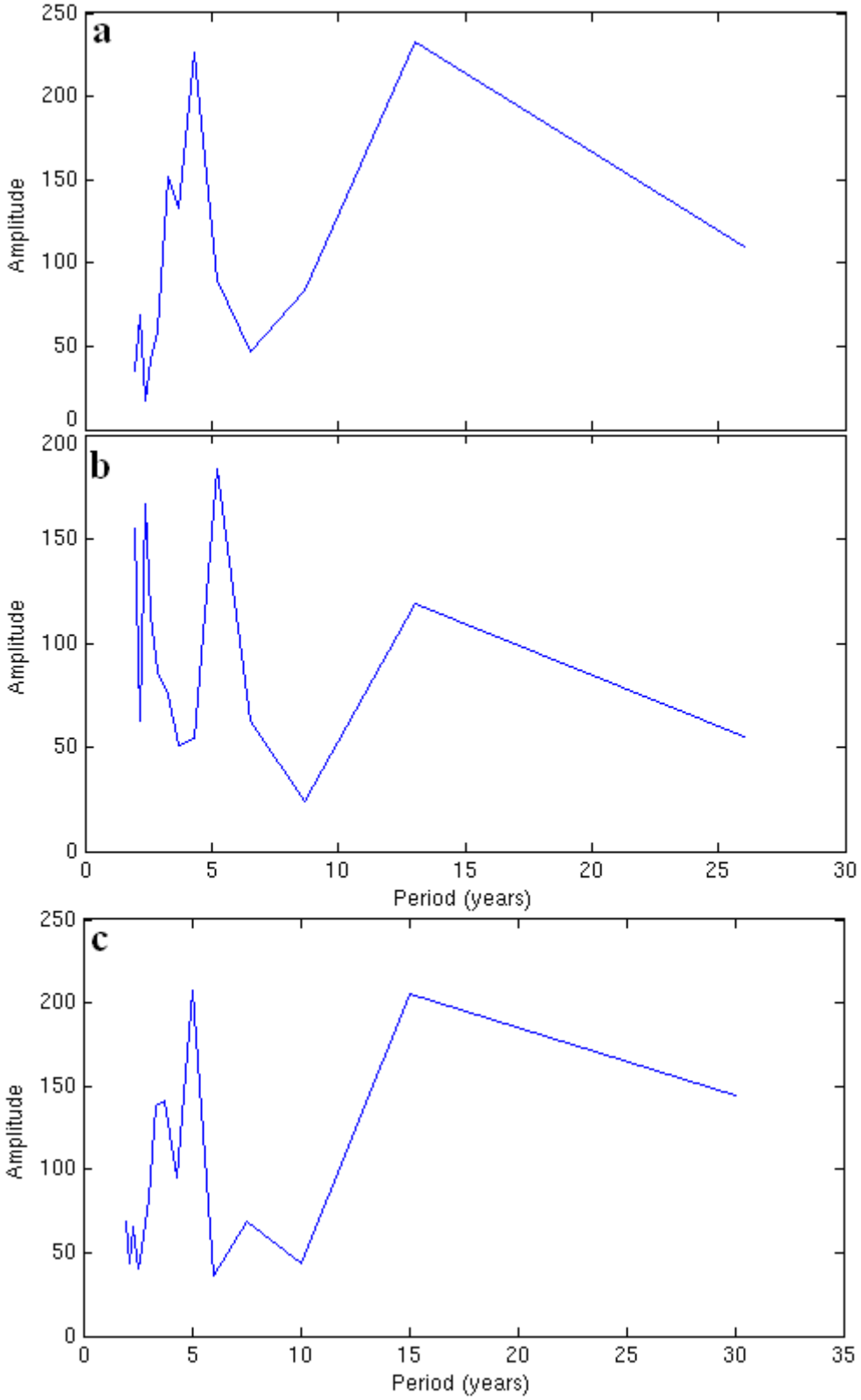

Figure 4.40: Fourier transform spectra of monsoon season (May to November) total rainfall based on 29 years (1978 to 2006) of data: (a) central , (b) southern and (c) same as (a) but based on 32 years (1975 to 2006).

4.4 Onset and withdrawal characteristics of the monsoon over the Maldives

The Asian monsoon is an annual event, and the onset of summer monsoon rain is one of the most important sub-seasonal phenomena within the monsoon annual cycle, as it characterises the abrupt transition from the dry season to the rainy season (Ding and Chan 2005; Mao and Wu 2007; Webster et al. 1998);(Zeng and Lu 2004). For example, the onset of the Indian summer monsoon (ISM) marks the beginning of the rainy season over the Indian sub-continent (Chakraborty et al. 2006). Mao and Wu (2007) pointed out that the timing of onset (late or early) of the monsoon may have devastating effects on the agricultural community even if the mean annual rainfall is normal, as crops are planted relative to the anticipated onset of the rainy season (Liebmann et al. 2007). Identification or forecasting of the timing of onset is critical as it determines ploughing and planting times for the agricultural communities in the monsoon regions (Webster et al. 1998). As Fasullo and Webster (2003) pointed out, an objective definition of the monsoon season depends on objective definition of the monsoon onset (first onset date) and withdrawal (last withdrawal date) of the southwest monsoon.

Conventionally, the monsoon season (southwest monsoon) for the Maldives has been considered as the May to November period. The official normal monsoon onset date for the Maldives has been considered to be 17 May (Ramiz 2007). However, this is arbitrary and exact prescription of the monsoon season has been lacking for the Maldives region. Xavier et al. (2007) pointed out that the onset and withdrawal dates determine the length of the rainy season, which in turn is related to the interannual variability (IAV) of the monsoon. A better understanding of the variability of onset and withdrawal dates should lead to a better understanding of the IAV of the monsoon. The aim of this section is to define monsoon onset and withdrawal criteria and to determine monsoon onset and withdrawal dates (hence to define the length of the monsoon or rainy season, objectively) for the Maldives. This analysis is the first of its kind in the context of the Maldives. Objective determination of onset and withdrawal dates of the southwest monsoon will be beneficial for agriculture and for the management of floods and water resources of the country.

According to Ding and Chan (2005), it is difficult to obtain a unified and consistent picture of the climatological onset dates of the Asian summer monsoon in different regions due to differences in data, monsoon indices and definitions of monsoon onset used in

different studies. The south Asian summer monsoon average onset dates are shown in Figure 4.41.

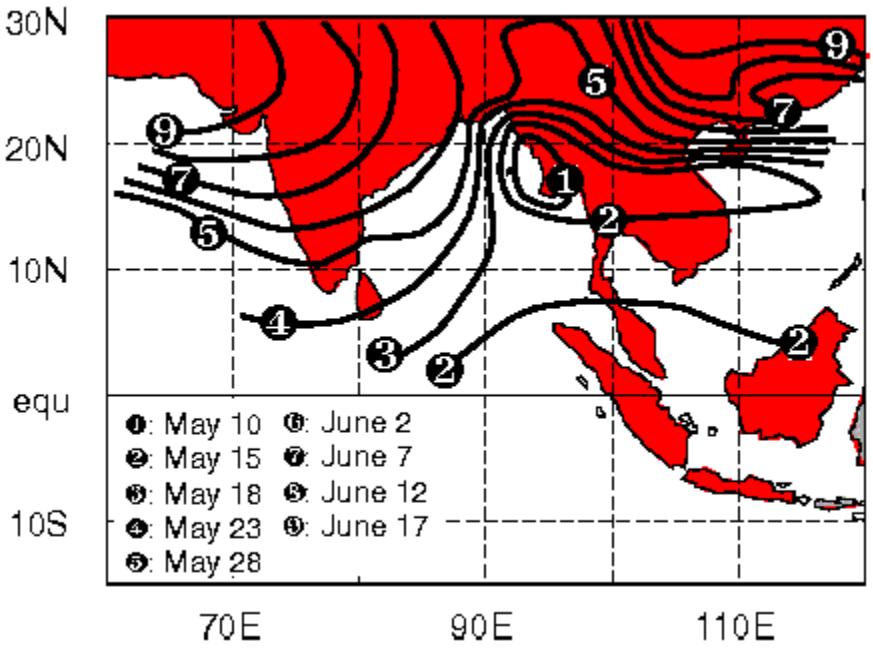

Figure 4.41: Climatological onset dates for the south Asian summer monsoon region. Taken from from Webster et al. (1998).

It has been suggested that the rainy season generally lasts longer (from late April to November) towards the equator. Large scale onset dates for the Asian monsoon region are shown in Figure 4.42. Over the Asian monsoon regions, the earliest onset of the rainy season is found in late April (over the Bay of Bengal region) and it runs through to November (over the southern Bay of Bengal) (Mao and Wu 2007; Qi et al. 2008; Wang and LinHo 2002).

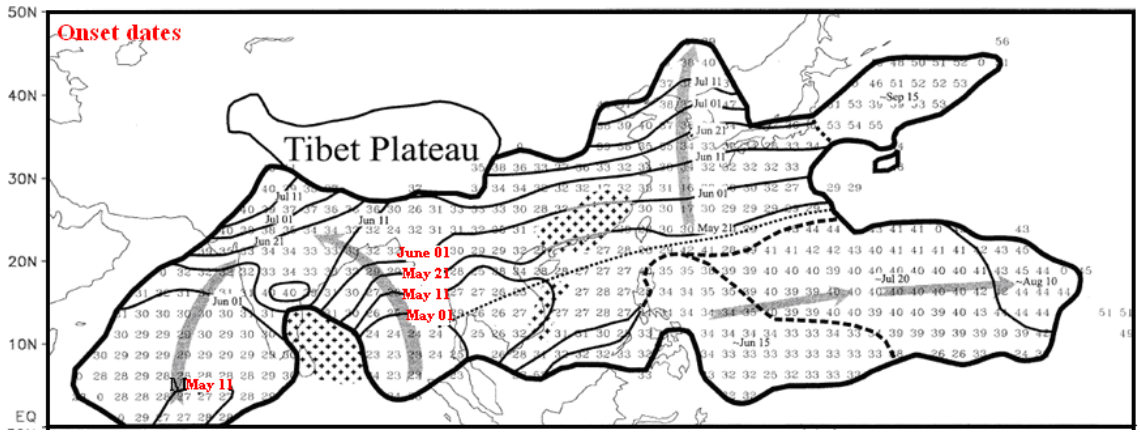

Figure 4.42: Large scale onset patterns for the Asian monsoon region. The thick dashed lines denote discontinuities. The arrows indicate the directions of rain-belt propagation. Adapted from Wang and LinHo (2002).

The onset of the summer monsoon is generally concurrent with a reversal or major change in the wind field, an abrupt rise in precipitation and water vapour (Zeng and Lu 2004). Characteristics of the monsoon, such as onset, retreat and geographical extent, have been studied extensively for a long time (e.g., Ramage 1971). Zeng and Lu (2004) proposed criteria to define globally unified summer monsoon onset (or retreat) dates using a single meteorological variable (i.e., the global daily 1° × 1° normalized precipitable water data). Various methods have been proposed to determine monsoon onset date over different monsoon regions (Fasullo and Webster 2003; Hendon and Liebmann 1990) (Marengo et al. 2001). Different criteria have also been defined for different parts of the same monsoon regions (Higgins et al. 1999; Minoura et al. 2003).

Methods that identify the monsoon's withdrawal date are few, while different parts of the Asian monsoon have defined onset dates using different methods. Some studies have used local rainfall or convective activity using satellite-observed data (Fasullo and Webster 2003; Lau and Yang 1997; Wang and LinHo 2002). On the other hand, the criteria used by others include change of prevailing winds or a combination of wind and convection (Zhang et al. 2002). Zhang et al. (2000) defined onset date over the Indochina Peninsula as the day on which the 5-day running mean rainfall index satisfies the following criteria:

1. Total daily rainfall exceeds 5 mm/day and persists continuously for 5 days;
2. Within 20 consecutive days, the number of the days with rainfall greater than 5 mm/day exceeds 10 days.

The onset of the Indian summer monsoon first occurs over Kerala (southern tip of the peninsula) and marks the beginning of the rainy season for the Indian subcontinent. The two principal methods that identify onset date over the Indian region include the objective method developed by Ananthakrishnan and Soman (1991) and the more subjective declarations of onset by the Indian Meteorological Department (IMD) (Fasullo and Webster 2003; Goswami and Gouda 2007). On an operational basis, the onset of the monsoon over Kerala is based on rainfall over Kerala. If any five stations out of seven selected stations (Colombo, Minicoy, Thiruvananthapurm, Alapuzha, Cochi, Kozhikode, Mangalore) receive 1 mm of rainfall (within a 24 hour period) for two consecutive days after 10 May, the onset of monsoon over Kerala is declared on the second day, provided that the lower tropospheric westerly wind over Kerala is strong and deep and the relative humidity of the air is high from the surface to at least 500 hPa.

According to Syroka and Toumi (2004), the mean characteristics of the Indian summer monsoon (ISM) withdrawal are mentioned in the literature. However, the only guidelines that exist for defining the withdrawal date of the ISM are the working rules of the India Meteorological Department (IMD). The IMD classifies the recession of the monsoon with reference to the sharp change in rainfall totals over the regional meteorological subdivisions. However, it is known that, in terms of rainfall, the onset is better defined than the withdrawal, especially over southern India (Syroka and Toumi 2004). Syroka and Toumi (2004) defined the withdrawal of the ISM from northern and central India based on a daily circulation index that includes the difference in average 850 hPa zonal winds between a southern region (5° N–15° N, 50° E–80° E) and a northern region (20° N–30° N, 60° E–90° E). The withdrawal dates of the monsoon from northern and central India are defined as the first of seven consecutive days for which the circulation index becomes negative.

Ahmed and Karmakar (1993) proposed criteria based on daily rainfall amount and daily prevailing wind (direction and speed) to determine the onset and withdrawal date of the summer monsoon over Bangladesh. They have identified onset dates of the summer monsoon in Bangladesh from 1958 to 1987 for 19 stations. The arrival date of the summer monsoon in Bangladesh was taken as the first day of three or more consecutive days of rainfall, with daily rainfall of 5 mm or more, accompanied by southerly or southeasterly winds. The withdrawal date of the southwest monsoon in Bangladesh was identified as the last day of the last period of three or more consecutive days of rain, after which the wind

direction changed from southerly or south-easterly to north-westerly or northerly (Ahmed and Karmakar 1993).

4.4.1 Monsoon onset and withdrawal criteria for the Maldives

As pointed out above, over the Asian monsoon regions the rainy season runs from late April through to November or even December (Wang and LinHo 2002; Zhang and Wanga 2008), the rainy season for the Maldives generally falls into this period. Due to large latitudinal extent and monsoon rainfall variability of the Maldives, onset and withdrawal dates of monsoon for the north, central and southern Maldives were determined separately for three regions, following a similar approach to that used by Ahmed and Karmakar (1993).

Before defining the criteria, preliminary analysis was carried out using daily total rainfall and the wind vector (both speed and direction) between 18 April (one month before the official date of monsoon onset: 17 May) and 31 December. Preliminary analysis indicated that the southern part of the Maldives is dominated by southwesterly to northwesterly winds and maintains high wind speeds in April, and occurrence of rain becomes more frequent from late April onwards, indicating the beginning of the southwest monsoon for the southern parts of the Maldives. Average wind speed and direction for the southern parts is shown in Figure 4.43. On the other hand, analysis indicated that in November the prevailing wind direction in northern parts of the Maldives changes from southwesterly or northwesterly to a variable or northeasterly direction and occurrence of rain become less frequent in late November, indicating cessation of the southwest monsoon from the northern parts of the Maldives.

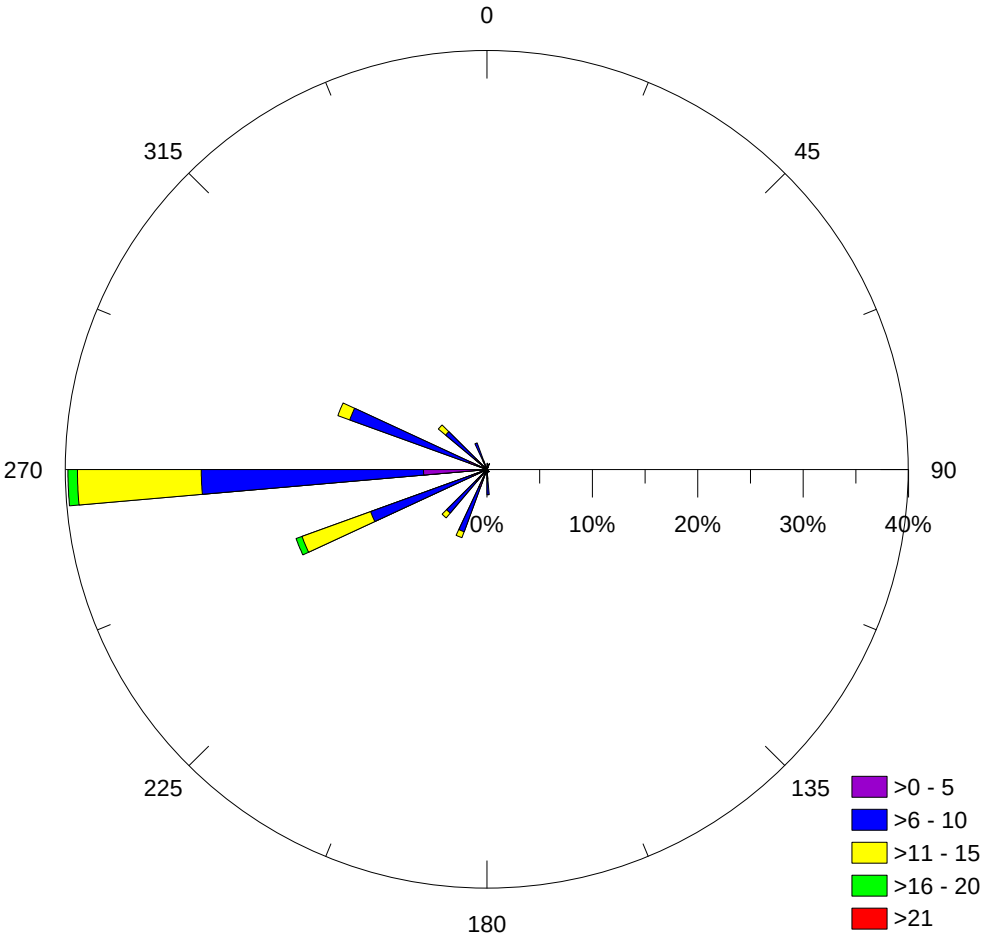

Figure 4.43: Average wind speed (knots) and direction (1992-2006) for the southern parts of the Maldives for the month of April, based on Gan data.

Due to lack of long term observational data for different meteorological parameters over the Maldives, monsoon onset and withdrawal criteria are defined following Ahmed and Karmakar (1993). For the individual years, the first day when the following conditions were met between 18 April and 15 June was considered as the onset date of the southwest monsoon over that region for that particular year.

1. **Three or more consecutive days of wet weather (more than 1 mm of rainfall on each day)**
2. **Daily wind speed equals or exceeds long term mean wind speed (for the period between 18 April and 15 June for that particular region) for at least 3 consecutive days**
3. **Accompanied by southwesterly to northwesterly wind for at least 3 consecutive days**

On the other hand, withdrawal dates of the southwest monsoon or cessation of the rainy period over the Maldives were taken as the first day when the following conditions were met between 1 November and 31 December for the region and year.

1. **Three or more consecutive days of dry spells (rainfall less than 1 mm of rainfall on each day)**
2. **Wind speed is less than long term mean wind speed (for the period between 1 November and 31 December for that particular region) for at least 3 consecutive days**
3. **Accompanied by northwesterly to northeasterly or variable wind for at least 3 consecutive days**

To define the first criterion for the onset and withdrawal (three or more consecutive days of wet/dry period, respectively), different threshold values (2.5, 2 and 1.5 mm/day) for rainfall were tried initially for each region. Higgins et al. (1999) pointed out that it is necessary to use different threshold criteria to define monsoon onset for three regions of the United States and Mexico (Arizona–New Mexico, northwest Mexico, and southwest Mexico) because rainfall amounts in each of these regions are different. However, initial analysis of total daily rainfall for the north, central and southern parts of the Maldives indicated that different threshold values of rainfall give inconsistent onset and withdrawal dates. Hence, a final threshold value of 1 mm/day (over three consecutive days) was used for all three regions. Figure 4.44 shows the cumulative frequency of daily rainfall from 1992 to 2006 for the north, central and southern Maldives for the onset phase of the monsoon. As can be seen from the figure, daily rainfall begins to pick up first for the southern Maldives and subsequently the central and northern Maldives. Furthermore, Figure 4.45 shows the cumulative frequency of total rainfall from 1992 to 2006 for the north, central and southern Maldives for the withdrawal phase of the monsoon. The long-term wind speed between 18 April and 15 June and 1 November to 31 December were determined for the north, central and southern Maldives to define the second criteria for onset and withdrawal, respectively. The long term wind speeds between 18 April and 15 June for the north, central and southern Maldives were found to be 4.6, 5.3 and 4.2 m/s respectively. Furthermore, the long term wind speeds between 1 November and 31 December for the north, central and southern Maldives were found to be 2.9, 4.9 and 3.8 m/s, respectively. By assuming that the monsoon arrives first in southern parts, in order to determine onset dates, the variables (rainfall, wind vector) were analyzed for the southern

part first and then subsequently for central and northern parts of the Maldives. On the other hand, by assuming that the withdrawal begins from the north, in order to determine withdrawal dates, the data were analyzed first for the northern part and subsequently the central and south of the region.

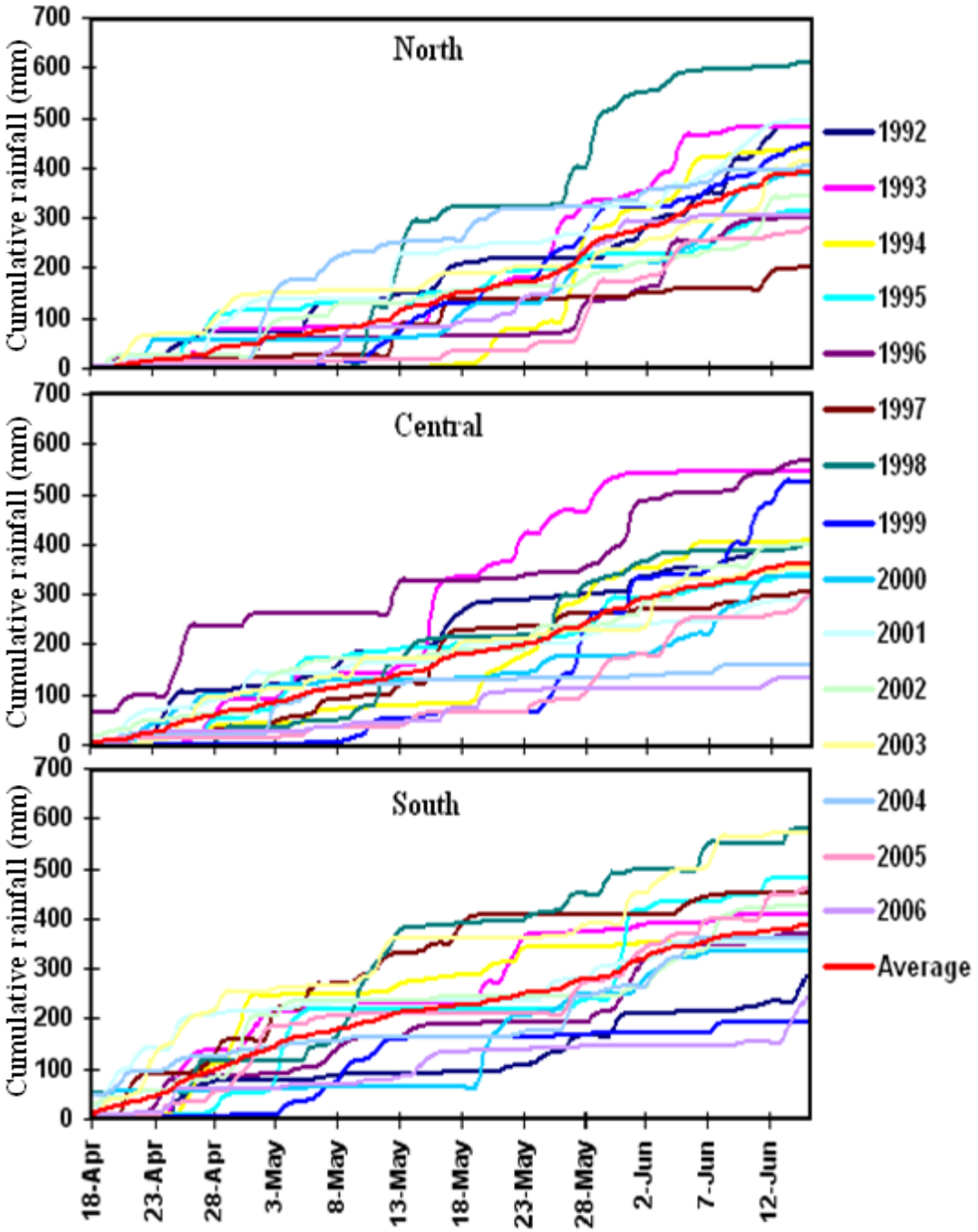

Figure 4.44: Cumulative daily total rainfall for the onset phase of the monsoon from 1992 to 2006 for the north, central and southern parts of the Maldives.

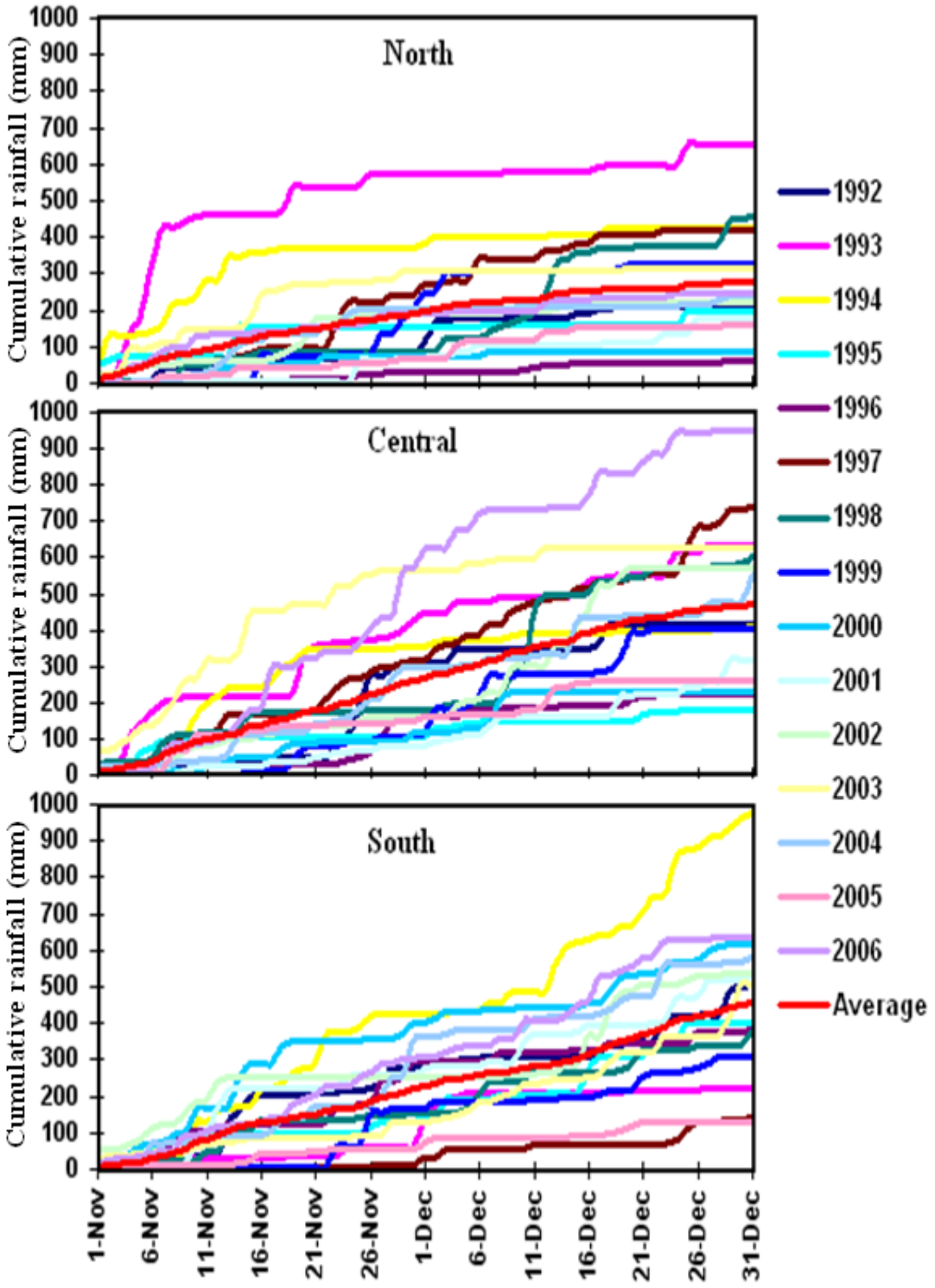

Figure 4.45: Cumulative daily total rainfall for the withdrawal phase of the monsoon from 1992 to 2006 for the north, central and southern parts of the Maldives.

According to the above definition, the monsoon onset and withdrawal dates for each individual year were determined objectively for north, central and southern parts of the Maldives for the period 1992 through to 2006 and are presented in Table 4.6 and, Table 4.7 respectively. In some years the onset and withdrawal episodes were characterized by the

absence of the three consecutive days of rain, and wind (speed and direction) criteria defined above.

Table 4.6: Monsoon onset dates for the Maldives from 1992 to 2006. The * indicates the years where three criterions were not met and where S.D. = Standard deviation.

Monsoon Onset dates for the Maldives			
Years	**Southern**	**Central**	**Northern**
1992	23 April	08 May	16 May
1993	24 April	20 May	24 May
1994	19 May	23 May	24 May
1995	28 April	04 May	13 May
1996	*	28 May	01 June
1997	06 May	16 May	*
1998	08 May	13 May	25 May
1999	04 May	09 May	10 May
2000	18 April	03 June	17 May
2001	21 April	29 April	28 April
2002	05 June	*	13 May
2003	09 May	*	14 May
2004	30 April	03 May	07 May
2005	02 May	28 May	28 May
2006	*	*	23 May
Mean	**04 May**	**15 May**	**17 May**
S.D.(days)	**13**	**11**	**9**

Clarke et al. (2000) pointed out that the timing of the onset date of the summer rainfall in a particular location can vary considerably from year to year. This is true for the Maldives, as can be seen from Table 4.6 the monsoon onset dates differ from one year to another for the same region and for different regions of the Maldives. The earliest and latest onset date was for the southern Maldives: 18 April (2000) and 5 June (2002), respectively. For the central Maldives, the earliest and latest onset dates were 25 April (2003) and 3 June (2000), while the earliest and latest onset dates for the north were 28 April (2001) and 1 June (1996), respectively (Table 4.6). The mean onset dates for the southern, central and northern Maldives are 4, 15 and 17 May with standard deviations of 13, 11 and 9 days, respectively (Table 4.6). It is interesting to note that the mean onset date for the northern Maldives coincides with the official onset date (17 May).

During the 15 year period (1992-2006), the onset for the southern parts occurred about 46.6, 46.6 and 6.6 % of the time in April, May and June, respectively. Furthermore, during the same period for the central and northern parts of the Maldives, about 6.6, 86.6 and 6.6 % of the time the onset occurred in April, May and June, respectively. This

suggests that the onset of the monsoon rain is first established for the southern parts of the Maldives (in late April or early May) and progressively moves northwards, establishing the monsoon for the whole of the Maldives in May. The rain then migrates further northward rapidly, reaching the southern parts of the Indian subcontinent by late May, establishing the monsoon in Kerala, the southern tip of India, around 1 June (Wang and LinHo 2002). Fasullo and Webster (2003) suggested that the northward progression of the monsoon onset is symptomatic of a large scale transition of deep convection from the equatorial to continental regions. Figure 4.46 shows climatological advancement of the Asian monsoon onset and pentad averaged precipitation rates (mm/day) from 1 May to 10 June. The black dots shown in the figure denote the location of the onset of the monsoon. The onset dates shown in Table 4.6 agree with the onset pattern shown in Figure 4.46.

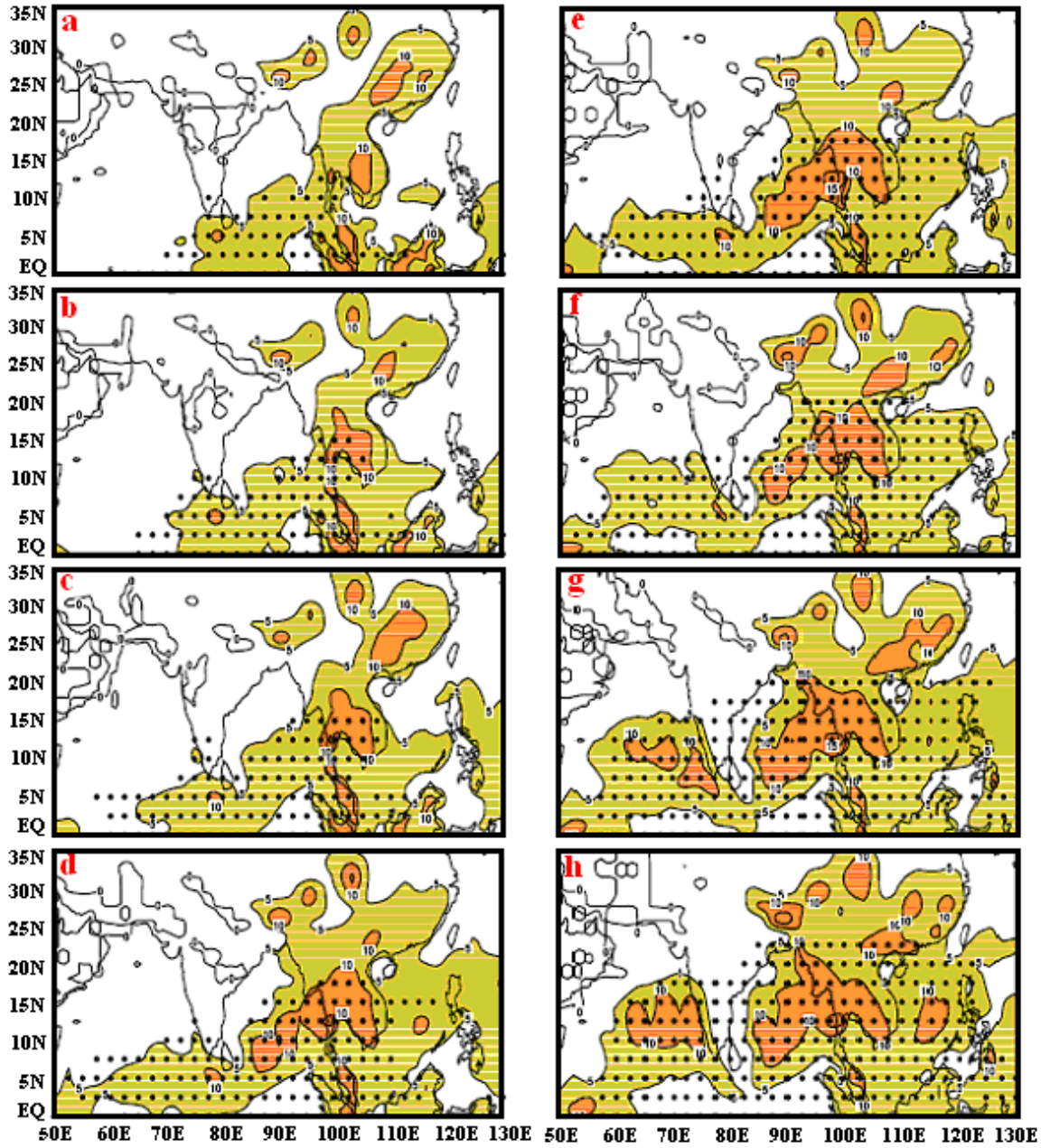

Figure 4.46: Climatological advance of the Asian summer monsoon onset (denoted by dots) and pentad averaged precipitation rates (mm/day) for : (a) 1-5 May, (b) 6-10 May, (c) 11-15 May, (d) 16-20 May, (e) 21-25 May, (f) 26-30 May, (g) 1-5 June to 6-10 June. Light and dark shading indicate regions where precipitation rate is > 5mm/day and 10 mm/day, respectively. Adapted from Zhang et al. (2004b).

The interannual variability of monsoon onset dates for northern, central and southern Maldives from 1992 to 2006 based on official monsoon onset date (17 May) is shown in Figure 4.47, while Figure 4.48 shows interannual variability of onset dates of the summer monsoon for the southern tip (Kerala) of India from 1947 to 1998. Furthermore, interannual variability of onset dates of the summer monsoon over Indochina from 1951 to

1996 is shown in Figure 4.49. The earliest and most delayed onset dates of the summer monsoon over India during the 1947 to 1998 period were 17 May (1962) and 18 June (1972), respectively (Raju et al. 2005). However, according to Fasullo and Webster (2003), the earliest and most delayed onset dates of the summer monsoon over the Indian region during the years between 1948-2000 were 19 May (1990) and 20 June (1997) respectively. The earliest and latest onset years for the Indochina region were 1988 (13 April) and 1958 (4 June), respectively, based on a mean date of 9 May (Figure 4.49). From these figures, it is clear that the onset dates can differ remarkably from one year to another and from one location to another (Clarke et al. 2000; Zhang et al. 2002). Xavier et al. (2007) stated that the earliest and latest onset for the Indian region differs by 46 days. For the Maldives, earliest and latest onset date of the monsoon differs by 49 days. The monsoon onset dates are more variable for the southern Maldives with a coefficient of variation of 76%, while the onset dates are least variable for the northern Maldives with a coefficient of variation of 29%.

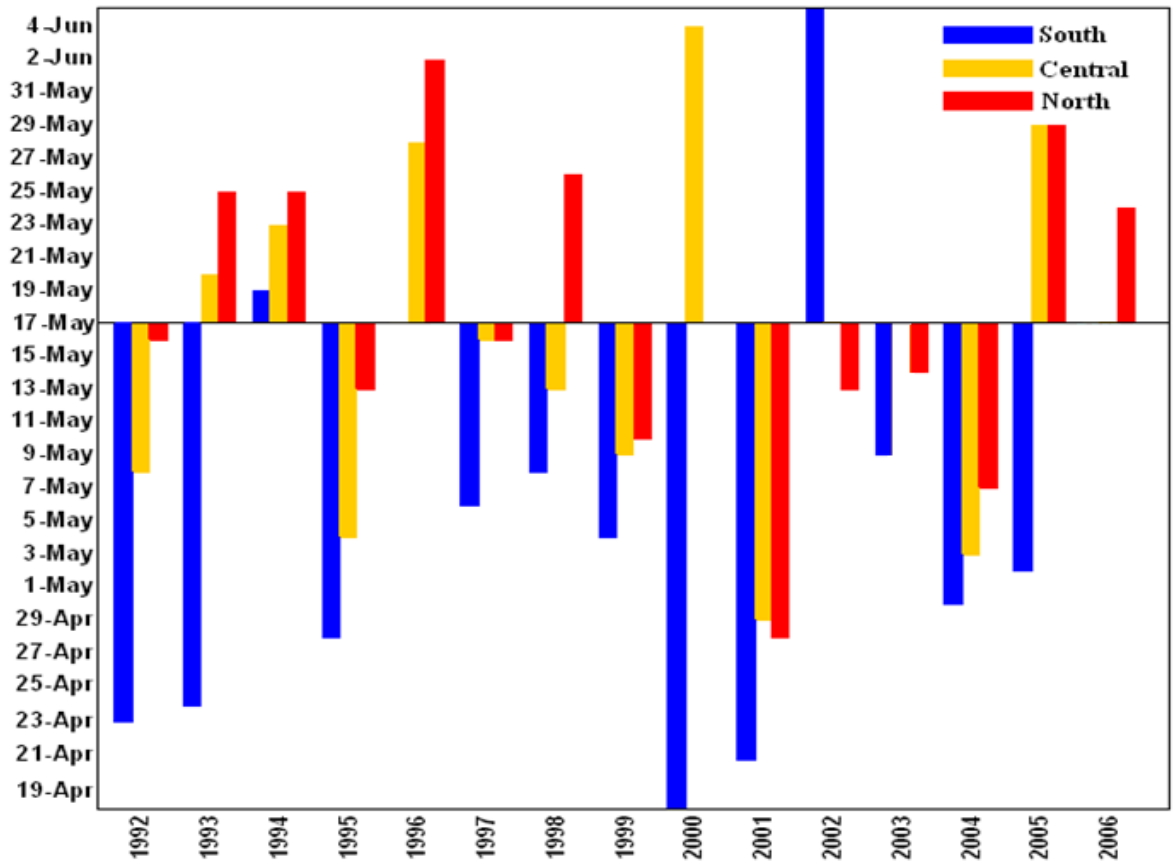

Figure 4.47: Interannual variability of southwest monsoon onset dates for northern, central and southern Maldives from 1992 to 2006.

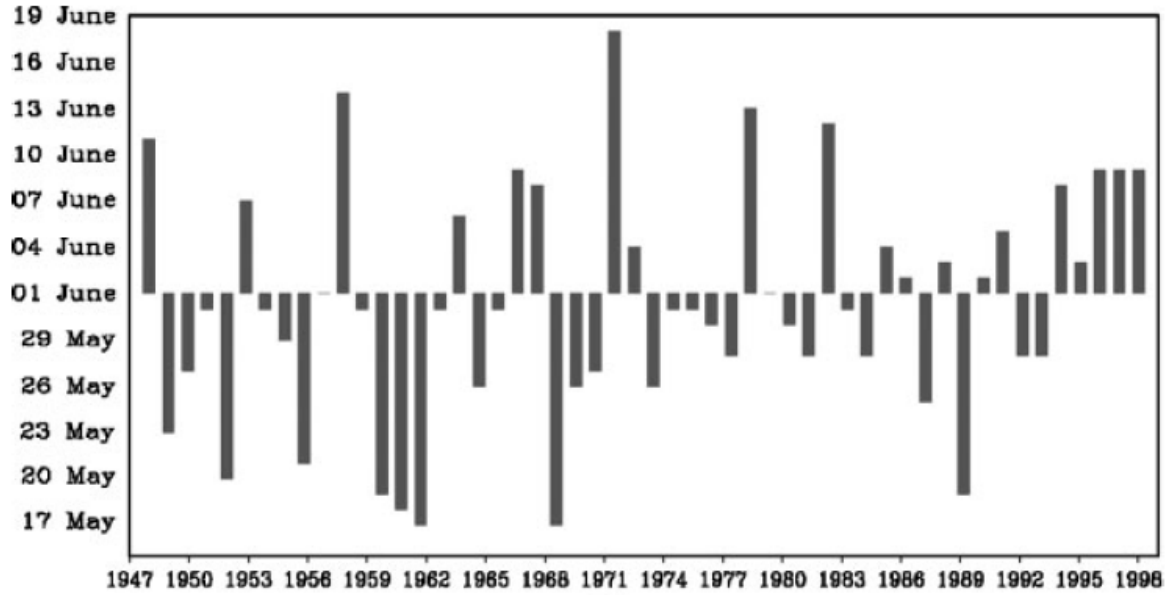

Figure 4.48: Interannual variability of onset dates of the summer monsoon over India (Kerala) from 1947 to 1998. Taken from Raju et al. (2005).

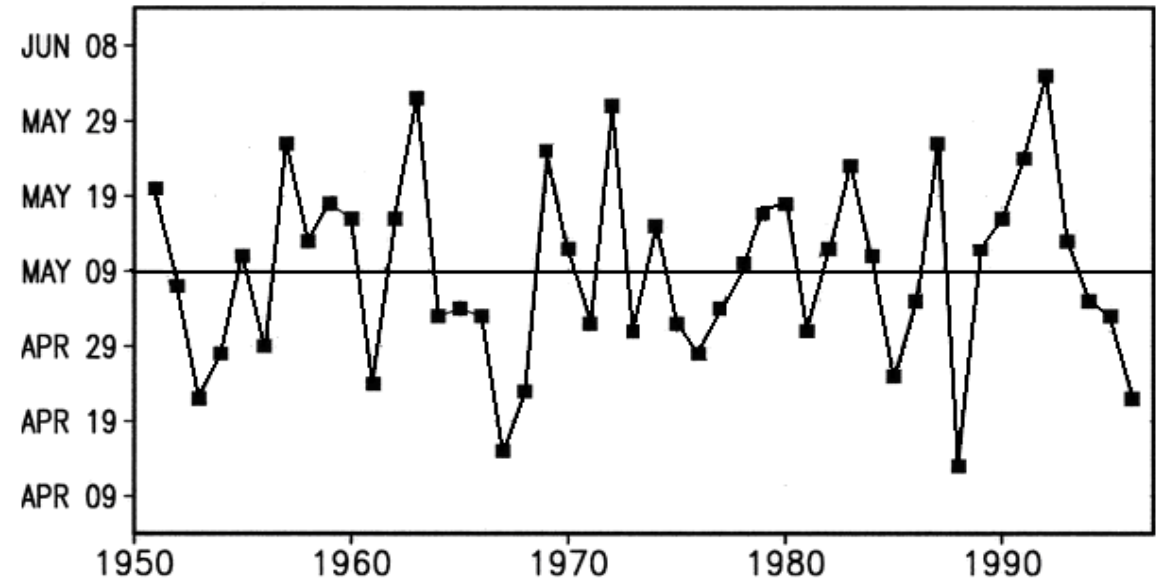

Figure 4.49: Interannual variability of onset dates of the summer monsoon over Indochina from 1951 to 1996. Modified from Zhang et al. (2002).

Ahmed and Karmakar (1993) pointed out that the monsoon withdrawal dates were found to be less obvious than those of the onset dates in Kerala and Bangladesh. As is shown in Table 4.7, the monsoon withdrawal dates for northern, central and southern Maldives are also found to be less obvious than those of the onset dates listed in Table 4.6. It is instructive to note that, for the central Maldives, in 2006 there is no withdrawal date that satisfies the criteria defined above (Table 4.7). During the 15-year period, the earliest withdrawal date was 1 November 2000 for the northern Maldives and most delayed

withdrawal date was 24 December 2002 and 2003 for the southern and central Maldives, respectively. The latest date of withdrawal for the northern Maldives was in 1992 (25 November). The earliest withdrawal date for the central Maldives was 5 November 2000. The earliest withdrawal date for the southern Maldives was 2 November 2004.

For the northern Maldives 86.7 % of the time withdrawal occurred in November, and about 13.3% of the time a withdrawal date for the northern Maldives was unidentified since the three criterions were not met. On the other hand, for the central part of the Maldives about 60% and 13.3% of the time withdrawal occurred in November and December, respectively, while 26.7 % of the time a withdrawal date for the central Maldives was unidentified. For the southern Maldives about 33.3% of the time withdrawal occurred in November and December, respectively, while 33.3 % of the time a withdrawal date for the southern Maldives was unidentified. These results also indicate that the withdrawal of the monsoon begins from the northern parts of the Maldives in November and subsequently from the central and southern Maldives in November or December. However, withdrawal of the monsoon should not be considered a gradual process (Syroka and Toumi 2004). The monsoon withdrawal dates listed in Table 4.7 for the Maldives agree with the Asian monsoon withdrawal pattern shown in Figure 4.50.

Table 4.7: Monsoon withdrawal dates for the Maldives from 1992 to 2006. NA and S.D. stand for not applicable and standard deviation, respectively.

Monsoon withdrawal dates for the Maldives			
Years	**Southern**	**Central**	**Northern**
1992	10 December	09 November	25 November
1993	12 November	13 November	13 November
1994	NA	22 November	25 November
1995	NA	25 November	17 November
1996	17 November	07 November	08 November
1997	NA	NA	06 November
1998	27 November	20 November	21 November
1999	NA	08 November	07 November
2000	04 December	05 November	01 November
2001	12 December	NA	21 November
2002	02 December	24 December	30 November
2003	24 December	14 December	24 November
2004	02 November	18 November	02 November
2005	27 November	NA	NA
2006	NA	NA	NA
Mean	**29 November**	**20 November**	**15 November**
S.D.(days)	**15**	**16**	**10**

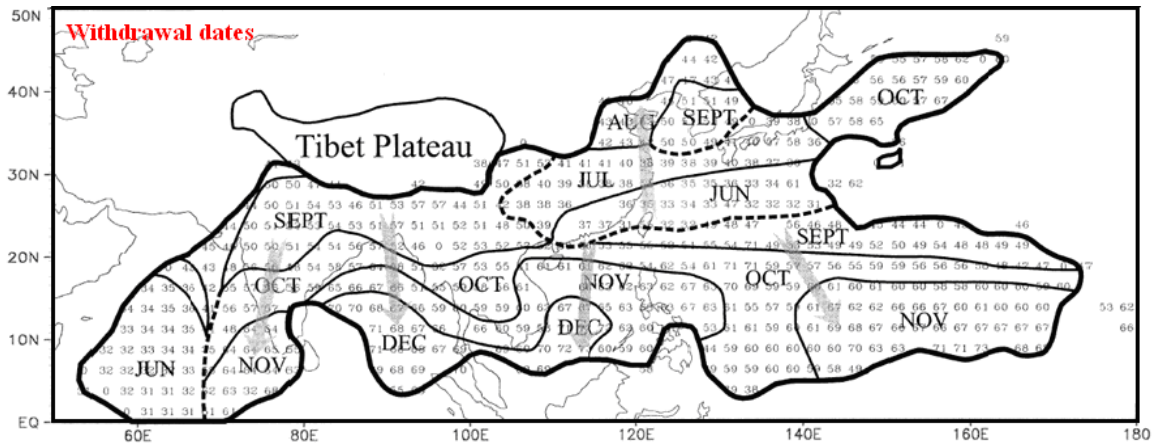

Figure 4.50: Large scale withdrawal patterns for the Asian monsoon region. The thick dashed lines denote discontinuities. The arrows indicate the direction of rain-belt propagation. Adapted from Wang and LinHo (2002).

The interannual variability of monsoon withdrawal dates for northern, central and southern Maldives from 1992 to 2006 is shown in Figure 4.51. The monsoon withdrawal date for the Maldives has significant interannual variability, with the earliest and most delayed withdrawal differing by 57 days. Unlike the onset dates, monsoon withdrawal dates are more variable for the central and least for the south, with coefficients of variation of 76.8 and 53.5%, respectively. The mean withdrawal dates of the monsoon for the northern, central and southern Maldives between 1992 and 2006 are 15, 20 and 29 November with standard deviations of 10, 16 and 15 days, respectively. According to Syroka and Toumi (2004), the mean date of withdrawal for the Indian region between 1958-2000 is 19 October with a standard deviation of 14 days. The mean date of 19 October for India is about a month earlier than the mean withdrawal date (18 November) from the northern Maldives (Table 4.7). Interannual variability of withdrawal dates for the Indian region is shown in Figure 4.52. During the 43-year period, the earliest and most delayed withdrawal dates for the Indian region were 23 September (1994) and 23 November (1998), respectively (Syroka and Toumi 2004). On the other hand, Prasad and Hayashi (Prasad and Hayashi 2005) found that the earliest and most delayed withdrawal dates for the Indian region between 1958-2001 were 23 September (1994) and 12 November (1964), respectively.

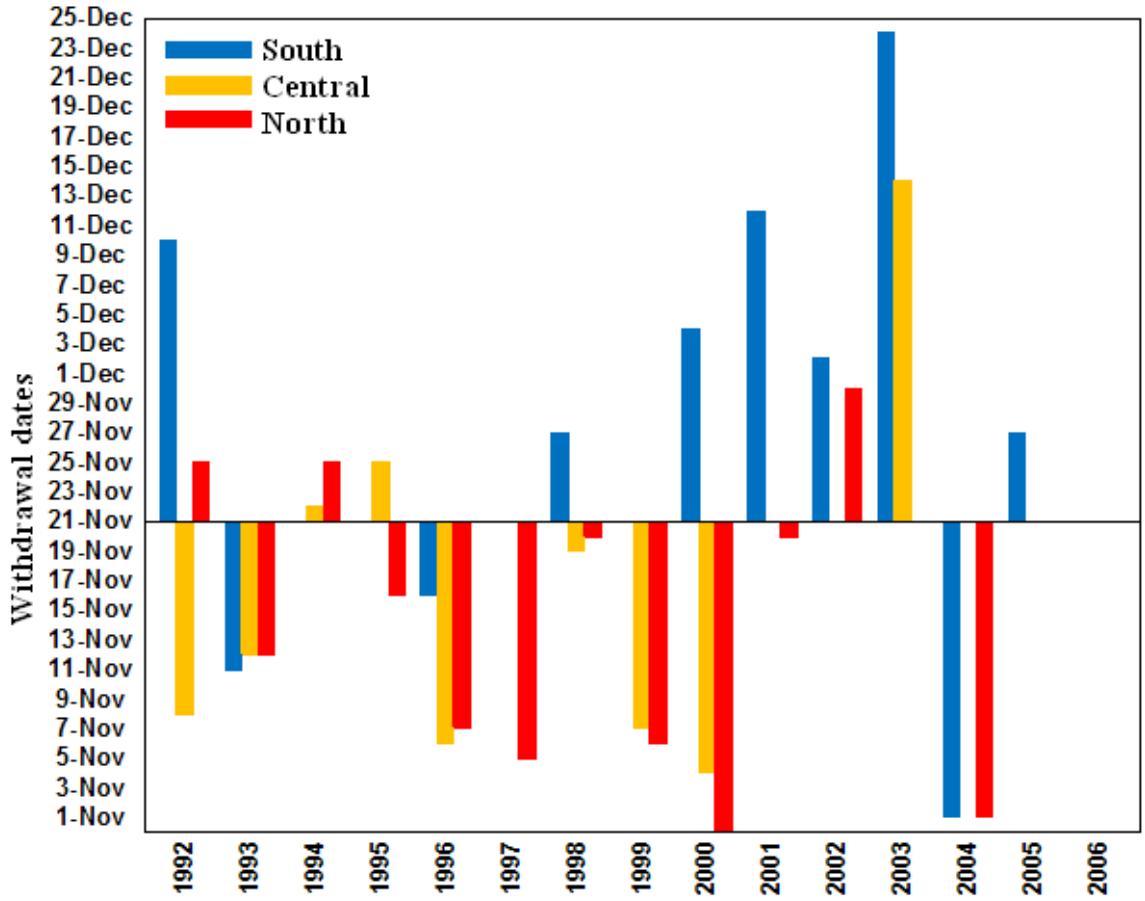

Figure 4.51: Interannual variability of monsoon withdrawal dates for northern, central and southern Maldives from 1992 to 2006.

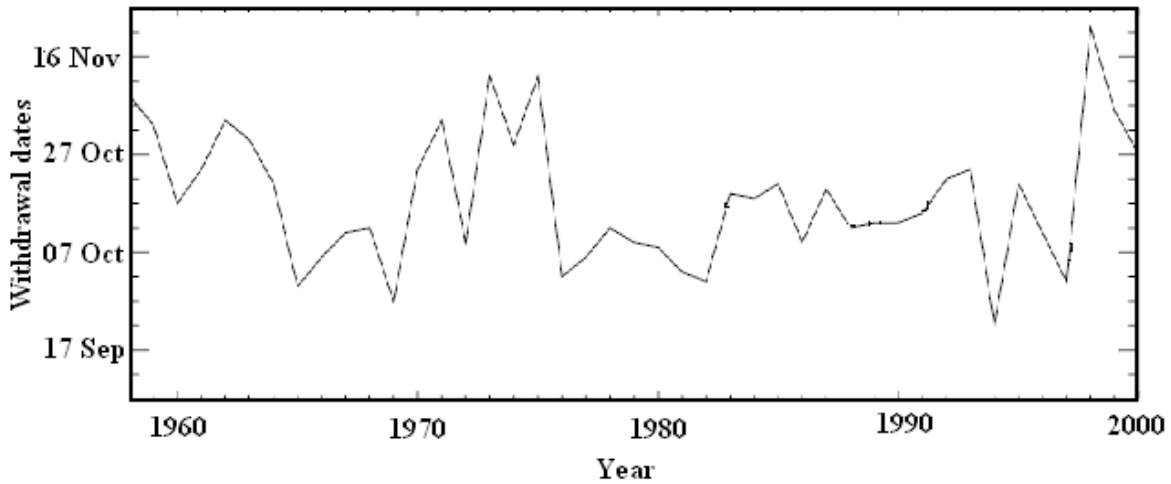

Figure 4.52: Interannual variability of Indian summer monsoon withdrawal dates from 1958 to 2000. Adapted from Syroka and Toumi (2004).

From the above discussion, it is clear that the onset and withdrawal dates vary greatly from one year to another and from one location to another (Ahmed and Karmakar 1993; Clarke et al. 2000). Depending on the criteria used, earliest and latest onset and

withdrawal dates can also differ for the same region (e.g., Fasullo and Webster 2003; Prasad and Hayashi 2005; Syroka and Toumi 2004). It has been noted in the literature that the bogus onset (the appearance of the monsoon like feature far ahead of the normal dates) occurs associated with pre-monsoon thundershowers and it is difficult to distinguish the monsoon rains from the thundershowers (Flatau et al. 2003; Prasad and Hayashi 2005). Xavier et al. (2007) argued that the onset definition based on rainfall over a small region (such as Kerala) may be sensitive to small-scale or higher-frequency fluctuations, such as synoptic disturbances and intraseasonal oscillations, and could lead to 'bogus' monsoon onsets as suggested by Flatau et al. (2001) and Flatau et al. (2003).

The Maldives is much smaller in terms of land area and the rainfall network is far smaller than the rainfall network of Kerala. The onset and withdrawal dates identified for the northern, central and southern Maldives are based on data (rainfall and wind vector) from only one station per region. Some of the onset and withdrawal dates identified above for the Maldives may be due to small-scale or higher-frequency fluctuations such as synoptic disturbances and intraseasonal oscillations (Flatau et al. 2001; Flatau et al. 2003; Prasad and Hayashi 2005; Xavier et al. 2007). To further substantiate the choice of the criteria (based on rainfall and wind vector) defined above and the identified onset and withdrawal dates for the Maldives using data from a single location (per region), onset and withdrawal dates were also identified based on an outgoing longwave radiation (OLR) index (based on a 5 day pentad) for the whole Maldivian region and were compared with the onset and withdrawal dates listed in Table 4.6 and Table 4.7, respectively.

Kousky (1988) determined the climatological onset date at every point on a 2.5° grid using satellite-based OLR measurements for the South American region. Kousky defined onset dates based on an OLR threshold value of 240 W m^{-2} and identified onset dates when the OLR is less than 240 W m^{-2} in a given 5-day average (pentad) and when 10 of the 12 previous pentads had OLR above 240 W m^{-2} and 10 of the 12 subsequent pentads had OLR below 240 W m^{-2}. On the other hand, Zhang et al. (2004b) used a combination of OLR (pentad mean OLR < 240 W m^{-2}) and establishment of zonal vertical shear between low-level westerlies and upper level easterlies to determined monsoon onset over the tropical Asian region (south of 20° N). Furthermore, Wu and Wang (2000) defined monsoon onset for the western North Pacific using pentad mean OLR and identified onset dates based on transition time over which the pentad mean OLR becomes lower than 240 W m^{-2}. Wu and Wang (2000) suggested that the selection of 240 W m^{-2} is subjective but relates to a precipitation rate of 6 mm/day for the western North Pacific region. Haque and

Lal (1991a) used OLR data to determine onset and withdrawal dates of the summer monsoon for seven selected regions on the Indian sub-continent (Figure 4.53).

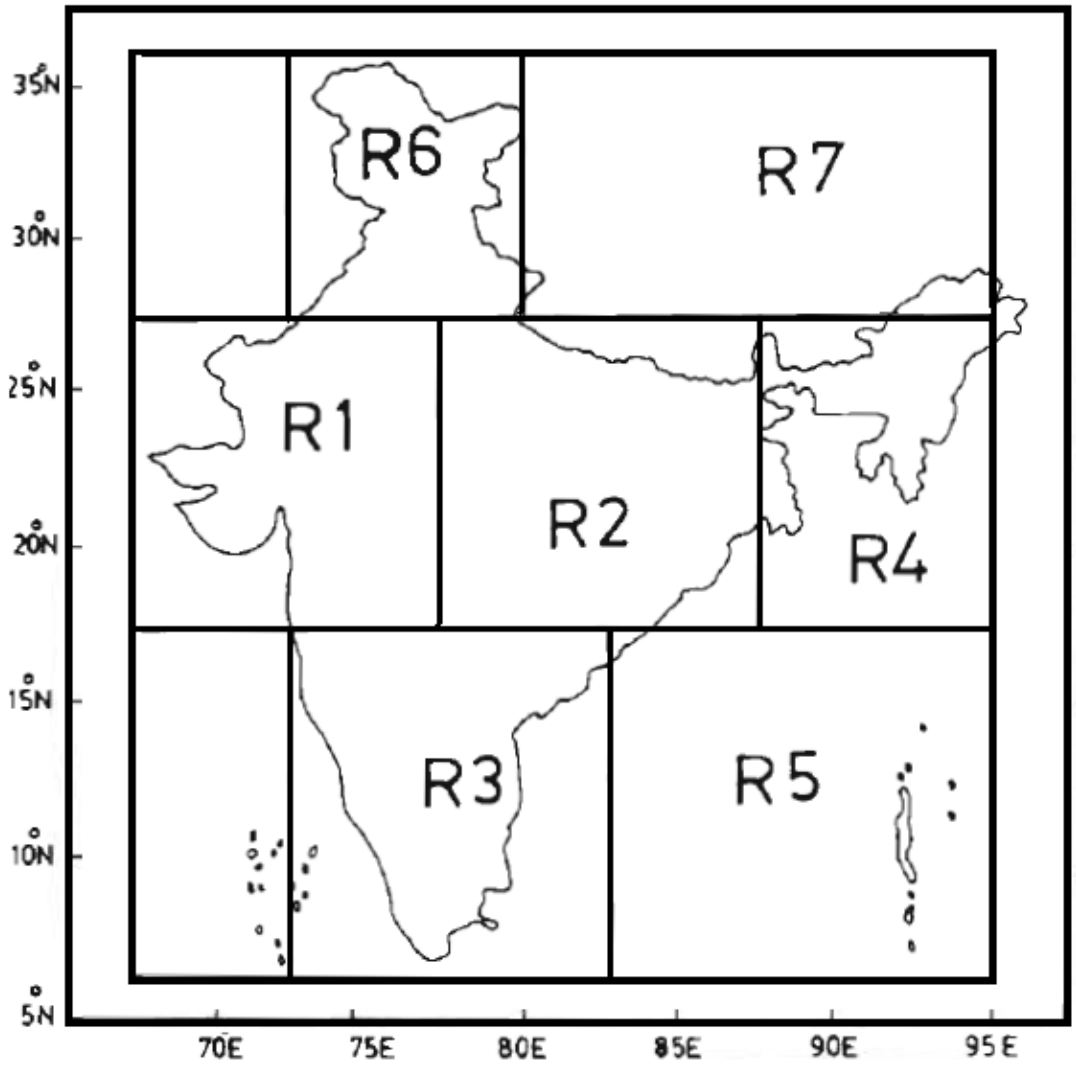

Figure 4.53: Seven selected regions (R1 to R7) over the Indian subcontinent for which Haque and Lal (1991a) identified onset and withdrawal dates using outgoing longwave radiation. Adapted from Haque and Lal (1991a).

In order to determine onset and withdrawal dates based on an OLR index, global OLR daily data for 15-years (1992-2006) were obtained from (Liebmann and Smith 1996). Details of the OLR data can be found in Section 2.1.6. The daily data were extracted for the Maldives domain defined by a 10° × 10° grid box (extending from 2.5° S – 7.5° N and 67.5° E - 77.5° E) shown in Figure 1.2. Following Haque and Lal (1991a), an OLR index for the Maldives region was computed. First, 5 day means were calculated for every grid point for each year (i.e. 73 pentads for every year). In leap years (1992, 1996, 2000 and 2004) the last pentad (73rd) is a 6 day mean. Haque and Lal (1991a) argued that the

threshold value of 240 W m^{-2} (long-term mean OLR for the Indian subcontinent) defines the large-scale annual cycle in monsoon area rainfall reasonably well. Secondly, the number of grid points having OLR values less than the threshold value of 240 W m^{-2} for every pentad was obtained. Thirdly, the resulting value (number of grid points having OLR values below 240 W m^{-2}) was divided by the number of grid points (25 grid points) to obtain an OLR index for each pentad. Time series of average outgoing longwave radiation (pentad mean for the period 1992 to 2006) (blue curve) and average OLR index (red curve) for the Maldives region is shown in Figure 4.54. Horizontal dashed lines (blue and red) show the OLR threshold value of 240 W m^{-2} and OLR index of 0.4, respectively. It is clear from the figure that the average OLR is below threshold value of 240 W m^{-2} from mid-April to mid-December. On the other hand, the average OLR index is above threshold value of 0.4 between mid-April and late December.

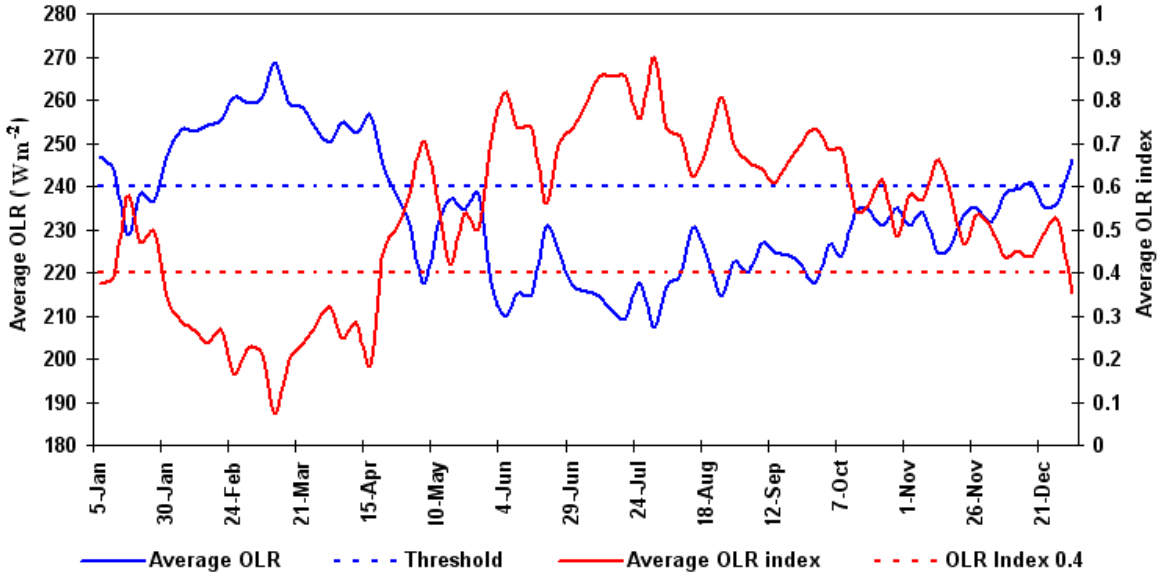

Figure 4.54: Time series of the pentad climatology of average outgoing longwave radiation (OLR - blue curve) and average OLR index (red curve) for the Maldives region. Horizontal dashed lines (blue and red) show OLR threshold value of 240 Wm^{-2} and OLR index of 0.4, respectively. Based on 15 years (1992 to 2006) of OLR data.

Haque and Lal (1991a) suggested that if more than 40% of a region (shown in Figure 4.53) had OLR values less than 240 W m^{-2} (OLR index 0.4) for a continuous 15 day period (i.e. 3 consecutive pentads) between 25 May and 15 June, the area was considered to be covered by convective clouds and under the influence of an active monsoon. Accepting the same threshold value of 240 W m^{-2} and following Haque and Lal (1991a), a criterion was adopted to determine monsoon onset dates for the Maldives. From the 3 consecutive pentads having an OLR index greater than the threshold index of 0.4 between 18 April and

15 June, the third day of the first pentad was taken as the monsoon onset date for each year from 1992 to 2006. Similarly, a criterion was adopted following Haque and Lal (1991a) to determine monsoon withdrawal dates for the Maldives. According to Haque and Lal (1991a), if more than 90% of a region (R1-R7 shown in Figure 4.53) had OLR values higher than 240 W m^{-2} (an OLR index less than 0.1) and there was no indication of a strengthening of monsoon activity (the OLR index did not exceed 0.4 for 3 consecutive pentads) the region can be considered to have become free from large scale convective clouds associated with the monsoon circulation. Initial analysis indicated that it is not possible to determine withdrawal dates based on an OLR index less than 0.1 as a threshold value for the Maldives region. As can be seen from Figure 4.54, the mean OLR index hardly falls below an OLR index of 0.1 (OLR index is less than 0.1 only between the 13 and 14 pentads: 6-11 March). Based on an OLR index of 0.1, it was possible to determine withdrawal dates for only 20% of the time (1992, 1994 and 2006) during the 15-year period and about 80% of the time the criteria was not met. Therefore, another approach (Haque and Lal 1991b) was taken to identify the monsoon withdrawal dates for the Maldives. The date of monsoon withdrawal was taken as the third day of the lowest pentad value between 1 November and 31 December of every year. The monsoon onset and withdrawal dates for each individual year between 1992 and 2006 for the Maldives, based on these OLR index criteria are listed in Table 4.8.

Table 4.8: Monsoon onset and withdrawal dates for the Maldives from 1992 to 2006 based on the OLR index.

Monsoon onset and withdrawal dates		
Year	**Onset**	**Withdrawal**
1992	11-May	2-Dec
1993	27-Apr	7-Nov
1994	22-May	12-Nov
1995	2-May	7-Nov
1996	1-May	2-Dec
1997	27-Apr	7-Dec
1998	12-May	12-Dec
1999	7-May	2-Dec
2000	21-May	12-Nov
2001	23-Apr	12-Nov
2002	23-Apr	17-Nov
2003	23-Apr	12-Nov
2004	21-Apr	2-Dec
2005	2-May	17-Dec
2006	22-May	17-Nov

Based on the OLR index criteria, the earliest and delayed onset dates for the Maldives were 21 April (2004) and 22 May (1994 and 2006), respectively. The earliest and delayed withdrawal dates for the Maldives based on OLR index criteria were 7 November (1993 and 1995) and 17 December (2005). It should be noted from Table 4.8, showing onset and withdrawal dates for the whole Maldives region, that it is not possible to determine onset and withdrawal dates for northern, central and southern Maldives separately using the OLR indices. Hence, it is not possible to compare the onset and withdrawal dates shown in Table 4.8 with the onset and withdrawal dates listed in Table 4.6 and Table 4.7, respectively. To compare the onset dates obtained based on the OLR index with onset dates identified based on rainfall and wind vector criteria, onset dates listed in Table 4.6 for three regions (north, central and south) were averaged to obtain a single date for each year for the whole Maldives. Similarly, withdrawal dates listed in Table 4.7 for north, central and south were averaged to obtain a single date for each year for the whole of the Maldives. The resulting onset and withdrawal dates were compared with the onset and withdrawal dates listed in Table 4.8. Figure 4.55 shows the interannual variability of the onset dates based on rain and wind criteria (blue line: average of north, central and south) and onset dates based on the OLR index (red line). On the other hand, Figure 4.56 shows the interannual variability of the withdrawal dates for the Maldives based on the rain and wind criteria, and OLR index. It is clear from these figures that the onset dates in some years were in close agreement between the two methods (e.g. 2000 and 1993), while in other years the onset differs by more than one month between the two methods. The biggest difference between the onset dates obtained from the two method was 32 days (in 2002), while the withdrawal differs by up to 31 days (in 1997) when the two methods were compared. Based on the OLR index, the 15-year average onset date was 4 May with a standard deviation of 11 days. The 15-year average withdrawal date was 23 November with a standard deviation of 13 days (Table 4.9). Furthermore, the average onset date for the whole of the Maldives based on rain and wind criteria was 13 May (an 9 day difference when compared with the average onset date based on the OLR index), while the average withdrawal date was 21 November, which is very close to the average withdrawal date obtained based on the OLR index (23 November: Table 4.9).

Table 4.9: Comparison of statistics of the onset and withdrawal dates obtained with the two methods described in the text.

	Onset date		Withdrawal date	
	Rain & Wind based	OLR based	Rain & Wind based	OLR based
Earliest	26 April	21 April	6 November	7 November
Latest	30 May	22 May	11 December	17 December
Mean	13 May	4 May	21 November	23 November
S. Deviation	9 days	11 days	12 days	13 days

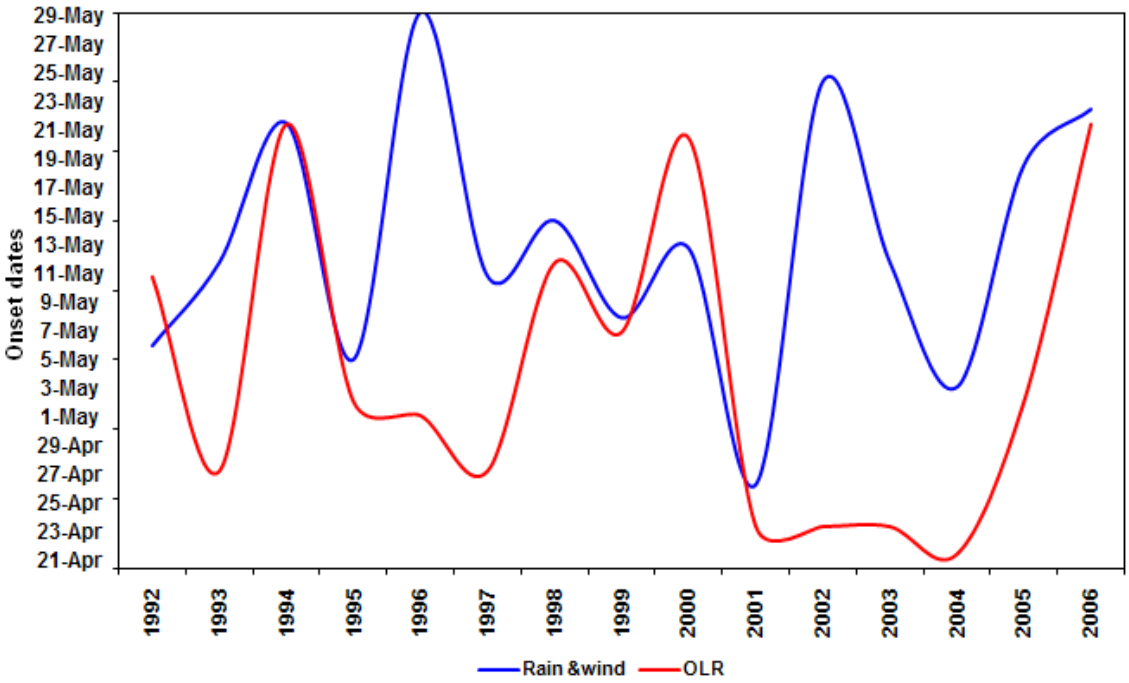

Figure 4.55: Interannual variability of onset dates of the monsoon over the Maldives based on rain and wind (blue) and OLR index (red) criteria.

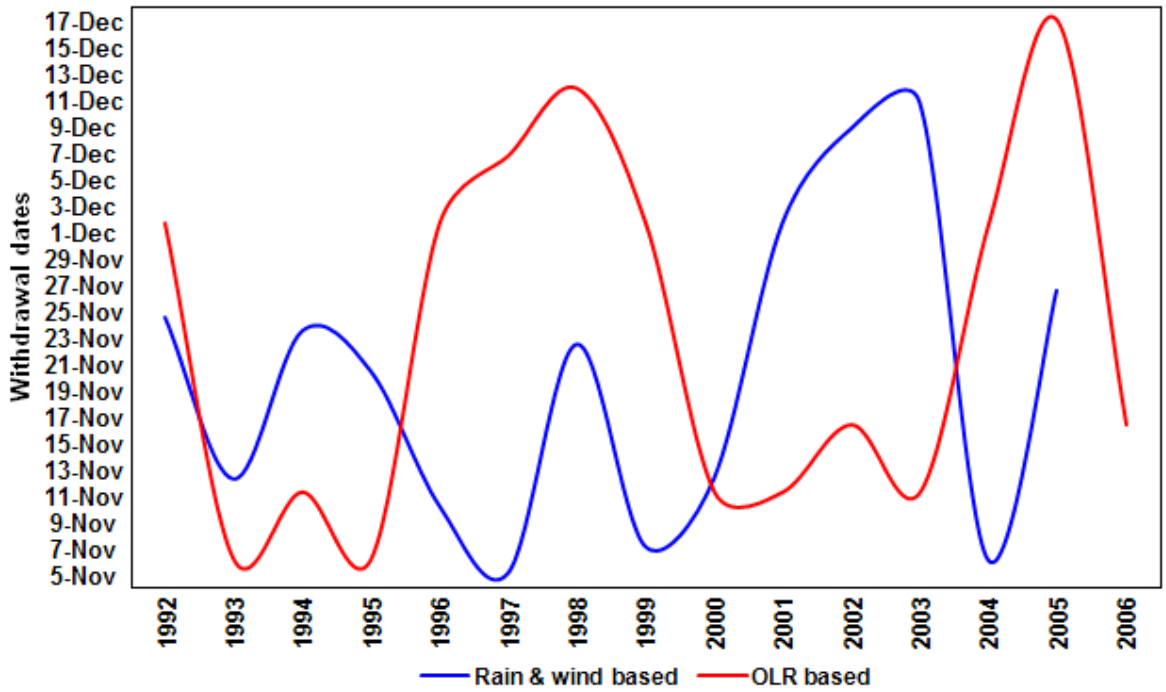

Figure 4.56: Interannual variability of withdrawal dates of the monsoon from the Maldives based on rain and wind (blue) and OLR index (red) criteria.

From the above graphs and tables it is evident that the onset and withdrawal dates determined by these two methods (rain & wind, and OLR index based) are reasonably consistent and thus considered to be useful for determining onset and withdrawal dates for the Maldives region. It is noted that the withdrawal dates have higher interannual variability than the onset dates when the two methods were compared. Based on onset and withdrawal dates obtained above, the length of rainy season (LRS) for the Maldives can be defined as the difference between onset and withdrawal dates (Xavier et al. 2007). LRS for the Maldives was calculated based on onset and withdrawal dates obtained from the above two methods. Interannual variability of LRS for the Maldives based on the two methods described above is shown in Figure 4.57 together with its linear trend. The equations shown in the figure indicate that there is no significant increasing trend of LRS for both methods. The mean LRS for the Maldives based on OLR index criteria is 204 days, with a standard deviation of 18 days. On the other hand, mean LRS based on the rain and wind criteria is 11 days shorter (193 days, with a standard deviation of 14 days). Since the obtained LRS was based on onset and withdrawal dates, it can be concluded that the rainy season on average commences between 4 May and 13 May (mean onset dates based on OLR index and rain and wind criteria, respectively) and terminates in late November (21 and 23 November: mean withdrawal dates based on rain and wind, and OLR index criteria, respectively) for

the Maldives. The correlation coefficient between the two methods of LRS shows a very weak negative correlation (CC = -0.11, insignificant at 5% level).

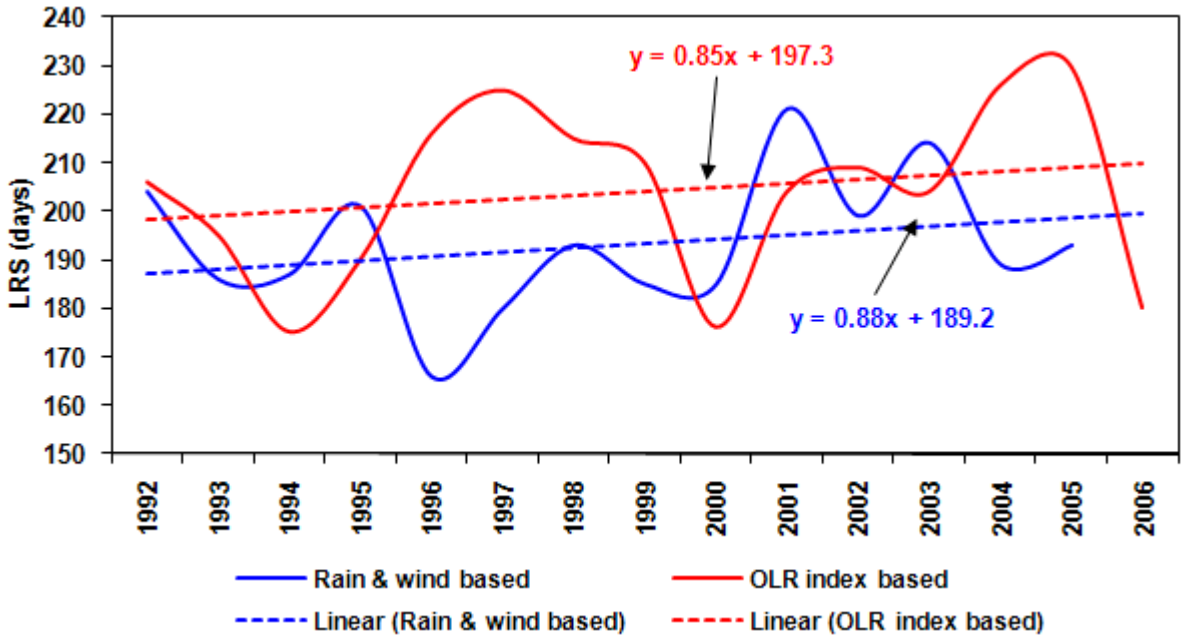

Figure 4.57: Interannual variability of the length of the rainy season (LRS) for the Maldives based on the rain & wind criteria, and OLR index discussed in the text.

4.5 Summary

The objective of this chapter was to characterize monsoon rainfall over the Maldives and to determine monsoon season objectively. Results indicate that the Maldives monsoon rainfall (as well as the Asian monsoon) is characterized by interdecadal, interannual and intraseasonal variability. On the interdecadal time scale, the Maldives monsoon rainfall is characterised by a periodicity of 12-15 years. Interannual monsoon rainfall over the Maldives is characterised by significant peaks with periodicities of about 2-7 years, which can be attributed to the tropospheric biennial oscillation (TBO) and remote forcings, such as ENSO. Intra-seasonal variability of monsoon rainfall during the monsoon season is characterized by the occurrence of active-break cycles of wet or dry phases and is characterized by 10-20 and 30-60 day periodicities. Criteria definition of monsoon onset and withdrawal dates lead to the determination of monsoon season or the length of the rainy season objectively for the Maldives. Monsoon onset and withdrawal dates based on wind/rain and an OLR index clearly demonstrates that the onset and withdrawal dates vary greatly from one year to another and between the two methods and hence that the Maldives monsoon season or length of rainy season is characterized by large interannual variability.

5 Parameters influencing monsoon variability

This chapter investigates the parameters involved in the variability of monsoon precipitation. It has been pointed out in the literature that spatial and temporal variability in monsoon rainfall is associated with variations in such surface and upper air meteorological parameters as temperature, pressure, geopotential height and wind. Mohapatra and Mohanty (2006) suggested that an understanding of the characteristics of surface and upper air meteorological fields is essential for a complete understanding of the Indian monsoon and its variability. The objective of this chapter is to investigate the relationship between various meteorological parameters (sea surface temperature, mean sea level pressure, outgoing long-wave radiation, air temperature, humidity and wind) and spatio-temporal variability of monsoon precipitation over the Maldives. An attempt is made to identify those parameters that influence monsoon precipitation variability using correlation. The significant parameters are then used to develop a regression model to predict core monsoon season (June-September: JJAS) precipitation for the Maldives. These predictions will be useful for water resources and agricultural planning as discussed later in Chapter 8.

5.1 Identification of parameters

The Asian monsoon is the result of the land-sea heating contrast, involving large-scale seasonal reversals of pressure, temperature and winds. A significant correlation between surface and upper level circulation parameters in the Indian region and summer monsoon rainfall has been established (Cannon and McKendry 1999). The parameters used here therefore include both surface and upper level parameters. The surface parameters are surface air temperature, mean sea level pressure and sea surface temperature. The upper level circulation parameters include zonal wind (at 1000, 850, 500 and 250 hPa levels), relative humidity (1000, 850, 500 and 250 hPa levels) and outgoing longwave radiation (top of the atmosphere). Details of the selected parameters are tabulated in Table 5.1. All these parameters were identified based on their relationship with monsoon precipitation for different regions of Asia, described elsewhere in the literature. For example, sea surface temperature (SST) throughout the tropical Indian Ocean correlates positively with subsequent monsoon rainfall in the boreal fall and winter preceding the summer Indian monsoon. Clarke et al. (2000) found a strong correlation (0.53) between the summer All-India Rainfall Index (AIRI) and the preceding December–February Arabian Sea SST for

the period 1945-94. Furthermore, a correlation of 0.58 was found between the AIRI and the SST to the northwest of Australia for the same period. Prasad et al. (2000) also found that the SST over the southern Indian Ocean during April is positively associated with the all-India summer monsoon rainfall (ASMR) and suggested that the outgoing longwave radiation (OLR) in this region appears to represent variation in sea surface temperature (SST) of the region during April. The SST and the OLR of the region have a significant positive association with the ASMR. A high OLR over the region during April enhances the subsequent summer monsoon activity through a complex ocean–atmospheric interaction (Prasad et al. 2000).

5.2 Correlation analysis

Correlation analysis (details provided in Chapter 2) provides a measure of the relative strength and direction of the relationship between two variables. The primary datasets used for this part of the analysis are the National Oceanic and Atmospheric Administration (NOAA) outgoing longwave radiation, OLR, (Liebmann and Smith 1996) and the National Centers for Environmental Prediction–National Center for Atmospheric Research (NCEP-NCAR) reanalysis (Kalnay et al. 1996) for the period 1979 to 2007. In recent years, NCEP/NCAR reanalysis has improved the geographical coverage and availability of the data. Linear correlations between the monsoon precipitation and other parameters have been evaluated using NOAA and NCEP/NCAR gridded data, over the entire Asian region (30-120 °E: 30 °N-15 °S), to identify parameters that influence variability of monsoon over the Maldives region and then to use these parameters to develop a scheme for predicting monsoon precipitation for the Maldives.

As a first step, the data were explored to find correlations between precipitation over the Maldives and various other parameters listed in Table 5.1. The core monsoon season precipitation (from June to September) for each grid point spanning 70-75 °E and 0.5 °S-7.75 °N (Maldives region) was filtered for each year and a time series of June-July-August-September (JJAS) total precipitation for the Maldives region was extracted. The JJAS total precipitation for the Maldives region was correlated with the individual variables separately for each grid point over the whole area shown in Figure 4.28 for January, February, March, April and May of the current year. Spatial correlation maps were produced for individual months and for all parameters. Based on correlation maps, spatially coherent regions having maximum significant correlation with the Maldives JJAS total precipitation have been identified. The areas with correlation coefficients (CCs) of at least 5% level of significance

were identified for each parameter and contours were drawn on CC maps to enclose areas of significant correlation. The contour areas are restricted to a minimum of 2° × 2°, to avoid isolated patches of significant areas. There were some isolated areas having significant CCs. However, these regions were too small and not considered here.

Table 5.1 shows CCs between precipitation over the Maldives and the other parameters for the period from 1979 to 2007. The JJAS total precipitation over the Maldives is positively correlated with the May mean sea level pressure in the Arabian Sea region (52.5 °E-62.5 °E: 10 °N-20 °N), with a maximum correlation coefficient of 0.42, significant at 5% level (Table 5.1), as shown in Figure 5.1b. This positive correlation (Figure 5.1b) may be linked to the occurrence of El Niño years. In the pre-monsoon month of May and during the monsoon season (June-September), significantly higher mean sea level pressure anomalies occur over India, the Arabian Sea, parts of Arabia and the southwest equatorial Indian Ocean in El Niño years compared with La Niña years (Bhatla et al. 2006). Mean sea level pressure anomaly maxima occur over the north Arabian Sea and the usual region of monsoon heat low (Arabia, Pakistan and northwest India) (Bhatla et al. 2006). The land mass of the Asian subtropical regions becomes warm due to intense solar heating during April and May resulting in low surface pressure over the Indian subcontinent. The low surface pressure over India is evident from the May mean sea level pressure shown in Figure 5.1a.

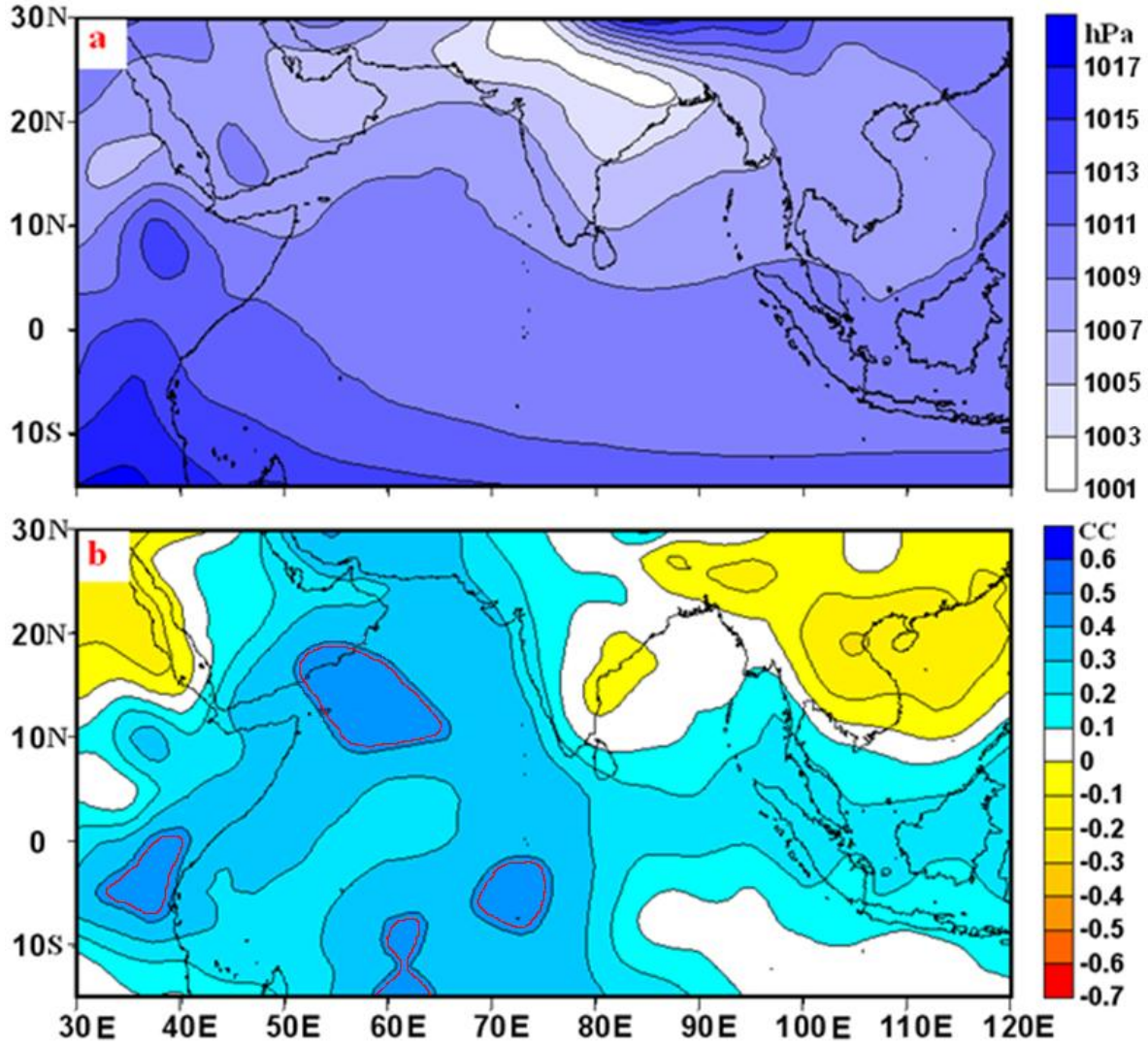

Figure 5.1: Mean sea level pressure (hPa) for May (a) and correlation between JJAS total precipitation over the Maldives and May mean sea level pressure (b), from 1979 to 2007. The red contour lines indicate areas of significant correlation (5% level).

Table 5.1: Correlation coefficient (CC) between JJAS total precipitation over the Maldives and the parameters analysed.

Parameters	Levels/Month	Parameter label	Areas of significance	CC
Sea level pressure	Surface/May	SLPMAY	52.5-62.5E; 12N-20N	0.42*
Air temperature	Surface/February	ATPFEB	47.5-50E; 2.5S-7.5S	0.44*
Sea surface temperature	Surface/January	SSTJAN	48-76E; 2S-6S	0.45*
Outgoing long wave radiation	Top of Atmosphere/May	OLRMAY	55-60E; 2.5N-7.5N	0.46*
Zonal wind	Surface/January	SUWJAN	65-75E; 5N-5S	-0.62**
	850 hPa/January	850UWJAN	50-62.5E; 7.5N-2.5S	-0.64**
	500 hPa/January	500UWJAN	32.5-45E; 7.5-15N	0.55**
	250 hPa/January	250UWJAN	102.5-120E; 27.5-30N	-0.52**
Relative humidity	Surface/April	SRHAPR	107.5-120E; 2.5S-5S	0.53**
	850 hPa/May	850RHMAY	92.5-97.5E; 0-5N	-0.56**
	500 hPa/May	500RHMAY	52.5-65E; 10-15N	-0.59**
	250 hPa	-	-	-

**** Significant at 5% level; ** significant at 1% level***

The availability of hemispheric mean surface temperatures in the early 1980s made it possible for Verma et al. (1985) to use the Northern Hemisphere (NH) winter surface air temperature anomaly (January and February) for the prediction of all-India summer monsoon rainfall, and identified it as one of the most important parameters, with a CC of

0.56 for the period 1951-80, noting its significance even during the more recent years. Figure 5.2b shows the correlation between JJAS total precipitation over the Maldives and mean surface air temperature for February for the period from 1979 to 2007. The highest significant correlation between surface air temperature for February and monsoon precipitation for the Maldives region is 0.44 (Table 5.1), located in the southern Indian Ocean (Figure 5.2b). As can be seen from Figure 5.2a, the mean surface air temperature for February for the same period shows very uniform temperature across the whole Asian region, except for the Tibetan region (80-115 °E; 28-30 °N). The low air temperature in the northern Indian region could be due to excessive snow cover, thus reducing the net solar radiation absorbed by the ground surface (due to high reflectivity) or absorbed solar energy being used to melt the snow and evaporate water in this region rather than to heat the ground directly (Zhang et al. 2004a).

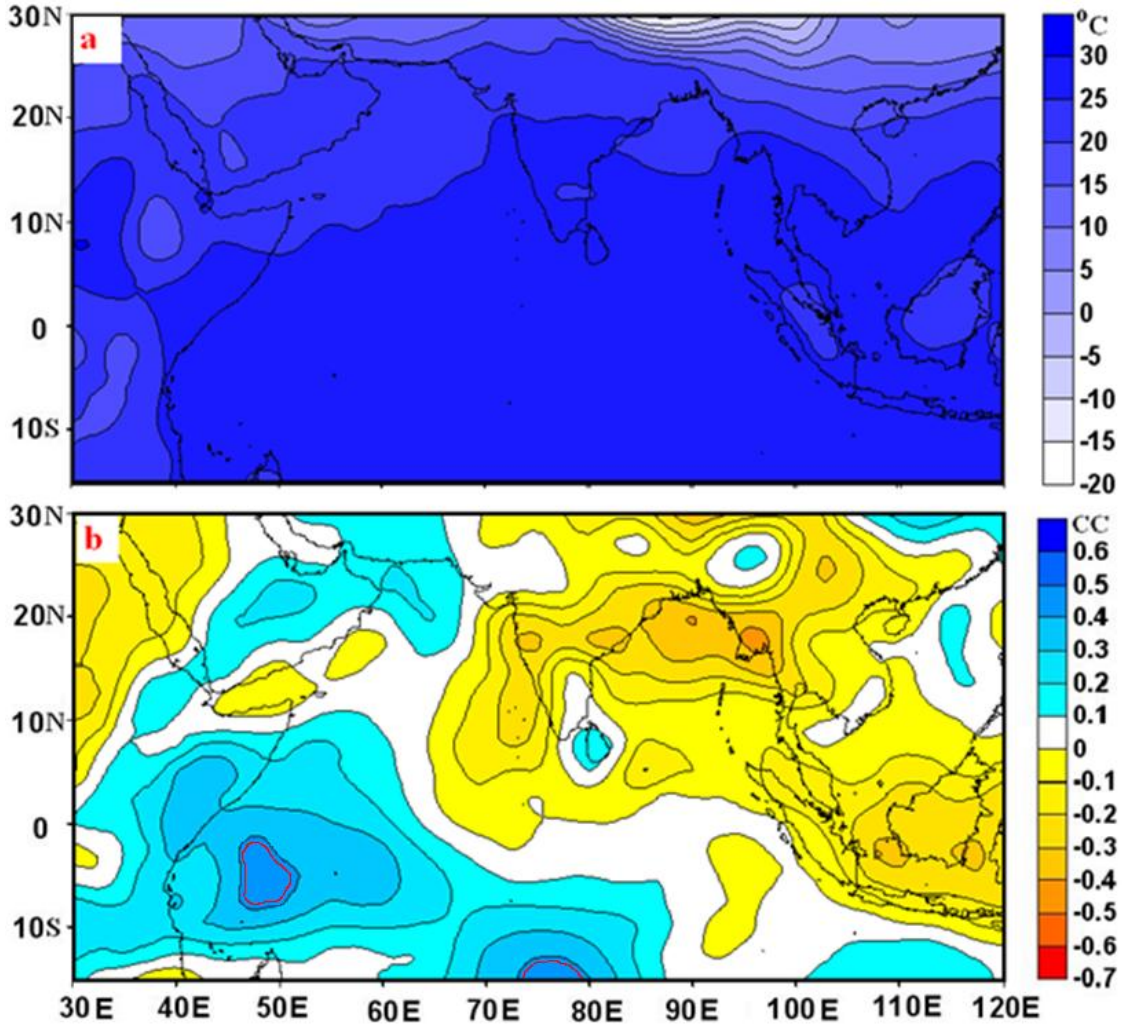

Figure 5.2: Mean surface air temperature (°C) for February (a) and correlation between JJAS total precipitation over the Maldives and February surface air temperature (b), from 1979 to 2007. The red contour lines indicate areas of significant correlation (5% level).

Convective activity is closely linked to sea surface temperature (SST) (Pattanaik 2007) . It has been suggested that the SSTs in different regions (e.g. in the western Pacific and Indian Oceans) can influence the Asian monsoon. Regional sea surface temperatures (SSTs) influence the Asian monsoon through changes in surface energy and moisture supply, and thermal contrast between land and ocean through ocean-atmosphere interaction. The sea surface temperature may play a feedback role with the monsoon and therefore acts as both an external and internal factor. A rise in SST can lead to increase in moisture (through evaporation) in the atmosphere and hence an increase in monsoon rainfall. SST can also influence the intensity of the monsoon circulation by reducing the summertime land-sea thermal contrast (Wang 2006) .

Past studies have indicated that the SST for different months in the tropical Indian Ocean and Arabian Sea correlates with the Indian summer monsoon (JJAS) rainfall. SST over the southern Indian Ocean during April is positively correlated with the all-India summer monsoon rainfall, while the preceding December–February Arabian Sea SST strongly correlates with the summer all-India rainfall index (Clarke et al. 2000; Prasad et al. 2000). March–April (MA) SST anomalies in the south-eastern Arabian Sea are significantly correlated with the JJAS rainfall over India, while the correlation between SST and JJAS rainfall changes with the season. The correlation of rainfall varies between significantly positive with the pre-monsoon SST, very small with SST during the monsoon season, and significantly negative with SST during the post-monsoon months (Rao and Goswami 1988; Reddy and Salvekar 2003). January SST over the southern Indian Ocean (48 °E-76 °E; 2 °S-6 °S) shows a positive correlation (CC = 0.45, significant at 5%) with the core monsoon season (June-September) rainfall over the Maldives (Figure 5.3b). Figure 5.3a shows SST over the Asian region (Arabian Sea and Indian Ocean) for the month of January. In most of the Arabian Sea and Indian Ocean the mean SST is quite uniform and high (24-28 °C: Figure 5.3a) for the whole ocean domain, except coastal regions close to land, where the SST is low compared to open ocean. In a recent study, Pattanaik (2007) suggested that the JJAS mean SST over most of the Arabian Sea and the entire Bay of Bengal is higher than 27 °C, which can create favourable conditions for the occurrence of deep convection and hence increase rainfall.

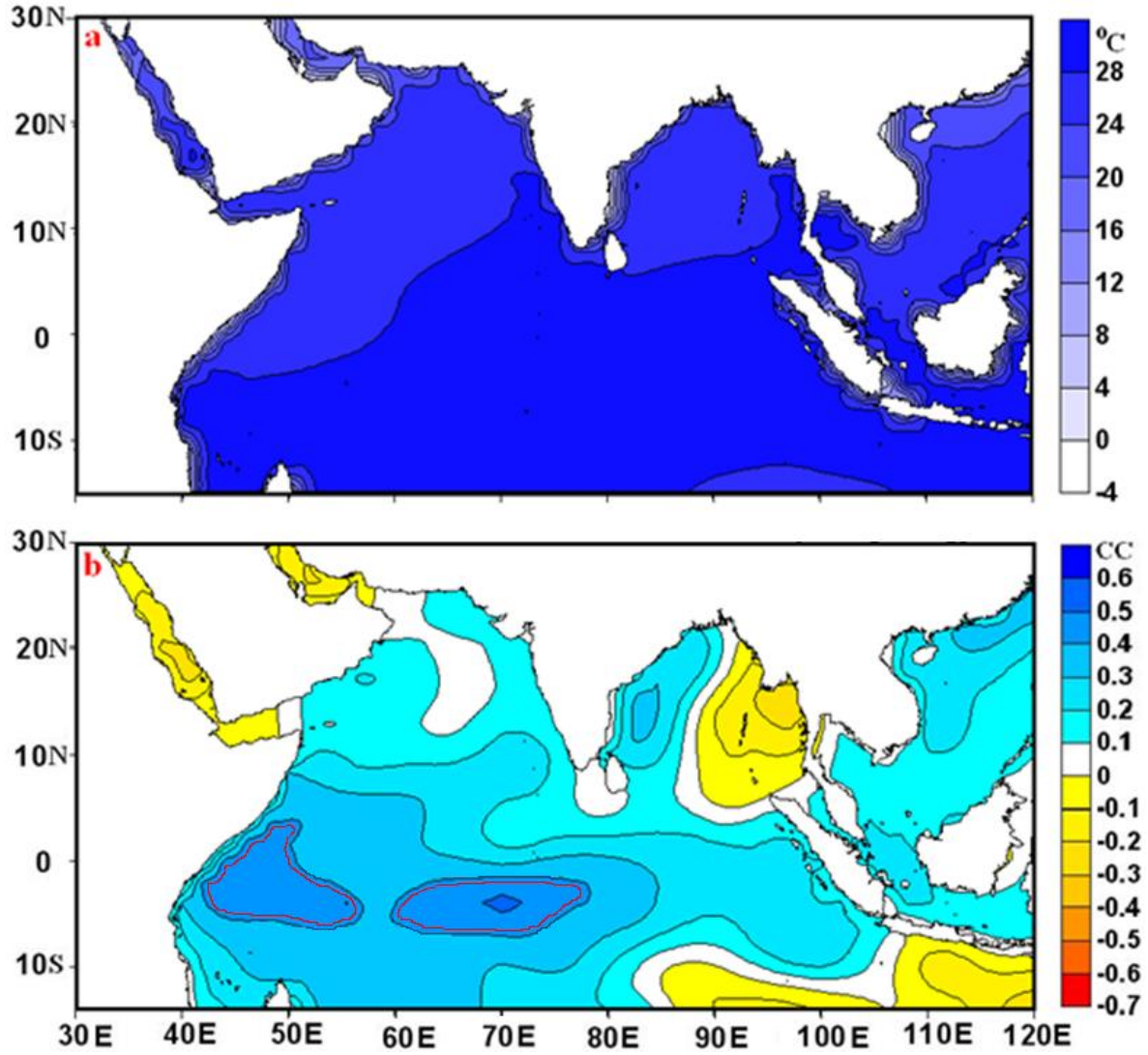

Figure 5.3: Mean sea surface temperature (°C) for January (a) and correlation between JJAS total precipitation over the Maldives and January sea surface temperature (b), from 1979 to 2007. The red contour lines indicate areas of significant correlation (5% level).

Pattanaik et al. (2005) found that the negative OLR anomalies that originate in the western Pacific region in the months of January gradually strengthen in a west-northwest direction and become established by the month of May over the Southeast Asian region and adjoining eastern equatorial Indian Ocean in monsoon rainfall excess years. On the other hand, negative OLR anomalies established over the western Pacific region in January during the deficient monsoon years almost remain active over the same region until the month of May. Prasad et al. (2000) correlated all-India summer monsoon total rainfall (ASMR: June-September) with OLR for the preceding monsoon months (i.e. January-May) over the Indian Ocean (30°N-30 °S and 40 °E-100°E). They found significant correlation

between OLR in February over the region 17.5°S-20 °S and 55 °E-60 °E, April over the region 27.5°S–30°S and 92.5°E-97.5°E, and in May over the head of the Bay of Bengal (20°N-22.5°N and 90°E–92.5°E) with ASMR. It is shown here (Figure 5.4b) that the JJAS total rainfall over the Maldives positively correlates with the proceeding May OLR, with a maximum CC of 0.46 (significant at 5%) over 55 °E-60 °E and 2.5 °N-7.5 °N. The spatial pattern of mean OLR for the month of May is shown in Figure 5.4a. Low values of mean OLR can be seen over the Bay of Bengal, the Andaman Sea and the Indian Ocean, while higher mean OLR values over north-western parts of India can also be seen. Pattanaik (2007) found that low and high long-term mean OLR during the monsoon season in these regions corresponds to areas of deep convection and reduced convective activity, respectively. This is also evident from the mean OLR for the month of June (figure not shown), which shows a similar OLR pattern to that shown in Figure 5.4a, except that the low OLR regions shown in Figure 5.4a were located further north and the high OLR over the north-western parts of India were further west.

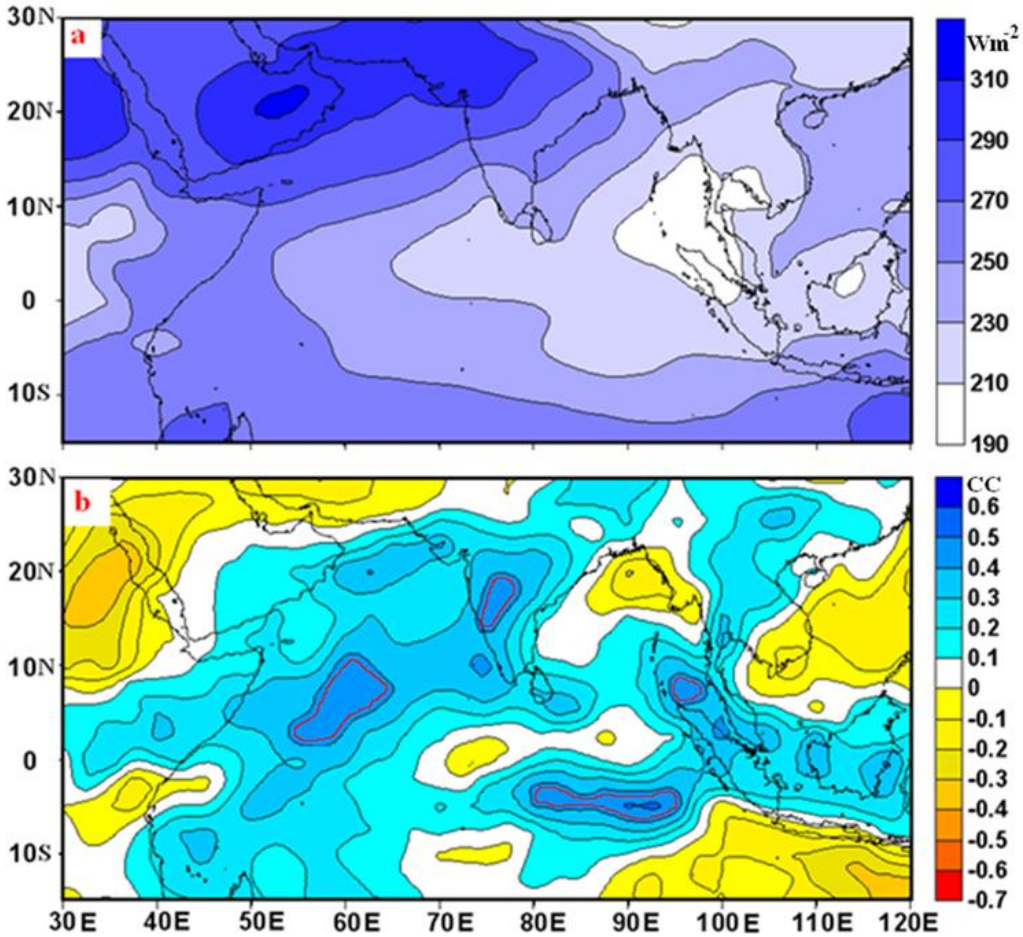

Figure 5.4: Mean outgoing longwave radiation (W m-2) for May (a) and correlation between JJAS total precipitation over the Maldives and outgoing longwave radiation for May (b), from 1979 to 2007. The red contour lines indicate areas of significant correlation (5% level).

According to Senan et al. (2003), the surface zonal wind in the equatorial Indian Ocean is westerly in direction almost all year round. Li et al. (2003) suggested that there is a close relationship between zonal wind and SST, suggesting a strong air-sea coupling over the Indian Ocean (IO). The zonal wind anomaly over the central IO depends on a number of factors, including east-west sea surface temperature anomaly (SSTA) gradients, anomalous monsoon heating and the intensity of the local Walker cell controlled by the SSTA over the maritime continent (Li et al. 2003). The spatio-temporal link between sea surface temperatures and winds suggests a strong coupling through the precipitation field and ocean dynamics. According to Saji et al. (1999), the interaction between air and sea is unique to the Indian Ocean, and is shown to be independent of the El Niño/Southern Oscillation. The intensity of the SST dipole mode (SST anomaly between the tropical western Indian Ocean (50°E-70 °E, 10 °S-10 °N) and the tropical south-eastern Indian Ocean (90 °E-110 °E, 10 °S-Equator)) and the strength of the zonal wind anomaly over the equator (70°E-90°E, 5°S-5°N) are independent of each other (Saji et al. 1999). Figure 5.5 to Figure 5.8 show January mean zonal winds for the Asian region for different levels (Figure 5.5a: surface, Figure 5.6a: 850 hPa level, Figure 5.7a: 500 hPa level and Figure 5.8a: 250 hPa level). The corresponding correlation between JJAS total precipitation over the Maldives and January mean zonal winds for the levels are shown in (b) in each figure for the period from 1979-2007. At the surface level the Asian region is mostly dominated by the easterly wind (Figure 5.5a). A weak band of westerly zonal wind is located in the south Indian Ocean (50-90 °E; 5-10 °S). This weak band of westerly wind is also evident from the 850 hPa level zonal wind (Figure 5.6a). At the 850 hPa level, the north Indian Ocean (equator to 20 °N) is dominated by easterly zonal wind (Figure 5.6a). As it can be seen from the zonal wind distribution for the upper levels (500 hPa and 250 hPa), the westerly wind dominates from latitudes greater than about 10 °N, and it increases from 10 °N to further north (Figure 5.7a and Figure 5.8a). On the other hand, easterly wind dominates from about 10 °N to further south, with a strong band of easterly located around equator (Figure 5.7a and Figure 5.8a). Clift and Plumb (2008) suggested existence of westerly subtropical jets straddling the equator at altitudes of about 12 km. The change in wind direction around 10 °N may be related to these subtropical jets.

There is an inverse relationship between the zonal winds at different level with JJAS precipitation over the Maldives, except for 500 hPa zonal wind, which is positively correlated with the precipitation over the Maldives with a correlation coefficient of 0.55 (significant at 1% level: Table 5.1). Correlation between JJAS precipitation and January

zonal wind is highest for the 850 hPa level (around 50-62.5 °E; 7.5 °N-2.5 °S: Figure 5.6b), with a CC of -0.64 (Table 5.1), which is significant at 1%. Maximum correlation between JJAS precipitation and surfrace zonal wind occurs over the Indian Ocean, with a maximum CC of -0.62, while maximum correlation between JJAS precipitation and 250 hPa level zonal wind occurs around 102.5-120 °E; 30 °N-25 °S with a maximum correlation coefficient of -0.52. These CCs are also significant at 1% level.

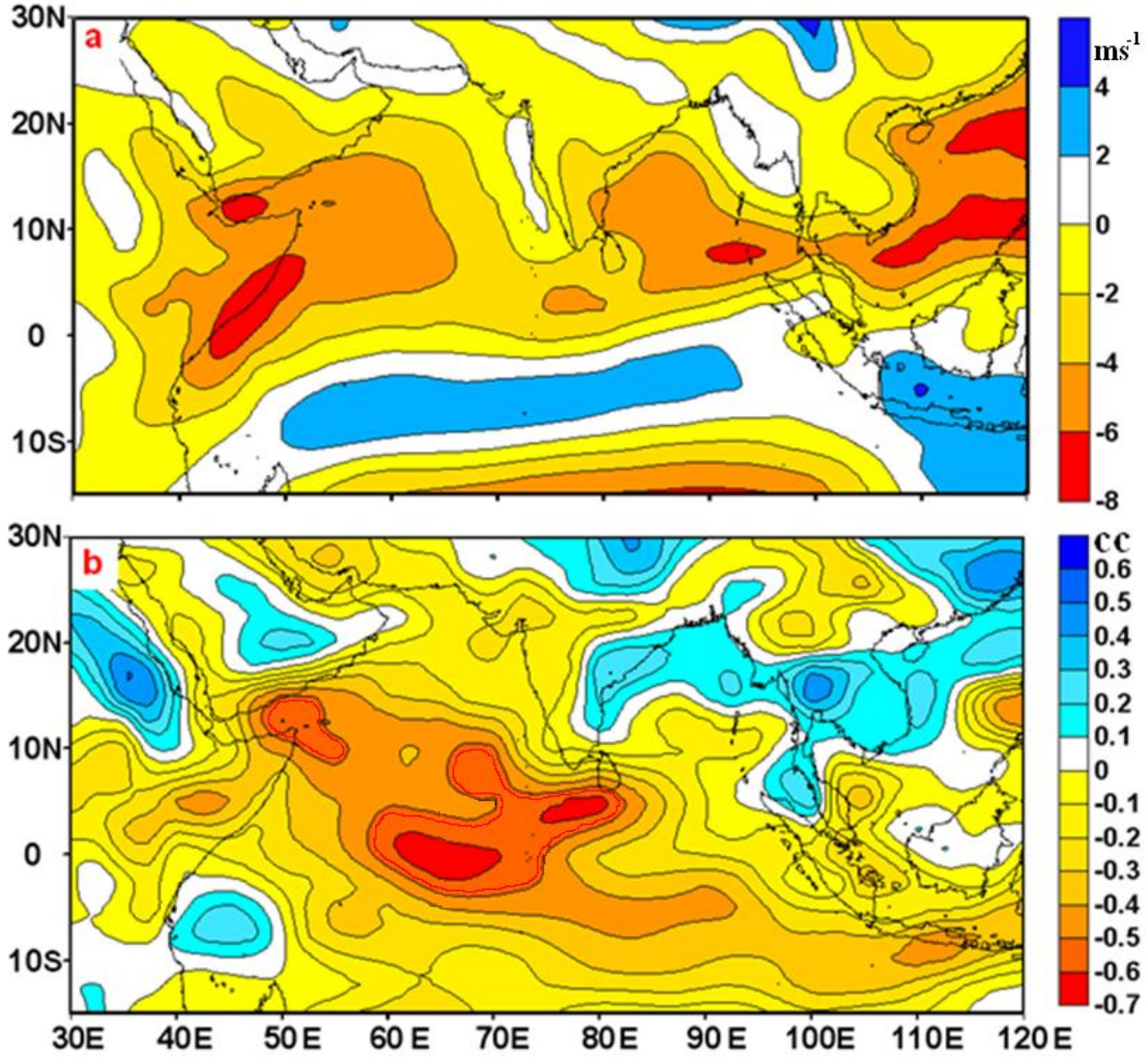

Figure 5.5: Surface mean zonal wind (m/s) for January (a) and correlation between JJAS total precipitation over the Maldives and surface mean zonal wind for January (b), from 1979 to 2007. The red contour lines indicate areas of significant correlation (1% level). The negative/positive values of zonal wind indicates easterly/westerly direction, respectively.

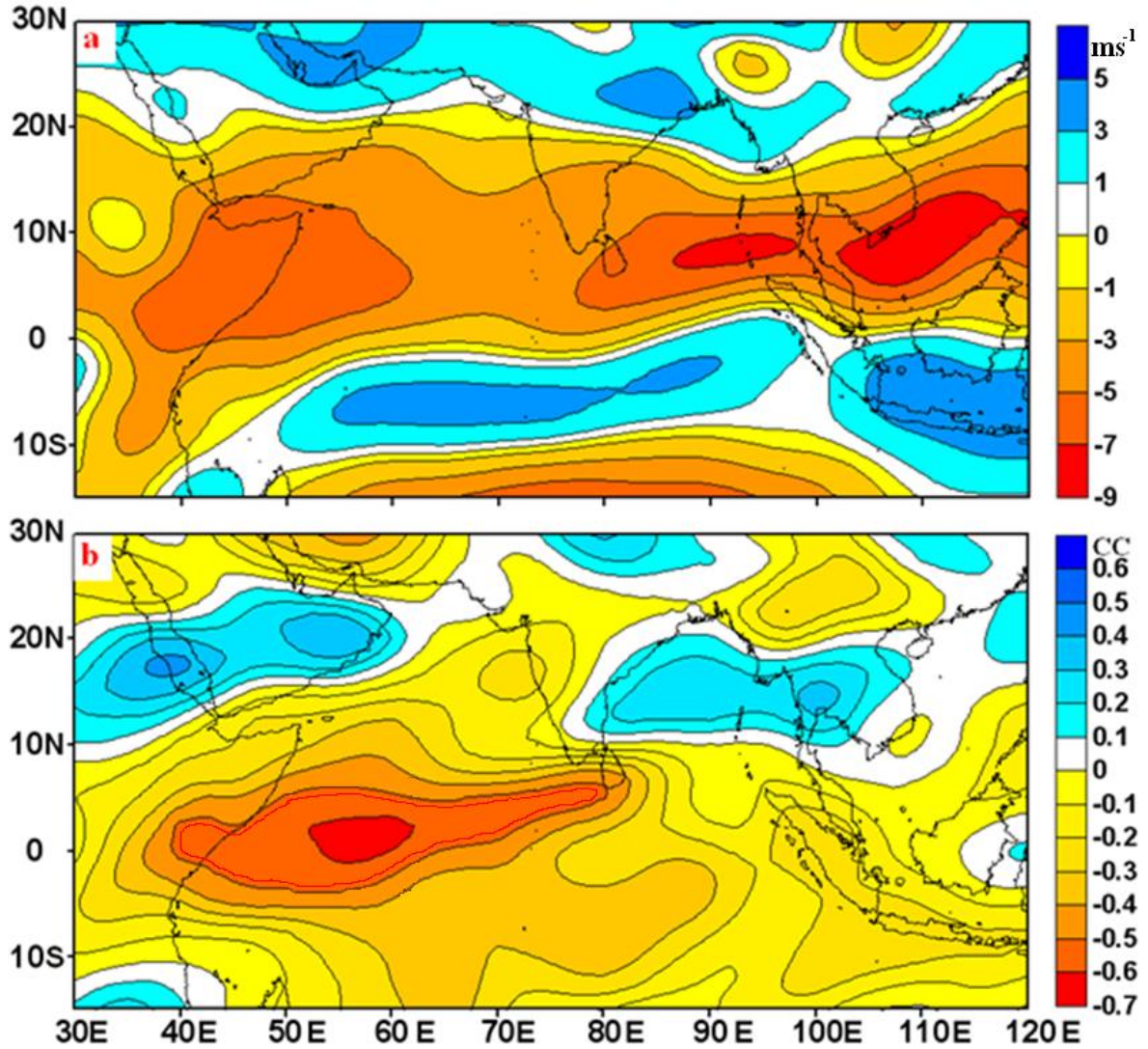

Figure 5.6: 850 hPa mean zonal wind (m/s) for January (a) and correlation between JJAS total precipitation over the Maldives and 850 hPa mean zonal wind for January (b), from 1979 to 2007. The red contour lines indicate areas of significant correlation (1% level). The negative/positive values of zonal wind indicates easterly/westerly direction, respectively.

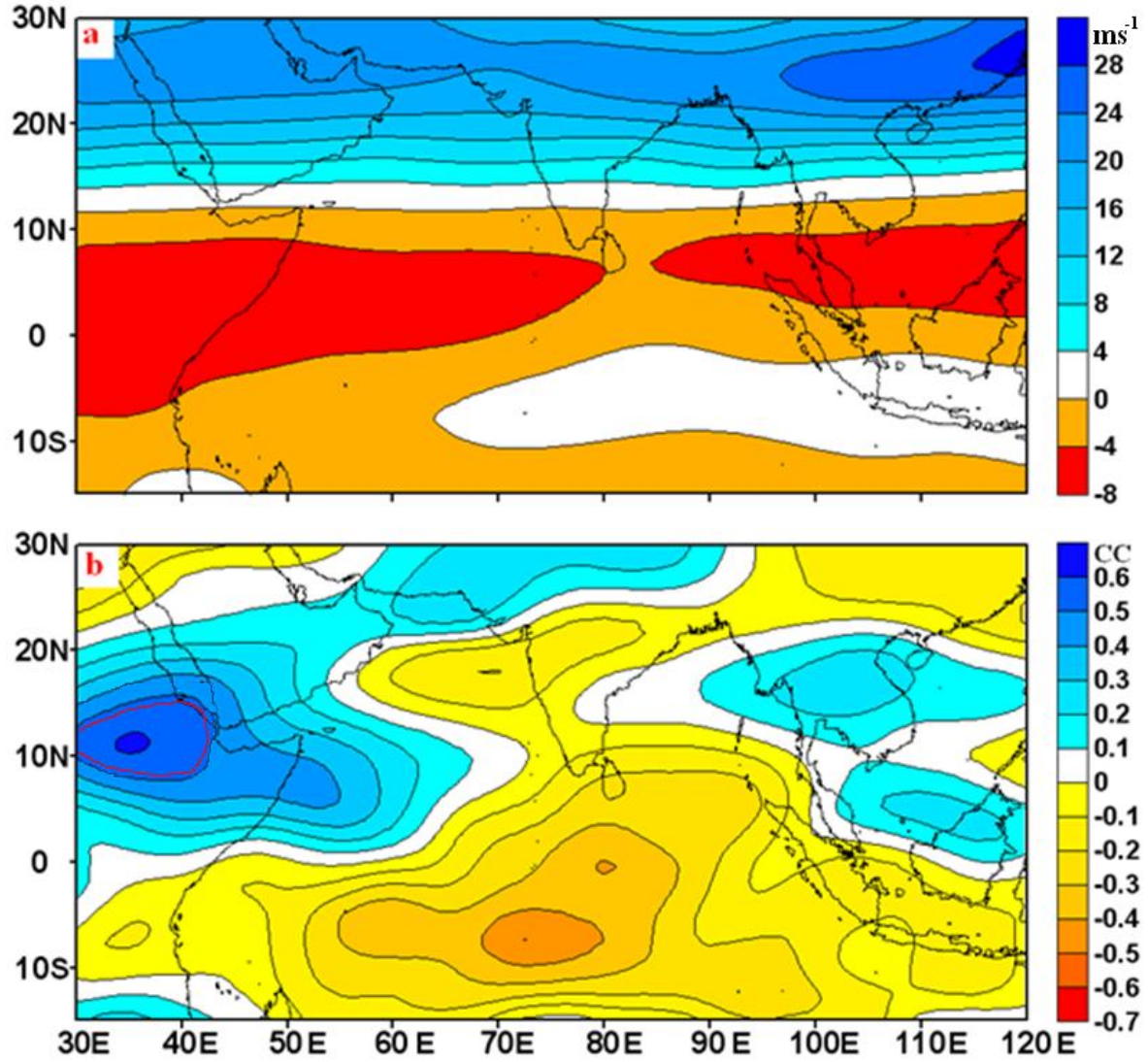

Figure 5.7: 500 hPa mean zonal wind (m/s) for January (a) and correlation between JJAS total precipitation over the Maldives and 500 hPa mean zonal wind for January (b), from 1979 to 2007. The red contour lines indicate areas of significant correlation (1% level). The negative/positive values of zonal wind indicates easterly/westerly direction, respectively.

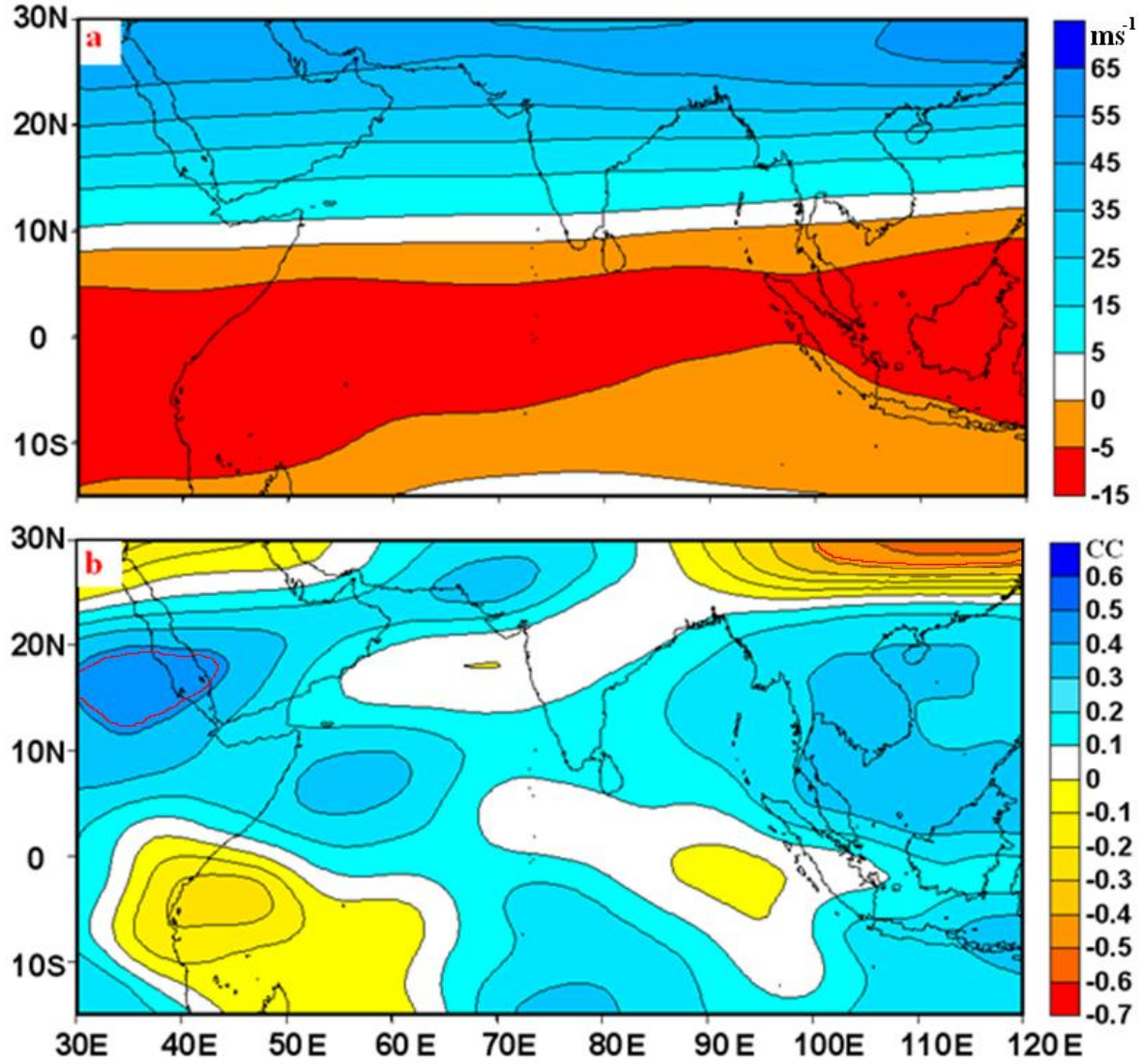

Figure 5.8: 250 hPa mean zonal wind (m/s) for January (a) and correlation between JJAS total precipitation over the Maldives and 250 hPa mean zonal wind for January (b), from 1979 to 2007. The red contour lines indicate areas of significant correlation (1% level). The negative/positive values of zonal wind indicates easterly/westerly direction, respectively.

Relative humidity near the surface hardly varies across the globe. The average relative humidity lies in the range of 65 to 85% and there is a general decrease of relative humidity with height (Clift and Plumb 2008), as shown in Figure 5.9. Manabe et al. (2004) pointed out that the decrease in precipitation in many semiarid regions of the world is due to the decrease in relative humidity in the lower troposphere. Gadgil (2008) suggested that the relative humidity of surface air over the tropical oceans is about 80% and this also can be seen from Figure 5.11a. April mean relative humidity is highest over the ocean, especially south of the equator and the northeastern part of the Indian Ocean and over China. As can be seen from Figure 5.11a, April mean relative humidity is quite low over

most of the Indian subcontinent and part of the African continent. The air over most of the Indian subcontinent is very dry during pre-monsoon months (Lal et al. 1995). Around mid-May, the low level monsoon circulation picks up moisture from the eastern Arabian Sea. As the monsoon current travels across the Arabian Sea, the moist layer deepens due to an increase in moisture absorption, resulting in cloud development and hence an increase in precipitation. Using the distribution of the relative humidity difference between the excess and deficit rainfall seasons over India, it has been shown that the air above the sea surface contains more moisture over the Arabian Sea and small areas of the southern Indian Ocean (65 °E, 90 °E and 100 °E) (Mohanty and Ramesh 1993). An increase in moisture associated with the monsoon circulation over the Indian region also has been supported by model-simulated relative humidity at 850 hPa during the months of April and July (Lal et al. 1995), as shown in Figure 5.10.

Figure 5.11-5.13 (a) show the mean relative humidity for the surface (April), 850 hPa (May) and 500 hPa levels (May), respectively for the Asian region, while Figure 5.11-5.13b show corresponding spatial correlations between relative humidity over Asia and JJAS total rainfall over the Maldives region. May mean relative humidity (for all levels) is negatively correlated with the Maldives monsoon precipitation. The highest correlation between relative humidity and precipitation over the Maldives was found over the Arabian Sea region (52.5-65 °E; 10-15 °N: Figure 5.13b) in the month of May (500 hPa mean relative humidity), with CC = -0.59, significant at 1% level (Table 5.1). The highest correlation for the 850 hPa level mean relative humidity was observed over the eastern Indian Ocean (92.5-97.5 °E; 0-5 °N: Figure 5.12b), with a CC of -0.56, significant at 1% level. The southeast Indian Ocean (107.5-120 °E; 2.5 °S-5 °S) shows the highest correlation between April surface mean relative humidity (Figure 5.11) and the JJAS total rainfall over the Maldives, with a CC of 0.53, significant at 1% (Table 5.1). In addition to these levels (surface, 850 and 500 hPa), 250 hPa level relative humidity for the months of January, February, March, April and May were also correlated with the JJAS total rainfall over the Maldives. No significant correlation was found between these parameters.

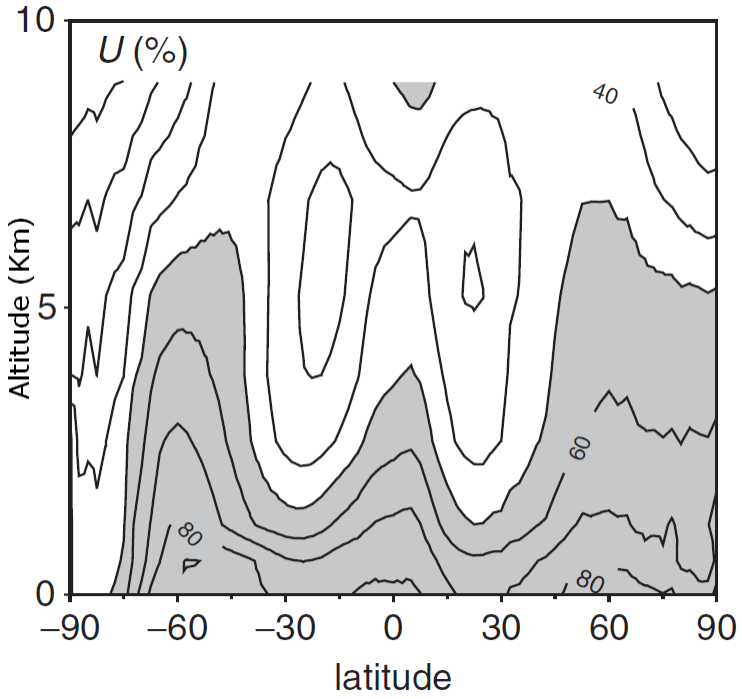

Figure 5.9: Global climatological zonal-mean relative humidity (%), values greater than 50% are shaded. Taken from Clift and Plumb (2008), Figure 1.3).

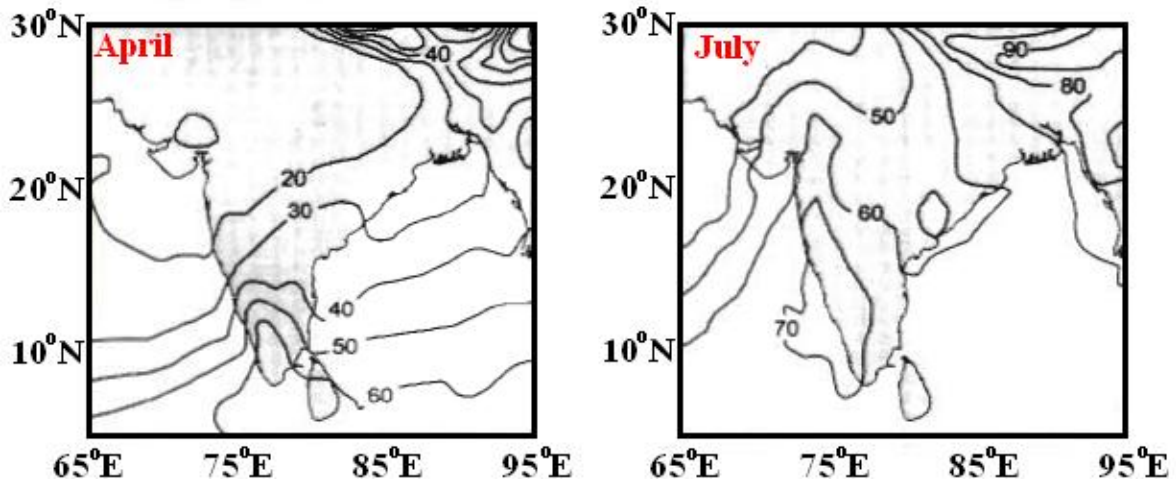

Figure 5.10: Model-simulated spatial distribution of the 850 hPa relative humidity for the months of April and July for the Indian region. Taken from Lal et al. (1995), Figure 4).

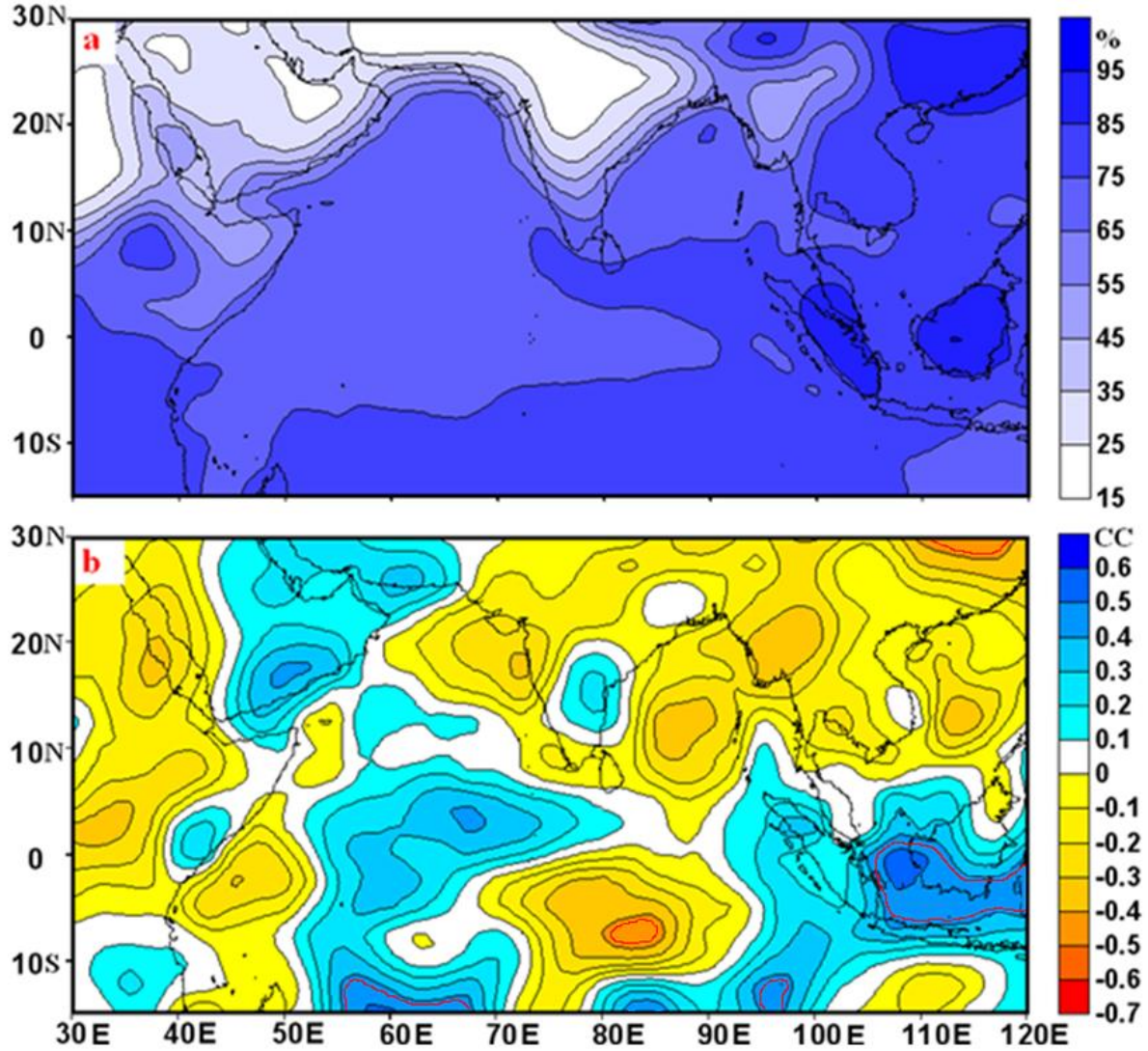

Figure 5.11: Surface mean relative humidity (%) for April (a) and correlation between JJAS total precipitation over the Maldives and surface mean relative humidity for April (b), from 1979 to 2007. The red contour lines indicate areas of significant correlation (1% level).

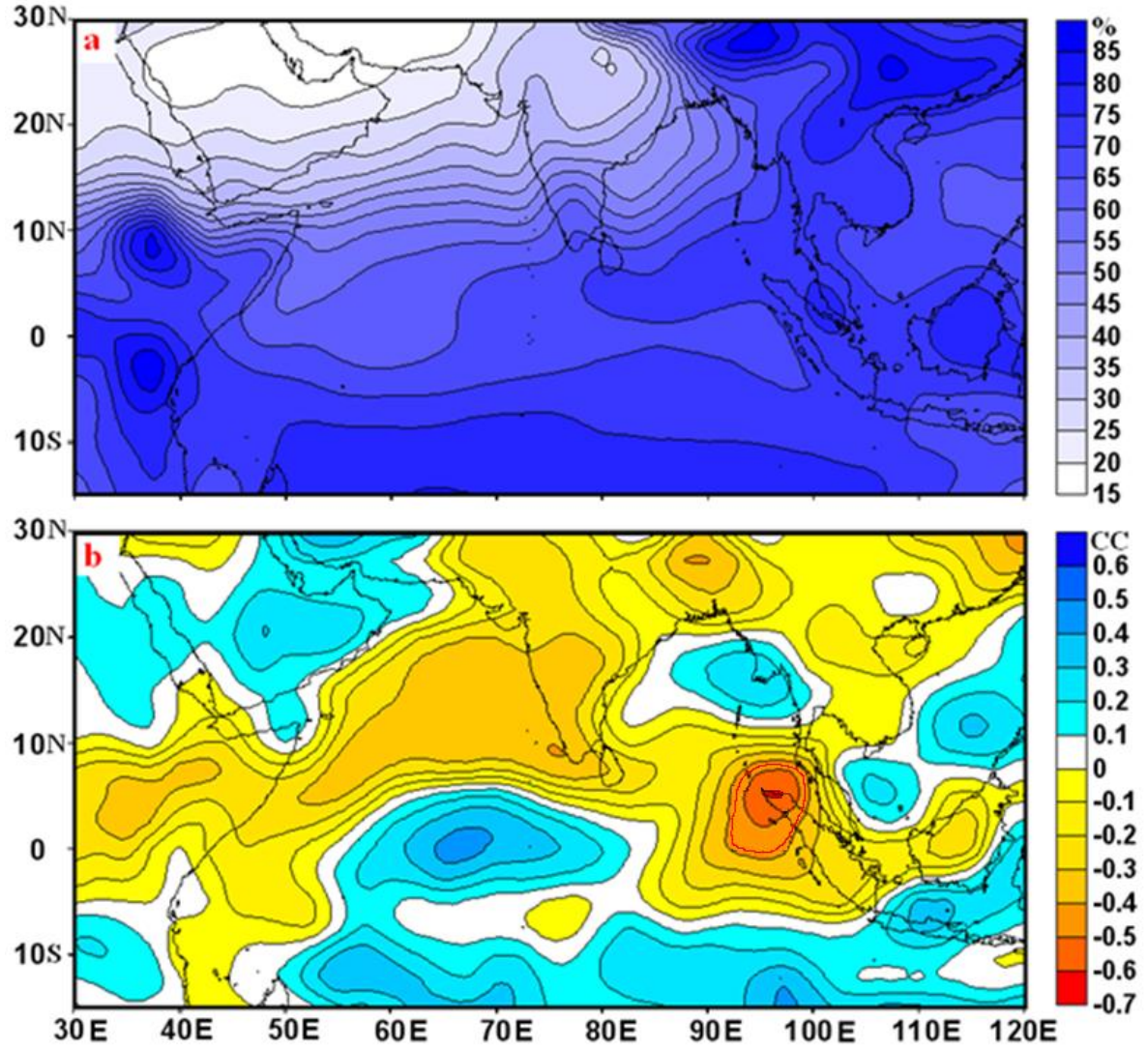

Figure 5.12: 850 hPa mean relative humidity (%) for May (a) and correlation between JJAS total precipitation over the Maldives and 850 hPa mean relative humidity for May (b), from 1979 to 2007. The red contour lines indicate areas of significant correlation (1% level).

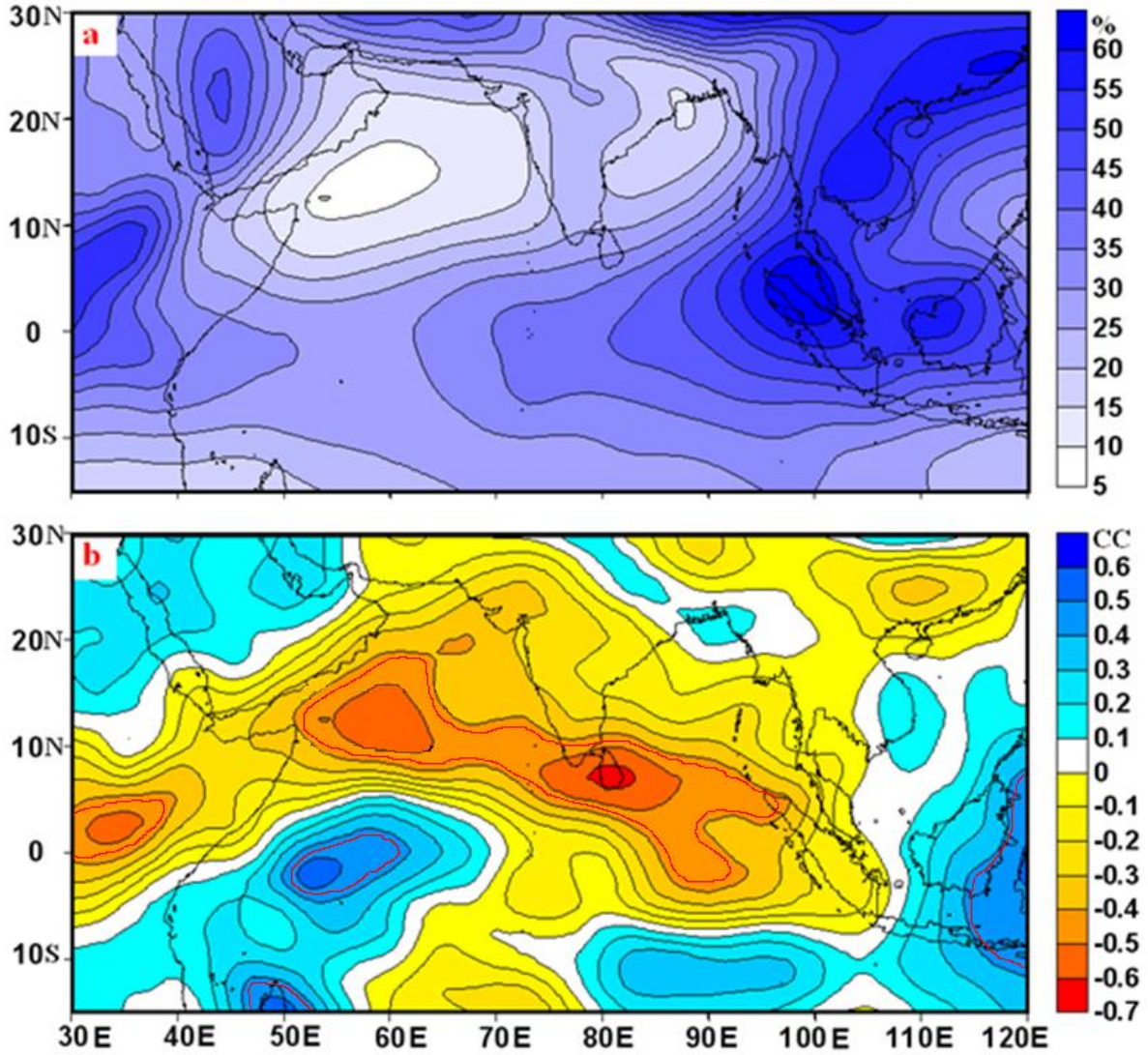

Figure 5.13: 500 hPa mean relative humidity (%) for May (a) and correlation between JJAS total precipitation over the Maldives and 500 hPa mean relative humidity for May (b), from 1979 to 2007. The red contour lines indicate areas of significant correlation (1% level).

5.3 Temporal consistency of correlations

Figure 5.14 shows the year-to-year standardised JJAS total rainfall over the Maldives, as well as the other meteorological parameters discussed above, depicting their interannual variability. The time series are standardised based on the mean and standard deviation of the whole data period (1979-2007). As is depicted in the figure, most of the time series show year-to-year random fluctuations. However, it should be noted that there appears to be signs of an epoch of positive anomalies of rain, together with the May mean sea level pressure (Figure 5.14a) and April surface mean relative humidity (Figure 5.14f) from 1992 to 1998. On the other hand, January surface zonal wind shows an epoch of negative anomalies (Figure 5.14e) for the same period.

Correlation between parameters can change from one period to another. It is essential to examine the temporal consistency of correlation between predictor variables, before using as new predictor parameter in a forecast model (Kumar et al. 1997). In order to assess the variability of the correlation coefficient (CC) between JJAS total rainfall over the Maldives and the parameters used above, the time series of these parameters were divided into six different time periods (1979-1988, 1989-1998, 1999-2007, 1979-1998, 1989-2007 and 1979-2007: Table 5.2) to see whether the influence of these parameters changes over time. The correlation between JJAS total rainfall over the Maldives and other parameters varies for different periods, as depicted in Table 5.2. It should be noted that the last column in Table 5.2 is the same as the last column in Table 5.1. It is interesting to note that the correlations between rainfall over the Maldives and the parameters (except surface air temperature) are significant for the period 1979-1998 (Table 5.2, column 6). Parameters sea level pressure, zonal wind and relative humidity are significant at the 1% level, while parameters sea surface temperature and outgoing longwave radiation are significant at the 5% level (Table 5.2, column 6). It is also worth pointing out that none of the parameters are significant for all the time periods considered, indicating temporal inconsistency of correlations between parameters and monsoon rainfall over the Maldives. However, it should be noted that the longer the period, more of the parameters are significantly correlated with the monsoon precipitation over the Maldives. Although the significance of correlations changes between different time periods, signs of the relationship (from positive to negative or from negative to positive) do not change (Table 5.2). Changes in the correlation coefficients over different periods may be related to the slow varying large-scale changes in the monsoon circulation (Kumar et al. 1997).

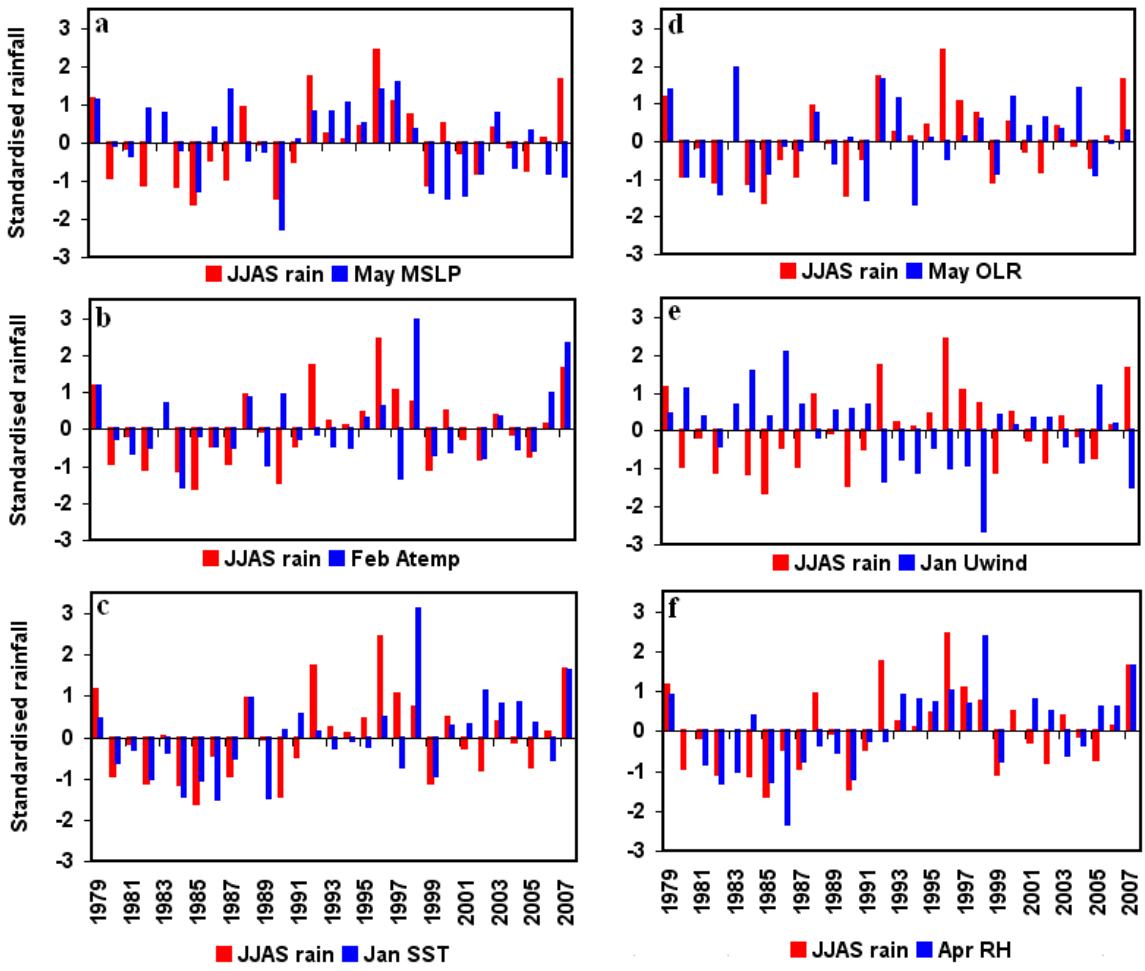

Figure 5.14: Time series of standardised rainfall (red bar) with other standardised parameters: (a) May mean sea level pressure (MSLP), (b) February mean surface air temperature (Atemp), (c) January mean sea surface temperature (SST), (d) May mean outgoing longwave radiation (OLR), (e) January surface mean zonal wind (Uwind) and (f) April surface mean relative humidity (RH).

Table 5.2: Correlation coefficients (CCs) between parameters and JJAS total rainfall for different time periods.

Parameters	Level/month	CCs 1979-1988	CCs 1989-1998	CCs 1999-2007	CCs 1979-1998	CCs 1989-2007	CCs 1979-2007
Sea level pressure	Surface/May	0.26	0.79**	0.02	0.57**	0.59**	0.42*
Air temperature	Surface/February	0.77**	0.03	0.82**	0.32	0.31	0.44*
Sea surface temperature	Surface/January	0.83**	0.13	0.55	0.46*	0.21	0.45*
Outgoing long wave radiation	Top of atmosphere/May	0.76	0.32	0.39	0.50*	0.28	0.46*
Zonal wind	Surface/January	-0.23	-0.61	-0.78*	-0.59**	-0.69**	-0.62**
	850 hPa/January	-0.47	-0.69*	-0.31	-0.70**	-0.63**	-0.64**
	500 hPa/January	0.50	0.69*	0.30	0.61**	0.63**	0.55**
	250 hPa/January	-0.67*	-0.42	-0.27	-0.57**	-0.40	-0.52**
Relative humidity	Surface/April	0.38	0.50	0.49	0.56**	0.50*	0.53**
	850 hPa/May	-0.73*	-0.63	-0.67*	-0.63**	-0.44	-0.56**
	500 hPa/May	-0.41	-0.75*	-0.22	-0.67**	-0.59**	-0.59**

**** Significant at 5% level; ** Significant at 1% level.***

5.4 Relationship between various parameters and monsoon rainfall for sub-regions of Asia

Previous studies have investigated the spatial coherence of the correlation coefficients between various parameters and rainfall over India (Clarke et al. 2000; Nayagam et al. 2008; Prasad et al. 2000). The high correlation coefficients are located over

northwestern and central India, while the lowest correlation coefficients are located over northeast and the western peninsula of India. Rainfall in some areas of India has negligible correlation with that in some other parts of India, suggesting rainfall is not spatially homogeneous. For example, India summer monsoon rainfall (India taken as a single unit) is significantly correlated with the regional rainfall of northwest and central India, but a very weak relationship exists over the southern part of the peninsula and to the northeast (windward side of the Western Ghats and the Himalayas) (Nayagam et al. 2008). Correlation analysis carried out here shows that core monsoon season (JJAS) total rainfall over the Maldives is significantly correlated with the JJAS total rainfall for the whole Asian region and Western Ghats (WG) region of the Indian west coast (CC = 0.50 and 0.59, respectively, significant at 1%). No significant relation exists between JJAS total rainfall over the Maldives and other sub-divisions of Asia (see Figure 4.28). In order to see whether the parameters used above correlate with the JJAS total rainfall for the Asian region as a whole and sub-regions of Asia (Western Ghats, Bay of Bengal, East Asia and central India: see Figure 4.28 for these regions), a correlation analysis was carried out. The only parameters that significantly correlate with the JJAS total rainfall for the Asian region as a whole are the surface air temperature and sea surface temperature with a CC of 0.66 and 0.42 (significant at 1%), respectively. It is interesting to note here that most of the parameters show significant correlation with the WG region rainfall (Table 5.3), and a maximum correlation with the surface air temperature (CC = 0.59), significant at 1% level. It is also worth noting that the parameters (sea level pressure, air temperature, sea surface temperature, outgoing longwave radiation, zonal wind and relative humidity) have no significant correlation with total rainfall for BoB, EA and CI (Table 5.3).

Table 5.3: Correlation between various parameters and JJAS total rainfall for different regions (ASIA = as a whole, WG = Western Ghats, BoB = Bay of Bengal, EA= East Asia and CI = central India: see Figure 4.28 for these regions).

Parameters	Level/month	ASIA	WG	BoB	EA	CI
Sea level pressure	Surface/May	0.08	0.25	-0.07	-0.05	-0.14
Air temperature	Surface/February	0.66**	0.59**	0.23	0.01	0.27
Sea surface temperature	Surface/January	0.42*	0.43*	0.20	-0.14	0.06
Outgoing long wave radiation	Top of atmosphere/May	0.31	0.22	0.15	-0.10	-0.23
Zonal wind	Surface/January	-0.22	-0.39*	-0.04	0.20	0.03
	850 hPa/January	-0.24	-0.29	-0.03	0.21	0.13
	500 hPa/January	0.35	0.46*	0.21	-0.04	-0.06
	250 hPa/January	-0.09	-0.39*	-0.11	0.26	0.15
Relative humidity	Surface/April	0.35	0.44*	0.06	-0.03	0.05
	850 hPa/May	-0.28	-0.26	-0.13	0.21	0.11
	500 hPa/May	-0.09	-0.24	-0.04	0.21	0.20

**** Significant at 5% level; ** Significant at 1% level.***

5.5 Regression model for the prediction of monsoon rainfall for the Maldives

Seasonal prediction of monsoon precipitation over the Asian-Australian region remains one of the most challenging tasks in climate prediction (Wu and Li 2008). The most commonly used method for the prediction during the last 100 years has been through the use of empirical and statistical models (Cannon and McKendry 1999; Pai and Rajeevan 2006; Rajeevan et al. 2007). According to Nayagam et al (2008), prediction of monsoon precipitation over a small area or shorter periods is difficult and use of statistical methods has become necessary. In 1909, Sir Gilbert Walker formulated a linear regression model based on correlation and regression analysis for the prediction of the Indian summer monsoon (Gadgil et al. 2005). In recent years, use of statistical models such as linear regression has become very common for forecasting of monsoon rainfall on various time scales: interannual, intraseasonal, monthly or even weekly time scales. Most of these models use a linear combination of one or more predictors with precipitation (Cannon and McKendry 1999).

Here an attempt is made to predict the core monsoon season (June-September) precipitation over the Maldives by using multiple linear regression. This is the first attempt to formulate a linear regression model for the prediction of Maldives monsoon rainfall (MMR). According to Nayagam et al. (2008), development of a regression model includes: (1) the selection of predictors based on empirical relations between various parameters and precipitation, (2) their careful and optimum selection in a stepwise regression analysis, (3) formulation of the regression equation and (4) verification of the model with independent samples. These steps are described in the following sections.

5.5.1 Selecting predictors based on empirical relationships with Maldives monsoon rainfall (MMR)

To identify the parameters that may have predictive potential for Maldivian monsoon rainfall (MMR), correlation coefficient maps between MMR and other parameters were prepared for the period 1979-2007. The most significant and influential parameters for inter-annual variability of the Maldives monsoon rainfall are mean sea level pressure for May, surface air temperature for February, outgoing longwave radiation for May, sea surface temperature for January, surface and 850, 500 and 250 hPa zonal wind for January, surface relative humidity for April, and 850 and 500 hPa level relative humidity for May. Figure 5.15 shows the geographical distributions of these parameters. The parameter grid

points within the grid boxes shown in the figure are significant to at least the 5% level and do not include any non-significant grid points. These significant boxes were averaged for computing parameter indices (area averages of the parameter over the respective significant area) and to form corresponding time series. The temporal consistency of these parameters with the MMR was checked for different time periods, as depicted in Table 5.2. Temporal inconsistency can be seen for the shorter periods, compared with the longer periods. Hence, parameters that have a significant CC at the 5% level for longer time periods (1979-1998 and 1979-2007) were retained. The parameter selected were: (1) mean sea level pressure for May, (2) outgoing longwave radiation for May, (3) sea surface temperature for January, (4) surface zonal wind for January, (5) 850 hPa zonal wind for January, (6) 500 hPa zonal wind for January, (7) 250 hPa zonal wind for January, (8) surface relative humidity during April, (9) 850 hPa relative humidity during May and (10) 500hPa level relative humidity during May, as presented in Table 5.4. These parameter time series were used to formulate a regression model to predict core monsoon rainfall for the Maldives.

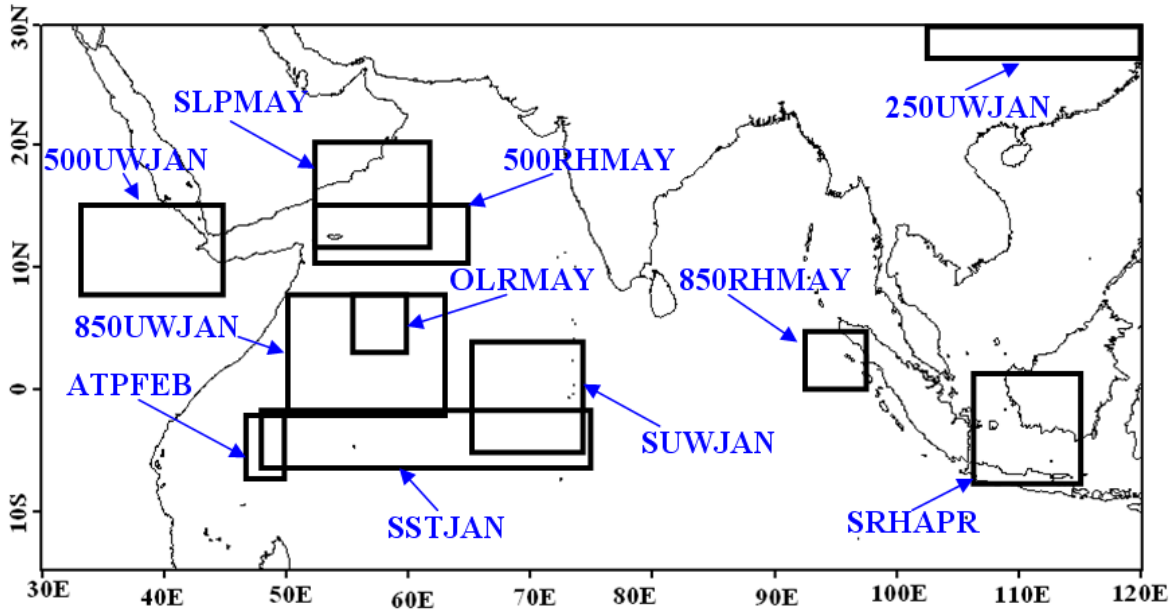

Figure 5.15: Geographical locations of the indices derived from the correlation analysis: SLPMAY = mean sea level pressure for May, ATPFEB = surface air temperature for February, OLRMAY = outgoing longwave radiation for May, SSTJAN = sea surface temperature for January, SUWJAN = surface zonal wind for January, 850UWJAN = 850 hPa level zonal wind for January, 500UWJAN = 500 hPa level zonal wind for January, 250UWJAN = 250 hPa level zonal wind for January, SRHAPR = surface relative humidity for April, 850RHMAY = 850 hPa level relative humidity for May and 500RHMAY = 500 hPa level relative humidity for May.

Table 5.4: Predictors used for the stepwise regression analysis.

Parameters	Level/month	CCs 1979-1998	CCs 1979-2007
Sea level pressure	**Surface/May**	**0.57****	**0.42***
Sea surface temperature	**Surface/January**	**0.46***	**0.45***
Outgoing long wave radiation	**Top of atmosphere/May**	**0.50***	**0.46***
Zonal wind	**Surface/January**	**-0.59****	**-0.62****
	850 hPa/January	**-0.70****	**-0.64****
	500 hPa/January	**0.61****	**0.55****
	250 hPa/January	**-0.57****	**-0.52****
Relative humidity	**Surface/April**	**0.56****	**0.53****
	850 hPa/May	**-0.63****	**-0.56****
	500 hPa/May	**-0.67****	**-0.59****

5.5.2 Regression analysis

Regression analysis is a statistical empirical technique that is widely used in many disciplines, including climate prediction (Zaw and Naing 2008). This technique utilizes the relationship between two or more quantitative variables (independent and dependent) from an observational database so that an outcome variable (dependent) can be predicted through a mathematical equation, a regression model. Multiple regression is an extension of simple, bi-variate regression, it allowing additional factors to enter the analysis separately so that the effect of each can be estimated (Hair et al. 2006; Pallant 2007). There are a number of different types of multiple regression, with the three main types being standard or simultaneous, hierarchical or sequential and stepwise (Pallant 2007). Most commonly used

method of multiple regression is performed using the stepwise method (details provided in Chapter 2).

For the medium-range forecasting of the Maldives monsoon rainfall (MMR), time series of the ten predictor candidates identified above (Table 5.4) were used as the input to a stepwise regression analysis, with the Maldives monsoon rainfall (MMR) as the predictant. DelSole and Shukla (2002) pointed out that no unique regression equation exists for a fixed set of predictors and argued that the model should be limited to as small a number of predictors as possible, and suggested that a large number of predictors in a model should to lead to artificial skill and poor forecasts of the independent data. Statistically derived prediction equations are developed from a number of predictors, and these equations are subjected to sampling errors (in practice the sample size is always limited). The sampling errors increase as the number of predictors increase. As more and more predictors are used in the regression model, these sampling errors give the impression that the model fits the data better and better. The aim of the regression model is not to fit the dependent data exactly, but to predict or forecast new independent data (DelSole and Shukla 2002). Furthermore, according to Rajeevan et al. (2004) about 8–10 predictors are required to explaining a good amount of variation (70–75%) in the model development period, and also to keep the root mean square error (RMSE) of the results over the independent period to a minimum. On the other hand, some studies suggested that three or four predictors are adequate to develop a statistical model with useful predictive skill for monsoon forecasting and that the regression models that utilize two-four predictors produced better forecasts on average than the model that utilizes a large number of predictors (DelSole and Shukla 2002; Rajeevan et al. 2007).

According to Draper and Smith (1981) stepwise regression analysis reduces the dimensionality of parameters/indices. The backward stepwise regression method uses the amount of unique variance a predictor adds to the complete model (all remaining predictors) as the criterion for exclusion from the model. In this method, the full model (with all predictor variables included) is computed first. Secondly, the predictor variable that causes the least reduction in accounted variance by its removal from the model is eliminated. This stepping is continued until all remaining predictors contribute a significant amount of unique variance to the final multiple regression model. Before applying the backward regression, the multiple linear regression assumptions (linearity, independence of residuals, homoscedasticity and normality of residuals) outlined in Section 2.4.1 were checked.

5.5.3 Assumptions

Although atmospheric processes are not linear, linearity of the model is ensured since the parameters entered into the regression analysis were identified through linear correlation analysis (Nayagam et al. 2008). Independence of the residuals was tested by the Durbin–Watson (DW) statistic and expressed as (Nayagam et al. 2008):

$$DW = \frac{\sum_{t=2}^{n}(e_t - e_{t-1})^2}{\sum_{t=1}^{n} e_t^2}$$

where e_t is the residual at the time t and e_{t-1} that at time $t-1$. This statistic checks the significance of the assumption that the residuals for successive observations are uncorrelated. The DW value ranges from 0 to 4; a value above 2 suggests that there exists some negative autocorrelation, while a value below 2 indicates existence of a positive autocorrelation. The DW value computed here is 2, suggesting that lag 1 autocorrelation does not exist and the assumption of independence of the residuals is not violated. The constant variance property (homoscedasticity) of the residuals is assessed using residual plots. If there is an organized pattern in the residuals, it means that there is a relationship between the fitted values and the residuals (Nayagam et al. 2008). The residual plots (standardised residuals vs. standardised predicated values) do not show (figure not shown) any organised pattern, indicating that the homoscedasticity assumption is met. The assumption of normal distribution of the errors was checked by visual examination of the normal probability plots of the residuals. The normal probability plots of the residuals (expected vs. observed: figure not shown) shows that the values fall along the diagonal with no substantial or systematic departure. This suggests that the assumption of normality of the error term is met. All the four assumptions evaluated here indicate that the assumptions are not violated, so that assumptions of linearity, independence of residuals, homoscedasticity and normality of residuals can be accepted.

Nayagam et al.(2008) stated that the inter-correlation between the predictors leads to multicolinearity (the parameters are non-orthogonal) and suggested that the model lacks accuracy if multicolinearity exists between the variables, and may lead to unclear interpretation of the regression coefficients. A high degree of multicolinearity produces unacceptable uncertainty (large variance) in the regression coefficient estimates. As multicolinearity increases, the interpretation of the model becomes more complicated because it is more difficult to ascertain the effect of any single variable, owing to their

interrelationships (Hair et al. 2006). In order to reduce complexity and to increase the reliability of the parameters in the prediction, the multicolinearity was studied. The easiest way to check colinearity is to examine the correlation matrix of the predictor variables, with correlation > 0.90 and higher indicating substantial colinearity (Hair et al. 2006). The correlation matrix between the variables suggests that they are not significantly inter-correlated with each other (correlations not shown). The multicolinearity is also studied here using the variance inflation factor (VIF) method, defined as (Nayagam et al. 2008):

$$VIF(a_i) = \frac{1}{1 - r_i^2}$$

Where r_i^2 is the unadjusted r^2 when predictors are regressed against all other explanatory variables in the model. According to Nayagam et al. (2008), the VIF measures how much the variance of the estimated coefficients are inflated compared to the situation when the independent variables are uncorrelated, and a VIF greater than 10.0 could significantly affect the stability of the regression coefficients. The computed VIF for the predictors are presented in Table 5.5, which suggests that only very weak multicolinearity exists.

Since all the assumptions were met, using a backward stepwise elimination method, predictors with less influence in the variance of MMR were eliminated (Nayagam et al. 2008) and the predictors that explained a significant amount of variance in the MMR were retained to formulate the regression equation.

5.5.4 Formulation of regression equation

The above analysis led to the identification of the ten predictors that are potential predictors for the MMR. The time series of the core monsoon season rainfall (June-September) and the ten predictor candidates identified above were derived for the period 1979-1998 as the training period for formulating the regression equation. The remaining nine years' data (1999-2007) were used as the testing period (for the independent verification of the model), in the next section. After eliminating the predictors with less influence in the variance of MMR, the predictors that explained a significant amount of variance in the MMR were surface relative humidity during April (SRHAPR), 850 hPa level relative humidity during May (850RHMAY) and 500 hPa relative humidity for May (500RHMAY). The final regression model derived from the backward regression analysis is:

$$\boldsymbol{MMR = 14.4SRHAPR - 26.3RHMAY_{850} - 12.7RHMAY_{500} + 1689.4}$$

where MMR is Maldives monsoon rainfall (June-September total rainfall), SRHAPR is surface relative humidity for April, $RHMAY_{850}$ is 850 hPa level relative humidity during May and $RHMAY_{500}$ is 500 hPa relative humidity for May. As the model suggests, the MMR is positively related to the April mean surface relative humidity, while May mean relative humidity at 500 and 850 hPa level are negatively related. It is worth noting that the latter two parameters are located over the Arabian and Indian Oceans, respectively and the month of May is the pre-monsoon month for India. The mean relative humidity at 500 hPa level shown in Figure 5.13a indicates that the parameter ($RHMAY_{500}$) values entered for the model are low on average (mean relative humidity is less than 10%). On the other hand, $RHMAY_{850}$ values entered for the model are higher on average (mean relative humidity is greater than 70%) as shown in Figure 5.12a. As depicted in Figure 5.16, the mean relative humidity at the surface during the month of May for the regions used for the calculations of the parameter indices ($RHMAY_{850}$and $RHMAY_{500}$: see Figure 5.15) are greater than 70%. The mean surface relative humidity in this month over the Indian continent and Arabian Peninsula is quite low (average relative humidity is less than 30%). Although the relative humidity at upper levels (500 and 850 hPa level) in May is negatively related to the Maldives monsoon rainfall as suggested by the regression model above, the surface mean relative humidity in May indicates that the mean relative humidity over the Maldives region is in excess of 70%. This may be due to low level southwesterly winds bringing more moisture from the southern oceanic regions, leading to onset of the monsoon in the month of April/May and an increase in rainfall over the Maldives.

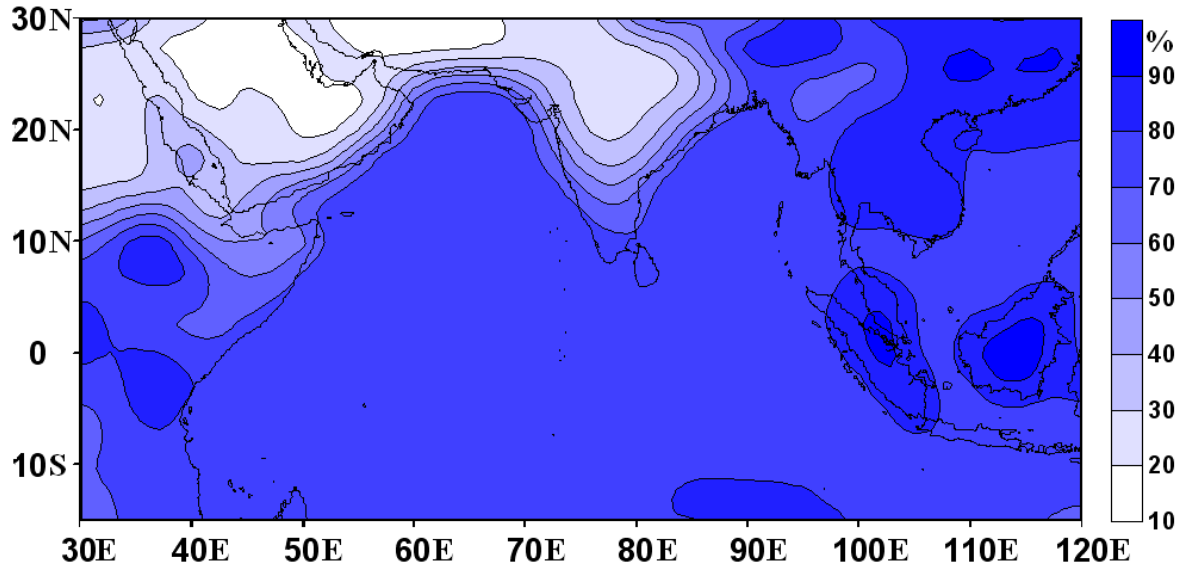

Figure 5.16: Surface mean relative humidity (%) for May, from 1979 to 2007.

Student's t-test was conducted to see whether the coefficients of the predictors ($SRHAPR$, $RHMAY_{850}$ and $RHMAY_{500}$) in the regression equation above are significant and the results are presented in Table 5.5. The t-test results indicate that the predictors in the regression equation are highly significant. The regression model above explains about 76.6% of the variation (adjusted r^2, which takes into account the number of predictors in the model and the number of observations the model is based on) in the dependent variable (Maldives monsoon rainfall) and has a multiple correlation coefficient of 0.90. The significance of the model was tested using the $\boldsymbol{F}$ statistic. The analysis of variance (ANOVA) gave a value of $\boldsymbol{F_{3,16}}$ = 21.7 and a very small p-value (<0.0001). The ANOVA test indicates the model is significant at 1% significance level. These tests strongly suggest that the predictors included in the model account for the significant part of the variance (76.6%) in the MMR and indicates the usefulness of the model for the long-range prediction of the MMR (Nayagam et al. 2008).

Table 5.5: Results of the t-test for the predictors used in the regression model.

Parameters	t-test	p-value	VIF
Surface relative humidity (April)	2.4	0.028	1.17
850 hPa level relative humidity (May)	-4.3	0.0006	1.05
500 hPa relative humidity (May)	-4.2	0.0007	1.15

5.5.5 Verification of the model

Validation or verification of the model is an important component of model construction, and the most recommended method of model validation is to construct the model using a subset of the data (training period) and to then test the model over the remaining period (test period) (Mason 1998; Wilks 1995). The above model was therefore constructed using the data for the period 1979-1998 as the training period and data for 1999-2007 were used as the testing period, for the independent verification of the model. The observed and forecasted JJAS rainfall for the training and test period and their corresponding standardized rainfalls are shown in Figure 5.17 (a and b, respectively), while Figure 5.18 shows the scatter plot of the observed and forecast MMR for the test period. The observed and the model forecast values of MMR appear to be in close agreement with each other. In general, Figure 5.18 indicates that if the observed rainfall is higher, the forecast MMR is also higher. It should be noted from Figure 5.17a that the MMR forecast by the model is higher than the observed MMR in all the years (except 2006, when rainfall forecast and observed values are almost the same) during the testing period. In some years the observed and forecast rainfall are out of phase, as depicted in Figure 5.17b. Although the observed MMR in 2000 was normal (rainfall within ± one standard deviation), the model forecast MMR in 2000 was above +1 S.D. (Figure 5.17b). During the test period, 2000 is the only year where the forecast MMR is above + 1 S.D., while the observed MMR is within ± 1 S.D. On the other hand, during the training period, 1980 forecast MMR is more than -1 S.D. when compared with the observed MMR, which is just within ± 1 S.D. In 1992 and 1997, the observed MMR are above +1 S.D., while the forecast MMR are within ± 1 S.D. (Figure 5.17b).

The model forecast performance was verified using the coefficient of correlation (CC) between observed and forecasted MMR, root mean square error (RMSE), mean absolute error (ABSE) and bias in the model forecast (BIAS) for the training and test period using the following equations (Munot and Kumar 2007; Rajeevan et al. 2007; Sadhuram and Murthy 2008):

$$RMSE = \sqrt{\frac{\sum (Y' - Y)^2}{n}}$$

$$ABSE = \sum |Y' - Y| / n$$

$$BIAS = \frac{\sum (Y' - Y)}{n}$$

where Y is the observed rainfall, Y' is the forecast rainfall and n the number of years. The computed statistics are depicted in Table 5.6. As can be seen from the correlation coefficients (CCs), a strong positive relationship exists between observed and model forecast rainfall for the training (model development period) and test period, with CC of 0.90 and 0.76, respectively, significant at 1% level. The CC was also calculated for the entire period (1979-2007) and the value dropped from 0.9 to 0.80, significant at 1% level. As can be seen from Table 5.6, the forecast appears to be positively biased for the entire period (BIAS = 26.1 mm), negatively biased for the training period (BIAS = -3.7 mm) and strongly positively biased for the test period (BIAS = 87.5). The root mean square errors (RMSE) for all the time periods are lower than their respective standard deviation (S.D.), except for the test period. RMSE for the test period is about twice that of the training period (Table 5.6). Furthermore, the mean absolute errors (ABSE) for all the periods are less than their respective S.D. Despite strong positive BIAS (87.5) in MMR for the test period, these statistics indicate that the model presented above (i.e. the regression equation) represents the interannual variability of MMR well and that it is useful in medium long-range forecasting of the MMR. As depicted in Figure 5.19, there are systematic epochal changes in rainfall and relative humidity (for the three levels). It is clear from Figure 5.19a, that the rainfall anomaly is positive for several years (from 1992-1998) before the model test period and then changes anomaly sign. Furthermore, the standardised surface relative humidity anomaly also shows the same pattern (i.e., positive anomaly from 1992 to 1998 and then changes to a negative anomaly: Figure 5.19b). Although, relative humidity at 850 hPa during the same period shows an overall positive anomaly for the same period, in some years (1992, 1996 and 1997) the anomaly is negative (Figure 5.19c). On the other hand, standardised relative humidity at 500 hPa for the same period (1992 to 1998) shows a negative anomaly and then the anomaly sign changes to positive (Figure 5.19d). The positive BIAS in the model forecast MMR for the test period (1999 to 2007) may be related to changes in the relative humidity regime around the late 1990s. Changes in relative humidity may again be due to changes in climatic factors, such as Eurasian snow cover (ESC) and winds in the Asian region. From the satellite data, a significant reduction in Eurasia snow cover has been observed since 1997 and it has been suggested that the winds in the Arabian Sea had increased during the southwest monsoon phase since 1997 due to

these changes (Lindsey and Simmon 2006). Decrease in snow cover has also been verified by Lindsey and Simmon (2006) with independent station observational air temperature data, concluding that the air temperature is increasing. Changes in the Eurasian snow cover and wind in the Arabian Sea since 1997 could have played a crucial role in redistributing the moisture in this region and hence relative humidity. This may have lead to the overestimation of the MMR by the model during the test period and may have caused positive BIAS (87.5) in the model for the test period.

Table 5.6: Measures of forecast performance.

Measures	Whole period	Training period	Test period
CC	0.80*	0.90*	0.76*
RMSE†	74.7	53.0	107.0
ABSE†	59.0	44.0	87.5
BIAS†	26.1	-3.7	87.5
Mean†	891.4	866.2	947.5
S.D†	111.6	111.4	94.9

Indicates significant at 1% level and † indicates that the measures are in mm.

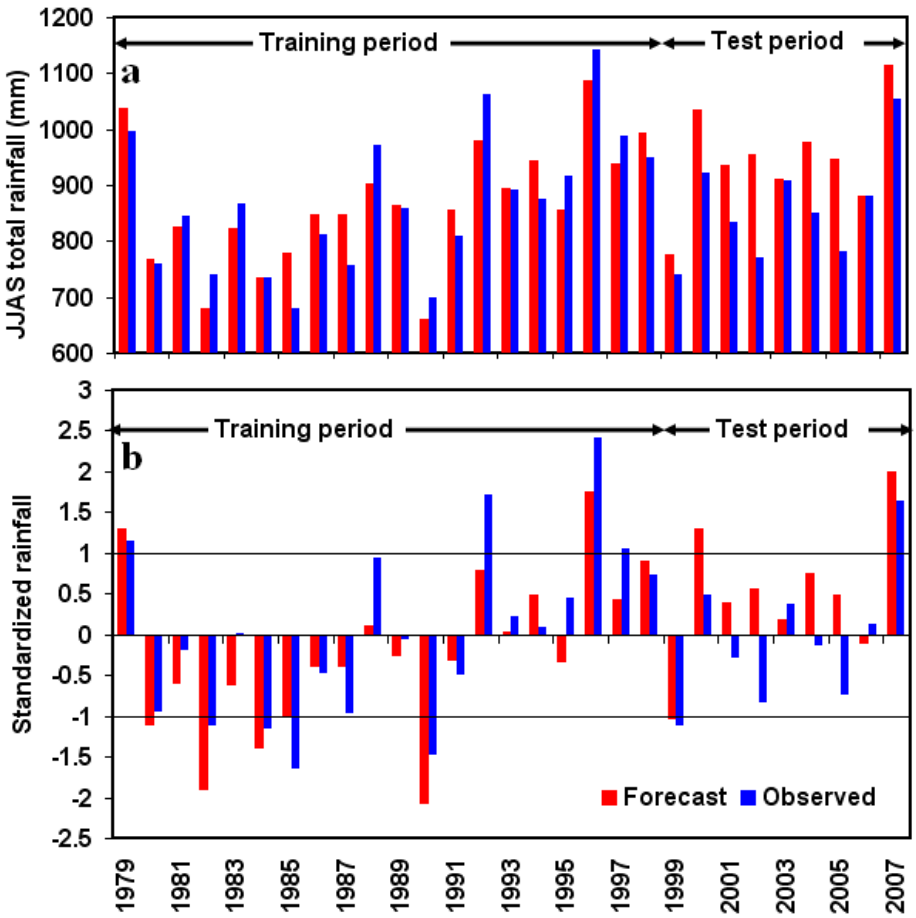

Figure 5.17: Observed (blue) and forecast (red) June-September (JJAS) total rainfall (a) and corresponding standardized rainfall (b) for the Maldives regions.

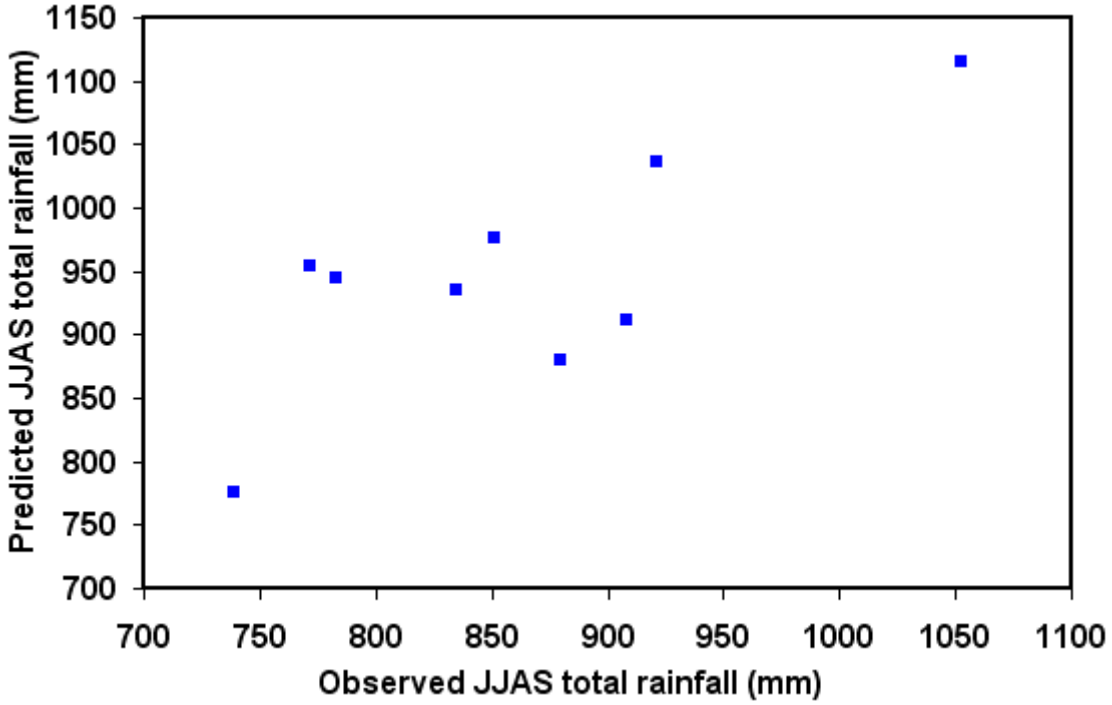

Figure 5.18: Scatter plot of observed and predicated June-September (JJAS) total rainfall for the test period (1999 to 2007).

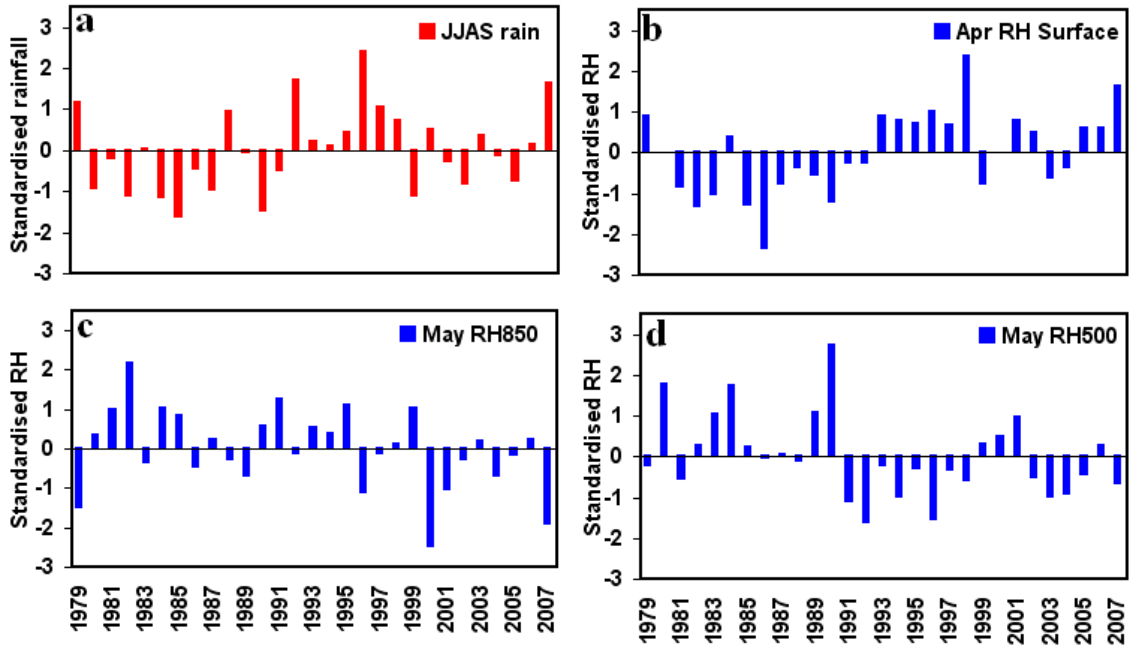

Figure 5.19: Time series of standardised: (a) June-September (JJAS) rainfall, (b) April surface mean relative humidity (Apr RH surface), (c) May 850 hPa level mean relative humidity (May RH850) and (d) May 500 hPa level mean relative humidity (May RH500), from 1979 to 2007.

5.6 Summary

This chapter investigated the relationship between spatio-temporal variability of monsoon precipitation over the Maldives and various meteorological parameters. The correlation results indicate that variability of the Maldives monsoon rainfall on interannual time scales is influenced by mean sea level pressure for May, February surface air temperature, outgoing longwave radiation (for May), January sea surface temperature, surface and 850, 500 and 250 hPa zonal wind for January, surface relative humidity for April, and May 850 and 500 hPa level relative humidity, which are significant at 5% level. These significant parameters are used as inputs to stepwise regression to develop a regression model for the prediction of core monsoon season (June-September) rainfall for the Maldives. The obtained regression model is significant at 1% significance level and explains about 76.6% of the variation in Maldives monsoon rainfall, indicating usefulness of the model for the prediction of monsoon rainfall before the monsoon season commences.

6 Monsoon circulation processes (global scale: ENSO)

The monsoon circulation may be viewed as the circulation responding to the annual cycle in the differential solar heating between ocean-atmosphere-land systems. Besides interactions between ocean-atmosphere-land systems, the monsoon circulations are influenced by other climate systems such as ENSO and the extra-tropical regime. The physical processes that govern the coupled and variable ocean-atmosphere-land systems are complex (Webster et al. 1998), as shown in Figure 6.1. The objective of this chapter is to investigate whether variations in the observed precipitation pattern over the Maldives are due to the global scale systems, such as ENSO. Regional scale systems, such as Eurasian snow cover and TBO that may influence the Maldives monsoon rainfall will be investigated in next Chapter.

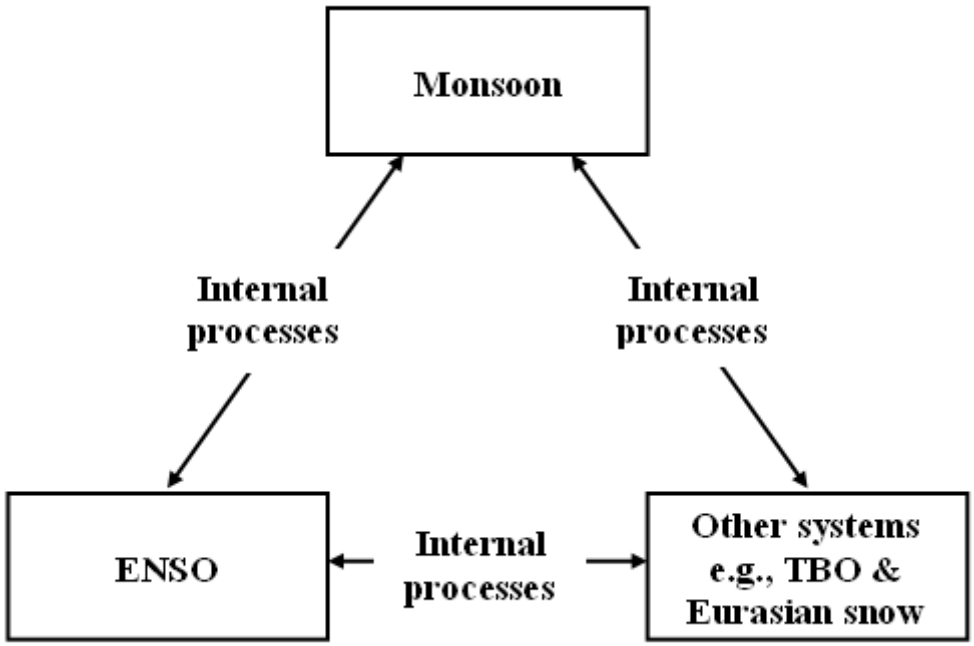

Figure 6.1: Schematic diagram showing possible relationships between the monsoon, the El Niño Southern Oscillation (ENSO), and other climate factors, such as the tropospheric biennial oscillation (TBO) and Eurasian snow cover. Modified from Webster et al. (1998).

6.1 The impact of El Niño-Southern Oscillation (ENSO) on Maldives monsoon rainfall variability

The El Niño-Southern Oscillation (ENSO) phenomenon is the strongest natural fluctuation of climate on interannual time-scales that influences the weather and climate around the globe (Stocker et al. 2001). Originally, the term "El Niño" (Niño means "the boy Christ-child" in Spanish) is recognised as a weak warm ocean current that flows southwards along the coast of Peru and Ecuador about Christmas-time (Guilyardi et al. 2009; Trenberth 1997). However, now it is applied to denote the large-scale warming in the tropical Pacific Ocean basin which occurs and alternates at an interval of 2-7 years with an opposite cold phase called "La Niña" ("the girl" in Spanish) (Guilyardi et al. 2009; Trenberth 1997). The atmospheric component of the El Niño-La Niña cycles is referred to as the "Southern Oscillation", which is associated with a large-scale tropical east-west seesaw pattern in sea level surface pressure over the southern Pacific. The phenomenon associated with atmosphere and ocean coupling in the tropical Pacific is often referred as El Niño-Southern Oscillation or simply ENSO (Guilyardi et al. 2009; Trenberth 1997). Due to the seasonal variation in El Niño and La Niña extreme phases, identification of El Niño and La Niña years is highly problematic (Trenberth 1997). According to Chou et al. (2003) and Wallace et al. (1998), due to the complexity of the ENSO evolution, there is no consensus on the definition of ENSO phases. Different indices or criteria have therefore been used to identify El Niño and La Niña events (Chou et al. 2003; Trenberth 1997; Wu et al. 2009).

A monsoon-ENSO relationship has been suggested by many studies (e.g., Chen 1994; Goswami 1998; Ju and Slingo 1995; Lau and Nath 2000; Li and Yanai 1996; Pillai and Mohankumar 2009; Wang et al. 2001; Wang et al. 2003; Webster and Yang 1992). Among a range of factors, the El Niño-Southern Oscillation plays a key role in modulating the Indian Ocean (IO) interannual variability. The influence of ENSO on the IO sea surface temperature is associated with the large scale warming in the positive phase of El Niño and cooling associated with La Niña (Bracco et al. 2007). According to Pillai and Mohankumar (2009), the El Niño-Southern Oscillation plays a crucial role in determining the variability of Indian summer monsoon rainfall (ISMR) on the interannual time-scale. ENSO affects the Indian summer monsoon through changes in large-scale east-west circulation over the equatorial Indo-Pacific Ocean and due to Rossby wave interaction over the northern Indian Ocean and western north Pacific (Pillai and Mohankumar 2009; Wu and Kirtman 2007). Shift of the Walker circulation associated with El Niño related wind anomalies over the Indian basin cause the preferred location of deep convection to move from the west Pacific

warm pool to the central Pacific, leading to subsidence and reduced precipitation over Indonesia and off Sumatra, and generally below-normal rainfall over India (Bracco et al. 2007; Webster and Yang 1992). Suppiah (1997) also argued that strong interannual variability of rainfall in the tropics is the result of the ENSO phenomenon, which causes droughts and floods due to El Niño and La Niña events over different parts of the globe, causing a negative impact on the economies of the countries affected. Suppiah (1997) also pointed out that the magnitude of climate anomalies in various regions of the tropics can be influenced by the strength and duration of El Niño and La Niña events, which can vary from one event to another. The magnitude and location of western Pacific sea surface temperature and tropical convection determine monsoon strength and the occurrence of warm or cold ENSO events (Soman and Slingo 1997; Torrence and Webster 1999). According to Wang et al. (2003), ENSO related year-to-year variability of the Asian–Australian monsoon exhibits noticeable regionality. For example, India experiences a deficit in rainfall during the El Niño evolution phase, while Australia experiences deficient monsoon rainfall during the mature phase of ENSO (Wang et al. 2003). Considerable work has been done investigating climate variability (particularly rainfall) of India, but the nature of climate variability over other countries (Sri Lanka, Nepal, Pakistan or the Maldives) is not well documented (Chowdhury 2003). This is the first attempt to investigate large-scale features of ENSO events in the context of Maldives monsoon rainfall (MMR: June-September) variability.

In order to understand the association between the Maldives monsoon rainfall and ENSO events, in this study El Niño and La Niña events were identified using the most recent version of the Extended Reconstruction Sea Surface Temperature (SST) Version 3B (ERSST V3B) analysis data. ERSST V3 is described in Smith et al. (2008). The only difference between the ERSST V3 and ERSST V3B is that satellite SST data are not used in the latter since addition of the satellite SSTs introduces a small residual cold bias in the order of 0.01º C (Smith et al. 2008). Wu (2008) used the older version of the data set (ERSST V2 – update of this data set is being discontinued) to identify El Niño and La Niña events. Here, ENSO events are determined following the definition of the Climate Prediction Centre (CPC), who uses the Niño 3.4 region (5ºS-5ºN, 170º-120ºW) SST anomalies for monitoring ENSO events. According to Trenberth (1997), the Niño 3.4 region refers to 40% of the way between the Niño 3 and Niño 4 regions, as shown in Figure 6.2. Warm ENSO events are categorised as El Niño events when the 3 month running mean of ERSST V3B SST anomalies in the Niño 3.4 region equalled or exceeded +0.5^{o}C for a

minimum of 5 consecutive overlapping seasons, while periods when the 3 month running mean of ERSST V3B SST anomalies in the Niño 3.4 region equalled or exceeded -0.5^{o}C for a minimum of 5 consecutive overlapping seasons are considered to be La Niña events. The ERSST V3B SST anomalies are computed based on the 1971-2000 period (Wu 2008). Identified ENSO episodes from 1979-2007 are shown in Figure 6.3.

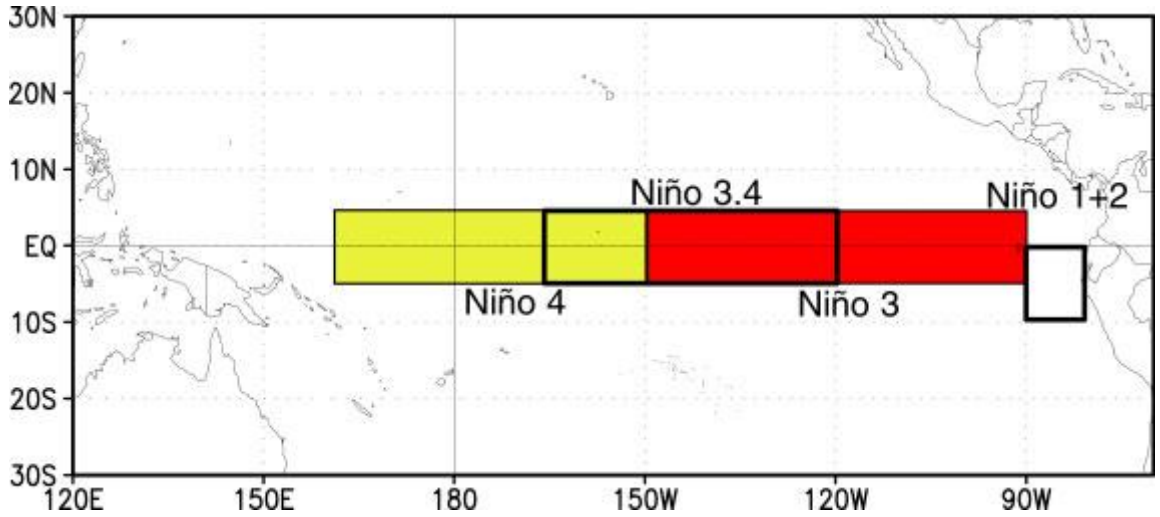

Figure 6.2: Geographical locations of the four Niño regions. Obtained from Climate Prediction Centre: http://www.cpc.noaa.gov/products/analysis_monitoring/ensostuff/nino_regions.shtml.

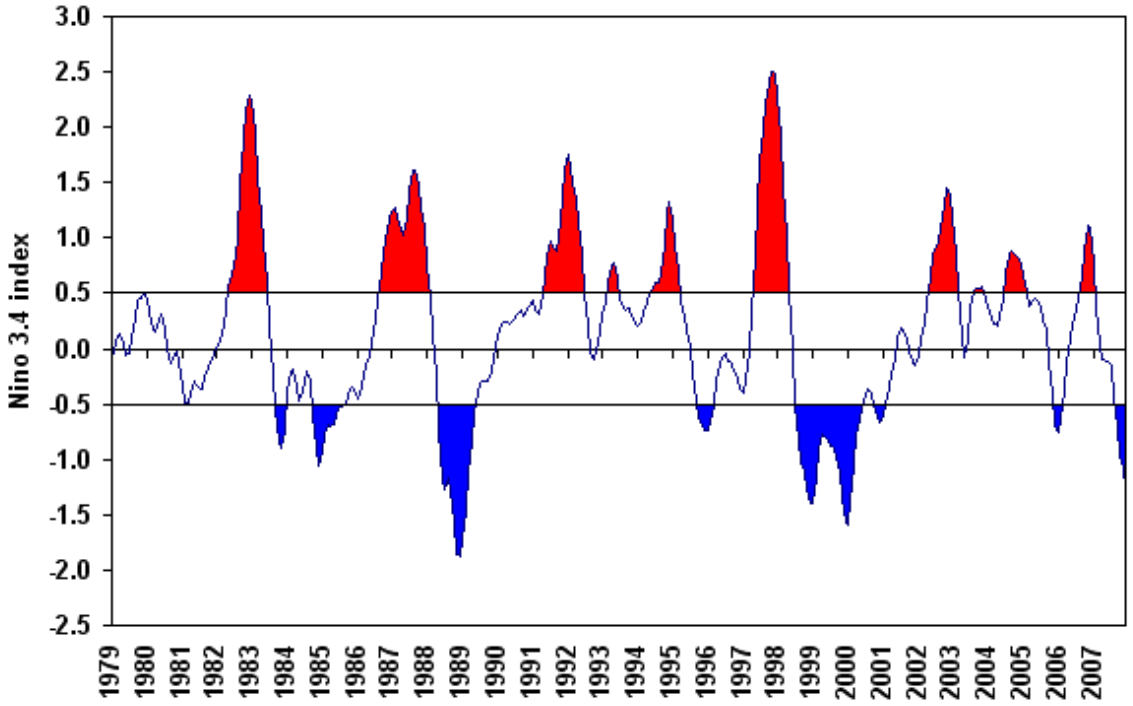

Figure 6.3: Identified El Niño (indicated in red) and La Niña (indicated in blue) events based on Niño 3.4 region (5ºS-5ºN, 170º-120ºW) SST anomalies. The anomalies are computed using 1971-2000 as a base period.

All the ENSO events (except 1995-1996) identified in this study are in agreement with the El Niño and La Niña events identified by Chou et al. (2003). Chou et al. (2003) considered 1995 as only an El Niño decaying year and 1996 as a non-ENSO year. However, in this study, 1995-1996 was considered as a La Niña event, in agreement with Wu (2009). Lists of non-ENSO, El Niño and La Niña years are provided in Table 6.1. The difference between the classification of 1995-1996 used here and that of Chou et al. (2003) could be due to the old and new ERSST data sets used. As Chowdhury (2003) pointed out and as can be seen from Figure 6.3 and Table 6.1, some El Niño and La Niña events extended across more than one calendar year (1982-1983, 1986-1987, 1991-1992, 1994-1995 and 1997-1998), and in other cases El Niño (decaying) and La Niña (developing) events can occur in the same calendar year (e.g. 1995 and 1998). The identified El Niño and La Niña events are sub-classified as strong and moderate events based on the severity of events. Here, the classification system of Golden Gate Weather Services (GGWS: http://ggweather.com/enso/oni.htm) is used. When the SST anomalies in the Niño 3.4 region equalled or exceeded +1.5 ºC and/or lie between +1.0 and +1.4 ºC for a minimum of three months, there are considered to be strong and moderate El Niño events, respectively. On the other hand, strong and moderate La Niña events are considered when the SST anomalies in the Niño 3.4 region are less than or equal to -1.5 ºC or between -1.0 to -1.4 ºC, respectively, for a minimum of three months. The years identified as strong and moderate El Niño and La Niña events are shown in Table 6.2. There is a total of 3 strong and 4 moderate El Niño events, while there were 1 strong and 3 moderate La Niña events (1/3) during the period 1979-2007. Since the total number of El Niño and La Niña events are not equal, the latest 3 deficient monsoon rainfall years corresponding to El Niño events (1987, 1991 and 2002: Table 6.2 and Figure 6.4) and 3 latest excess monsoon rainfall years corresponding to La Niña events (1988, 1998 and 2007: Table 6.2 and Figure 6.4) are used for the composite analysis.

Table 6.1: Non-ENSO, El Niño and La Niña years from 1979-2007.

Categories of ENSO types		
Non-ENSO	**El Niño (warm)**	**La Niña (cold)**
1979,1980,1981, 1984, 1990, 1993, 2001, 2003, 2005	1982-1983, 1986-1987, 1991-1992, 1994-1995 1997-1998, 2002, 2004, 2006	1985, 1988-1989, 1995-1996, 1998-2000, 2007

Table 6.2: The El Niño and La Niña years classified as strong and moderate events following Golden Gate Weather Services classification (http://ggweather.com/enso/oni.htm). The 3 El Niño and La Niña events used in the composite analysis are underlined.

El Niño categories		La Niña categories	
Strong	Moderate	Strong	Moderate
1982	1986	1988	1998
1991	1987		1999
1997	1994		2007
	2002		
Strong/Moderate El Niño: 3/4		Strong/Moderate La Niña: 1/3	

Figure 6.4 shows the association between the percentage departure of Maldives monsoon rainfall (MMR: based on the 1979-2007 mean) and strong/moderate El Niño and La Niña events, together with the All-India monsoon rainfall (AIMR) departure. It is evident that during strong/moderate El Niño years, except 1994 and 1997, the Maldives experienced a deficiency of monsoon rainfall. During the strong/moderate El Niño years of 1994 and 1997 MMR experienced excess rainfall (Figure 6.4) and hence provided some inconsistency in the El Niño and rainfall relationship. Although the correlation between MMR and AIMR is weak (CC = 0.26, insignificant at the 5% level), it is interesting to note that the AIMR also tended to have deficient/excess rainfall during the same strong/moderate El Niño years when MMR experienced a deficit/excess in monsoon rainfall. The same time series (Figure 6.4) shows that during strong/moderate La Niña events, there is a tendency for the Maldives and the AIMR to be associated with excess rainfall. The 1999 La Niña event is an exception to this relationship between La Niña and rainfall, when MMR experienced a significant deficiency in monsoon rainfall (14.6%) and AIMR also experienced a slight deficiency (Figure 6.4). It is worth noting that both MMR and AIMR tend to have deficient/excessive rainfall during the same strong/moderate La Niña events (Figure 6.4). Occurrence of deficient and excess monsoon rainfall for the Maldives during strong/moderate El Niño and La Niña events is depicted in Table 6.3. The percentage occurrence of deficient and excess monsoon rainfall shown in Table 6.3 holds true for AIMR, as the AIMR also tends to have deficient/excessive rainfall during the same strong/moderate El Niño and La Niña events. It is clear from the table that the Maldives/India region experiences deficiencies in monsoon rainfall about 71.4% of the time

during strong/moderate El Niño events, while the Maldives/India region experience excessive monsoon rainfall about 75% of the time during strong/moderate La Niña events. This suggests that the deficient/excess monsoon rainfall over the Maldives and India region is linked to the strong/moderate El Niño and La Niña events, respectively. This finding is consistent with previous findings that most of the drought years over India are associated with El Niño events, while the La Niña events are associated with flood events (Kane 1998; Kumar et al. 1995; Rajeevan and Pai 2006). Rajeevan and Pai (2006) also suggested that severe droughts over India are not always associated with El Niño events, and pointed out that the 21st century's most severe El Niño event was in 1997 when Indian summer monsoon rainfall was excessive. Further, Rajeevan (2006) stated that during a 126 year period (1880-2005), less than half of the time deficient rainfall over India was associated with El Niño events. It is interesting to see that excess and deficient monsoon rainfall for India and over the Maldives region occurred during non-ENSO events (Figure 6.4) and Kane (1998) indicated that factors unrelated to ENSO events (perhaps a combination of factors) may play an important role in some years. It should also be noted that during most of the non-ENSO events (55.5% of the time), monsoon rainfall over the Maldives and India are out of phase, indicating that monsoon rainfall over the Maldives and India during non-ENSO events are influenced by different factors. One other noticeable thing in Figure 6.4 which is worth highlighting is that during the period 1980-1987 and 1992-1998 monsoon rainfall over the Maldives is below normal and above normal, respectively, whereas AIMR does not show such a deviation (below normal/above normal) over an extended period.

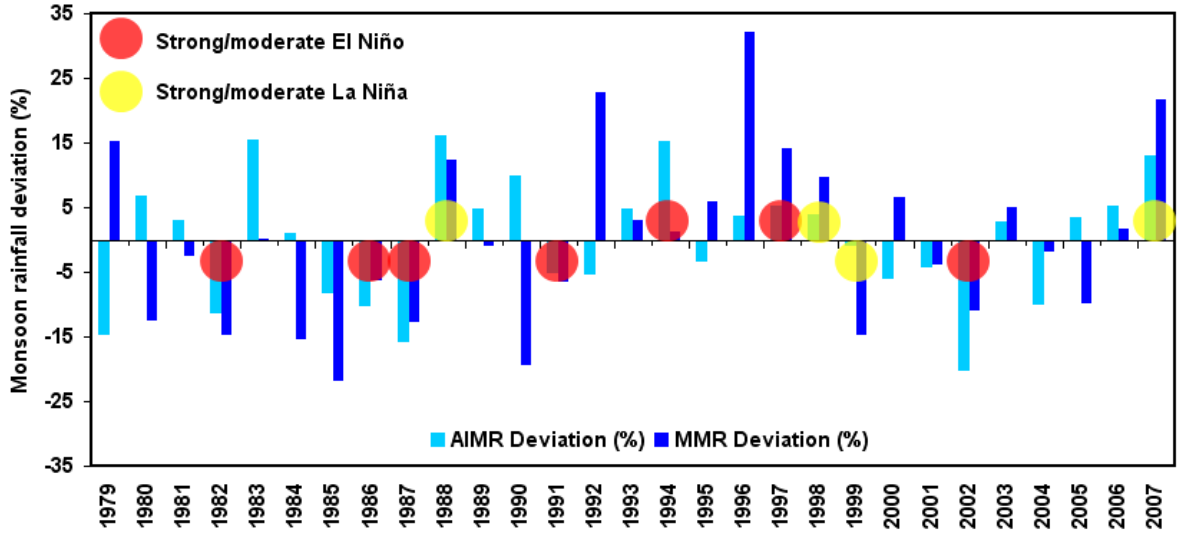

Figure 6.4: Association between strong/moderate El Niño and La Niña events and All-India monsoon rainfall (AIMR) and Maldives monsoon rainfall (MMR) deviation (%) based on the 1979-2007 mean. Strong/moderate El Niño and La Niña events are marked in red and yellow circles, respectively.

Table 6.3: Occurrence of deficient and excess monsoon rainfall for the Maldives/India during strong/moderate El Niño and La Niña conditions. The numbers in parenthesis indicate percentage occurrence of deficient and excess monsoon rainfall.

	Deficient monsoon	Excess monsoon	Total
Strong/moderate El Niño	5 (71.4%)	2 (29.6%)	7 (100%)
Strong/moderate La Niña	1 (25%)	3 (75%)	4 (100%)

In addition to the 'whole of Maldives' monsoon rainfall-ENSO relationship explored above, the association between ENSO and regional and individual station monsoon rainfall for the period 1979-2007 was investigated. The regions (northern and southern) were identified based on correlation analysis in the previous section. The station rainfall data used here are from Hulhule and Gan (shown in Figure 2.1), since only these two stations have data for the 1979-2007 period. Figure 6.5 shows association between ENSO events and north/south and Hulhule/Gan monsoon rainfall deviation based on the 1979-2007 period. The association between strong/moderate El Niño years and MMR (north) reveals very similar results as obtained above, except that the northern region experienced a slight excess in monsoon rainfall during the 1991 El Niño event (Figure 6.5a). Furthermore, association between strong/moderate La Niña events and MMR (north) reveals exactly the same results obtained above. Compared to the MMR-El Niño relationship obtained above, the only disagreement between strong/moderate El Niño events and MMR (south) is that during the 2002 El Niño event, southern Maldives experienced excess monsoon rainfall (Figure 6.5a). Association between ENSO and regional (north and south) monsoon rainfall over the Maldives is in agreement with the findings of Chowdhury (2003), who explored the association between ENSO and regional rainfall over Bangladesh and found similar results. High-to-moderate rainfall deficits were experienced in strong/moderate El Niño years, whle during strong/moderate La Niña years high-to-moderate excess rainfall was experienced. As can be seen from Figure 6.5b, the association between ENSO events and monsoon rainfall at the Hulhule and Gan stations provided a poor insight into the relationship between individual station monsoon rainfall and strong/moderate El Niño and La Niña events.

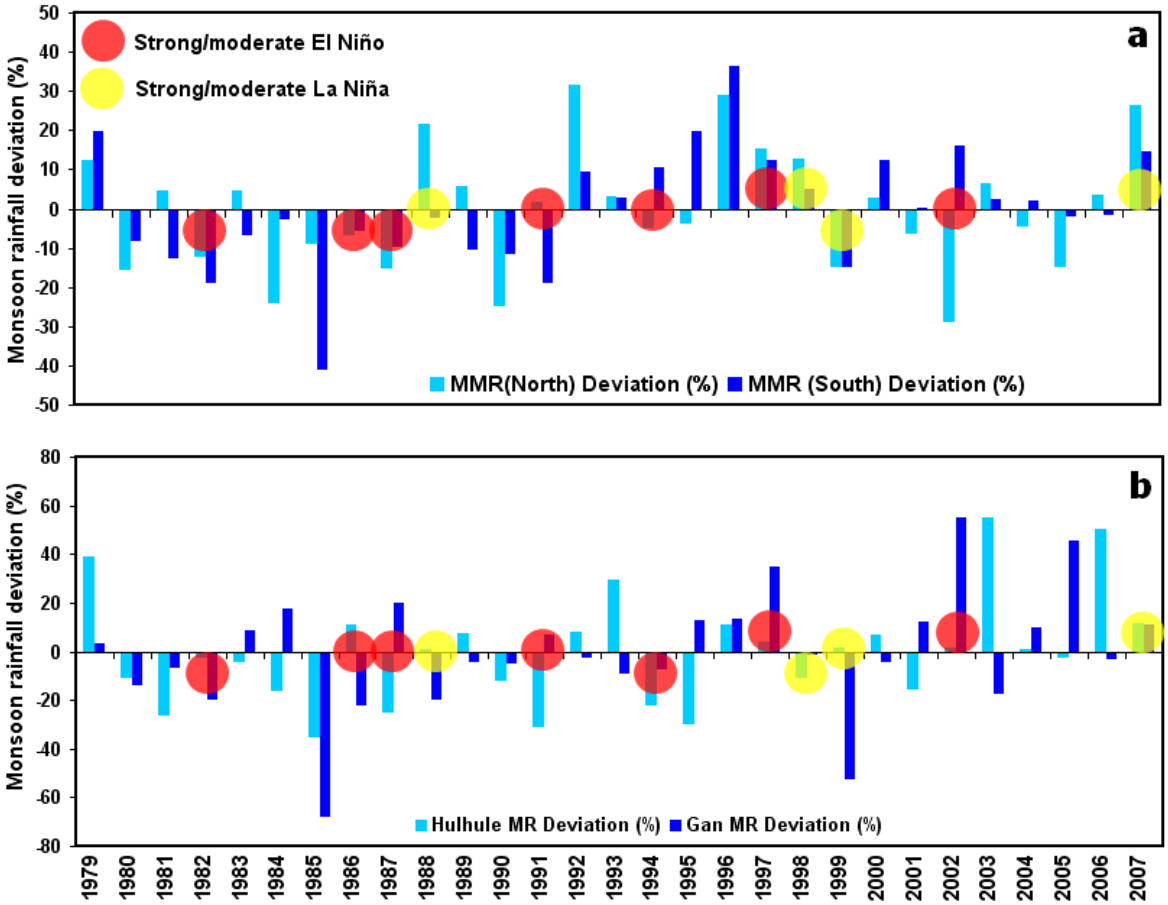

Figure 6.5: Association between strong/moderate El Niño and La Niña events with regional (a: northern and southern) and station monsoon rainfall deviation (b: Hulhule and Gan) based on the 1979-2007 mean. Strong/moderate El Niño and La Niña events are marked in red and yellow circles, respectively.

6.1.1 Physical link between ENSO and Maldives monsoon rainfall

Several studies have attempted to understand the physical mechanism by which ENSO-related SST anomalies in the Pacific region are related to the precipitation over the Indian monsoon region (Goswami 1998; Krishnamurthy and Goswami 2000; Nigam 1994; Webster and Yang 1992). It has been suggested that during El Niño events the eastern Pacific experiences anomalous sea surface temperatures which cause the movement of the ascending branch of the Walker circulation towards the eastern Pacific (Goswami 1998). However, Goswami (1998) stated that it has not been established exactly how a shift of the Walker cell and its associated circulation changes leads to reduction of continental precipitation over India. In addition to the large-scale circulation associated with ENSO, the monsoon is also affected by regional-scale circulations (Goswami 1998). On the other hand, Krishnamurthy and Goswami (2000) pointed out that the shift in the ascending branch of the Walker circulation towards the eastern Pacific results in enhanced low level

convergence over the Indian Ocean region and this in turn helps to drive an anomalous Hadley circulation with descent over the Indian continent and therefore decreased monsoon rainfall there (Krishnamurthy and Goswami 2000). Hence, ENSO influences the Indian monsoon through an interaction between the Walker circulation (WC) and the regional monsoon Hadley circulation (Krishnamurthy and Goswami 2000).

6.1.2 Evolution of ENSO related warm episodes

Spatial patterns of June-September (JJAS) mean sea surface temperature (SST) over the long-term (1979-2007: Figure 6.6a), for the non-ENSO years (1979, 1980, 1981, 1984, 1990, 1993, 2001, 2003 and 2005: Figure 6.6b), for the El Niño years (1987, 1991 and 2002: Figure 6.6c) and for the La Niña years (1989, 1998, 2007: Figure 6.6d) are depicted in Figure 6.6. The long-term mean SST, the non-ENSO mean SST and El Niño mean SST patterns are very similar, where the equatorial Indian Ocean and Pacific Ocean mean sea surface temperature is in excess of 25° C compared to other areas (Figure 6.6a-c). Mean SST for the La Niña years shows maximum SST in the Indian and Pacific Ocean (Figure 6.6d), but the Niño3.4 region shows lower sea surface temperature compared to other cases, which is consistent with the previous findings that the Niño3.4 region experiences a negative SST anomaly during La Niña events. There appears to be no variation in mean SST for the long-term and for the non-ENSO years in the Niño3.4 region (Figure 6.6a-b). The maximum mean SST for the Niño3.4 region is shifted to east for the case of El Niño years (Figure 6.6c).

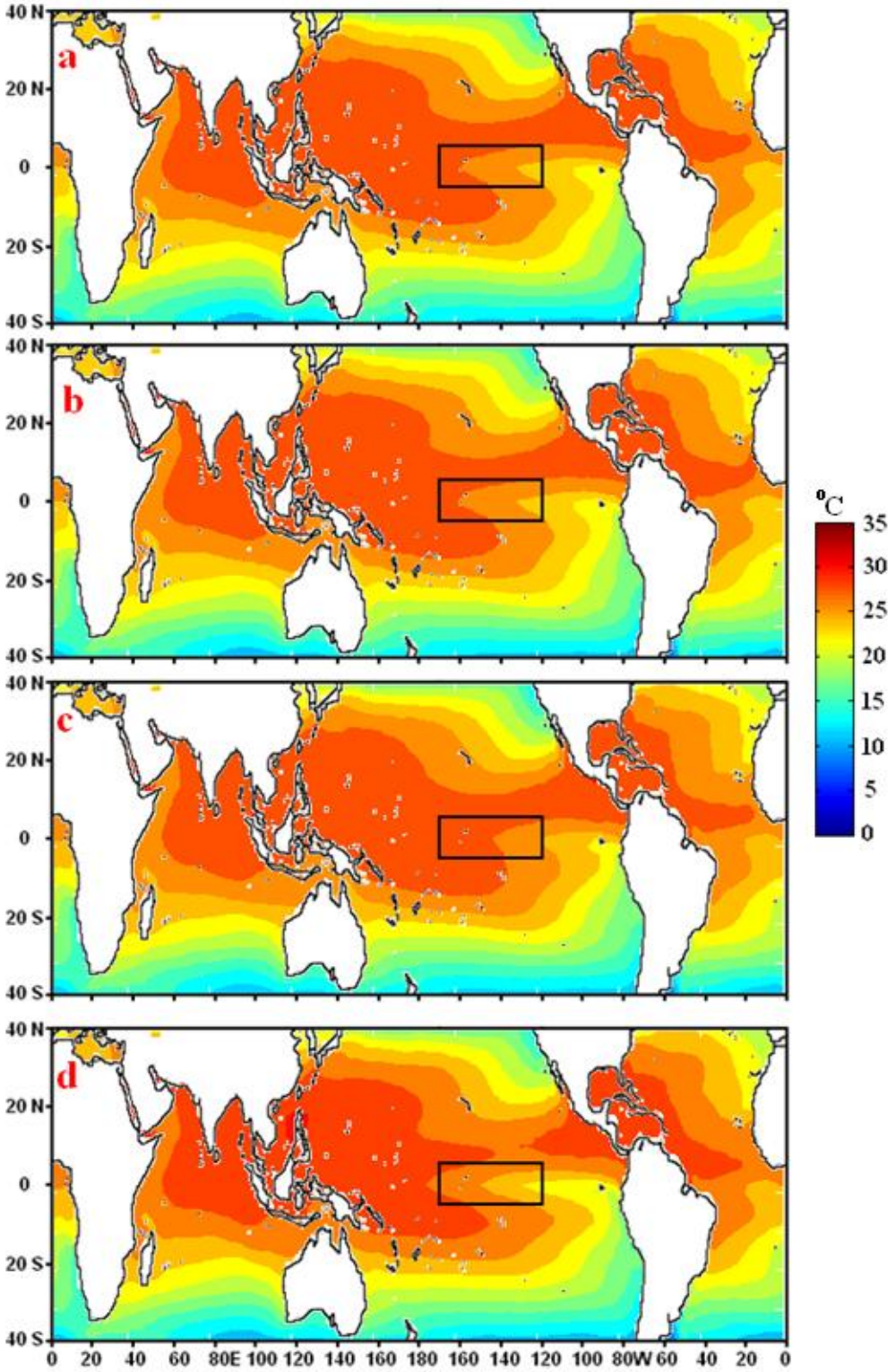

Figure 6.6: Spatial pattern of June-September (JJAS) mean sea surface temperature (SST): (a) 1979-2007 period, (b) non-ENSO years, (c) strong/moderate El Niño years (1987, 1991 and 2002) and (d) strong/moderate La Niña years (1988, 1998 and 2007). The Niño 3.4 region (5ºS-5ºN, 170º-120ºW) is highlighted as a rectangular box.

The temporal evolution of the sea surface temperature anomaly (SSTA) in the Niño 3.4 region for the strong/moderate El Niño and La Niña cases is shown in Figure 6.7 for the three year period from one year prior (year -1) to the onset of an ENSO event (mature phase: year 0) to one year after (year +1) the onset of an ENSO event. As depicted in Figure 6.7 and pointed out by Okumura and Deser (2009), in some years the El Niño and La Niña events tend to last for about 1-2 years. The 1987 ENSO warm event was a multi-year event. The SSTA started to evolve in year -1 (1986) and continued to grow in year 0, reaching its mature phase around the middle of year 0, before decaying in year +1. Furthermore, the 1999 La Niña was also a multi-year event. It developed in year -1 and maintained La Niña conditions during year 0, before reaching its mature phase towards the end of year 0 (Figure 6.7b). The amplitude of El Niño SST anomalies in Niño3.4 tends to be greater than those during La Niña cases. Except for 1987 the SSTA in most of the El Niño cases lies between +1 and -1 during year -1 (prior to ENSO onset). As Figure 6.7 (a-b) depicts that, except for the 1987 El Niño and 1999 La Niña events, the ENSO events started to evolve around March (year 0) and matured (maximum anomaly) towards the end of year 0 or at the beginning of year +1. Okumura and Deser (2009) also suggested that the El Niño and La Niña events mostly develop in late spring-summer (for Northern Hemisphere), during this time the Pacific cold tongue intensifies and peaks toward the end of the calendar year, resulting in a SSTA peak in December. Although the physical processes responsible for this phase-locking are still unclear, it has been suggested that "the nonlinear modulation of the annual cycle by interannual displacement of the thermocline, seasonal migration of the ITCZ and associated atmospheric heating, delayed negative feedback from the Indian Ocean and influence of the North Pacific Oscillation might play a role" (Okumura and Deser 2009).

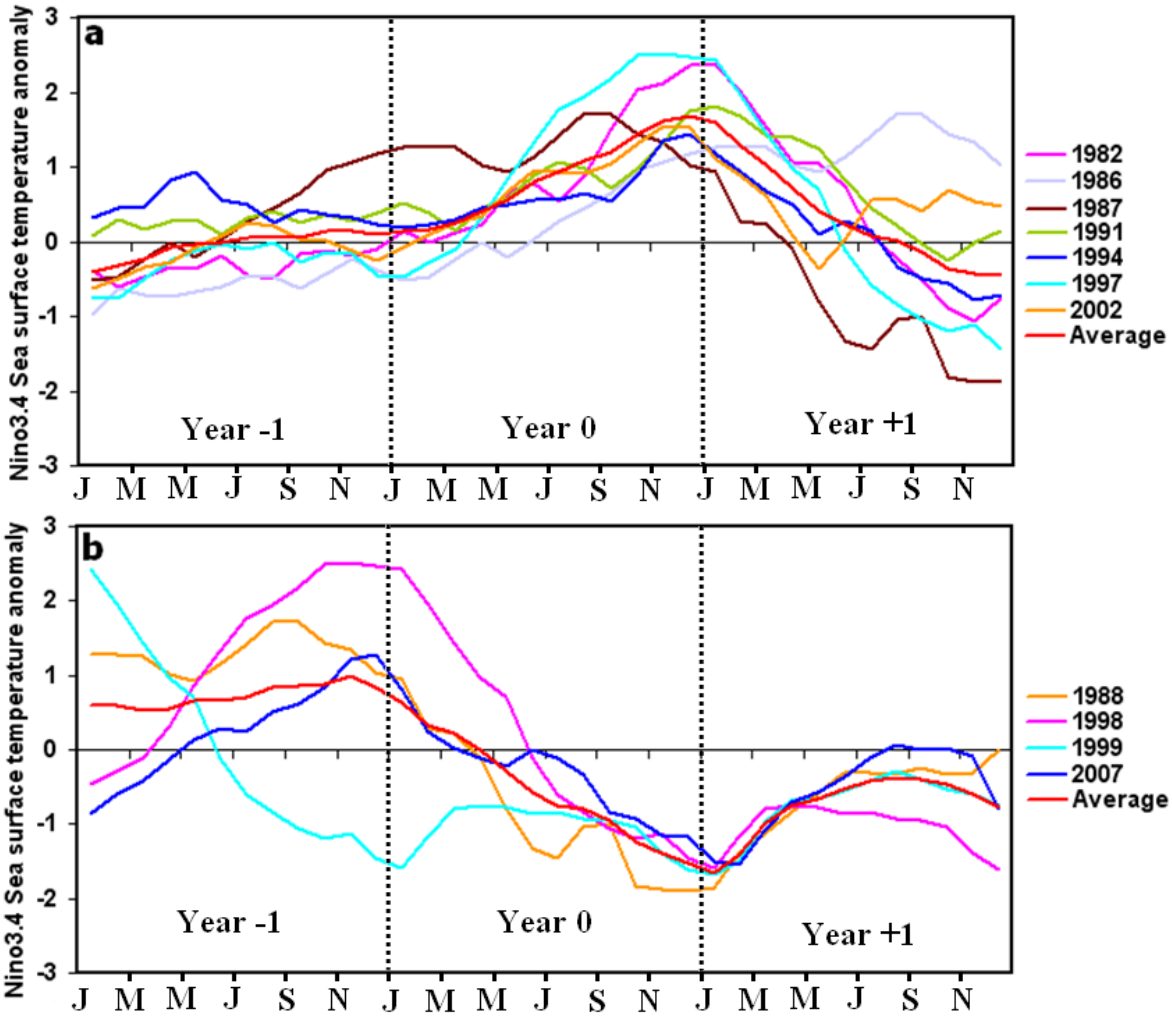

Figure 6.7: Niño 3.4 (5ºS-5ºN, 170º-120ºW) sea surface temperature anomaly (in degress Celcius) for: (a) strongest El Niño events and (b) strongest La Niña events occurred during the 1979-2007 period (one year prior (year -1) to the onset of an ENSO event (mature phase: year 0) and one year after (year +1) the onset of an ENSO event). Beginning of each year is indicated with vertical dashed lines.

Spatial evolution of mean sea surface temperature anomalies (SSTA) for the strong/moderate El Niño years (1987, 1991 and 2002) for the months of January, April, July and October are shown in Figure 6.8. It is quite noticeable that the maximum SSTA occurs around the central Pacific Ocean for all the months during El Niño events (Figure 6.8). Anomalous SST evolution is more evident around the Niño 3.4 region and a strong warm tongue (mature phase) develops during the months of July and October, which is characteristic of warm ENSO events. During the month of July, an anomalous cold region is also evident along the west coast of North America, and by the month of October the cold area has moved to the central north Pacific, which is seen as a "circular hole" in Figure 6.8d.

Figure 6.9 depicts the mean SSTA for the strong/moderate La Niña years (1988, 1998 and 2007) for the months of January, April, July and October. In contrast to the El Niño positive SST anomaly shown in Figure 6.8, very similar patterns can be seen but a with negative SST anomalies, especially for the La Niño mature phase (Figure 6.9c-d) in the Niño 3.4 region. The anomalously high positive SST anomaly for the month of January for the case of La Niña is due to the influence of ENSO warm conditions existing from the previous El Niño years (1987, 1997 and 2006). It is apparent from Figure 6.7a, that the 1987 and 1997 El Niño warm conditions persisted at the beginning of La Niña years 1988 and 1998, while 2006 El Niño warm conditions persisted at the beginning of the La Niña year 2007 (not shown). The cold "circular hole" which was observed in the central north Pacific in the El Niño mature phase (October: Figure 6.8d) is also present in the January SSTA pattern for La Niña years (Figure 6.9a). This also indicates that anomalously warm conditions existed from the previous El Niño conditions. The January warm condition (positive SSTA) weakened by April and evolution of anomalously cool conditions is apparent in July (Figure 6.9 c). In the mature phase, a cool tongue developed in October (Figure 6.9d) in the Pacific Ocean, especially in the Niño 3.4 region, which is the characteristic of La Niña. A "circular hole" very similar to that observed in the El Niño October case can also be seen in La Niña October case, but opposite in sign (a positive SST anomaly) in the central north Pacific Ocean region (Figure 6.9d).

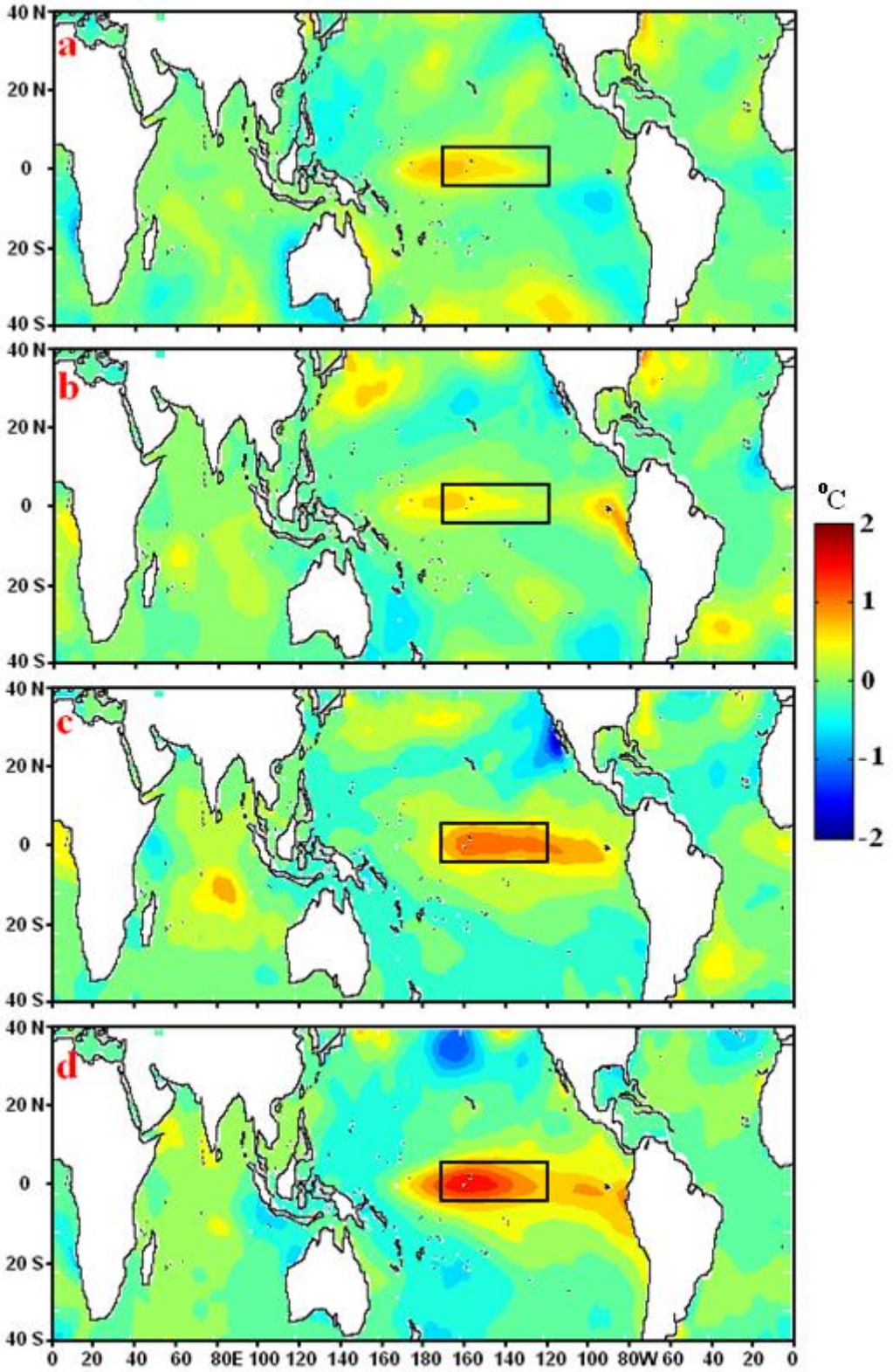

Figure 6.8: Sea surface temperature anomaly for: (a) January, (b) April, (c) July and (d) October. Each month is an average of strong/moderate El Niño years (1987, 1991 and 2002). Anomalies are based on the 1979-2007 period. The Niño 3.4 region (5ºS-5ºN, 170º-120ºW) is highlighted as a rectangular box.

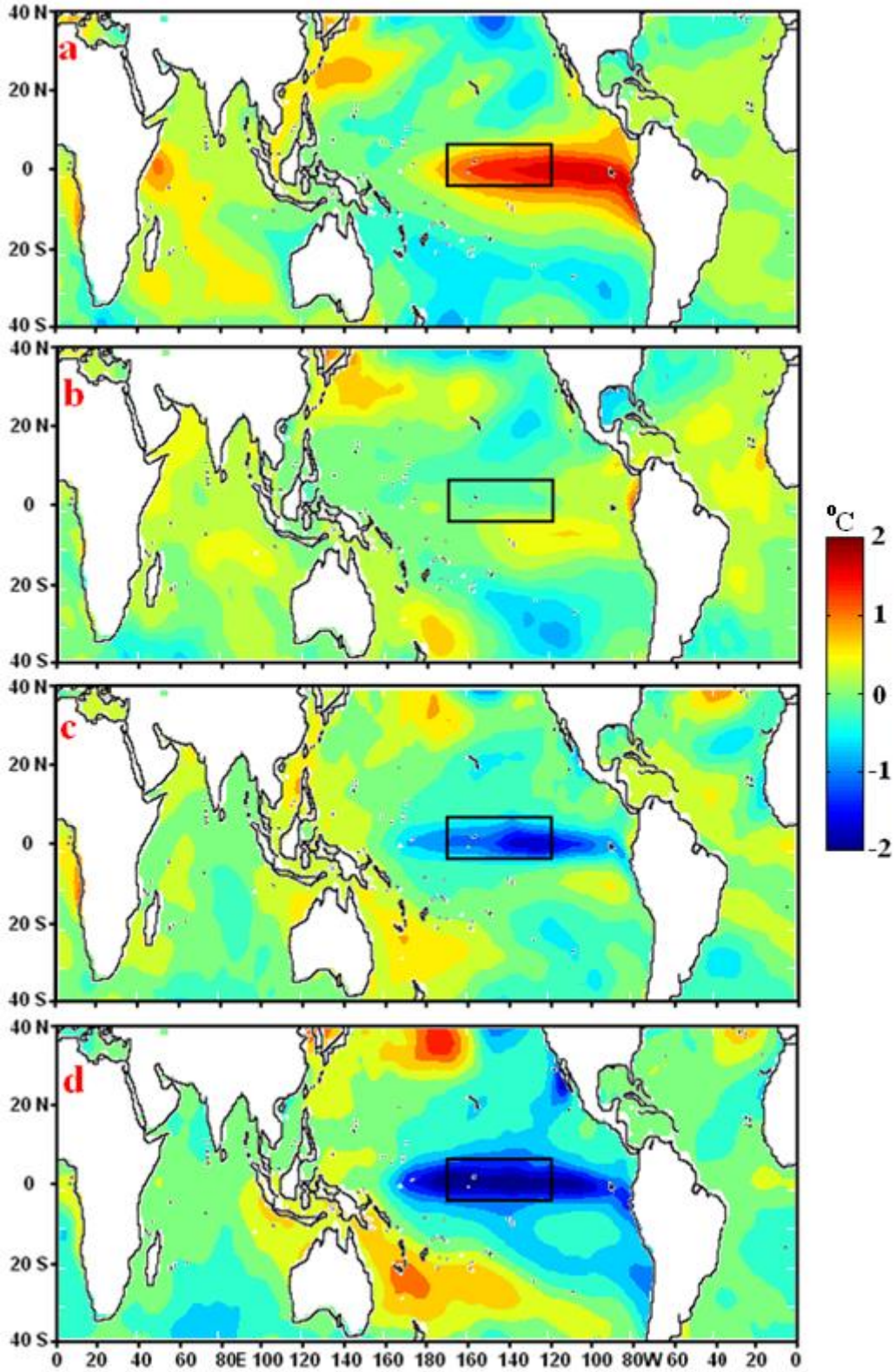

Figure 6.9: Sea surface temperature anomaly for: (a) January, (b) April, (c) July and (d) October. Each month is an average of strong/moderate La Niña years (1988, 1998 and 2007). Anomalies are based on the 1979-2007 period. The Niño 3.4 region (5ºS-5ºN, 170º-120ºW) is highlighted as a rectangular box.

June-September composites of SSTA for the non-ENSO years, El Niño years and La Niña years are depicted in Figure 6.10. According to Kang and Kug (2002), the amplitude of El Niño SST anomalies tends to be greater than that during La Niña events. This is clearly evident from the composite difference between El Niño and La Niña presented in Figure 6.10d. SST anomaly skewness, with large positive values in the eastern equatorial Pacific and small negative values in the western Pacific Ocean region, has also been noted by Burgers and Stephenson (1999), who suggested that the positive SST anomaly skewness in the eastern equatorial Pacific is due to the proximity of the thermocline to the ocean surface. These non-linear oceanic processes create a large positive SST anomaly in the eastern equatorial Pacific with small negative values in the western Pacific Ocean, and are responsible for the asymmetry in the strength of El Niño and La Niña (Burgers and Stephenson 1999; Okumura and Deser 2009). Furthermore, Jin et al. (2003) also pointed out that non-linear vertical and zonal advection in the equatorial upper ocean generates larger amplitudes of SSTA during the ENSO warm phase compared to the amplitude of the ENSO cold phase.

In comparison to the non-ENSO composite anomaly, a very distinct anomalously positive (warming) and negative (cooling) SSTA pattern is evident in the central Pacific Ocean for the case of El Niño/La Niña composites (Figure 6.10b and c), especially in the Niño3.4 region. Changes in SST, associated with El Niño/La Niña conditions in the eastern equatorial Pacific can influence the monsoon through changes in atmospheric circulation, namely via the large-scale Walker circulation (Pillai and Mohankumar 2009). According to Kinter et al. (2002), the most significant and strongest large-scale atmospheric vertical motion in the world is associated with the Walker circulation (WC). The anomalously cool SST in the eastern tropical Pacific during La Niña (Figure 6.10c) are accompanied by a shallow equatorial thermocline in the east and strong trade winds blowing towards the west, as shown in Figure 6.11b. The equatorial upwelling due to strong easterly winds induces stronger surface cooling in the eastern basin creating an east-west SST gradient (Okumura and Deser 2009). This in turn drives the equatorial easterly winds and builds up heat in the western tropical Pacific. Heat and moisture (water vapour) gathered during this process helps intensification of the atmospheric deep convection and upper-atmospheric westerly winds over the western Pacific warm pool (Okumura and Deser 2009). This leads the westerly flow back to the east (warm air rising over the warmer waters of the western Pacific and descending over the cooler eastern Pacific (Figure 6.11b)), thus establishing a strong WC during La Niña events and enhanced precipitation in the Asian region. The

reverse happens during El Niño events (Figure 6.11a). The trade winds around the equatorial region weaken, warm surface waters flow eastward and the slope of the thermocline decreases. Associated with anomalously warm SST in the tropical Pacific during El Niño events (Figure 6.10b), the tropical Pacific region experiences unusually warm waters. As a result, warm air rises over the entire equatorial Pacific, thus weakening the Walker circulation (Philander 1999). Due to the weakened Walker circulation during El Niño events, the atmospheric deep convection is suppressed over the tropical Indian Ocean (Chowdhury 2003; Okumura and Deser 2009) and El Niño related wind anomalies over the Indian basin cause deep convection to move from the west Pacific warm pool to the central Pacific, causing subsidence and reduced precipitation over Indonesia and off Sumatra, and below-normal rainfall over India (Bracco et al. 2007; Webster and Yang 1992).

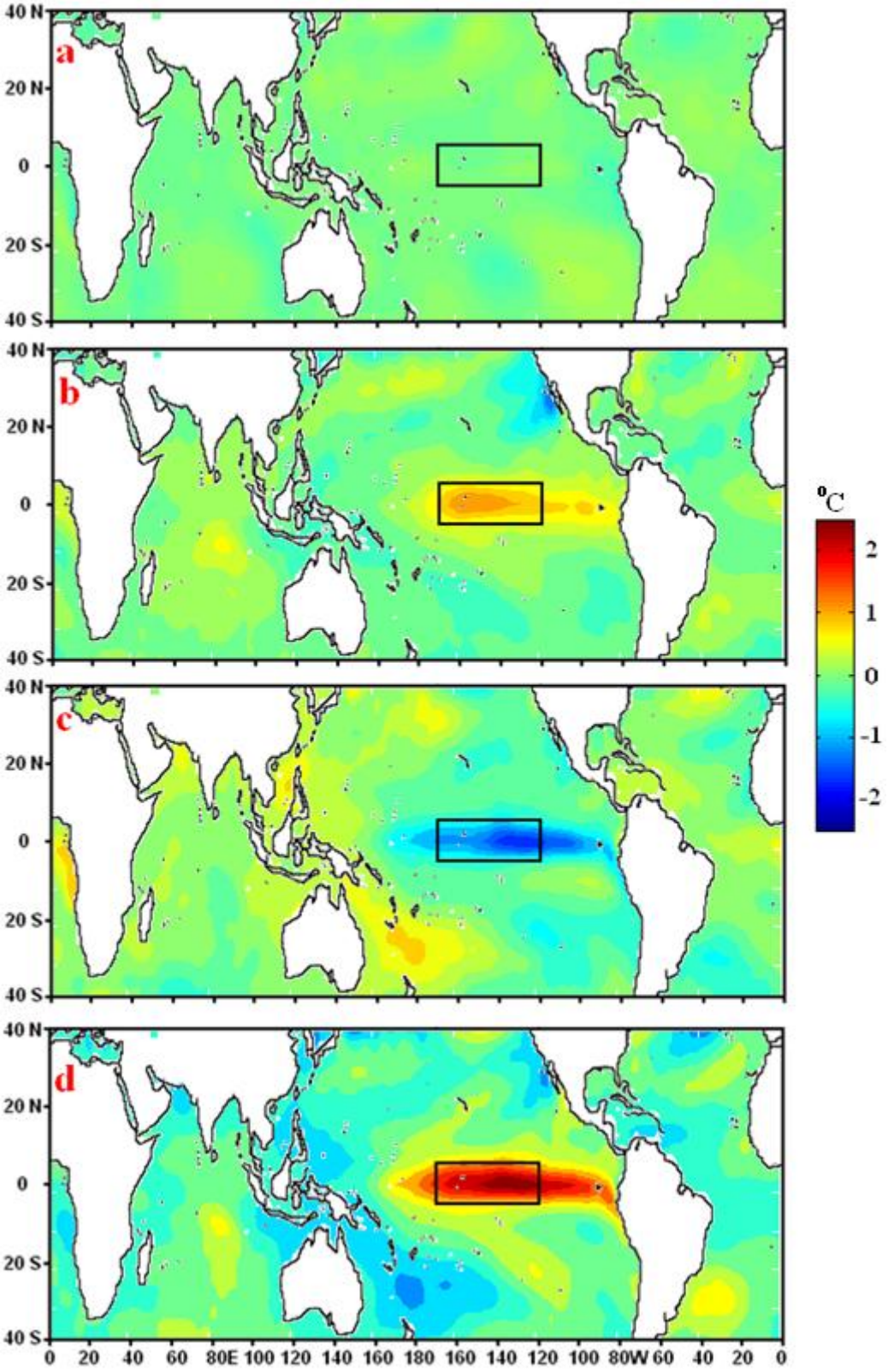

Figure 6.10: Spatial pattern of June-September (JJAS) composite sea surface temperature (SST) anomaly for: (a) Non-ENSO years, (b) El Niño deficient monsoon rainfall years (1987, 1991 and 2002), (c) La Niña excess monsoon rainfall years (1988, 1998 and 2007) and (d) the difference between b and c. Anomalies are based on the 1979-2007 period. The Niño 3.4 region (5ºS-5ºN, 170º-120ºW) is highlighted as a rectangular box.

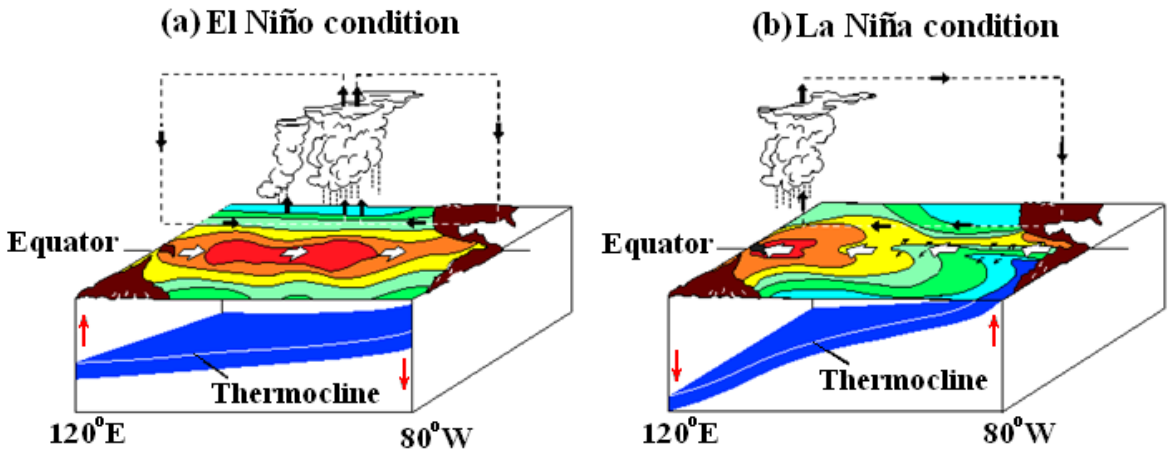

Figure 6.11: Schematic diagram of El Niño (a) and La Niña (b) conditions in the Pacific Ocean region. Taken from NOAA (2010).

6.1.3 Atmospheric circulation patterns associated with SSTA

To understand the atmospheric circulation patterns associated with the El Niño warm and La Niña cold events, various atmospheric fields were analyzed, including the horizontal wind velocity, velocity potential, vertical velocity, outgoing longwave radiation and vertically integrated moisture transport. According to Fu et al. (2008), moisture transported by the monsoon plays an integral part in maintaining the moisture balance in the monsoon regions. Vertically integrated moisture transport (VIMT) is directly linked to the basic monsoon forcings and monsoon rainfalls (Fasullo and Webster 2003; Fu et al. 2008). Outgoing longwave radiation (OLR) and mid-tropospheric (500 hPa) vertical velocity patterns are good indicators of large scale rising (deep convection) and sinking (subsidence) regions (Bony and Dufresne 2005; Bony et al. 2004; Wang and Hendon 2007). The velocity potential pattern at 200 hPa (upper tropospheric) represents the Walker circulation well, indicating the centres of upper level convergence and divergence (Pillai and Mohankumar 2009). In the tropics, the divergent outflow is partly driven by diabatic heating. Three-dimensional heating anomalies related to the sea surface temperature anomalies are represented by the velocity potential (Thomas et al. 2000). The horizontal wind velocity was partitioned into non-divergent (eddy or rotational) and divergent (non-eddy or irrotational) parts, following the methods described by Mancuso (1967), Krishnamurti (1971) and Krishnamurti et al. (1973):

$$\mathrm{v} = \mathrm{v}_{\psi} + \mathrm{v}_{\phi} = \mathrm{k} \times \nabla\psi + \nabla\phi$$

where ψ is streamfunction and ϕ is velocity potential. Although the streamfunction (non-divergent or rotational part) component is larger than the second component (velocity potential of the divergent wind: irrotational part), it does not contribute to atmospheric vertical motion. The fact that the Walker and Hadley cells are developed thermally due to atmospheric convergence-divergence, the irrotational part of velocity potential plays a significant role in the atmospheric vertical circulation (Semenov et al. 2008; Wang 2002).

Velocity potential and divergent wind at 200 and 850 hPa pressure levels were computed for the monsoon season (June-September) to understand the circulation patterns during El Niño and La Niña events. The 200 and 850 hPa levels were selected to represent the upper and lower troposphere, respectively. Spatial patterns of the velocity potential, together with the divergence for these two levels are shown in Figure 6.12 and Figure 6.13, respectively. As the figures indicate, the low velocity potentials are associated with divergent outflow, while high velocity potential regions are associated with convergent inflow. The 200 hPa level divergence outflow patterns are mainly concentrated around the equatorial region, while the convergence inflow patterns are located south and north of equator. A very similar pattern of divergent outflow is apparent from the upper tropospheric level (200 hPa) velocity potential and divergent wind pattern for the non-ENSO and La Niña case (Figure 6.12a and c). Both figures show east-west dipole patterns of divergent outflow; one over South America and the second one centred over the Indonesian region. The 200 hPa divergent wind for the El Niño case shows a weak elongated divergent outflow pattern (instead of the east-west dipole that was observed for the non-ENSO and La Niña cases), originating from the central Atlantic Ocean and reaching the Indian Ocean (Figure 6.12b). This is consistent with observations that the warm air rises over the entire equatorial Pacific during El Niña events, thus weakening Walker circulation (Philander 1999).

The distribution of atmospheric heat sources (convergence areas) and heat sinks (divergence areas) is often represented by the velocity potential in the lower troposphere (D'Abreton and Tyson 1995). The lower tropospheric level (850 hPa) velocity potential and divergent wind shows a similar but opposite pattern (Figure 6.13) to the 200 hPa level velocity potential and divergent wind shown in Figure 6.12. The 200 hPa level convergence corresponds to 850 hPa level divergence, while the 200 hPa level divergence corresponds to 850 hPa level convergence (Pillai and Mohankumar 2009). Zones of high velocity potential are in the equatorial region, where convergence inflow is noticeable, especially in the eastern Pacific and in the Indian Ocean region. The El Niño velocity potential pattern

(Figure 6.13b) shows a similar pattern to the non-ENSO and La Niña velocity potential patterns (Figure 6.13a and c), but the velocity potentials are higher in the central Pacific region and sinking air (convergent inflow) is more evident in the region when compared to the non-ENSO and La Niña patterns for the same level. Spatial patterns of velocity potential for El Niño minus La Niña (Figure 6.13d) clearly show that during the El Niño events the velocity potential is higher in the Pacific region, originating from the South Pacific Ocean. The positive velocity potential anomalies (El Niño minus La Niña: Figure 6.13d) over the entire equatorial Pacific suggest that the convergent inflow occurs across the entire equatorial Pacific region during El Niño events (Figure 6.13d) and is consistent with the SSTA. Due to the basin wide convergence inflow, the Walker circulation becomes weak, influencing the monsoon flow during El Niño conditions. The higher velocity potential and strong divergence wind flow pattern for the El Niño case indicates that the flow pattern is influenced by the underlying sea surface conditions. Convergence centres are associated with warm SSTA in the eastern Pacific during El Niño and divergence is associated with cold SSTA in the Pacific during La Niña.

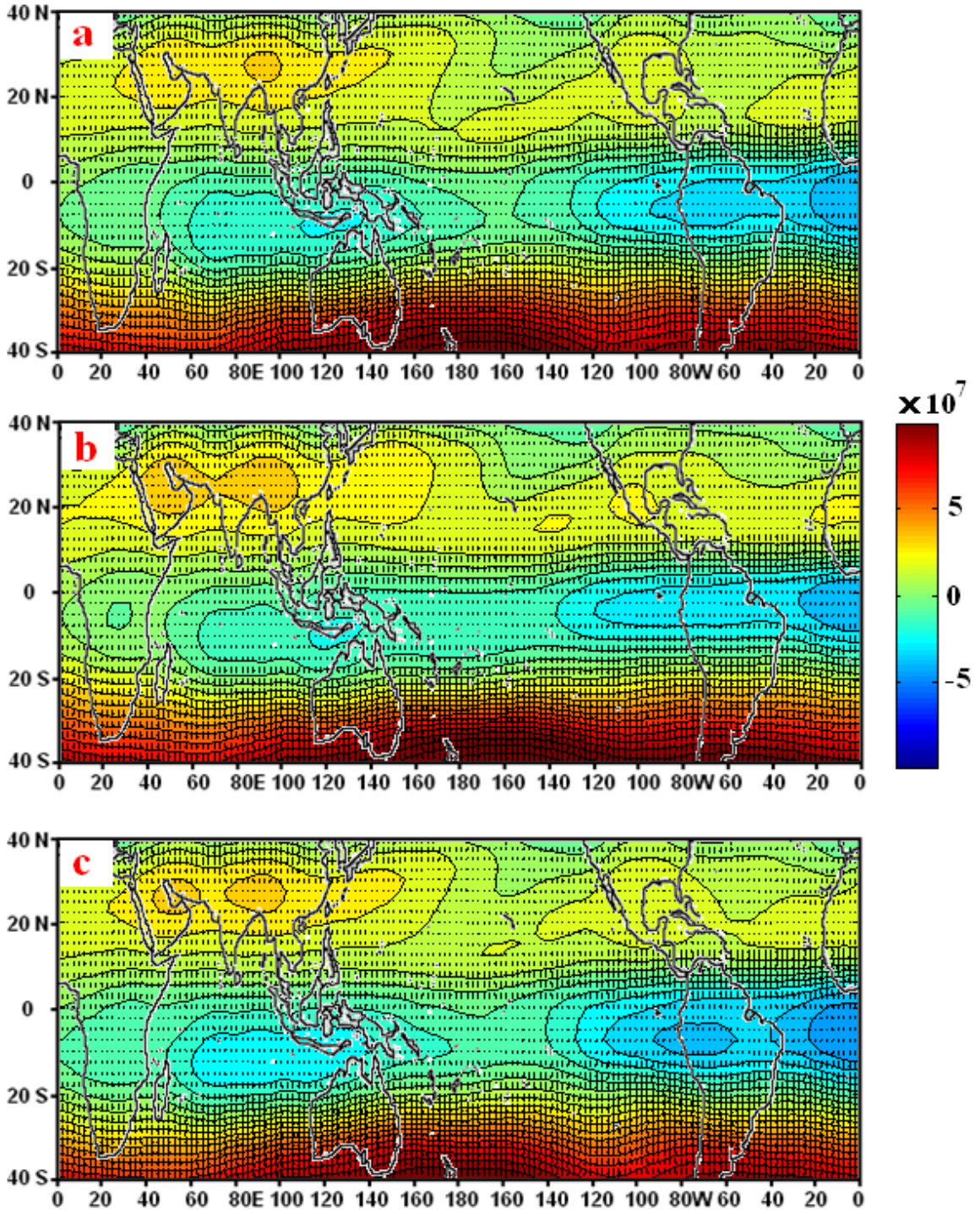

Figure 6.12: 200 hPa June-September mean velocity potential (m^2/s: contour shadings) and divergent wind (m/s: arrows) for: (a) Non-ENSO years, (b) El Niño deficient monsoon rainfall years (1987, 1991 and 2002) and (c) La Niña excess monsoon rainfall years (1988, 1998 and 2007).

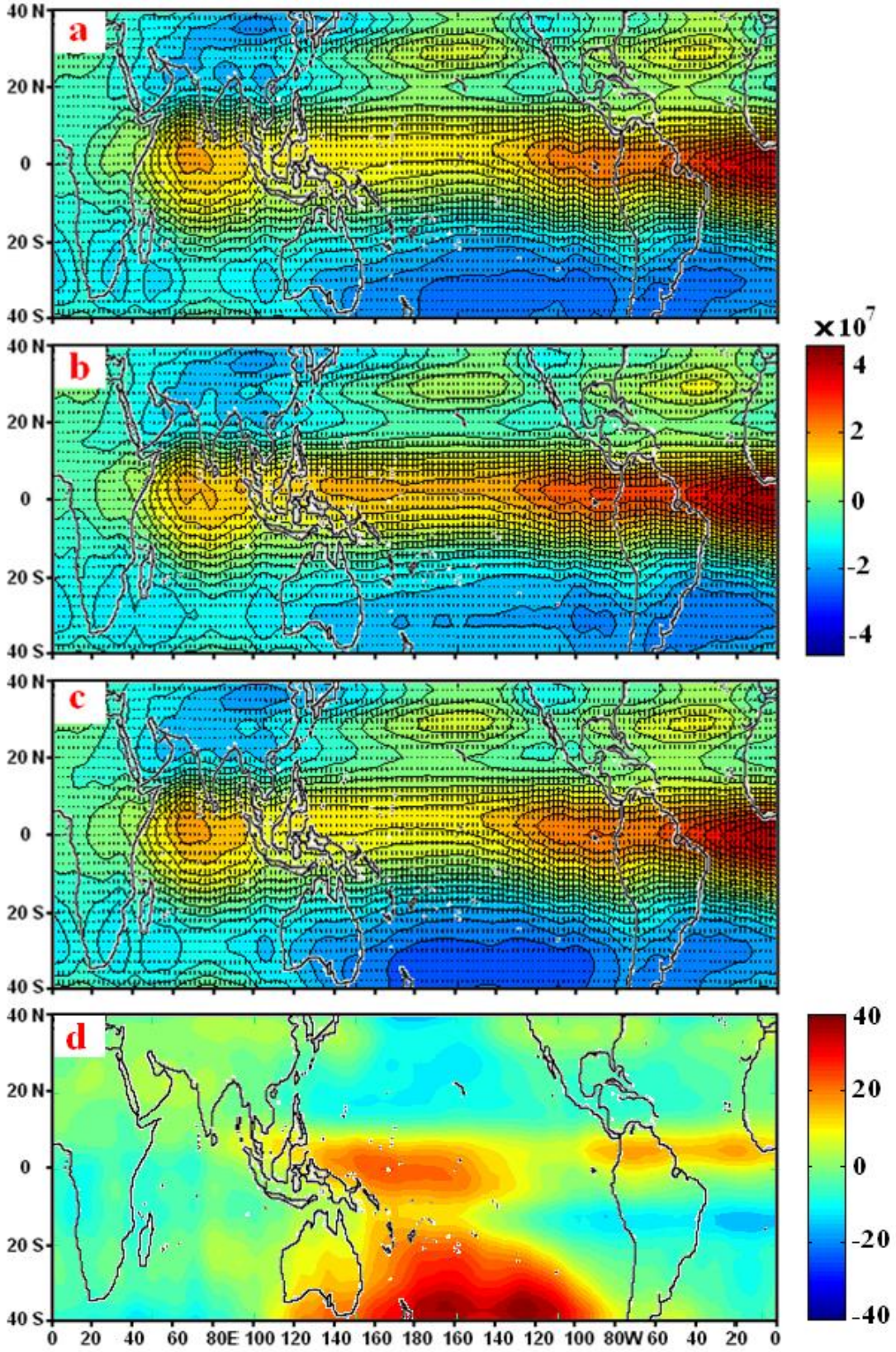

Figure 6.13: 850 hPa June-September mean velocity potential (m^2/s: contour shadings) and divergent wind (m/s: arrows) for: (a) Non-ENSO years, (b) El Niño deficient monsoon rainfall years (1987, 1991 and 2002), (c) La Niña excess monsoon rainfall years (1988, 1998 and 2007) and (d) Difference between El Niño years and La Niña years (b minus c) velocity potential magnitude (m^2/s).

Figure 6.14 depicts the lower-tropospheric (850 hPa level) monsoon mean wind flow (June-September) for the El Niño and La Niña episodes. The most striking feature is the existence of the strong Somali jet in both cases (Figure 6.14a and b). It should be noted that the cross-equatorial flow in the Indian Ocean region is weaker during the El Niño condition (Figure 6.14a), compared to the La Niña condition (Figure 6.14b). The higher wind that exists in the central Pacific during La Niña is not fully established during El Niño episodes. Annamalai et al (1999) also indicated that monsoon flow during the La Niña is stronger than normal and the monsoon flow during El Niño episodes are weaker than normal. Lower-tropospheric (850 hPa level) mean monsoon seasonal wind anomaly (based on the 1979-2007 period) patterns for the El Niño and La Niña episodes shown in Figure 6.15a and b, respectively, clearly indicate that the monsoon flow is weaker than normal during El Niño conditions and the flow is stronger than normal during La Niña episodes. A closer look at the wind flow in the Asian region also reveals that the wind anomaly direction pattern for the El Niño is the opposite of its counterpart La Niña condition. The most noticeable difference between wind anomaly patterns for the El Niño and La Niña episodes is that two strong maxima occur over the Pacific Ocean during La Niña conditions (Figure 6.15b), the centre of one maxima is located in the western Pacific (5º N and 140º E) with the second one in the south-eastern Pacific region (30º S and 120º W). These two maxima closely resemble the El Niño minus La Niña velocity potential pattern (Figure 6.13d). In the case of El Niño, the maximum wind anomaly in the western Pacific is much weaker and more shifted towards the east (Figure 6.15a). The second maximum that is seen in La Niña conditions is absent from the El Niño wind anomaly pattern. Another interesting feature that should be pointed out is that the flow is opposite, especially in the heart of the maxima mentioned. During La Niña, the easterly flow dominates where the maximum wind anomaly occurs (Figure 6.15b), whereas during El Niño episodes westerly flow dominates in the region of maximum wind anomaly (Figure 6.15a) causing the atmospheric deep convection to be suppressed over the tropical Indian Ocean during El Niño events. The El Niño related wind anomalies over the Indian Ocean cause deep convection to move from the western Pacific to the central Pacific during El Niño events (Bracco et al. 2007; Webster and Yang 1992).

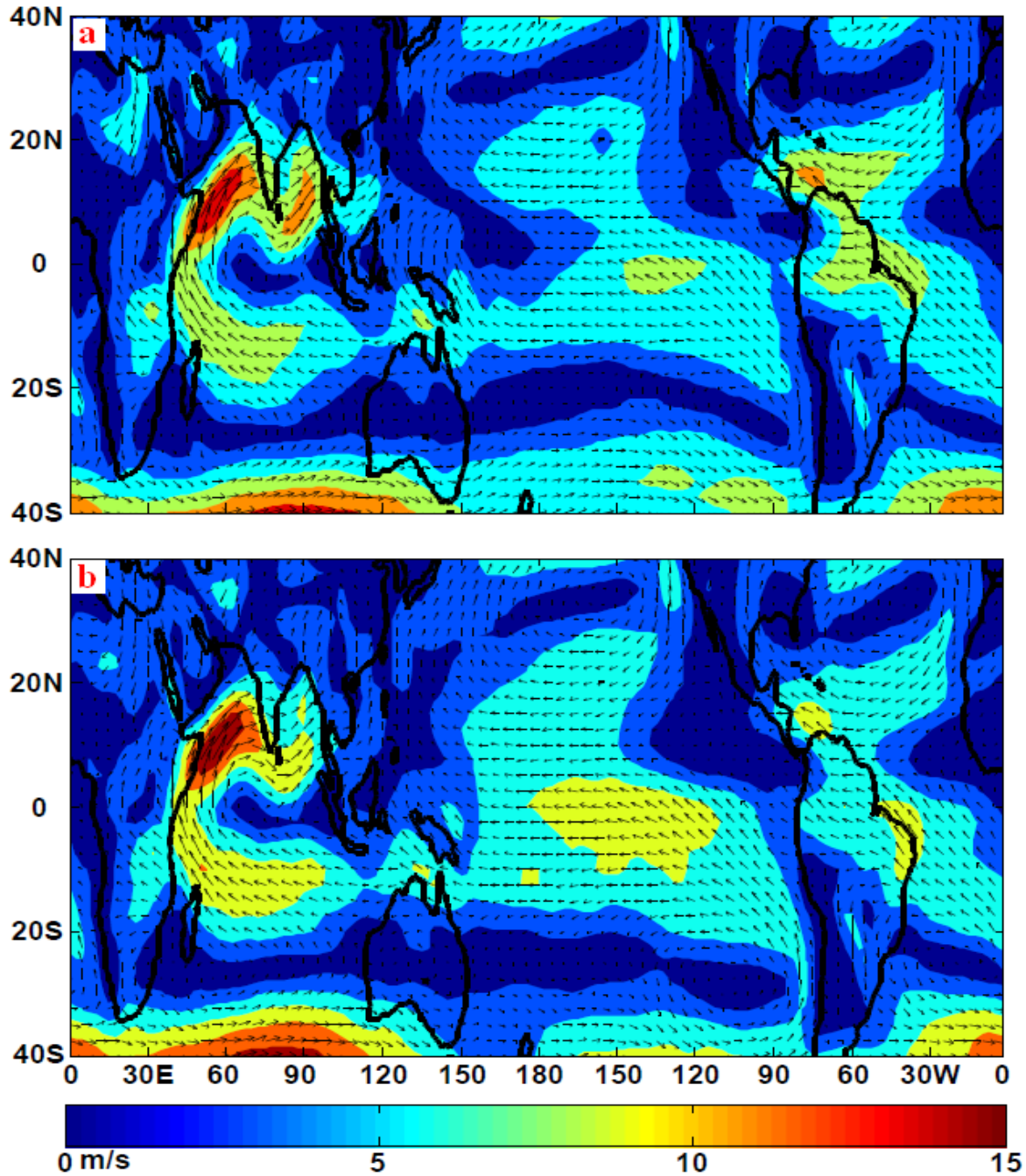

Figure 6.14: 850 hPa June-September mean wind (magnitude: contour shadings and direction: arrows) for: (a) El Niño deficient monsoon rainfall years (1987, 1991 and 2002), (b) La Niña excess monsoon rainfall years (1988, 1998 and 2007).

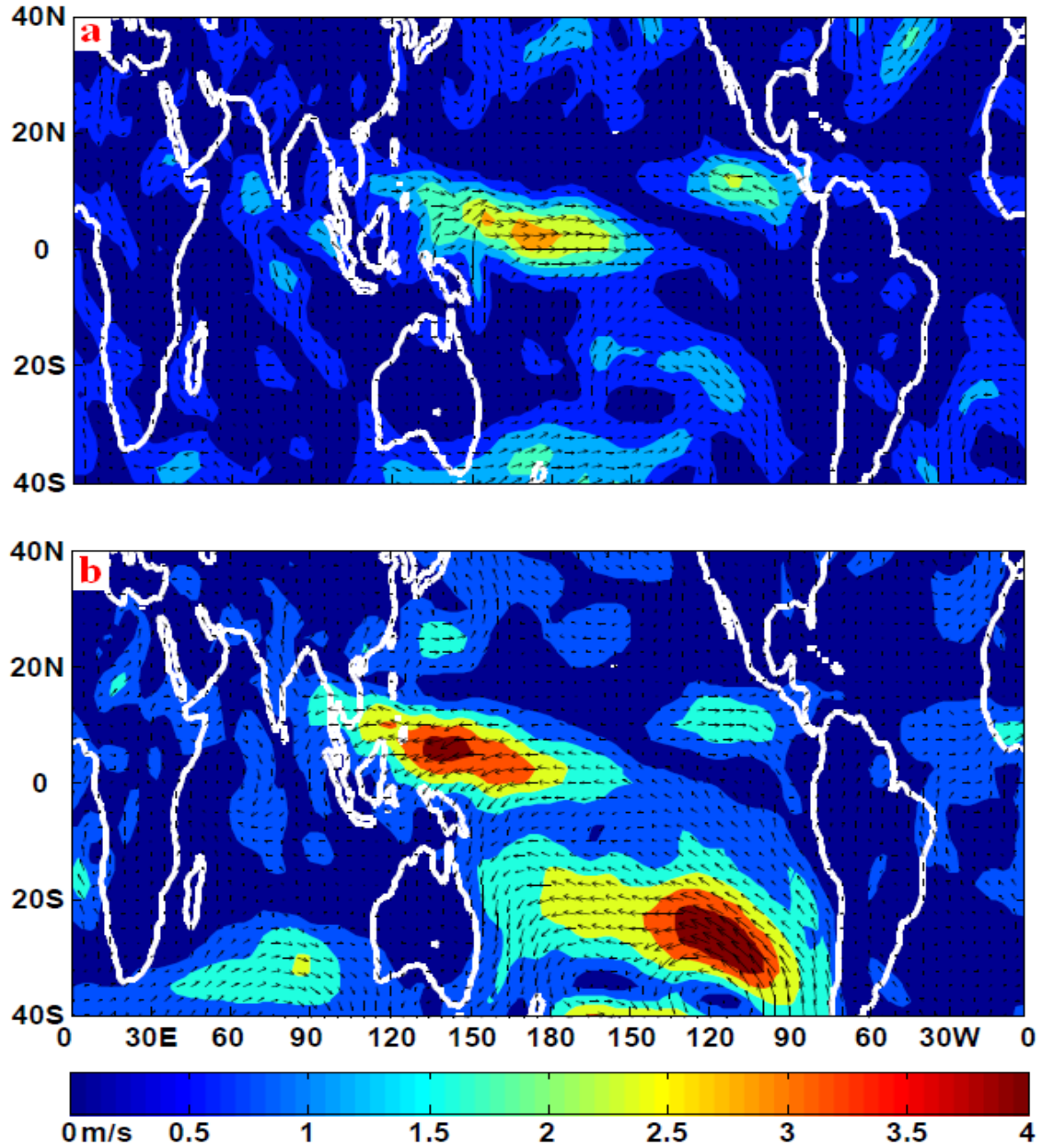

Figure 6.15: 850 hPa June-September wind anomaly (magnitude: contour shadings and direction: arrows) for: (a) El Niño deficient monsoon rainfall years (1987, 1991 and 2002), (b) La Niña excess monsoon rainfall years (1988, 1998 and 2007).

Global atmospheric deep convection inferred from outgoing longwave radiation (Wang and Hendon 2007) for the monsoon season (June-September) during El Niño and La Niña conditions are depicted in Figure 6.16a and b respectively. Both figures indicate persistent deep convection (low OLR) over the Indian and China Sea region. However, convection activity for the Indian region, including the Maldives area, during the El Niño conditions is less compared to the La Niña episodes. The deep convection in the Pacific Ocean is more pronounced and extends more to the east and covers most of the equatorial

Pacific region during El Niño conditions (Figure 6.16a), compared to the La Niña case (Figure 6.16b). Areas of low OLR (deep convection) and higher OLR (suppressed convection) can be seen more clearly from the OLR composite anomaly patterns shown in Figure 6.17. A very distinct but contrasting OLR anomaly pattern is evident for El Niño and La Niña episodes. Anomalously higher OLR (suppressed convection) dominates in the southwest Indian region (including the Maldives area) and Indonesian region for the case of El Niño (Figure 6.17a). Furthermore, an extended area of deep convection (anomalously low OLR) dominates in the Pacific Ocean region for the same scenario (El Niño case). On the other hand, the counterpart scenario (La Niña episode) shows the opposite pattern; positive anomalies occupy the Pacific region, while the Indian and Indonesian regions are dominated by anomalously low OLR during La Niña conditions (Figure 6.17b). The difference between El Niño and La Niña condition (El Niño minus La Niña: Figure 6.17c) also clearly shows that the Pacific region is dominated by a strong negative anomaly (deep convection) and the Asian region has a strong positive OLR anomaly, suggesting suppressed convection during El Niño episodes. This is consistent with the observed El Niño velocity potential pattern (Figure 6.13b and d). Velocity potentials are higher in the central Pacific region and sinking air (convergent inflow) is more evident during El Niño. This is also in agreement with the findings of Webster and Yang (1992) and Bracco et al. (2007). Deep convection moves from the western Pacific to the central Pacific during El Niño, due to the El Niño related wind anomalies over the Indian Ocean.

Evolution of convective activity for the El Niño situation is presented by means of monthly (January, April, July and October) outgoing longwave radiation anomalies based on long-term monthly mean values, as shown in Figure 6.18. Before the El Niño condition develops (in the month of January: Figure 6.18a), convective activity is quite strong (strong negative OLR anomaly) in the Indian and Pacific Oceans. It can be seen from Figure 6.18b, that the convective activity becomes less active in the Indian and Pacific Oceans as the El Niño starts to evolve (El Niño starts to evolve around March: Figure 6.7a). As Figure 6.18c depicts, convection is significantly suppressed during the monsoon season (July) in the Indian region during El Niño conditions. However, the convective activity is strengthened over the Pacific region over the same period. Towards the mature phase of El Niño (Figure 6.18d), low OLR anomalies (convective activity) appear in the Indian Ocean, associated with the migration of the Intertropical Convergence Zone (ITCZ) from the Northern Hemisphere to the Southern Hemisphere. During the same month, the convective activity further strengthened over the Pacific region. Evolution of convective activity (as inferred

from OLR anomaly patterns) is very consistent with the SSTA shown in Figure 6.8, suggesting that monsoon activity is closely linked to the SSTA in the Pacific.

El Niño and La Niña OLR anomaly amplitude averaged over the latitude band (2.5º S – 7.5º N: Maldives region) for all longitudes is shown in Figure 6.19. A very distinctive OLR anomaly amplitude pattern is evident for El Niño and La Niña episodes. During El Niño conditions, anomalously high OLR anomalies persist for the latitude band extending from West Africa (10º E) to the western Pacific Ocean (150º E), suggesting that convection is suppressed for the Maldives during El Niño conditions. Unusually low OLR anomalies persist in the Pacific region for the same scenario, indicating enhanced convection in the region. For the case of La Niña, opposite OLR anomalies dominate these regions. Unusually low OLR anomalies persist for the latitude band extending from about 0º E - 140º E longitude, indicating increased monsoon activity during La Niña conditions (Krishnamurti et al. 1990). On the other hand, the Pacific region is dominated by anomalously high OLR, associated with reduced convection in the region. A very contrasting and opposite OLR anomaly for the Maldives area (as indicated by the arrows in Figure 6.19) is evident and hence supporting that El Niño is associated with suppressed (reduced) convection, while the La Niña condition enhances monsoon activity for the Maldives area. Another feature that should be noted here is that the negative OLR anomaly is shifted more to the west during El Niño (Figure 6.19), suggesting that the deep convection moves from the western Pacific to the central Pacific during El Niño, further supporting the findings of Webster and Yang (1992) and Bracco et al. (2007).

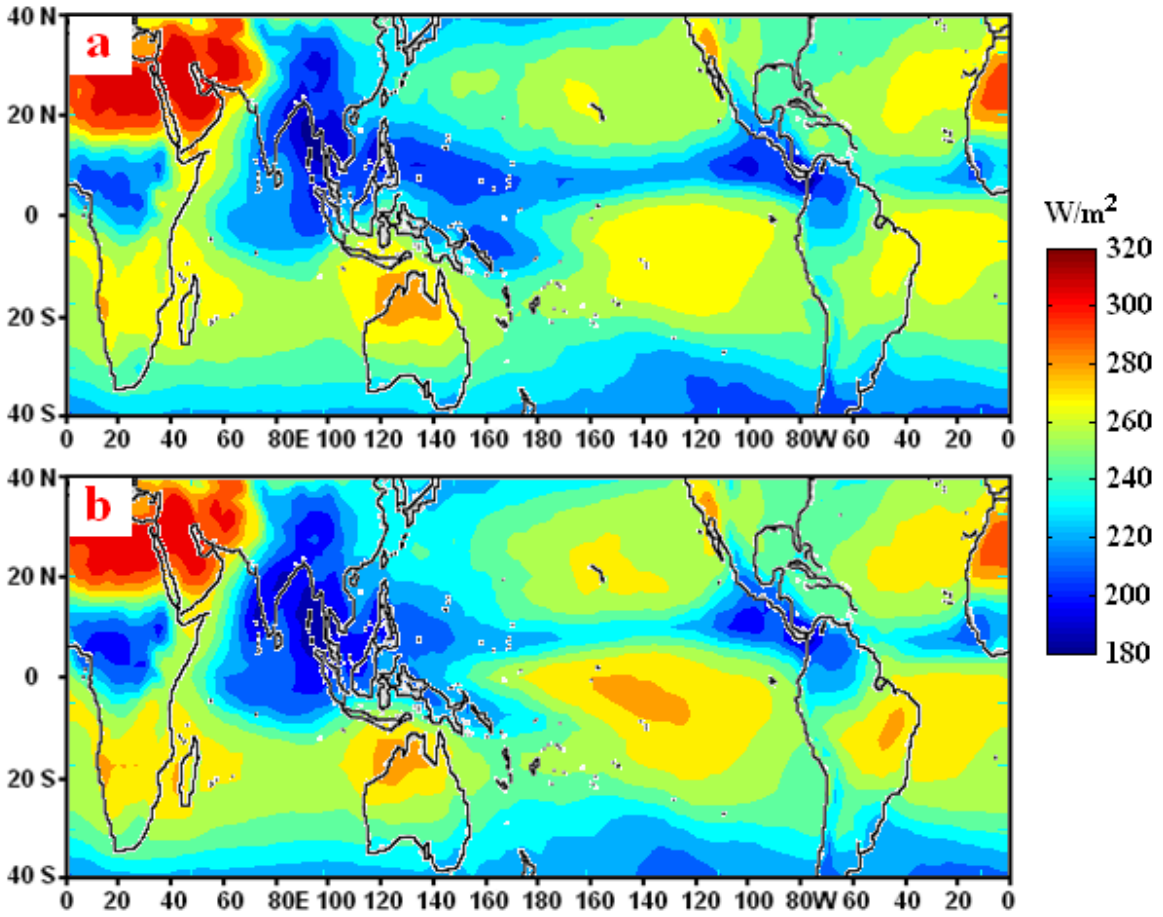

Figure 6.16: Spatial pattern of June-September (JJAS) mean outgoing longwave radiation (OLR) for: (a) El Niño deficient monsoon rainfall years (1987, 1991 and 2002) and (b) La Niña excess monsoon rainfall years (1988, 1998 and 2007).

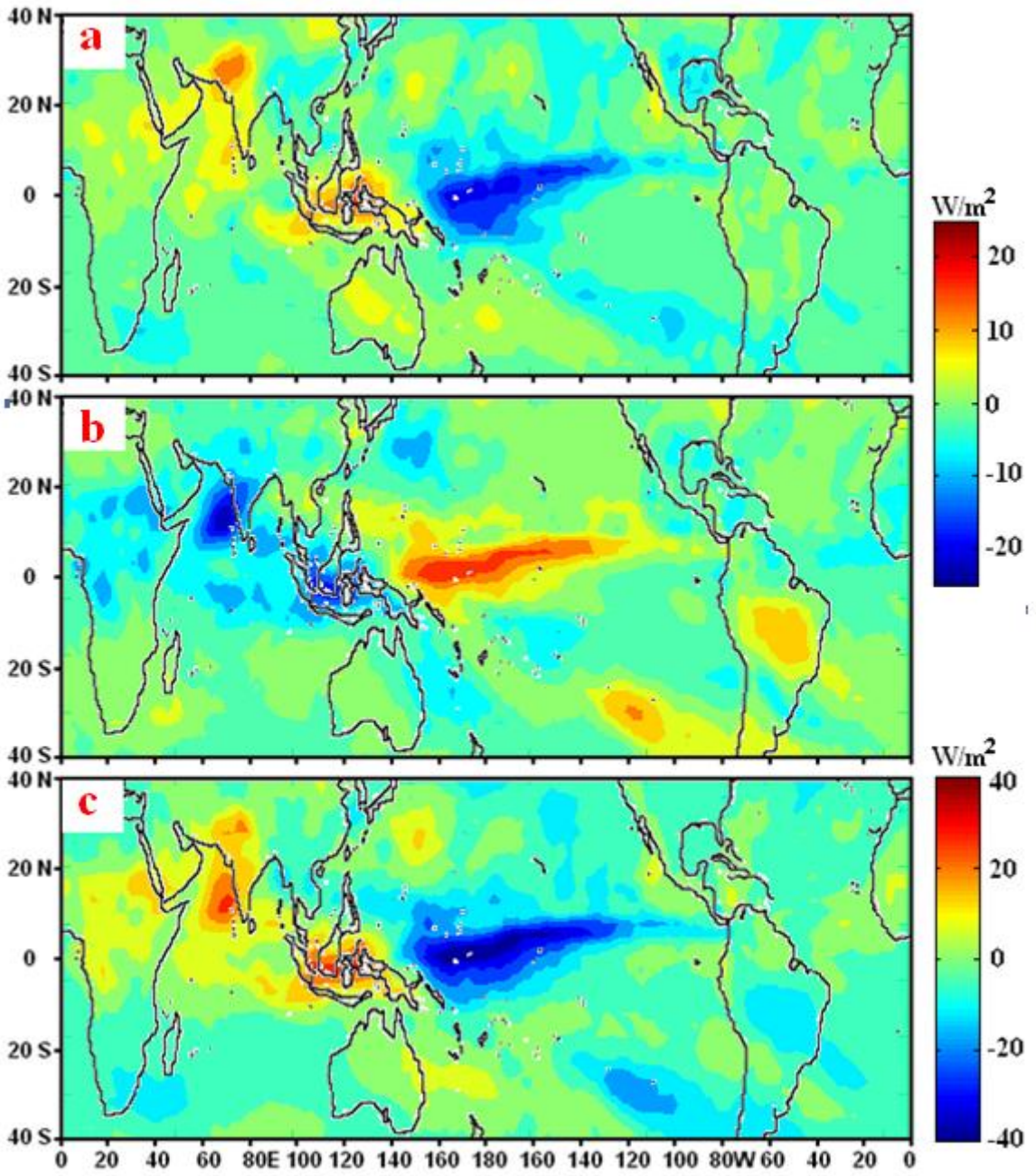

Figure 6.17: Spatial pattern of June-September (JJAS) composite outgoing longwave radiation (OLR) anomaly for: (a) El Niño deficient monsoon rainfall years (1987, 1991 and 2002), (b) La Niña excess monsoon rainfall years (1988, 1998 and 2007), and (c) difference between (a) and (b). Same colour bar is shown for (a) and (b) but a different colour bar is shown for (c). Anomalies are based on the 1979-2007 period.

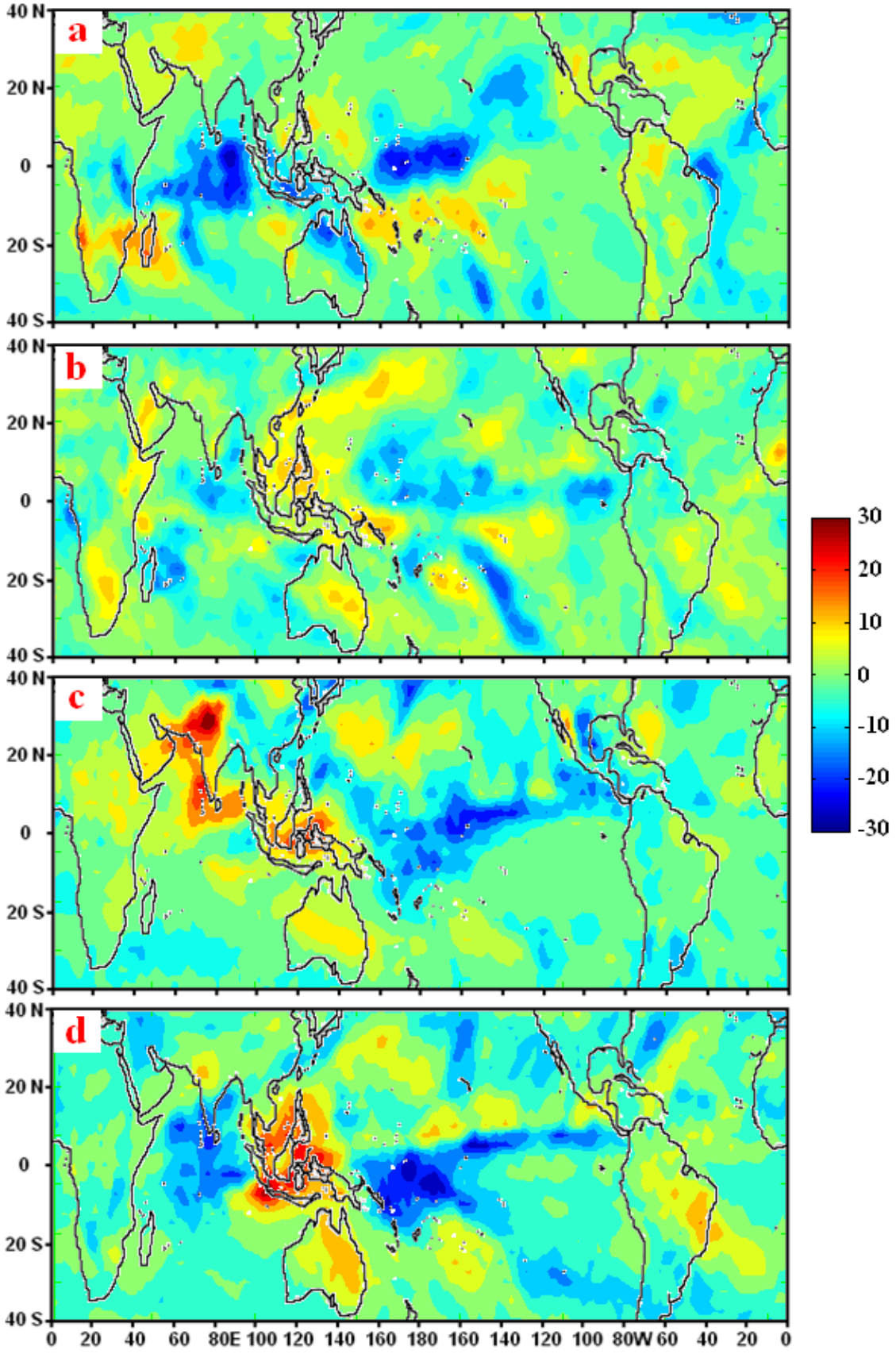

Figure 6.18: Evolution of outgoing longwave radiation (OLR): (a) January, (b) April, (c) July and (d) October. Each month is an average of El Niño years (1987, 1991 and 2002). Anomalies are based on the 1979-2007 period.

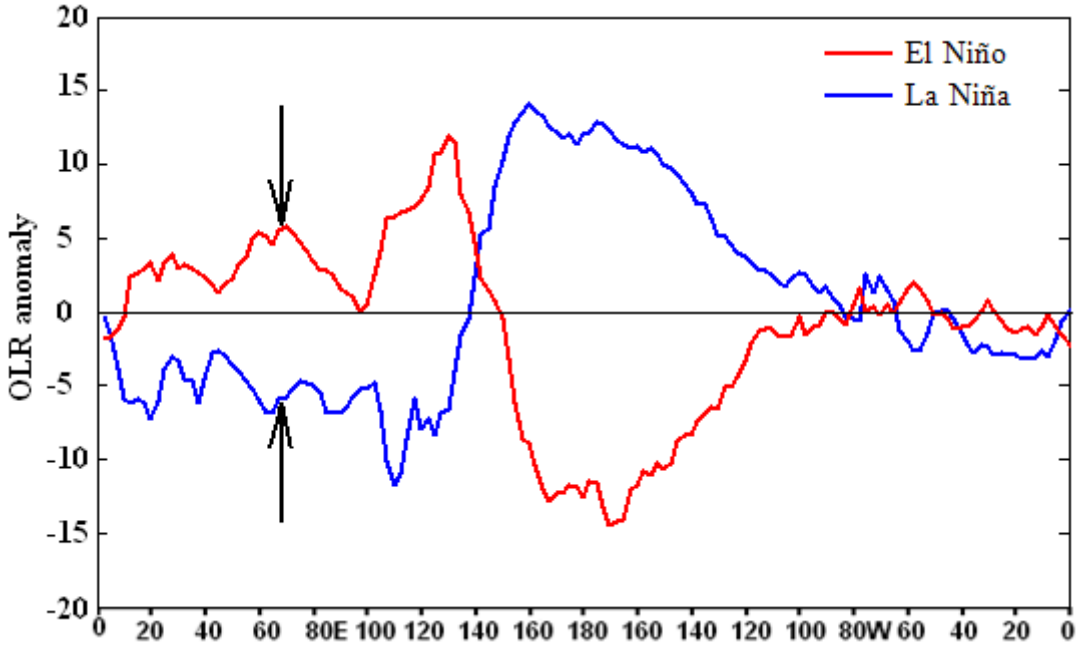

Figure 6.19: June-September (JJAS) outgoing longwave radiation (OLR: Wm^{-2}) anomaly averaged for the Maldives region (2.5º S-7.5º N: indicated by the arrows) for El Niño years (red curve) and La Niña years (blue curve). Anomalies are based on the 1979-2007 period.

Another way of assessing large scale rising and sinking (subsidence) regions is through analysis of vertical velocity (ω: omega) patterns. When 500 hPa level (mid-tropospheric level) vertical velocity is less than zero (ω500 < 0), it represents rising air/deep convection and when 500 hPa level vertical velocity is greater than zero (ω500 >0), it indicates sinking action/subsidence (Bony and Dufresne 2005; Bony et al. 2004). Mid-tropospheric mean vertical velocity for the monsoon season is depicted in Figure 6.20. Negative vertical velocities in the figure indicate upward motions, while positive velocities indicate downward motion. A very similar pattern can be seen for the 500 hPa level long-term vertical velocity climatology (Figure 6.20a) and for the El Niño and La Niña mean velocity for the monsoon season (Figure 6.20b and c, respectively). The most noticeable pattern is the occurrence of rising air/deep convective regions in the equatorial region, especially over Africa, India, China and Pacific Ocean. Compared to the El Niño conditions, the upward motion (rising air) is suppressed during the La Niña case, especially over China and the west and central Pacific Ocean. 500 hPa spatial patterns of composite vertical velocity anomaly shown in Figure 6.21 clearly indicate regions of rising air/deep convection or sinking action/subsidence compared to the normal/average condition. A strong ascending motion (rising air) region is located in the central Pacific during El Niño

episodes (Figure 6.21a). Areas of ascending motion are also located around China and the west Pacific. On the other hand, vertical velocity maxima are located over southwest India, the Maldives and the Indonesian region for the same scenario. Composite anomalies of mid-tropospheric vertical velocity for the monsoon season during La Niña conditions show opposite anomaly patterns (Figure 6.21b). This is especially true for the Pacific region. Regions of strong ascending motion (rising air) that are apparent during El Niño conditions are reversed in La Niña conditions. Upward motion is also apparent around 65º E (at the equator), along the east coast of Australia and in the south Pacific (around equator and 165 ºE-130 ºW) during La Niña. The strong ascending motion over the Pacific during El Niño is shifted more to the east compared to descending motion during La Niña. This is an indication that weak Walker circulation associated with the El Niño causes the deep convection to move from the western Pacific warm pool to the central Pacific. The ascending (rising air/deep convection) or descending (sinking action/subsidence) motions in the Pacific during El Niño and La Niña episodes, respectively, are closely linked to the warm and cold SST anomaly conditions over the Pacific ocean, during El Niño and La Niña episodes, respectively (Veiga et al. 2005), as was depicted in the SST anomaly pattern for El Niño and La Niña episodes (Figure 6.10).

A better way of representing ascending (rising air/deep convection) or descending (sinking action/subsidence) motions for a particular location is through analysis of vertical sections (cross-sections of longitude-height) of vertical velocity. Figure 6.22 shows cross-sections of longitude-height vertical velocity composites for El Niño and La Niña (Figure 6.22a and b, respectively) and their corresponding composite anomaly patterns (Figure 6.22c and d, respectively) averaged for the Maldives area (2.5° S -7.5° N latitude band). The most noticeable features along this latitude band are regions of significant ascending motions ($\omega 500 < 0$: rising air/deep convection) during both El Niño and La Niña conditions. Double cells of strong ascending motion ($\omega 500 < 0$) are located in the Pacific during El Niño, originating from 130º E and extending to 140º W, starting from about 900 hPa and reaching up to the 100 hPa level. The ascending motion observed over the west coast of South America and the Atlantic Ocean region in the 500 hPa vertical velocity (Figure 6.20) pattern also appear as double cells in the longitude-height vertical velocity cross-section for both scenarios (Figure 6.22a and b), extending from 900 hPa up to the 250 hPa pressure level. A region of rising air is also located between 700 and 100 hPa levels for the Indian Ocean region (75º E and 105º) during El Niño episodes. Although the areas of negative vertical velocity (ascending motion) appear during both episodes over Africa

(Figure 6.22a and b), it is more widespread over Africa during La Niña, but stronger during El Niña conditions at the 700 hPa and 400 hPa pressure levels. During the La Niña case, an extensive area of strong ascending motion dominates the 2.5° S -7.5° N latitude band, extending from 60º E-170º E, originating from the lower troposphere up to the 100 hPa level. The ascending motion that occupies the Indonesian region during the La Niña episode is absent for the case of the El Niño episode (Figure 6.22a and b). As is evident from Figure 6.22a and b, regions of descending motion ($\omega 500 > 0$) are less extensive compared to the ascending motion ($\omega 500 < 0$) observed for both El Niño and La Niña conditions. As can be seen from the figure, a small area of sinking air appears at around 40º E-50º E, from the surface to upper levels. A weak extensive area of sinking motion (strongest between 600 hPa and 300 hPa levels) dominates the east Pacific region during La Niña conditions (Figure 6.22b), which is almost absent during El Niño episodes.

Vertical cross-sections of vertical velocity composite anomaly for the El Niño and La Niña episodes presented in Figure 6.22c and d, respectively, show regions of rising air/deep convection or sinking action/subsidence compared to the mean conditions. A region of strong ascending motion (negative vertical velocity anomaly) occupies from the dateline to the eastern Pacific (120º W), between 900 and 100 hPa pressure levels, during El Niño condition (Figure 6.22c). Veiga et al. (2005) also observed similar negative anomalies of vertical velocity between 180º and 120º W and between 700-200 hPa pressure levels for El Niño composites (1972-73, 1982-83, 1986-87, 1991-92 and 1997-98). During La Niña, the opposite anomaly pattern is evident for the same region, but the descending motion located between 900 and 100 hPa pressure levels is more extensive, crossing the dateline and reaching as far as 150º E (Figure 6.22d). Another significant pattern that should be noted is the very contrasting opposite anomaly pattern over the Maldives (indicated by the arrows in Figure 6.22) and Indonesian region during El Niño and La Niña conditions. Over the Maldives and Indonesian region, significant enhancement of descending (sinking action/subsidence) motions occurs during El Niño (Figure 6.22c) compared to the La Niña condition (when rising air/deep convection dominates: Figure 6.22d). Vertical cross-sections (longitude-height) of vertical velocity composite anomaly pattern for the El Niño and La Niña events averaged over the Maldives (2.5° S -7.5° N latitude band) clearly show that during El Niño, the Maldives region is dominated by positive vertical velocity anomaly, or increased downward motion (descending/sinking/subsidence).

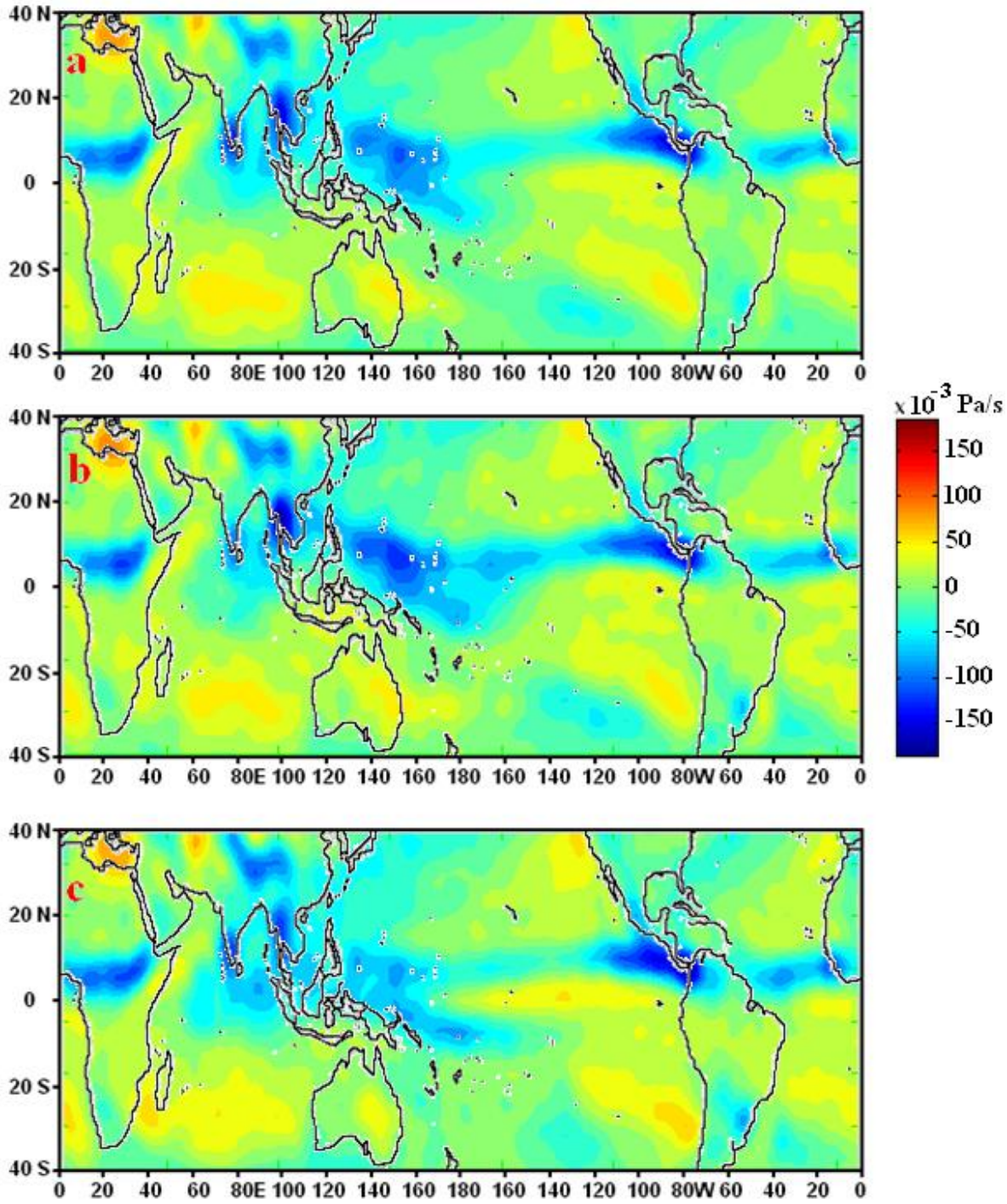

Figure 6.20: June-September mean vertical velocity for the 500 hPa level: (a) mean for the period 1979-2007, (b) mean for El Niño deficient monsoon rainfall years (1987, 1991 and 2002), and (c) mean for La Niña excess monsoon rainfall years (1988, 1998 and 2007).

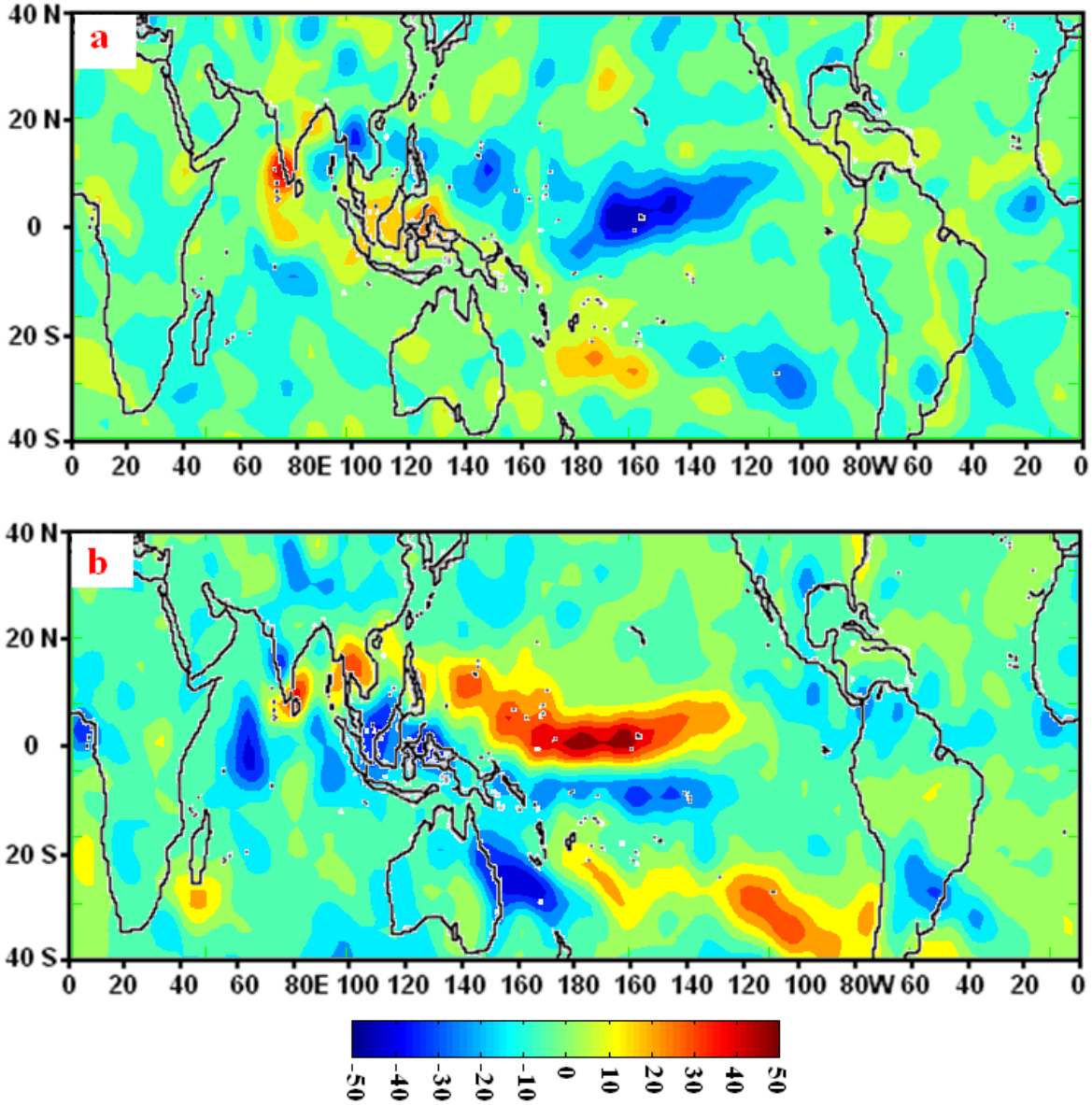

Figure 6.21: 500 hPa June-September composite vertical velocity anomalies (×10^{-3} Pa/s): (a) El Niño years (1987, 1991 and 2002) and (b) La Niña years (1988, 1998 and 2007). Anomaly based on the 1979-2007 period.

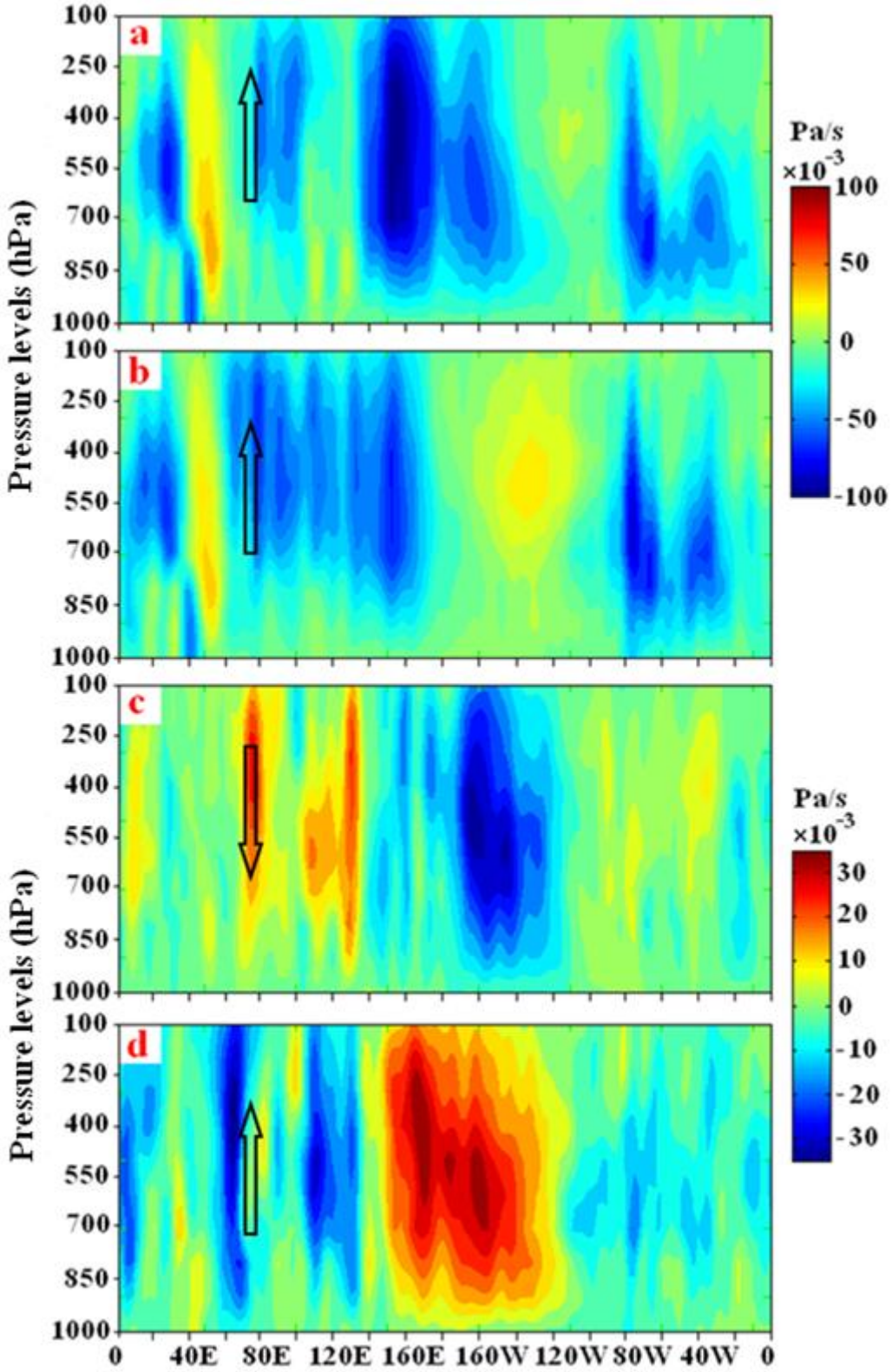

Figure 6.22: Longitude-height sections of June-September vertical velocity composite (averaged over the Maldives region: 2.5° S -7.5° N latitude band): (a) mean for El Niño deficient monsoon rainfall years (1987, 1991 and 2002), (b) mean for La Niña excess monsoon rainfall years (1988, 1998 and 2007), and (c) and (d) their corresponding anomaly based on 1979-2007 period. The Maldives region is represented by the arrows.

The water vapour flux or vertically integrated moisture transport is an important component of the global hydrological cycle, since it redistributes moisture and latent heat (Liu and Tang 2005). The release of latent heat from moisture is a major source of heat for the atmosphere and zonal variation of latent heat plays a crucial role in the tropical circulation (D'Abreton and Tyson 1995). Vertically integrated moisture transport in the north Indian Ocean accounts for about half of the variability in the moisture convergence in the region during ENSO events (Fasullo and Webster 2002). Since fluctuations of the moisture content (integrated over the depth of the atmosphere) can significantly influence flood and drought events (Liu and Tang 2005), changes in the hydrological cycle associated with the El Niño and La Niña conditions can be analysed through water vapour flux measurements (vertically integrated moisture transport). Fasullo (2005) found that changes in vertically integrated moisture transport over the Arabian Sea and India associated with the disturbed Walker and Hadley circulations played a key role in causing drought over Indian in 2002. Since the monsoon forcings are directly linked to the vertically integrated moisture transport (He et al. 2007)(VIMT) it is calculated following Peixoto and Oort (1983) and the zonal and meridional components of the Q vector are expressed as:

$$Q_u = \frac{1}{g} \int_{Psurface}^{Ptop} qu \, \mathrm{dp}$$

$$Q_v = \frac{1}{g} \int_{Psurface}^{Ptop} qv \, \mathrm{dp}$$

where g is acceleration due to gravity, Psurface = 1000 hPa (the surface pressure), Ptop = 300 hPa (pressure at the top of the atmosphere), q is the specific humidity and u and v are the zonal and meridional wind components, respectively. Above 300 hPa, specific humidity values are poorly know and the calculation of the VIMT is negligibly influenced by the use of 300 hPa pressure, since over the tropics specific humidity at that level is two orders of magnitude less than at the surface (Fasullo and Webster 2003; Kalnay et al. 1996). Composites of VIMT for El Niño and La Niña were estimated by means of Riemann sum integration using vertical profiles of monthly NCEP/NCAR specific humidity and wind

vector data for the 1000, 925, 850, 700, 600, 500, 400 and 300 hPa vertical levels (Fernandez et al. 2003).

Figure 6.23 shows the computed vertically integrated moisture transport for the whole globe. It is very interesting to note that the vertically integrated moisture transport depicted in the figure resembles very closely the lower-tropospheric (850 hPa level) wind flow pattern shown in Figure 6.11. Strong cross-equatorial easterly flow of moisture in the Asian region is evident for both El Niño (Figure 6.23b) and La Niña (Figure 6.23c) cases. However, it should be noted that the magnitude of the VIMT is weaker during El Niño conditions, compared to the mean (Figure 6.23a) and La Niña conditions. This is also clear from the composite anomaly shown in Figure 6.24 for El Niño and La Niña cases. The most noticeable anomaly occurs in the Pacific region. During El Niño, the Pacific region shows anomalously negative VIMT, while during La Niña the same region is dominated by positive anomalies. Anomalously negative VIMT also occupies the South Pacific Ocean region, China and India. The anomaly pattern for El Niña and La Niña is consistent with the El Niña and La Niña vertical velocity anomaly patterns shown in Figure 6.21a and b, suggesting that areas of negative vertical velocity (ascending motion/rising air) during El Niño are associated with a decrease in VIMT (Figure 6.24a). On the other hand, vertical velocity anomalies during La Niña conditions are associated with enhanced moisture. Godfred and Reason (2002) pointed out that the extreme states of ENSO (El Niño and La Niña) redistribute preferred areas of low-level moisture convergence and deep convection in the Indo-Pacific region due to changes in the Walker circulation in association with sea surface temperature anomalies in the region. The vertically integrated moisture transport anomaly during El Niño and La Niña for the 2.5ºS-7.5ºN latitude band (Maldives region: Figure 6.25) is very similar to the OLR anomalies (Figure 6.19) averaged for the same latitude band. It is evident from Figure 6.25 that during El Niño conditions moisture is suppressed over the Maldives area, while during La Niña conditions the Maldives region experiences enhanced VIMT. There is therefore a tendency for a decrease in precipitation over the Maldives during El Niño episodes and enhanced precipitation during La Niña conditions. From Figure 6.25, it interesting to note that the increased moisture occurs to the west of the Maldives, while to the east there is a negative anomaly (during La Niña).

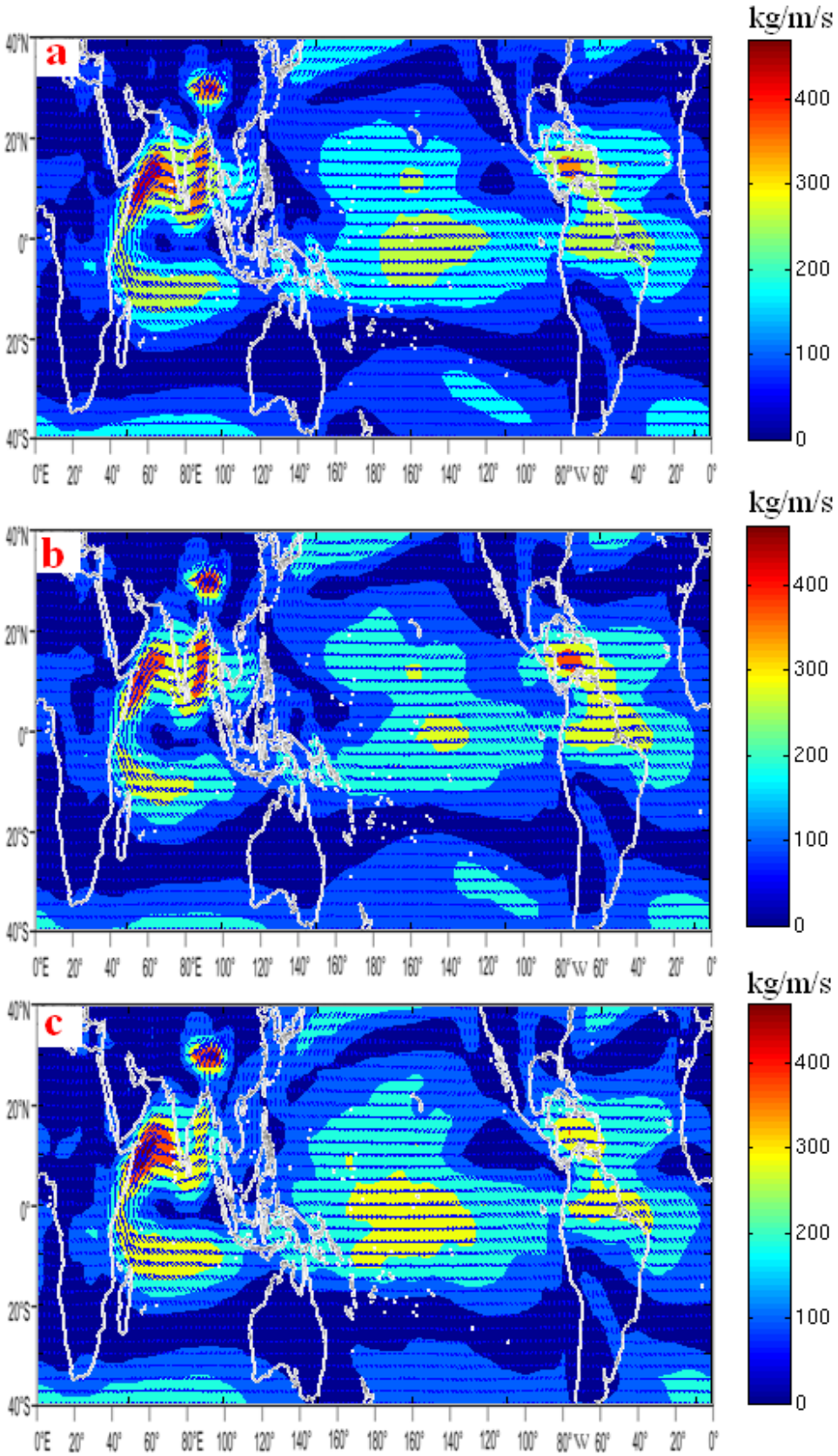

Figure 6.23: Vertically integrated moisture transport: (a) June-September mean for the period 1979-2007, (b) June-September composite for El Niño years (1987,1991 and 2002) and (c) June-September composite for La Niña years (1988, 1998 and 2007).

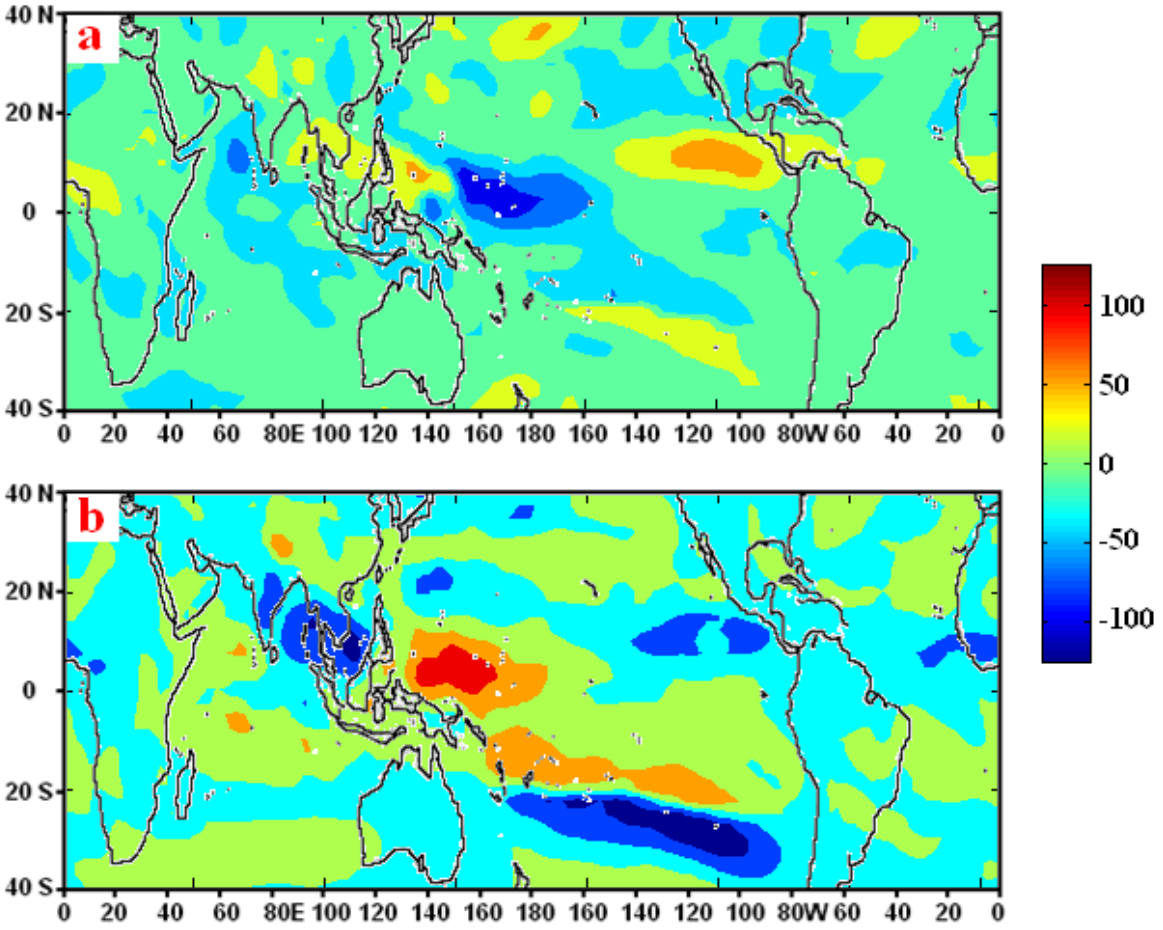

Figure 6.24: Vertically integrated moisture transport ($kgm^{-1}s^{-1}$) composite anomaly for: (a) El Niño years (1987, 1991 and 2002) and (b) La Niña years (1988, 1998 and 2007). Anomaly based on the 1979-2007 period.

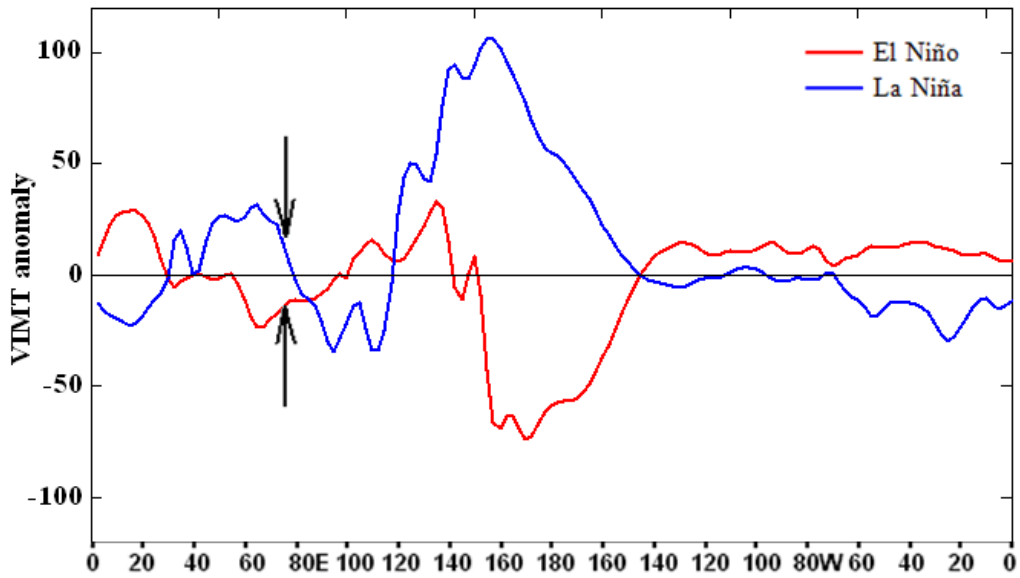

Figure 6.25: June-September (JJAS) vertically integrated moisture transport (VIMT: $kgm^{-1}s^{-1}$) anomaly averaged for the Maldives region (2.5º S-7.5º N: indicated by the arrows) for El Niño years (red curve) and La Niña years (blue curve). Anomalies are based on the 1979-2007 period.

The results presented above for various atmospheric fields (horizontal wind velocity, velocity potential, vertical velocity, outgoing longwave radiation and vertically integrated moisture transport) clearly indicate that the SSTA over the Pacific region brings very contrasting atmospheric circulation patterns for the El Niño warm and La Niña cold events. Anomalous circulation patterns during El Niño and La Niña events are associated with negative rainfall anomalies during El Niño and anomalously positive rainfall during La Niña for the Asian region as a whole, as depicted in Figure 6.26a and b, respectively. The association between strong/moderate El Niño and La Niña events and All-India monsoon rainfall (AIMR) and Maldives monsoon rainfall (MMR) depicted in Figure 6.4 agrees well with the negative rainfall anomaly and anomalously positive rainfall for the Asian region. This is an agreement with the previous findings that India experiences a deficit in rainfall (drought) during most of the El Niño events, while most of the La Niña episodes are associated with enhanced precipitation (flooding) over India (Bracco et al. 2007; Webster and Yang 1992). The area averaged fields for the Maldives region clearly shows opposite signs during El Niño and La Niña conditions, suggesting teleconnections between the Maldives monsoon rainfall and El Niño/La Niña conditions. Strong/moderate El Niño and La Niña events are associated with deficit/excess rainfall for the Maldives during the monsoon season (Figure 6.4), which is in agreement with the large-scale atmospheric circulation patterns for the Asian region.

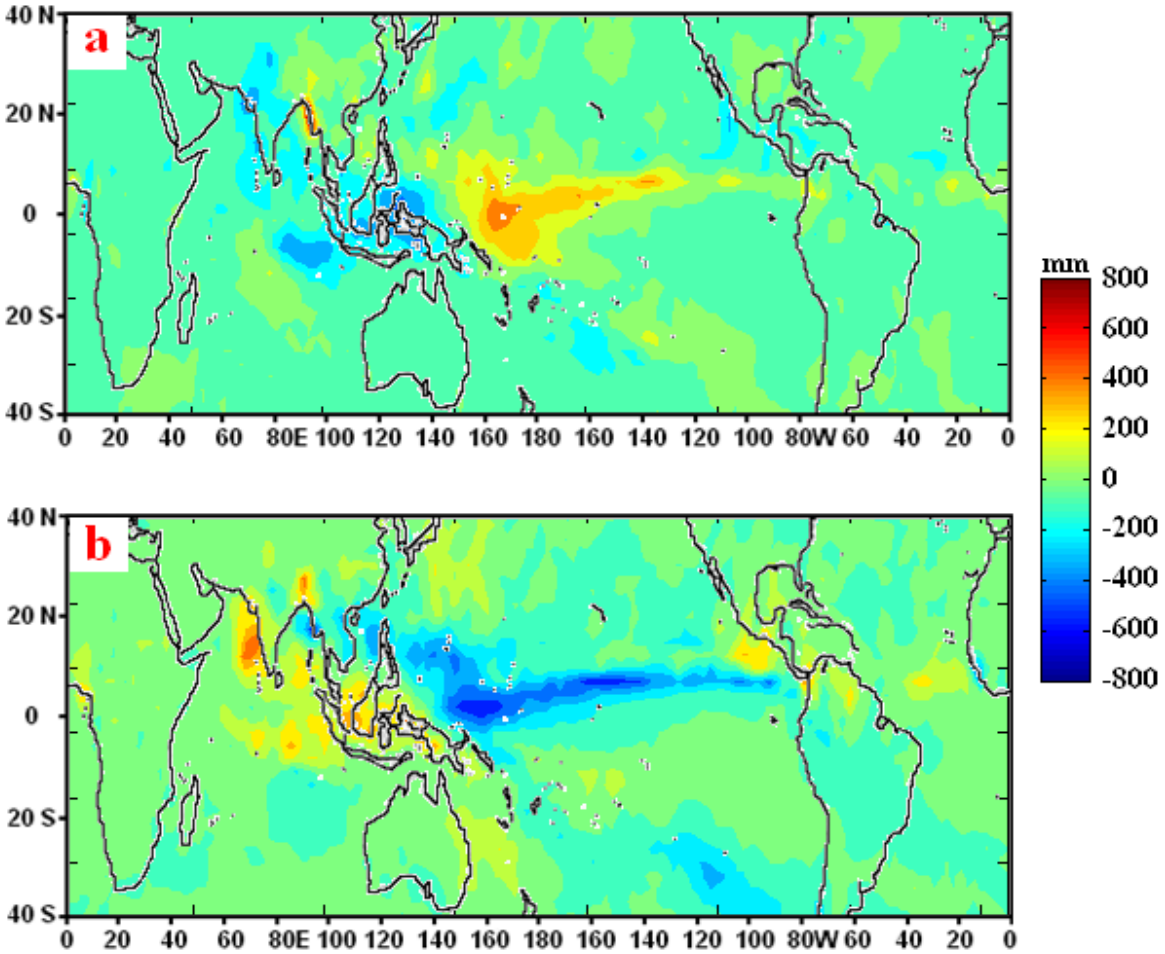

Figure 6.26: June-September (JJAS) precipitation composite anomaly for: (a) El Niño years and (b) La Niña years. Anomalies are based on the 1979-2007 period.

6.2 Summary

The aim of this chapter was to understand the association between the Maldives monsoon rainfall and ENSO events. To determine the connection between ENSO and the monsoon, El Niño and La Niña events were identified using Extended Reconstruction Sea Surface Temperature (SST) Version 3B (ERSST V3B) data. Since no studies have looked at the connections between ENSO and monsoon variability over the Maldives, evolution of various features and changes in large-scale atmospheric circulation patterns were investigated using various atmospheric fields (including the horizontal wind velocity, velocity potential, vertical velocity, outgoing longwave radiation and vertically integrated moisture transport) over the equatorial Indo-Pacific Ocean in relation to the Maldives monsoon rainfall, to understand the atmospheric circulation patterns associated with the El Niño and La Niña events and to determine the role they play in bringing normal/abnormal rainfalls over the Maldives and Asian region as a whole. The results indicate that there was

a total of 3 strong and 4 moderate El Niño events (3/4) and 1 strong and 3 moderate La Niña events (1/3) for the period 1979-2007. Composite analysis carried out on various atmospheric fields based on Maldives monsoon rainfall for strong/moderate El Niño and strong/moderate La Niña years, clearly demonstrates significant contrasting opposite anomaly patterns during El Niño and La Niña events. Associated with El Niño and La Niña anomaly patterns, the Maldives/India region experiences deficiencies in monsoon rainfall about 71.4% of the time during strong/moderate El Niño years. Furthermore, during strong/moderate La Niña events the Maldives/India regions experience excessive monsoon rainfall about 75% of the time, suggesting that the deficient/excess monsoon rainfall over the Maldives and India regions is linked to the strong/moderate El Niño/La Niña events, respectively. Not only during El Niño and La Niña events do the Maldives and India experience excessive and deficit monsoon rainfall, but during some of the non-ENSO years these areas experience excessive and deficit monsoon rainfall. This demonstrates that factors unrelated to ENSO events also play an important role in bringing excessive and deficit monsoon rainfall to this region in some years. During most of the non-ENSO events, monsoon rainfall over the Maldives and India is out of phase. This suggests that the monsoon rainfalls over the Maldives during non-ENSO events are influenced by different factors from those affecting India during the same events. Therefore, processes influencing monsoon rainfall over the Maldives during non-ENSO events needs to be investigated in future.

7 Regional scale processes

Global scale processes such as ENSO, discussed in Chapter 6, can impact on the Eurasian continent through changes in land surface conditions, which in turn can influence the following monsoon (Meehl 1997; Wang 2006). The tropospheric biennial oscillation (TBO) plays an important role in the interannual variability of the monsoon in the Indo-Pacific region, while ENSO may interact with the TBO (Izumo et al. 2008). Variations in the precipitation pattern over the Maldives in relation to regional scale processes (Eurasian snow cover and TBO), as mentioned in Chapter 6, will be investigated further here.

7.1 Eurasian snow cover and monsoon (Regional scale processes: Part A)

The monthly mean snow cover over the Northern Hemisphere land area ranges from about 7-40% (Wu and Qian 2003). Snow covered surfaces are one of the most rapidly varying natural surfaces both spatially and temporally, and snow on a large scale can have a profound impact in modifying the regional hydrological cycles through snowmelt due to diabatic heating (Cohen 1994; Wu and Qian 2003). According to Ye and Bao (2001), anomalous snow cover/volume over Eurasia can influence the monsoon circulation due to the following: snow reduces solar absorption due to snow's high albedo, it uses more solar energy for snow melting (thus reducing available energy for heating the surface or the air above it) and increases soil moisture (after melting), which also increases heat consumption for evaporation (again reducing available energy for surface heating or the air above it). These factors reduce warming over land, which in turn reduces the thermal gradient between land and ocean, thus influencing the monsoon circulation (Ye and Bao 2001). The influence of Eurasian snow cover on the South Asian monsoon has been studied for more than a century and it has been found that the spring snow cover anomaly can play a major role in Asian summer monsoon variability (Liu and Yanai 2002; Shaman et al. 2005).

Many studies have indicated (based on observational data) that there is an inverse relationship between Eurasian snow cover/depth and the Indian summer monsoon rainfall, with excessive snow cover in winter/spring associated with deficient Indian monsoon rainfall and vice versa (Bamzai and Shukla 1999; Kripalani and Kulkarni 1999). Using modelled and simulated results, Vernekar et al. (1995) further supported observed evidence that a strong positive anomaly in winter/spring Eurasian snow cover is associated with

deficient rainfall over India in the following summer monsoon. They have shown that excessive snow cover in February is characterized by higher sea level pressure over India, a weak Somali jet, weaker lower and upper tropospheric westerlies and easterlies, respectively, and reduces monsoon precipitation over India.

Until today, much of the research on the snow-monsoon relationship has focused on the Indian or Chinese monsoon, without examining a possible snow-monsoon relationship in summer rainfall over other parts of the Asian continent (Liu and Yanai 2002; Shaman et al. 2005). Liu & Yanai (2002) attempted to explore the influence of snow anomalies on Asian summer rainfall by considering a large part of Asia (extending from 5-65° N and 60-140° E). However, none of these studies directly examined the possible relation between Eurasian snow and the Maldives monsoon rainfall (MMR: June-September). Here, an attempt has been made for the first time to explore the possible relationship between Eurasian snow cover and Maldives monsoon rainfall.

The possible relationship between Eurasian snow and the rainfall over the Maldives is investigated using composite and correlation analyses. Robock et al. (2003) also used composite and correlation analyses to examine the relationship between snow cover, the North Atlantic Oscillation (NAO), soil moisture, and all-India rainfall (AIR). In order to investigate the relationship between Eurasian snow cover and monsoon rainfall, lag correlations will also be considered.

7.1.1 Eurasian snow cover and Maldives monsoon rainfall teleconnections

To describe teleconnections between the Eurasian snow cover (ESC) and Maldives monsoon rainfall, the data employed here includes monthly snow cover from The Rutgers University Global Snow Lab (at http://climate.rutgers.edu/snowcover/), enhanced gridded precipitation (http://www.cdc.noaa.gov/cdc/data.cmap.html) to estimate the Maldives monsoon rainfall (June-September) index (MMRI), and monthly mean zonal and meridional NCEP/NCAR reanalysis wind data obtained from http://www.esrl.noaa.gov/psd/data/gridded/data.ncep.reanalysis.derived.html. Details of these data sets are described in Chapter 2. Since there are only five raingauges (over short time periods) in the Maldives, it is not possible to estimate an area averaged monsoon rainfall index using rain gauge data. Hence Maldives monsoon rainfall index (MMRI) was calculated by averaging gridded precipitation data obtained from Climate Prediction Center (CPC) merged analysis of precipitation (CMAP) for the monsoon season (June-September)

for the period 1979-2007, covering the Maldives area (68.75° E-76.25° E and 8.75° N-1.25° S) with a total of 20 grid points, as shown in Figure 7.1. Area averaged monsoon rainfall obtained for the period 1979-2007 is shown in Figure 7.2.

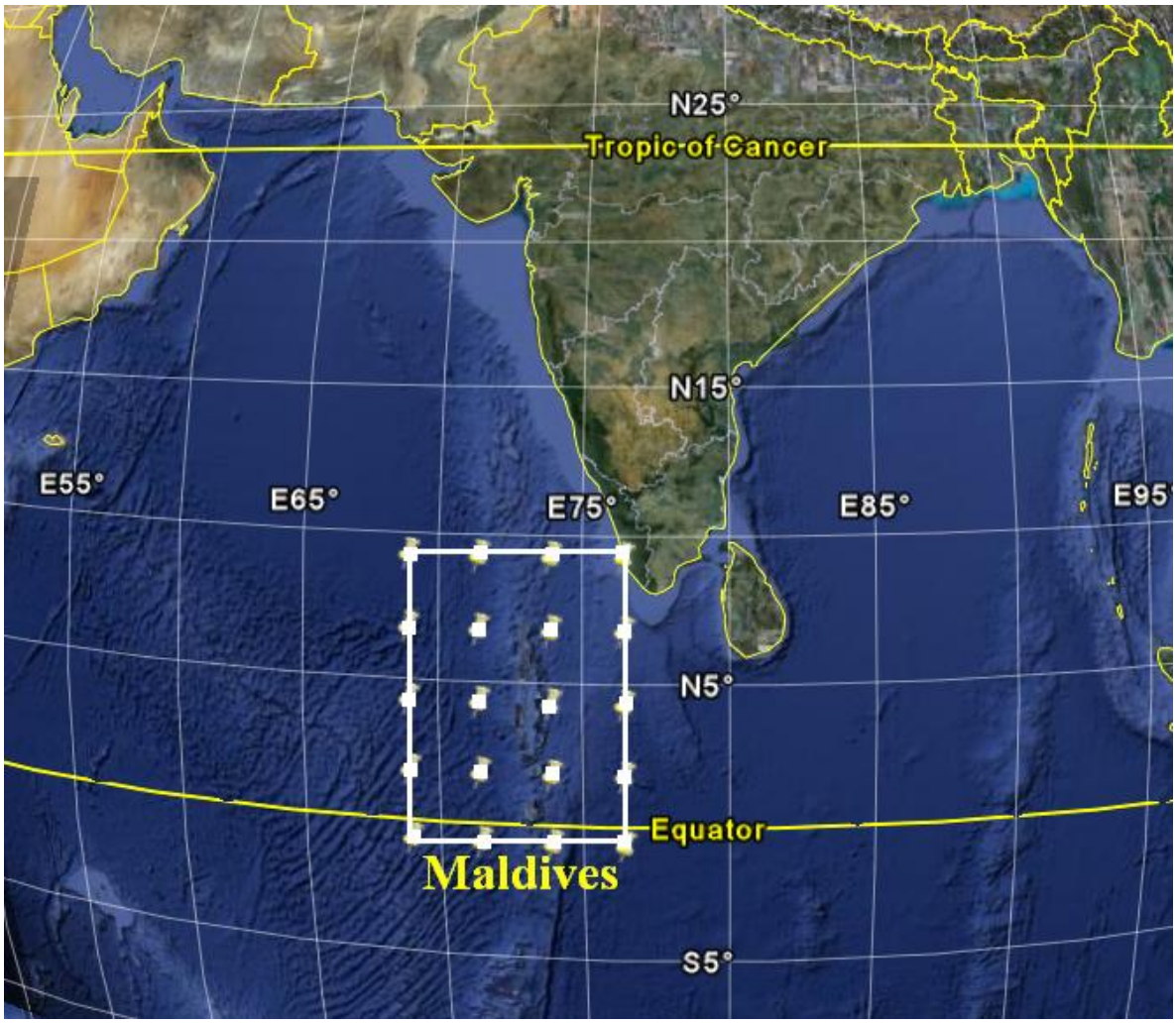

Figure 7.1: Map showing the grid points used to calculate an area weighted Maldives monsoon rainfall index (modified map from Google Earth).

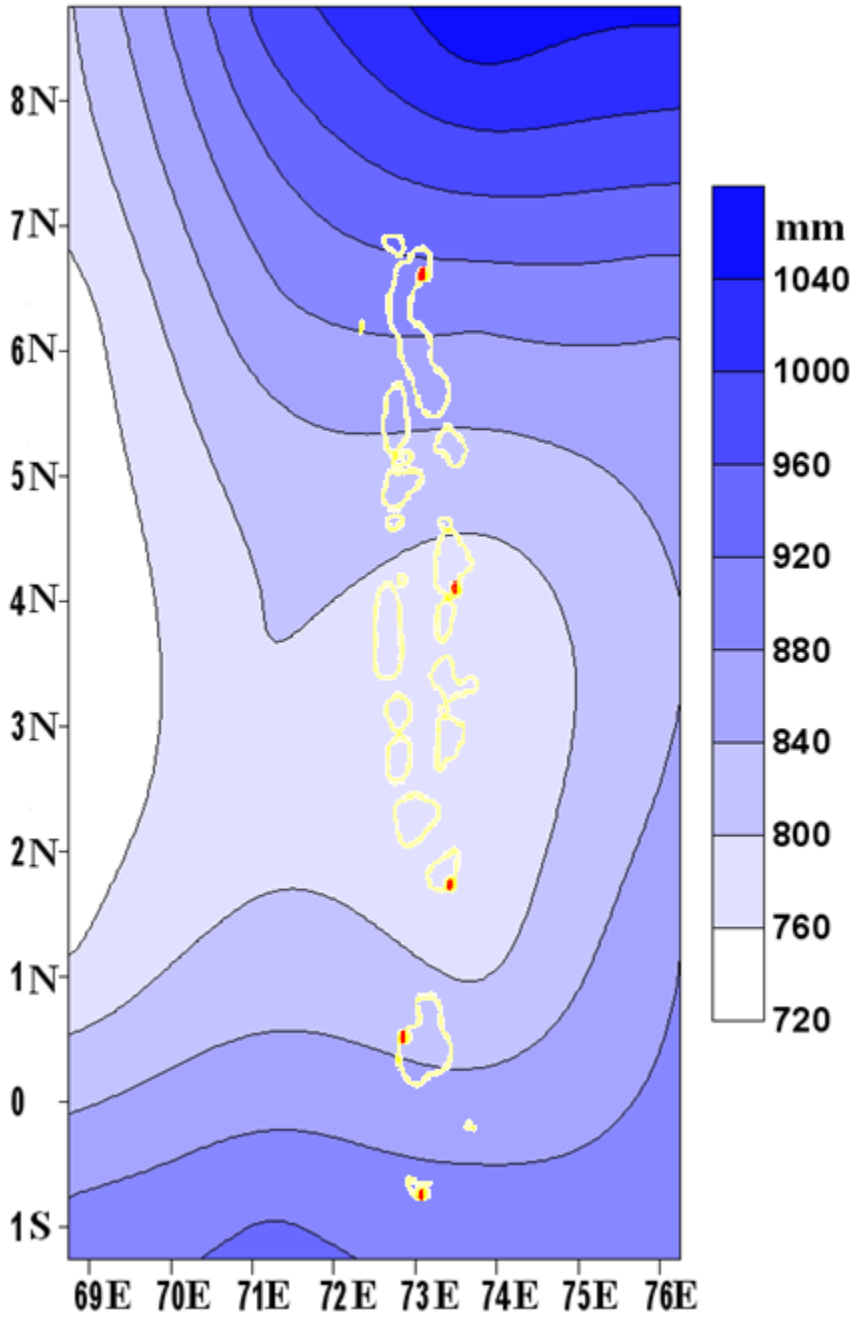

Figure 7.2: June-September average total rainfall for the period 1979-2007 for the Maldives region, based on CMAP data.

To determine teleconnections between the Eurasian snow cover (ESC) and Maldives monsoon rainfall (MMR) objectively, anomalies of area averaged MMRI have been correlated with the anomalies of ESC for October-December (previous year) and rainfall during the months January-May immediately preceding the monsoon. Before applying correlation, the time series were detrended to minimize the influence of time series trends on the strength and significance of the correlations between the variables (Qian and Saunders 2003). According to Qian and Saunders (2003), the presence of trends

in a time series may lead to a false significant correlation even though there is no physical linkage between interannual variability in the two variables. Therefore, unless otherwise stated, all the time series were detrended.

Figure 7.3 shows the year-to-year variability of the Maldives monsoon rainfall anomaly together with the yearly averaged standardized Eurasian snow cover anomaly for the period between 1979 and 2007. As depicted in Figure 7.3, there exists interannual variability among the two variables, with the MMR showing mainly negative anomalies in the 1980s and positive anomalies in the 1990s. It is interesting to note that the greatest negative MMR anomaly (1985) corresponds to the highest positive anomaly of ESC. On the other hand, the greatest negative ESC anomaly (1990) corresponds to the second highest negative anomaly of MMR. Furthermore, the highest positive MMR anomaly (1996) corresponds to a positive ESC anomaly. There appears to be no correlation between these two variables (CC = 0.01, insignificant at 5% level).

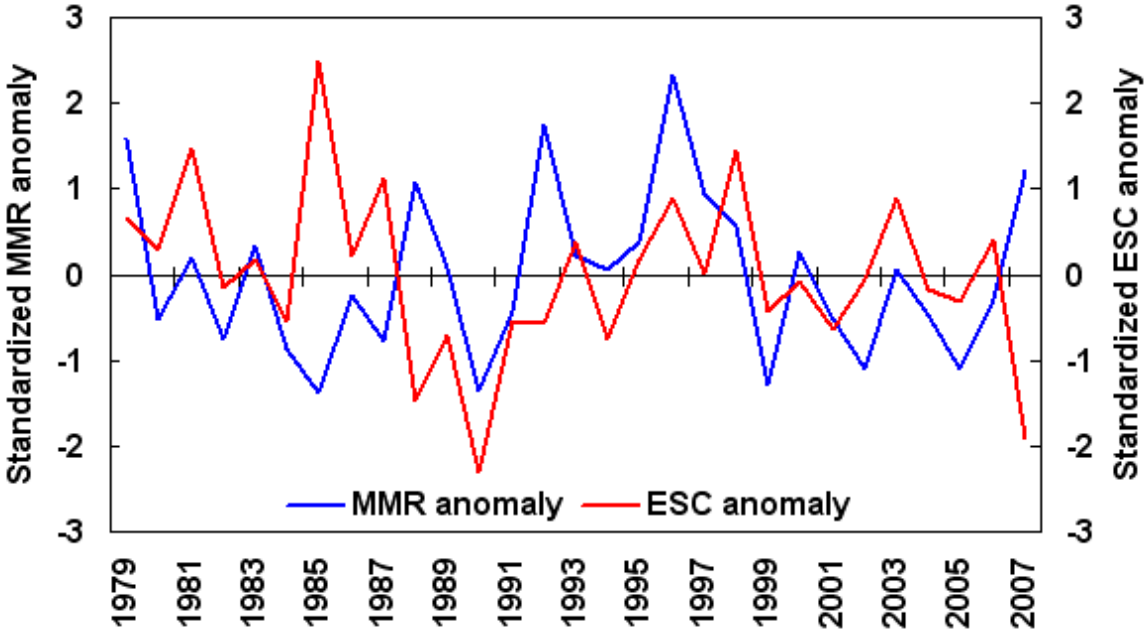

Figure 7.3: Interannual variability of standardized Maldives monsoon rainfall (MMR) and yearly averaged standardized Eurasian snow cover (ESC) anomaly from 1979-2007.

Figure 7.4 shows interannual variability in the detrended Maldives monsoon rainfall anomaly and Eurasian snow cover anomaly (detrended) for January-May in the current year, and October-December of the previous year. Very weak correlations were found between the MMR and ESC anomalies for these months. The calculated correlation coefficients between the Maldives monsoon rainfall anomaly and ESC anomaly for these

months are shown in Figure 7.4 and Table 7.1 and correlation coefficients between subsequent months of ESC anomalies are shown in Table 7.2. The highest correlation (CC = -0.15, insignificant at 5% level) between MMR and ESC was found for the month of February. Even though there appears to be no significant relationship between MMR and ESC, a strong correlation exists between months October-May of ESC anomalies, as depicted in Table 7.2. The highest correlation (CC = 0.80) is between the rainfall anomalies for April and May, significant at the 1% level. It is also worth noting that a significant correlation exists between the previous year's December ESC anomaly and the ESC anomaly for all other months, except for the preceding February, as shown in the last column of the Table 7.2.

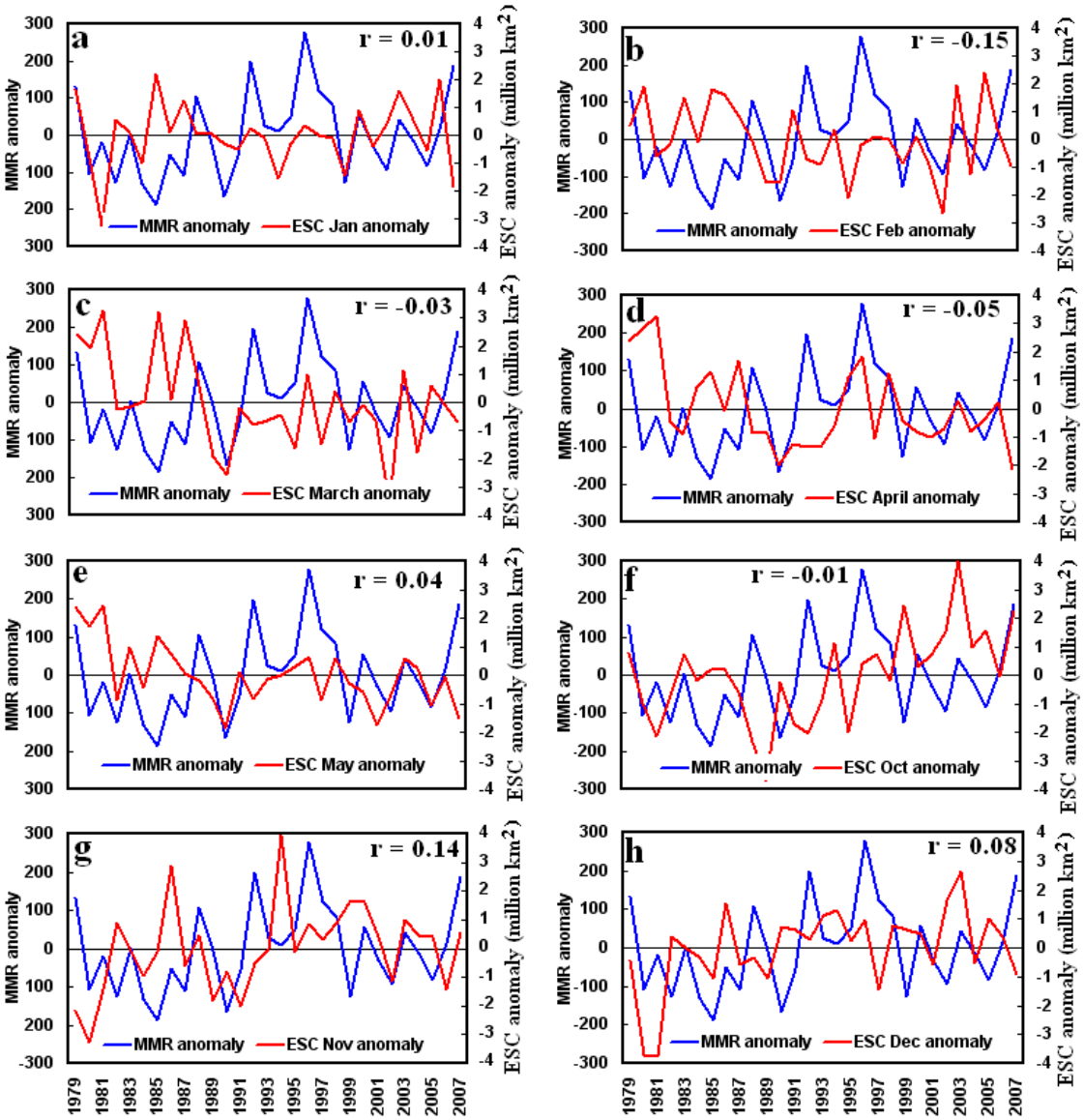

Figure 7.4: Interannual variability of Maldives monsoon rainfall (MMR) anomaly and Eurasian snow cover anomaly for the preceding months (January-May immediately preceding the monsoon period and October-December of the previous year).

Table 7.1: Correlation coefficients between the Maldives monsoon rainfall (MMR) anomaly and Eurasian snow cover anomaly for the months of October-December of the previous year and the months preceding the monsoon (January-May).

	Oct	Nov	Dec	Jan	Feb	Mar	Apr	May
MMR	**- 0.01**	**0.14**	**0.08**	**0.01**	**- 0.15**	**- 0.03**	**- 0.05**	**0.04**

Table 7.2: Correlation coefficients between different months of Eurasian snow cover anomaly for the preceding months (January-May) and October-December of the previous year.

	Feb	Mar	Apr	May	Oct	Nov	Dec
Jan	**0.25**	**0.11**	**0.04**	**0.08**	**0.12**	**- 0.09**	**0.34***
Feb		**0.66****	**0.30**	**0.40***	**0.24**	**0.07**	**- 0.01**
March			**0.74****	**0.69****	**- 0.04**	**- 0.14**	**- 0.39***
April				**0.80****	**- 0.14**	**- 0.32***	**- 0.44****
May					**- 0.09**	**- 0.23**	**- 0.34***
Oct						**0.43****	**0.43***
Nov							**0.54****

*** = Correlations significant at the 5% level and ** = Correlations significant at the 1% level.**

The Eurasian winter and spring snow cover anomaly has been cited as an important factor in influencing seasonal-to-interannual variability of the succeeding Asian summer monsoon and rainfall due to a colder ground temperature in the subsequent summer. These occur since a large proportion of the available solar energy during spring and early summer is consumed for melting the snow and evaporating water from the wet soil instead of heating the ground (Bamzai and Shukla 1999; Liu and Yanai 2002). As pointed out earlier, excessive snow cover in winter/spring is associated with deficient Indian monsoon rainfall (Bamzai and Shukla 1999; Kripalani and Kulkarni 1999). The Eurasian snow cover anomaly for winter/spring, as well as snowmelt was correlated with the MMR. December-February (DJF) and March-May (MAM) mean snow cover are taken to represent the winter and spring season, respectively, while snowmelt is taken as the difference between the February and the following May snow cover. Figure 7.5 shows the interannual variability of these parameters (a: winter snow cover anomaly, b: spring snow cover anomaly, and c: snowmelt anomaly). As can be seen from Table 7.3, the only significant correlation is between the winter snow cover anomaly and the snowmelt anomaly, with a correlation coefficient of 0.54, significant at the 1% level. Correlations between MMR and the snow cover anomaly for winter, spring and with snowmelt are -0.02, -0.02 and -0.18, respectively, as shown in Figure 7.5 and in Table 7.3. Very weak correlation coefficients

(insignificant at the 5% level) between MMR and snow variables suggest that there are no teleconnections between MMR and winter/spring snow cover and snowmelt. This contradicts the findings of previous studies on the winter/spring snow cover relationship with Asian rainfall and also with the Indian rainfall, where strong significant inverse relationships have been found (Bamzai and Shukla 1999; Kripalani and Kulkarni 1999). Bamzai and Shukla (1999) undertook a comparative study of the correlation between Eurasian snow cover and monsoon rainfall found in previous studies with their results. They found a correlation coefficient of -0.34 between winter snow cover and monsoon rainfall for the period 1973-94, while Hahn and Shukla (1976) found a correlation coefficient of -0.54 using a much shorter period of data (1967-76). Furthermore, Dickson (1984; 1983) found a correlation coefficient of -0.59 between Eurasian snow cover and Indian monsoon rainfall using 1967-80 data, while SankarRao et al. (1996) found a correlation coefficient of -0.41 for the period 1973-90. According to Bamzai and Shukla (1999), the difference between their correlation coefficient and those of Hahn and Shukla (1976) and Dickson (1983; 1984) was mainly due to exclusion of the 1967-72 period. When compared to the SankarRao et al. (1996), Bamzai and Shukla (1999) included an additional four years (1991-94) in their study and found very similar results. The low correlation coefficient obtained by Bamzai and Shukla (1999) between Eurasian snow cover anomalies and Indian monsoon rainfall could be due to the inclusion of 1991-94 data, and the studies that included the 1967-71 data showed a higher correlation (Bamzai and Shukla 1999). The low correlation coefficients found between MMR and winter/spring snow cover and snowmelt may be due to the data period used (1979-2007) in this study. Although the ESC data covers the period November 1966 to the present, the MMR data covers only 1979 to present, limiting the analysis to the period from 1979. Another explanation for the low correlation coefficients found here could be related to the difference in MMR data used. The MMR index is derived from satellite data (calculated by averaging gridded precipitation data for the Maldives area, as shown in Figure 7.1), whereas the all-India monsoon rainfall index used by others (e.g; Bamzai and Shukla, 1999) is based on the observed area-weighted average rainfall from 306 rain gauge stations across the Indian subcontinent (Bamzai and Shukla 1999). To overcome this problem, the all-Maldives rainfall (AMR) was calculated using available long-term (from 1979-2006) rainfall station data from two stations (Gan and Hulhule, 1979-2006: see station location map: Figure 2.1). No significant correlations between AMR and winter/spring snow cover or snowmelt were obtained (not shown).

The results of lag-lead correlation between the Maldives monsoon rainfall (MMR) anomaly and snow cover variables are shown in Figure 7.6. The MMR anomaly shows an inverse correlation with the spring snow cover (Figure 7.6b). However, the only significant inverse correlation is at lag -6, with a correlation coefficient of -0.51, with the spring snow cover leading the MMR. Although the snowmelt does not show a significant inverse relationship with MMR, it shows a positive correlation at lag -6 (CC = 0.38). On the other hand, winter snow cover shows a strong inverse correlation with the MMR at lag +1, with a correlation coefficient = -0.34.

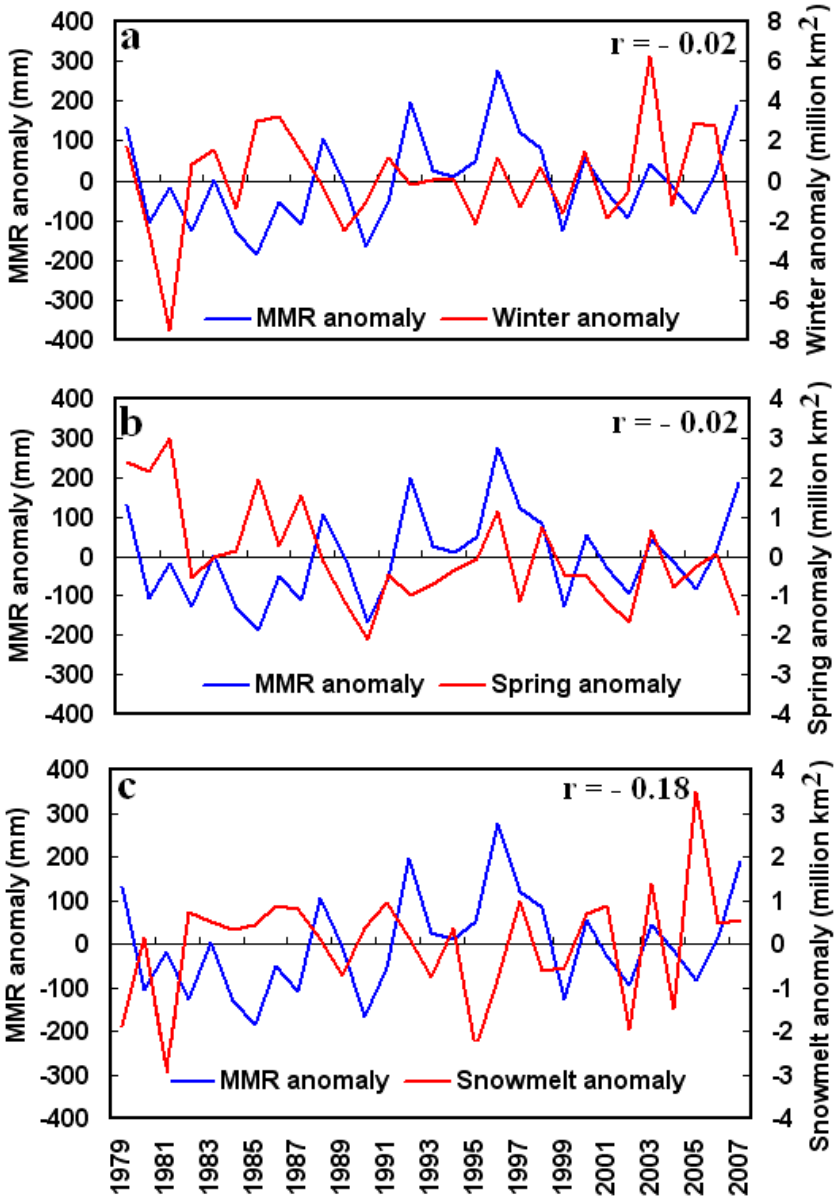

Figure 7.5: Year-to-year variability in the Maldives monsoon rainfall (MMR) anomaly and Eurasian snow cover anomaly for: (a) winter, (b) spring, and (c) snowmelt together with their correlation coefficients.

Table 7.3: Correlation coefficients between the Maldives monsoon rainfall (MMR) anomaly and Eurasian snow cover (winter, spring and snow melt) anomalies, and correlations between snow cover variables (winter, spring and snow melt anomaly).

	Winter anomaly	Spring anomaly	Snowmelt anomaly
MMR anomaly	**- 0.02**	**- 0.02**	**- 0.18**
Winter anomaly		**0.06**	**0.54****
Spring anomaly			**- 0.24**

**** = Correlations significant at the 1% level.**

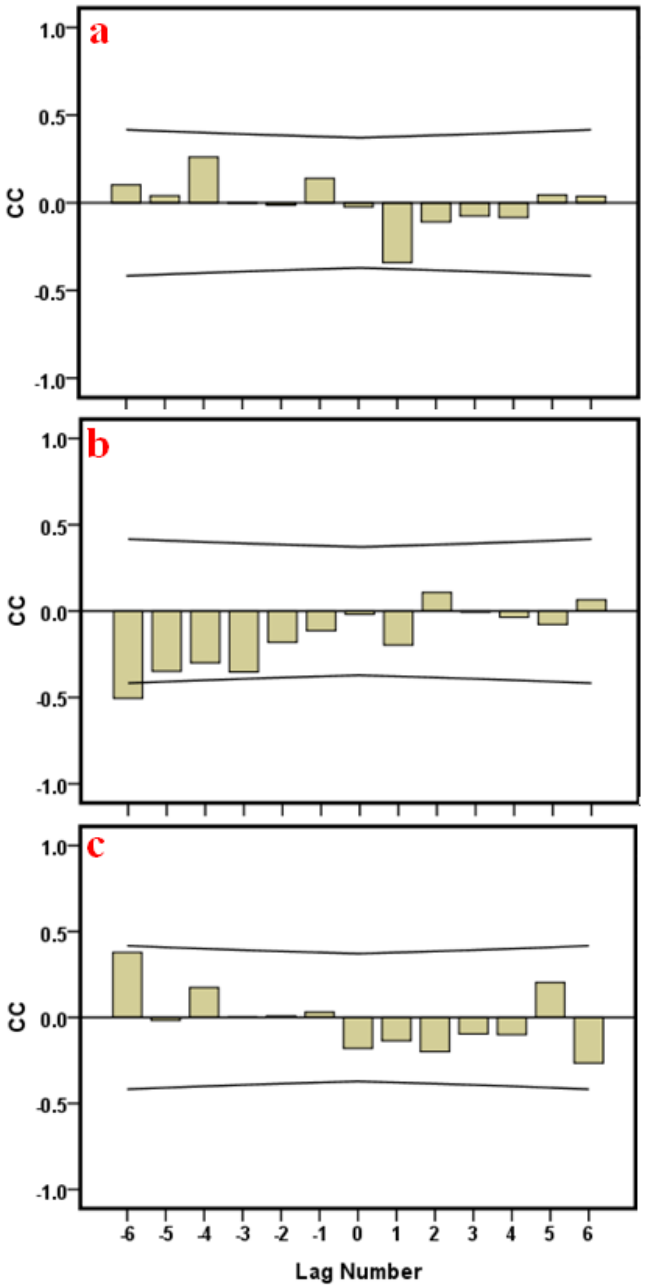

Figure 7.6: Lag-lead correlations between Maldives monsoon rainfall and (a) winter snow cover anomaly, (b) spring snow cover anomaly, and (c) snowmelt for the period 1979-2007. The upper and lower lines show upper and lower confidence limits, respectively.

For the composite analysis, years with high and low snow cover (for winter, spring and snowmelt) were identified. High snow cover is defined as years where the snow cover value is greater than one standard deviation above the mean, while the low snow cover is defined as the years where the snow cover value is less than -1 standard deviations (Pang et al. 2005). The identified high and low snow cover years are shown in Figure 7.7. Composites of monsoon rainfall averaged for the years of high winter snow cover (e.g. 1985 and 1986) years minus rainfall averaged for the years of low winter snow cover (e.g. 1981 and 2007) show a dipole pattern (Figure 7.8a) similar to the one shown in Figure 7.2. This suggests that monsoon rainfall in years with high and low snow cover in winter favour a normal monsoon rainfall distribution over the Maldives, where southern and northern areas of the Maldives receive higher rainfall on average. On the other hand, years with high spring snow cover (1979, 1980, 1981, 1985 and 1987) and low snow cover in spring (1990, 2002 and 2007) create a deficit in rainfall for southern and central regions over the Maldives, as shown in Figure 7.8b. Furthermore, composites of monsoon rainfall for the years of high snowmelt (2003 and 2005) minus years of low snowmelt (1979, 1981, 1995, 2002 and 2004) show an east-west dipole like pattern, with the western region experiencing monsoon rainfall deficit while the eastern region receives excess rainfall (Figure 7.8c). This indicates that association with the snow cover in different seasons may lead to a complex monsoon rainfall patterns over the Maldives region.

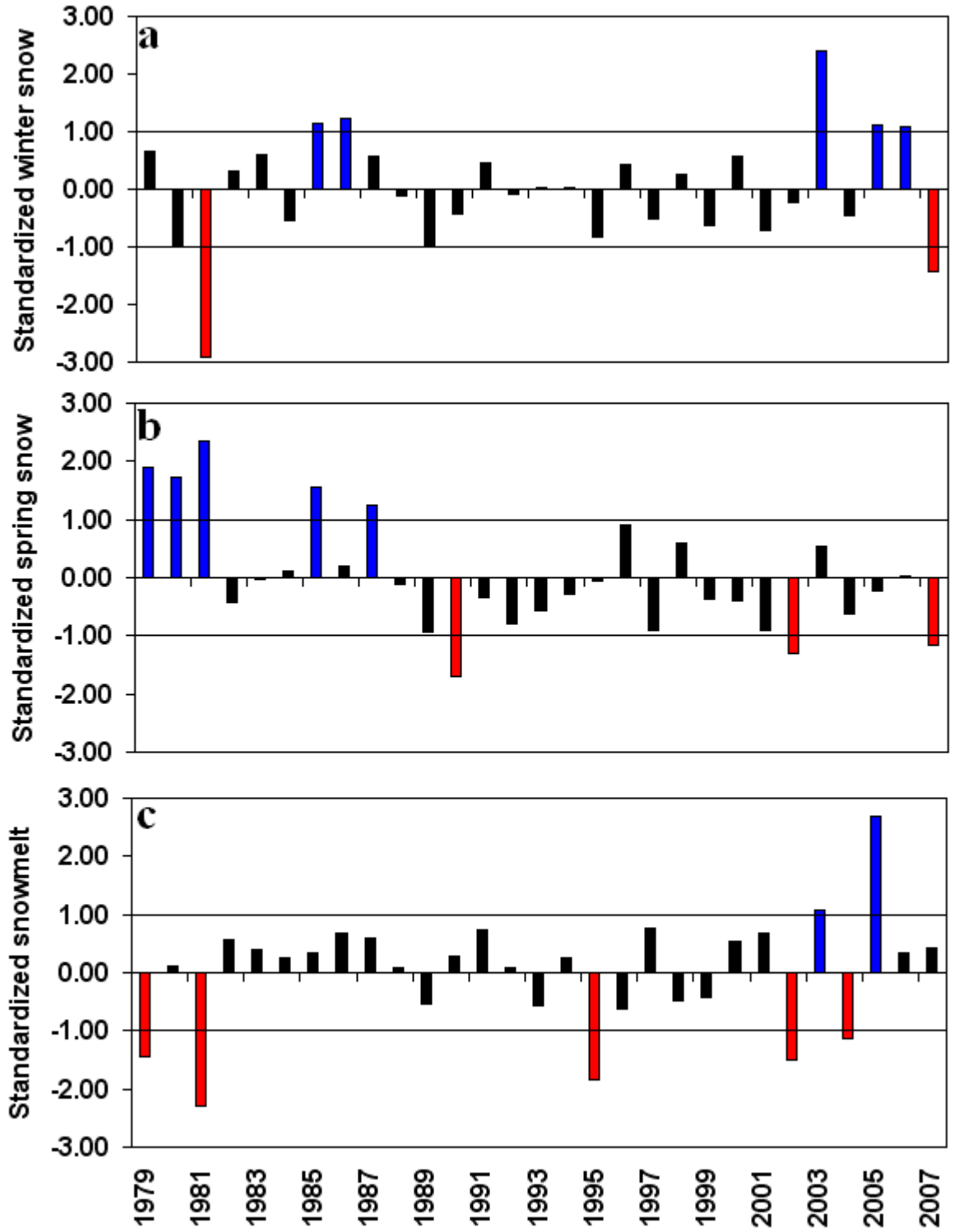

Figure 7.7: Standardized snow cover for (a) winter, (b) spring and (c) snowmelt. Blue and red bars indicate high and low snow cover or snowmelt, respectively. The horizontal lines show plus and minus one standard deviation from the mean.

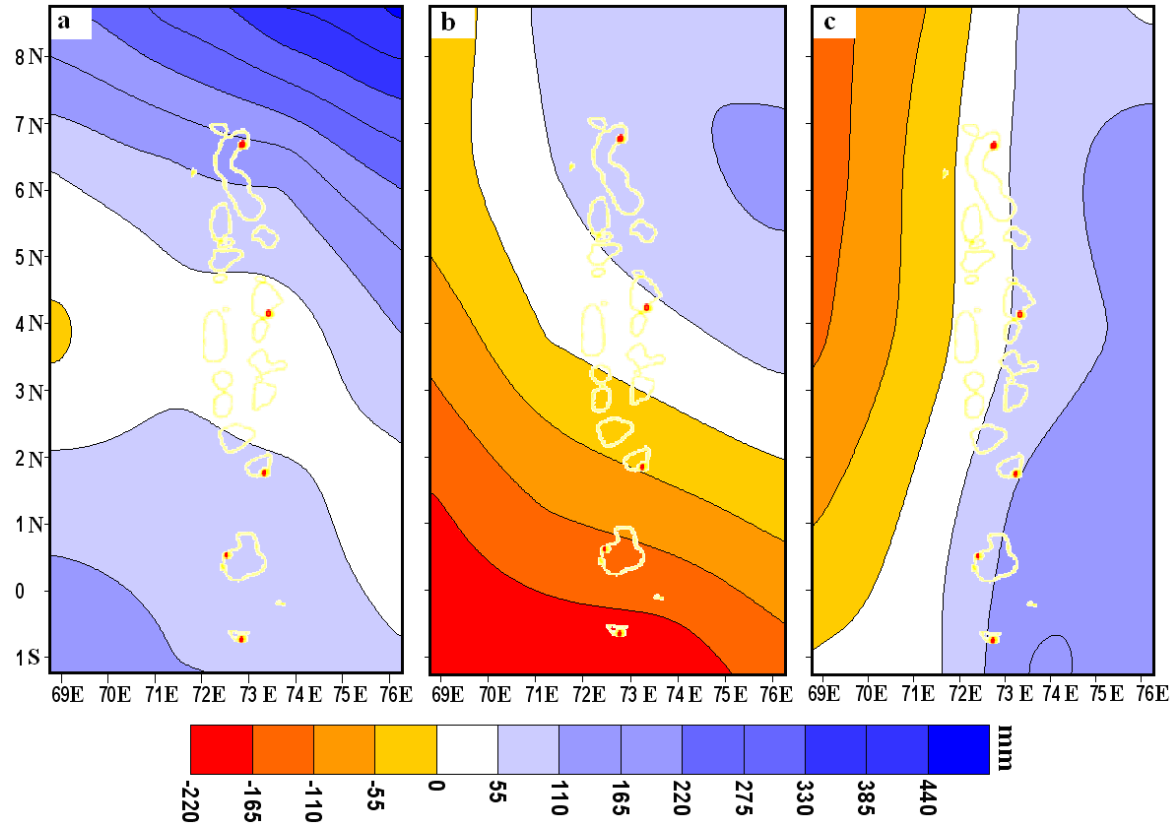

Figure 7.8: Composites of Maldives monsoon rainfall for years of heavy snow cover minuse light snow cover years for: (a) winter (heavy snow cover years: 1985 and 1986 and low snow cover years: 1981 and 2007), (b) spring (heavy snow cover years: 1979, 1980, 1981, 1985 and 1987 and low snow cover years: 1990, 2002 and 2007), and (c) snowmelt (high snowmelt years: 2003 and 2005 and low snowmelt years: 1979, 1981, 1995, 2002 and 2004).

In an attempt to compare the results (correlation coefficients) obtained for the MMR with the all-India summer monsoon rainfall (AISMR) and snow cover, correlation coefficients between AISMR and snow cover variables (winter/spring snow cover and snowmelt) were calculated for the same period (1979-2007). Although the magnitude of the correlation coefficients between the AISMR and other variables is higher (Table 7.4), when compared with the correlation coefficients obtained between MMR and winter/spring snow cover and snowmelt (Table 7.3), none of the correlation coefficients were significant at the 5% level. It is worth noting that the magnitude of the correlation between the snowmelt anomaly and MMR and AISMR are very similar, but they show opposite signs. It should be noted that the winter snow cover (December-February) anomaly used here differs from what Bamzai and Shukla (1999) used. They used December-March snow cover to define the winter snow cover anomaly. Hence, the winter (December-March: DJFM) snow cover anomaly is recalculated for two separate periods (1973-94 and 1979-2007). The correlation coefficients between the winter (DJFM) snow cover anomaly and AISMR was computed

for the two periods to check what effect it would have on correlations if two separate time periods were used. The same correlation coefficient (-0.34) was obtained as found by Bamzai and Shukla (1999) for the 1973-94 period. However, the correlation coefficient dropped to -0.18 for the 1979-2007 period, suggesting that the inverse relationship between ESC and monsoon had weakened over the more recent time period. A significant reduction in Eurasia snow cover has been observed in recent years and it has been linked to the increased winds in the Arabian Sea during the southwest monsoon phase since 1997 (Goes et al. 2005; Lindsey and Simmon 2006). A decrease in snow cover has also been verified by Lindsey and Simmon (2006), using independent observational air temperature data, and they concluded that the measured air temperature is increasing and the snow cover is declining.

Table 7.4: Correlation coefficients between all-India summer monsoon rainfall (AISMR) anomaly and Eurasian snow cover (winter, spring and snow melt) anomaly. None of the correlation coefficients are significant at the 5% level.

	Winter anomaly	Spring anomaly	Snowmelt anomaly
AISMR	**- 0.20**	**- 0.14**	**0.21**

To gain insight into this new finding (the reduction in Eurasia snow cover and its link with increased winds in the Arabian Sea during the southwest monsoon phase) of Goes et al. (2005) and Lindsey and Simmon (2006), winds in the Arabian Sea during the monsoon season (June-September) were correlated with the Maldives region wind to examine possible teleconnections with the Maldives monsoon. According to Goes et al. (2005), the increase in wind over the Arabian Sea during the monsoon season is mainly due to the temperature difference between land and ocean (land-sea thermal gradient) that develops in the Arabian Sea in late spring and early summer. This, in turn, is related to the reduced Eurasian snow cover, as the reduced Eurasian snow cover strengthens the spring/summer land-ocean thermal difference. This results in stronger winds during the monsoon season and positive rainfall anomalies over the region (Goes et al. 2005). If a strong positive relationship exists between the Arabian Sea and the Maldives region wind, then it may be associated with the reduction of ESC in recent years. To examine the connection between the Arabian Sea and Maldives region wind, NCEP/NCAR reanalysis monthly mean zonal (u) and meridional winds (v) were extracted for the Arabian Sea region (47-50° E, 5-10° N) and the Maldives region (70-75° E, 7.5° N-2.5° S), and resultant

wind speed was computed from these u and v components. The region selected to represent the Arabian Sea (the western Arabian Sea) is the same as that used by Goes et al. (2005) in their analysis.

Figure 7.9 shows the resultant wind pattern for the Arabian Sea and Maldives region. The wind distribution over the Maldives varies from north to south. The southern Maldives is dominated by a south-esterly wind, while the northern Maldives is dominated by a south-westerly wind. The interannual variability of the resultant wind speed for the two regions (a: for the western Arabian Sea, and b: for the Maldives region) are shown in Figure 7.10. There is a decreasing trend of wind speed in both regions for the period 1979-2007, with a correlation coefficient of 0.26, insignificant at the 5% level. It is interesting that the magnitude of wind speed for the entire period is twice as much for the Arabian Sea region, compared to the Maldives region. The higher wind in the western Arabian Sea region may be associated with the Somali Jet. After the onset of the summer monsoon, the Somali Jet appears along the coast of east Africa and passes over the western Arabian Sea during the summer season (Seo et al. 2008). Vecchi et al. (2004) further stated that during the monsoon season, the western Arabian Sea is dominated by large-scale and strong surface wind forcing linked to the large SST gradients at the oceanic mesoscale due to vigorous dynamical ocean response. As Goes et al. (2005) suggested, the western Arabian Sea wind had increased for the period 1997-2004 during the monsoon season (Figure 7.10a). A similar trend can be seen for the Maldives region (Figure 7.10b) for the same period. However, the correlation between the resultant wind speed in the Arabian Sea and Maldives region has weakened during recent years, with the correlation coefficient dropping from 0.26 (1979-2007 period) to 0.067 for the 1997-2004 period. The insignificant correlation between these two regions could be due to the inhomogeneity of wind in the Maldives region.

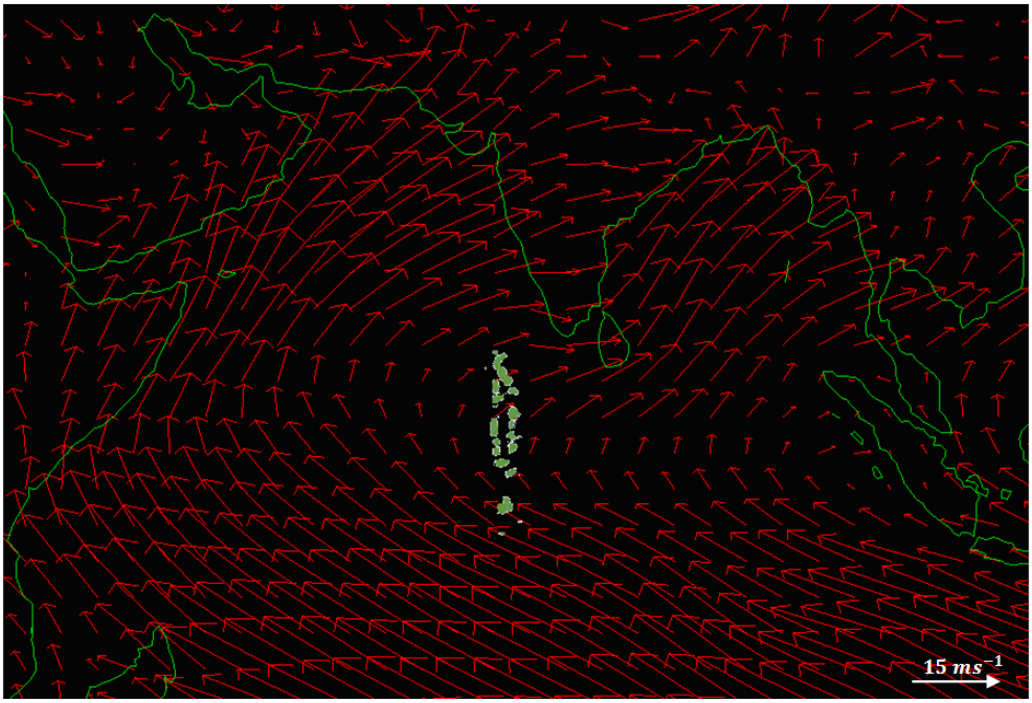

Figure 7.9: Resultant wind pattern over the Arabian Sea and Maldives region for the month of June, 1979 based on NCAP data.

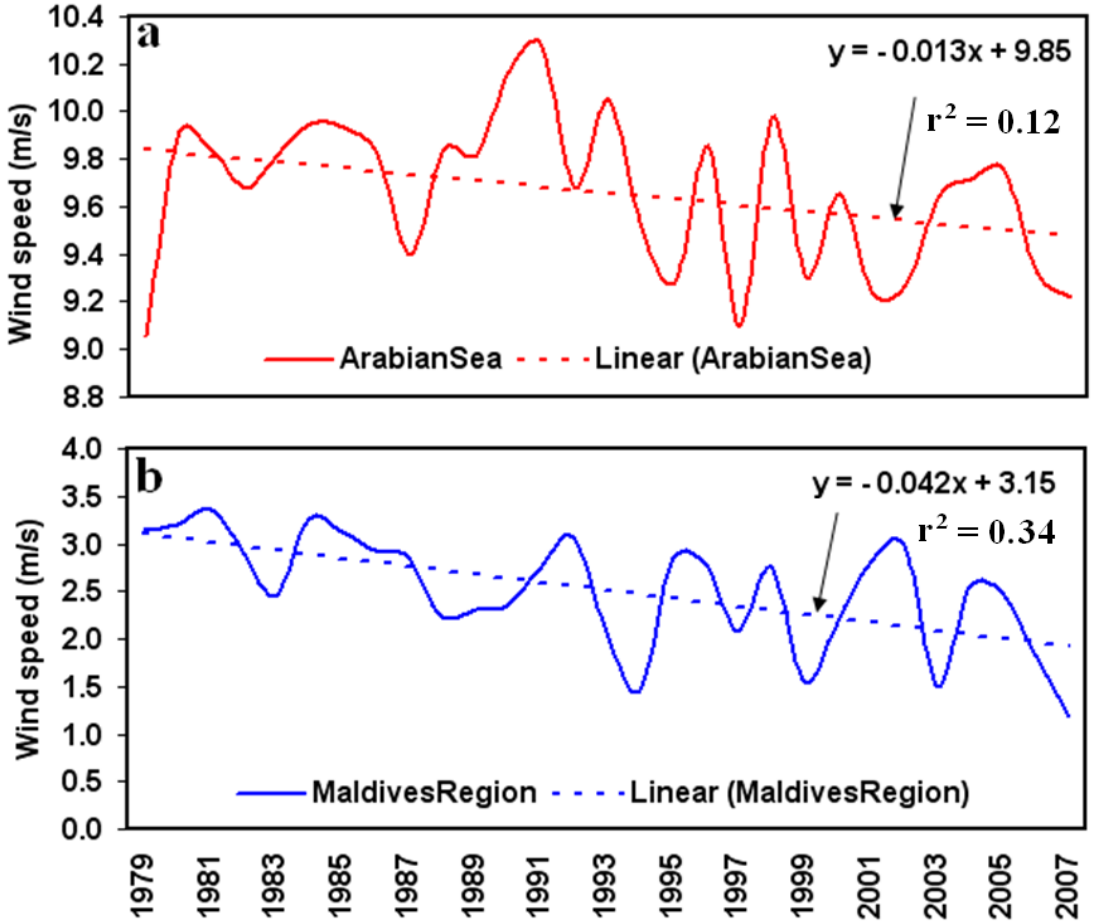

Figure 7.10: Monsoon season (June-September) mean resultant wind speed for the western Arabian Sea (a) and Maldives region (b), together with their linear trends from 1979-2007 (same period as used by Goes et al. (2005)).

To examine inhomogeneity in wind, the Maldives region resultant wind at each grid point is correlated with each other. Results of the correlation coefficients between grid points are depicted in Table 7.5. The correlation between the wind over the Maldives region at different latitudes and longitudes indicates that the winds south of the equator are highly inter-correlated, but are not well correlated with the wind at most of the latitude and longitude points north of the equator, suggesting that there is spatial variability (inhomogeneity) in the wind field over the Maldives region. The Maldives region is dominated by two wind regimes: (I) the region north of the equator is dominated by weak south-easterly flow while further north of the equator is dominated by strong south-westerly flowand (II) the region south of the equator are mainly dominated by southeasterly flow. Figure 7.11 shows spatial correlation between wind speed at 2.5° S/75° E (a) and 2.5° N/75° E (b). A very distinct spatial contrast between north and south (with a break at around 1° N) is evident, where the wind speed at 2.5° S/75° E is positively correlated with southern region. On the other hand, wind speed at 2.5° S/75° E is negatively correlated with

northern region wind speed. Furthermore, wind speed at 2.5° N/75° E is strongly correlated (positively) with northern areas of the Maldives, while it negatively correlates with the southern region. This indicates that the Maldives region cannot be considered as a single area. Hence, the Maldives region can be divided into two parts (north and south). Resultant wind speed for the north and south were generated and again correlated with the western Arabian Sea region wind. Significant correlation exists between the northern Maldives and the western Arabian Sea region for the period 1979-2007, with a correlation coefficient of 0.46 (Table 7.5), significant at the 5% level. A very weak inverse relationship (correlation coefficient = -0.11, insignificant at 5% level) can be seen between the southern Maldives and the western Arabian Sea region for the same period. Similarly, a very weak inverse relationship (correlation coefficient = -0.12, insignificant at the 5% level: Table 7.6) can be seen between the southern Maldives and the western Arabian Sea region when recent years (1997-2004) are considered. Furthermore, the correlation coefficient increased to 0.47 (Table 7.6) between the western Arabian Sea wind and Maldives northern region wind for the later period. Figure 7.12 shows wind for the western Arabian Sea (a), and the northern (b) and southern (c) Maldives. Although there is an overall decreasing trend of wind for the western Arabian Sea, the northern and southern Maldives for the longer period (1979-2007, not shown), the western Arabian Sea and northern Maldives region wind shows an increasing trend over 1997-2004 period. This is in agreement with the findings of Goes et al. (2005) and Lindsey and Simmon (2006), who found that the western Arabian Sea wind had increased for the period 1997-2004 and linked this to the observed decrease in Eurasian snow cover. The increasing trend of wind for the Maldives northern region for the 1997-2004 period and significant strong correlation between western Arabian Sea winds and northern Maldives winds for the same period suggests a connection between the Maldives region wind (especially for the northern region) and the western Arabian Sea wind. The increased wind over the northern Maldives region in turn could be related to the decrease in ESC in recent years (1997-2004), as suggested by Goes et al. (2005).

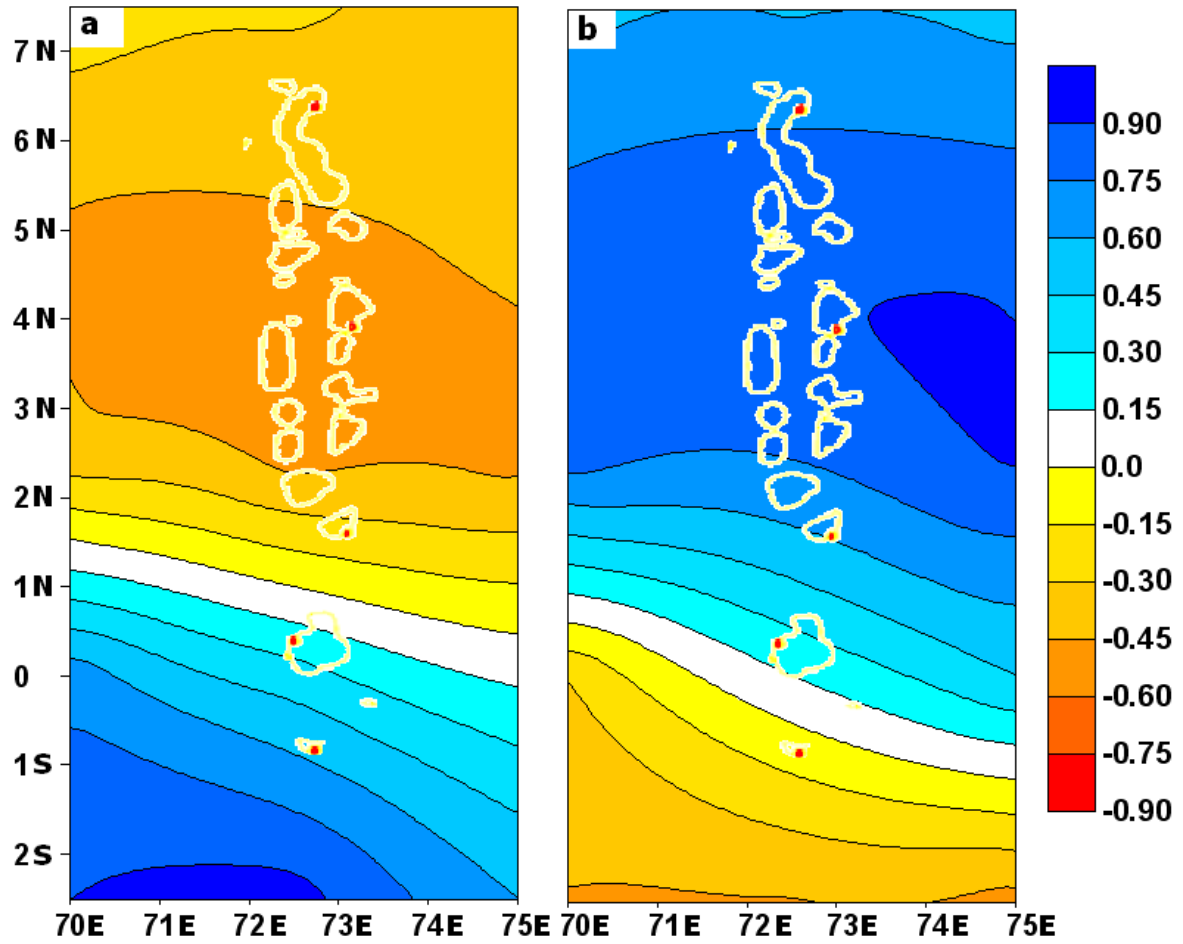

Figure 7.11: Spatial correlation coefficients between wind at 2.5° S/75° E (a) and 2.5° N/75° E (b) with all other grid points showing inhomogeneity in resultant wind speed over the Maldives region.

Table 7.5: Correlation coefficients for June-September resultant wind speed derived from mean zonal and meridional winds from 1979-2007 for the Maldives region grid points (70-75° E: 7.5° N-2.5° S). Correlation coefficients significant at the 5% level are shown by a single asterisk (*) and correlation coefficients significant at 1% level are shown by double asterisks (**).

Lat/ long	7.5/ 70.0	7.5/ 72.5	7.5/ 75.0	5.0/ 70.0	5.0/ 72.5	5.0/ 75.0	2.5/ 70.0	2.5/ 72.5	2.5/ 75.0	0.0/ 70.0	0.0/ 72.5	0.0/ 75.0	-2.5/ 70.0	-2.5/ 72.5
7.5/72.5	0.96**													
7.5/75.0	0.87**	0.93**												
5.0/70.0	0.74**	0.69**	0.60**											
5.0/72.5	0.79**	0.79**	0.74**	0.95**										
5.0/75.0	0.79**	0.81**	0.79**	0.81**	0.94**									
2.5/70.0	0.55**	0.53**	0.45*	0.90**	0.82**	0.70**								
2.5/72.5	0.42*	0.42*	0.37*	0.84**	0.79**	0.69**	0.92**							
2.5/75.0	0.56**	0.59**	0.55**	0.82**	0.88**	0.86**	0.83**	0.92**						
0.0/70.0	-0.07	-0.10	-0.08	-0.24	-0.27	-0.19	-0.05	-0.24	-0.30					
0.0/72.5	0.01	0.01	-0.01	0.06	0.00	0.04	0.35	0.26	0.14	0.76**				
0.0/75.0	0.06	0.10	0.04	0.18	0.17	0.19	0.45*	0.50**	0.44*	0.28	0.79**			
-2.5/70.0	-0.13	-0.20	-0.23	-0.37*	-0.37*	-0.30	-0.33	-0.47*	-0.46*	0.75**	0.35	0.01		
-2.5/72.5	-0.14	-0.21	-0.23	-0.40*	-0.39*	-0.30	-0.34	-0.49**	-0.46*	0.76**	0.39*	0.07	0.98**	
-2.5/75.0	-0.23	-0.28	-0.33	-0.47**	-0.47*	-0.38*	-0.40*	-0.52**	-0.51**	0.69**	0.37	0.12	0.90**	0.96**

Table 7.6: Correlation coefficients between the western Arabian Sea region June-September resultant wind with the Maldives north and south region wind. * = correlation coefficients significant at the 5% level.

	1979-2007 period		1997-2004 period	
	Maldives north	**Maldives south**	**Maldives north**	**Maldives south**
Western Arabian Sea	**0.46***	**-0.11**	**0.47***	**-0.12**

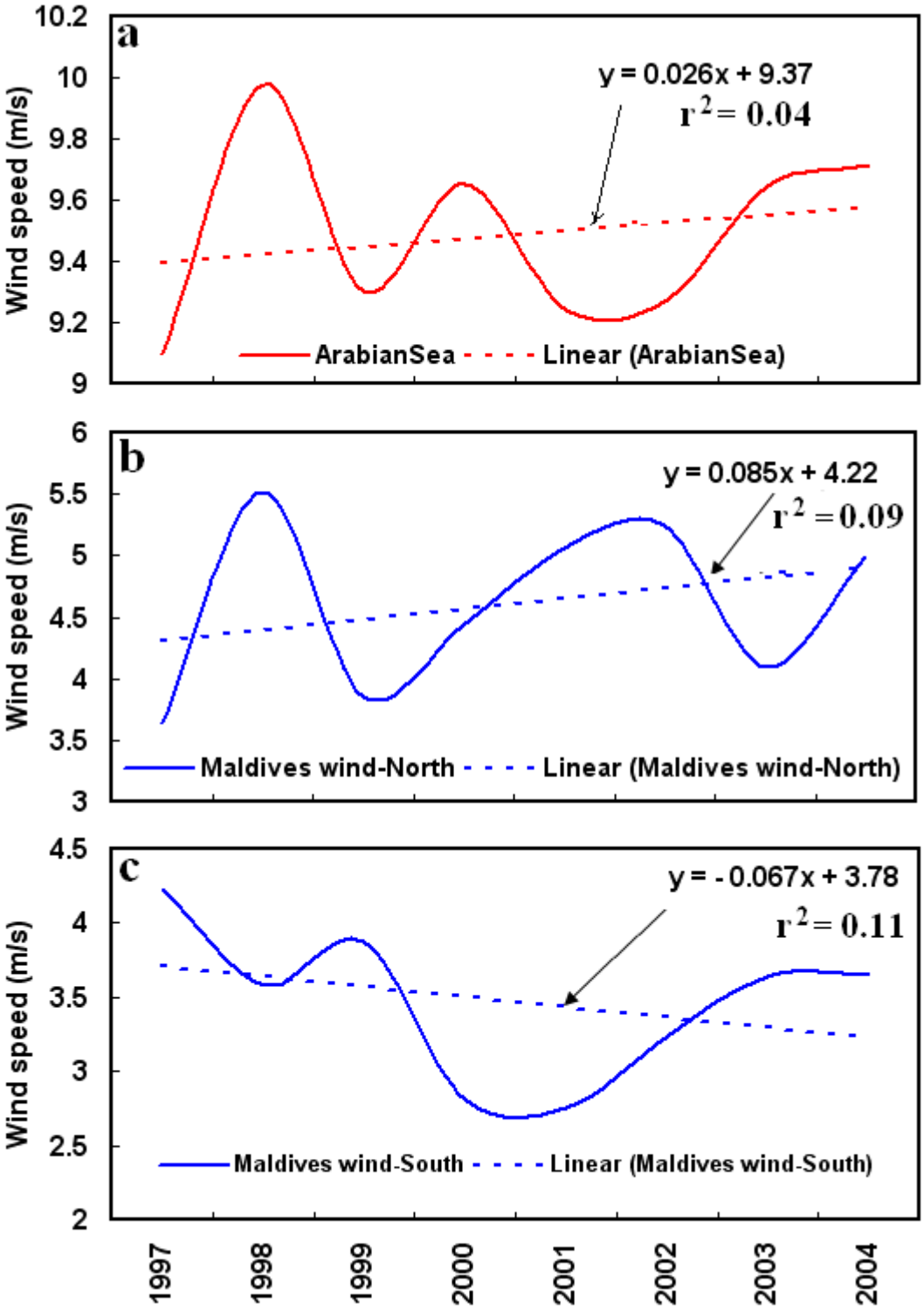

Figure 7.12: Monsoon season (June-September) mean resultant wind speed for the western Arabian Sea (a), Maldives northern region (b) and Maldives southern region (c), together with their linear trends from 1997-2004.

The weak inverse relationship found between the MMR and ESC variables found previously (Table 7.3) could be due to the fact that the Maldives monsoon rainfall was generated from an area average of the whole Maldives region. As the wind for the Maldives

region suggested, the MMR may also have spatial inhomogeneity. The average monsoon rainfall (June-September) indicates that the monsoon rainfall has dipole-like spatial variability, where the central region has the lowest rainfall, and the northern and southern regions receive higher rainfall during the monsoon period (Figure 7.2). To check whether there is a clear pattern of spatial variability in monsoon rainfall, the Maldives region monsoon rainfall at each grid point shown in Figure 7.1 was correlated with each other and the results of the correlation analysis are shown in Table 7.7. As can be seen from this table, most of the longitudinal grid points over the northern region (latitude points greater than 3.75 °N) correlate well with each other, while most of the longitudinal grid points over the southern region (latitude points less than 1.25 °N) correlate well with each other. Furthermore, only a few grid points in the northern region correlate with the grid points in the southern region, and vice versa. This suggests that the Maldives monsoon rainfall can be divided into two regions: north and south.

Table 7.7: Correlation coefficients for monsoon rainfall from 1979-2007 for the Maldives region grid points (70-75° E, 7.5° N-2.5° S). Correlation coefficients significant at 5% level are shown by a single asterisk (*) and correlation coefficients significant at 1% level are shown by double asterisks (**).

Lat/long	8.75/68.75	8.75/71.25	8.75/73.75	8.75/76.25	6.25/68.75	6.25/71.25	6.25/73.75	6.25/76.25	3.75/68.75	3.75/71.25
8.75/71.25	0.93**									
8.75/73.75	0.78**	0.89**								
8.75/76.25	0.58**	0.61**	0.64**							
6.25/68.75	0.85**	0.76**	0.60**	0.42*						
6.25/71.25	0.77**	0.78**	0.71**	0.42*	0.86**					
6.25/73.75	0.76**	0.81**	0.84**	0.53**	0.72**	0.91**				
6.25/76.25	0.67**	0.78**	0.84**	0.69**	0.53**	0.73**	0.90**			
3.75/68.75	0.63**	0.56**	0.32	0.31	0.79**	0.60**	0.46*	0.28		
3.75/71.25	0.65**	0.61**	0.40*	0.33	0.81**	0.75**	0.64**	0.47*	0.84**	
3.75/73.75	0.64**	0.60**	0.41*	0.32	0.75**	0.79**	0.75**	0.61**	0.72**	0.91**

(Continuation of the above table)

Lat/long	3.75/73.75	3.75/76.25	1.25/68.75	1.25/71.25	1.25/73.75	1.25/76.25	-1.25/68.75	-1.25/71.25	-1.25/73.75
3.75/76.25	0.89**								
1.25/68.75	0.47*	0.29							
1.25/71.25	0.68**	0.45*	0.86**						
1.25/73.75	0.76**	0.64**	0.70**	0.82**					
1.25/76.25	0.79**	0.71**	0.47*	0.71**	0.87**				
-1.25/68.75	0.34	0.30	0.81**	0.57**	0.55**	0.38*			
-1.25/71.25	0.37	0.24	0.79**	0.66**	0.66**	0.49**	0.88**		
-1.25/73.75	0.28	0.22	0.67**	0.60**	0.67**	0.58**	0.70**	0.82**	
-1.25/76.25	0.36	0.39*	0.33	0.49**	0.59**	0.74**	0.33	0.43*	0.74**

Maldives monsoon rainfall indices were computed again for the north and south separately and the detrended monsoon rainfall anomaly time series were correlated with the ESC variables (winter, spring snow cover and snowmelt) and the results are shown in Table 7.8. The correlation coefficients between ESC variables and MMR over northern and southern areas are insignificant at the 5% level, but MMR over the southern region shows higher correlation when compared with correlation coefficients between snow cover variables and MMR for the whole Maldives region (as shown in the second row of Table 7.3). Very low CC values obtained here for the Maldives monsoon rainfall (for the whole Maldives (Table 7.3), and north and south (Table 7.8) separately) contradicts the previous findings for Indian rainfall, where a strong significant inverse correlation was found between Indian monsoon rainfall and Eurasian winter and spring snow cover and snowmelt (Bamzai and Shukla 1999; 1984; Dickson 1983; Hahn and Shukla 1976). However, lag-lead correlation results (Figure 7.13) show that the monsoon rainfall over the southern region is inversely related to the spring snow cover. The spring snow cover leading by lags -6, -5 and -4 (Figure 7.13b) shows a significant inverse relationship (CC = -0.51, -0.45 and -0.45, respectively) with monsoon rain over the southern region. Furthermore, winter snow cover also shows a significant inverse correlation at lag +1 (CC = -0.38: Figure 7.13a) with monsoon rainfall over the northern Maldives. In this case the monsoon rainfall leads the winter snow cover, which is consistent with the reported relationship between Eurasian winter snow cover and Indian monsoon rainfall. From this, it can be concluded that Eurasian snow cover does influence the Maldives monsoon rainfall to some extent.

Table 7.8: Correlation coefficients between Maldives monsoon rainfall (MMR) anomaly and Eurasian snow cover (winter, spring and snow melt) for the period 1979-2007. None of these correlations are significant at the 5% level.

	Winter snow cover anomaly	Spring snow cover anomaly	Snowmelt anomaly
MMR anomaly (North)	**0.10**	**0.06**	**- 0.12**
MMR anomaly (South)	**-0.04**	**-0.15**	**- 0.26**

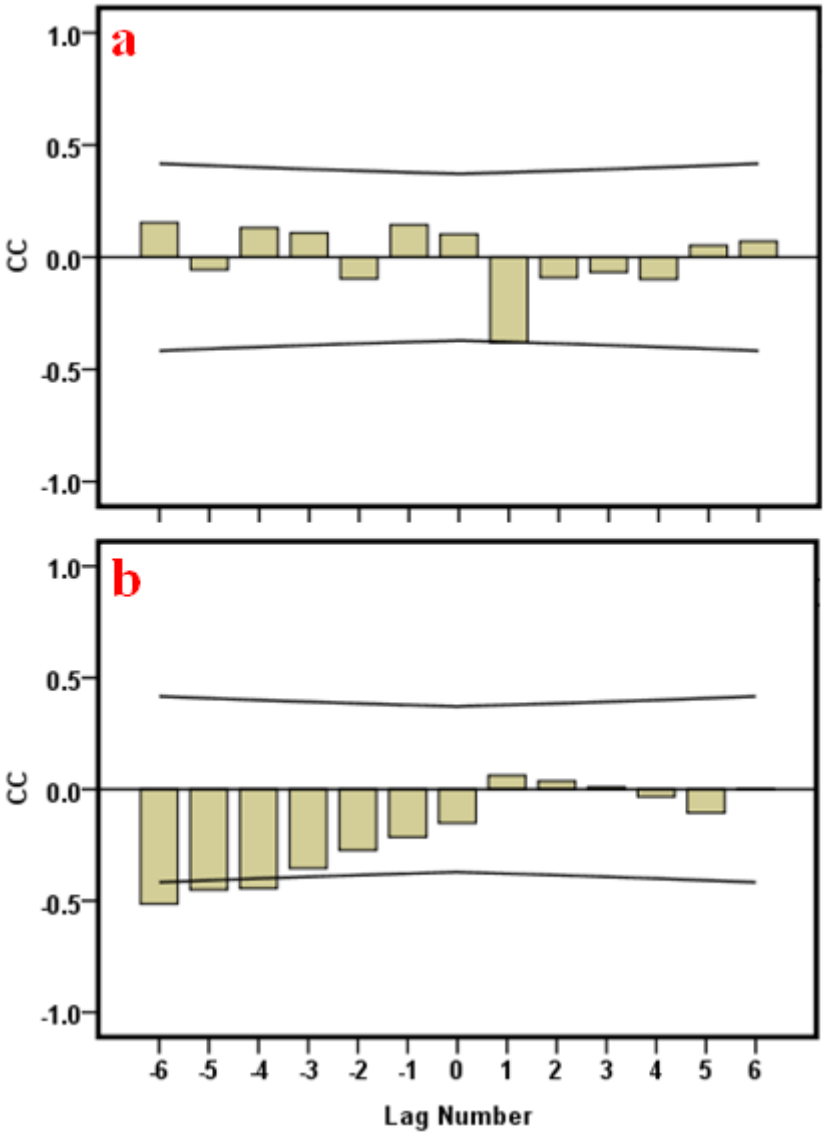

Figure 7.13: Lag-lead correlation between: (a) winter snow cover and monsoon rainfall (north) and (b) spring snow cover and monsoon rainfall (south) for the period 1979-2007. Negative (positive) lags represent spring snow cover leading (lagging) monsoon rainfall at the lags indicated. The upper and lower lines show upper and lower confidence limits, respectively.

7.2 Summary

One of the aims of this chapter (Part A) was to study the variations in the precipitation pattern over the Maldives in relation to the Eurasian snow cover. Correlation analysis indicates that there exists only a very weak relationship between MMR and snow variables. Very weak correlation coefficients between MMR and winter snow cover anomaly, spring snow cover anomaly and snowmelt (with CC = -0.02, -0.02 and -0.18, respectively, insignificant at the 5% level) demonstrate that there are no teleconnections between MMR and winter/spring snow cover and snowmelt. Although this is not in

agreement with the findings of previous studies (where strong significant inverse relationships have been found between winter/spring snow and Asian monsoon and also with the Indian monsoon rainfall), the lag-lead correlation results suggest that a significant teleconnection exists between monsoon rainfall over the southern region of the Maldives and spring snow cover, with rainfall inversely related to spring snow cover. The fact that inconsistent results were obtained between ESC variables and Maldives monsoon rainfall compared to previous studies suggests that the influence of Eurasian snow cover on the Maldives monsoon rainfall needs to be further investigated using long-term data and with the aid of numerical models.

7.3 Tropospheric biennial oscillation (TBO) (Regional scale processes: Part B)

In the same way that the Asian monsoon returns with remarkable regularity each summer, the interannual variability of the Indian and Australian monsoon rainfall experiences a remarkable biennial oscillation, which has been referred to as the tropospheric biennial oscillation, in order to distinguish it from the stratospheric quasi-biennial oscillation (Chang and Li 2000; Mooley and Parthasarathy 1984; Webster et al. 1998; Yasunari 1990). In addition to the tropical Indian and Pacific Ocean intersections, Chang and Li (2000) argued that the TBO is due to the interactions between northern summer and winter monsoons and acts as an important part of tropical ocean–atmosphere interaction, which acts separately from the El Niño–Southern Oscillation interactions. Chang and Li (2000) further suggested that the eastern Pacific plays only a passive role in the TBO mechanism, but the western Pacific-Maritime Continent region is important as well. Spatially and temporally it acts by connecting the convection anomaly from the northern summer (northern summer explicitly means that the Northern Hemisphere is in the summer phase) to the northern winter (northern winter explicitly means that the Northern Hemisphere is in winter phase) monsoon, thus playing a major role in channelling the feedback of the northern winter monsoon to the Indian Ocean (Chang and Li 2000).

7.3.1 Impact of the tropospheric biennial oscillation (TBO) on Maldives monsoon variability

The tropospheric biennial oscillation is one of the most unique components of the interannual variability of the Asian monsoon (Wang 2006). In the context of the monsoon regions of Asia/Australia, the TBO is defined as the tendency for a relatively strong monsoon to be followed by a relatively weak monsoon, and vice versa, with the transitions

occurring due to the interactions involving land-atmosphere-ocean processes over a large area of the Indo-Pacific region in the seasons prior to the monsoon (Meehl 1997; Meehl and Arblaster 2002b). The TBO is not an oscillation, but a tendency of the system, such as the monsoon system, to flip-flop back and forth from year to year. If the monsoon system is more alternating (between strong and weak years), or flip-flopping, the system will be more biennial. The large-scale interactions between land-ocean–atmosphere in the Indian and Pacific Ocean regions is believed to be responsible for the monsoon system alternating between strong and weak years (Chang and Li 2000; Meehl 1993). It is believed that the land and ocean surface conditions in March-May (MAM) over the Indo-Pacific region play an important role in TBO monsoon transitions. These include (Meehl and Arblaster 2002a):

- Atmospheric circulation-related anomalous south Asian land temperatures and resulting meridional temperature gradients
- Anomalous SSTs in the Indian Ocean
- Anomalous tropical Pacific SSTs.

Power spectral, composite, time filtering and singular value decomposition analysis were employed to study the role of the TBO in Maldives monsoon variability, using NCAR/NCEP re-analysis products (zonal and meridional wind, geopotential height, outgoing longwave radiation and vertical velocity) and extended re-constructed sea surface temperature (constructed using the most recently available International Comprehensive Ocean-Atmosphere Data Set (ICOADS) for SST data and improved statistical methods that allow stable reconstruction using sparse data) as described in Chapter 2.

7.3.1.1 Power spectrum analysis

The power spectrum of the Maldives monsoon rainfall was carried out to see whether the area averaged Maldives monsoon rainfall exhibits quasi-biennial time scale periodicities. The power spectrum shown in Figure 7.14 reveals three significant peaks. The first two correspond to the interannual time scale, with the first peak resembling a quasi-biennial time scale (2-3 year period, known as the TBO scale) and the second peak a longer time scale (3-7 years), which is often considered to be an ENSO time scale. Li and Zhang (2002) obtained two distinctive peaks on the interannual time scale using domain averaged Indian rainfall for the period 1949-1998. Furthermore, Li et al. (2001) carried out spectral analysis on the all-India rainfall for a 127-year period (1871-1997) and NCAR/NCEP re-analysis data for a 48-year period (1950-1997), and found that the 2-3 year peak is the only significant peak at 90% white noise level for both periods. The interannual time scale

periodicities (2-3 for TBO and 3-7 for ENSO) obtained for the Maldives monsoon rainfall also appear in the global precipitation field (Lau and Sheu 1988; Li and Zhang 2002) and are consistent with the periodicities frequently observed in the Asian-Australian monsoon region (Li et al. 2001).

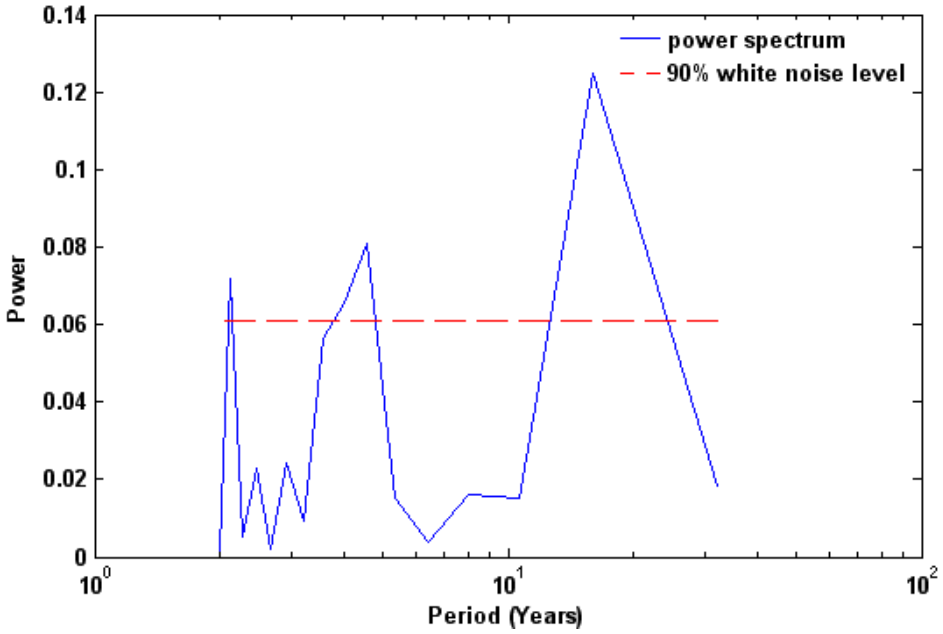

Figure 7.14: Power spectrum of Maldives monsoon season rainfall for the period 1979-2007. The red line shows the 90% white noise level.

Figure 7.15 illustrates the biennial tendency of Maldives monsoon rainfall transition from a relatively strong/weak to a relatively weak/strong monsoon in consecutive years that is related to the TBO. The degree to which Maldives monsoon rainfall is relatively greater or less than the preceding or following years was identified following the definition of Meehl and Arblaster (2002b). Relatively strong and weak monsoon years are defined, respectively as:

$$P_{i-1} < P_i > P_{i+1}$$

$$P_{i-1} > P_i < P_{i+1}$$

where P_i is area-averaged monsoon precipitation for a given year i. Following this definition, 17 out of 29 years (1979-2007) are considered to be TBO years. Among TBO years identified in relation to the Maldives monsoon, a TBO strong year accounts for 47.1% of the total TBO years and a weak TBO year accounts for 52.9% of the total TBO years. El Niño (1982, 1987, 1991, 1997 and 2002) and La Niña (1984, 1988, 1998 and 2000) onset years were identified using five month running means of sea surface temperature anomalyies in the Niño3.4 region (Figure 6.2) with a threshold value of ±0.5º C for two consecutive seasons after the March-April-May (MAM) transition season during the following one year

period. ENSO onset years (El Niño onset: 1982, 1987 and 2002 and La Niña onset: 1988 and 2000) that correspond to TBO only years are depicted in Figure 7.15. This indicates that not all El Niño or La Niña onset years correspond to TBO years, as first noted by Meehl (1987). As illustrated in Figure 7.15, El Niño onset years (1982, 1987 and 2002) frequently correspond to weak TBO years, while La Niña onset years (1988 and 2000) correspond to strong TBO years. Composites of strong (1988 and 2000: La Niña onset years) minus weak (1982, 1987 and 2002: El Niño onset) ENSO only TBO years (hereafter referred to as ENSO TBO years) and composites of strong non-ENSO only TBO years (1981, 1983, 1986, 1992, 1996 and 2003) minus weak non-ENSO only TBO years (1980, 1985, 1990, 1994, 1999 and 2005) (hereafter referred to as normal TBO years) were created separately and mathematical expression composites are presented below:

$$\textbf{ENSO TBO year composite} =$$

$$\text{strong } (1988 + 2000) - \text{weak } (1982 + 1987 + 2002)$$

$$\textbf{Normal TBO year composite} =$$

$$strong\ (1981 + \ 1983 + 1986 + 1992 + 1996 + 2003) -$$

$$weak\ (1980 + 1985 + 1990 + 1994 + 1999 + 2005)$$

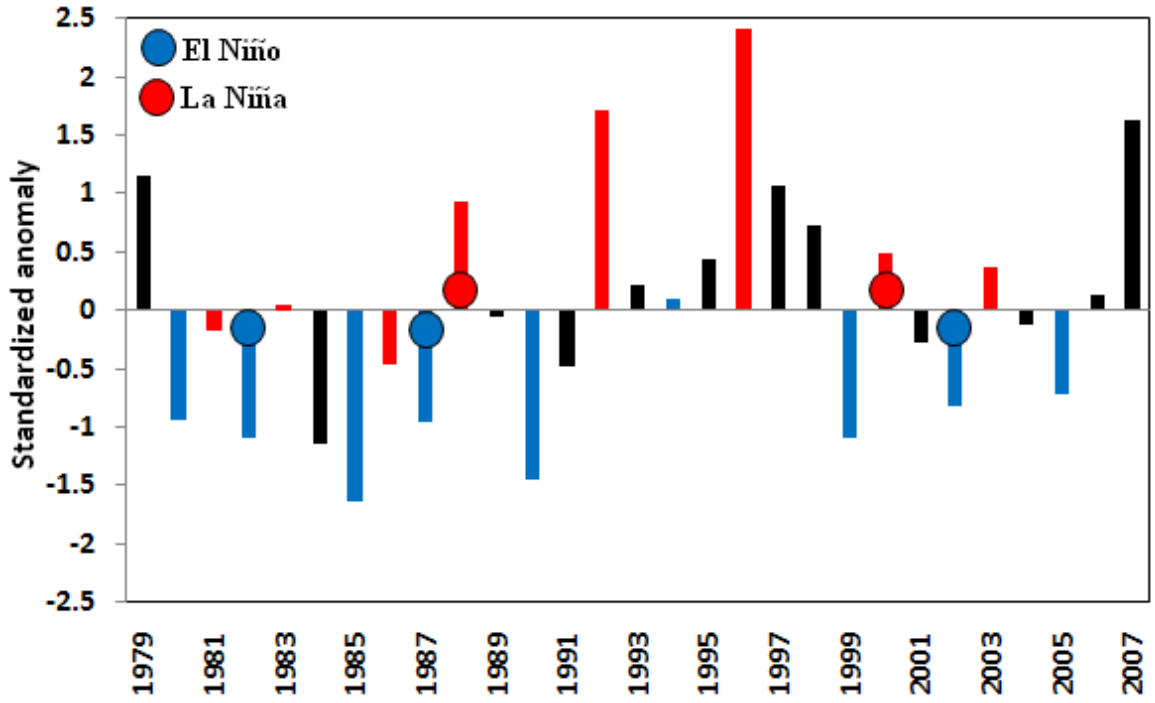

Figure 7.15: Time series of Maldives monsoon season rainfall (June-September) averaged over the region 1.25ºS – 8.75º N, 61.25ºE – 86.25º E. Red and blue bars indicate TBO strong/weak years when monsoon rainfall was relatively greater/less than preceding and following years respectively, while blue and red circles indicate TBO El Niño and La Niña onset years, respectively.

7.3.1.2 Composite analysis

Composites of sea surface temperature for the strong minus weak ENSO TBO years and for normal TBO years are shown in Figure 7.16. Starting from the strong monsoon season (JJA: 0), a very distinctive east-west dipole in the SST gradient can be seen for the following seasons for the case of the ENSO TBO composite (Figure 7.16: left panel), where the Indian Ocean (IO) gets progressively cooler with cool water extending more to the east from one season to another and warmer SST anomalies occuring north of Australia. In the case of the normal TBO year composite, the east-west dipole SST gradient is absent in all seasons (Figure 7.16 right panel). The SST composites for strong minus weak ENSO TBO years and for normal TBO years are consistent with the spatial pattern of convective activity displayed for the strong minus weak ENSO TBO years and for normal TBO years in Figure 7.17 and Figure 7.18, respectively. For the ENSO TBO case, strong convective activity dominates most of the Asian region and extends to the Indonesian region during the JJA (0) season, with maximum convection occurring in the Indonesian and Philippines region. During the same season, convectively active regions in the IO were dominated by westerlies (JJA 0: Figure 7.17). Associated with strong convection, the SST in the IO remains relatively cool during this season and positive SST anomalies prevail over the western Pacific (JJA 0: Figure 7.16 left panel). Following the JJA (0) season, convective activity further strengthens over the eastern Asian and Indonesian region and remains active during the SON (0) season. The westerlies in the IO region intensify and extend towards the Indonesian region, where maximum ascending occurs. Negative SST anomalies setup in the previous season are further intensified in the IO region during the SON (0) season (Figure 7.16 left panel) and maximum warming occurs north of Australia during the SON (0) season. It has been noted that the strong Indian monsoon is often followed by a strong Australian monsoon in the following DJF (Meehl and Arblaster 2002b; Webster and Yang 1992). This is consistent with the evolution of convective activity depicted for the case of the ENSO TBO composite (Figure 7.17). As the seasons progress from northern summer (JJA 0) to northern winter (DJF 0) convective activity in the IO region weakens, and moves further west with the centre of maximum convection occurring in the western Pacific and the Australian region. Another noticeable feature that starts developing in this season is easterly flow in the IO (DJF 0: Figure 7.17). Cooling in the IO region further intensifies and maximum positive SST observed in the previous season (SON 0) north of Australia weaken by this time (DJF 0: Figure 7.16 left panel). Prior to the next Asian monsoon season, in MAM (+1), convection weakens over Australia, but convective activity covers most of the

Indian region during MAM (+1), extending from the equator to 20º N. The easterly flow that originates from the southern IO gets deflected after reaching the African continent and changes to westerly flow covering the Arabian Sea and northern IO region, and westerly flow converges in the northern Pacific region (MAM (+1): Figure 7.17). Although the magnitude of maximum cooling observed over the southern IO during the previous season, DJF (0), has weakened by MAM (+1), the overall spatial patterns remain the same (MAM (+1): Figure 7.16 left panel). By the following Asian summer monsoon, JJA (+1), most of the Asian region becomes convectively inactive, especially the southern India and Arabian Sea region. However, an active region lies in the vicinity of the Bay of Bengal. Although easterlies occupy the western and southern IO, westerlies dominate much of the central IO during the JJA (+1) season (Figure 7.17). By this season, the maximum cooling centres have moved further north and lie close to the Asian continent (JJA (+1): Figure 7.16 left panel).

As the normal TBO strong monsoon season (JJA 0) indicates, maximum convection occurs southwest of India (in the Arabian Sea region), with the westerly dominating north of the equator during this season (JJA (0): Figure 7.18). During this season, much of the domain is occupied by homogeneous positive SST anomalies as depicted in Figure 7.16 right panel (JJA (+1)). Convection centres setup during the monsoon season move from the western region to the Indonesian and Philippines region by the following season, SON (0), and strong easterlies occupy the Indonesian region. Although the spatial patterns of SST anomaly remain unchanged during the post-monsoon season (SON 0), an overall cooling pattern is evident for the Indian Ocean and Arabian Sea regions, especially close to the African continent (SON 0: Figure 7.16 right panel). During the Australian monsoon season, DJF (0), zones of convective activity are seen over the IO region, over Australia and around Madagascar for the case of the normal TBO OLR composites, as shown in Figure 7.18 (DJF 0). During the same season, a strong northwesterly exists near the Madagascar region and westerlies prevail over most of the central IO. Compared to the previous season, SON (0), during the Australian monsoon season the sea surface temperature is cooler near the Australian continent and cooling patterns from the previous season remain unchanged in the IO region (DJF 0: Figure 7.16 right panel). Convection remains active over the southern Indian Ocean and over Australia during the following season (MAM +1: Figure 7.18). Easterlies dominate north of the equator, while a narrow band of westerlies lie over the southern IO (MAM +1: Figure 7.18). SST anomalies for MAM (+1) remain unchanged compared to the previous season, except for some warming over the southeastern IO

(MAM+1: Figure 7.16 right panel). By the following monsoon season, JJA (+1), the convective activity almost disappears from the Indian region and active areas lie close to the Indonesian region. Much of northern Asia is dominated by strong westerly flow during the monsoon season, while south of the equator (up to 10^{o} S) is dominated by easterly wind (JJA +1: Figure 7.18). During this season, most of the Indian Ocean and Arabian Sea region is warmer compared to the MAM (+1) season, while the north-western Pacific Ocean (north of Australia) is dominated by negative SST anomalies (JJA+1: Figure 7.16 right panel).

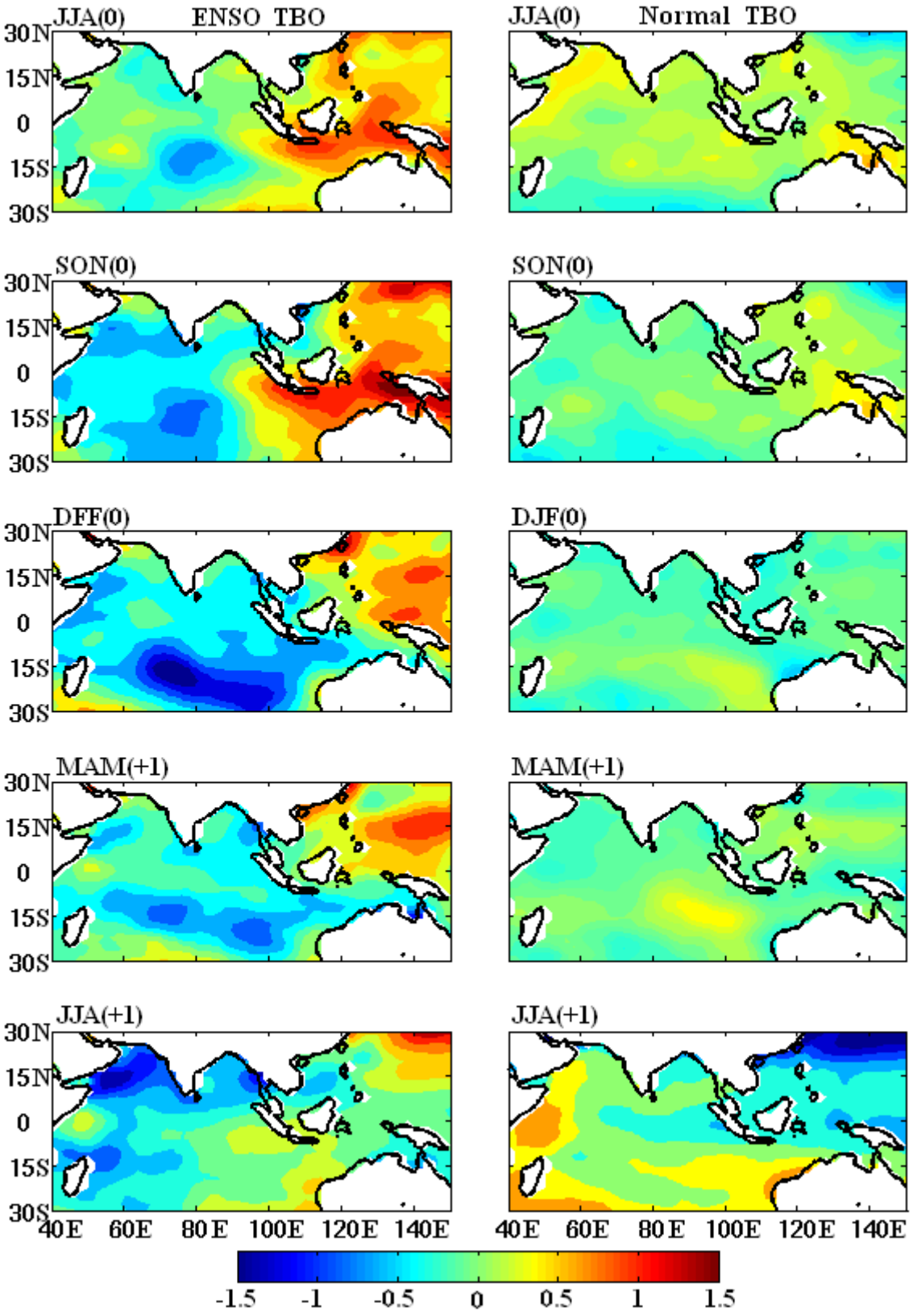

Figure 7.16: Strong minus weak ENSO TBO year (left panel) and strong minus weak normal TBO year (right panel) composites of sea surface temperature, starting from strong monsoon, JJA (0), to the next year monsoon, JJA (+1).

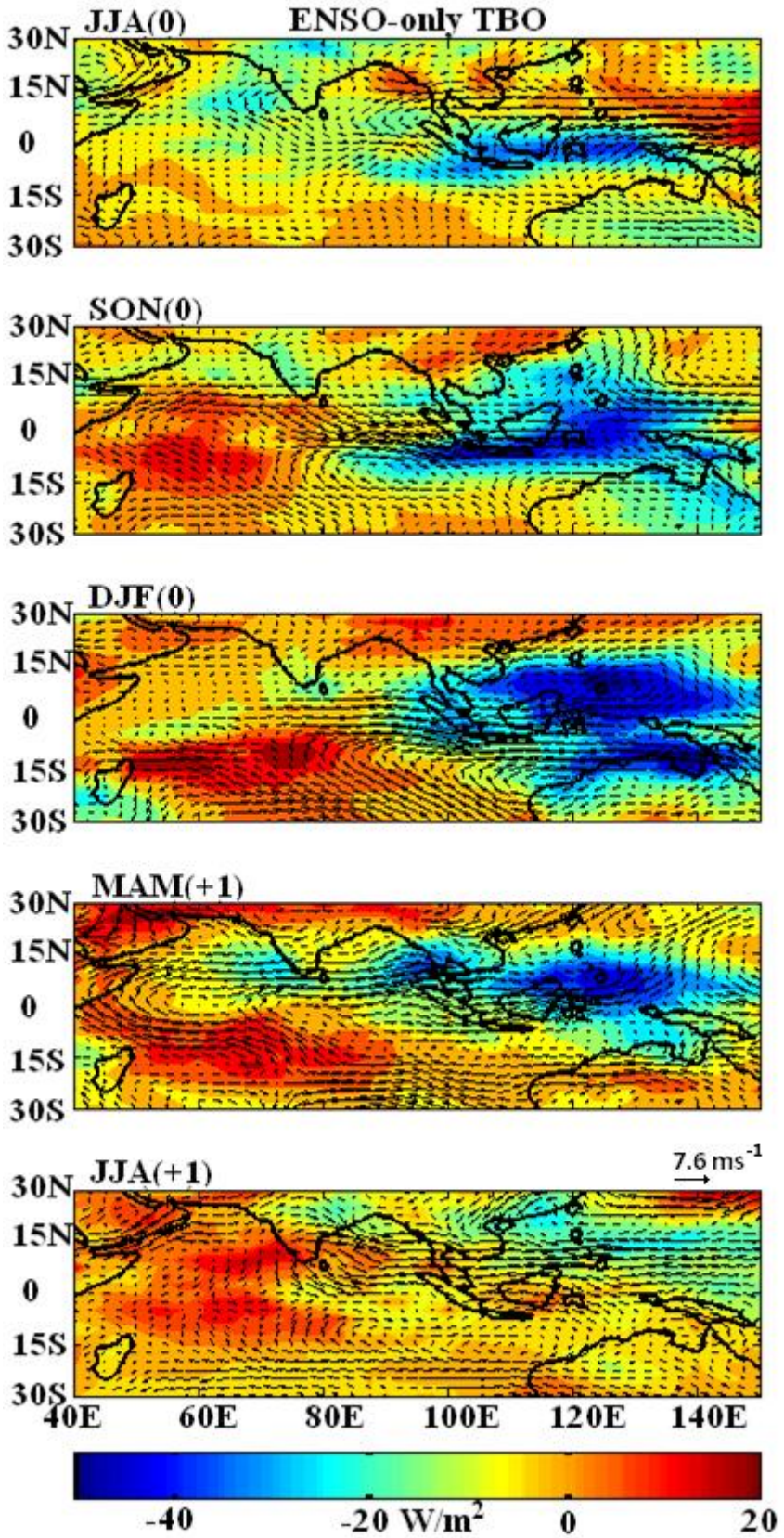

Figure 7.17: Strong minus weak ENSO TBO composites of outgoing longwave radiation (OLR: shaded) and 850 hPa wind (arrows: key is indicated at the bottom plot), starting from strong monsoon, JJA (0), to the next year monsoon, JJA (+1).

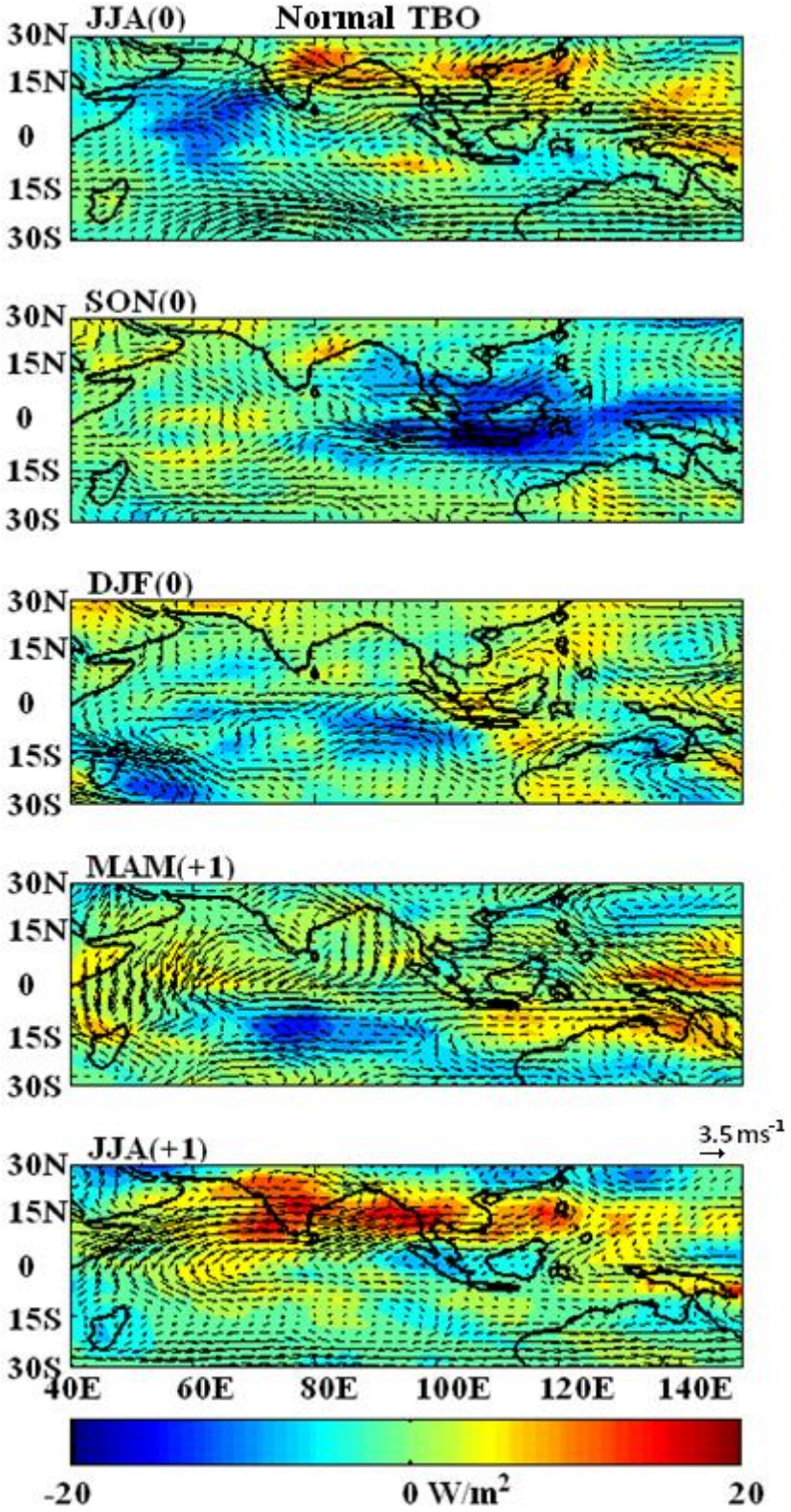

Figure 7.18: Strong minus weak normal TBO composites of outgoing longwave radiation (OLR: shaded) and 850 hPa wind (arrows: key is indicated at the bottom plot), starting from strong monsoon, JJA (0), to the next year monsoon, JJA (+1).

Longitude-time evolution of convective activity from the previous year's monsoon, starting from the month June (-1) through the strong monsoon year (June 0) to the end of

the following year's monsoon season (Sep+1) across the longitudes extending from 30º E to 180º E and latitudes averaged between 20ºN-20ºS is illustrated in Figure 7.19 for ENSO TBO years (left panel) and for normal TBO years (right panel). From the strong minus weak ENSO TBO year composite depicted in Figure 7.19 (left panel), very strong convective activity is evident for the ENSO TBO years compared to the normal TBO case. For the ENSO TBO years, as the previous year's monsoon progresses, a convective region develops in the western IO. When the convective activity diminishes in the IO, strong convective activity develops between 90º E-130º E by the time of the Australian monsoon (December-January-February). By the following monsoon, the convective zone reaches the western Pacific and also a convective region develops over the western IO. Convective activity in the western IO region joins the maximum convective activity that develops over the eastern IO and further advances in time and moves further east covering the western Pacific by the time of the Australian monsoon (December-January-February). Although the western IO region becomes cloud free by the following monsoon, weak convection occupies much of the eastern IO and Pacific region (Figure 7.19 left panel) indicating biennial variability.

Longitude-time evolution of convective activity for the normal TBO years (Figure 7.19 right panel) indicates that convective activity is weaker during all months. However, for the normal TBO case, occurrence of convective activity over the IO region is evident during monsoon seasons. The weak convective activity established over the IO region during the previous monsoon moves east, with the maximum convective activity occupying the area between 90º E-120º E after the previous monsoon. Between January (0) and May (0) the entire longitude section remains relatively cloud free, with monsoon cloud re-appearing in the western IO associated with increasing wind strength by the following monsoon. As the season progress, the maximum convection centre moves further east, starting from 60º E and reaching 120º E by the end of post-monsoon season (September-November: SON 0). By the following monsoon season, weak convective activity re-appears in the IO and as the monsoon advances the convective activity extends almost to 100º E (Figure 7.19 right panel). The re-occurrence of convective activity each monsoon season over the IO region in normal TBO years indicates a biennial tendency (a relatively strong monsoon followed by a relatively weak monsoon, and vice versa).

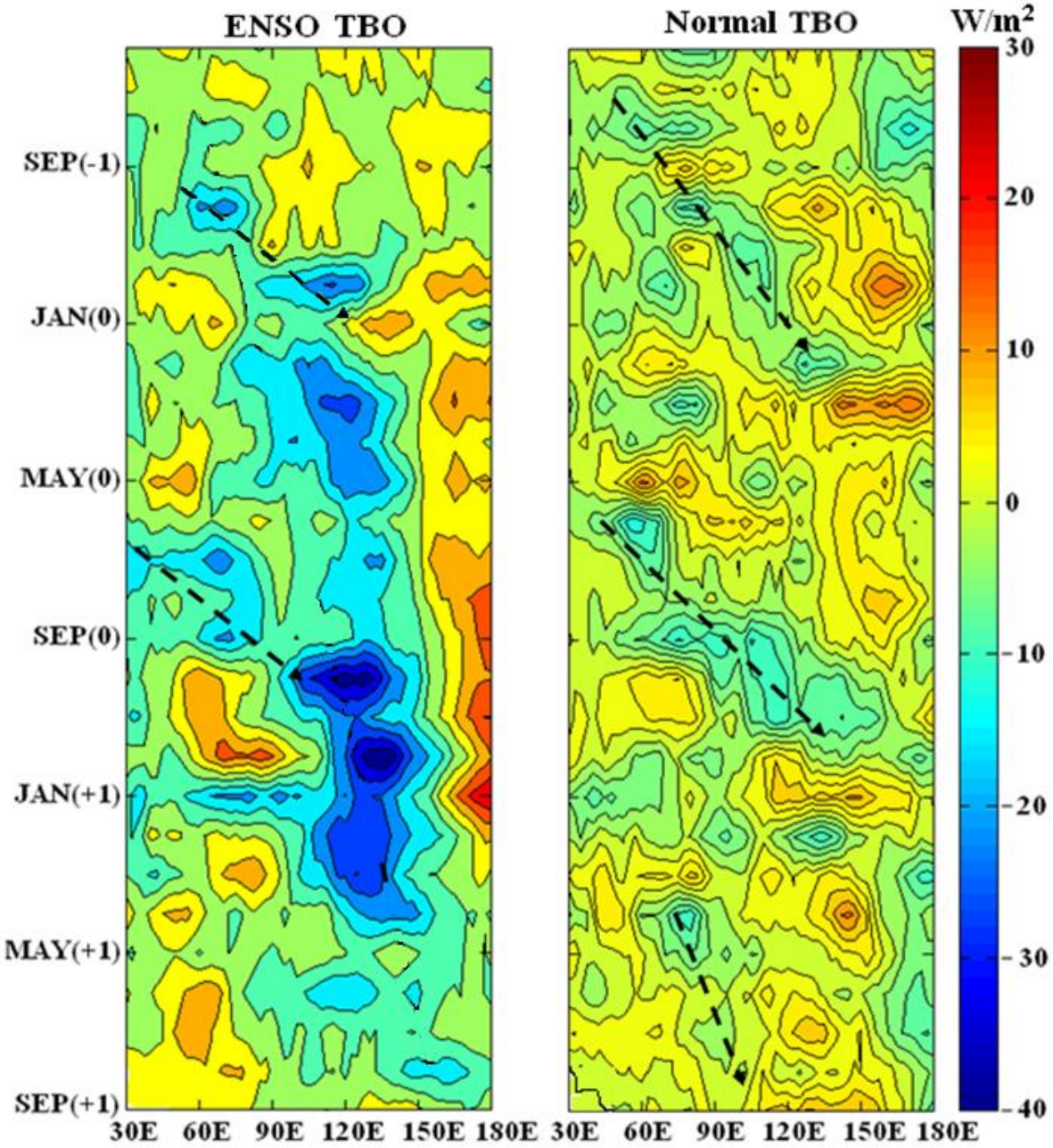

Figure 7.19: Longitude-time cross-section (averaged over latitudes from 20º N to 20º S) of outgoing longwave radiation (OLR) for strong minus weak composites for ENSO TBO years (left panel) and for normal TBO years (right panel), starting from the previous year monsoon (June-1) to the end of the next year's monsoon season (Sep+1). Arrows indicated movement of convection zones.

To understand the evolution of meridional circulation associated with changes in SST, OLR and wind anomalies previously discussed, composites of the local Hadley circulation for strong minus weak ENSO TBO and for normal TBO years was carried out. In relation to the circulation associated with the monsoon and its interannual variability, it has been suggested that the local meridional circulation (local Hadley circulation) plays a

more important role than the mean meridional circulation of the tropical atmosphere (Pillai and Mohankumar 2008; Slingo and Annamalai 2000). Local Hadley circulation was derived from meridional velocity and omega (represents rate of chage of pressure over time and represented by the symbol, ω), since the vertical velocity (w) is not measured directly and hence has to be derived from fields that are measured directly (Holton 2004). Using the hydrostatic equation, the omega and vertical velocity can be related to each other and the vertical motion can be inferred from the isobaric coordinate system as the total time derivative of the pressure (Holton 2004):

$$dp = -\rho g\, dz$$

$$w = \frac{dz}{dt}$$

$$\omega = \frac{dp}{dt} \approx -w\rho g$$

where ρ is the air density and g is gravity, and ω and w are defined above. The vertical velocity is thus derived as:

$$w = -\frac{\omega}{\rho g}$$

and is a good approximation (Holton 2004).

Strong minus weak ENSO TBO and normal TBO year composites of local Hadley circulation (height-latitude cross-sections of meridional velocity and vertical velocity averaged over the longitudes from 60-95º E) for the previous year (JJA-1), reference year (JJA0) and following year (JJA+1) monsoon seasons are illustrated in Figure 7.20. In the ENSO TBO mode, a strong descending motion is located around 20º N during the previous monsoon season (JJA-1) and further to the north lies a band of ascending motion during the same season. Weak descending motion also occurs near the surface close to the equator during the JJA (-1) season. Pronounced ascending motion occupies the Northern Hemisphere during the reference monsoon season (JJA0: Figure 7.20 left panel) together with a narrow descending branch between 5-15º S. During the next monsoon season (JJA+1), anomalous descending motion occupies between 10-20º N for the case of the ENSO TBO mode (Figure 7.20 left panel). The Hadley circulation for strong minus weak normal TBO year composite (Figure 7.20 right panel) for the previous monsoon season (JJA-1) reveals descending motion in most of the Northern Hemisphere, except in the region 25-35º N, where ascending motion is evident aloft. During the strong monsoon season (JJA0), the region between 5º S-20º N is occupied by weak upward motion for the case of the normal TBO. The equatorial region (5º S-10º N) experiences downward motion

during the following weak monsoon season (JJA+1: Figure 7.20 right panel) and also weak descending motion lies between 30-40º N.

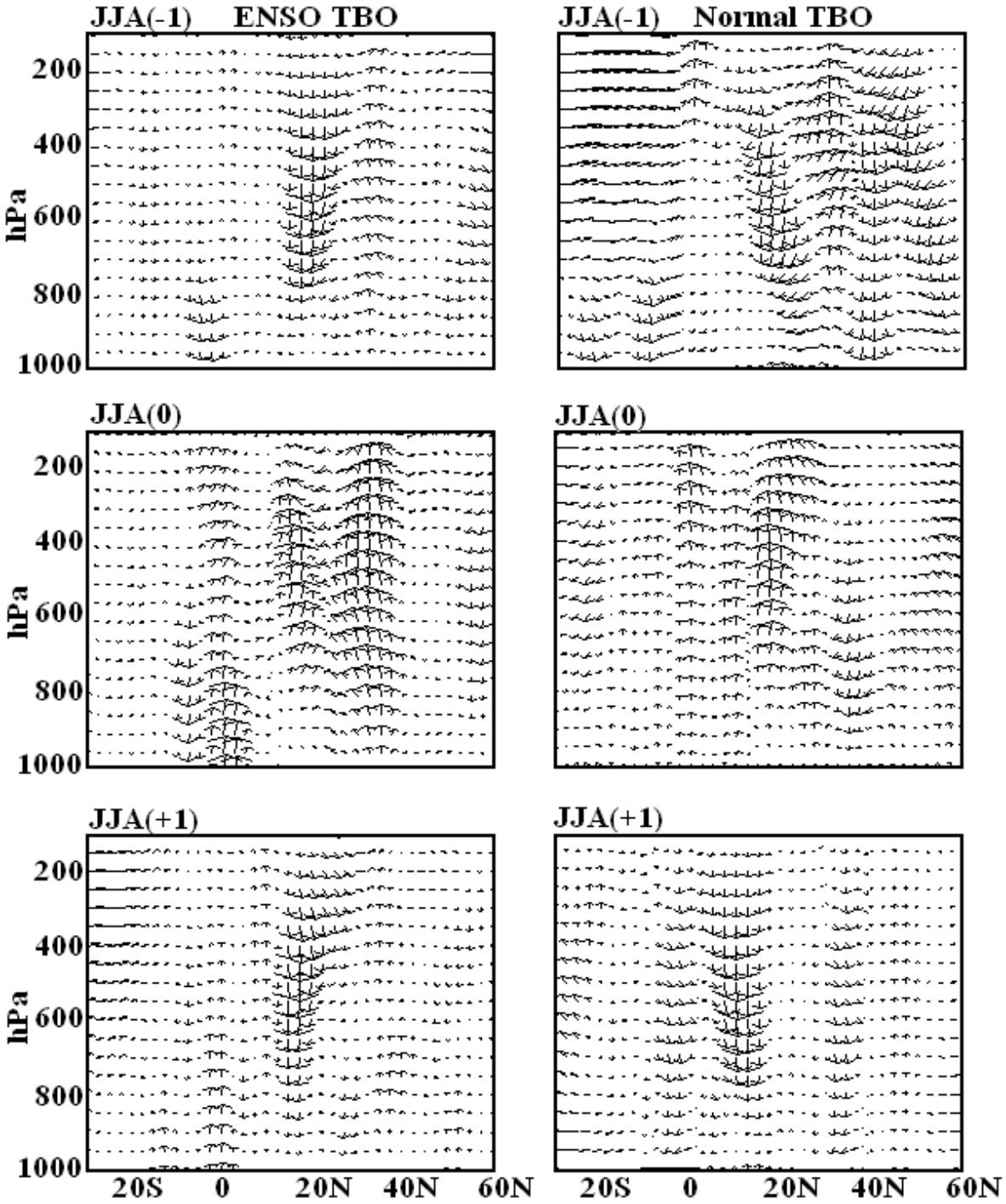

Figure 7.20: Height-latitude cross section of the strong minus weak composite of meridional velocity and vertical velocity averaged over longitudes 60-95º E for ENSO TBO (left panel) and normal TBO (right panel) years, for the previous year monsoon season (JJA-1), reference monsoon season (JJA0) and following monsoon season (JJA+1).

The composites shown above indicate differences in the formation and propagation of seasonal SST, OLR and wind anomaly patterns for strong minus weak ENSO TBO and

for normal TBO years. The SST composites for ENSO TBO years reveal the presence of dipole patterns (Indian Ocean dipole: IOD), which has been identified as an inherent factor of the IO influencing the Asian monsoon and TBO (Loschnigg et al. 2003; Meehl and Arblaster 2002a; Pillai and Mohankumar 2007). The dipole pattern is absent from the non-ENSO TBO year SST composite. This suggests that the IOD does not play a role in Maldives monsoon rainfall biennial variability during normal TBO years, as indicated by Pillai and Mohankumar (2007) for the case of Indian monsoon rainfall. During normal TBO years, propagation of the convective zone is mostly limited to the IO region, re-occurring during each monsoon season. On the other hand, for ENSO TBO years, the maximum convective activity lies in the western Pacific region during the Australian monsoon season (Figure 7.17 and Figure 7.19 left panel) and a biennial tendency of convective activity can be seen from one monsoon season to the next for the IO region, as well. Wind anomalies for the strong minus weak ENSO TBO and for normal TBO year also indicate a biennial cycle. The local Hadley circulation also suggests existence of biennial variability for ENSO TBO and for normal TBO year cases, with the upward motion during a strong monsoon season and downward motion during previous and following monsoon seasons (Figure 7.20). This indicates that the local Hadley circulation influences the Maldives monsoon rainfall. The discrepancies between ENSO TBO and normal TBO year anomalies for SST, OLR, wind and the local Hadley circulation suggests that factors other than ENSO play a role in biennial variability in non-ENSO TBO years (Pillai and Mohankumar 2007). Li and Zhang (2002) suggested that variability of the monsoon on the TBO scale is mainly due to local processes in the Indian Ocean, while ENSO scale monsoon variability is associated with more remote forcings. These processes will be investigated below.

7.3.1.3 Time-filtering analysis

In order to differentiate the processes responsible for TBO and ENSO forcings, a band-pass filter (Murakami 1979) was used to separate the data into approximately 2-3 year (TBO time scale) and 3-7 year (ENSO time scale) series, with the spectral peak-power points of these two time scales located at 2 and 5 years, respectively (Li and Zhang 2002; Li et al. 2001; Pillai and Mohankumar 2009). These two time scales represent significant interannual time scale peaks for the Maldives monsoon rainfall (Figure 7.14) and area-averaged Indian rainfall (Li and Zhang 2002). Details of the filter and filtering techniques are provided in Chapter 2.

Maldives monsoon rainfall was filtered using the TBO and ENSO time scales separately, to determine strong and weak years for the TBO and ENSO time scales. A strong/weak year is when the filtered standardized anomaly of monsoon rainfall is more than +1 SD/-1 SD, respectively. Figure 7.21 illustrates strong minus weak year SST anomaly composites for the TBO (right panel) and ENSO time scale (left panel), starting from the previous year winter (DJF-1) to the following year winter (DJF+1). With the TBO time scale, significant changes in SST anomaly over the Indian and Pacific Ocean region are evident. The maximum warming occurs over the Pacific Ocean during the DJF (-1) season for both TBO and ENSO time scales. However, the ENSO related warming over the Pacific Ocean is weaker during the DJF (-1) compared to the TBO time scale for the same season. The whole of the IO experiences a positive SST anomaly during the same season on the TBO time frame (DJF-1: Figure 7.21 left panel). By the following season (MAM 0), the warming setup in the previous season in the Pacific becomes weaker on the TBO time scale. For the case of ENSO, the SST anomalies remained relatively unaltered during the MAM (0) season compared to the previous season (DJF-1). With the onset of the monsoon season, JJA (0), significant cooling is evident in the Indian and Pacific Oceans. No significant changes in SST are noted for the ENSO time scale during the monsoon season (JJA 0: Figure 7.21 right panel). During the next two seasons (SON 0 and DJF+1), the cooling over Indian and Pacific Oceans further intensifies for the TBO mode. On the ENSO time scale, during the same seasons (SON 0 and DJF+1), no significant changes in sea surface temperature are observed, except some cooling over the western Pacific and weakening of warming in the eastern Pacific (SON0 and DJF+1: Figure 7.21 right panel) compared to the JJA (0) season. Strong minus weak year SST anomaly composites for different seasons suggests that the evolution of anomalies is different for the TBO and ENSO time scales. The difference in evolution of SST anomalies has previously been suggested by Pillai and Mohankumar (2009) based on strong and weak years identified using the ISMR index.

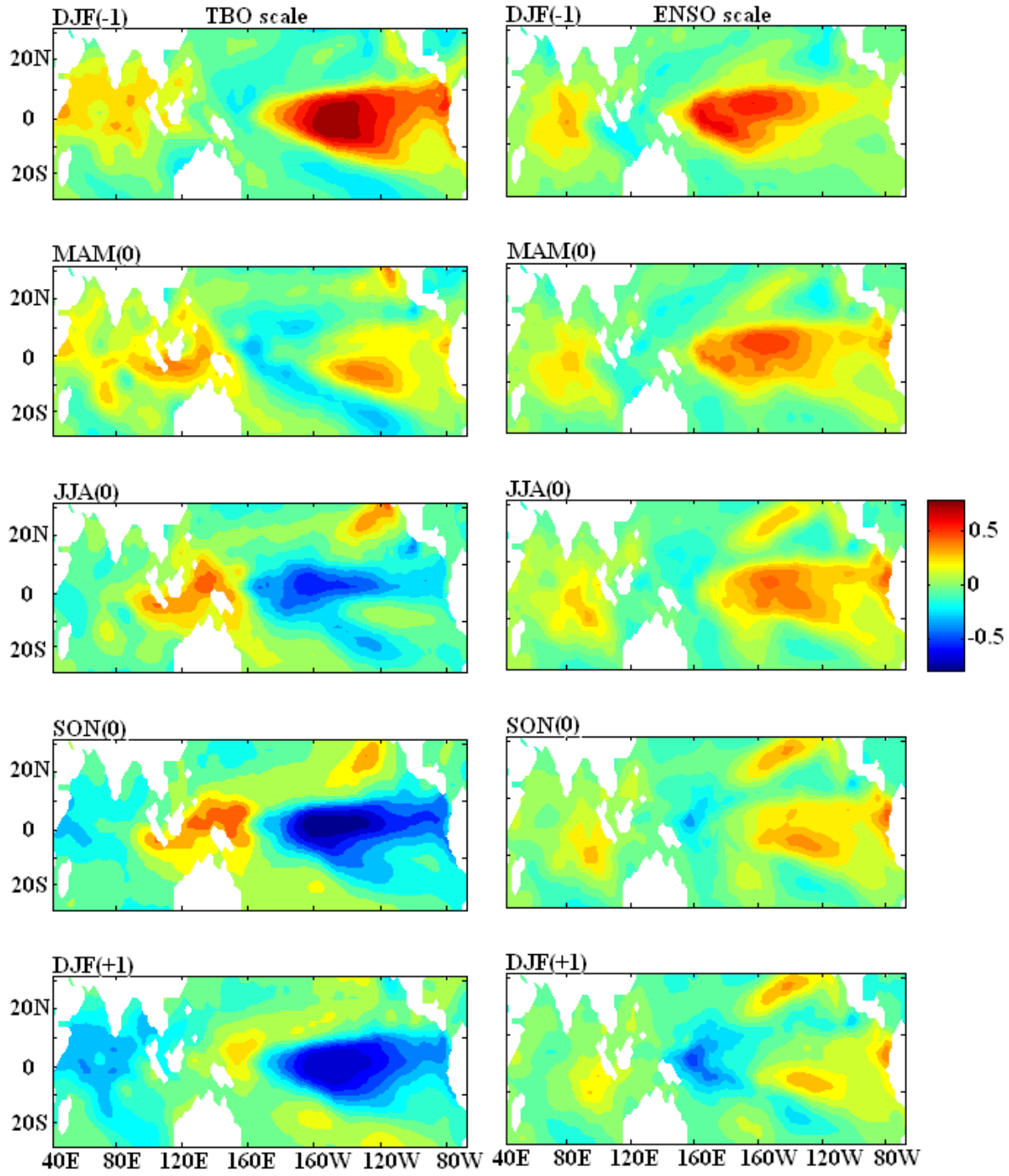

Figure 7.21: Strong minus weak composites of sea surface temperature (SST: ºC) for TBO (left panel) and ENSO time scales (right panel), starting from the previous winter season (DJF (-1)) to the following winter (DJF (+1)), taking the monsoon season (JJA (0)) as the reference season.

The spatial correlations between filtered Maldives monsoon season rainfall and filtered SST anomalies is depicted in Figure 7.22 for the TBO (left panel) and ENSO time frames (right panel), starting from previous winter to the following winter. The evolution of the TBO time frame correlation (Figure 7.22 left panel) is very similar to the TBO mode SSTA evolution shown above (Figure 7.21 left panel). During the preceding winter (DJF-1)

and spring (MAM 0), the Maldives monsoon rainfall positively correlates with the SSTA in the Indian and eastern Pacific Oceans, while a weak negative correlation exists between SSTA in the western Pacific region in TBO time frame. With the onset of the monsoon, the correlation becomes weak in the Indian and eastern Pacific Ocean region, but significantly negative correlations develop between Maldives monsoon season rainfall and SSTA in the central Pacific region for the case of the biennial time scale (JJA0: Figure 7.22 left panel), with the maximum positive and negative correlations occurring north of Australia and in the central Pacific, respectively. During the next two seasons (SON 0 and DJF+1), the inverse relationship that started to develop in the previous season over the IO is further strengthened. For the ENSO time frame (Figure 7.22 right panel), the positive correlations in the IO region become weaker as the seasons progress from winter (DJF-1) to the next winter (DJF+1), while the correlation in the eastern Pacific region strengthen around the summer season through to the next monsoon season. No other significant changes in correlation are evident over the Pacific Ocean region for the case of the ENSO time frame as the seasons progress from DJF-1 to DJF+1 (Figure 7.22 right panel). The leading (winter and spring) strong correlation between Maldives monsoon rainfall and SSTA in the IO for the TBO suggests that the SSTA in the IO play a significant role in strengthening the subsequent monsoon over the Maldives, as indicated for the Indian monsoon by Li et al. (2001). Singh and Oh (2007) pointed out that the regional SST warming over the IO enhances monsoon precipitation over south peninsula India, west peninsula India and the IO. The evaporation and resultant moisture transport associated with the sea surface temperature anomaly may influence the monsoon rainfall (Chang and Li 2000; Li et al. 2001; Meehl 1997).

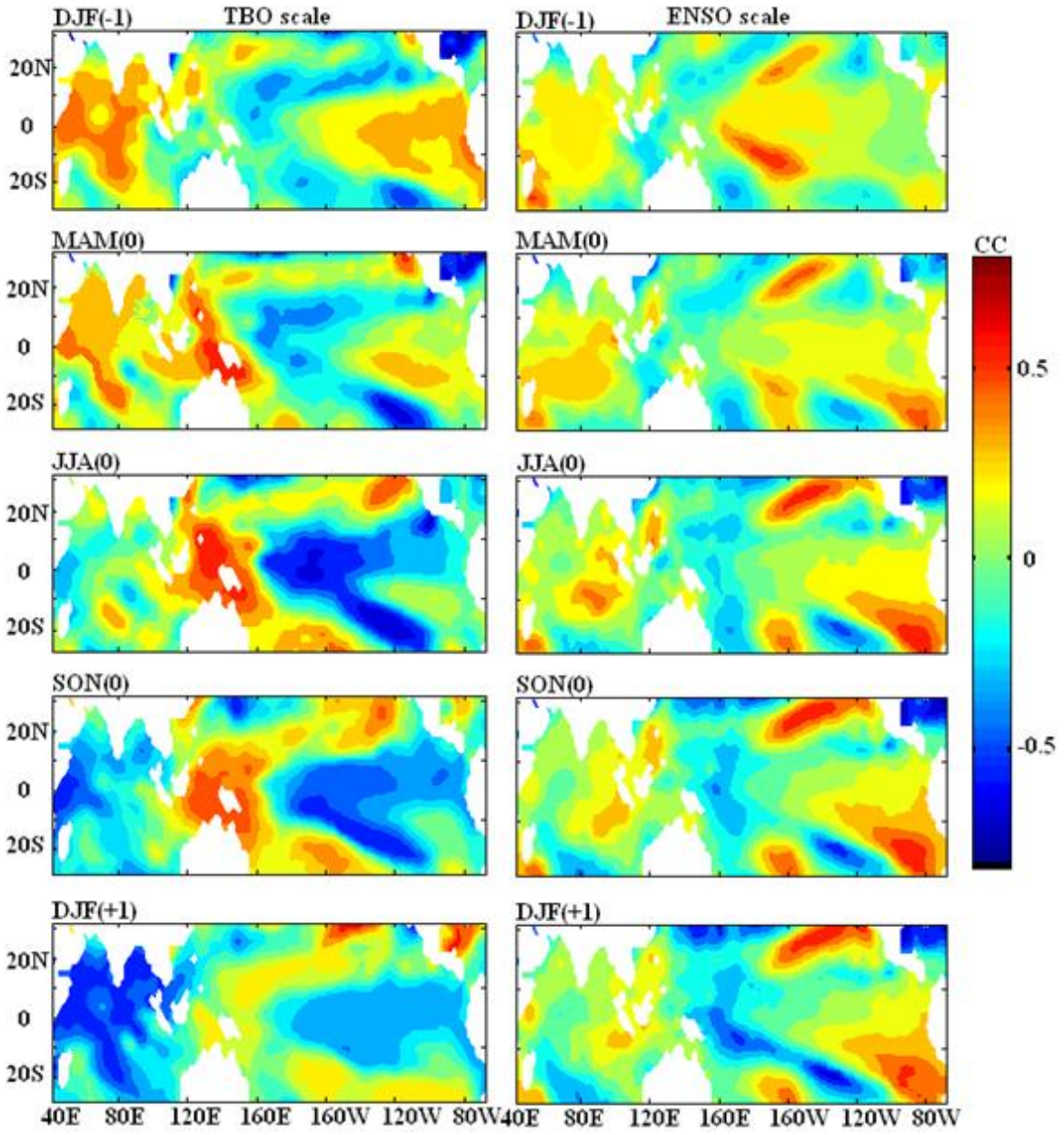

Figure 7.22: Lag correlation between filtered Maldives monsoon season (JJAS) rainfall and filtered sea surface temperature anomalies (SSTA) in DJF (-1), MAM (0), JJA (0), SON (0) and DJF (+1) for the TBO (2-3 year) and ENSO (3-7 year) time scales. "0" indicates reference monsoon year and "-1" and "+1" represents year before and after reference monsoon year, respectively.

Strong minus weak composites of moisture flux at 1000 hPa for the TBO and ENSO modes starting from the Northern Hemisphere winter season (DJF-1) to the following monsoon season (JJA 0) are depicted in Figure 7.23, together with the direction of moisture flux. On the ENSO time frame the only region with anomalously higher moisture flux during Northern Hemisphere winter and spring (MAM 0) is located over Indonesia and west of Indonesia. The TBO time frame shows anomalously higher moisture flux over the

central IO region during the winter and spring season, indicating build-up of moisture prior to the monsoon season (Figure 7.23 left panel). This indicates a positive correlation between the monsoon and the transport of moisture to the region during the winter and spring season, and the sea surface temperature anomaly. On the ENSO time frame, there is little correlation between the prior season's moisture transport and the monsoon, as no persistent anomalously higher moisture flux was observed over the IO region during DJF(-1) and MAM(0).

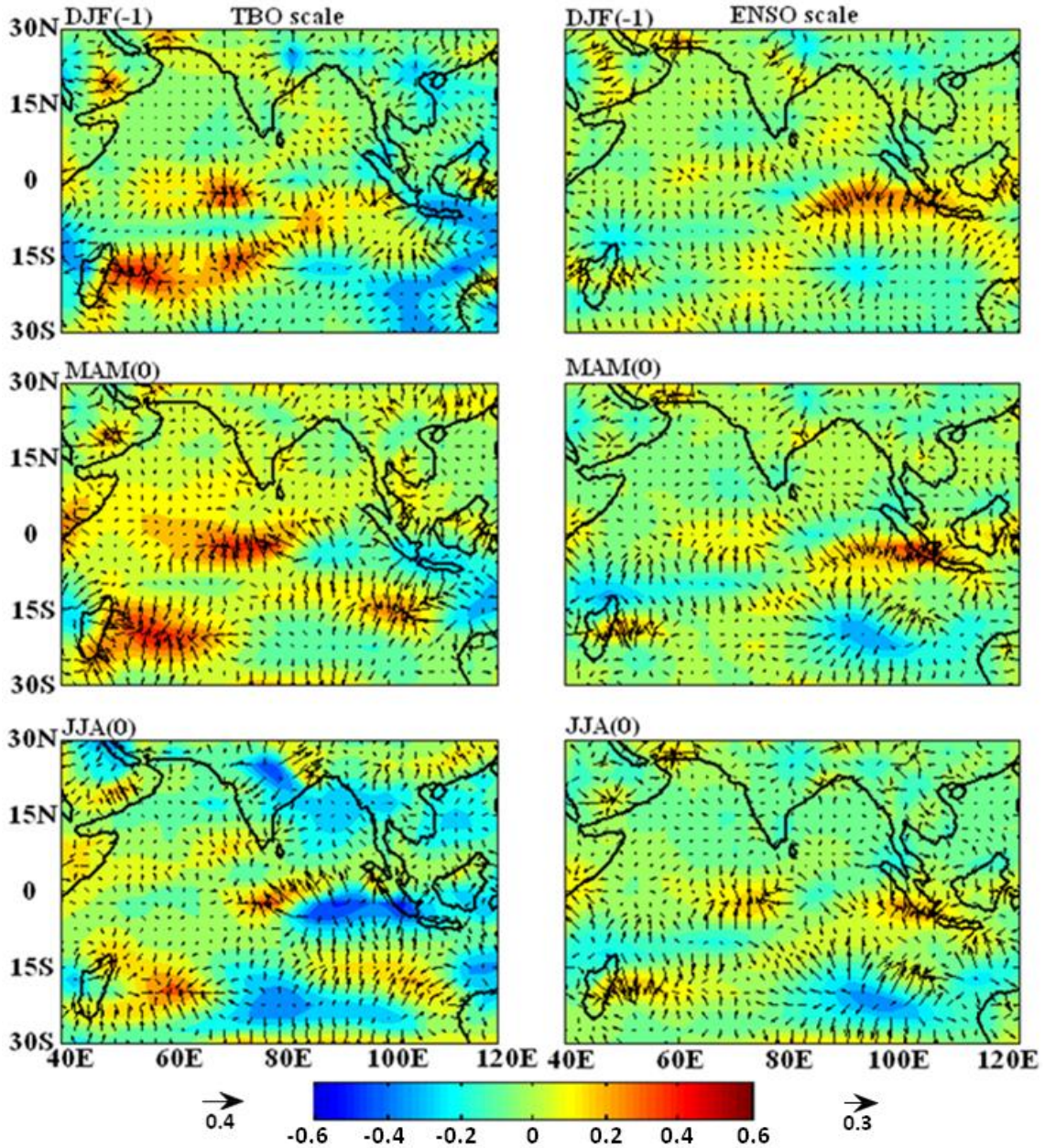

Figure 7.23: Strong minus weak moisture flux (m s^{-1} g kg^{-1}) composite anomaly at 1000 hPa for TBO (left panel) and ENSO time frame (right panel), starting from the previous winter season (DJF (-1)) to the following monsoon season (JJA (0)). The arrows indicate the direction of moisture flux and the magnitude of the arrows is indicated at the bottom of the figure for both time frames.

To crosscheck whether the spatial composites and correlations are the result of an artificial outcome of the band-pass filter used to separate the data into the TBO and ENSO time frames, SST composites of unfiltered data were derived. Figure 7.24 illustrates sea surface temperature anomaly composites from the preceding winter (DJF-1) to spring (MAM0) during peak El Niño events (based on the five month running mean of Niño3.4 SSTA being greater than ±0.5ºC: see Chapter 6 on ENSO) for wet, normal and dry years (Table 7.9) of Maldives monsoon rainfall, whereas Figure 7.25 depicts sea surface temperature anomaly composites for the same three categories of Maldives monsoon rainfall for the same seasons. Over the IO region there is a notable difference in SSTA between wet and dry conditions for these seasons. During the wet conditions most of the IO experiences anomalously high SST, while during dry conditions the IO experiences cooling. Positive sea surface temperature anomalies dominate most of the central and eastern Pacific region for the three categories depicted in Figure 7.24 during the two seasons. Spatial and temporal evolution of sea surface temperature anomalies for the La Niña case shows the opposite pattern (Figure 7.25) compared to the El Niño case SSTA (Figure 7.24). For the La Niña case, during winter and spring, most of the IO and Pacific region is affected by negative SSTA in the wet composite. On the other hand, the dry conditions for the La Niña are associated with positive SSTA in the Indian and Pacific Ocean region in the winter season (DJF-1) and the SSTA persists into spring in the IO region, although in some parts of the Pacific region, the positive SSTA setup during winter and spring changes its sign (Figure 7.25).

Li and Zhang (2002) suggested that the anomalous warming over the IO in the preceding winter/spring is a precursory signal for a wet monsoon. The warming over the IO observed for the Maldives monsoon wet conditions and cooling over the IO observed for the Maldives monsoon dry conditions using unfiltered data supports the positive lag correlation obtained for the northern winter and spring season (DJF-1 and MAM0: Figure 7.22 left panel) between filtered Maldives monsoon rainfall and SSTA for the TBO time frame. The preceding winter season warming/cooling over the IO for the wet/dry conditions further supports the observed build-up of moisture in the IO region one to two seasons prior to the monsoon onset, for the case of the TBO time scale depicted in Figure 7.23 (left panel). According to Li and Zhang (2002), warm sea surface temperature anomalies in the eastern Pacific in the preceding winter is associated with a strong/weak monsoon for the TBO/ENSO time frame, respectively. The anomalous SSTA found during the winter and spring season over the eastern Pacific for the wet (El Niño case: Figure 7.24) and dry

conditions (the La Niña case: Figure 7.25) using unfiltered data are consistent with the preceding winter and spring correlation obtained above between filtered SSTA and Maldives monsoon rainfall for the TBO and ENSO time frame (Figure 7.22 left and right panel, respectively), suggesting that the relationship is not an artificial outcome of the band-pass filter (Li and Zhang 2002; Li et al. 2001).

Table 7.9: Wet, normal and dry years of Maldives monsoon rainfall (MMR) corresponding to El Niño and La Niña events. Wet, normal and dry years are defined when the MMR > +0.7 SD, -0.70 < MMR < 0.7 SD and MMR < -0.7 SD, respectively.

	El Niño events	La Niña events
Wet years	1988, 1992, 1997	1998, 1996, 2007
Normal years	1983,1995, 2004, 2006	1989, 2000
Dry years	1987, 2002	1985, 1999

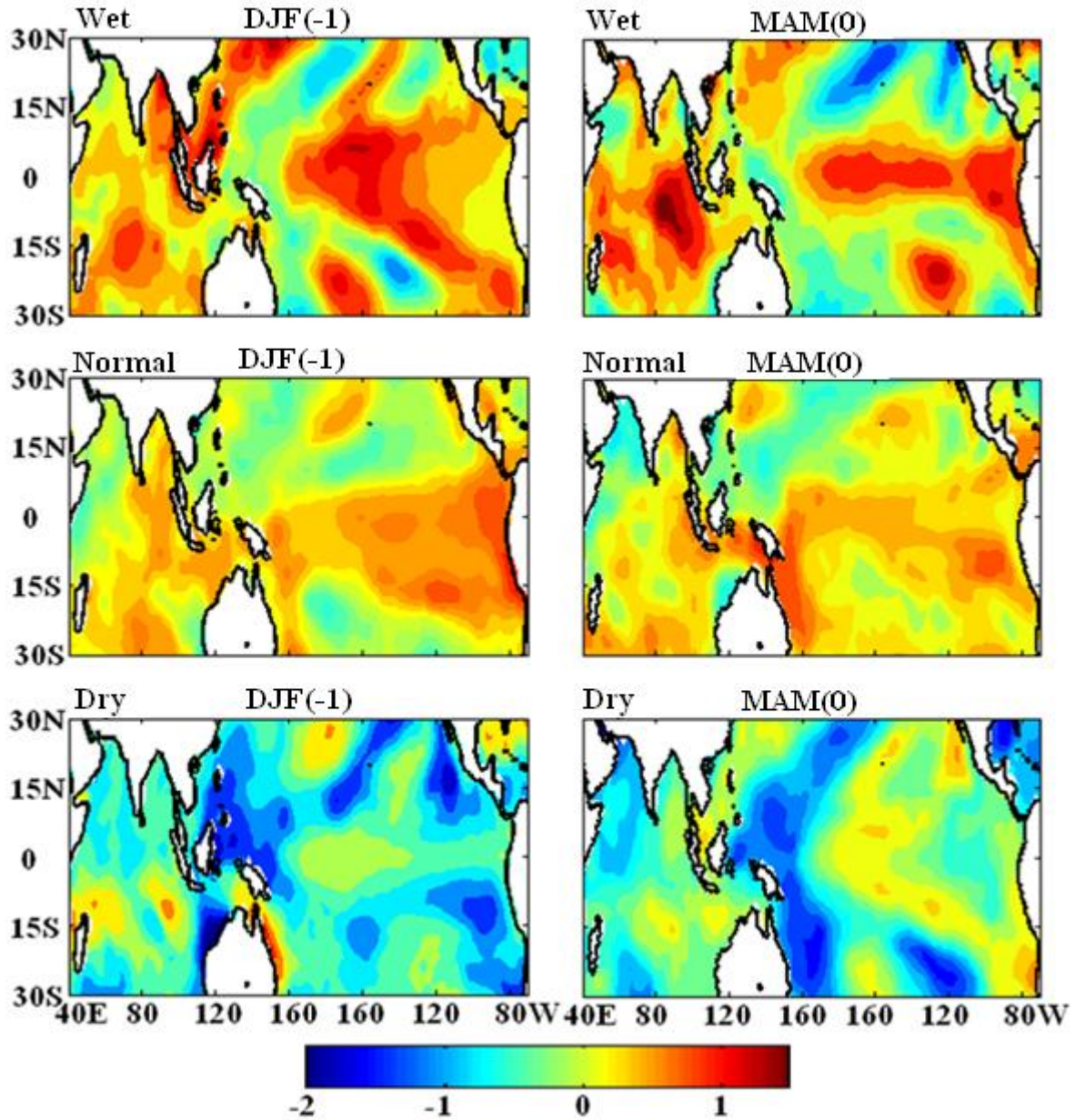

Figure 7.24: Sea surface temperature anomaly (SSTA) composites for the winter (DJF-1) and spring (MAM0) season associated with peak El Niño events for three categories of Maldives monsoon rainfall (MMR): wet, normal and dry. Wet, normal and dry categories are defined above (see Table 7.9). SST at each grid point has been normalized by its respective standard deviation.

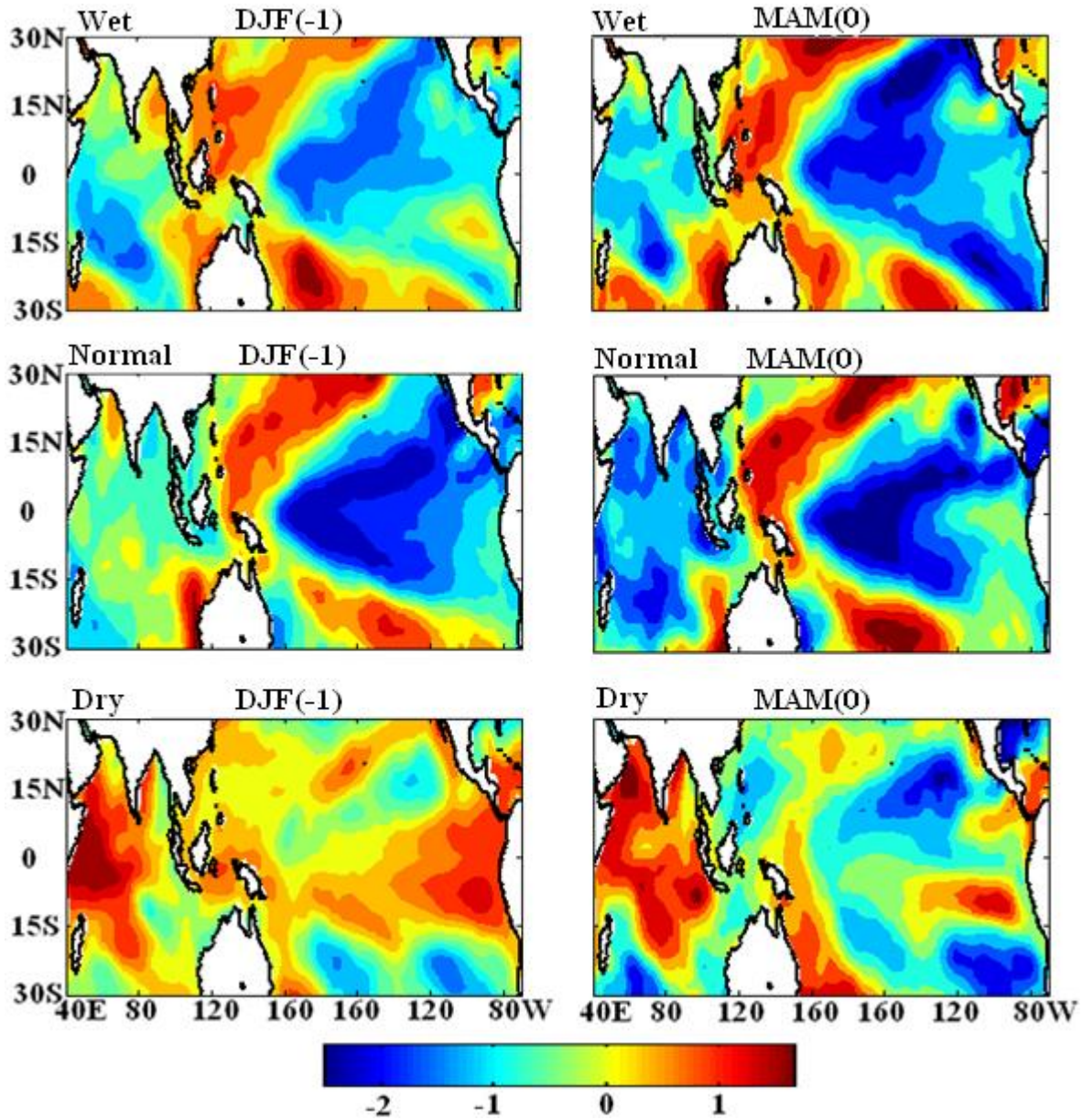

Figure 7.25: Sea surface temperature anomaly composites for the winter (DJF-1) and spring (MAM0) season associated with peak La Niña events for three categories of Maldives monsoon rainfall (MMR): wet, normal and dry. Wet, normal and dry categories are defined above (see Table 7.9). SST at each grid point has been normalized by its respective standard deviation.

Comparison between ENSO TBO and normal TBO composites indicates a difference in movement and formation of anomalies. The time-filtering analysis carried out above further indicates that the Maldives monsoon rainfall on TBO and ENSO time frames differs significantly and is associated with different processes. The Maldives monsoon rainfall is highly correlated with the SSTA in the IO 3-6 months prior to the onset of monsoon in the TBO time frame, but on the ENSO time frame very weak correlation exists. Anomalous positive SST in the IO increases evaporation, thus increasing surface moisture in the region (moisture flux into the region associated with the south-westerly flow)

resulting in a strong monsoon (Chang and Li 2000; Li et al. 2001). A strong monsoon in turn increases surface wind and leads to cooler than normal SSTA in the IO. This will result in reduction of moisture build-up in the region in the seasons leading up to the next monsoon, resulting in a weak monsoon the following year (Li and Zhang 2002; Li et al. 2001). On the other hand, the SSTA in the eastern and western Pacific influence the monsoon rainfall on an ENSO time scale. The eastern Pacific SSTA influence the monsoon through the vertical overturning of the east-west circulation, while warm SSTA in the western Pacific influence the local convection and tropospheric circulation (Li and Zhang 2002; Li et al. 2001). Another process that influences the monsoon on an ENSO time scale is related to the remote tropical SSTA forcing of mid-latitude circulation due to the establishment of a meridional temperature gradient between land and ocean. Lagged correlations between monsoon rainfall and the geopotential height thickness (200 minus 500 hPa) depicted in Figure 7.26 indicates establishment of a north-south thermal contrast across Asia 6 months prior to the onset of the monsoon for the case of the ENSO time frame, with the warm core region occurring over the Tibetan Plateau (DJF-1: Figure 7.26 right panel). The spatial correlation pattern for the TBO time scale (Figure 7.26 left panel) for the winter and spring is markedly different from the winter and spring seasons for the ENSO time scale. In TBO mode, an elongated warm anomaly originating from the African continent covers the Indian subcontinent and the Indian Ocean region during DJF (-1) and MAM (0) seasons. This suggests that an enhanced/reduced land-ocean thermal contrast in preceding months is followed by a strong/weak monsoon related to the ENSO signal, but not with the TBO case (Li and Zhang 2002; Li et al. 2001).

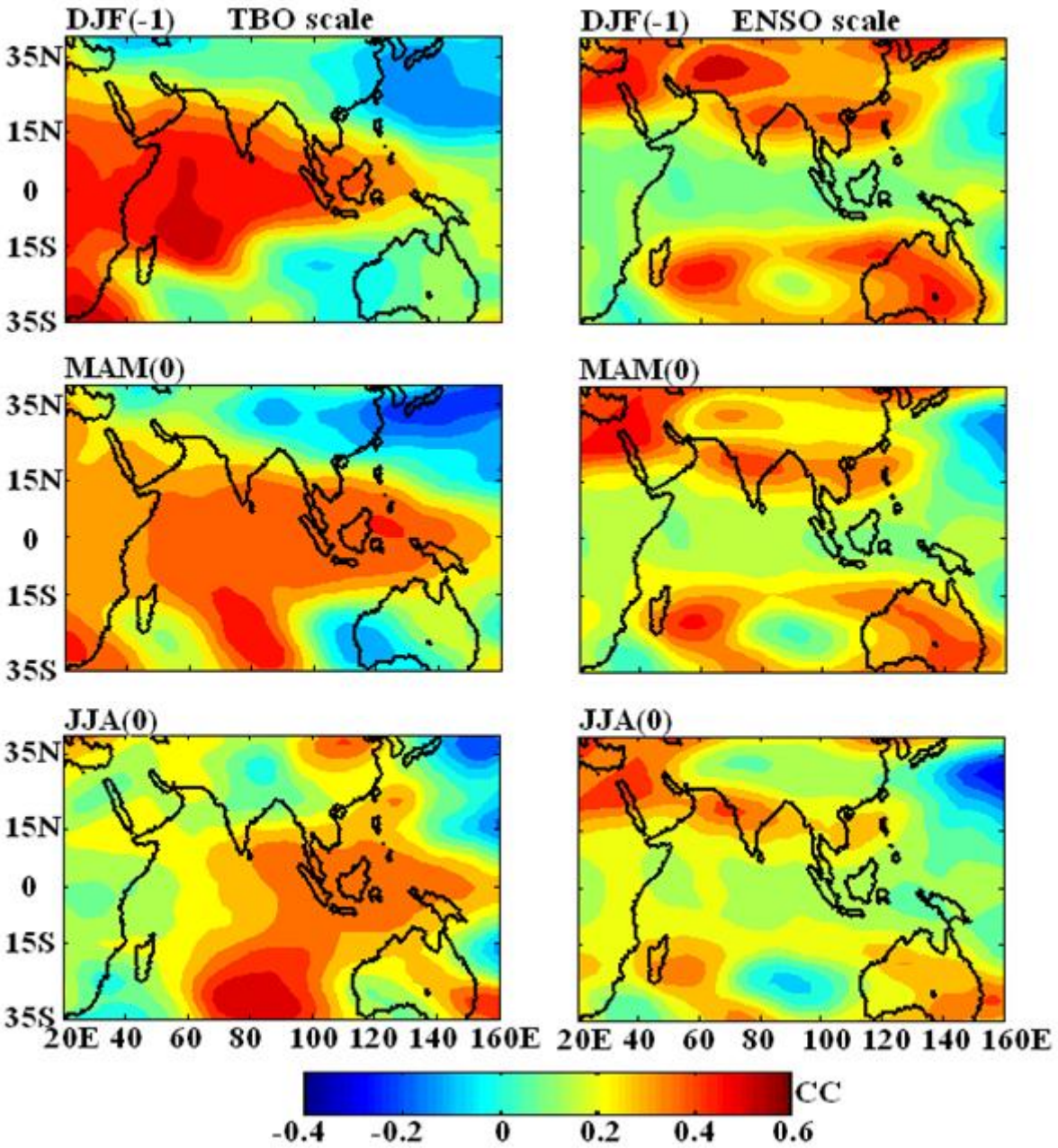

Figure 7.26: Lag correlation between Maldives monsoon season rainfall and geopotential height (200-500 hPa thickness) for TBO (left panel) and ENSO (right panel) time scales starting from the previous winter season, DJF (-1), to the following monsoon season, JJA (0).

The influence of the local Hadley circulation (height-latitude cross-section of meridional velocity and vertical velocity averaged over the longitudes from 60-95º E) on TBO and ENSO time frames is depicted in Figure 7.27. During the strong monsoon season (JJA0), the region between the equator and 45º N is dominated by ascending motion, while south of the equator lies a narrow belt of weak descending motion, for the case of the TBO time frame, indicating local circulation over the Maldives region. By the weak monsoon season (JJA+1), the circulation anomaly reverses, with strong downward motion occurring

between 25-45º N. A weak ascending region is located between the equator and 5º S during the same season (JJA+1: Figure 7.27 left panel). The strong monsoon season (JJA0) on the ENSO time frame (Figure 7.27 right panel) is dominated by strong ascending motion over most of the Northern Hemisphere and weak ascending motion is over the Southern Hemisphere (close to the equator). During the same season, strong descending motion lies over the Southern Hemisphere between 20-30º S on the ENSO time frame. The opposite anomaly pattern can be seen for the ENSO window during the weak monsoon season, as depicted in Figure 7.27, right panel (JJA+1). The ENSO scale weak monsoon season is dominated by ascending motion from 15º S-45º N, without local circulation, indicating that the location Hadley circulation plays an important role in the TBO time scale variability of the Maldives monsoon season rainfall. This is in agreement with Pillai and Mohankumar (2009), who concluded that the Indian Ocean fluxes and the local Hadley circulation and their interannual variability are limited to the TBO time scale only.

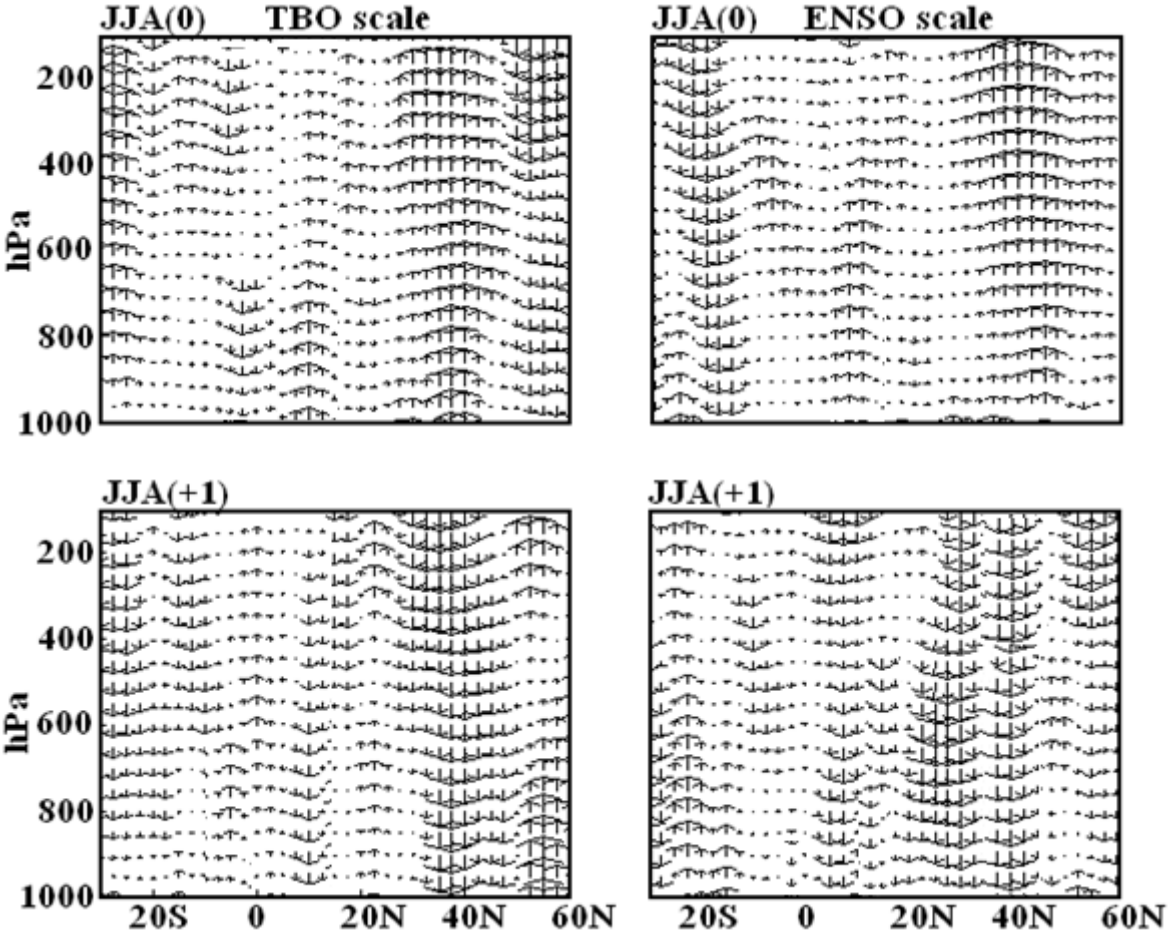

Figure 7.27: Height-latitude cross-section of the strong minus weak composite of meridional velocity and the vertical velocity averaged over longitudes 60-95º E for TBO (left panel) and ENSO time scales (right panel), for the reference monsoon season (JJA0) and following monsoon season (JJA+1).

7.3.1.4 Singular value decomposition analysis

Singular value decomposition (SVD) analysis was carried out to determine spatial association between the transition conditions in the March-May (MAM) season with the Maldives monsoon season (June-September) rainfall. Details of the SVD method are provided in Chapter 2. The transition conditions used here are 500 hPa geopotential height, and equatorial Indian Ocean and eastern equatorial Pacific SST. Positive height anomalies over Asia represent atmospheric circulation anomalies, leading to warm air advection from the south. This in turn strengthens subsequent monsoon rainfall due to the anomalously warm land temperatures and enhanced meridional temperature gradient (Li and Yanai 1996; Meehl and Arblaster 2001; 2002a; b). Anomalously higher SST in the equatorial Indian Ocean could enhanced evaporation, thus increasing moisture in the region, resulting in enhanced monsoon rainfall (Chang and Li 2000; Li et al. 2001; Meehl 1997; Meehl and Arblaster 2001; 2002b). On the other hand, anomalously cold SST in the eastern Pacific could enhance monsoon rainfall through changes in the large scale east-west circulation (Meehl and Arblaster 2001; 2002b).

The first SVD modes for the Indian Ocean SST, eastern Pacific Ocean SST and 500 hPa height for the MAM season using the data for the period 1979-2007 are illustrated in Figure 7.28a-c, while their corresponding first SVD modes for precipitation are depicted in the same figure (d-f), respectively. The positive SST in the Indian Ocean in MAM is associated with positive monsoon rainfall anomalies over the western part of the Maldives region, while the eastern part is associated with negative precipitation anomalies originating from the Sri Lanka region (Figure 7.28d). The coupling between monsoon rainfall and Indian Ocean SST explained by the first SVD component is 33.28%, while the correlation between the first SVD expansion coefficient time series of these two variables is 0.44. The spatial pattern of the first SVD component for the eastern Pacific Ocean SST indicates that the region is mainly dominated by a negative anomaly (Figure 7.28b). Associated with the eastern Pacific Ocean SST, the monsoon rainfall shows a southwest-northeast gradient and the negative SST anomaly in the eastern Pacific is associated with a positive rainfall anomaly in the southwestern part of the Maldives region (Figure 7.28e). The first SVD component between the eastern Pacific SST and monsoon rainfall explains 28.59% of the total squared covariance between the two variables and the corresponding expansion coefficient time series are correlated at the 0.62. The first SVD component of the 500 hPa height is quite different from the other two transition consitions and indicates that the southern East Asia area is dominated by positive anomalies in MAM (Figure 7.28c).

Patterns of convective heating anomalies stretching from eastern Africa to the western equatorial Pacific associated with an anomalous ridge of positive 500-hPa height anomalies over Asia and warmer Asian land temperatures, has been noted in earlier studies (e.g. Meehl 1997; Meehl and Arblaster 2001; 2002b). The positive height anomalies of 500 hPa height are associated with positive anomalies of monsoon rainfall west of Sri Lanka (Figure 7.28f). The variance explained by the first SVD component between 500 hPa height and the Maldives monsoon season rainfall is 24.87% and the correlation coefficient between their corresponding expansion coefficient time series is 0.39.

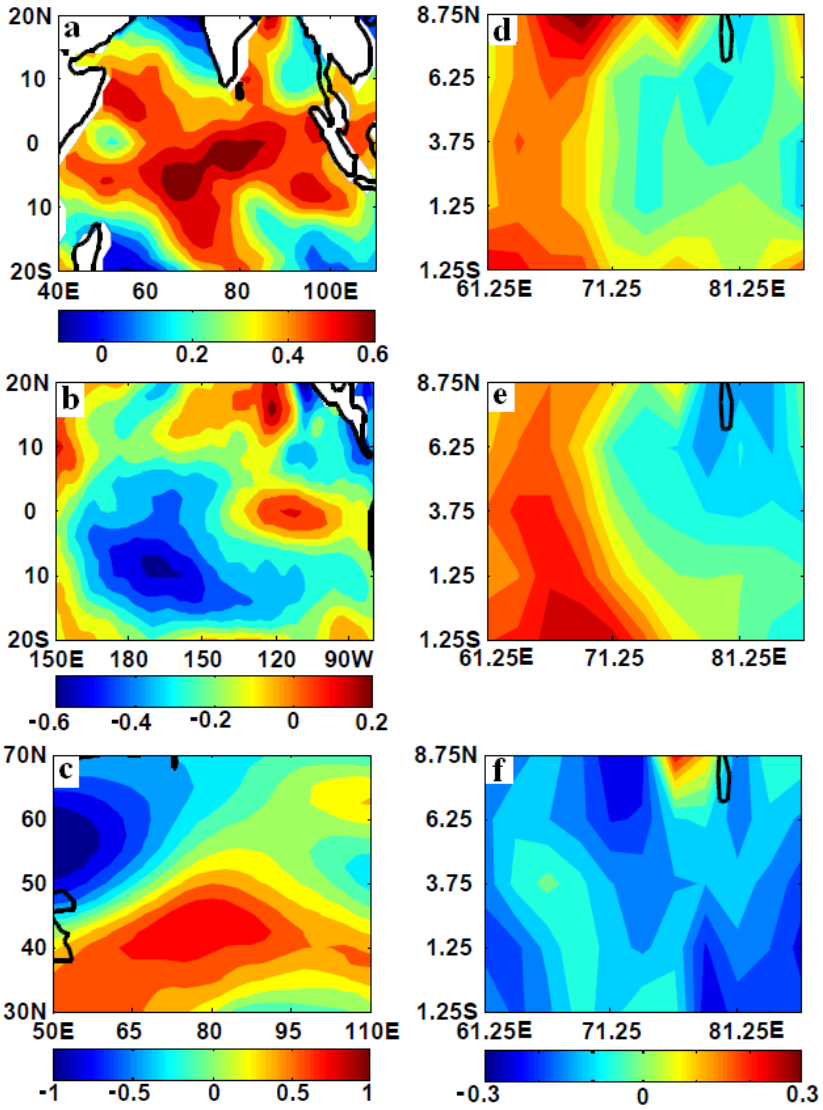

Figure 7.28: Spatial patterns of the first SVD mode for three transition conditions in MAM: (a) Indian Ocean SST, (b) Pacific Ocean SST, (c) 500 hPa height and (d-f) their corresponding first SVD modes for the Maldives monsoon rainfall (JJAS: in mm/day). The colour bar for SVD mode precipitation is given at the bottom of (f), which is common for (d-f), and the colour bar for each transition condition is given below each figure.

The squared covariance (r^2) explained by the second SVD components for the Indian Ocean SST, eastern Pacific Ocean SST and 500 hPa height for the season MAM, account for 12.08, 15.48 and 12.29%, respectively. The subsequent components account for considerably less. Since the first components for the mentioned conditions account for the majority of the squared covariance, first SVD components of the MAM transition conditions were used to quantify the individual associations year by year to identify which years the MAM transition conditions are working independently and in which years they are connected (Meehl and Arblaster 2001; 2002b). The spatial anomaly pattern correlations between the observed monsoon rainfall patterns and the SVD projections individually and cumulatively are calculated separately, following Lau and Wu (1999) and Meehl and Arblaster (2001; 2002b). The cumulative contribution from the first SVD components of the three transition conditions to the actual observed monsoon rainfall anomaly for the kth year is given by:

$$\boldsymbol{A_{i,j} = \langle O_j, \sum_{k=1}^{i} S(k) * C(k)_j \rangle,}$$

where $\langle \quad \rangle$ is the spatial anomaly pattern correlation over the Maldives region, i is the number of transition conditions (here i = 3 for three separate conditions), S is the normalized precipitation pattern for JJAS associated with MAM transition conditions, C is the precipitation SVD expansion coefficient for that year, and O is the observed Maldives monsoon rainfall anomaly. The calculated individual and cumulative anomaly correlation patterns are depicted in Figure 7.29a and b, respectively. It is quite interesting to see that the Indian Ocean and Pacific SST transition conditions follow each other quite closely (Figure 7.29a). In some years the associations between the Maldives region monsoon rainfall and the transition conditions in the Indian Ocean and Pacific SST during MAM are large. For example, the El Niño year 1987 and the La Niña year 2000 have pattern correlations of about 0.4 in both years. On the other hand, association between the transition conditions in the Indian Ocean and Pacific SST during MAM and the Maldives region monsoon rainfall in some years are weak (e.g. 1994 and 2002: Figure 7.29a). This suggests that in some years the transition conditions act independently and in some years the Indian Ocean can provide a regional input to the Maldives monsoon season rainfall, which is separate from the large scale influence from the Pacific region (Meehl and Arblaster 2002b).

In many years, the MAM regional 500 hPa height acts independently from the other two transition conditions (e.g. 1982, 1985, 1986, 1987, 2000, 2003 and 2005: Figure 7.29a). In some other years, the association between the three transition condition associations are large (e.g. 1983, 1992 and 1999: Figure 7.29a). This indicates that in some years the three transition conditions act independently, while in some years they follow each other and can provide an input to the Maldives monsoon rainfall.

The combined effects (cumulative anomaly correlation patterns) of the transition conditions are highest in 2003, with the cumulative anomaly correlation of about +0.8 (Figure 7.29b). This accounts for more than 60% of the spatial variance of the Maldives monsoon rainfall in 2003. During this year, individually Pacific SST accounts for the highest spatial variance followed by the transition conditions in the Indian Ocean, with the least contribution from the 500 hPa height. In 1999, all three transition conditions showed negative anomaly pattern correlations (Figure 7.29b). Associated with this, the only negative cumulative correlation pattern during the entire period can be seen in 1999, with the correlation of about -0.46, explaining only 21% of spatial variance in monsoon rainfall (Figure 7.29b). Although year 2000 transition conditions in Indian Ocean and Pacific SST are large (correlation value near to or greater than 0.4), the cumulative pattern correlation is near zero (Figure 7.29b), suggesting that other processes or internal dynamics can play a crucial role in monsoon rainfall in some years (Meehl and Arblaster 2001; 2002b).

The first components of SVD rainfall patterns associated with the transition conditions and their corresponding expansion coefficient time series were used to derive a cumulative area-averaged Maldives monsoon rainfall index, similar to the method used by Meehl and Arblaster (2001; 2002b), which is depicted in Figure 7.29c. Standardized monsoon rainfall index for the Maldives region obtained from the observed data is also illustrated in Figure 7.29c. The monsoon rainfall index derived from SVD and that obtained from the observed data are highly correlated, with a correlation coefficient of 0.95, indicating that the SVD generated Maldives monsoon rainfall index can explain more than 90% of the variance of the full index and indicates the strength of the monsoon (Meehl and Arblaster 2001; 2002b).

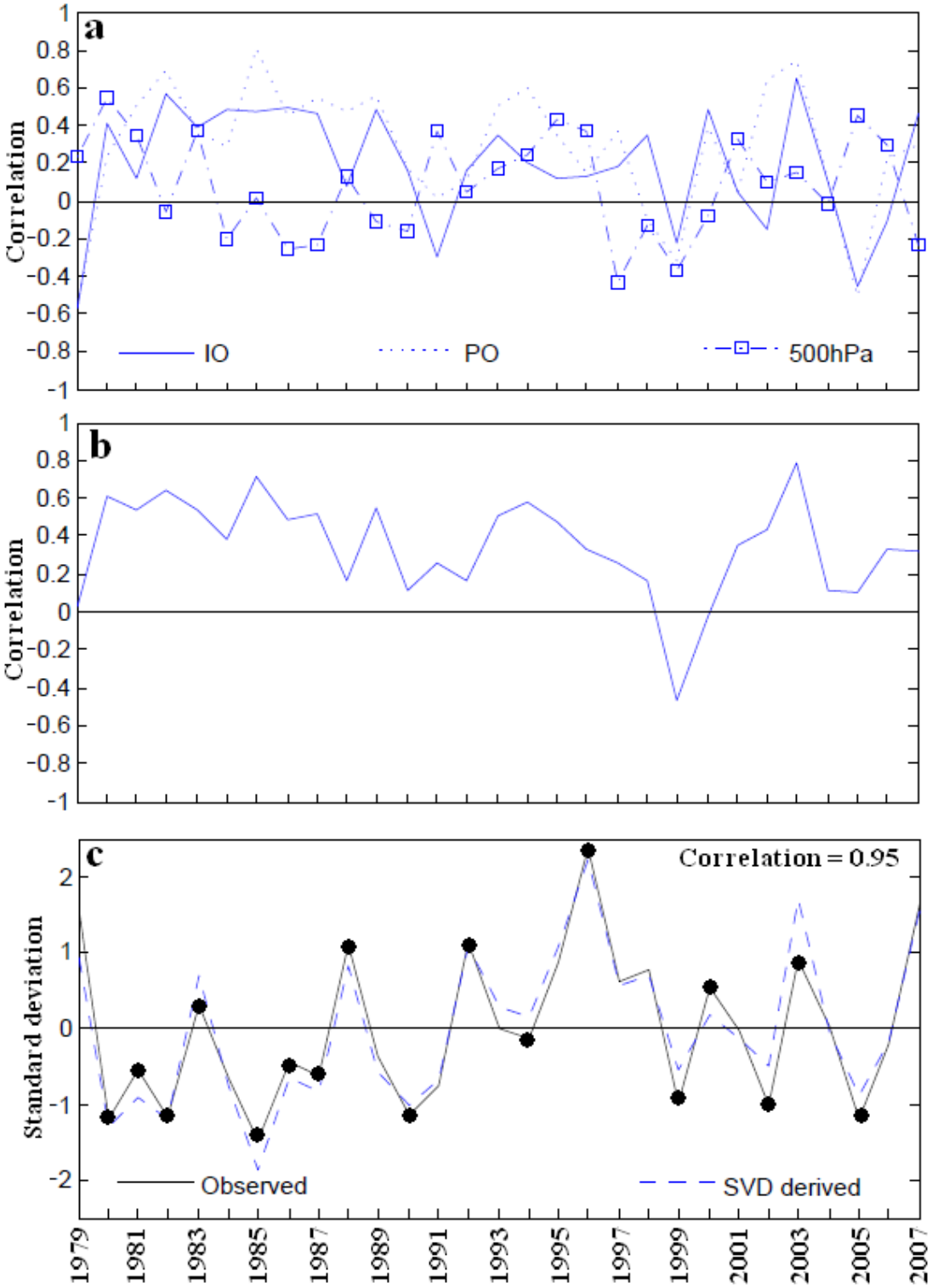

Figure 7.29: (a) Anomaly correlation patterns derived from the March-April-May (MAM) first SVD individual transition conditions (Indian Ocean (IO) SST, Pacific Ocean (PO) SST and 500 hPa height) presented in Figure 7.28 and the observed monsoon rainfall over the Maldives region, (b) cumulative anomaly pattern correlations derived from the three transition conditions combined for monsoon rainfall over the Maldives region, and (c) normalized Maldives monsoon rainfall index from observed data (Observed) and cumulative monsoon rainfall derived from SVD (SVD derived). The dots in (c) indicate TBO years identified in Figure 7.15.

After removing ENSO onset years identified in Figure 7.15, SVD analysis was carried out for the same transition conditions (Indian Ocean SST, eastern Pacific Ocean SST and 500 hPa height) in MAM with the Maldives monsoon rainfall (June-September) season, in order to check whether the ENSO years influence the SVD associations presented above (Meehl and Arblaster 2002b). Meehl and Arblaster (2002b) suggested that, similar processes are contributing in ENSO and non-ENSO years, if the results of the SVD patterns are similar between ENSO and non-ENSO years. The first SVD component spatial patterns for the three transition conditions and their corresponding first SVD components of precipitation shows a very similar pattern when ENSO years are include (Figure 7.28), compared with the first SVD components obtained for when ENSO years are removed (Figure 7.30). The pattern of correlations between different transition conditions and corresponding pattern correlations for monsoon rainfall with and without ENSO are depicted in Table 7.10. Significantly higher pattern correlations indicated that the transition conditions in MAM are highly related with the monsoon rainfall over the Maldives region with and without ENSO years, and similar processes are contributing to TBO in ENSO and non-ENSO years (Meehl and Arblaster 2002b).

Table 7.10: Pattern correlation for the transition conditions and for the corresponding monsoon rainfall with and without ENSO years.

Pattern correlation between:	Correlation
Indian Ocean SST with and without ENSO (Figure 7.28a and Figure 7.30a)	0.94
Corresponding precipitation with and without ENSO (Figure 7.28d and Figure 7.30d)	0.97
Pacific Ocean SST with and without ENSO (Figure 7.28b and Figure 7.30b)	0.86
Corresponding precipitation with and without ENSO (Figure 7.28e and Figure 7.30e)	0.98
500 hPa height with and without ENSO (Figure 7.28c and Figure 7.30c)	0.98
Corresponding precipitation with and without ENSO (Figure 7.28f and Figure 7.30f)	0.95

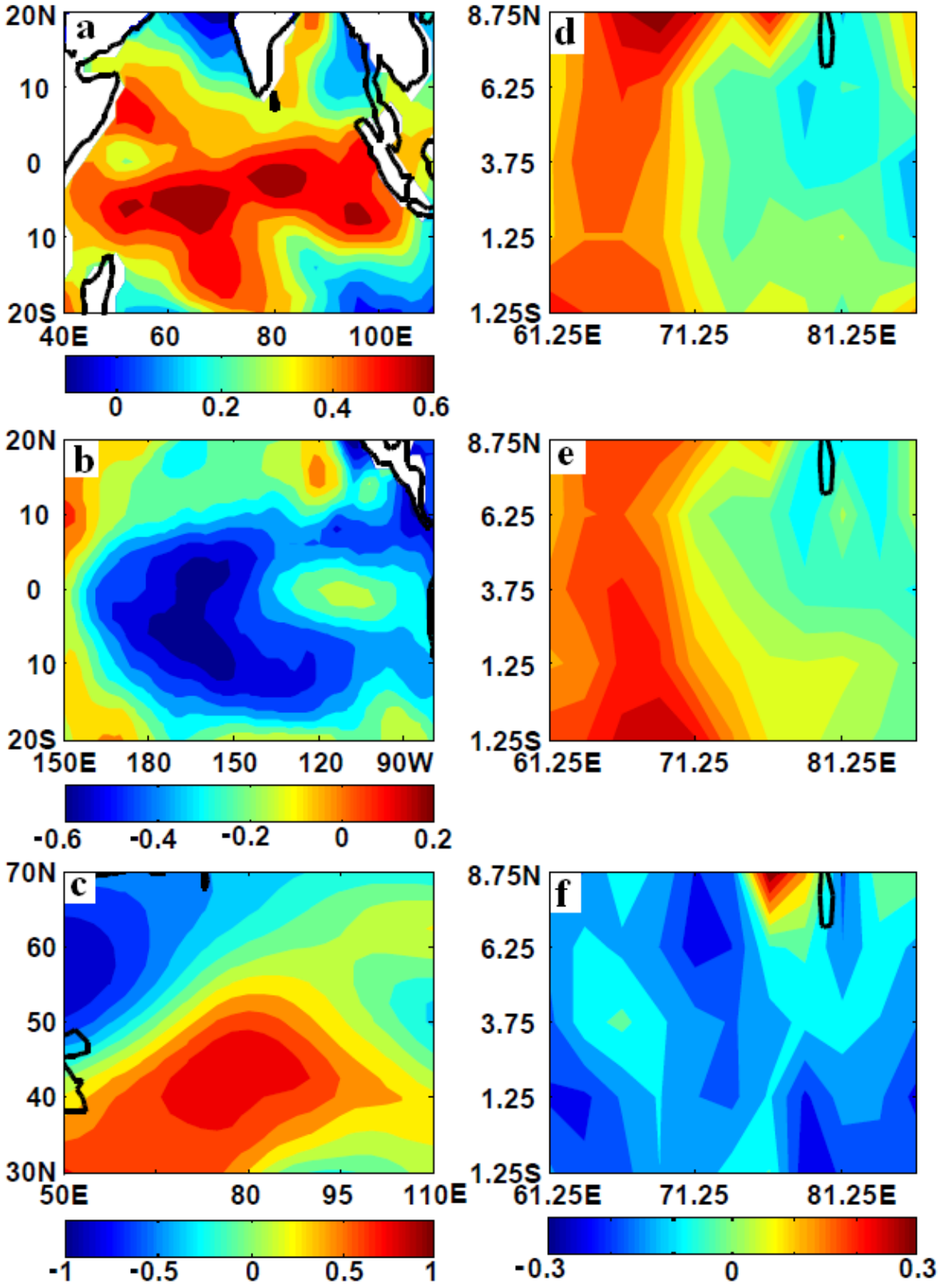

Figure 7.30: Same as in Figure 7.28 except that the ENSO years are removed.

7.4 Summary

The aim of this part of the chapter (Part B) was to examine role of the TBO in Maldives monsoon variability. Results indicate that there exists a biennial tendency in the Maldives monsoon rainfall to go through a transition from relatively strong/weak to relatively weak/strong monsoons in consecutive years in relation to the TBO. The results indicate that not all El Niño or La Niña onset years correspond to TBO years and the formation and propagation of seasonal SST, OLR and wind anomaly patterns for the strong minus weak ENSO TBO and normal TBO year composites demonstrates considerable differences, and the discrepancies between ENSO TBO and normal TBO year anomalies suggests that factors other than ENSO play a role in biennial variability in non-ENSO TBO years. Investigation of the local Hadley circulation indicates existence of biennial variability for both ENSO TBO and normal TBO year cases, with upward motion during a strong monsoon season and downward motion during previous and following monsoon seasons, suggesting that the local Hadley circulation influences the Maldives monsoon rainfall over a biennial time frame. The spatial correlations between filtered Maldives monsoon season rainfall and filtered SST anomalies for the TBO and ENSO time frames shows very similar spatial patterns to the TBO mode SSTA evolution, and the Maldives monsoon rainfall positively correlates with the SSTA in the Indian and eastern Pacific Ocean during the proceeding winter (DJF-1) and spring (MAM 0), while a weak negative correlation exists between SSTA in the western Pacific region at TBO time frames. However, with the onset of the monsoon, a significant negative correlation develops between Maldives monsoon season rainfall and SSTA in the central Pacific region for TBO time scale (JJA 0). The inverse relationship further strengthens for the season SON (0) and DJF+1. This leading (winter and spring) strong correlation between Maldives monsoon rainfall and SSTA in the IO for TBO suggests that the SSTA in the IO plays a significant role in strengthening the subsequent monsoon over the Maldives. Anomalously high moisture flux over the central IO region during the winter and spring seasons of the TBO time frame are also evident, further demonstrating build-up of moisture prior to the monsoon season for the TBO time frame. The local Hadley circulation on TBO and ENSO time scales for the reference monsoon season (JJA0) and following monsoon season (JJA+1) also indicates differences in local circulation between the two time scales. The ENSO scale weak monsoon season is dominated by ascending motion from 15º S-45º N, without the effect of the local circulation, indicating that the location of the Hadley circulation plays an important role in the TBO time scale variability of the Maldives

monsoon season rainfall. Singular value decomposition (SVD) analysis indicates that coupled interactions between transition conditions (500 hPa geopotential height, and equatorial Indian Ocean and eastern equatorial Pacific SST) in the season prior to the monsoon (the MAM season) can influence the Maldives monsoon rainfall. When the first SVD components of the MAM transition conditions were used to quantify the individual associations year by year to identify which years the MAM transition conditions are working independently and in which years they are connected, the results indicate that the Indian Ocean and Pacific SST transition conditions follow each other quite closely, but in some years the association between Maldives region monsoon rainfall and the transition conditions in the Indian Ocean and Pacific SST during MAM are large. The results also indicate that in many years the MAM regional 500 hPa height acts independently from the other two transition conditions demonstrating that in some years the three transition conditions act independently, while in some years they follow each other and can contribute to variation in the Maldives monsoon rainfall.

8 Impacts associated with monsoon rainfall variability

Floods and droughts can be regarded as the key extreme climatic events for the Maldives. These two extreme conditions have negative impacts on water resources (through prolonged dry periods together with sea level rise) and the agricultural sector (floods, drought and sea level rise) of the Maldives. According to UN-OHRLLS (2009b), impacts of climate change and its associated changes in precipitation have the potential to make the island nations, such as the Maldives, uninhabitable in the future due to drought events, since droughts would impact on the supplies of drinking water and food security.

The role of the ENSO and TBO in the Maldives monsoon rainfall variability was established in Chapters 6 and 7. Since ENSO has a dominant influence on monsoon variability (Annamalai et al. 2007), any changes in the magnitude or frequency of the ENSO cycle would impact on the Maldives monsoon season rainfall. Also, given the known strong biennial component of TBO on the Asian monsoon rainfall, the tropospheric biennial oscillation (TBO) may have a role to play in future monsoon variability (Turner et al. 2007b), and any changes in TBO would have an impact on Maldives monsoon season rainfall. The most direct impacts related to monsoon rainfall variability may be associated with the increase in frequency of extreme flood and drought events. The aim of this chapter is to explore the flood, drought events and water resource issues faced by the Maldives based on data obtained from a field survey carried out in the Maldives (described in Section 8.3) and other available local data.

8.1 Occurrence of flood and drought events

Internationally, flood and drought events are the most common and important natural disasters and are associated with hydrological extreme conditions (Sharma and Singh 2007). Climate change is expected to bring changes in average temperature and precipitation, and variability of precipitation events, resulting in more intense and frequent flood and drought events (Houghton et al. 2001; Kay et al. 2006). Climate models predict increases in both the frequency and intensity of heavy rainfall in the high latitudes of the Northern Hemisphere under enhanced greenhouse conditions (Jones and Reid 2001; McGuffie et al. 1999). More than two billion people across Asia (India, China and the rest of Southeast Asia) rely on the timing, duration and strength of the summer monsoon rainfall

for water resources and agricultural production, and any changes in rainfall patterns of the Asian monsoon will impact millions of people in Asia, through floods and drought events (Stern 2007; Turner et al. 2005). Stern (2007) argued that it is the changes in the timing and variability of rainfall, both within the wet season (intraseasonal) and between years (interannual) that are likely to cause most significant impacts on lives and livelihoods of the people in this region. Stern (2007) pointed out that even a 10% reduction in average rainfall associated with year-to-year fluctuations could lead to food and water shortages. According to Stern (2007), large uncertainty exists regarding changes in the variability of rainfall within the monsoon season (wet season), but these rains are crucial for the economy and livelihoods of this region. For example, during the month of July 2002 (core-monsoon season), India experienced below average rainfall, resulting in a seasonal rainfall deficit of 20%, which caused severe hardship for millions of people due to the reduction in agricultural production (Stern 2007). At the other extreme, Mumbai, India's financial capital, was devastated on 26 July 2005 when the city received a record-breaking 944 mm of rainfall within a 24 hour period and the city was flooded to a depth of 3 m (Figure 8.1). This event took 1000 lives and affected more than 20 million people (AAI 2005; UNESCO 2006). This indicates that more irregular or extreme monsoon conditions (drought/flood) could lead to water and food shortages, resulting in malnutrition during drought conditions or an increase in water-borne disease and damage to local infrastructure associated with flooding (Stern 2007; Turner et al. 2007a).

Figure 8.1: 26 July 2005 Mumbai flood event, which took 1000 lives and affected more than 20 million people. Top and bottom photos taken from UKIER (2007) and FDMG (2006), respectively.

Knowledge of floods and droughts and their frequencies and magnitudes are required to achieve effective management and mitigation measures to combat the impacts associated with flood and drought events. No proper mechanism exists for collecting or recording data on floods and especially for drought events in the Maldives, and hence data

on drought or prolonged dry periods are lacking. Furthermore, no criteria exist for the case of the Maldives for declaring flood or drought events and hence it is difficult to determine flood and drought intensity (severity) and trends for the Maldives. According to McGregor and Nieuwolt (1998), the Indian Meteorological service classifies drought events based on monsoon season rainfall (June-September) deficiency. In this classification a moderate and severe drought is declared when a rainfall deficiency of 26-50% and deficiencies in excess of 50% of normal rainfall occur, respectively, for in a particular region.

For the Maldives, an excess (wet) or flood year and a deficient (dry) or drought year is identified following Parthasarathy et al (1994). Here an excess (wet) or flood year has been defined when the Maldives monsoon season rainfall (MJJASON total rainfall) is $R_i \geq \overline{R} + S$ and a deficient (dry) or drought year is defined as when MJJASON total rainfall is $R_i \leq \overline{R} + S$, where R_i is the monsoon rainfall of the ith year, $\overline{R}$ is the mean and S is the standard deviation of the data series. The identified flood and drought years for the three regions of the Maldives are depicted in Figure 4.25. The figure indicates that the central region is most vulnerable to flood (5 years with excess rainfall), while the southern region is least vulnerable to both flood (2 years with excess rainfall) and drought (2 years with deficit rainfall) events (Figure 4.25 c). The northern and central regions show an equal number of years (3 years) with deficit rainfall, indicating that these two regions are equally prone to drought events.

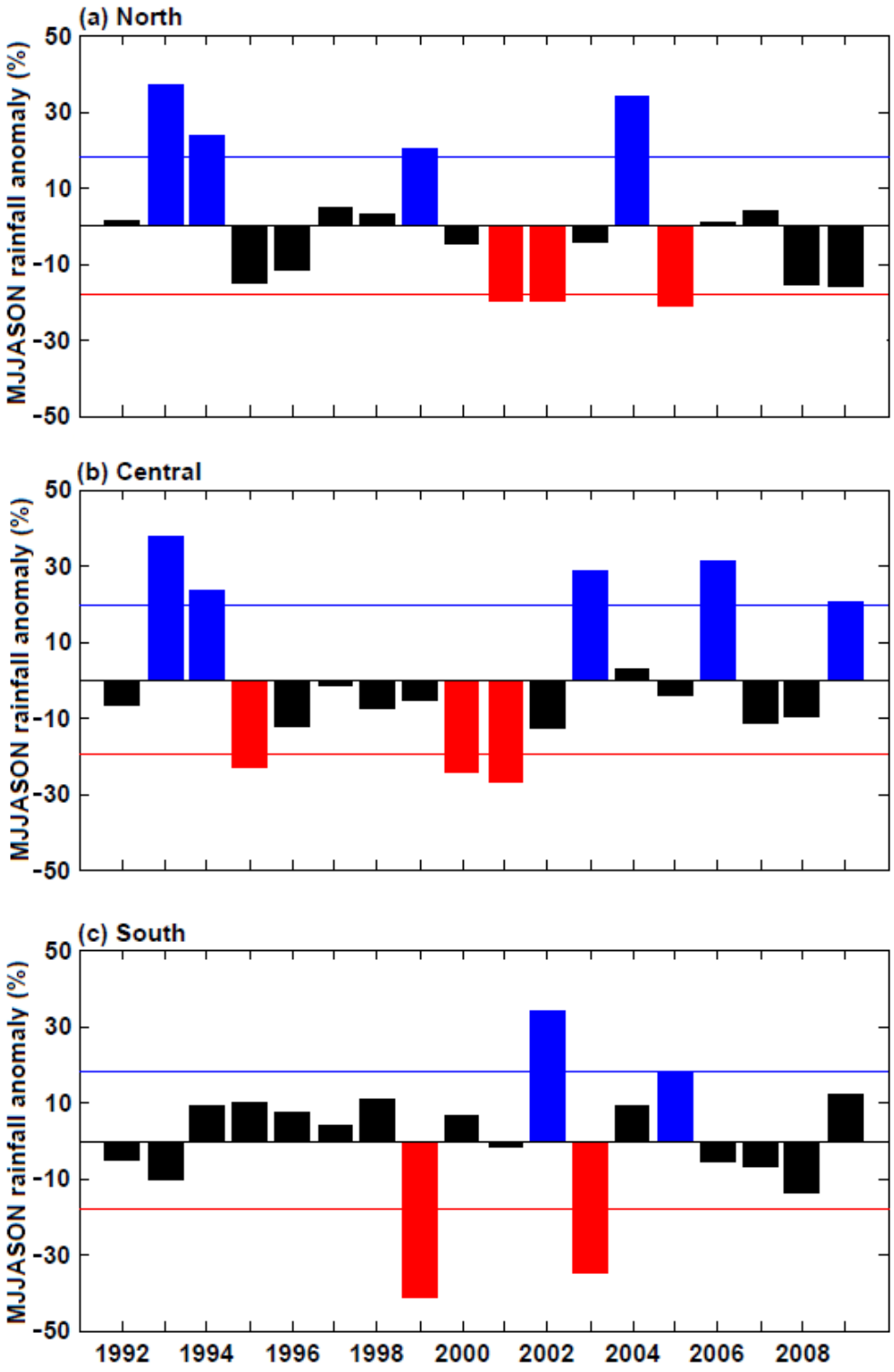

Figure 8.2: Flood and drought years for: (a) northern, (b) central and (c) southern Maldives based on Maldives monsoon rainfall (May-November: MJJASON) for the period 1992 to 2009. Blue and red lines indicate $\overline{R} + S$ and $\overline{R} - S$ (where $\overline{R}$ and S is mean and standard deviation, respectively), while blue and red bars indicate flood and drought years, respectively. Normal years are indicated by black bars.

The return period, sometimes referred to as the recurrence interval, is often used to determine how often an extreme event of a given magnitude occurs. It is a statistical estimate of how often an extreme event, such as a rainfall event, of a given magnitude and, for a given duration, is likely to be equalled or exceeded once (Hay 2006; McGregor and Nieuwolt 1998). For example, the hundred-year flood event is an event which will on average be equalled or exceeded once over a hundred year period. However, it should be noted that such an event might not occur every hundred years and there is a 1% chance that a 100 year event may occur in any given year (Hay 2006). Based on daily rainfall, occurrence of flood events (return periods) for the northern, central and southern regions of the Maldives was computed and is presented in Figure 8.3. Table 8.1 also depicts return periods for different categories of rainfall. Figure 8.3 and Table 8.1 also illustrate modelled return periods for years 2025, 2050, 2075 and 2100. Modelled return periods are based on observed daily rainfall from respective regions, and the United Kingdom Hadley Model and A1B emission scenario (a balance across all sources, where balanced is defined as not relying too heavily on one particular energy source, on the assumption that similar improvement rates apply to all energy supply and end-use technologies (IPCC 2007)) estimates. As can be seen from Figure 8.3 and Table 8.1, at present a daily rainfall of 150 mm for the northern region is a 300 year event, but by year 2050 and 2100, it is likely that 150 mm rainfall events will become quite frequent with a return period of 66 and 23 years (Figure 8.3a and Table 8.1), respectively. For the central region, currently a 190 mm rainfall event is about a 387 year event, but by 2050 and 2100 such events are likely to occur every 140 and 62 years, respectively. At present, daily rainfall of 210 mm is a very rare event, with a return period of about 437 years, for the case of the southern Maldives. By the year 2050 and 2100, an extreme daily rainfall event of 210 mm is likely to occur every 166 and 77 years on average, respectively (Table 8.1 and Figure 8.3c). Figure 8.4 and Table 8.2 depict return periods based on the same emission scenario but using three-hourly rainfall for the period 1990-2008 for the central Maldives only, since 3-hourly rainfall data is available for this region only. For this region, at present a three-hourly rainfall of 120 mm currently has return period of 460 years. However, three-hourly rainfall events of 120 mm are likely to become less than a 100 year event by 2050, and by 2100 such events are predicted to become quite frequent, with a return period of about 30 years (Figure 8.4 and Table 8.2).

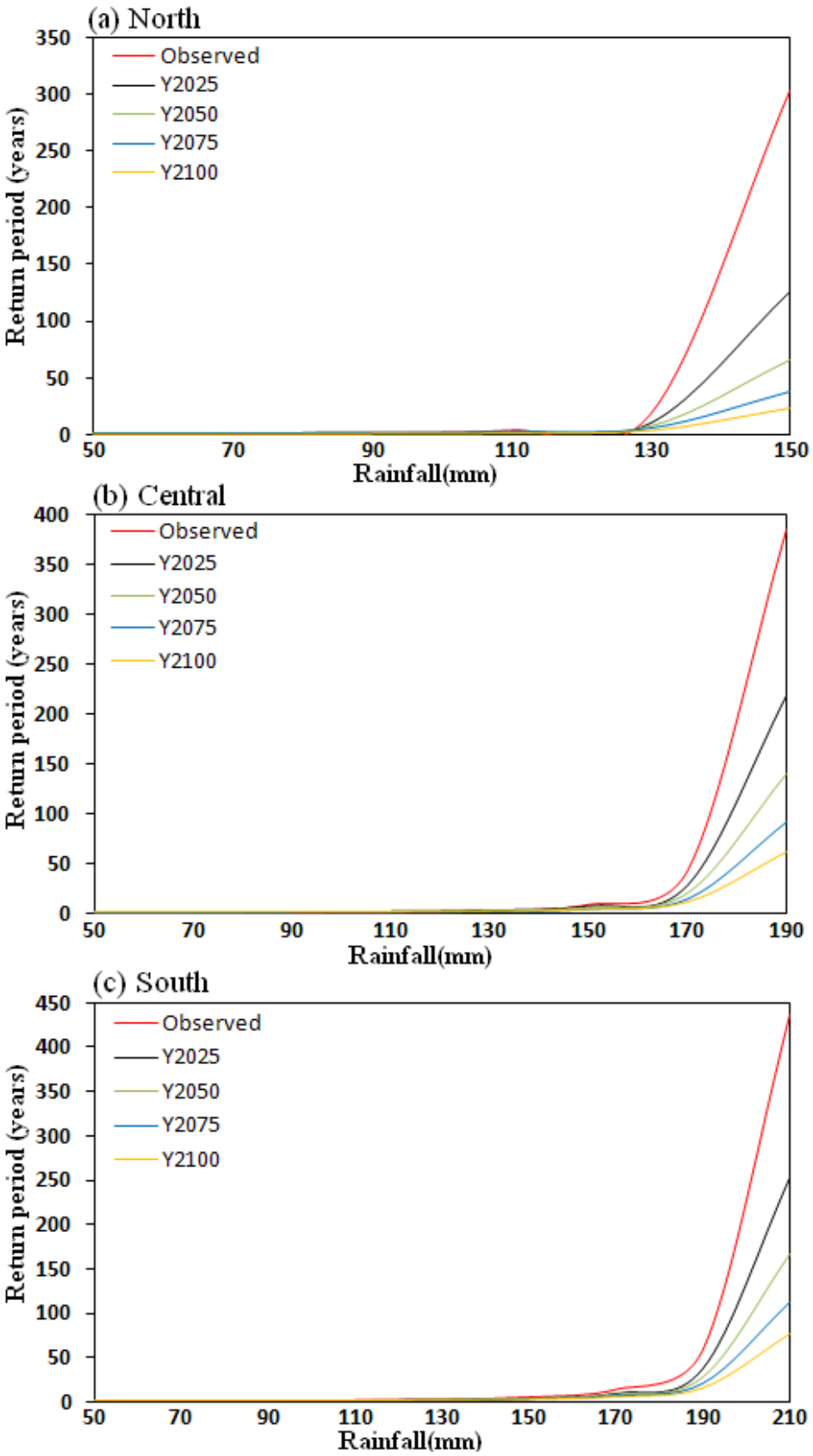

Figure 8.3: Observed and predicted (for years 2025, 2050, 2075 and 2100) return periods for: (a) northern, (b) central and (c) southern Maldives regions based on daily rainfall for the periods 1992-2009 (northern), 1975-2009 (central) and 1980-2009 (southern).

Table 8.1:Observed and predicated return periods computed for a range of rainfall categories, based on daily rainfall data from the northern, central and southern Maldives for the periods 1992-2009, 1975-2009 and 1980-2009, respectively.

Daily rainfall categories (mm): northern	Return period (Years): northern				
	Observed	Y2025	Y2050	Y2075	Y2100
50	1.0	1.0	1.0	1.0	1.0
70	1.2	1.1	1.1	1.1	1.0
90	1.6	1.4	1.3	1.2	1.2
110	3.7	2.7	2.3	1.9	1.7
130	17.9	10.4	7.2	5.2	4.0
150	303.5	125.8	66.2	37.6	23.0
Daily rainfall categories (mm): central	**Return period (Years): central**				
	Observed	**Y2025**	**Y2050**	**Y2075**	**Y2100**
50	1.0	1.0	1.0	1.0	1.0
70	1.1	1.1	1.1	1.0	1.0
90	1.3	1.2	1.2	1.2	1.1
110	1.9	1.7	1.5	1.4	1.3
130	3.5	2.9	2.5	2.2	2.0
150	9.6	7.0	5.6	4.5	3.8
170	43.8	28.2	20.1	14.8	11.2
190	386.5	219.4	140.1	91.8	62.0
Daily rainfall categories (mm): southern	**Return period (Years): southern**				
	Observed	**Y2025**	**Y2050**	**Y2075**	**Y2100**
50	1.0	1.0	1.0	1.0	1.0
70	1.1	1.1	1.0	1.0	1.0
90	1.2	1.2	1.1	1.1	1.1
110	1.6	1.4	1.4	1.3	1.2
130	2.4	2.1	1.9	1.7	1.6
150	4.8	3.8	3.3	2.8	2.5
170	13.4	9.7	7.7	6.2	5.1
190	58.2	37.9	27.3	20.3	15.4
210	436.8	253.7	166.0	111.6	77.2

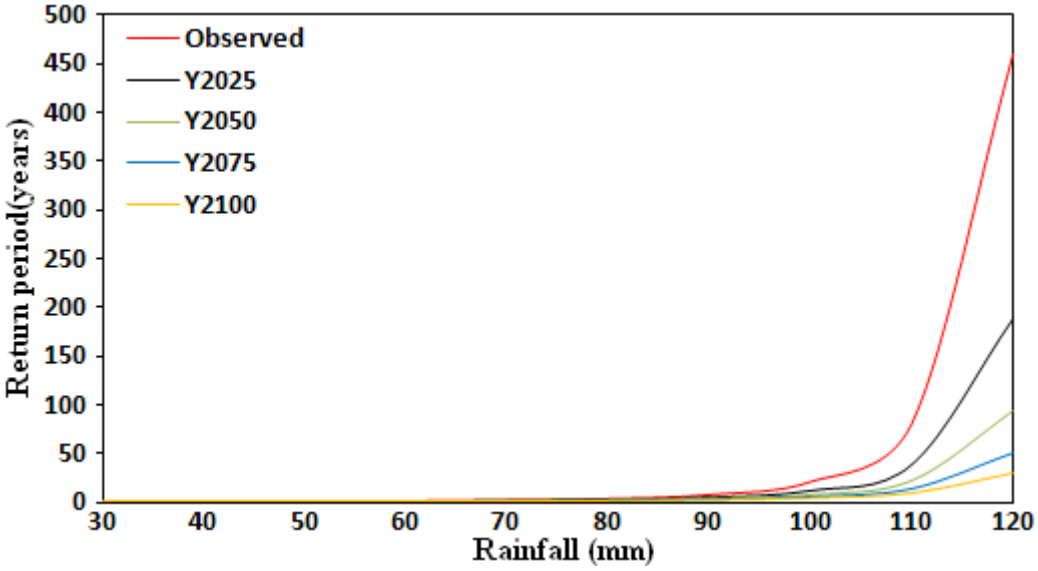

Figure 8.4: Observed and predicted (for years 2025, 2050, 2075 and 2100) return periods for central parts of the Maldives based on 3 hourly rainfall for the period 1990-2008.

Table 8.2: Observed and predicated return periods computed for a range of rainfall categories, based on 3 hourly rainfall data from the central Maldives for the period 1990-2008.

3 Hourly rainfall categories (mm)	Return period (Years)				
	Observed	Y2025	Y2050	Y2075	Y2100
30	1.0	1.0	1.0	1.0	1.0
40	1.1	1.1	1.0	1.0	1.0
50	1.2	1.1	1.1	1.1	1.0
60	1.5	1.3	1.2	1.2	1.1
70	2.2	1.8	1.5	1.4	1.3
80	3.7	2.7	2.2	1.8	1.6
90	7.7	4.9	3.6	2.8	2.3
100	21.1	11.7	7.7	5.4	4.0
110	80.9	38.5	22.3	13.8	9.1
120	460.3	187.7	94.2	50.5	29.0

Based on field observations and correlations with severe weather reports, UNDP (2007b) and UNDP (2007a) identified rainfall related flash flood events for different threshold levels for Sh. Funadhoo and L. Gan, respectively, as depicted in Table 8.3. It should be noted that threshold values used for identifying flood related impacts for Sh. Funadhoo differ from the threshold values used for identifying flood related impacts for L. Gan. This indicates that the flash flood impacts associated with particular rainfall threshold values can have different impacts on different islands. The flood impacts associated with a particular rainfall threshold may depend on geography (whether the island has low lying

and flood prone areas), shape, soil type and the depth of the water lens of that particular island.

Table 8.3: Flooding associated with different threshold levels of daily rainfall for Sh. Funadhoo and L. Gan, modified from UNDP (2007b) and UNDP (2007a), respectively.

Rainfall threshold levels (mm)	Possible impacts for Sh. Funadhoo
70	Puddles on road, flooding in low houses, occasional minor damage to household goods
110	Moderate flooding in low houses; minor damage to household items, damage to household crops, temporary (minor to moderate) disruptions to socio-economic functions for less than 24 hours
150	Widespread flooding on roads and low lying areas. Moderate damage to household goods, disruptions to socio-economic functions for more than 24 hours.
175+	Widespread flooding on roads, low areas and houses. Moderate damage to household goods, sewerage network, backyard crops, disruption to socio economic functions for more than 24 hours, gullies created along shoreline, possible damage to road and harbour infrastructure.
Rainfall threshold levels (mm)	**Possible impacts for L. Gan**
50	Puddles on road, flooding in low houses, occasional minor damage to household goods in most vulnerable locations, disruption to businesses and primary school in low areas.
100	Moderate flooding in low houses; all low lying roads flooded; moderate damage to household items especially in the backyard areas
150	Widespread flooding on roads and low lying houses. Moderate to major damage to household goods, school closure.
200	Widespread flooding on roads and houses. Major damages to household goods, sewerage network, backyard crops, school closure, gullies created along shoreline, possible damage to road infrastructure.
230+	Widespread flooding around the island. Major damages to household goods and housing structure, schools closed, businesses closed, damage to crops, damage to road infrastructure, sewerage network and quay wall.

Table 8.4 presents the frequency of occurrence of rainfall events for different threshold categories of daily rainfall. Over the last 18 year period, on average the islands of the Maldives experienced about 6-8 daily events of rainfall between 50-99 mm each year.

On the other hand, the northern region experienced rainfall events with a magnitude of 100-149 mm about once every two years, while the central and southern region experienced such events about once every year. When a daily rainfall threshold value greater than 50 mm is considered as the criterion for defining flood events, then the southern region is most vulnerable to flood events. The southern region had 166 rainfall events greater than 50 mm, while the northern region is least vulnerable to flood events, with only 123 rainfall events greater than 50 mm (Table 8.4). According to Shaig (2006), more than 90 islands of the Maldives (45% of all the inhabited islands) experienced flash flooding at least once during the last six years, and about 37 islands have experienced inundation regularly or at least once a year. Furthermore, about 71 inhabited islands were flooded in 2004 alone due to severe weather events (Shaig 2006). The frequencies of occurrence of rainfall events or flash flood events (Table 8.4) are consistent with the return periods presented in Table 8.1.

Table 8.4: Frequency of occurrence of rainfall events for the three regions of the Maldives for different daily rainfall threshold categories for the period 1992-2009.

Rainfall threshold category (mm)	**Northern**		**Central**		**Southern**	
	Frequency	**Average events per year**	**Frequency**	**Average events per year**	**Frequency**	**Average events per year**
50-99	113 (88%)	6.3	109 (59%)	6.1	147 (65%)	8.2
100-149	10 (80%)	0.6	13 (92%)	0.7	16 (56%)	0.9
150-199	None	None	3 (100%)	0.2	3 (67%)	0.2
>200	None	None	None	None	None	None
Total no. of events > 50 mm	**123**		**125**	**-**	**166**	**-**

Note: The values in brackets indicate the percentage of occurrence during the monsoon season (May-November).

The most direct impacts that are related to monsoon rainfall variability may be associated with the increase in frequency of extreme flood and drought events. According to Kundzewicz et al. (2007), droughts can impact rain-fed agriculture (decrease in

agricultural production), and domestic, industrial and agricultural water supplies. With the projected increase in sea level and higher frequency of extreme events, such incidents of flash flooding, are likely to be more frequent and severe (MEEW 2007).

8.2 Global and local sea level rise

Due to the likelihood of impacts on the human population living in coastal regions and on small islands, sea level rise or change is of considerable interest (Bindoff et al. 2007). According to Bindoff et al. (2007), there is empirical evidence that the global mean sea level has been rising over past decades and that there is high confidence that the rate of sea level rise has increased between the mid-19th and mid-20th centuries. The global average sea level rise for the period from 1961 to 2003 was 1.8 ± 0.5 mm/year, whereas for the 20th century, the average rate was 1.7 ± 0.5 mm/year (Bindoff et al. 2007). Figure 8.5 illustrates past and future global mean sea level. It is predicted that global sea level will reach 0.22 to 0.44 m by 2090s, when compared to 1990 levels. This equates to sea level rise of about 4 mm/year, but future sea level changes will not be spatially uniform. In some regions rate of rise will be higher than the global mean, while in other regions it is predicted that the sea level will fall (Bindoff et al. 2007). Vulnerability assessments associated with global sea level rise can highlight the overall significance of sea level rise for coastal societies and could facilitate comparison of regional sea level related risks (Sterr 2008). Furthermore, Nicholls and Cazenave (2010) pointed out that accurate estimates of future regional sea level rise are required in order to carry out coastal impact assessment and adaptation measures. Tekken et al. (2009) suggested that small-scale analysis of climate change impacts and sea level rise should be undertaken in a deductive way and individually to account for national or sub-national characteristics. The global mean sea level rise may be of little use to assess local or regional vulnerability associated with sea level rise. The use of regional or local sea level data is important to assess local or regional vulnerability.

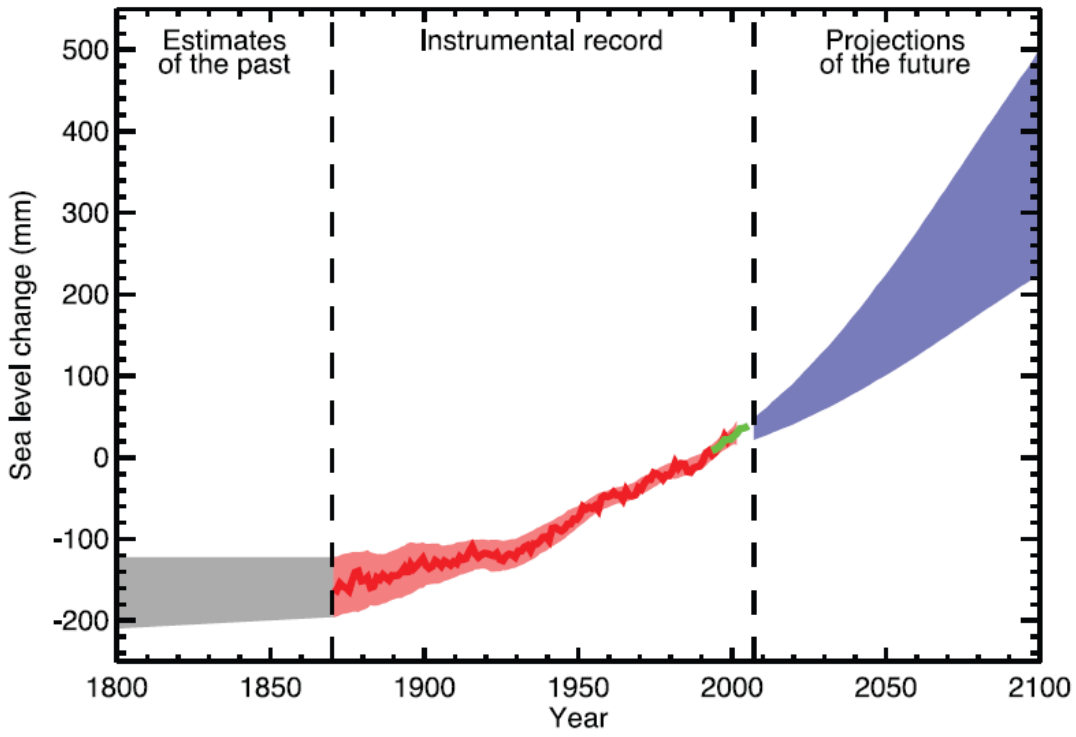

Figure 8.5: Global mean sea level (deviation from the 1980-1999 mean) in the past and as projected for the future. The grey shading shows the uncertainty in the estimated long-term rate of sea level change (for the period before 1870, global measurements of sea level are not available). The red line is a reconstruction of global mean sea level from tide gauges and the red shading denotes the range of variations from a smooth curve. The green line shows global mean sea level observed from satellite altimetry. The blue shading represents the range of model projections for the SRES A1B Scenario for the 21st century, relative to the 1980 to 1999 mean, which has been calculated independently from the observations. Beyond 2100, the projections are increasingly dependent on the emissions scenario. Taken from Bindoff et al. (2007), FAQ 5.1, Figure 1, page 409).

When sea level rise around Maldives area is considered, increasing trends of mean tidal level of about 4.1 mm/year and 3.9 mm/year for the central (for the period 1991-1999) and southern Maldives (for the period 1989-1999), respectively, have been found (Khan et al. 2002; UN-OHRLLS 2009a). Figure 8.6 shows daily and maximum hourly sea level changes for the central Maldives. Using daily sea level data, Hay (2006) found a long term trend in sea level of 1.7 mm/year for the central Maldives for the period 1989-2005. Furthermore, Hay (2006) also found a 7 mm/year increase in maximum hourly sea level and pointed out that this is far in excess of the observed local and global trends in mean sea level. According to Bindoff et al. (2007), between the mid-19th and mid-20th centuries an increase in the occurrence of extreme sea level worldwide related to storm surges is evident. Currently, an hourly sea level of 70 cm above current mean sea level is a 100 year event, but by 2025 an hourly sea level of 70 cm is likely to be at least an annual event for

the central Maldives. Such exceptionally high sea levels will cause flooding, accelerated coastal erosion and salt water intrusion into groundwater (Hay 2006).

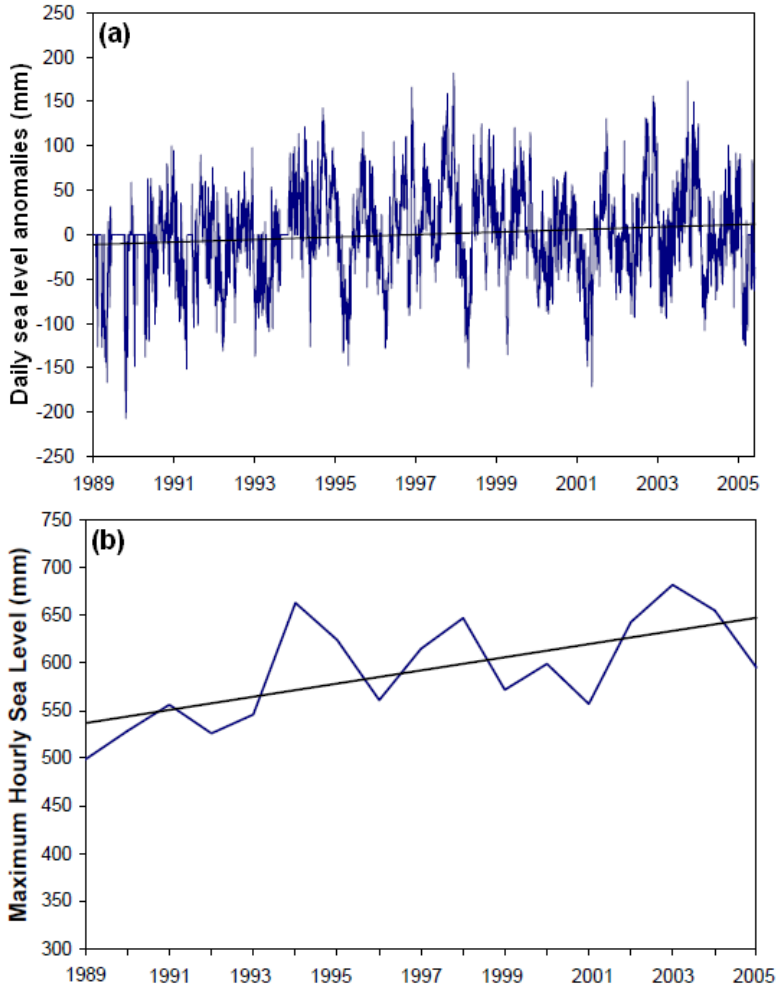

Figure 8.6: Sea level changes in the central Maldives (Hulhule) for the period 1989-2005 for: (a) daily sea level anomalies, and (b) maximum hourly sea level relative to the mean sea level. Modified from Hay (2006).

The floods and droughts combined with sea level rise will have negative impacts on water resources and the agricultural sector of the Maldives. As part of this research, a field survey (described below) was undertaken in the Maldives to examine these impacts.

8.3 Field survey

A field survey (structured questionnaire-interview) was conducted in the Maldives during March-May, 2009, to determine to what extent the water resources and agricultural sector depend on monsoon rainfall, and to determine how often these two sectors are currently impacted by floods and droughts (prolonged dry periods). An attempt has also been made to determine water resources impacts in the tourism sector of the Maldives.

Figure 8.7 summaries the components of the field survey and details are provided in the following sections.

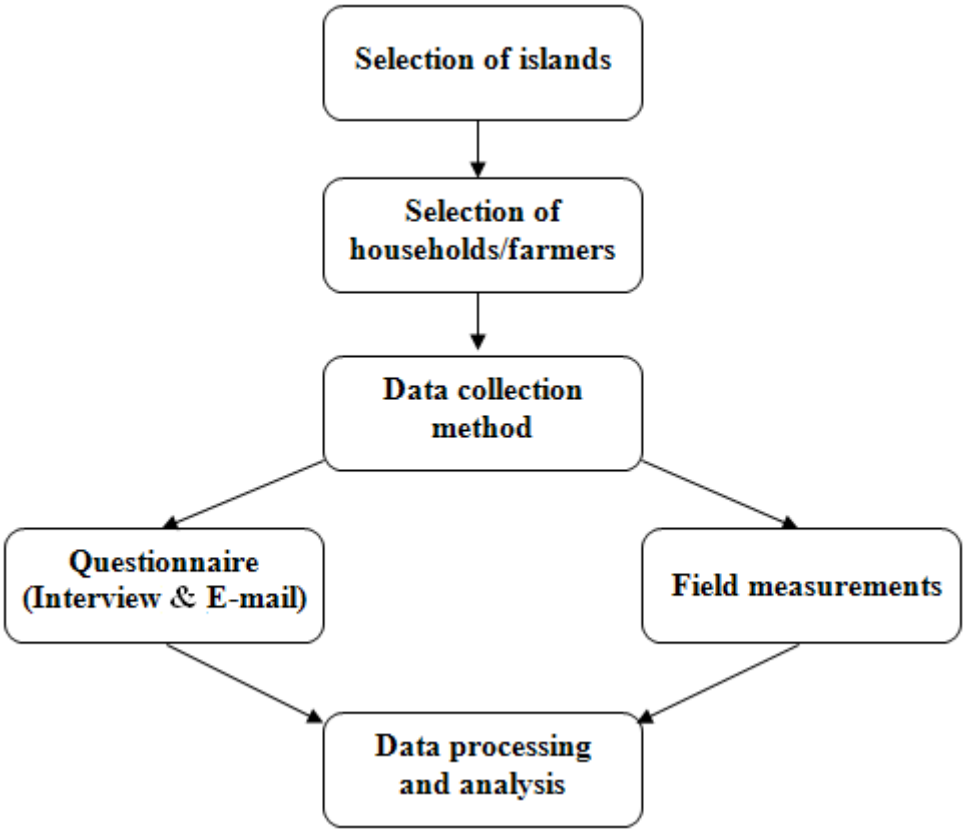

Figure 8.7: Field survey components used to determine to what extent different sectors depend on monsoon rainfall and its associated impacts.

8.3.1 Selection of islands

There were about 200 inhabited islands in the Maldives, scattered across 840 km. It would be too costly and time consuming to visit each of the 200 inhabited islands to undertake a field survey. The survey questionnaire aimed to collect information at island, household and farmer level. Since the analysis aims to compare results from different regions (to assess spatial variability across the Maldives), the Maldives was divided into three regions; northern, central and southern. The number of islands was narrowed down to inhabited islands where significant farming operations occur. The agricultural master plan of the Maldives (2006-2020) identifies 13 islands as the main agricultural islands (MFAMR 2006). Based on the agricultural master plan and discussions held with officials from the Ministry of Fisheries and Agriculture, four islands from the northern (Ha. Kelaa, Ha. Baarah, Hdh. Finey and Sh. Feevah), central (K. Kaashidhoo, Aa. Thoddoo, L. Gan and L. Hithadhoo) and southern (GDh. Vaadhoo, Gn. Fuvahmulah, S. Hithadhoo and S. Meedhoo) regions were selected as survey islands, and are shown in Figure 8.8.

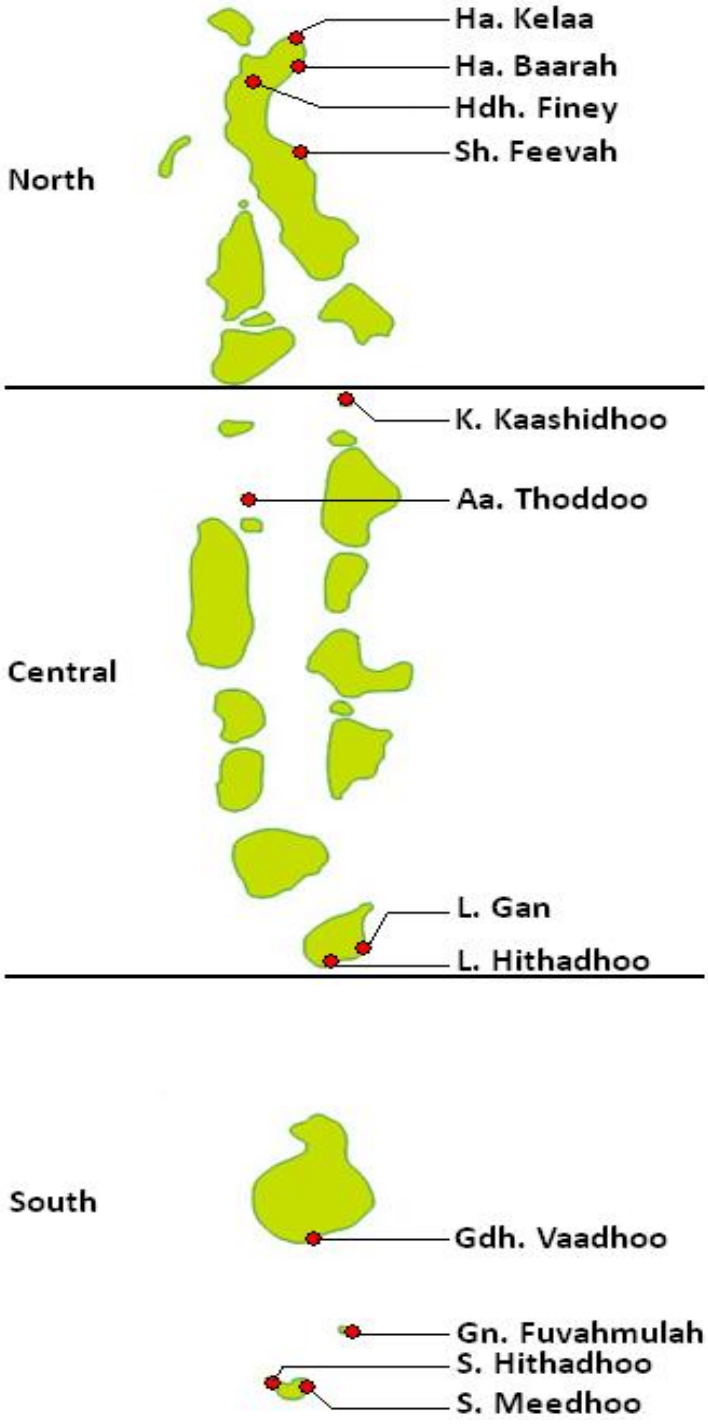

Figure 8.8: Inhabited main agricultural islands selected (indicated in red dots) for the field survey. Four islands were selected for each region (northern, central and southern). The green shaded areas indicate the atoll boundaries.

8.3.2 Selection of households (HHs)

The total number of households for each island was obtained from the 2006 census (DNP 2006). Total household (HH) numbers for each region were computed by summing

respective household numbers from the four islands in each region. Sample sizes for each region were calculated using a web-based sample size calculator (HRSA 2010) that is expressed as:

$$\boldsymbol{Sample\ size} = \boldsymbol{n}/[\mathbf{1} + (\boldsymbol{n}/\boldsymbol{Population})]$$

$$\boldsymbol{n} = \boldsymbol{Z} \times \boldsymbol{Z}[\boldsymbol{P}(\mathbf{1} - \boldsymbol{P})/\boldsymbol{D} \times \boldsymbol{D}]$$

where P = true proportion of factor in the population, or the expected frequency value, D = maximum difference between the sample mean and the population mean and Z = 1.96 (area under normal curve corresponding to the 95% confidence level). Based on the 95% confidence level and error level of 7.5% (how much error willing to tolerate), the calculated regional sample size and total HH is depicted in Table 8.5.

Table 8.5: Regional total household (HH) numbers from the 2006 census, recommended regional sample sizes computed based on 95% confidence level, and actual regional total household number used in the survey.

	North	Central	South
Total HH (regional)	710	1005	3275
Sample size (regional)	138	146	162
Actual HH interviewed	154	154	181
Total farmers interviewed	31	33	31

Based on the recommended regional sample size obtained using the above formulae, the actual household sample size for each island was calculated using the following expression:

$$\boldsymbol{Island\ HH\ sample\ size} = \frac{\boldsymbol{Island\ total\ HH}}{\boldsymbol{Regional\ total\ HH}} \times \boldsymbol{regional\ sample\ size}$$

The calculated household sample size for each island is illustrated in Table 8.6. When visiting each island, the HH list was obtained from the island office and a number was given to each HH. From the list, HHs were selected randomly. In the case where an adult cannot be found for the interview, new HH samples were selected randomly from the remaining HHs, for substitution for the missing HHs. In most of the cases, daily transfers

from one island to another are not available and the interviewer was forced to stay on some of the islands for longer. In such cases, more HHs were interviewed to provide a more representative sample population. Hence, the actual HHs interviewed were more than the sample sizes calculated for each region (Table 8.5).

Table 8.6: Island household (HH) number and sample sizes.

North			
Island Name	**HH no**	**HH sample size**	**No of farmers interviewed**
HA. Kelaa	262	51	5
HA. Baarah	241	47	16
HDh. Finey	74	14	3
Sh. Feevah	133	26	7
Total	**710**	**138**	**31**
Central			
K. Kaashidhoo	277	40	13
AA. Thoddoo	183	27	7
L. Gan	399	58	8
L. Hithadhoo	146	21	5
Total	**1005**	**146**	**33**
South			
GDh. Vaadhoo	147	7	7
Gn. Fuvammulah	1332	66	16
S. Hithadhoo	**1493**	**74**	**2**
S. Meedhoo	303	15	6
Total	**3275**	**162**	**31**

8.3.3 Selection of farmers

A list of farmers and number of farm sites is not available, since no such list exists. Island maps were obtained from each island and agricultural areas were identified. The islands office and local people indicated that it would be best to visit the farms to meet the farmers, and indicated that most of the farmers will be working at the farm sites in the evening. During the stay in each island, the farm areas were therefore visited in the evening to meet the farmers. The farmers were asked whether other farmers work in the area (who are not available on that particular day). If it is indicated that more farmers are in the area, the same farm area was visited the next day. Hence, the farmers selected for interview were mainly the farmers available at the farm sites when the interviewer visited the site. In most of the cases, the researcher was accompanied by a local resident during the farm visits and

if a farmer is known to the resident and was not in the farm, the farmers were contacted directly (via mobile phone) and were requested to come to the farm for the interview. The number of farmers interviewed from each region and island is depicted in Table 8.5 and Table 8.6, respectively.

8.3.4 Data collection method

Two main methods were employed for the collection of the primary data, namely field survey through structured questionnaire (mainly qualitative) and field measurement (quantitative). Secondary data were collected from official documents, websites, reports, review of the literature and personal communication.

8.3.4.1 The questionnaire

Four sets of questionnaires were prepared for the field survey (see Appendices 1-4). The field survey questionnaire had been approved by the Human Ethics Committee (see Appendix 5), University of Canterbury and permission to conduct the survey was also obtained from the Maldives Department of National Planning (see Appendix 6) prior to surveys and interviews commencing. The first questionnaire (Appendix 1) was targeted at the individual islands. The aim of this part of the survey was to gather information regarding water resources (drought or prolonged dry periods) and agricultural issues related to flood/drought or prolonged dry periods, and salinity problems at the island level. After arriving at each island, interviews were held with the island office officials (Figure 8.9, top photo) to get responses to the questionnaire and to obtain the household list and map. The second questionnaire (see Appendix 2) was targeted at individual houses to quantify the amount and type of water resources used for different household purposes, and also to obtain information regarding salinity problems, water shortage and flood events. Randomly selected houses were visited from 9 am to 4 pm, until all the selected households were interviewed. From each household, an adult was requested to provide responses for the questionnaire (Figure 8.9, bottom photo). The third questionnaire (see Appendix 3) was targeted at the farmers. The aim of this part of the survey was to determine to what extent the agricultural sector of the Maldives depends on monsoon rainfall and to quantify the amount of water usage by the farms. Furthermore, the survey aimed to gather information on salinity, drought and flood events faced by the agricultural sector. The farm sites were visited from 4 pm until sunset and all the farmers were interviewed at their farm sites. The electronic mail (e-mail) based questionnaire (fourth questionnaire: see Appendix 4) was

targeted at the tourism sector of the Maldives. This questionnaire aimed to determine the main water resources in the tourism sector and whether the tourism sector faces water resource problems. The questionnaire was e-mailed to the tourist resort islands, as an attachment.

Figure 8.9: Interviewing an official from the L. Gan island office (top) and household occupant (bottom) to obtain responses to the structured questionnaire.

8.3.4.2 Quantitative measurements

Some components of the questionnaire required quantitative measurements. During the interview process an attempt was been made to estimate the following parameters and this will be discussed in more detail under the following headings:

1. Salinity measurement
2. Groundwater depth

3. Effective roof area
4. Water flow rate (household tap, showerhead and hose)
5. Water consumption by households (for different uses)
6. Water consumption by farm sites

In addition to the data collected from field surveys, other data such as precipitation data (the station precipitation data set used in previous analysis was updated from 2007-2009 by obtaining data from the meteorological service of the Maldives) and other information was sourced from government technical reports, textbooks, journals, the internet and through personal communications.

8.3.4.3 Validity of the data

During the fieldwork, every effort was made to ensure that the data collected during the interview process and measurements were accurate and valid. It has been argued that the positionality of the researcher may influence the data collection and interpretation, and finally the information that is coded as "knowledge" (Madge 1993; Rose 1997). In the research context, the positionality refers to the social location of the researcher (the awareness of the researcher to his/her own background) and how the respondents (or the people being interviewed) may perceive the researcher and, may influence how the participants interact or respond to the researcher, hence affecting the interpretation and findings of the study (O'Connor 2004; Rijal 2009; Sultana 2007).

Since the fieldwork that I carried out was a vital part of this research, careful consideration was given to minimising the positionality issue (how the interviewees or respondents perceived me and how this may have influenced their responses to the questions that I presented during the interviews). The reflexivity or process of thinking through the power relations between the researcher and the researched recommended by Rose (Rose 1997) was adhered in this research to minimise potential biases due to previously developed relations with the respondents (Rijal 2009). According to O'Connor (2004), for an apparent positionality, the researcher needs to engage in critical reflexivity throughout the project. This involves reflection of self, process and representation, and critical examination of power relations and politics in the research process, as well as researcher accountability in data collection and interpretation (Falconer et al. 2002; Jones et al. 1997; Sultana 2007). Furthermore, Sultana (2007) pointed out the importance of reflexivity from the beginning until the end of the research, and suggested by considering

the reflexivity at the end of research process is a mere introspection which can leave positivist methodologies intact.

Knowledge I have acquired from previous fieldworks (in preparing environmental impact assessment reports for various agencies) and discussions held with Maldivian colleagues (Ali Shareef and Mizna Mohamed, aslo in the Geography Department) greatly helped me to design the research questions in local context and to reflect on the positionality in designing my fieldwork. As a result of exposure to some of these communities long before conducting the field survey, I had introduced some aspects of myself to these communities, and my understanding of the local people greatly helped in carrying out the surveys without much difficulty. Furthermore, the common grounds (common culture, religion and language) shared by the researcher and interviewees helped participants to interact with me and share their opinions freely (Ahmed et al. 2010; Gibson and Abrams 2003). The participants were by and large willing to participate in the survey and welcomed me to their homes to conduct the survey and expressed their gratitude towards me for carrying out 'useful' research. Being a native researcher (insider) allowed me to understand and gain insights into interviewees' perspectives and the respondents literal and body language that an outside researcher may not have had (Ahmed et al. 2010; Gilgun and Abrams 2002; Labaree 2002). Previous experience, accountability and ability to put all the data (information) collected into a research perspective, together with the critical interpretation of the information gathered, facilitated the minimising of potential biases due to positionality and hence to improve the quality of data.

8.3.4.4 Data cross-checking

Information collected during the interview process (during day time) were checked (each night) for any obvious errors, and were corrected next day by re-visiting the respondent where necessary. An attempt was also made to cross-check the estimates of water consumption by households and farm sites with another method. A household water use log sheet (see Appendix 2) was given to the respondents (or another person from the household) who agreed to record the water usage for the household. The number of log sheets given and received (from each island a person was arranged to collect the log sheets after 5 days and if water consumption was not recorded, additional days were given to allow completion of the form) from the islands and for the regions are presented in Table 8.7. Similar log sheets were prepared for the agricultural and tourism sector (see Appendices 3 and 4, respectively). None of the farmers agreed to record their farm water

usage. Most of the household water use log sheets received were incomplete and the number of log sheets was far too few (none from some islands) to draw any meaningful conclusion, and hence they were omitted from the analysis.

Table 8.7: Number of "household water use log sheets" given and number of returned log sheets by island and region.

North		
Island Name	**No. of log sheets given**	**No. of log sheets returned**
HA. Kelaa	30	7
HA. Baarah	25	none
HDh. Finey	13	7
Sh. Feevah	14	none
Total	**82**	**14**
Central		
K. Kaashidhoo	6	4
AA. Thoddoo	5	5
L. Gan	36	5
L. Hithadhoo	4	none
Total	**51**	**14**
South		
GDh. Vaadhoo	8	none
Gn. Fuvammulah	45	14
S. Hithadhoo	71	15
S. Meedhoo	19	11
Total	**143**	**40**

8.3.5 Data processing and analysis

Although the questionnaires were in English, the interviews (with island office officials, households and farmers) were conducted (presented) in the local language (Dhivehi). The responses to the questionnaire from the island offices were recorded on the soft-copy of the questionnaire (Microsoft Excel sheet on the laptop) and the responses to the questionnaire from the households and the farmers were recorded on the printed questionnaire. These data were transferred later to Excel sheets for analysis. The processed data were analysed with the use of percentages and mass curve analysis.

8.4 Maldives water resources sector

The economic and social development of the small state nations, such as the Maldives, depends on water resources. The availability of water resources is a limiting

factor for development, since most of the small states depend almost entirely on a single water resource, such as groundwater, rainwater, surface reservoirs or imported water (McCarthy et al. 2001). In the capital island of Maldives (Male'), heavy abstraction (due to high population density) of groundwater as the main source of potable (drinking) and non-potable uses, coupled with poor sanitation facilities (more sewerage being disposed off into the ground) has depleted the freshwater lenses of Male' (Ibrahim 2008). Furthermore, salinity of the aquifer increased sharply due to the increased volume of groundwater used to flush toilets being discharged to the sea, hence limiting the groundwater as a reliable source of water. Due to the small roof catchment areas together with the limited available space for rainwater storage in Male', one of the few options available for providing reliable safe water for Male' was desalinated water (Ibrahim 2008). Due to high contamination of groundwater in Male', domestic water demand (for drinking as well as for other domestic purposes such as dishwashing, cooking, clothes washing and showering) for 96% of the population in Male' is now met by desalinated water distributed via piped network (Ibrahim 2008). Unlike the capital island (Male'), the outer islands of the Maldives strongly depend on groundwater for non-potable use, and rainfall as a source of water for potable use (cooking and drinking). It can be seen from Table 8.8, that 100% of the non-potable and potable water demand is met by groundwater and rainwater, respectively. However, it should be noted that 4, 1 and 12% of households in the northern, central and southern regions, respectively, indicated use of bottled water for children and 6, 3 and 24% of the households from the northern, central and southern regions, respectively, indicated use of bottled water for at least one person due to health related issues (Table 8.8). It is also worth noting that during shortage of rainwater households use groundwater, desalinated water, and bottled water for cooking and drinking. This will be discussed in more detail in relevant places.

Table 8.8: Groundwater and rainwater usage (percentage) for household purposes for the three regions of the Maldives during normal conditions based on field survey data. Percentage usage of bottled water is also presented for the three regions.

Type/purpose of water used	Northern (%)	Central (%)	Southern (%)
Groundwater (for dishwashing, clothes washing, hand washing, hygiene, shower and toilet flushing)	100	100	100
Rainwater (for drinking)	100	100	100
Bottled water (for children)	4	1	12
Bottled water (due to health related issues)	6	3	24

8.4.1 Water use by households

The household water requirements (especially non-potable use) of the outer islands in the Maldives were met by rainwater (harvested from roof catchment) and groundwater extracted from wells dug within household compounds. Table 8.9 indicates that each household surveyed is equipped with at least one well. In general, groundwater is extracted from the wells in two ways, manually using containers connected to a long stick (locally knows as *dhaani*) and electrical pumps (Figure 8.10). The percentage use of manual and electrical pumps for extracting groundwater in the households by regions is presented in Table 8.9, together with the groundwater depth (the method used for groundwater depth calculation is provided below). The extracted groundwater is commonly used for non-potable use, such as dishwashing, clothes washing, hygiene (tooth brushing, hand washing, ablution, post-defecation), showering and toilet flushing. Some households also use groundwater for watering plants (backyard farming or gardening). The daily total quantities of household water usage (consumption) for these purposes are estimated below.

Figure 8.10: Containers connected to a long stick (locally knows as *dhaani*) and electrical pumps (bottom photo) are commonly used for extracting groundwater from wells. Bottom photo taken from MWSA (2005).

Table 8.9: Statistics of household dug wells and groundwater extraction methods in the three regions.

Parameters		Northern	Central	Southern
No. of wells/HH	Minimum	1	1	1
	Average	1.4	1.5	1.7
	Maximum	3	3	4
Average depth (m)	Minimum	0.5	0.8	0.1
	Average	1.1	1.2	1.1
	Maximum	1.5	1.7	2.5
Method of extraction (%)	Pump	66	88	54
	Manual	86	64	66
	Both	52	51	20

***Southern: 17% also said sometimes they use neighbours wells**

Groundwater depth (m): Measurements were taken from household wells to calculate groundwater depth (GWD: from surface to groundwater level). First the depth from the groundwater level to the top of the well (H_1) was measured and then from the ground surface to the top of the well (H_2) (Figure 8.11, top) was measured using a measuring tape. The GWD is calculated as:

$$\boldsymbol{GWD = H_1 - H_2}$$

In many farm sites, the well height is ground surface level (Figure 8.11, bottom). In such cases, the GWD is given by:

$$\boldsymbol{GWD = H}$$

where H is the height from the groundwater level to the ground surface.

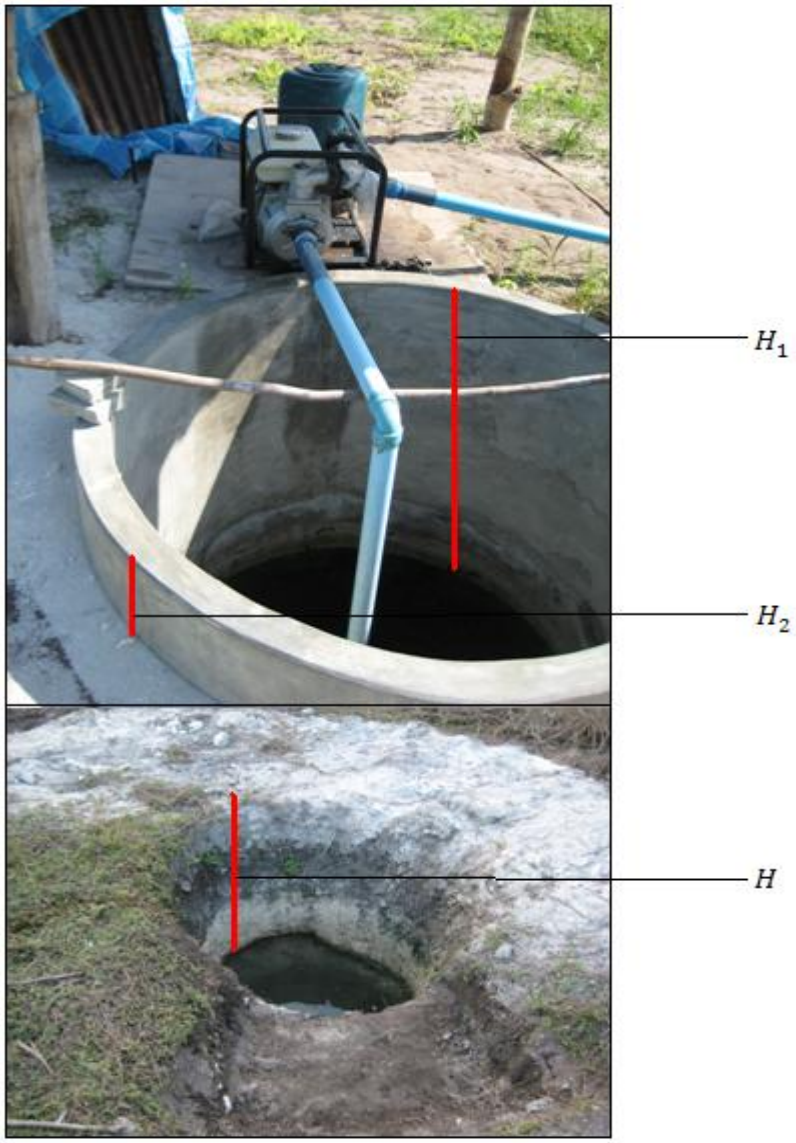

Figure 8.11: Groundwater depth is the difference between the depth from the groundwater level to the top of the well (H_1), where it exists, and from the ground surface to the top of the well (H_2).

8.4.1.1 Estimation of quantity of water usage by household occupants

There is little existing information relevant to the islands of the Maldives with regard to the average quantity of water usage by household occupants for different purposes. Available estimates are presented in Table 8.10. The estimates available differ considerably and Falkland (2001b) indicated that some of the estimates appear to be questionable. Based on this review and due to the difference between the estimates, during the field survey, information was gathered to quantify the water usage by household occupants.

Table 8.10: Available estimates of water consumption (litre per capita per day: lpcpd) for the islands of the Maldives.

Purpose	Amount (lpcpd)		
Clothes washing	4	35	
Dishwashing	6	-	
Bathing & hygiene and toilet flushing	60 (if PT*) or 90 (if CT*)	113	
Drinking & cooking	10	14	
Others	-	13	
Total	80 (if PT)	175	59 (if PT)
	110 (if CT)		80 (if CT)
Source	(Falkland 2001b)	(Beswick 2000)	(West and Arnell 1976)

***PT = pour flush toilet and *CT = cistern flush toilet**

In order to estimate the quantity of water usage by household occupants for different purposes, first water flow rates from household taps and showerheads were estimated (described below), since more than 50% of the households from each region use electrical pumps for extracting groundwater from household dug wells (Table 8.9). The estimated regional average water flow rate (representing at least 12 readings taken from each region) presented in Table 8.11 were used (when applicable) for calculating some of the components described below.

Water flow rate (household tap and showerhead): In cities in developed country, household water use has been measured using a flow meter fixed to each tap in the sampled households (Sivakumaran and Aramaki 2010). None of the houses visited during the field survey had water meters installed at the property and no data were available for the capacity or flow rate of the pumps (Falkland 2001b) or taps/showerheads. Falkland (2001b) indicated that it would be useful to collect flow rate data in future surveys. From each island visited during the survey, household water flow rates from the tap and showerheads were estimated for at least 3 houses. The flow rates were estimated by measuring the time taken to fill a container of known volume (bucket or bottle) by opening the tap/showerhead at normal flow rate (PDHO 2010). This simple method of estimating water flow rate has also been suggested by Falkland (2001b). The water flow rate for both the taps and showerheads were determined using the following equations, respectively:

$$\boldsymbol{W_{FRT}} = \frac{\boldsymbol{V_c}}{\boldsymbol{T_t}}$$

$$\boldsymbol{W_{FRS}} = \frac{\boldsymbol{V_c}}{\boldsymbol{T_t}}$$

where W_{FRT} and W_{FRS} represent tap and showerhead water flow rates (litre/min), V_c is volume (litres) of the container and T_t is the time taken (minutes) to fill the container. Another way of estimating water flow rate is to find the amount of water collected from the tap or showerheads in a given time (for example in one minute time period). These two methods were used in estimating the water flow rate from households, depending on the type and size of the container most readily available. In addition to this, water flow rate for a hose was estimated using the same method as for the tap/showerhead and is given by:

$$\boldsymbol{W_{FRH}} = \frac{\boldsymbol{V_c}}{\boldsymbol{T_t}}$$

where W_{FRH} is hose water flow rate (litre/min), and V_c and T_t are defined above. However, it should be noted that the use of hoses is not common (even when pumps are used for extraction of water, plants are watered by filling a watering jug or bucket: Figure 8.12) for watering the plants, and hence in some islands it was not possible to take three readings from the hoses. Estimated water flow rates (minimum, average and maximum) for household taps, showerheads and hoses are depicted in Table 8.11. Water flow rates for the

Maldives (for any islands) could not be found from any available reports. Hence, for comparison, water flow rates obtained from the literature for other countries are illustrated in Table 8.12. The water flow rates estimated here appear to be lower for showers and higher for taps, than the flow rates for the other countries. The difference in flow rates could be due to the difference in water pressure. The water flow rates presented in Table 8.12 were based on mains water supply, while the water flow rates depicted in Table 8.11 were based on individual household electrical pumps (Figure 8.10, bottom photo). For the case of electrical pumps, the taps or showers need to be released to some extent before water can be pumped to the tap, and if another tap/shower is used at the same time the pressure of the water would fall. Hence, the flow rates estimated here appear to be reasonable for the Maldives conditions.

Figure 8.12: Watering jug is being filled by water using a container (dhaani). 10 litre watering jugs are commonly used for watering plants.

Table 8.11: Water flow rate (L/min) from household showerheads, taps and hose for the three regions.

Parameters		Northern	Central	Southern
Showerhead (L/min)	Minimum	6.50	6.00	5.75
	Average	**7.56**	**7.67**	**7.88**
	Maximum	9.00	10.00	10.00
Tap (L/min)	Minimum	4.00	4.00	4.25
	Average	**5.31**	**5.15**	**5.44**
	Maximum	6.25	6.50	6.75
Hose (L/min)	Minimum	6.75	6.25	6.75
	Average	**8.13**	**8.25**	**8.29**
	Maximum	9.50	10.00	9.50

Table 8.12: Water flow rates (L/min) obtained from the available literature (for Australia, New Zealand and Thailand).

Showerhead (L/min)	Tap (L/min)	Country	Source
11.8	3.79	New Zealand (Kapiti Coast)	(Heinrich 2007)
7.6 (efficient showerhead) 10.5 (normal showerhead)	3.3	Australia (Queensland)	(Stewart et al. 2005)
8.5	4.5	USA (Seattle)	(Mayer et al. 2000)

Cooking and drinking: Information on the volume of water (quantity) used for cooking and drinking was not readily available. During the interview process, discussions were held with respondents, together with the head female of the household and other

family members (whenever possible) regarding household water usage for cooking (food preparation) and drinking.

It was evident from the observations and discussions that household cooking was normally done together for the entire family (common cooking arrangements). Quite often, the water used for cooking (food preparation) was collected from the rainwater tank using containers such as a bucket (Figure 8.13, top) or jars. Questions were asked regarding the size (in litres) of the container the household normally uses for collecting water and number of containers used daily. If the volume of the container was not known, the size of the container was measured by filling the container with water using a known sized container, such as a jar or bottle. The daily total household water consumption for cooking was estimated as:

$$\boldsymbol{C_{dc} = N_c \times S_c}$$

where C_{dc} is the daily water consumption for cooking (in litres), N_c is the no of containers used (per day) and S_c is the size of the container (in litres). If the same water collected in the containers was used for both cooking and drinking, the above equation represents daily total household water consumption for both cooking and drinking. If the drinking water is different from the above, then consumption of water for drinking was estimated as below.

From the observations and discussions held with household occupants, it was clear that most of the time bottles were filled from the rainwater tank or container (Figure 8.13, bottom left) and put in the fridge for cooling and later used for drinking. In such cases, respondents were asked about the size of the bottles (litres) and the number of bottles used daily. In this case, the daily total household water usage for drinking was estimated as follows:

$$\boldsymbol{D_{wc} = N_b \times S_b}$$

where D_{wc} is the daily water consumption for drinking (in litres), N_b is the no of bottles used (per day) and S_b is the size of the bottle (in litres). In some cases, a glass is filled directly from the tap (rainwater tank: Figure 8.13, bottom right) and consumed. If that is the case, the respondents (and other family members) were asked how many glasses of water were consumed each day on average, and the average number of glasses per capita per day (pcpd) was recorded together with the average size of the glass used for drinking water.

Hence, total daily household water consumption for drinking was estimated using the equation below:

$$\boldsymbol{D_{wc} = N_o \times N_g \times S_g}$$

where D_{wc} is defined above, N_o is the number of occupants, N_g is the no of glasses (per day) and S_g is the size of the glass (in litres).

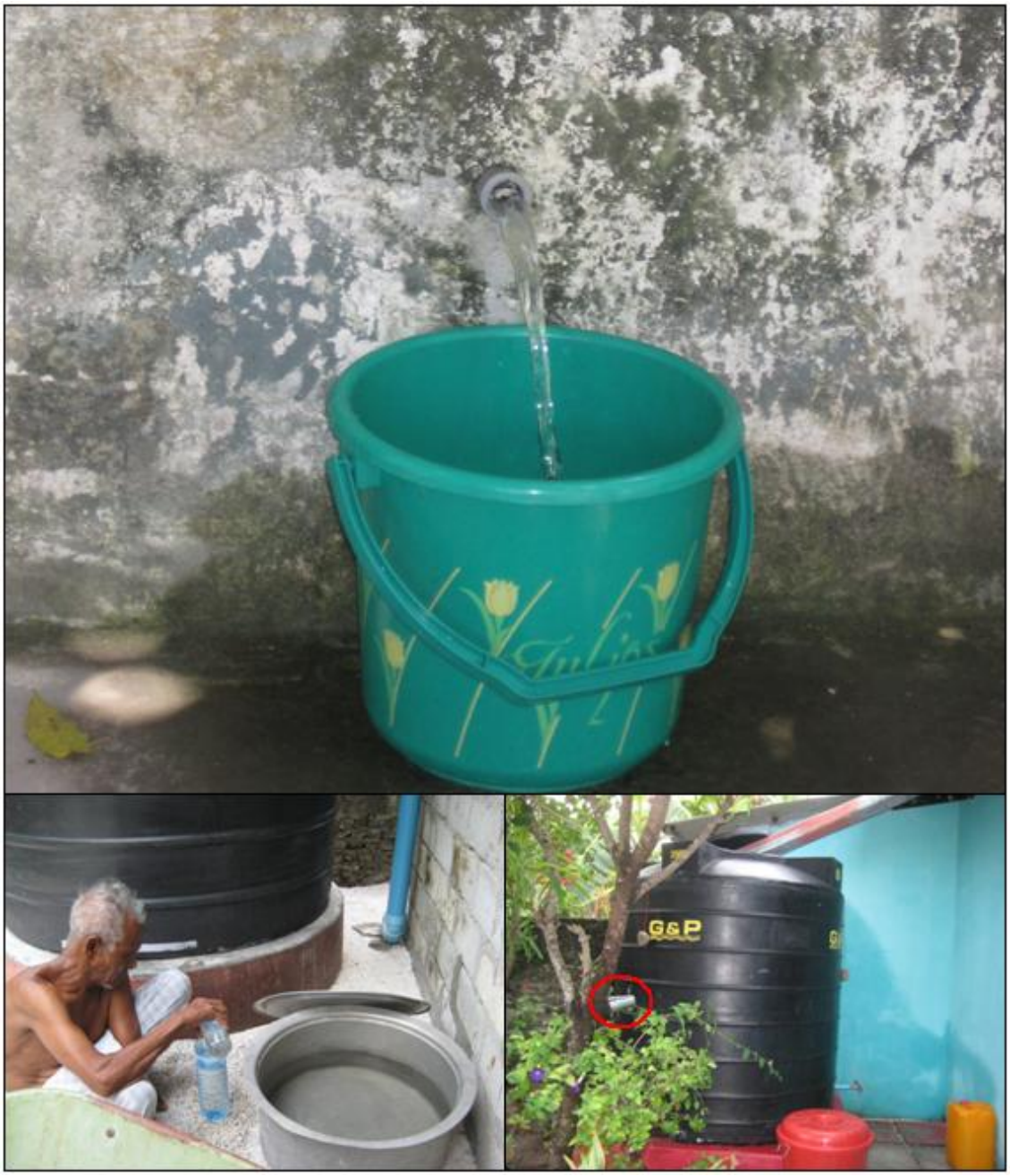

Figure 8.13: Bucket being filled with rainwater from a communal rainwater tank and commonly stored until it is used for cooking (top). Quite often, bottles were filled from the rainwater tank and later used for drinking (bottom left). Sometimes, a glass is used to obtain water from the tank for drinking (indicated by the red circle: bottom right) and consumed directly. The yellow bottle (bottom right) is often used to fill washing machines.

Dishwashing: It is very rare to use a dishwasher for washing dishes in the Maldives. None of the households visited during the survey had dishwashers and all the household dishes were done by hand. The two commonly used methods of dishwashing observed during the field survey were:

1. A container (bucket, basin, tub or bowl) is first filled with water by dhaani (manual extraction) or tap and then used for dishwashing (Figure 8.14)
2. Sink tap is directly used for washing dishes.

For the first method, the quantity of water used for household dishwashing was estimated based on the information provided by the respondents (and other residents) regarding the size of the container used (it was measured if the size was not known) and the number of containers used per day, and using the following equation:

$$\boldsymbol{Q_{dw} = N_c \times S_c}$$

where Q_{dw} is the quantity of water used for diswashing (per day in litres), N_c is the no of containers used (per day) and S_c is the size of the container (in litres). For the second method, discussions were held with the respondents (and female head and other residents) to quantify average tap running time (number of minutes) for dishwashing per day. Based on this, the quantity of water used for household dishwashing was estimated as below:

$$\boldsymbol{Q_{dw} = W_{FRT} \times T_{RT}}$$

where Q_{dw} is defined above, W_{FRT} is the water flow rate (tap)(L/min) and T_{RT} is the average tap running time (minutes) per day (in litres).

Figure 8.14: A filled bucket, tub or bowl is commonly used for dishwashing in the outer islands of the Maldives.

Clothes washing: On the outer islands of the Maldives, clothes washing is done both by washing machines and by hand. The most common types of washing machine are top-load machines. In some households the washing machines are filled manually (using a container such as the yellow bottle shown in Figure 8.13, bottom right, or using a basin, bucket or tub), while in other households it is filled directly from the tap. The respondents indicated that, clothes washing was not done every day (normally it is done on Friday). The

days when washing was done often involved several loads on a day. The respondents were asked about the number of days and number of times clothes washing was done per week. In the case of where washing machines are used and filled manually, the quantity of water used was estimated based on the number of times the washing machines are used (filled) per week (number of cycles/week), and the number and the size of the container used to fill the washing machine. Thus, daily household water usage (quantity) for clothes washing was estimated as:

$$\boldsymbol{Q_{cw} = \frac{N_{cycles} \times N_c \times S_c}{7}}$$

where Q_{cw} is the quantity of water used for clothes washing (in litres/day), N_{cycles} is the number of cycles per week, N_c is the no of containers used (per day) and S_c is the size of the container (in litres) and 7 is the conversion factor from week to days. When taps are used directly to fill the machines, the respondents were asked about how many minutes it takes for the washing machine to fill on average. Based on tap flow rate and the average number of minutes, the quantity of water used for household clothes washing per day was estimated as below:

$$\boldsymbol{Q_{cw} = \frac{N_{cycles} \times W_{FRT} \times T_t}{7}}$$

where Q_{cw}, N_{cycles}, T_t and 7 are defined above and W_{FRT} is the tap flow rate (litre/minute) and 7 is the conversion factor from week to days. In the case of household clothes washing being done by hand, the quantity of water usage for clothes washing per day was estimated using the following equation:

$$\boldsymbol{Q_{cw} = \frac{N_t \times N_c \times S_c}{7}}$$

where Q_{cw} is the quantity of water used for clothes washing (in litres), N_t is the number of times clothes washing was done per week, N_c is the no of containers used (per day) and S_c is the size of the container (in litres) and 7 is the conversion factor from week to days.

Bathing and hygiene: In order to estimate the household water usage for bathing (showering) and hygiene purposes (tooth brushing, hand washing, face washing, ablution and post-defecation), first the quantity of water usage for a single person (usually for the

respondent) for each household was estimated. In the case of where electrical pumps are used for the extraction of water from the wells, the respondents are asked on average how many minutes the shower head is turned on (shower running time) during showering (and how many showers per day), and information regarding total tap running times for hygiene purposes per caita per day (pcpd) was recorded. Based on this information, daily total household water usage for bathing (showering) and hygiene purposes was estimated as follows:

$$\boldsymbol{Q_{BH} = W_{FRS} \times S_{RT} \times N_o + W_{FRT} \times T_{RT} \times N_o}$$

where Q_{BH}, W_{FRS}, S_{RT}, N_o, W_{FRT} and T_{RT}, N_o is the quantity of water used for bathing and hygiene (in litres), showerhead water flow rate (L/min), shower running time (minutes), number of occupants, tap water flow rate (L/min) and tap running time, respectively. Similarly, for the case of where manual methods (dhaani: Figure 8.10 or other types of containers) are used for extracting water from the well, the respondents are asked on average how many dhaani (containers) are used each for a shower and how many showers are taken per day, and also about the number of dhaani's used for hygiene purposes per day. In this case, daily total household water usage for shower and hygiene purposes was estimated as follows:

$$\boldsymbol{Q_{BH} = N_o \times N_c \times S_c}$$

where Q_{BH} and N_o are defined above, N_c is the number of containers (dhaani) and S_c is the size of the container (in litres).

Toilet flushing: On the outer islands of the Maldives, the household toilets are flushed in two ways:

1. Using a pail (manual pour flushing)
2. Using flush tanks (cistern flush toilet)

In the case of pour flushing, for each island, the average size of the pail (in litres) used for pour flushing was determined from 3 households. The quantity of water used for toilet flushing (pcpd) was determined by asking the respondents (and other occupants where possible) about the number of times the toilet is flushed per day. Hence, the total quantity of water used for toilet flushing (or pour flushing) is estimated using the following expression:

$$\boldsymbol{Q_{TF} = N_o \times N_{tt} \times S_p}$$

where Q_{TF}, N_o, N_{tt} and S_p are daily household water use for toilet flushing per day (in litres), number of occupants, number of times toilet is flushed (per day) and size of the pail (in litres), respectively. For the case of cistern flush toilets, the average flush tank sizes were determined by collecting information from the suppliers (shops) about the most common size of toilet flush tanks sold and the type of the tanks (single or dual flush). Based on supplier's information and observations made during the field survey, the total household water consumption for toilet flushing (cistern flush toilets) was estimated as follows:

$$\boldsymbol{Q_{TF} = N_o \times N_{tt} \times S_t}$$

where Q_{TF}, N_o and N_{tt} are defined above and S_t is the average size of the tank (in litres), and the average size of the container and tank size presented in Table 8.13 is used for estimating daily total household water consumption for toilet flushing. For the household where two types of toilets are used, the average of pail and tank size was taken.

Table 8.13: Average size of the pail (container) and tank size (same for all regions: based on suppliers information) used for estimating water used for toilet flushing.

	Northern	Central	Southern
Pail (container) size (L)	8.0	8.5	8.75
Tank size (L)	12.0	12.0	12.0

Water usage for watering plants: Backyard farming or gardening is practiced in some households and the plants are not watered every day. Mostly the watering of plants was done by hand using a watering jug/can (Figure 8.12). However, in some households a hose is used. In order to estimate the quantity of water used for watering the plants (for the days when plants were watered), the respondents were asked about the average time the tap is released (where a hose is used for watering) or the number of watering jugs/cans (containers) used. Hence, the quantity of water used for watering plants (using a hose) is estimated as:

$$\boldsymbol{Q_{pw} = W_{FRH} \times T_{RT}}$$

where Q_{pw} is the quantity of water used for plant watering (for the days when plants were watered), W_{FRH} is the hose water flow rate (L/min) and T_{RT} is the average time that the hose is turned on (minutes). In the case where watering jugs are used, the quantity of water used for watering plants is estimated as:

$$\boldsymbol{Q_{pw} = N_c \times S_c}$$

where Q_{pw} is defined above, N_c is the number of containers (watering jug/can) and S_c is the size of the jug/can.

8.4.1.2 Estimated quantity of water usage by households

Due to the fact that only very limited information is readily available regarding the average quantity of water usage by household occupants for different purposes, water usage for the above purposes was computed separately for each household and all the components were summed to obtain the daily total household water consumption, except water usage for watering plants (water used for backyard farming was excluded, since not all the households surveyed use water for watering plants and in those households who use water for watering plants, plants were not watered every day). In estimating the household water usage, it was assumed that same quantity of water was used by each of the occupants within the household). To obtain per capita per day (pcpd) water consumption, household daily total water consumption was divided by the number of occupants in the household. Average pcpd water consumption for each region was obtained by averaging the four islands in each region and is depicted in Figure 8.15 and Table 8.14. The per capita per day water consumption estimated here appears to be higher than the estimates presented in Table 8.10. The estimated pcpd used provided by Beswick (2000) is reasonably similar to the estimates obtained here. With the improved access to electricity during the past decade, significant behavioural changes might have occurred regarding the use of water in the outer islands of the Maldives, due to the use of more electrical pumps, washing machines and cistern flush toilets in the islands, resulting in higher water usage pcpd. For example, in the outer islands (atolls) the use of washing machines increased from 57% to 84% during the period 2000-2006 (MPND 2008). The difference between Beswick's estimate and the estimate here could be due to the difference in behavioural changes that might have occurred during the past decade. It is not clear whether Beswick (2000) included pcpd water use for ablution. It is estimated about 15-26 L/person is used per day for the ablution process (Oyegun 1985; Taleb and Sharples 2010). The pcpd water consumption estimates given in Table 8.14

include daily water usage for the ablution process. The slight increase in pcpd water consumption estimated here (Table 8.14) compared to the Beswick's (2000) pcpd water consumption estimates presented in Table 8.10 could be due to behavioural changes over the past decade and inclusion of water usage for ablution. Total daily water consumption per person for other countries (and for different cities) and are depicted in Table 8.15. Otaki et al. (2008) provided a comparison of daily water consumption per person for different purposes and for different counties (cities) as illustrated in Figure 8.16. These values clearly indicate that pcpd water consumption can vary from country to country and from city to city, and water consumption for different purposes also varies from one country (city) to another.

It is evident from Figure 8.15 and Table 8.14, that bathing and hygiene accounts for the highest pcpd water consumption (105, 110 and 107 L for the northern, central and southern regions, respectively), accounting for about 55% (Figure 8.15b and Table 8.14) of daily total usage (186, 199 and 195 L pcpd for the northern, central and southern regions, respectively) for each region. It is interesting to see that about 97-98% of the total household water demand (100% of all the non potable use: Table 8.8) is met by groundwater, while the remaining 2-3% of the total household water demand is met by rainwater (rainwater accounts for 100% of water usage for cooking and drinking: Table 8.8). The similar pcpd values of water consumption for cooking and drinking (5, 5 and 6 lpcpd for northern, central and southern regions, respectively) could be due to common cooking practices (normally cooking was done together for the entire family) in the islands of the Maldives. It is clear that the outer islands of the Maldives completely rely on these two water resources for normal household purposes and that total pcpd water usage for the three regions is comparable with pcpd water consumption for other countries (cities). Taking account of water used for ablution and behavioural changes the pcpd consumption for the three regions is consistent with the pcpd consumption estimated by Beswick (2000).

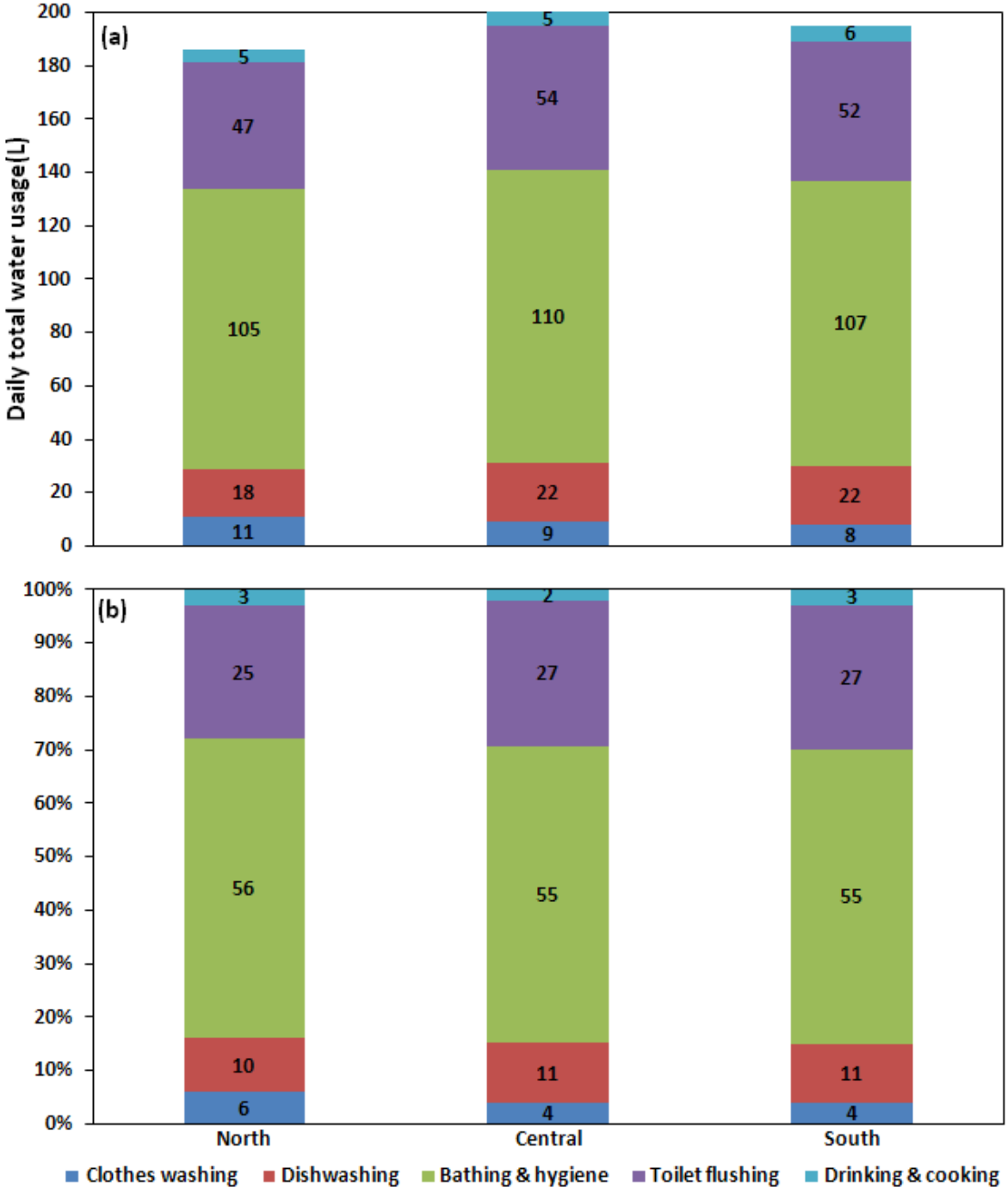

Figure 8.15: Total household water usage (a) and corresponding percentage (b) per capita per day (pcpd) for different purposes and regions. The key shown is common for the two plots.

Table 8.14: Household average water consumption (litres per capita per day: lpcpd) for different purposes and their corresponding percentages for the three regions (does not include water used for watering plants and agriculture water use).

Purposes	Northern		Central		Southern	
	lpcpd	%	lpcpd	%	lpcpd	%
Clothes washing	11	6	9	4	8	4
Dishwashing	18	10	22	11	22	11
Bathing & hygiene	105	56	110	55	107	55
Toilet flushing	47	25	54	27	52	27
Drinking & cooking	5*	3	5*	2	6*	3
Total	**186**	**100**	**199**	**100**	**195**	**100**

Note: lpcpd values are rounded off to the nearest whole number. For rainwater supply and demand calculation, the values indicated by * (5, 5 and 6) were rounded off from 5.0, 4.8 and 5.7, respectively.

Table 8.15: Total consumption (litres per capita per day) for different countries (cities).

Country (City)	lpcpd	Source
Thailand (Bangkok)	217	Otaki et al.(2008)
Thailand (Chiang Mai)	77	Otaki et al.(2008)
Singapore	175 (in 1994) and 156 (in 2008)	ADB (2010)
Sri Lanka	139	Sivakumaran and Aramaki (2010)
Malaysia	310	Weng and Nittivatananon (2006)
Saudi Arabia	498	Taleb and Sharples(2010)
Australia (Sydney)	506	Birchfield and Easton (2007)
New Zealand (Christchurch)	280	Heinrich (2006)
New Zealand (Auckland)	185	Heinrich (2006)
New Zealand (Wellington)	240	Heinrich (2006)
New Zealand (Kapiti)	600	Birchfield and Easton (2007)

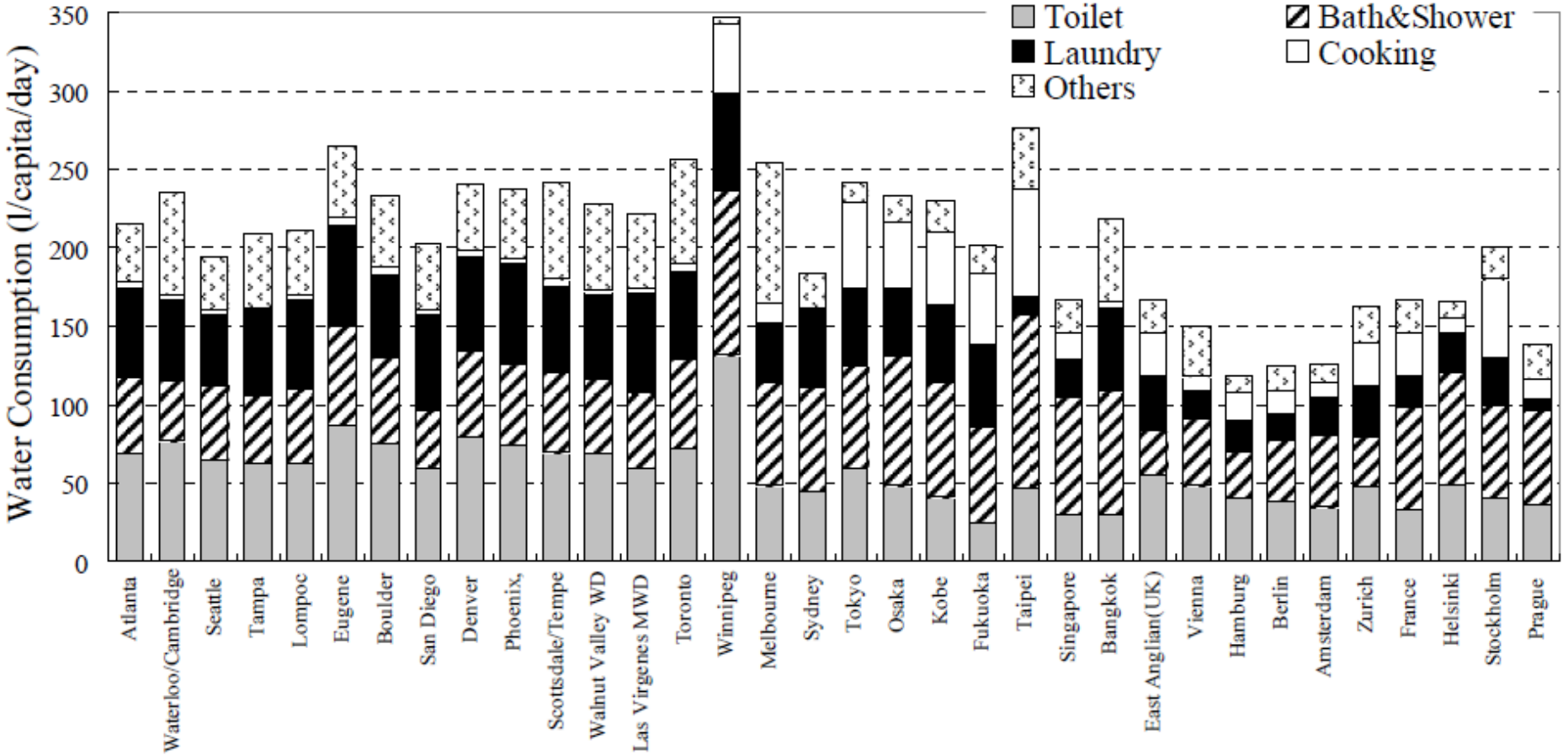

Figure 8.16: Comparison of per capita per day (pcpd) water consumption for different purposes. Taken from Otaki et al. (2008).

8.4.2 Availability of groundwater resources

Bailey et al. (2008) pointed out that knowledge of the quantity and quality of groundwater is not readily available for the vast majority of atoll islands around the world, which is true for most of the Maldivian islands. During the field survey, information on quantity and quality of groundwater was collected. Due to the geographic (low-lying) nature of the islands of the Maldives, very few surface water resources exist. Only limited numbers of island have surface water in the form of swampy areas or freshwater ponds/rivers, locally known as kulhi (Figure 8.17). The majority of freshwater resources in the islands of the Maldives exist as groundwater. This fresh groundwater is the result of rainfall and the amount that infiltrates into the islands' sandy coral soils and accumulates as fresh groundwater (Figure 8.18). This fresh groundwater is found in the form of freshwater lenses underlying the islands and floating on top of the saline water due to the density difference (Ibrahim 2008; Millar 2002; Woodroffe 1989) and the maximum freshwater lens occurs towards the middle of the island (Figure 8.18). Traditionally, the islands of the Maldives depended on groundwater resources for both potable and non-potable use (Ibrahim 2008), and groundwater has been viewed as a "free resource" which can be extracted from the household well easily (all the households have at least one well dug in the compound: Table 8.9).

Figure 8.17: Kulhudhuffushi island of the Maldives is one of few islands where surface water resources exist in the form of ponds, locally known as Kulhi.

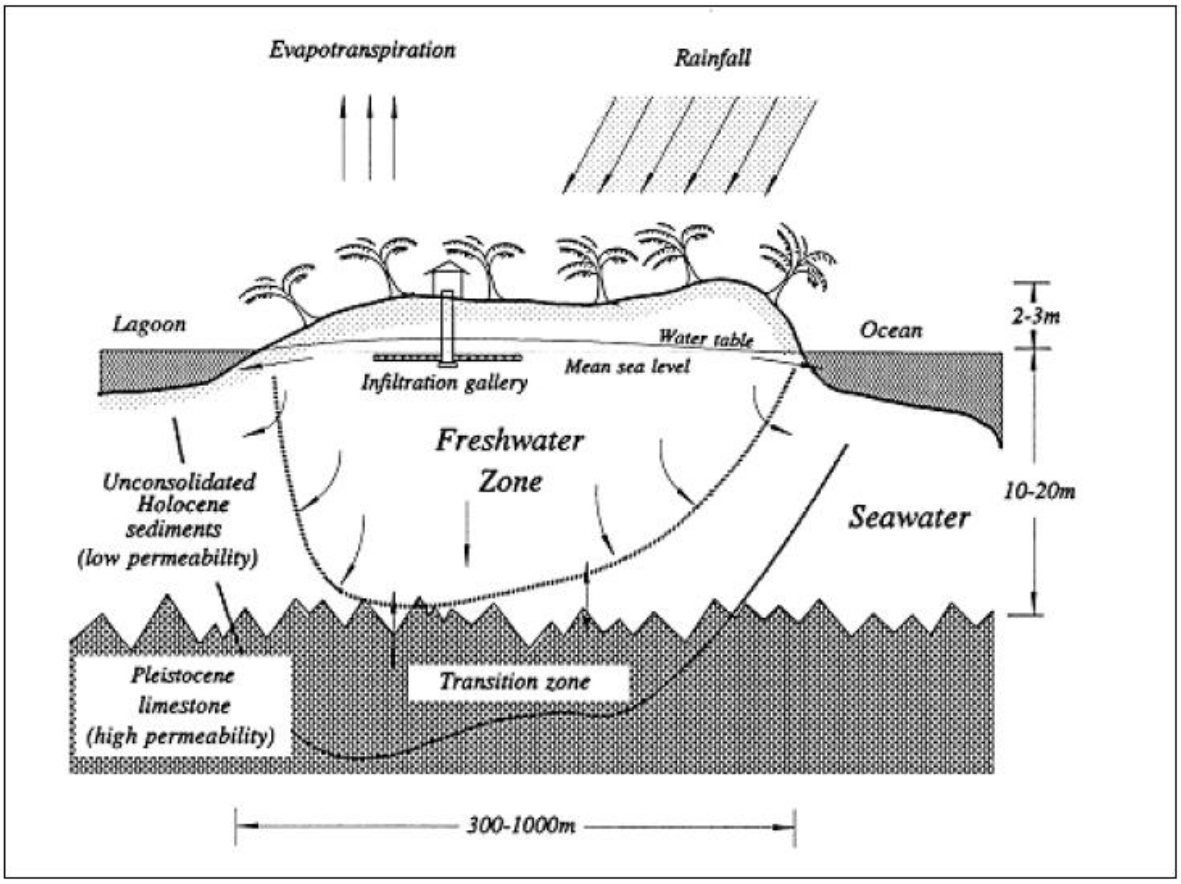

Figure 8.18: Schematic diagram showing flow of groundwater and the freshwater zone beneath reef islands. Taken from Falkland (2001b).

8.4.3 Estimation of groundwater resources

The thickness of a freshwater lens (hence available groundwater for extraction) is influenced by a number of factors such as island width, island geology/geometry (aquifer permeability and porosity), rainfall recharge rate, abstraction rate (groundwater withdrawal), evapotranspiration (depends on soil type and vegetation cover of the island) and tidal movement (Bailey et al. 2008; Falkland 1993; Falkland 2001b; Ibrahim 2008; Woodroffe 1989). According to Woodroffe (1989), the freshwater lens exists or develops only when the width of the island is large enough (with a threshold width of 200, but 300-400 m is a more realistic minimum width for a lens to develop). The relationship derived between freshwater lens thickness, annual rainfall and island width for small coral islands suggests that a permanent freshwater lenses can only occur where the island width is more than 120 m (Falkland 1994; Oberdorfer and Buddemeier 1988; Woodroffe 1989) and this relationship is presented below (Falkland 1994):

$$\frac{H}{P} = 6.94 log W - 14.38$$

where H = freshwater lens thickness (measured from water table to sharp interface or mid-point of transition zone in metres), P = annual rainfall (metres) and W = island width (metres). For the Maldivian islands, typically for every 250 m of island width, the freshwater lens is expected to be about 1 m thick and hence where an island width is 500 m it can be expected that the freshwater lens will be about 2 m thick, but there are islands where the freshwater lens thickness is greater or less than this (Ibrahim 2008). Based on field studies carried out in some of the islands of the Maldives, Ibrahim (2008) suggested that the freshwater lens thickens further away from the coastline and in general maximum freshwater lens thickness occurs in the middle of the islands, and hence freshwater lens thickness is controlled by the width of the island, but not the island length. One of the most important factors determining the thickness of a freshwater lens is the amount and variability of recharge to the groundwater. Groundwater recharge is the balance between rain falling onto the island (input) and evapotranspiration (output of water from the surface of the island) (Bailey et al. 2008; Falkland 2001b; Woodroffe 1989), and the simple water balance given by Bailey et al. (2008) is presented below:

$$R = P - I - ET \pm \Delta S$$

However, there are clearly islands that have more water than this, as well as those with less.

Where R = recharge to the freshwater lens, P = total precipitation, I= intercepted precipitation, ET = evapotranspiration (evaporation from the surface, transpiration from the root zone, and extraction from the lens by deep-reaching coconut roots), and ΔS = change in soil storage. It has been estimated that approximately 15% of total rainfall is intercepted by vegetation before it reaches the ground (Bailey et al. 2008; Falkland 2001b). On the other hand, evapotranspiration could have a major effect on recharge, and it has been estimated that coconut trees can transpire about 70-130 L of water/coconut tree per day. For the Cocos (Keeling) Islands, the estimated recharge rate is 48% and 25% of the rainfall where there are no coconut trees and where there is 100% cover of coconut trees, respectively (Woodroffe 1989). Recharge to the freshwater lens has been estimated to be less than 50% of rainfall, and in typical limestone islands the recharge can vary between 25-30% of the rainfall (Bailey et al. 2008; Woodroffe 1989). On the other hand, for Home

Island, Ghassemi et al. (1998) estimated the annual recharge rate as 44% based on mean annual rainfall for 1953-1987. Based on a number of small island groundwater recharge studies, Falkland (2001b) provided a relationship between annual rainfall and annual recharge rate as illustrated in Figure 8.19, which takes account of average vegetation cover of the islands, since vegetation cover has a major effect on recharge, as discussed above. In the absence of field estimates of recharge, Falkland (2001b) used this simple method to estimate recharge rates for some of the islands of the Maldives.

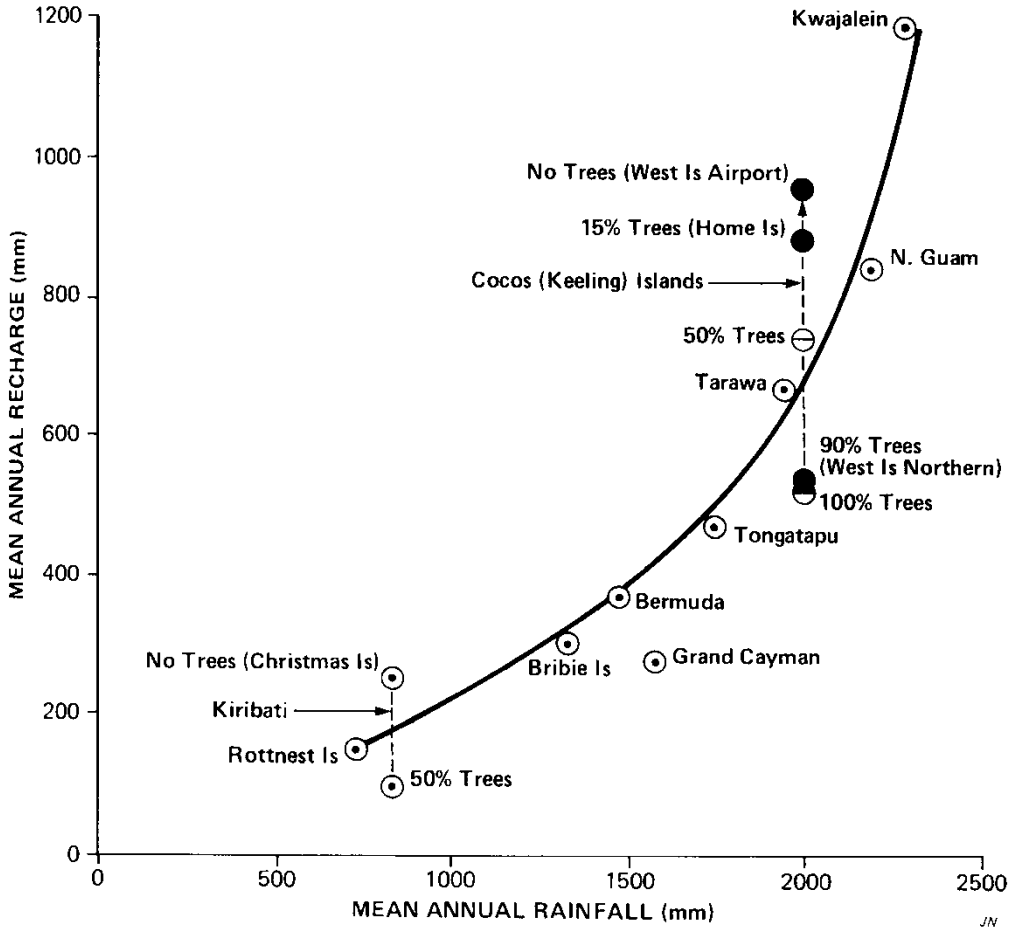

Figure 8.19: Relationship between mean annual rainfall and mean annul recharge on coral islands. In the absence of field estimates of recharge, this simple method could be applied to estimate recharge. Taken from Falkland (2001b).

In order to estimate recharge (and hence groundwater resources) for the islands surveyed, a similar approach used by Falkland (2001b) was adopted here. Based on regional rainfall (for the period 1992-2009), the graph in Figure 8.19, and observations made during the field survey regarding vegetation cover, recharge was estimated for the 12 islands as well as estimates of other parameters (as depicted in Table 8.16). Moderate vegetation cover was observed for all the islands, except S. Hithadhoo, where vegetation

cover was largely absent. Based on this observation, it was assumed that the recharge rate is 40% of the rainfall for the islands where the vegetation cover is greater than average, and 50% of the annual rainfall (where the vegetation cover is less than average). Falkland (2001b) also used a similar conservative approach in estimating recharge. Hence, recharge rate was calculated by multiplying corresponding regional rainfall with proportional recharge (0.4 and 0.5). Assuming that permanent freshwater lenses only exist where the island width is greater than 200 m and freshwater lenses do not exist within 50 m of the shoreline, freshwater lens areas for each island were estimated from Google earth maps (Tony Falkland, pers. comm.), and are illustrated in Table 8.16. Falkland (2001b) also used the minimum island width approach for estimating freshwater lens areas for some of the islands of Maldives. The island area presented in the table was obtained from DNP (2010). From the freshwater lens area and recharge rate, recharge volume was estimated as follows, and presented in Table 8.16:

$$\boldsymbol{R_{vol} = L_{area} \times R_{rate}}$$

Where R_{vol} = recharge volume (m^3/year), L_{area}= lens area (m^2) and R_{rate} = recharge rate (mm/year). Daily recharge volume is computed by dividing the yearly recharge by number of days (365), and is also provided in Table 8.16.

Table 8.16: Estimated groundwater parameters based on regional rainfall and field observations.

	Island Name	Regional rainfall (mm)	Island area (ha)	Estimated freshwater lens area (ha)	Recharge rainfall (%)	Recharge rate (mm/year)	Recharge volume (m^3/year)	Recharge volume (m^3/day)
Northern	Ha.Kelaa	1789.0	213.4	114	40	715.6	815784	2235
	Ha.Baarah	1789.0	248.8	89	40	715.6	636884	1745
	Hdh.Finey	1789.0	118.4	92.5	40	715.6	661930	1814
	Sh.Feevah	1789.0	79.2	64.5	40	715.6	461562	1265
Central	K.Kaashidhoo	2086.2	276.5	209	40	834.5	1744063	4778
	Aa.Thoddu	2086.2	142.2	118	40	834.5	984686	2698
	L.Gan	2086.2	516.6	348	40	834.5	2903990	7956
	L.Hithadhoo	2086.2	108.7	58	40	834.5	483998	1326
Southern	Gdh.Vaadhoo	2226.3	167.3	117	40	890.5	1041908	2855
	Gn.Fuvahmulah	2226.3	420	399.5	40	890.5	3557627	9747
	S.Hithadhoo	2226.3	467.3	327	50	1113.2	3640001	9973
	S.Meedhoo	2226.3	166	125	40	890.5	1113150	3050

Not all the recharge volume calculated above is available for extraction. The volume of fresh groundwater that is available for extraction from the island aquifer is referred as sustainable yield, and depends on both groundwater storage and recharge, and represents the amount of freshwater that can be extracted without causing long-term depletion of the freshwater lens (Falkland 2001b). Since much of the recharge volume is required to maintain the groundwater, sustainable yield could only represent a small proportion of recharge volume. In the absence of field data, Falkland (2001b) considered 30% of the average recharge volume as sustainable yield. The estimated sustainable groundwater yield for each of the islands surveyed is given in Table 8.17, together with other estimated parameters. Sustainable yield (litre per capita per day: lpcpd) varies considerably from island to island, with the highest and lowest lpcpd being 1036.3 and 208.9 for Hdh. Finey and S. Hithadhoo, respectively. It is interesting to note that these two islands correspond to the lowest and highest population density (Table 8.17). Another parameter that is important for groundwater resource management is freshwater lens volume (groundwater storage). Using freshwater lens thickness information available from the literature (for Ha. Kelaa, Ha. Baarah and S.Hithahdoo), the freshwater lens volume was estimated for the three islands as below:

$$\boldsymbol{L_{vol} = L_{area} \times L_{thickness} \times S_{porosity}}$$

where L_{vol} = freshwater lens volume (m^3), L_{area}= lens area (m^2), $L_{thickness}$ = freshwater lens thickness (m) and $S_{porosity}$ = sand porosity (taken as 30% – Falkland (2000) used this estimate in the absence of field data). Since the freshwater lens thickness is not available for other islands, average freshwater lens thickness for the known islands (Ha. Kelaa, Ha. Baarah and S.Hithahdoo) was used (shown in Table 8.17) to get rough estimates of the freshwater lens volume for other islands (Table 8.17). However, it should be noted that the freshwater lens thickness can vary from island to island. For example, freshwater lens thickness as small as 0.5 m (Hoarafushi) and as large as 15 m (S. Gan) have been estimated from field observations by Falkland (2000; 2001a), respectively. The estimated freshwater lens volume for these islands (estimated by using average freshwater lens thickness zone) should be used cautiously. Another important parameter shown in Table 8.17 is residence time, which represents the number of years of rainfall recharge the freshwater lens volume holds and is computed as below:

$$\boldsymbol{RT = \frac{L_{vol}}{R_{vol}}}$$

Where RT = residence time (years), L_{vol} = freshwater lens volume (m^3) and R_{vol} = recharge volume (m^3/year). The average residence time varies from 2.2 (S.Hithadhoo) to 3.4 years (Ha. Kelaa). The larger the residence time, the longer the freshwater will exists for extraction and it will take more time for groundwater to become saline. The residence time shown in Table 8.17 suggests that the groundwater resources in these islands are not vulnerable to a single drought year. However, it should be noted that some of these residence times are based on average freshwater lens volume, and hence should be used with caution. Furthermore, Falkland (2000; 2001a) pointed out that freshwater zone thickness values are average conditions (based on field investigation of groundwater) and do not take consideration of critical zones (such as towards shoreline or narrow areas of islands), and suggested further monitoring is needed to check the validity of the use of the average freshwater zone thickness assumption. Residence time estimated by Falkland (2001a) for some of the islands of the Maldives ranges from 0.26 (Hoarafushi) to 4.4 years (Kumundhoo). Groundwater in islands with such a small residence time (for example Hoarafushi) is likely to face salinity problems, and will be more susceptible, even during single dry periods, seasons or drought years.

Table 8.17: Estimated sustainable yield and residence time for islands in the Maldives.

Island Name	Population	Population density (per ha)	Estimated Freshwater lens area (ha)	Recharge volume (m^3/day)	Sustainable yield (m^3/day)	Sustainable yield (lpcpd)	Freshwater lens thickness zone (m)	Freshwater lens volume (m^3)	Residence time (years)
Ha.Kelaa	2097	9.8	114	2235	670.5	319.7	8*	2736000	3.4
Ha.Baarah	1794	7.2	89	1745	523.5	291.8	6*	1602000	2.5
Hdh.Finey	966	4.4	92.5	1814	544.1	1036.3	7.3†	2025750	3.1
Sh.Feevah	525	12.2	64.5	1265	379.4	392.7	7.3†	1412550	3.1
K.Kaashidhoo	2116	7.7	209	4778	1433.5	677.4	7.3†	4577100	2.6
Aa.Thoddu	1609	11.3	118	2698	809.3	503.0	7.3†	2584200	2.6
L.Gan	3233	6.3	348	7956	2386.8	738.3	7.3†	7621200	2.6
L.Hithadhoo	1011	9.3	58	1326	397.8	393.5	7.3†	1270200	2.6
Gdh.Vaadhoo	1413	8.4	117	2855	856.4	606.1	7.3†	2562300	2.5
Gn.Fuvahmulah	2634	26.4	399.5	9747	2924.1	264.1	7.3†	8749050	2.5
S.Hithadhoo	14323	30.7	327	9973	2991.8	208.9	8**	7848000	2.2
S.Meedhoo	11073	15.9	125	3050	914.9	347.3	7.3†	2737500	2.5

*Taken from Falkland (2001a), ** taken from Falkland (2000) and †7.3 is the average freshwater lens thickness obtained from 8, 6 and 8 for Ha. Kelaa, Ha. Baarah and S.Hithahdoo, respectively.

When average water consumption pcpd for each region (186, 199 and 195 L pcpd for the northern, central and southern regions, respectively: Figure 8.15a and Table 8.14) is compared with the sustainable yield computed for each island (Table 8.17) and indicates that the groundwater resources in all the islands are sufficient to meet the normal daily household water demand, especially for non-potable uses (without taking into consideration gardening/backyard farming water needs). Table 8.18 shows the percentage number of households who use water for gardening/backyard farming and the average quantity of water used per day for the three regions. About 93% of the households from the southern region indicated use of groundwater for gardening/backyard farming, with an average of 117 L of water/day (for the days when plants are watered). Taking account of gardening/backyard farming and agriculture sector water needs (the agricultural sector also may require a substantial amounts of water, but this will be discussed later), it should be noted that the sustainable yield for S. Hithadhoo (208.9 lpcpd: Table 8.17) is very close to the average water consumption pcpd for the southern region (195 lpcpd: Figure 8.15a and Table 8.14), and groundwater resources in this island may not be sufficient to meet the normal daily household. None of the islands surveyed are likely to have problems in terms of the quantity of water required for normal household uses (non potable) at present (since every household has at least one dug well in the compound for extraction of groundwater (Table 8.9)), but some indicated difficulty in obtaining groundwater due to tidal variations (Table 8.19), and the quality of water has deteriorated in recent years due to sanitation practices. None of the islands surveyed have central sewerage systems (See Appendix 1) and the sanitation of the islands mainly consists of flush latrines connected to septic tanks, and the septic tanks are largely soak pits, from which sewage leaks through the porous soil and contaminates the groundwater, thus making the groundwater unfit for most household purposes (Falkland 2000; 2001a; Falkland 2001b; Ibrahim 2008).

Table 8.18: Statistics of groundwater usage for gardening and backyard farming by the households (based on field survey data).

Groundwater related issues	Northern	Central	Southern
Does your household use groundwater for gardening/backyard farming? Yes/No			
Yes (%)	68	64	93
No (%)	32	36	7
Average quantity of groundwater use per day (for the days when it is used) by the households			
Water quantity (L)	85	129	117

Despite high reliance on groundwater by the outer islands of the Maldives (97-98% of pcpd water consumption is met by groundwater resources: Figure 8.15b and Table 8.14) many islands are now facing groundwater problems caused by human activities, such as over-abstraction and sewage pollution (Falkland 2000; 2001a; Falkland 2001b; Ibrahim 2008). The responses received from the island office (see Appendix 1) also suggest that the groundwater in the islands is contaminated. Indication of the widespread nature of the groundwater problem is indicated in Table 8.19. The list of groundwater related issues presented in the table is generated from the responses received from the respondents when they were asked "would you like to add anything regarding the water resources in your household?". The responses received for this indirect question clearly show that households face groundwater problems, with about 37.6, 33.7 and 40.8% of the households in northern, central and southern regions having problems with groundwater. About 36.4, 37.0 and 43.9% of households in northern, central and southern regions, respectively, responded with "no comment" for this question and responses received for the remaining percentage of households include "shortage of rain", "more rainwater storage tanks needed" and "no problem with water". The problem is more widespread than this. According to UNSM (2007) groundwater in 162 islands of the Maldives is unfit for potable use, with 54 islands due to high salinity problems, 46 islands due to pollution, including faecal contamination. MEC (2004) also indicated that groundwater was suitable for drinking in only 39 of the 200 inhabited islands of the Maldives prior to the December 2004 tsunami. The porous nature of soils of the Maldives islands and proximity of groundwater to the surface (the freshwater aquifer lies about 0.5-2.5m below the surface: Table 8.9) makes the groundwater resources of the islands of the Maldives highly susceptible to pollution due to both human activities

(over-pumping and sewage) and natural causes (storm surge floods, causing salt water intrusion) (UNSM 2007).

Table 8.19: Indication of groundwater problems faced by households and their percentage by region (based on field survey data).

Groundwater related issues	Northern (%)	Central (%)	Southern (%)
Would you like to add anything regarding the water resources in your household?			
Groundwater is not suitable for use due to contamination	19.5	19.5	25.6
Smells and colour from groundwater	7.1	7.1	13.4
Not sure whether groundwater is safe	1.9	2.6	-
Alternative clean water is needed	9.1	4.5	1.8
Total %	37.6	33.7	40.8
Other groundwater related issues			
Shortage or difficulty in extracting groundwater due to low tide (%)	5	11	15
Respondents who indicated salinity in household well (%)	8	9	5
Actual measurements of salinity in household wells (%)	32	27	24
Average salinity (ppm*)	1100	1000	1100
Maximum salinity (ppm)	2000	1800	1100
Water quality related illness (%)	3	5	6

*ppm = parts per million

The respondents were asked whether their household wells experience groundwater salinity problems. The results are summarised in Table 8.19. In order to determine actual groundwater salinity of the islands visited during the field survey, groundwater from household wells and farm sites was tested for salinity using an EcoScan hand-held salinity meter (Figure 8.20, top left figure). The meter can read salinity values between 0.1 - 5.00% (1000 - 50,000 parts per million (ppm)), with a resolution of 0.01%. The results of salinity measurements are illustrated in Table 8.19 for household wells (results for agricultural sites will be presented later). The actual percentages of observed salinity in household wells are

higher than the perceived salinity. For example, only 8% of the respondents from the northern region indicated salinity in their household well, but the actual percentage of measured salinity for the same region is 32% (Table 8.19). The average salinity in household wells ranges from 1000-1100 ppm, with the maximum salinity (2000 ppm) observed for the northern region. According to drinking water guidelines published by the World Health Organisation (WHO 1993), the desirable limit of chlorine in freshwater is 250 mg/L (250 ppm), which is another measure of salinity (Falkland 2000). Furthermore, Al-Turki (2009) pointed out that when the groundwater salinity is greater than 500 ppm, the taste of water is poor, and when salinity is less than 500 ppm it is acceptable for household use. The salinity meter can only read salinity values greater than 1000 ppm and about 32, 27 and 24% for the northern, central and southern regions showed salinity measurements of 1000 ppm or more. Taking the threshold salinity value of 250 for drinking and 500 ppm as a guideline for household use, it is clear that the islands surveyed experience quite high levels of salinity, which might not be suitable for household purposes. Although the percentage of reported cases of illness associated with water is quite low (3, 5 and 5% for northern, central and southern regions, respectively), it has been suggested that waterborne disease has increased in recent years. For example, gastroenteritis (a waterborne disease) has increased from 15,000 cases in 2004 to 21,000 cases in 2005 and it is suggested that the island community (compared to the capital island Male') is more vulnerable to diarrhoeal diseases, indicating inadequate access to safe water and sanitation (Moosa 2006). Changes in precipitation patterns (associated with climate change) are likely to increase incidence of waterborne diseases like cholera and other diarrhoeal diseases in the future due to limited access to safe water (MHTE 2009).

Figure 8.20: A hand-held EcoScan salinity meter (top left) was used for testing groundwater from household wells (top right) and farm site wells (bottom).

8.4.4 Rainwater resources

It is evident from the above, that the island community relies heavily on rainwater for most of their potable use (cooking and drinking). Although, the amount of rainwater used for cooking and drinking accounts for only 2-3% of total pcpd water consumption, it is vital for the islands of the Maldives, since most of the islands groundwater resources are impacted by salinity (due to over-pumping) and pollution (due to sewerage contamination),

as discussed above. Even though the islands surveyed completely depend on rainwater normally for cooking and drinking, and despite the small quantity of rainwater used (5, 5 and 6 lpcpd for northern, central and southern regions, respectively) for potable uses, all the islands indicated shortage of rainwater (Table 8.20). At the other extreme, about 23-37% of the households experienced flood events (Table 8.20). Table 8.21 shows the years together with percentage occurrence of shortage of rainwater and occurrence of flood events. As can be seen from the table, shortage of rainwater and flood events do not occur in all the years. When the flood (excess rainfall) and drought (deficit) years identified for the three regions in Figure 4.25 is compared with the flood and drought events experienced by the households (Table 8.21), there appears to be no one-to-one relationship. This could be due to the fact that the flood and drought years identified in Figure 4.25 are based on monsoon season rainfall, whereas the flood years experienced by the households (Table 8.21) are due to flash flood events and drought (prolonged dry periods) years identified based on household respondents due to shortage of rainwater during the dry season.

The percentage number of households who experienced rainwater shortages is highest for the southern region (Table 8.20), despite that this region of the Maldives receives higher rainfall (Figure 3.9a). Compared to the other regions, the southern region had the least percentage of ownership of rainwater tanks in households (88%), which could be one reason for the reported higher percentage of rainwater shortages for the region. The average size of the rainwater collecting tank for the southern region is 3700 L, while the northern and central regions had 4000 L and 3800 L, respectively (Table 8.24). Hence this could be another reason for a larger percentage indicating shortage of rainwater for this region. About 78-97% of the respondents indicated that the shortage is due to the prolonged dry period, while 28-40% indicated it is due to small tank size. During shortage of rainwater, most of the households depended on either rainwater obtained from communal/neighbours' tanks or groundwater. Furthermore, it is clear from the table that the three regions experience shortage of rain during the dry season (December-April) only and shortage of rainwater can last for up to 3-4 months (northern and central regions). Table 8.20 suggests that all the households harvest their rainwater during the extended wet season (May-November: 100% for the three regions) and the harvested rainwater is not enough to meet the dry season potable water demand. According to MPND (2007a), in many islands of the Maldives shortage of rainwater (drinking water) is increasing. It is clear from Table 8.20, that the majority of the island communities depend on a communal/neighbours' rainwater tank and groundwater as an alternative source of potable water during shortage of

rainwater (when the household rainwater tank becomes empty). Furthermore, about 16 and 9% of the household from the northern and central part of the Maldives indicated using desalinated water during shortages of rainwater. About 60 inhabited islands (30% of all inhabited islands) experienced shortage of rainwater in 2009 (by mid-March 2009) alone and the national disaster management centre (NDMC) of the Maldives had to supply desalinated water to these islands (Haleem 2009). About 3-14% of the households used bottled water for drinking during shortages of rainwater. In order to supply the necessary amount of water for the dry season (the cumulative shortfall during the dry months) and to ensure rainwater is available through the year, for cooking and drinking, enough rainwater should be harvested during the wet season to last the dry season. In other words, the total rainwater harvested must exceed the total demand and there must be sufficient rainwater storage tanks to allow enough surplus water collected during the wet season to be carried over to meet the rainwater demand during the dry season (Gould and Nissen-Peterson 1999). Considering the high annual rainfall for the islands of the Maldives (Figure 2.29 and Table 2.11), it might be feasible (provided that no major changes occur regarding precipitation patterns over the Maldives) to harvest rainwater to meet the growing demand (due to contamination of groundwater by sewage) for potable uses by the households in the outer islands of the Maldives. However, to achieve this, the households should be equipped with the right size of rainwater storage tank(s) and should have the right size of effective roof area. Roof catchment area and appropriate rainwater storage tank size will be discussed below.

Figure 8.21: Actual (top) and schematic diagram (bottom) showing typical rainwater harvesting systems observed in the Maldives. Most of the households use only part of the roof (the gutter is only connected to a part of the roof) for harvesting rainwater.

Table 8.20: Household rainwater statistics based on field survey data.

Description	Northern	Central	Southern
Shortage of rainwater (%)	53	49	63
What type of water is used during shortage (%)?			
Rainwater from other sources (communal or neighbour)	43(7)*	40 (1)*	57 (7)*
Groundwater	44	51	36
Bottled water (drinking)	5	3(1) †	14
Desalinated water	16	9	-
Rainwater tank availability (%):			
Uses own tank	97	94	88
Uses communal	1	5	9
Uses neighbour's tank	2	1	2
During which period of the year is rainwater harvested (%)?			
December-April (dry season)	-	-	-
May-November (wet season)	100	100	100
Shortage during which period of the year (%)?			
December-April (dry season)	100	100	100
May-November (wet season)	-	-	-
How long shortage of rainwater lasts for (%)?			
<1 month	0	0	13
1-2 months	59	89	81
2-3 months	22	11	4
3-4 months	13	1	2
4-5	6	1	-
Reason for shortage of rainwater (%)?			
Tank size (small)	28 (12)**	40(23)**	10 (9)**
Prolonged dry period	78	83	97
Other	6	0	2
Flood related damage by the households (%)?			
Yes	23	31	37
No	77	69	63

Note: The common percentage value for both rainwater and groundwater is indicated as ( )*, common percentage value for bottled water and desalinated water is indicated as ( )† and common percentage value for tank size and prolonged dry period indicated as ( ).**

Table 8.21: Percentages showing drought (prolonged dry period) and flood years since 1992, among respondents who indicated shortage of water (both groundwater and rainwater) and experienced flood in households (based on field survey data).

Description	Northern	Central	Southern
In which years since 1992 did your household experience shortage of groundwater?			
Years and percentage	All the years (100%)	2008 (29%) All the years (71%)	2008 (12.5%) 2009 (12.5%) All the years (75%)
In which years since 1992 did your household experience drought/prolonged dry period/ shortage of rain?			
Years and percentage	2001 (6%) 2003 (10%) 2003 & 2008 (1%) 2005 (9%) 2005 & 2009 (1%) 2006 (1%) 2007 (5%) 2008 (11%) 2009 (43%) All the years (13%)	2000 (5%) 200 & 2009 (1%) 2001 (8%) 2003 (5%) 2004 (4%) 2005 (3%) 2006 (3%) 2007 (8%) 2008 (12%) 2009 (51%)	2000 (6%) 2003 (7%) 2004 (9%) 2005 (4%) 2006 (2%) 2006 & 2008 (1%) 2007 (7%) 2008 (21%) 2009 (41%) All the years (3%)
In which years since 1992 did your household experience flood related damages?			
Years and percentage	1999 (9%) 2000 (11%) 2004 (26%) 2005 (14%) 2006 (6%) 2008 (17%) All the years (17%)	1994 (4%) 2000 (4%) 2001 (2%) 2002 (9%) 2003 (17%) 2004 (6%) 2005 (2%) 2006 (28%) 2007 (21%) 2008 (2%) 2009 (4%)	2000 (2%) 2001 (12%) 2001 & 2007 (2%) 2002 (13%) 2003 (7%) 2004 (10%) 2005 (15%) 2006 (15%) 2007 (2%) 2008 (5%) All the years (18%)

8.4.4.1 Roof area (catchment size) and runoff coefficient

It was observed during the field survey that the gutter is mostly only attached to a part of the household roof for harvesting rainwater. The roof area connected to the gutter is referred to as the effective roof area (ERA: the term roof size will also be used inter-changeably) and sometimes the word "catchment" is used to mean roof. Since the effective roof area connected to the gutter is not readily available, ERA is estimated. First, the respondents (or any other person from the HH) were asked whether they know about the effective roof area, and if it is not known then the length (L) and width (W) of the roof connected to the gutter (Figure 8.21) was measured using a measuring tape. ERA **(**m^2) was calculated as:

$$\boldsymbol{ERA = L \times W}$$

where L = length (m) and W = width (m). The average roof sizes (average effective roof area) for the three regions are presented in Table 8.22. The table also provides a common roof runoff coefficient (C_R) of 0.8, which is the ratio of the volume of water that runs off from a surface (in this case runoff volume from roof surface) to the total volume of rainfall falling on to the roof surface (rainwater volume) and is given by (Gould and Nissen-Peterson 1999):

$$\boldsymbol{C_R = \frac{Runoff\ volume}{Rainwater\ volume}}$$

The roof runoff coefficient accounts for losses due to spillage, leakage, infiltration, catchment surface wetting and evaporation, and it is indicated that it is appropriate to use a runoff coefficient of 0.8 when designing roof catchment systems (Gould and Nissen-Peterson 1999; Khastagir and Jayasuriya 2010). Hence, a common roof runoff coefficient of 0.8 and the respective regional average roof size depicted in Table 8.22 were used in estimating rainwater supply (rainwater volume).

Table 8.22: Regional average roof size (catchment area), roof runoff coefficient (based on literature).

Parameters	Northern	Central	Southern
Average roof size (m^2)	39	44	39
Roof runoff coefficient	0.8		

8.4.4.2 Household rainwater supply and demand

It was shown above that about 88-97% of the households are equipped with their own rainwater storage tanks. The rainwater in the islands of the Maldives is harvested on a small scale (on a household basis) from the house roof catchment (Figure 8.21), mostly during the monsoon rainfall season. Four different scenarios were considered in calculating household rainwater supply and demand, to check whether the rainwater supply can meet the household rainwater demand for potable use for the scenarios defined below:

Scenario A (average): Average roof size and average per capita per day water consumption (5.0, 4.8 and 5.7 lpcpd for northern, central and southern) was used.

Scenario B (10 lpcpd): Same as scenario A, except that per capita per day water consumption of 10 lpcpd was used for the three regions. According to the Health Master Plan (1996-2005), the government aims to provide access to 10 lpcpd of safe water for cooking and drinking for the whole population of the Maldives (Falkland 2000; 2001a).

Scenario C (most common): Same as scenario A, but instead of average roof size, the most common roof size (30 m^2) is used, since about 60% of the households from each region had a roof size between 20 and 40 m^2.

Scenario D (most common and 10 lpcpd): The most common roof size and average per capita per day water consumption of 10 L is assumed.

Using the roof area obtained from the field survey (Table 8.22) and using the roof runoff coefficient (0.8), annual harvestable rainwater (rainwater supply) was computed (CEHI 2009; Gould and Nissen-Peterson 1999; Rahman and Yusuf 2000) :

$$\boldsymbol{S = ERA \times R \times C_R}$$

where S = annual rainwater supply (litres), ERA= effective roof area (m^2), R = annual rainfall (mm) and C_R = roof coefficient (taken as 0.8). In order to take prolonged dry spells into account and to ensure the design of the rainwater harvesting system is more reliable, annual rainfall for the worst year (the data period 1992-2009) for each region was used (CEHI 2009; Gould and Nissen-Peterson 1999). The worst rainfall year (lowest total rainfall years) for the northern, central and southern regions are 2002, 1995 and 1999,

respectively. Based on these years, the calculated annual rainwater supply (volume of rainwater captured from the roof) for each region is depicted in Table 8.23. Based on average household size (number of occupants) and rainwater consumption (litres per capita per day: lpcpd) for the three regions given in Table 8.23, the annual household rainwater demand was estimated as follows (CEHI 2009; Cresti 2007; Gould and Nissen-Peterson 1999), and values are presented in Table 8.23:

$$\boldsymbol{D = WC_{pcpd} \times N_0 \times 365}$$

where D = annual household rainwater demand (for cooking and drinking, in litres), WC_{pcpd} = rainwater consumption pcpd (litres), N_0= number of occupants (given in Table 8.23) and 365 = number of days in a year. The annual household rainwater demand presented in Table 8.23 assumes that the same number of occupants and the same quantity of rainwater is used per day, throughout the year. The values in brackets give the percentage of rainwater (average annual household rainwater demand/annual rainwater supply*100) that is utilized by the households. scenario A suggests that only 23-24% of the annual rainwater supply (harvestable rainwater) is utilized by the households, while scenario B indicates that households utilize less than 50% of the annual rainwater that can be captured. When most common roof area is considered (scenario C), households utilize about 30-34% of rainwater supply that is harvestable from the roof catchment area. Furthermore, scenario D (most common roof area and 10 lpcpd is used) indicates that about 54-71% of harvestable rainwater is utilized for cooking and drinking. From this, it is clear that the supply exceeds household average demand for the four scenarios considered, hence there is potential to provide a total year-round water supply. However, it should be noted that the rainwater supply can vary from month to month and in some months the demand could exceed the supply, while in other months, the rainwater supply can exceed the monthly or even yearly demand. Since, 100% of the households harvest rainwater during the rainy season, the monsoon rainfall prediction model formulated in Section 5.5.3 could be used to quantify the rainwater supply during the monsoon season before the monsoon season begins, thus quantifying possible rainwater that can be harvested during the monsoon season.

Table 8.23: Computed harvestable rainwater (rainwater supply) and demand for different scenarios. Average household water demand (for cooking and drinking) for each region was estimated based on respective average household number and rainwater consumption (litre per capita per day: lpcpd).

Parameters	Northern	Central	Southern
Average household occupants	5.3	6.6	7.1
Scenario A (average condition)			
Average roof size (m^2)	39	44	39
Average rainwater consumption (lpcpd)	5.0	4.8	5.7
Annual rainwater supply (L)	42000	49400	62500
Average annual household rainwater demand (L)	9700 (23%)	11600(23%)	14800(34%)
Scenario B (10 lpcpd)			
Average roof size (m^2)	39	44	39
Average rainwater consumption (lpcpd)	10	10	10
Annual rainwater supply (L)	42000	49400	62500
Average annual household rainwater demand (L)	19300 (46%)	24100(49%)	25900 (41%)
Scenario C (most common)			
Average roof size (m^2)	30	30	30
Average rainwater consumption (lpcpd)	5.0	4.8	5.7
Annual rainwater supply (L)	32300	33700	48000
Average annual household rainwater demand (L)	9600 (30%)	11600 (34%)	14800 (31%)
Scenario D (most common and (10 lpcpd)			
Average roof size (m^2)	30	30	30
Average rainwater consumption (lpcpd)	10	10	10
Annual rainwater supply (L)	32300	33700	48000
Average annual household rainwater demand (L)	19300 (60%)	24100 (71%)	25900 (54%)

Note: lpcpd given in Table 8.14 ***is rounded to nearest whole number, whereas here lpcpd is rounded off to one decimal place.***

Monthly rainwater supply and household rainwater demand for scenarios A/B and C/D are illustrate in Figure 8.22 and Figure 8.23, respectively for the three regions. For

scenario A, it is interesting to note that the supply for the southern region during the month of August (14795 litres: Figure 8.22, left bottom) exceeds the yearly household demand of 14772 litres (Table 8.23), and showed the highest number of months (three months: January, March and April) when the household rainwater demand exceeded the rainwater supply. On the other hand, for northern and central regions, monthly demand exceeds the rainwater supply during only one month (March) for the same scenario. When scenario B is considered, the northern region shows the highest number of months (5 months: January-March and December) where the household demand exceeds the rainwater supply. The central and southern regions show that the household rainwater demand exceeds the supply in January and March only for the central region and during January-April for the southern region (Figure 8.22). Scenarios C and D also indicate that the household rainwater demand can exceed the supply in some months (Figure 8.23). For scenario C, the southern region shows the highest number of months (4 month: January-April) where the demand exceeds the rainwater supply, while the northern and central regions show only two months (March-April for the northern region, and January and March for the central region) where the household rainwater demand exceeds the supply for scenario C. For the case of scenario D, it is interesting to note that household rainwater demand exceeds supply during some months of the core monsoon season (June-September) also – June for the central and September for the southern region (Figure 8.23). It is also worth pointing out that about 50% of the time (6 months), the household rainwater demand exceeds the supply for the central parts of the Maldives for scenario D (Figure 8.23 right middle). Although the monthly supply for some months is less than the monthly demand, there is a potential to capture enough rainwater to provide a constant year-round supply, as illustrated in Table 8.23, provided that the surplus water (during the months when the rainwater supply exceeds the household rainwater demand) is collected and stored, to be used during the months when the demand exceeds the monthly supply. This requires knowledge of appropriate rainwater storage tank size.

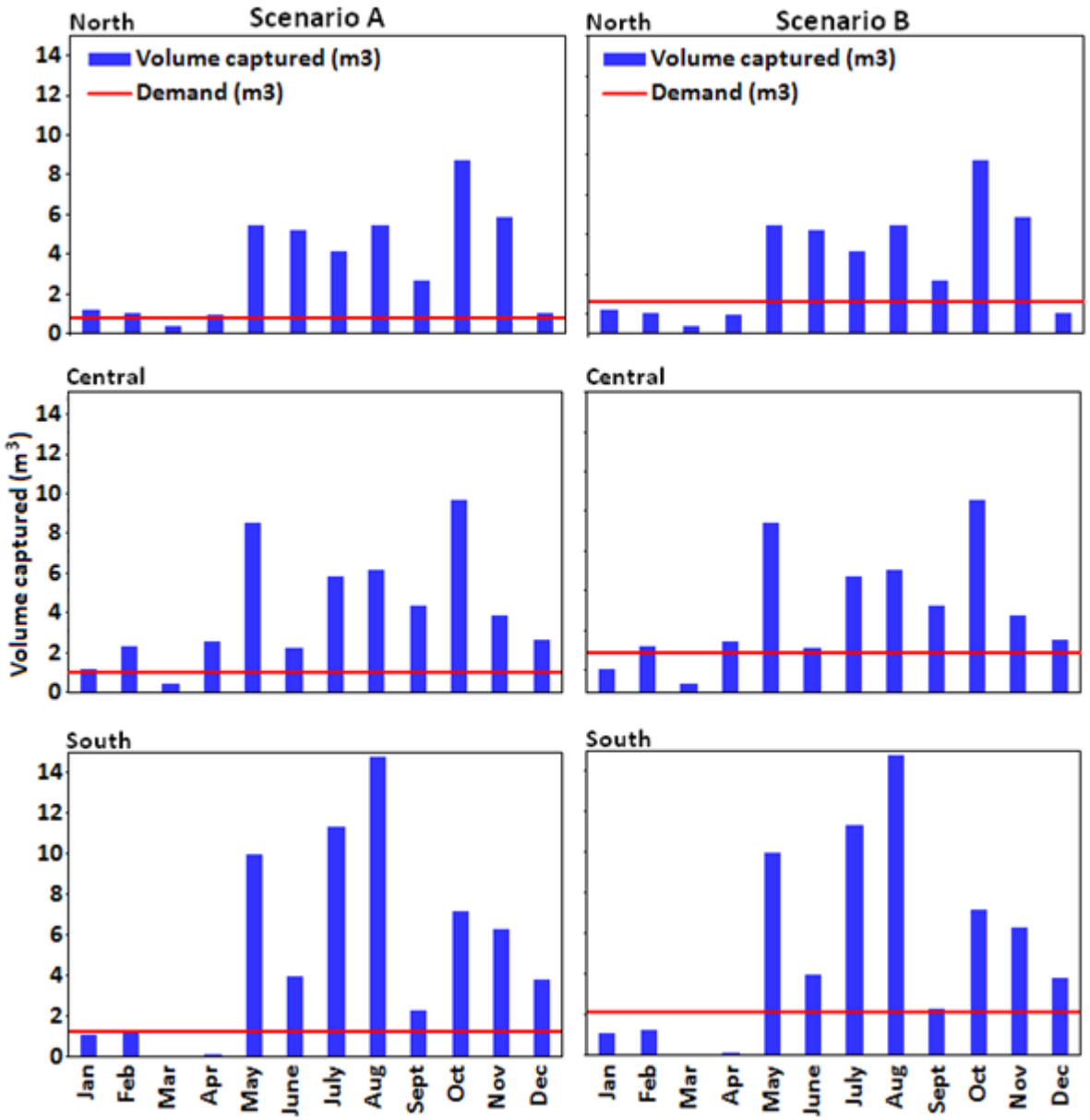

Figure 8.22: Monthly harvestable rainwater for scenarios A and B using lowest rainfall years 2002, 1995 and 1999 for the northern, central and southern Maldives, respectively. Average monthly household rainwater demand (potable) in cubic metres for each region (northern = 0.8 central = 1.0, and southern = 1.1 for scenario A, and northern = 1.6, central = 2.0, and southern = 2.2 for scenario B) is indicated by the horizontal line. Monthly harvestable rainwater (volume captured) and water demand for each region and each scenario were computed based on roof size, household size and water use per capita/day, as defined in Table 8.23.

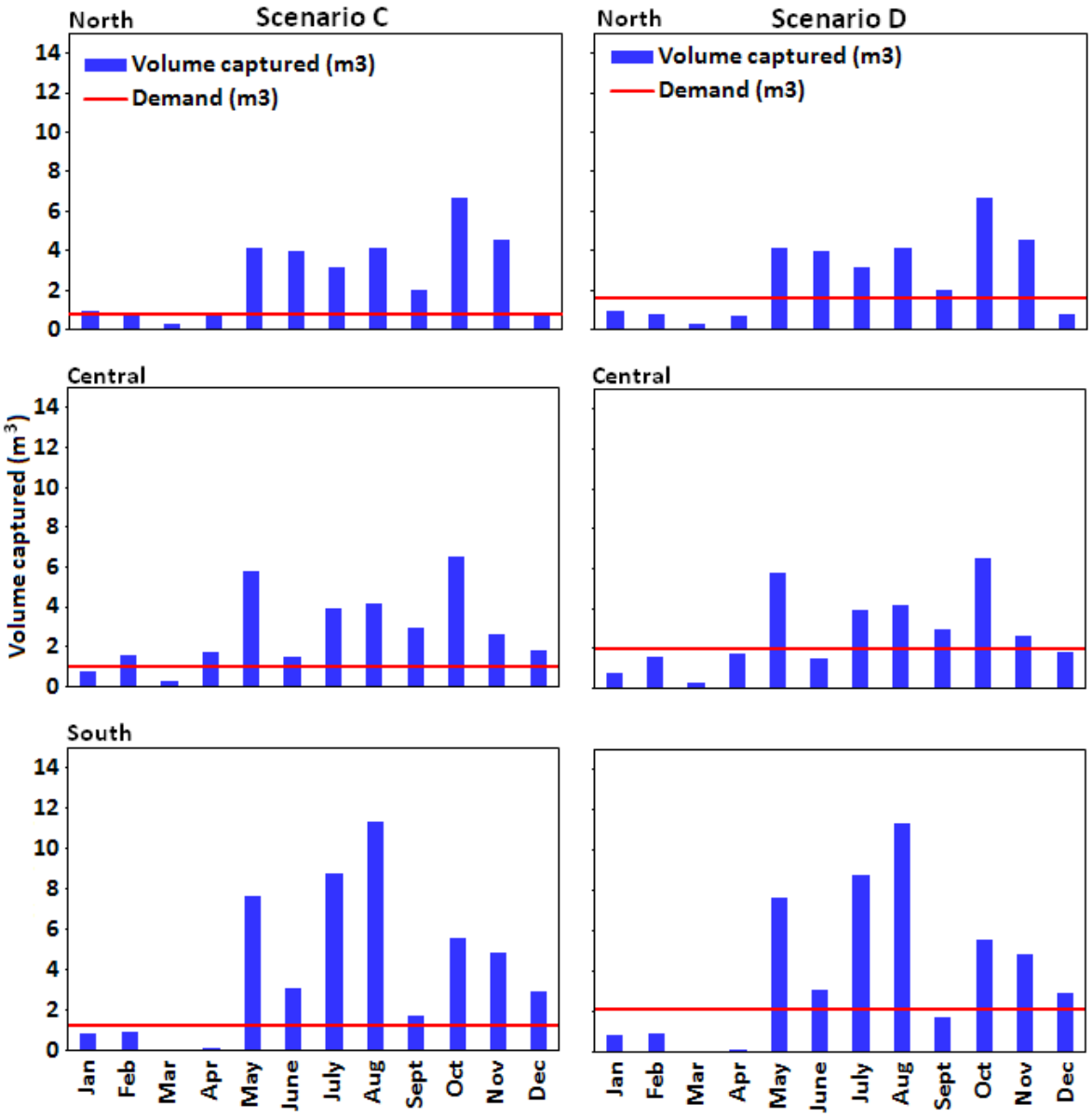

Figure 8.23: Monthly harvestable rainwater for scenarios C and D using lowest rainfall years 2002, 1995 and 1999 for the northern, central and southern Maldives, respectively. Average monthly household rainwater demand (potable) in cubic metre for each region (northern = 0.8 central = 1.0, and southern = 1.1 for scenario C, and northern = 1.6, central = 2.0, and southern = 2.2 for scenario D) is indicated by the horizontal line. Monthly harvestable rainwater (volume captured) and water demand for each region and each scenario were computed based on roof size, household size, and water use per capita/day as defined in Table 8.23.

8.4.4.3 Storage tank size determination

Although field surveys reveal the current average and most common rainwater tank size used by households (presented in Table 8.24 for each region), it is important to determine appropriate rainwater storage tank sizes to meet household rainwater demand throughout the year. Gould and Nissen-Peterson (1999) and Peters (2003) pointed out that there are several

methods or techniques available for estimating approximate storage sizes. These include dry period demand, tabular and graphical methods (CEHI 2009; Gould and Nissen-Peterson 1999). In the dry period demand method, the longest average dry period without any significant rainfall is considered and the tank size is determined by:

$$\boldsymbol{TS = N_d \times HD}$$

where TS = tank size (storage capacity in litres), N_d = no of dry days and HD = daily household rainwater demand (in litres). The daily household rainwater demand is estimated by multiplying lpcpd by the number of occupants. Although the dry period demand is easy to apply for estimating tank size roughly, it ignores the rainfall and roof size to deliver the necessary runoff to fill the tank and does not take account of the variations between different years, such as the occurrence of drought years, and hence it is not recommended to use this method if other methods and the necessary rainfall data are available (Gould and Nissen-Peterson 1999). Hence, determination of appropriate storage tank sizes using the dry period demand method is not considered in this research.

Table 8.24: Average and most common tank size used by households for collecting rainwater from roof catchments (based on field survey data).

Description	Northern	Central	Southern
Available average tank size (L)	4000	3800	3700
Most common tank size (L)	2500	2500	2500

It was clear from above (Figure 8.22 and Figure 8.23) that the monthly rainwater supply exceeds the monthly rainwater demand in the month of May for all scenarios discussed above and that this month represents the beginning of monsoon season (monsoon onset or commencement of the monsoon) for the Maldives, as discussed in Section 4.4.1. An example of estimating the minimum storage tank size using the tabular method for the southern region starting with the month of May is illustrated in Table 8.25 for scenario A. The minimum required storage size is the maximum volume stored (indicated in *) minus the volume left at the end of year (the last value in "volume stored" column, marked with * and sometimes called surplus water left at the end of the year) (CEHI 2009). The estimates of storage tank size for the four scenarios using the tabular method are presented in Table 8.26. As can be seen from these data, the estimated smallest minimum rainwater tank size (1200 L) is for the northern region for scenario A, which is smaller than the average and most common rainwater tank size available for the region (4000 and 2500 L, respectively:

Table 8.24). The largest minimum estimated tank capacity for the same scenario is for the southern region (2300 L). Estimated minimum tank size capacity for scenarios A and C are very similar, since the per capita per day consumption for both scenarios are the same and the small difference in tank size is due to the common roof size area ($30\ m^2$) used for scenario C. The estimated storage sizes for scenario C are smaller than the average and most common tank sizes available for northern and central regions, while the estimated tank size for the southern region (2900 L) is larger than the most common tank size (2500 L) but smaller than the average size available for the region (Table 8.24). Furthermore, estimated storage sizes for northern (3500 L) and central (3600 L) regions for scenario B is larger than the most common tank size of 2500 L, but smaller than the average size available for the northern (4000 L) and central (3800 L) regions. On the other hand, for the southern region, the minimum storage capacity estimated for the same scenario is larger (6000) than the regional average (3700 L) and most common tank size available (Table 8.24), but smaller than the average common tank size available for northern and central regions. The estimated tank size for the southern region (2900 L) is larger than the most common tank size (2500 L), but smaller than the average size available for the region (Table 8.24). For scenario D, the estimated minimum storage tank sizes are larger than the regional average and most common tank sizes available for the respective regions.

The estimated minimum storage tank sizes for the four scenarios are consistent with the monthly household rainwater demand shown in Figure 8.22 and 8.23. The minimum storage tank size estimated using the tabular method described here is based on target monthly demand and assumes that the rainwater is collected or harvested almost every month. For example, if rainwater is not collected every month, the storage tanks will become empty within 1.5-2 months time for scenarios A and C. According to Gould and Nissen-Peterson (1999), when demand estimates are being used as the basis for estimating rainwater storage capacity, the estimates should be treated with great caution, especially if the rainwater is the only source of water. As a rule of thumb, it is recommended to 'over-design' the rainwater collecting system to provide at least 20% more than the estimated demand (CEHI 2009; Gould and Nissen-Peterson 1999), and where there is no alternative source of water supply, the safety margin of 20% needs to be increased (Gould and Nissen-Peterson 1999). Gould and Nissen-Peterson (1999) also suggested that when the rainwater level in the household tank gets low, people will tend to use rainwater more sparingly and this informal rationing significantly reduces the chance of rainwater tank becoming completely empty and hence reduces empty tank duration (if it becomes empty). Despite this informal

rationing, it was shown earlier that about 49-63% of the respondents (Table 8.20) of the outer islands of the Maldives indicated shortage of rainwater (household rainwater tanks become empty). Furthermore, 100% of the respondents from each region suggested that rainwater is harvested during the wet season only (Table 8.20). If the estimated minimum storage capacity for different scenarios is used as a guide for storing rainwater to meet the household rainwater demand for cooking and drinking, there is greater chance that the rainwater tanks become empty quite often and may not provide enough rainwater for the dry season. The fact that 100% of the outer islands of the Maldives surveyed rely on the rainwater resource for cooking and drinking and experience shortages of rainwater quite often, and considering the limited alternative water resources available in the outer islands, it might be appropriate for the islands of the Maldives to determine storage tank size by maximising rainwater supply for a given roof area. The alternative mass curve technique determines storage tank capacity by maximising supply (Gould and Nissen-Peterson 1999) and is described below.

Table 8.25: An example of estimating minimum storage tank size required to meet the household rainwater demand for the southern region (scenario A). The first two rows of the table give assumed parameters.

Roof area = 39 (m^2)	**Average occupants = 7.1**	**Average no. of days/month = 30.4**				
Roof coefficient = 0.8	**Average pcpd = 5.7 L**					
Scenario A (southern region)						
Month/ rainfall (mm)	**Supply (m^3)**	**Cumulative supply (m^3)**	**Demand (m^3)**	**Cumulative demand (m^3)**	**Volume stored (m^3)**	**Surplus/ deficit volume (m^3)**
May / 321	10.0	10.0	1.2	1.2	8.8	8.8
Jun / 127.8	4.0	14.0	1.2	2.5	11.5	2.8
July / 364.6	11.4	25.4	1.2	3.7	21.7	10.1
Aug / 474.2	14.8	40.2	1.2	4.9	35.3	13.6
Sept / 72.6	2.3	42.4	1.2	6.2	36.3	1.0
Oct / 231.3	7.2	49.7	1.2	7.4	42.3	6.0
Nov / 202.9	6.3	56.0	1.2	8.6	47.4	5.1
Dec / 123.6	3.9	59.8	1.2	9.8	**50.0***	2.6
Jan / 35.7	1.1	61.0	1.2	11.1	49.9	-0.1
Feb / 40.1	1.3	62.2	1.2	12.3	49.9	0.0
Mar / 2.4	0.1	62.3	1.2	13.5	48.7	-1.2
Apr / 5.6	0.2	62.5	1.2	14.8	**47.7***	-1.1

Note: If correct month is not chosen to start the table, "volume stored" column may contain some negative values. In such cases, the minimum storage tank size can be obtained by finding the largest negative number and changing it to a positive value and adding it to the largest positive number in "volume stored" column. * indicates the maximum volume stored and surplus volume left at the end of the year, respectively. Hence minimum storage capacity required = 50.0-47.7 = 2.3 m^3.

Table 8.26: Estimated storage capacity required to meet the household rainwater demand for the four scenarios.

Description	Northern	Central	Southern
Scenario A			
Minimum storage tank capacity required (L)	1200	1600	2300
Scenario B			
Minimum storage tank capacity required (L)	3500	3600	6000
Scenario C			
Minimum storage tank capacity required (L)	1400	1600	2900
Scenario D			
Minimum storage tank capacity required (L)	4500	3900	6600

8.4.4.4 Mass curve analysis

Mass curve analysis can be used to calculate the storage tank size for meeting a known demand (for example daily, monthly or yearly demand) with a certain probability by maximising the supply (Gould and Nissen-Peterson 1999). This method was originally described by Rippl (1883) and since then the mass curve technique has been adopted and formed the basis for determining storage requirements for many purposes, such as for reservoirs (Gould and Nissen-Peterson 1999). Mass curve analysis involves identification of critical periods in the data (in this case rainfall) where the difference between cumulative supply from rainfall (inflows) and cumulative demand (water consumption or outflows) is at a maximum. This difference represents the maximum volume of rainwater available for future use and hence the maximum necessary rainwater storage capacity required to maximise supply (Gould and Nissen-Peterson 1999). The storage system will perform adequately when the following mathematical relationship is satisfied (Fewkes 2006):

$$\boldsymbol{TS \geq max\left\{\int_{t_1}^{t_2}[D_t - S_t]\mathrm{dt}\right\}}$$

where TS = tank size (storage capacity), D_t = household rainwater demand during the time interval (t), S_t = rainwater supply during the time interval (t) and $t_1 < t_2$. Gould and Nissen-Peterson (1999) provided an application of this method graphically by plotting cumulative supply (cumulative roof-runoff by summing the monthly runoff totals) bar

graphs and cumulative water usage (water demand) line graphs on the same plot. Application of the graphical method of estimating rainwater storage capacity (tank size) required to maximise supply in the Maldivian context for the above four scenarios is illustrated in Figure 8.24 and Figure 8.25. In order to allow some rainwater to remain in the tank at the start (residual volume), the cumulative supply and demand calculation was started with the month of May. As can be seen from these figures, the cumulative supply is far greater than the cumulative demand. For each plot, the maximum difference between cumulative rainwater supply and cumulative household demand (water consumption) is indicated by the red bar (Figure 8.24 and Figure 8.25) and the corresponding values (minimum storage tank capacity required) for the four scenarios are presented in Table 8.27. This represents the minimum rainwater tank size to store incoming rainwater and hence to maximise supply. It should be noted that the rainwater tank capacity required is significantly less than the yearly household rainwater demand (Table 8.23), since significant amount of rainwater is removed from the tank for household uses throughout the year or during the wet season while the tank is filling (Gould and Nissen-Peterson 1999). The only scenario where the minimum storage tank size is smaller than the annual rainwater demand is scenario D. For scenario D, the annual household demand values for northern and central regions are 19300 and 24100 L (Table 8.23), respectively, while the estimated minimum storage capacity to maximise supply for these two regions is 17500 L for the northern and 13500 L for the central region (Table 8.27), still providing enough rainwater to meet household demand. The estimated minimum tank size for the southern region (28800 L: Table 8.27) is larger than the annual demand of 25900 L (Table 8.23). For all other scenarios (A, B and C) and for all regions the estimated minimum required storage tank capacity is higher than the respective scenario annual demand. Hence the storage tanks may never become completely filled and/or they may never become empty/ or never be utilised fully (Peters 2003). One concern that is associated with sizing of storage tank capacity for maximising supply is the higher investment cost of the system. However, this method provides greater security. For the case of the Maldives this method can be justified, since fresh surface water is lacking and fresh groundwater resources are limited (in some of the islands groundwater is not suitable for human consumption) in the islands of the Maldives.

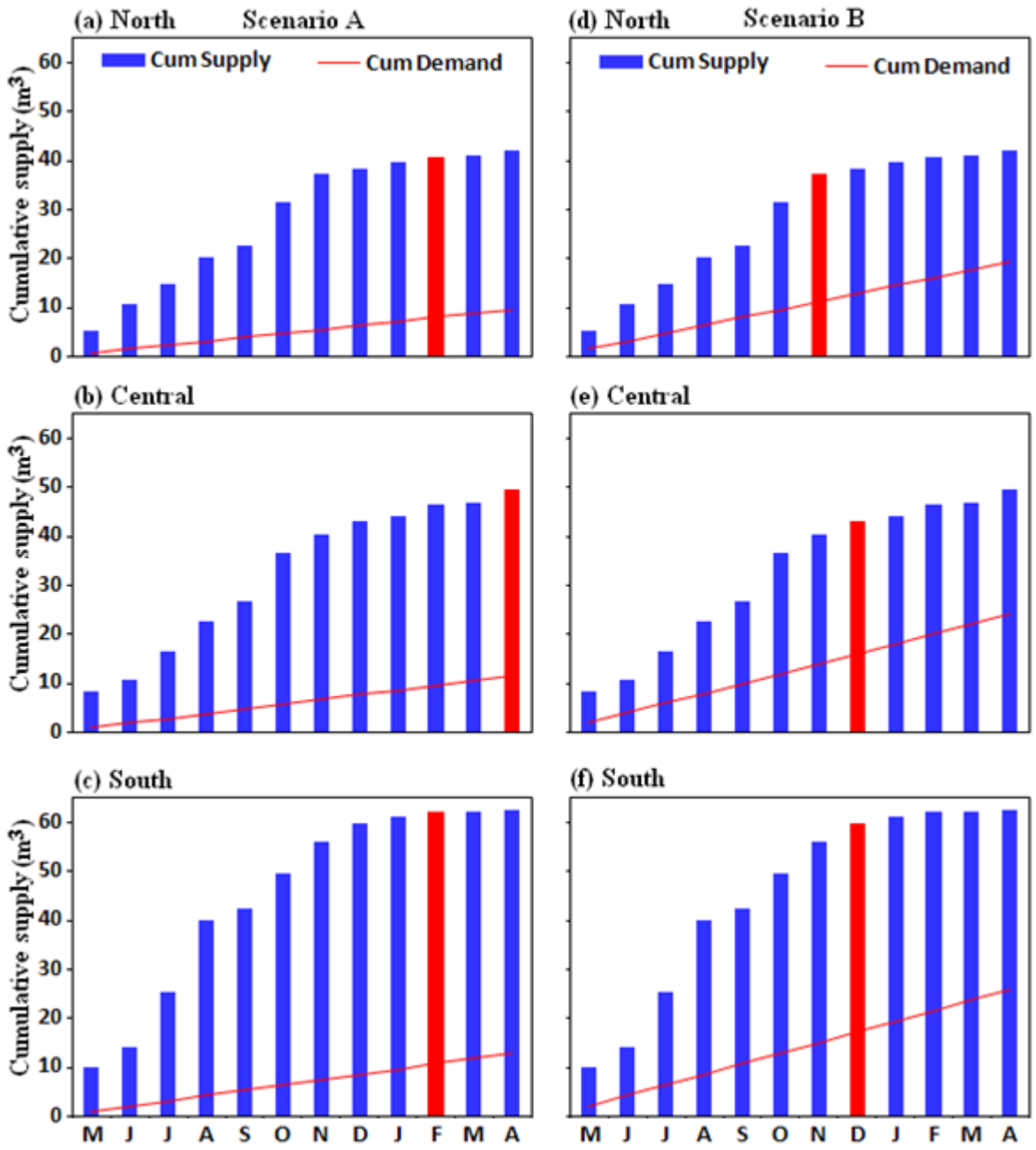

Figure 8.24: Cumulative supply for scenarios A and B (defined above) using lowest rainfall years 2002, 1995 and 1999 for the northern, central and southern Maldives, respectively, is shown by bars. Cumulative household rainwater demand in cubic metres for each region (northern = 0.8 central = 1.0, and southern = 1.1 for scenario A, and northern = 1.6, central = 2.0, and southern = 2.2 for scenario B) is indicated by the red line. Cumulative rainwater supply and demand for each region and each scenario was computed based on roof size, household size, water use per capita/day, as defined in Table 8.23. The bar in red in each plot indicates the month where the difference between cumulative supply from rainfall and cumulative demand is maximum.

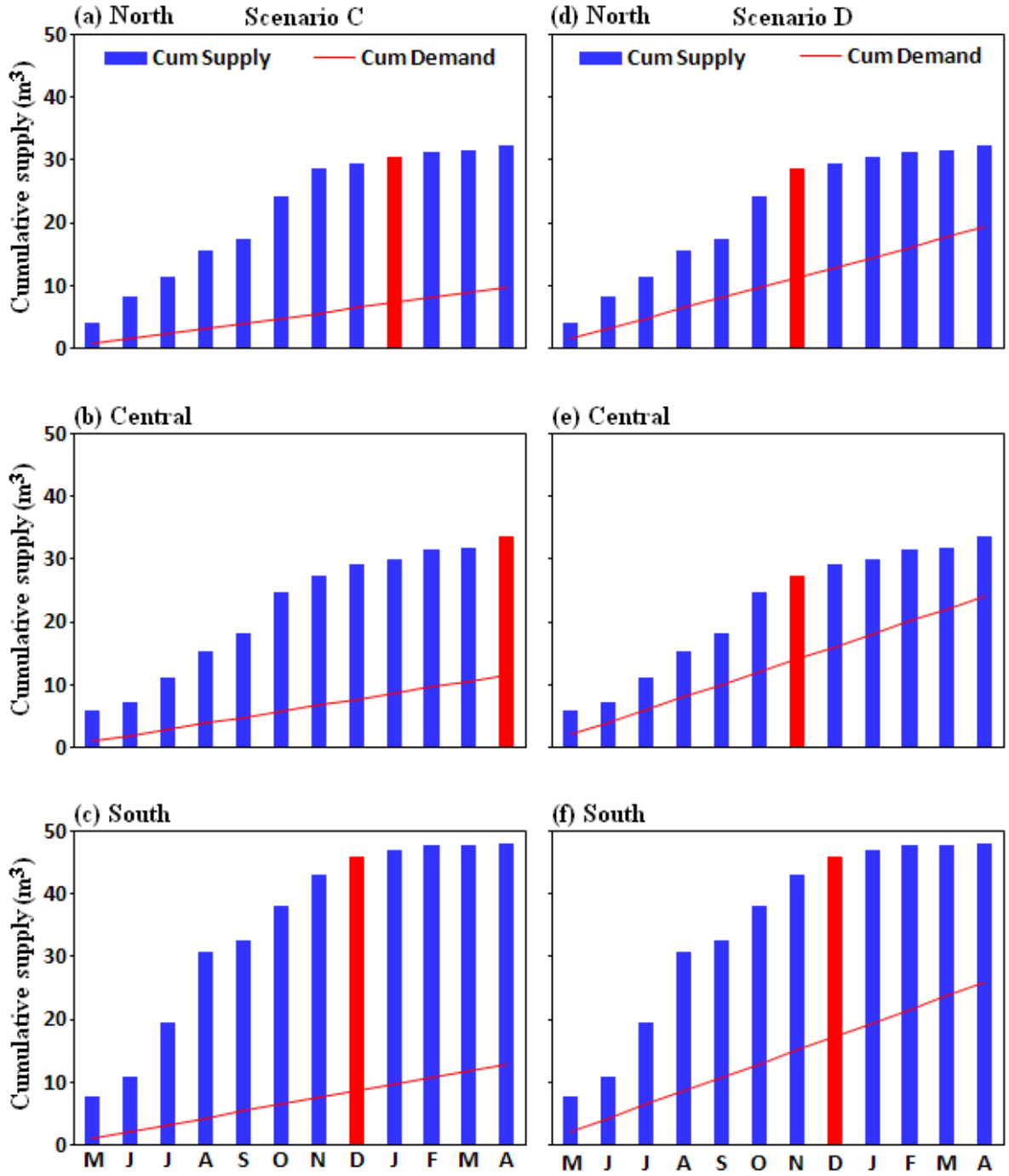

Figure 8.25: Cumulative supply (rainwater) for scenarios C and D (defined above) using lowest rainfall years 2002, 1995 and 1999 for the northern, central and southern Maldives, respectively, is shown by bars. Cumulative household rainwater demand (potable) in cubic metre for each region (northern = 0.8 central = 1.0, and southern = 1.1 for scenario C, and northern = 1.6, central = 2.0, and southern = 2.2 for scenario D) is indicated by the red line. Cumulative rainwater supply and demand for each region and each scenario was computed based on roof size, household size, water use per capita/day, as defined in Table 8.23. The bar in red in each plot indicates the month where the difference between cumulative supply from rainfall (inflows) and cumulative demand (water consumption or outflows) is maximum.

Table 8.27: Storage capacity required to maximise the supply for the four scenarios.

Description	Northern	Central	Southern
Scenario A			
Minimum storage tank capacity (L) required to maximise yearly supply	32600	37800	50000
Scenario B			
Minimum storage tank capacity (L) required to maximise yearly supply	26200	26900	42600
Scenario C			
Minimum storage tank capacity (L) required to maximise yearly supply	23300	22100	36200
Scenario D			
Minimum storage tank capacity (L) required to maximise yearly supply	17500	13500	28800

8.4.4.5 Behavioural analysis

The reliability of supply or, in other words, the probability of system failure (chances of storage tanks becoming empty) has not been analyzed so far in the context of the Maldives. This could be analysed through a combination of mass curve analysis and other statistical methods (Fewkes 2006; Gould and Nissen-Peterson 1999). The reliability of rainwater supply or chances of rainwater tanks becoming empty (rainwater storage tank fails to provide for household demand) is analysed below for different combinations of roof area, tank size and demand using daily rainfall from 1992-2009 for the three regions of the Maldives.

Behavioural analysis is a simulation technique in which inflow (supply) and outflow of various storage tanks are assumed and behaviour of the storage system is observed (Raheem and Khan 2006). The changes in volume of the storage or rainwater tank are calculated using a mass storage equation (Khastagir and Jayasuriya 2007; Khastagir and Jayasuriya 2010; Raheem and Khan 2006), which is mathematically expressed as:

$$\boldsymbol{S_{t+1} = S_t + Q_t - D_t},$$

provided that $0 \leq S_{t+1} \leq C$ is satisfied, where C is effective tank capacity (allowing for dead storage space below the outlet and any air space above the overflow to the tank), S_t is the storage value at the beginning of the t^{th} day, S_{t+1} is the storage volume in the tank at the end of t^{th} day, Q_t is the runoff from the roof (supply) into the tank on the t^{th} day, D_t is

the total rainwater demand on the t^{th} day. When $S_{t+1} = S_t + Q_t - D_t < 0$, it indicates that the tank is empty or cannot provide necessary supply to meet the daily water demand, hence the storage volume is set to zero and when the $S_{t+1} = S_t + Q_t - D_t > C$, it indicates that the water storage level is greater than the tank capacity (C) and is reset to C. Daily runoff from the roof (Q) for each time step is calculated using:

$$\boldsymbol{Q = R_{eff} \times C_R \times ERA}$$

where Q, C_R and ERA were defined previously and R_{eff} is = daily effective rainfall. Daily effective rainfall is defined as the difference between daily rainfall and first flush. The first flush is the initial discharge from the roof surface, which is allowed to go to waste to improve the quality of rainwater collected from the roof, since the initial discharge from the roof top is of poor quality due to dust, sediments, bird and animal droppings, and leaves and debris from the surrounding areas (Khastagir and Jayasuriya 2007; Khastagir and Jayasuriya 2010). According to Yaziz et al. (1989), subtracting the first 0.33 mm of rainfall from the total daily rainfall as the first flush significantly improves the quality of rainwater collected from the roof. On the other hand, AG-DHA (2004) suggested about 20-25 L should be diverted or discharged as first flush from an average roof catchment. According to CEHI (2009), rainfall depth equivalent to 0.5 mm is required to wash off the accumulated contaminants from the roof and this recommendation is adopted here. The water in the storage tank at the end of each day time step is computed using the storage equation above.

The computed volume of rainwater in the storage tank at the end of each day (starting from 16 May 1992) for northern, central and southern regions is depicted in Figure 8.26, 8.27 and 8.28, respectively, for the previously discussed scenarios. These figures indicate that the average and most common size tanks are quite reliable (the chance of storage tanks becoming empty is low) in supplying daily household rainwater demand (for cooking and drinking) when scenarios A and C are considered. On the other hand, the probability of system failure (chance of storage tanks becoming empty) is higher for scenarios B and D for all regions. For all the regions, in scenarios B and D, the rainwater storage tank fails to provide for household demand, since on some days the storage tank becomes empty.

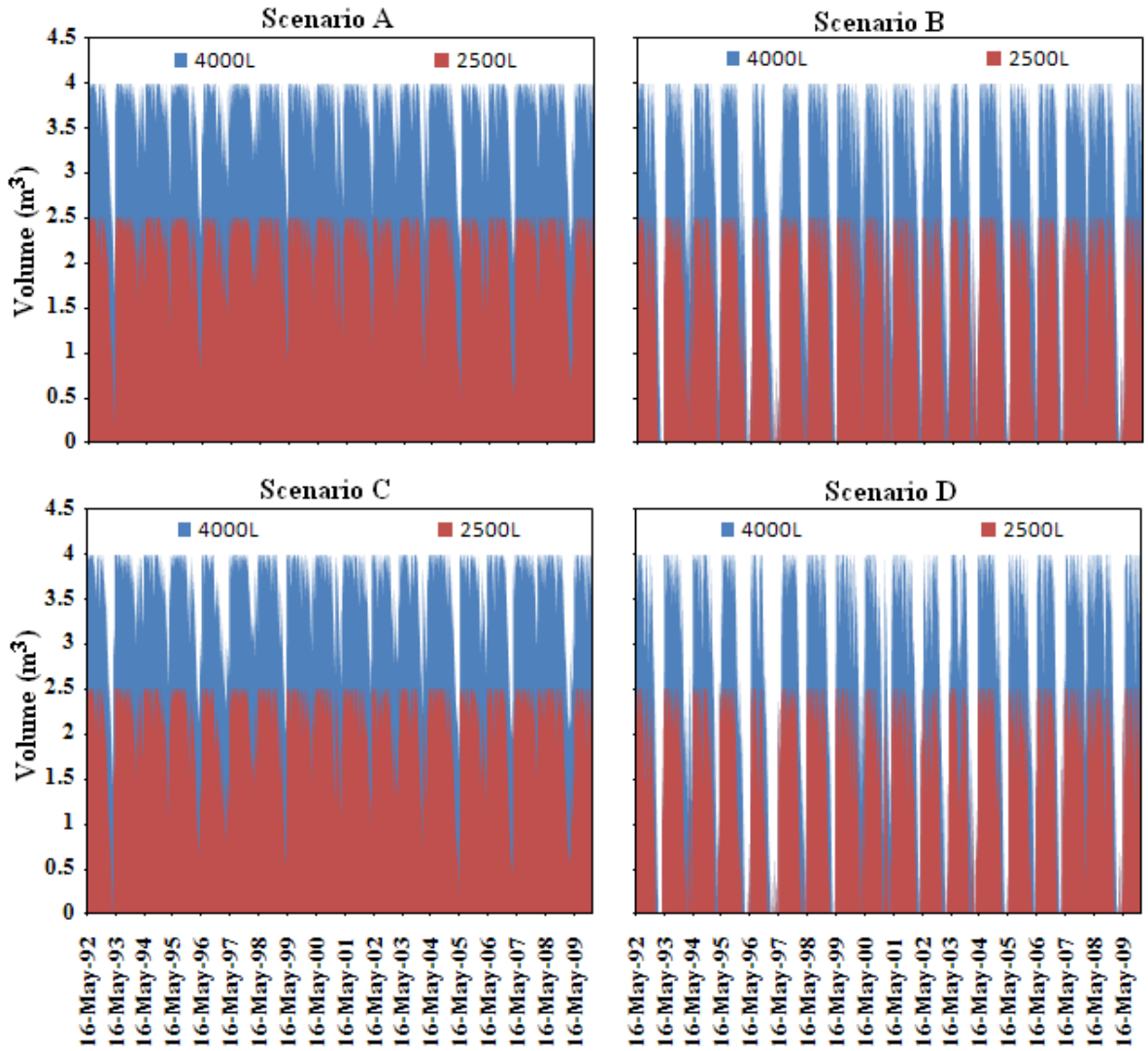

Figure 8.26: Daily changes in volume of rainwater in the tank for the northern region for the four scenarios. For each scenario, changes in volume for average tank size of 4000 L (blue) and most common tank size of 2500 L (red) is shown. The region between the x-axis and the shaded region (blue or red) indicates that the tank is not empty, while if the region between the x-axis and the un-shaded region (white) is zero then it indicates that the tank is empty.

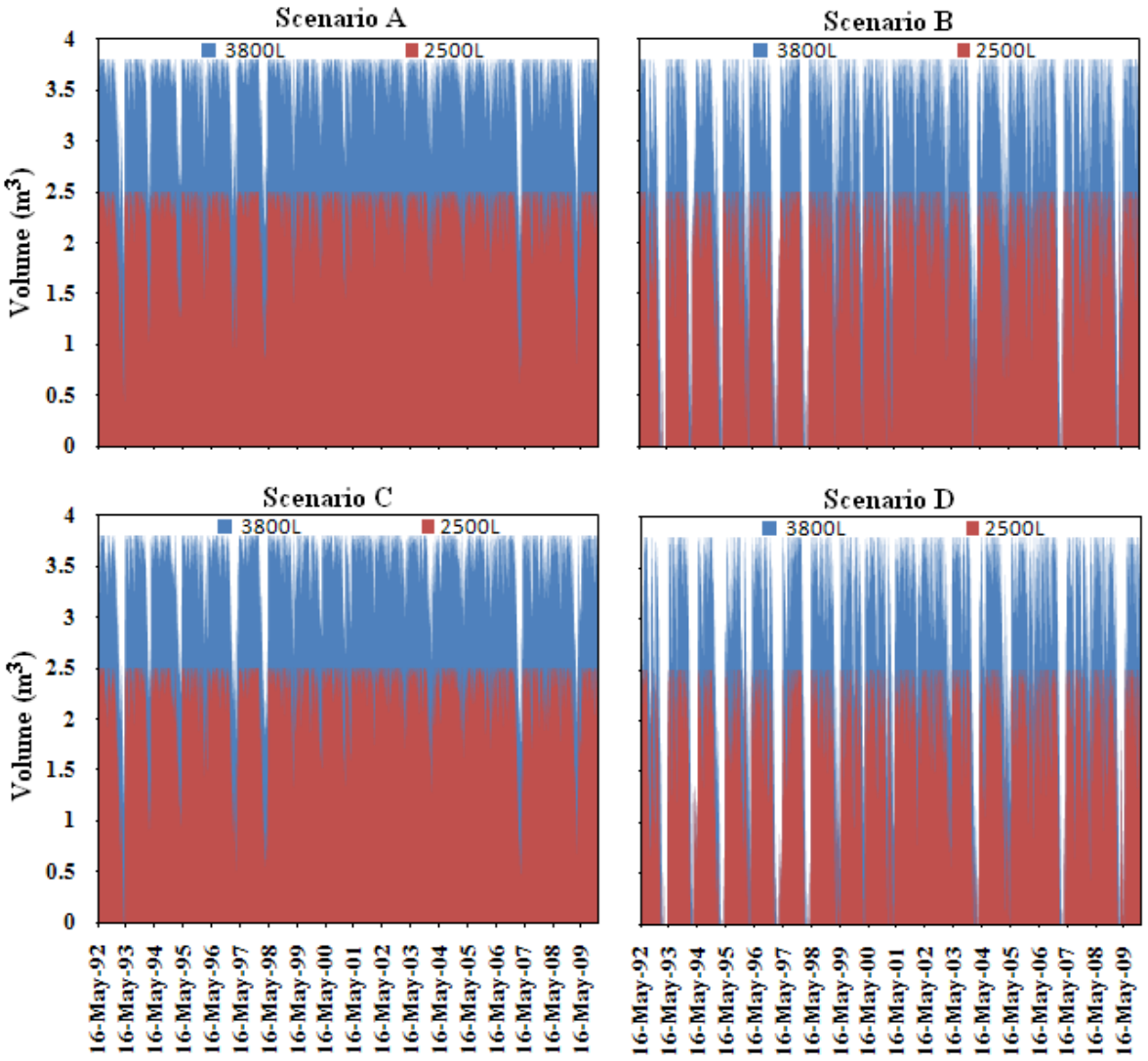

Figure 8.27: Daily changes in volume of rainwater in the tank for the central region for the four scenarios. For each scenario, changes in volume for average tank size of 3800 L (blue) and most common tank size of 2500 L (red) is shown. The region between the x-axis and the shaded region (blue or red) indicates that the tank is not empty, while if the region between the x-axis and the un-shaded region (white) is zero then it indicates that the tank is empty.

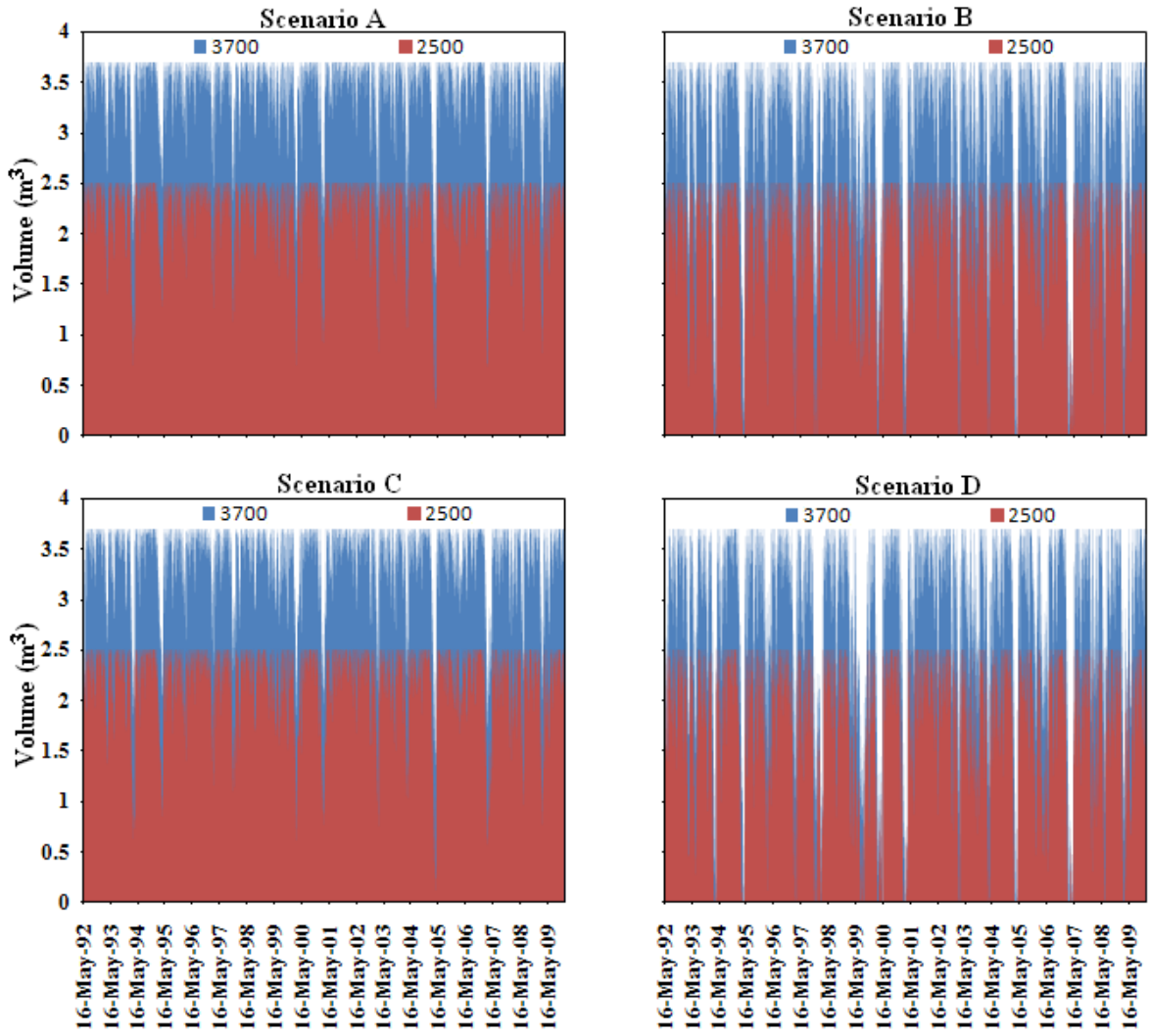

Figure 8.28: Daily changes in volume of rainwater in the tank for the southern region for the four scenarios. For each scenario, changes in volume for average tank size of 3700 L (blue) and most common tank size of 2500 L (red) is shown. The region between the x-axis and the shaded region (blue or red) indicates that the tank is not empty, while if the region between the x-axis and the un-shaded region (white) is zero then it indicates that the tank is empty.

The reliability of storage tanks or the probability of the storage tank having sufficient rainwater to meet the daily demand is computed by a reliability equation (Khastagir and Jayasuriya 2010):

$$Re = \frac{P}{N} \times 100$$

where Re is the probability of the tank being not empty as a percentage (reliability), P is the number of days the tank is not empty and N is the total number of days. The computed reliability for the four scenarios and for the average and most common tanks sizes for the

northern, central and southern region are presented in Table 8.28. As discussed above, for both tank sizes (average and most common tank size) scenarios A and C are 100% reliable in providing the household rainwater demand for all the regions except the central region (for scenario C), where the tank is 99.9% reliable based on today's climate, population and per capita demand. The lowest reliability for all the regions is seen for scenario D (Table 8.28) and hence chances of rainwater tanks becoming empty are highest for this scenario. For each scenario, minimum tank sizes required for 100% reliability were estimated and are illustrated in Table 8.29. For scenario A, the estimated minimum tank sizes for 100% reliability are less than the most common tank sizes available for each region (Table 8.29). Furthermore, for scenario C, the minimum tank sizes for 100% reliability are less than the regional average tank sizes, while for scenarios B and D, the estimated minimum tank sizes are greater than most common and regional average tank sizes.

Table 8.28: Percentage probability (reliability) of the rainwater tank not being empty (reliability of meeting the demand) using regional average tank size and most common tank size (2500 L) for different scenarios based on daily rainfall data.

Regions	Tank size (L)	Probability (reliability) of the tank not being empty (%)			
		Scenario A	Scenario B	Scenario C	Scenario D
Northern	4000	100.0	97.6	100.0	95.6
	2500	100.0	91.9	100.0	89.2
Central	3800	100.0	98.4	100.0	96.9
	2500	100.0	95.8	99.9	93.5
Southern	3700	100.0	99.8	100.0	99.0
	2500	100.0	97.7	100.0	96.2

Table 8.29: Minimum tank size required for 100% reliability for different scenarios based on daily rainfall data.

Regions	Tank size (L)			
	Scenario A	Scenario B	Scenario C	Scenario D
Northern	2400	5800	2600	6800
Central	2100	6500	2700	7100
Southern	2300	4400	2400	4800

From the above analysis it is clear that the most common and regional average tank sizes and average effective roof area could supply the estimated household rainwater demand if rainwater is collected effectively. However, as discussed previously all the regions experienced shortage of rainwater quite often. The newly built houses (built from the tsunami fund for those who were affected by the 2004 tsunami) in some of the islands are equipped with 1500 L rainwater tanks (Figure 8.29), which are smaller than the most common tank sizes and hence may not be 100% reliable for an average household even in present conditions. As it was pointed out previously, nearly 100% of the respondents harvest rainwater during the rainy season. This behaviour needs to be changed, since most of the islands rely completely on rainwater for potable uses. Hence, rainwater should be harvested throughout the year on a daily basis (whenever possible) after discarding the first flush. This would enhance the reliability (would minimise the number of days that the rainwater storage tank fails to provide for household demand) of the storage tank and would minimise chances of rainwater tanks becoming empty. It should be noted that the above minimum tank sizes required for 100% reliability are based on 1992-2009 rainfall data and it is wise to have tank sizes larger than the storage tanks estimated above to allow for unexpected variations in the patterns of rainfall and demand in the future. Furthermore, the above estimates assume that the same number of occupants live in the household throughout the year and the same quantity of rainwater is used per day by each occupant throughout the year. However, in reality, the demand will not remain static and needs to consider changes in water demand due to climate change (warming), population growth, changes in technology and changes in number of household occupants. Water demand analysis associated with these changes are beyond the scope of this study.

Figure 8.29: Newly built houses in Laamu Gan. The rainwater tank sizes in these houses are smaller than the most common tank sizes observed during the field survey.

8.5 Maldives agricultural sector

Despite the poor soil, limited arable land and limited water resources, the agricultural sector of the Maldives has been a fundamental sector in terms of providing crucial support to the livelihood of the people of the Maldives (MFAMR 2006). Although the agricultural sector of the Maldives accounts for only about 2.7 % of the GDP, it is important to the atoll and island communities in terms of generating employment opportunities and promoting food security and self-reliance (MFAMR 2006). The domestic agricultural products account for only 10% of the country's food requirements. Estimates indicate that the share of domestic fruit supply is relatively higher than that of vegetables, and it is estimated that the domestic fruit and vegetables account for 12% and 1% of the total quantity of available domestic fruit and vegetables, respectively, while 88% and 99% is accounted for by imported fruits and vegetables, respectively, in 2003 (MFAMR 2006). It is believed that 90% of Maldives food requirements are met through importation of staple food items such as rice, floor, potatoes, edible oil and sugar (the other 10% from the domestic agricultural products), and it is estimated that about US$ 32.4 million worth of

vegetable products were imported in 2003 alone (MFAMR 2006). In recent years, the agricultural sector of the Maldives has shown a steady growth, with the increase in both private and public sector investments, and has become commercially significant, with demand for fresh agricultural products increasing due to the expansion of the tourism sector of the Maldives (MFAMR 2006; UNEP 2005).

8.5.1 Crop growing season(s) and land allocation

The Maldivian farmers grow crops in two seasons. According to MFAMR (2006), the major growing season coincides with southwest monsoon season (wet season: from May to September) and crops are grown extensively during this season, since all the regions of the Maldives receive substantial rainfall (Figure 3.5) during this season. The minor crop growing season coincides with the northeast monsoon (dry season: from November to March). Due to the limited rainfall during this period of the year, crops are grown less extensively compared to the wet season. The most common crop locally produced in the Maldives is the coconut which is found in almost all the households in the outer islands of the Maldives and grown throughout the year. Table 8.30 shows the different types of crops grown on farm sites of the islands where significant farming is practiced. Figure 8.30 shows a papaya farm and its fruit. Island communities also grow cops within household compounds, referred to as backyard farming. Some of the crops grown in this way include breadfruit, banana, mango, chilli, papaya, pumpkin, cucumber, eggplant and cabbage.

Table 8.30: Most commonly grown crops on farm sites in the Maldives (based on field survey data).

Northern	Central	Southern
Banana, beans, cabbage, carrot, cassava, chillies, cucumber, eggplant, kale, lady's finger, lettuce, papaya, passion fruit, plantains, pumpkin, rock melon, snake gourd, sweet potato, tomatoes, water spinach and watermelon	Banana, betel, bitter gourd, cabbage, chillies, Chinese cabbage, cucumber, Dorset-Naga, eggplant, kale, papaya, passion fruit, pumpkin, radish, ridged gourd, snake gourd, sweet potato, tomatoes, and watermelon	Banana, beans, beetroot, cabbage, capsicum, cassava, cauliflower, chillies, Chinese cabbage, cucumber, eggplant, kale, lady's finger, leeks, lettuce, maize, onion, papaya, passion fruit, pumpkin, snake gourd, sponge gourd, sweet potato, taro, tomatoes and watermelon

Figure 8.30: Papaya are commonly produced in the islands of the Maldives and are consumed by the locals.

Due to the limited area of cultivable land area, communal land in inhabited islands was allotted free of charge by the government (Islands Offices) for growing crops (MFA 1996; MFAMR 2006). Table 8.31 shows allocated farm plot sizes for agricultural purposes together with well depth obtained from farm sites. In 1991, only 30 islands had been

identified as agricultural islands on the basis of the population engaged in agriculture, which rose to 42 in 1993, and by 1996 the number of agricultural islands increased to 60. Apart from this, by 2004, the government of the Maldives leased 32 uninhabited islands for commercial agriculture development (MFAMR 2006). The total cultivable land area is estimated to be about 2670 ha, which includes 1770 and 900 ha of land area in inhabited and uninhabited islands, respectively (MFAMR 2006).

Table 8.31: Plot sizes allocated to farmers for growing crops and depth of the wells within farm sites (based on field survey data).

Parameters		Northern	Central	Southern
Plot area **(m^2)**	Minimum	45	130	279
	Average	1616	8537	4040
	Maximum	10219	52024	23225
Well depth (m**)**	Minimum	0.6	0.9	1.0
	Average	1.0	1.2	1.2
	Maximum	1.3	1.5	2.0

8.5.2 Agricultural sector water resources

The Maldives agricultural sector depends on two types of water resources:

1. Rainwater: during the rainy season (May-November), especially during the days when it rains (rain-fed agriculture).
2. Groundwater: during the dry season (December-April).

As Table 8.32 indicates, no groundwater is used for watering crops if it rains, suggesting that the farmers depend on rainfall for watering crops, especially during the rainy season. However, some farmers pointed out that a small amount of groundwater is used for washing small crop plants on rainy days to eliminate fungal infection (some farmers believe that the rainwater causes fungal infection on small plants). It is clear from the table that 100% of the farmers depend on groundwater for watering crops, especially during the dry season. 100% of the farmers also suggested that groundwater is most commonly used during the dry season. Like households, on farm sites groundwater is extracted from the wells in two ways (Table 8.32); manually using containers connected to a stick ($dhaani$) (Figure 8.10) and using electrical pumps (Figure 8.11, top). Farmers use two methods for watering their crops:

1. Manually using watering jugs (Figure 8.31, top)

2. Manually using a hose (Figure 8.31, bottom).

Those farmers who extract groundwater manually use watering jugs, while those who have electric pumps on their farm sites use a watering hose for watering crops.

Table 8.32: Agricultural sector water resource statistics based on field survey data.

Description	Northern	Central	Southern
Number of farmers interviewed:	31	33	31
Do you use groundwater for watering crops? (%)			
Yes	100	100	100
No	-	-	-
How do you obtain groundwater? (%)			
Manually from farm site well	94	33	45 (6)*
Using electric pump	6	67	61
Is there any difference in ground water usage in your farm between May-November/December-April?			
Yes	100	100	100
No	-	-	-
During which period of the year is ground water used most commonly?			
December-April (dry season)	100	100	100
May-November (wet season)	-	-	-
Do you use groundwater for watering your crops if it rains? (%)			
Yes	-	-	-
No	100	100	100

Note: The common percentage value for both manual and electric pump is indicated as ( )*

Figure 8.31: The most common methods of watering the crops in the Maldives (the watering jugs are filled manually or a hand held hose is used).

8.5.3 Water consumption by the agricultural sector

With the intensification and commercialisation of agriculture, freshwater requirements for irrigation will increase in the Maldives (MFAMR 2006) and it is important to quantify the amount of water used by the farms. Currently no data are available regarding irrigable water (MFAMR 2006) and the quantity of water used for irrigation. In order to estimate the quantity of water used for watering the crops (for the days when plants were watered), observations were made at each farm site and discussions were held with the farmers. For the case of watering jugs used for watering crops, farmers indicated that a certain number of watering jugs were used per plant or 'plant well or hole' (Figure 8.32). Plant well or hole is referred to as the dip on the ground on which plants are grown. The number of plant wells or holes were obtained from the farmers (in some cases it was counted) and farmers were asked about how many times crops were watered per day. Based on this information, the quantity of water used per day by each farm site was estimated using the following equation:

$$\boldsymbol{Q_{cw} = N_{jug} \times S_{jug} \times N_{times}}$$

where Q_{cw} is quantity of water used for watering crops (for the days when plants were watered) , N_{jug} is the average number of jugs used per time and S_{jug} is the size of the jug used (litres) and N_{times} is the average number of times crops were watered per day. For the case of hoses being used for watering crops, the same approach is used for calculating the hose water flow rate. Hose water flow rate was determined for each farm site that uses hoses (since different size of the hoses were used by different farms) by filling a known volume container and by finding the time taken to fill the container (the type of container shown in Figure 8.13, bottom right (yellow bottle)) was readily available from most of the farms). Farmers were asked about the average time the farmers spend watering crops each day and the average number of times crops were watered per day. Based on this information, the daily total amount of water used per day was estimated using the following equation:

$$\boldsymbol{Q_{cw} = W_{FRH} \times T_{RT} \times N_{times}}$$

where Q_{cw} is quantity of water used for plant watering (for the days when plants were watered) , W_{FRH} is the hose water flow rate (L/min), T_{RT} is the average time that the hose is turned on (minutes) and N_{times} is the average number of times crops are watered per day.

The estimated quantity of water used for irrigation by each region is illustrated in Table 8.33, together with the quantity of water used per square metre per day. The amount of groundwater used for watering crops differs regionally and differs from farm to farm. This is because the plot size, type and amount of crops grown on each farm differ. According to Gould and Nissen-Peterson (1999), a small vegetable farm could easily require about 500 L per square metre (L/m^2) per year. When the daily average values were converted to yearly values, the quantity of water used varied between about 205 and 737 L/m^2 per year, with an average of about 483 L/m^2 per year, which is very close to Gould and Nissen-Peterson's (1999) estimate. The number of farms or plots obtained from the discussions held with the farmers and locals are presented in Table 8.34. The average quantity of water used by the farms for each island illustrated in Table 8.34 was computed based on regional average plot area (Table 8.31) and average amount of water use per square metre Q_{psm} (Table 8.33) and was obtained using the following expression:

$$\boldsymbol{Q_{AF} = A_p \times Q_{psm}}$$

where Q_{AF} is the total quantity of water use by the farms (L), A_p is plot area (m^2) and quantity of water per square metre (L/m^2). The island of Gn. Fuvahmulah uses the highest quantity of water /day (162852 L: Table 8.34) for agricultural operations. On the other hand, when the daily quantity of water used by the agricultural sector of each island is converted to lpcpd equivalent value (quantity of water per day divided by the population of respective island), the highest value of 131 lpcpd (Table 8.34) was obtained for HA. Baarah. When agricultural water use (lpcpd equivalent) is combined with the household water use (Table 8.34, right column), it further suggests that the groundwater extracted is very close to the lpcpd sustainable yield given in Table 8.17. For the case of HA. Baarah, the groundwater extracted (317 lpcpd: Table 8.34) exceeds the sustainable yield of 291.8 lpcpd (Table 8.17).

Figure 8.32: The marked circles indicated the dips on the ground for growing plant, which are referred as plant wells or holes by the Maldivian farmers. Most of the farmers indicated that they use one watering jug (10 L) per 3 holes or plant wells.

Table 8.33: Quantity of groundwater used per day per farm site based on field survey data.

Parameters		**Northern**	**Central**	**Southern**
Quantity of water used (L)	Minimum	160	243	729
	Average	1287	2257	1786
	Maximum	4453	11664	10000
Quantity of water used (L/m^2)	Minimum	0.20	0.02	0.07
	Average	2.02	0.56	1.39
	Maximum	7.75	1.87	5.16

Table 8.34: Estimated daily total quantity of groundwater usage by the farms for each island (based on field survey data) and combined estimates of groundwater usage by households and the agricultural sector (lpcpd equivalent). The combined estimates of water usage in lpcpd were computed by adding water used for agriculture (lpcpd) to respective regional estimates of household water usage (lpcpd) given Table 8.14.

Island name	No. of farm plots	Quantity of water (L)/island	Water usage for agriculture (lpcpd equivalent)	Combined water usage by households & agricultural farms (lpcpd equivalent)
Northern				
HA. Kelaa	11	35908	17	203
HA. Baarah	21	68551	131	317
Sh. Feevah	13	42436	44	230
HDh. Finey	8	26115	15	201
Average	**13.25**	**43252**	**52**	**238**
Central				
K. Kaashidhoo	23	109957	52	251
AA. Thoddoo	28	133860	83	282
L. Gan	17	81272	25	224
L. Hithadhoo	15	71711	71	270
Average	**20.75**	**99200**	**58**	**257**
Southern				
GDh. Vaadhoo	19	106696	115	310
Gn. Fuvammulah	29	162852	26	221
S. Hithadhoo	14	78618	7	202
S. Meedhoo	12	67387	7	202
Average	**18.50**	**103889**	**39**	**234**

8.5.4 Water resource related issues faced by the agricultural sector

According to MEEW (2007), the Maldives agriculture sector is already under stress due to poor soil, limited arable land for cultivation and due to water scarcity, and changes in precipitation patterns will provide extra pressure. There are two direct consequences for the Maldives agricultural sector associated with monsoon rainfall variability. An increase in frequency of extreme rainfall events will flood the agricultural lands, damaging the crops. According to Moosa (2006), the islands with agricultural activities are the islands which are more prone to flooding. Since the agricultural crops of the Maldives are mainly rain-fed (MFA 1996), an increase in drought events (prolonged dry periods) will reduce the

availability of water for crop growth. Droughts may decrease groundwater recharge (since recharge depends on rainfall as discussed previously) and may increase saltwater intrusion into freshwater lens, thus limiting groundwater availability for crops. As can be seen from Table 8.35, the agricultural sector of the Maldives currently also faces flood, prolonged dry periods and salinity problems. In addition to this, about 15-39% of the farmers indicated that they experience shortage of groundwater (Table 8.35), mostly during the dry season. This is consistent with the findings of Falkland (2001a), that the groundwater level in the wet season is higher than in the dry season and the water levels in wells increases after heavy rainfall, since recharge from rainfall increases after a rainfall event. Table 8.36 shows the years when the farmers experienced drought and flood events since 1992 and their corresponding percentage among those farmers who indicated shortage of water and flood events. The table indicates that the farmers do not experience shortage of water and flood events every year. Similar to the flood and drought events experienced by the households (Table 8.21)**,** there appears to be no one-to-one relationship between the flood and drought events identified for the three regions in Figure 4.25 and the flood and drought years identified by the farmers (Table 8.36), for the same reasons pointed out previously.

Table 8.35: Indication of water resource problems faced by the agricultural sector of the Maldives (based on field survey data). Number of farmers interviewed from each region is given in Table 8.32.

Description	Northern	Central	Southern
Have you experienced shortage of groundwater on your farm?			
Yes	15	33	39
No	85	67	61
Shortage of groundwater during which period of the year (%)?			
December-April (dry season)	100	100	100
May-November (wet season)	-	18	-
Have you experienced drought/ prolonged dry period/shortage of rain for your farm (%)?			
Yes	62	48	61
No	38	52	39
Shortage of rainwater during which period of the year (%)?			
December-April (dry season)	100	69	100
May-November (wet season)	-	31	-
How long does a shortage of rainwater last for (%)?			
1-2 months	48	50	42
2-3 months	33	31	53
3-4 months	19	19	5
Have you experienced flood related damage to your farm (%)?			
Yes	79	58	77
No	21	42	23
During which period of the year?			
December-April (dry season)	-	-	-
May-November (wet season)	100	100	100
Respondents who indicated salinity in farm wells (%)			
	3	12	16
Actual measured salinity in farm wells (%)			
	26	42	29
Salinity measurement (ppm)			
Average	0.15	0.14	0.11
Maximum	0.30	0.36	0.13

Note: The common percentage value is indicated as *.

Table 8.36: Year of occurrence of drought and flood events and their percentages among those farmers who indicated shortage of water and flood events (based on field survey data).

Description	Northern	Central	Southern
In which years since 1992 did your farm experienced shortage of groundwater?			
Years and percentage	1998 (20%) 2002 (20%) 2008 (20%) All the years (40%)	1998(18%) 2004(64%) All the years (18%)	2005 (25%) All the years (75%)
In which years since 1992 did your farm experience drought/prolonged dry period/ shortage of rain?			
Years and percentage	1992 (5%) 2002 (10%) 2007(10%) 2008(86%) All the years (5%)	1997 (19%) 1998 (6%) 2004 (13%) 2008 (44%) All the years (13%)	1998 (5%) 2000 (5%) 2005 (5%) 2005 & 2008 (5%) 2008 (79%)
In which years since 1992 did your farm experience flood related damages?			
Years and percentage	2007 (48%) 2008 (22%) All the years (33%) Not sure (4%)	2003 (5%) 2004 (5%) 2006 (5%) 2007 (37%) 2008 (32%) All the years (26%)	1998 (17%) 1998+2006+2007 (4%) 2003+2005 (4%) 2005(4%) 2006 (4%) 2006+2008 (4%) 2007 (29%) 2007+2008 (8%) 2008 (4%) All the years (21%)

The agricultural sector of the Maldives is likely to be impacted more frequently with prolonged dry events combined with an increase in the frequency of storm surges with the projected sea level rise. Increase in sea level rise will cause storms to be more intense, with higher flood heights (UNDP 2007b) causing saltwater intrusion further inland in the future, and thus leading to reduction of available groundwater.

8.6 Tourism sector water resource

The tourism sector of the Maldives plays a significant role in the economy, contributing about 33% to GDP and has created about 17,000 direct jobs (which is equivalent to half of the civil service jobs). The tourism sector of the Maldives caters for more than half a million people each year (655,852 people in 2009) (MTAC 2010), which is more than the total population of the Maldives. A major factor in choosing the Maldives as a destination by tourists is climate. The Maldives fragile ecosystem is threatened by global warming and natural disasters and any changes in climate could influence the viability and profitability of the Maldives tourism industry (Conrady and Bakan 2008; MEEW 2007). The Maldives tourism sector has been mostly developed on a one-island one-resort concept and these tourist islands are the most vulnerable and least defensible in the world (MEEW 2007). There is no information on tourism sector water resource impacts. Therefore an attempt was made to determine water resource impacts on the tourism sector of the Maldives.

An e-mail based questionnaire (see Appendix 4) was prepared to obtain information regarding the main water resources in the tourism sector and whether the tourism sector faces water resource problems. The e-mail based surveys cost considerably less, consumed less time and were more accessible (since e-mail communication among businesses, such as in the tourism industry, is popular and widely used) compared to traditional mail or personal interviews (Amira 2009; Meho 2006). Unlike the traditional face-to-face interview surveys, internet based (e-mail) survey questionnaires give more time to consider answers to particular questions rather than having to give an immediate response, and this can be considered an advantage (Amira 2009; Frankfort-Nachmias and Nachmias 1996). One of the disadvantages of an e-mail based questionnaire is that it is not guaranteed that the questionnaire will be completed and returned by the intended respondent to the researcher (Amira 2009; Bernard 2006). As with any survey method, an e-mail survey can be impacted by a low response rate. Low response rate survey research findings will be less valid and will have an effect on generalizing the research findings (Frankfort-Nachmias and Nachmias 1996; Simsek 1999). As far as response rate is concerned, as a means of gathering information, an e-mail survey has been used effectively in academic, scientific, and business contexts and has reported response rates ranging from 19.3% to 76% (Anderson and Gansender 1995; Simsek 1999).

At present nearly 100 tourist islands operate in the Maldives and are scattered along a length of about 830 km across the Maldives (MEEW 2007; MTAC 2010). At the time of

survey, 88 resort islands were in operation. For a country like the Maldives where the tourist islands are scattered over a large area (the islands are separated by sea), some of the the deciding factors for choosing an e-mail based questionnaire (survey) includes ease of distribution, less time consuming and low cost compared to other forms of survey (Amira 2009). The questionnaire was e-mailed (a list of tourist islands and contact details were obtained from the Maldives tourism promotion board, through personal communication) to the tourist resort islands, and they were requested to participate in the survey by completing the questionnaire, and the respondents were asked to return the completed questionnaire to the researcher. Due to the low response rate, the respondents were reminded by e-mail (after giving ample time to respond) and each time all the important material was included in the reminders (including the questionnaire), in case previously sent information and questionnaires had been deleted (Meho 2006). Some studies recommend limiting the number of reminders to one or two, suggesting that if more reminders were sent the respondents may construe this as successive pressure to continue participation Meho (2006). Two reminders resulted in only one resort island responding to the questionnaire, hence it is not possible to carry out tourism sector water resources analysis based on e-mail survey data.

8.6.1 Review of tourism sector water resources

During the field trip to the Maldives, I had discussions with a number of tourism sector personnel and also discussions were held with Ministry of Housing and Environment officials. From these discussions, it seems that the government has produced strict guidelines regarding the water resources in the tourism sector.

The regulations on the Protection and Conservation of Environment in the Tourism Industry (Maldives Tourism Act : Law No. 2/99) state that ((MTAC 2009):

1. Permission from the Ministry of Tourism and Civil Aviation should be obtained if anything which may adversely affect the vegetation or freshwater lens of the island is to be carried out (clause 2.1)
2. Groundwater shall not be extracted for the purpose of construction in an island or land leased for the development of tourism (clause 2.9).
3. For the purpose of provision of clean and safe water sufficient for use in the resort, every resort shall have a desalination plant. The plant shall be registered with the Maldives Water and Sanitation Authority in accordance with the

"Regulation on Desalination Plants", and shall comply with such regulation in the operation of the desalination plant (clause 6.1)

4. Clean and safe water that would be sufficient for 5 days, for use of tourists and staff and for all its purposes, shall be stored at every resort, Picnic island, marina or other place made for tourists (clause 6.3)
5. No resort, picnic island or marina shall do any activity that would contaminate the water table of the island (clause 6.4)
6. Groundwater taken from any resort, picnic island or marina shall not be used for drinking by guests or staff, and shall not be supplied to guest rooms or toilets of guest rooms or for use by staff (clause 6.5)
7. Drinking water shall be stored safely in a manner that it is not contaminated. The quality of drinking water shall not be lower than that set by the relevant government authority (clause 6.6).

Desalinated water has been used in the tourist resort islands since the beginning of the tourism industry in the Maldives in the early 1970s. Each island has its own desalination plant and desalinated water is most commonly used for cooking, washing and bathing, while imported or locally produced bottled water is used for drinking (Ibrahim 2008; Millar 2002). Table 8.37 outlines the results of a e-mail survey conducted by Millar (2002) of selected tourist resorts in the Maldives. Ibrahim (2008) pointed out that some of the tourist islands use wastewater for irrigation purposes. It appears that the tourist islands mainly use desalinated water for the tourists and some rainwater is used only for staff drinking purposes. From this it can be concluded that the water resources sector of the tourism industry of the Maldives is not under great threat. However, associated with climate change, water resources in the tourism sector might be impacted indirectly (MEEW 2007).

Table 8.37: Water resources used by the tourism industry for different purpose. Taken from taken from Millar (2002).

Purposes	**Type of water**
Toilets	Saltwater
Shower	Desalinated water
Cooking	Desalinated water
Drinking (tourists)	Bottled water
Drinking (staff)	Rainwater (treated)
Garden	Rainwater (tank)

8.6.2 Mitigation and adaptation measures

Rainfall deficiency over the last 18 years indicates that the Maldive islands are prone to drought and flood events, drought events occurring every 9 years, while flood events occur once every 6 years. Climate change is expected to increase the severity, duration and frequency of weather related extreme events, such as droughts and floods. As discussed above, the Maldives water resources and agricultural sector are vulnerable to these impacts. Since flash flood and drought events are the result of global, regional and local scale phenomena, they cannot be avoided. Hence, mitigation and adaptation strategies need to be identified, and have to be implemented from the individual household and farmer level to communities and to national government level to reduce the impacts. Full assessment of mitigation and adaptation options is beyond the scope of this study. Some general mitigation and adaptation measures are discussed below.

Mitigation measures: One of the most important non-structural mitigation measures to minimise impacts associated with flash floods is forecasting and issuing flood warnings. From the government level, the existing flash flood prediction/forecast system needs to be improved in order to provide accurate forecasts and timely dissemination of flood warnings. Timely forecasts and dissemination of warnings will help to make informed decisions by the concerned authorities and local people for better flood preparedness. According to Ammentorp et al. (2006), even a few hours of advance warning can reduce the losses of lives and property considerably. Another measure is flood hazard mapping. Due to the geographical nature of the islands (e.g. shape) some islands and some areas in some of the islands (such as wetland areas) are more prone to floods than other islands. Flood prone areas in these islands need to be identified and modelled for different rainfall threshold categories and flood-generating rainfall levels should be determined. Unlike floods, droughts develop over a longer period of time, and it is possible to reduce the impacts associated with droughts by implementing appropriate mitigation measures planned in advance, according to the indications provided by monitoring systems (Rossi et al. 2007). No drought monitoring system exists in the Maldives and strategic national policy for drought management is lacking. According to Rossi et al. (2007), formulation of guidelines for drought mitigation measures and for their appropriate use, in relation to different drought conditions, can be extremely helpful, and one of the important aspects of implementing an efficient drought management strategy includes identifying measures in advance, to mitigate drought impacts on the water resources sector, the productive sectors

and the environment. Hence, a national framework on drought management needs to be formulated and an effective drought forecasting and monitoring system for the evaluation of drought risk needs to be adopted, for timely implementation of drought mitigation measures. For an efficient strategy to cope with drought, three categories of drought mitigation measures identified include (Rossi et al. 2007):

1. **Measures oriented to increase water supply**

These measures include interventions that enable improvement of the water supply during drought through better use of the existing water system resources, the utilization of new water supply sources and the adoption of proper managing rules in the use of water resources.

2. **Measures oriented to reduce water demands**

These aim to reduce the water use in order to meet water requirements regardless of reduced water supplies. Such measures include legal restrictions, rationing (also based on a rational and fair re-allocation of limited water resources), economic incentives, as well as adoption of water re-cycling and water saving techniques.

3. **Measures oriented to minimize drought effects**

These measures are oriented to minimize drought impacts, and refer essentially to a reduction of damages or other negative consequences caused by a drought event, through risk spreading. It includes drought forecasting based on monitoring systems, public campaigns to increase awareness of drought events, insurance, and change in agricultural practices.

Adaptation measures: It is certain that adaptation measures taken in advance will reduce the impacts associated with drought or prolonged dry periods, as well as impacts associated with flash floods. A list of adaptation measures is given in Table 8.38. Apart from the adaptation measures identified in the table, provision of desalination plants of adequate capacity to supplement rainwater shortage, or where groundwater is not suitable for human consumption, should be considered as another adaptation measure. A comprehensive study into the feasibility of the identified adaptation options needs to be carried out in the context of the Maldives. Since about 23-37% of the households indicated flood related damages, it is important for household to adapt to flood events. Adaptation measures to minimise household flooding include avoiding settlement in flood prone areas, and building new houses that are elevated above the ground level. Another measure that could minimise household flooding is by establishing proper drainage systems in the islands.

Table 8.38: Adaptation measures to minimise impacts associated with drought and flood events.

Sector	Adaptation measures
Water resources (household)	**Groundwater resources:** 1. Promotion of indigenous practices for sustainable water use (manual extraction and washing clothes and dishes by hand) (Falloon and Betts 2010; Kundzewicz et al. 2007) 2. Enhance quality of groundwater resources through establishing sewerage systems on outer islands. 3. Minimise groundwater extraction and waste 4. Improve water saving techniques through use of water efficiency fixtures, such as efficacy taps and shower heads 5. Promotion of recycling of water and wastewater re-use (Falloon and Betts 2010; Kundzewicz et al. 2007) 6. Metering and pricing to encourage water conservation (Falloon and Betts 2010; Kundzewicz et al. 2007) 7. Legal restriction of groundwater resource use, especially during drought conditions **Rainwater resources:** 1. Standardising a legal minimum storage tank size based on household occupants. 2. Provision of more rainwater storage tanks 3. Increase rainwater storage tank capacity (Kundzewicz et al. 2007) 4. Increase in effective roof area (will help to fill the storage tanks more quickly) 5. Promotion of frequent rainwater harvesting (whenever possible)
Agriculture	1. Avoid farming in flood prone areas 2. Promote use of drought and heat, and saline-resistant crops 3. Promote early maturing crops and crops requiring less water use 4. Change crop sowing dates based on monsoon onset 5. Utilize pressurized water systems or underground or drainage water to avoid unnecessary water losses and apply mulch to reduce water losses due to evaporation. 6. Use of mini ponds to harvest rainwater

9 Summary and conclusions

The primary objective of this research is to understand the nature of the variability of the Asian monsoon and its influence on precipitation patterns over the Maldives, and the associated downstream impacts on water resources. Hence, the two main research aims defined in the introduction are:

1. To investigate the variability of the Asian Monsoon and its influence on precipitation patterns over the Maldives.
2. To examine possible downstream impacts of monsoon rainfall variability on the Maldives.

Various characteristics of the Asian monsoon and its influence on the monsoon precipitation patterns of the Maldives have therefore been investigated.

Because no previous studies have explored rainfall variability over the Maldives, this thesis began by providing a descriptive analysis of the rainfall regime over the Maldives. In this regard, temporal and spatial variability of the yearly and monthly rainfall across the Maldives was explored together with the relationship between rainfall and other meteorological variables.

Characterisation of monsoon variability on different time scales (interdecadal, interannual and intra-seasonal) for the whole Asian, Indian and Maldives region was investigated. Despite most of the countries in the Asian monsoon region having criteria for identifying monsoon onset and withdrawal dates, no objective criteria existed in the case of the Maldives and hence objective assessment of the actual monsoon season was lacking. This research has therefore developed criteria for determining the monsoon season objectively for the Maldives.

It is obvious that surface and upper air meteorological parameters such as temperature, pressure, geopotential height and wind could influence the spatial and temporal variability of monsoon rainfall. The influence of various meteorological parameters (sea surface temperature, mean sea level pressure, outgoing long-wave radiation, air temperature, humidity and wind) on the spatio-temporal variability of monsoon precipitation over the Maldives was investigated. The most significant of these parameters were then used to develop the first ever regression model to predict core monsoon season (June-September: JJAS) precipitation for the Maldives. Monsoon rainfall

prediction for the Maldives is very important for the water resource and agricultural planning purposes, so this is a key achievement.

The monsoon circulation is the result of atmospheric circulation responding to the annual cycle in the differential solar heating that occurs within the ocean-atmosphere-land system. Among the interactions that take place within the ocean-atmosphere-land system, global scale processes such as the El Niño-Southern Oscillation (ENSO) play a key role in modulating the Indian Ocean (IO) interannual climate variability. ENSO acts as the strongest natural fluctuation of climate on interannual time-scales that influences the weather and climate around the globe. Connections between the observed precipitation patterns over the Maldives and ENSO related circulation patterns were therefore investigated.

Snow cover influences the continental surface energy budget and is regarded as a crucial component of regional climate systems. Both observational and numerical studies suggest that the Eurasian winter/spring snow cover is an important factor affecting the Asian summer monsoon. In particular, the Eurasian winter/spring snow cover has been considered an important regional factor influencing the thermal conditions of the Asian continent, and hence the seasonal-to-interannual variability of the succeeding Asian summer monsoon and rainfall. None of the previous studies have examined the possible relationship between Eurasian snow and the Maldives monsoon rainfall (MMR: June-September), so that this relationship was explored for the first time in this thesis.

The monsoon has its own interannual variability, called the Tropospheric Biennial Oscillation (TBO) which is considered to be a major feature of the Indo-Pacific region due to strong coupling between the ocean and atmosphere over the Asian-Australian monsoon area. The large-scale interactions between land, ocean and atmosphere in the Indian and Pacific Ocean regions plays an important role in the monsoon system alternating between strong and weak years. Furthermore, it is believed that the land and ocean surface conditions in March-May (MAM) over the Indo-Pacific region play an important role in TBO monsoon transitions. There is no documentation of observed monsoon rainfall variability over the Maldives and its relationship with TBO. Hence, the role of the TBO in the context of the Maldives monsoon rainfall variability has been investigated for the first time.

Being one of the main aims of this research, the rest of the thesis examined the downstream impacts on the Maldives associated with monsoon rainfall variability. Any changes in global and regional processes, such as ENSO and TBO, now and in the future,

could impact on monsoon season rainfall over the Maldives, and in turn have negative consequences for the country. The most direct downstream impacts related to monsoon rainfall variability are likely to be associated with the increase in frequency of extreme flood and drought events. Based on field surveys carried out in the Maldives (described in Section 8.3) and other available local data, the flood and drought impacts and related water resource issues faced by the Maldives were investigated.

9.1 Summary of main findings

9.1.1 Descriptive analysis of rainfall variability in the Maldives

- Analysis of spatio-temporal patterns of annual rainfall over the Maldives show considerable variability. The Maldives annual rainfall varied between 1346.5 mm (for the north: Hanimaadhoo) and 3185.7 mm (for the south: Gan). Although the annual rainfall shows an overall decreasing trend, results of the Spearman's non-parametric test indicate that there is no significant trend in Maldives annual rainfall (for any of the meteorological stations). Similarly, average monthly rainfall also varied from month to month, with most rain falling during the period May to November (extended monsoon season) and relatively little falling outside this period, especially for the northern (Hanimaadhoo) and central (Hulhule) areas. A significant positive relationship (CC = 0.98, obtained for the northern region, Hanimaadhoo) was found between monthly average rainfall and rainy days. Spatially, there is an increasing trend of annual rainfall from north to south (with an average rainfall of 1755.9, 2017.2 and 2243.9 mm for the northern, central and southern Maldives, respectively). This descriptive analysis (space-time distribution of annual rainfall) will serve to detect changes in rainfall patters (associated with climate change or due to natural variability) over the Maldives in the future.

9.1.2 Characterisation of monsoon variability

- This research has provided an objective determination of the Maldives monsoon season or the length of the rainy season for the Maldives based on monsoon onset and withdrawal dates. The results based on wind/rain and an OLR index clearly demonstrate that the onset and withdrawal dates vary greatly from one year to another, and hence that the Maldives monsoon season or length of rainy season is characterized by large interannual variability. The mean LRS based on the OLR index criteria is 204 days, with a standard deviation of 18 days, while the mean LRS based on the rain and wind

criteria is 11 days shorter (193 days, with a standard deviation of 14 days). The average onset date for the whole of the Maldives based on rain and wind criteria was 13 May (a 9 day difference from the average onset date based on the OLR index), while the average withdrawal date for the whole of the Maldives based on rain and wind criteria was 21 November, which is very close to the average withdrawal date obtained from the OLR index (23 November). The OLR index suggested that the average onset date was 4 May with a standard deviation of 11 days for the 15 year period. The results suggest that monsoon onset dates in some years were in close agreement between the rain/wind and OLR based criteria (e.g. years 2000 and 1993), while in other years the onset differed by more than one month between the two methods. The biggest difference between the onset date obtained using the two methods was 31 days (in 2002), while the withdrawal date differed by 29 days (in 2003) when the two methods were compared. The monsoon onset dates are more variable for the southern Maldives (coefficient of variation of 76%), while the onset dates are least variable for the northern Maldives with a coefficient of variation of 29%. On the other hand, monsoon withdrawal dates are more variable for the north and least for the south, with coefficients of variation of 70 and 53%, respectively. This result also demonstrates that the earliest monsoon onset for the Asian region occurs from south of the Maldives in April and then moves north to establish monsoon onset for the whole Asian region in June. Furthermore, the monsoon withdrawal starts from India in September/October and then moves south, with complete withdrawal from the southern parts of the Maldives in November/December.

- Fourier spectral analysis indicates that, on the interdecadal time scale, the Maldives monsoon rainfall is characterised by periods ranging from about 12-15 years. The Asian region also shows clear differences in spatial variability in monsoon rainfall on the same time scale, as inferred from spatial rainfall anomalies for different periods, specifically the decades 1979-1988 and 1989-1998, and the period 1999-2007. The time series of monsoon rainfall and percentage monsoon rainfall anomaly also reveal interdecadal variability, with the mean monsoon rainfall highest during the first decade (from 1979-1988) and lowest during the period 1999 to 2007. Furthermore, a 12.9 year periodicity found for the Asian region monsoon rainfall confirms the observed interdecadal variability of monsoon rainfall. It is interesting to note that the years with large negative monsoon rainfall anomalies (obtained by averaging monsoon season rainfall, JJAS, for the whole Asian region) correspond to El Niño years, suggesting that

ENSO has a significant influence on Asian monsoon precipitation. Spectral analysis indicates that on the interannual time scale, the Maldives monsoon rainfall is characterized by periods ranging from 2.5 - 4 years, similar to the periodicities discovered for the Indian summer monsoon rainfall. Despite the southern Maldives receiving the highest rainfall annually, the percentage contribution to yearly rainfall from monsoon rainfall is lowest for this region. On average, the southern, central and northern parts of the Maldives receive about 62.7, 71.9 and 85.0 % of their annual rainfall from monsoon rainfall. Through principal component analysis (PCA), it was found that the first five principal components (PCs) account for about 49% and 65% of the interannual monsoon rainfall variability, for the Asian and Indian regions (68.75-91.25 °E and 6.25-28.75 °N), respectively. Time series of the scores of the first four principal components show interannual variability for the two regions (Asian and Indian). Since the correlations between the first two principal components and corresponding monsoon rainfall for the Asian and Indian regions is greater than 0.59, the first two principal components represent the dominant mode of interannual monsoon rainfall variability for these two regions. On the interannual time scale, both Asian and Indian region monsoon rainfall show significant peaks with periodicities of about 2.4-3.7 years, which can be attributed to the tropospheric biennial oscillation (TBO). Another significant periodicity in monsoon rainfall (with a frequency of 5.2 years) for the two regions further supports the existence of temporal variability of the monsoon on an interannual time scale that can be attributed to remote forcings, such as ENSO. The Fourier transform analysis revealed existence of important intra-seasonal time scale periodicities (10-20 days and 30-60 day) in daily time series of monsoon rainfall for different regions of Asia (Western Ghats, Bay of Bengal, East Asia, central India and the Maldives Islands: Figure 4.28). Intra-seasonal variability of monsoon rainfall during the monsoon season is characterized by the occurrence of active-break cycles of wet or dry phases, which are revealed by time-latitude cross-sections of monsoon rainfall for the years 2002 and 2003 (identified as drought and normal monsoon rainfall years for India) for different regions of Asia. These results demonstrate that the Maldives monsoon rainfall (as well as the Asian monsoon) is characterized by significant interdecadal, interannual and intraseasonal variability.

9.1.3 Parameters influencing Maldives monsoon variability

- Investigation of different meteorological parameters in relation to spatio-temporal variability of monsoon precipitation over the Maldives led to the identification of factors influencing the Maldives monsoon rainfall as well as those that have predictive potential. Correlation coefficient maps generated for the period 1979 to 2007 between Maldives monsoon rainfall and other parameters reveal that the most significant and influential parameters affecting interannual variability of the Maldives monsoon rainfall (MMR) are mean sea level pressure for May, surface air temperature for February, outgoing longwave radiation for May, sea surface temperature for January, surface and 850, 500, and 250 hPa zonal wind for January, surface relative humidity for April, and 850 and 500 hPa level relative humidity for May. Temporal consistency of these parameters with the MMR was checked for different time periods and parameters that have a significant CC at least at the 5% level for longer time periods (1979-1998 and 1979-2007) were retained. After eliminating the predictors with less influence on the variance of MMR, the predictors which explained significant amounts of variance in MMR were surface relative humidity during April (SRHAPR), 850 hPa level relative humidity during May (850RHMAY) and 500 hPa relative humidity for May (500RHMAY). These parameters were used to formulate a regression model to predict core monsoon season (June-September) rainfall for the Maldives and the final regression model is:

$$MMR = 14.4SRHAPR - 26.3RHMAY_{850} - 12.7RHMAY_{500} + 1689.4$$

The predictors in the regression equation are highly significant and the ANOVA test indicates that the model is significant at the 1% significance level. It also has a multiple correlation coefficient of 0.90. These tests strongly suggest that the predictors included in the model account for a significant part of the variance (76.6%) in the MMR and indicate the usefulness of the model for medium range prediction of MMR. The model will be a valuable tool for water resource managers. However, the model results should be compared with other models (to be developed in the future) and should be re-evaluated in the future using long-term data to check model performance.

9.1.4 Global scale processes: ENSO and monsoon relationship

- To check the connection between ENSO and the monsoon, the ENSO episodes were identified for the period 1979-2007 based on Niño 3.4 region (5ºS-5ºN, 170º-120ºW) SST anomalies. The identified El Niño and La Niña events were sub-classified as strong

and moderate events based on the SST anomalies in the Niño 3.4 region (when the SST anomalies in the Niño 3.4 region equalled or exceeded +1.5 ºC and/or lay between +1.0 and +1.4 ºC for a minimum of three months, they were considered to be strong and moderate El Niño events, respectively, while strong and moderate La Niña events were considered to occur when the SST anomalies in the Niño 3.4 region are less than or equal to -1.5 ºC and between -1.0 to -1.4 ºC , respectively, for a minimum of three months). A total of 3 strong and 4 moderate El Niño events were identified, while there were 1 strong and 3 moderate La Niña events (1/3) during the period 1979-2007. It is evident from the association between the percentage departure of Maldives monsoon rainfall (MMR: based on the 1979-2007 mean) and strong/moderate El Niño and La Niña events that during strong/moderate El Niño years, except 1994 and 1997, the Maldives experienced a deficiency of monsoon rainfall. During the strong/moderate El Niño years of 1994 and 1997 MMR experienced excess rainfall and hence provided some inconsistency in the El Niño and rainfall relationship. Even though the correlation between MMR and AIMR is weak (CC = 0.26, insignificant at the 5% level), it is interesting to note that the All-India monsoon rainfall (AIMR) also tended to have deficient/excess rainfall during the same strong/moderate El Niño years that MMR experienced a deficit/excess in monsoon rainfall. The results also show that there is a tendency for the Maldives and the AIMR to be associated with excess rainfall during strong/moderate La Niña events. The 1999 La Niña event is an exception to this relationship, when MMR experienced a deficiency in monsoon rainfall (14.6%) and the AIMR also experienced a slight deficiency. It is worth noting that both MMR and AIMR tend to have deficient/excessive rainfall during the same strong/moderate La Niña events (Figure 6.4). The results clearly demonstrate that the Maldives/India region experiences deficiencies in monsoon rainfall about 71.4% of the time during strong/moderate El Niño events, while the Maldives/India regions experience excessive monsoon rainfall about 75% of the time during strong/moderate La Niña events, suggesting that the deficient/excess monsoon rainfall over the Maldives and India regions is linked to the strong/moderate El Niño/La Niña events, respectively. This finding is consistent with previous findings that most of the drought years over India are associated with El Niño events, while the La Niña events are associated with flood events (Kane 1998; Kumar et al. 1995; Rajeevan and Pai 2006). Changes in SST in the eastern equatorial Pacific can influence the monsoon through changes in atmospheric circulation, namely the large-scale Walker circulation (WC) which plays a major role in

large-scale atmospheric vertical motion. In comparison to the non-ENSO SST composite anomaly, a very distinct anomalously positive (warming) and negative (cooling) SSTA pattern was found in the central Pacific Ocean for the case of El Niño/La Niña composites, especially in the Niño3.4 region. The anomalously cool SST in the eastern tropical Pacific during La Niña is accompanied by a shallow equatorial thermocline in the east and strong trade winds blowing towards the west. The equatorial upwelling due to strong easterly winds induces stronger surface cooling in the eastern basin creating an east-west SST gradient, and helps to builds up heat in the western tropical Pacific. Heat and moisture (water vapour) gathered during this process helps intensification of atmospheric deep convection and upper-atmospheric westerly winds over the western Pacific warm pool, and this in turn leads to enhanced near-surface flow back to the east (warm air rising over the warmer waters of the western Pacific and descending over the cooler eastern Pacific), thus establishing a strong WC during La Niña events and enhanced precipitation in the Asian region, including the Maldives area. The reverse happens during El Niño events, when El Niño related wind anomalies over the Indian basin cause deep convection to move from the west Pacific warm pool to the central Pacific, causing subsidence and reduced precipitation over Indonesia and off Sumatra, and below-normal rainfall over India and the Maldives.

- Atmospheric heat sources (near-surface convergence areas) and heat sinks (near-surface divergence area) inferred from velocity potentials and divergent wind at 200 and 850 hPa pressure levels indicate that the low velocity potentials are associated with divergent outflow, while high velocity potential regions are associated with convergent inflow. The 200 hPa divergent wind for the El Niño case shows a weak elongated divergent outflow pattern (instead of the east-west dipole that was observed for the non-ENSO and La Niña cases), originating from the central Atlantic Ocean and reaching the Indian Ocean. This is consistent with observations that warm air rises over the entire equatorial Pacific during El Niño events, thus weakening the Walker circulation in El Niño events. Spatial patterns of velocity potential for El Niño minus La Niña (Figure 6.13d) clearly show that during the El Niño events the velocity potential is higher in the Pacific region, originating from the South Pacific Ocean. The positive velocity potential anomalies (El Niño minus La Niña: Figure 6.13d) over the entire equatorial Pacific suggest that the convergent inflow occurs across the entire equatorial Pacific region during El Niño events (Figure 6.13d) and is consistent with the SSTA. Due to the basin

wide convergence inflow, the Walker circulation becomes weak, influencing the monsoon flow during El Niño conditions. The higher velocity potential and strong divergent wind flow pattern for the El Niño case indicates that the flow pattern is influenced by the underlying sea surface conditions. Convergence centres are associated with warm SSTA in the eastern Pacific during El Niño and divergence is associated with cold SSTA in the Pacific during La Niña, causing enhanced and deficient rainfall over the Asian region, including the Maldives, during La Niña and El Niño events, respectively.

- The lower-tropospheric (850 hPa level) monsoon mean wind flow (June-September) for the El Niño and La Niña episodes indicates that the cross-equatorial flow in the Indian Ocean region is weaker during El Niño conditions (Figure 6.14a) compared to the La Niña conditions (Figure 6.14b), further supporting that the monsoon flow is different during El Niño and La Niña conditions. A closer look at the wind flow in the Asian region also reveals that the wind direction anomaly pattern for the El Niño is opposite from its counterpart La Niña condition, as has been suggested in previous studies. In the case of El Niño, the maximum wind anomaly in the western Pacific is much weaker and more shifted towards the east (Figure 6.15a). During La Niña, easterly flow dominates (Figure 6.15b) where the maximum wind anomaly occurs when compared to the El Niño, whereas during El Niño episodes westerly flow (Figure 6.15a) dominates in the region of maximum wind anomaly, causing the atmospheric deep convection to be suppressed over the tropical Indian Ocean during such events. The El Niño related wind anomalies over the Indian Ocean cause deep convection to move from the western Pacific to the central Pacific during El Niño events, thus reducing precipitation over the Indian Ocean region. Deep convective activity (low OLR, inferred from outgoing longwave radiation for the monsoon season, June-September, during El Niño and La Niña conditions) also indicates that the convection during El Niño conditions is less compared to La Niña episodes for the Indian region, including the Maldives area, while deep convection in the Pacific Ocean is more pronounced and extends more to the east and covers most of the equatorial Pacific region during El Niño conditions, compared to the La Niña case. The difference between El Niño and La Niña conditions (El Niño minus La Niña: Figure 6.17c) also clearly indicates that the Pacific region is dominated by a strong negative anomaly (deep convection) and the Asian region has a strong positive OLR anomaly, suggesting suppressed convection during El Niño episodes.

This is also consistent with the observed El Niño velocity potential pattern (Figure 6.13b and d). Velocity potentials are higher in the central Pacific region and sinking air (convergent inflow) is more evident during El Niño. Evolution of convective activity (as inferred from OLR anomaly patterns) is very consistent with the SSTA shown in Figure 6.8, further suggesting that monsoon activity is closely linked to the SSTA in the Pacific. More specifically, the amplitude of OLR anomalies averaged over the latitude band 2.5º S – 7.5º N (Maldives region) and for all longitudes for El Niño and La Niña cases indicates that during El Niño conditions, anomalously high OLR anomalies persist for the latitude band extending from West Africa (10º E) to the western Pacific Ocean (150º E), suggesting that convection is suppressed for the Maldives during El Niño conditions. A very contrasting and opposite OLR anomaly for the Maldives area (as indicated by the arrows in Figure 6.19) is evident during El Niño and La Niña conditions, hence supporting the notion that El Niño is associated with suppressed (reduced) convection, while La Niña conditions enhance monsoon activity for the Maldives area. The calculated vertically integrated moisture transport anomaly for the El Niño and La Niña cases for the Maldives region (2.5ºS-7.5ºN latitude band) is very similar to the corresponding El Niño and La Niña OLR anomalies (Figure 6.19) averaged for the same latitude band. During El Niño conditions moisture is suppressed over the Maldives area, while during La Niña conditions the Maldives region experiences enhanced VIMT, indicating that there is a tendency for a decrease in precipitation over the Maldives during El Niño episodes and enhanced precipitation during La Niña conditions. This is also further demonstrated by vertical velocity patterns at 500 hPa level (mid-tropospheric level) for El Niño and La Niña events. Analysis of patterns of vertical velocity indicate that upward motion (rising air) is enhanced during the La Niña case, especially over China and the western Pacific Ocean, compared to the El Niño conditions, while strong ascending motion (rising air) is located in the central Pacific during El Niño episodes (Figure 6.21a). At the same time, vertical velocity maxima (upward) are located over south-west India, the Maldives and the Indonesian region during the La Niña case. Regions of strong ascending motion (rising air) that are apparent during La Niña conditions are reversed in El Niño conditions. The strong ascending motion over the central Pacific during El Niño is shifted more to the west during La Niña. The weak Walker circulation associated with the El Niño causes the deep convection to move from the western Pacific warm pool to the central Pacific. Vertical cross-sections (longitude-height) of vertical velocity

composite anomaly patterns for the El Niño and La Niña events averaged over the Maldives (2.5° S-7.5° N latitude band) clearly demonstrate that during El Niño, the Maldives region is dominated by a positive vertical velocity anomaly, or increased downward motion (descending/sinking/subsidence action) and during La Niña the opposite is evident. This demonstrates that there is a tendency for a decrease in precipitation over the Maldives during El Niño episodes and enhanced precipitation during La Niña conditions. The fact that some of the excessive and deficit monsoon rainfall years for both the Maldives and India corresponds to non-ENSO events, demonstrates that factors unrelated to ENSO events also play an important role in some years (Kane 1998). The results show that during most of the non-ENSO events (55.5% of the time), monsoon rainfall over the Maldives and India is out of phase, indicating that monsoon rainfall over the Maldives during non-ENSO events is influenced by different factors from those affecting India during the same events. The processes influencing monsoon rainfall over the Maldives during non-ENSO events therefore needs to be investigated in future.

9.1.5 Regional scale processes: Part A - Eurasian snow cover and monsoon relationship

- Although previous studies have found strong significant inverse relationships between winter/spring snow cover relationship with both Asian and Indian rainfall, the correlations between Maldives monsoon rainfall (MMR) and the Eurasian snow cover anomaly variables (winter snow cover anomaly, spring snow cover anomaly (March-May, MAM) and snowmelt) indicate a very weak relationship with CC = -0.02, -0.02 and -0.18 (insignificant at the 5% level), respectively, demonstrating that there exists only very weak teleconnections between MMR and winter/spring snow cover and snowmelt. No significant correlations were found between all-Maldives rainfall (AMR: calculated using available long term (from 1979-2006) rainfall station data from two stations, Gan and Hulhule) and winter/spring snow cover or snowmelt, further demonstrating that only weak teleconnections exist between snow-cover variables and monsoon rainfall over the Maldives. Furthermore, there appears to be a very weak relationship (CC = 0.01, insignificant at 5% level) between the Maldives monsoon rainfall anomaly and yearly averaged standardized Eurasian snow cover (ESC) anomaly for the period between 1979 and 2007 and very weak correlations were found between the MMR and ESC anomalies for the months January-May in the current year, and

October-December of the previous year. To compare the results obtained between the MMR and snow cover variables, correlation coefficients between all-India summer monsoon rainfall (AISMR) and snow cover variables (winter/spring snow cover and snowmelt) for the same period (1979-2007) were calculated. Although the magnitude of correlation coefficients between the AISMR and other variables is higher when compared with the correlation coefficients obtained between MMR and winter/spring snow cover and snowmelt, none of the correlation coefficients were significant at the 5% level. This contradicts the findings of previous studies on the winter/spring snow cover relationship with both Asian and Indian rainfall, where strong significant inverse relationships have been found (Bamzai and Shukla 1999; Kripalani and Kulkarni 1999). To check the effect on correlations if a different time period was used, correlation coefficients between the winter snow cover anomaly and AISMR were recalculated for the period 1973-94 (the same data period used by Bamzai and Shukla, 1999). The same correlation coefficient (-0.34) was obtained as found by Bamzai and Shukla (1999) for the 1973-94 period. However, the correlation coefficient dropped to -0.18 for the 1979-2007 period, suggesting that the inverse relationship between winter ESC and monsoon had weakened over the more recent time period. A significant reduction in Eurasia snow cover has been observed in recent years and it has been linked to the increased winds in the Arabian Sea during the southwest monsoon phase since 1997. The fact that the monsoon and snow cover relationship has weakened over the more recent time period (the correlation between winter snow cover anomaly and AISMR dropped by a half) suggests that the weak teleconnections found between MMR and snow cover variables might be associated with this weakened relationship. The lag-lead correlation results suggest that a significant teleconnection exists between monsoon rainfall over the southern region of the Maldives and spring snow cover, with monsoon rainfall over the southern region inversely related to spring snow cover. This significant inverse relationship involves spring snow cover leading monsoon rain by lags -6, -5 and -4 (CC = -0.51, -0.45 and -0.45, respectively). Furthermore, winter snow cover also shows a significant inverse correlation at lag +1 (CC = -0.38) with monsoon rainfall over the northern Maldives. In this case, the monsoon rainfall leads the winter snow cover, which is consistent with the relationship between Eurasian winter snow cover and Indian monsoon rainfall and demonstrates that the Eurasian snow cover influences the Maldives monsoon rainfall to some extent. However, influence of Eurasian snow cover

on the Maldives monsoon rainfall needs to be further investigated with the aid of numerical models.

9.1.6 Regional scale processes: Part B - TBO and monsoon relationship

- Results indicate that the biennial tendency of the Maldives monsoon rainfall to go through a transition from relatively strong/weak to relatively weak/strong monsoons in consecutive years appears to be related to the TBO. Among 17 out of 29 TBO years identified for the Maldives monsoon, TBO strong years accounted for 47.1% and weak TBO years accounted for 52.9% of the total TBO years. The identified El Niño and La Niña onset years indicated that not all El Niño or La Niña onset years correspond to TBO years, although El Niño onset years (1982, 1987 and 2002) tend to correspond to weak TBO years, while La Niña onset years (1988 and 2000) tend to correspond to strong TBO years. The formation and propagation of seasonal SST, OLR and wind anomaly patterns for the strong minus weak ENSO TBO and normal TBO year composites demonstrates considerable differences. The discrepancies between ENSO TBO and normal TBO year anomalies for SST, OLR and wind suggest that factors other than ENSO play a role in biennial variability in non-ENSO TBO years (Pillai and Mohankumar 2007). Li and Zhang (2002) suggested that variability of the monsoon on the TBO scale is mainly due to local processes in the Indian Ocean, while ENSO scale monsoon variability is associated with more remote forcings. Although SST composites for ENSO TBO years revealed the presence of dipole patterns (Indian Ocean dipole, IOD, which has been identified as an inherent factor of the IO influencing both the Asian monsoon and TBO), absence of the dipole pattern from the non-ENSO TBO year SST composite suggests that the IOD does not play a significant role in Maldives monsoon rainfall biennial variability during normal TBO years, as indicated by Pillai and Mohankumar (2007) for the case of Indian monsoon rainfall. Despite convective activity re-occurring during each monsoon season in normal TBO years, propagation of the convective zone is mostly limited to the IO region, while for the case of ENSO TBO years, the maximum convective activity lies in the western Pacific region during the Australian monsoon season, and a biennial tendency of convective activity is evident for the IO region. Wind anomalies for the strong minus weak ENSO TBO and normal TBO years also demonstrated a biennial cycle, demonstrating the TBO influence on Maldives monsoon rainfall. Furthermore, the local Hadley circulation (represented by

the height-latitude cross-sections of meridional velocity and vertical velocity averaged over longitudes 60-95º E) indicate existence of biennial variability for both ENSO TBO and normal TBO year cases, with upward motion during a strong monsoon season and downward motion during previous and following monsoon seasons, suggesting that the local Hadley circulation influences the Maldives monsoon rainfall on a biennial time frame.

- Strong minus weak year SST anomaly composites (based on Maldives monsoon rainfall filtered on the TBO and ENSO time scales separately) for different seasons suggests that the evolution of anomalies is different for the TBO and ENSO time scales. Significant changes in SST anomaly over the Indian and Pacific Ocean region are evident from one season to another at the TBO time scale. The spatial correlations between filtered Maldives monsoon season rainfall and filtered SST anomalies for the TBO and ENSO time frames, starting from the previous winter to the following winter shows very similar spatial patterns to the TBO mode SSTA evolution. During the proceeding winter (DJF-1) and spring (MAM 0), the Maldives monsoon rainfall positively correlates with the SSTA in the Indian and eastern Pacific Ocean, while a weak negative correlation exists between SSTA in the western Pacific region at TBO time frames. With the onset of the monsoon, the correlation becomes weak in the Indian and eastern Pacific Ocean regions, but a significant negative correlation develops between Maldives monsoon season rainfall and SSTA in the central Pacific region for the case of the biennial time scale (JJA 0), with the maximum positive and negative correlations occurring north of Australia and in the central Pacific, respectively. The inverse relationship that started to develop in JJA (0) over the IO is further strengthened during SON (0) and DJF+1 seasons. This leading (winter and spring) strong correlation between Maldives monsoon rainfall and SSTA in the IO for TBO suggests that the SSTA in the IO play a significant role in strengthening the subsequent monsoon over the Maldives, as indicated for the Indian monsoon by Li et al. (2001). Anomalous positive SST in the IO increases evaporation, thus increasing surface moisture in the region (moisture flux into the region associated with the south-westerly flow) resulting in a strong monsoon. A strong monsoon in turn increases surface wind and leads to cooler than normal SSTA in the IO. This will result in reduction of moisture build-up in the region in the seasons leading up to the next monsoon, resulting in a weak monsoon the following year. Anomalously high moisture flux over the central IO region during

the winter and spring seasons of the TBO time frame is also evident from strong minus weak composites of moisture flux at 1000 hPa for the TBO and ENSO modes starting from the Northern Hemisphere winter season (DJF-1) to the following monsoon season (JJA 0), further demonstrating build-up of moisture prior to the monsoon season for the TBO time frame. The positive correlations between filtered Maldives monsoon season rainfall and filtered SST anomalies in the IO region weakens as the seasons progress from winter (DJF-1) to the next winter (DJF+1), while the correlation in the eastern Pacific region strengthened around the summer season through to the next monsoon season for the ENSO time frame. There is little correlation between the prior season's moisture transport and the monsoon, as no persistent anomalously higher moisture flux was observed over the IO region during DJF(-1) and MAM(0) for the ENSO time frame. The warming observed over the IO for the Maldives monsoon wet conditions and cooling observed over the IO for the Maldives monsoon dry conditions using unfiltered data support the positive lag correlation obtained for the northern winter and spring season between filtered Maldives monsoon rainfall and SSTA for the TBO time frame, and indicates that the results are not due to the artificial outcome of the filters used to separate the data into the TBO and ENSO time frames. The preceding winter season warming/cooling over the IO for the wet/dry conditions further supports the observed build-up of moisture in the IO region one to two seasons prior to the monsoon onset, for the case of the TBO time scale. On ENSO time scale, the eastern Pacific SSTA influences the monsoon through the vertical overturning of the east-west circulation, while the warm SSTA in the western Pacific influences the local convection and tropospheric circulation. Another process that influences the monsoon on an ENSO time scale is related to the remote tropical SSTA forcing of mid-latitude circulation due to the establishment of a meridional temperature gradient between land and ocean. Lagged correlations between monsoon rainfall and the upper tropospheric geopotential height thickness (200 minus 500 hPa) indicate that the spatial correlation pattern for the TBO time scale for the winter and spring is markedly different from the winter and spring seasons for the ENSO time scale and indicates establishment of a north-south thermal contrast across Asia 6-months prior to the onset of the monsoon for the case of ENSO time frame, with the warm core region occurring over the Tibetan Plateau during the DJF-1 season. An elongated warm anomaly originating from the African continent covers the Indian subcontinent and the Indian Ocean region during DJF (-1) and MAM (0) seasons in TBO mode. This suggests that an enhanced/reduced land-ocean thermal

contrast in preceding months is followed by a strong/weak monsoon related to the ENSO signal, but not with the TBO case. The local Hadley circulation on TBO and ENSO time scales for the reference monsoon season (JJA0) and following monsoon season (JJA+1) also indicates differences in local circulation between the two time scales. The ENSO scale weak monsoon season is dominated by ascending motion from 15º S-45º N, without the effect of the local circulation, indicating that the location of the Hadley circulation plays an important role in the TBO time scale variability of the Maldives monsoon season rainfall, in agreement with Pillai and Mohankumar (2009), who concluded that the Indian Ocean fluxes and the local Hadley circulation and their interannual variability are limited to the TBO time scale only. Coupled interactions between transition conditions (500 hPa geopotential height, and equatorial Indian Ocean and eastern equatorial Pacific SST) in the season prior to the monsoon (the MAM season) can influence the Maldives monsoon rainfall as indicated by the singular value decomposition (SVD) analysis. The first SVD component explains about 33.28% of the coupling between monsoon rainfall and Indian Ocean SST, and correlation between the first SVD expansion coefficient time series of these two variables is 0.44. The positive SST in the Indian Ocean in MAM is associated with positive monsoon rainfalls over the western part of the Maldives region, while the eastern part is associated with negative precipitation anomalies originating from the Sri Lanka region. The first SVD component between the eastern Pacific SST and monsoon rainfall explains 28.59% of the total squared covariance between the two variables and the corresponding expansion coefficient time series are correlated with a CC = 0.62. The first SVD component of the 500 hPa height indicates that the southern East Asia area is dominated by positive anomalies in MAM and the positive height anomalies are associated with positive anomalies of monsoon rainfall west of Sri Lanka, explaining 24.87% of the coupling between the first SVD component of 500 hPa height and the Maldives monsoon season rainfall, while the correlation coefficient between their corresponding expansion coefficient time series is 0.39. When the first SVD components of the MAM transition conditions were used to quantify the individual associations year by year to identify which years the MAM transition conditions are working independently and in which years they are connected, the results indicate that the Indian Ocean and Pacific SST transition conditions follow each other quite closely, but in some years the association between Maldives region monsoon rainfall and the transition conditions in the Indian Ocean and Pacific SST during MAM are large. Although the correlation between

Maldives region monsoon rainfall and transition conditions in the Indian Ocean and Pacific SST are large for the year 2000 (correlation value near to or greater than 0.4), the cumulative pattern correlation is near zero, suggesting that other processes or internal dynamics can play a crucial role in monsoon rainfall in some years (Meehl and Arblaster 2001; 2002b). In many years, the MAM regional 500 hPa height acts independently from the other two transition conditions (Figure 7.29a). This demonstrates that in some years the three transition conditions act independently, while in some years they follow each other and can contribute to the Maldives monsoon rainfall. Also, in some years the Indian Ocean can provide a regional input to the Maldives monsoon season rainfall, which is separate from the large scale influence from the Pacific region. SVD analysis was carried out for the same transition conditions (Indian Ocean SST, eastern Pacific Ocean SST and 500 hPa height) in MAM with the Maldives monsoon rainfall (June-September) season, after removing ENSO onset years (identified in Figure 7.15), in order to check whether the ENSO years influence the association between transition conditions and Maldives monsoon rainfall. The first SVD component spatial patterns for the three transition conditions and their corresponding first SVD components of precipitation show a very similar pattern to ENSO years, compared with the first SVD components obtained when ENSO years are removed. Significantly higher pattern correlations indicated that the transition conditions in MAM are highly related with the monsoon rainfall over the Maldives region with and without ENSO years, thus suggesting similar processes are contributing to TBO in ENSO and non-ENSO years.

9.1.7 Downstream impacts

- Investigation of occurrence of excess (wet) or flood years and deficient (dry) or drought years identified based on the Maldives extended monsoon season rainfall (MJJASON total rainfall) for the period 1992-2008 indicated that the central region is most vulnerable to flood, while the southern region is least vulnerable to flood. The return periods calculated based on daily rainfall indicate that at present daily rainfall events of 150-210 mm are quite rare (such events occur approximately once every 300-440 years), but by 2050 daily rainfall events of 150-210 mm are likely to occur once every 66-166 years, and by 2100 such events are likely to occur once every 23-77 years. The calculated return periods also demonstrate that at present a three-hourly rainfall of 120 mm has a return period of 460 years, but it is likely that such events will become less

than a 100 year event by 2050, and by 2100 such events will become quite frequent, with a return period of about 30 years, suggesting that the islands of the Maldives will face frequent flooding in the future. The field survey indicates that in the current conditions the households and farmers already experience flood events quite often. For example, the survey results indicate about 23, 31 and 37% households (respondents) from the northern, central and southern regions experienced flood events, while about 79, 58 and 77% of the farmers who participated in the field survey from the northern, central and southern regions responded that they have experienced floods on their farm. At the other extreme, the northern and central regions are most vulnerable to drought events, with an equal number of drought years (3 years over the 18 year period), while the southern region is least prone to drought events (2 years with deficit rainfall). Despite high reliance on rainwater by the outer islands of the Maldives for potable use (rainwater accounts for 100% of water usage for cooking and drinking: 5, 5 and 6 lpcpd for the north, central and south), the field survey indicates that 49-63% of households experience shortage of rain water and about 78-97% of the respondents indicated that the shortage is due to prolonged dry periods. In addition to the households, 48-62% of the farmers also experienced shortage of rain water on their farms. Monthly supply and demand also demonstrates that there is potential to capture enough rainwater to provide a constant year-round supply for cooking and drinking, provided that the surplus water during the months when the rainwater supply exceeds the household rainwater demand is collected and stored. The minimum rainwater tank size estimated for different scenarios also demonstrates that if the rainwater is collected on a monthly basis, minimum rainwater tank size of 1200-2300 L, 3500-6000 L, 1400-2900 L and 3900-6600 L is enough to meet household rainwater demand for scenarios A, B, C and D, respectively. But it is clear from household responses that nearly 100% of the households harvest rainwater during the extended monsoon season (May-November) on a small scale (on a household basis: about 88-97% of the households are equipped with their own rainwater storage tanks with an average tank size of 4000, 3800 and 3700 L for northern, central and southern regions) from the house roof catchment. Despite the island communities experiencing shortage of rainwater quite frequently, different scenarios demonstrate that there is potential to provide a total year-round water supply for cooking and drinking, since scenarios A, B, C and D suggest that 23-24%, less than 50%, 30-34% and 54-71%, respectively, of the annual rainwater supply (harvestable rainwater) is utilized by the households for cooking and drinking. Application of the

graphical method for the four scenarios further demonstrates that the cumulative supply is far greater than the cumulative demand and the rainwater tank capacity required is significantly less than the yearly household rainwater demand. Except scenario D, for all other scenarios (A, B and C) and for all regions the estimated minimum required storage tank capacity is higher than the respective scenario annual demand. Hence the storage tanks may never become completely filled and/or may never become empty/or never be utilised fully. The fact that 100% of the outer islands of the Maldives surveyed rely on the rainwater resource for cooking and drinking and experience shortages of rainwater quite often, and considering the limited alternative water resources available in these outer islands (in some of the islands groundwater is not suitable for human consumption), it might be appropriate for the islands of the Maldives to determine storage tank size by calculating the maximum rainwater supply for a given roof area.

- At present, most of the households of the outer islands of the Maldives depend on either rainwater obtained from communal/neighbours' tanks or groundwater during shortage of rainwater. Groundwater accounts for about 97-98% of the total household water demands (100% of all the non potable use, with an average water consumption of 186, 199 and 195 lpcpd for the northern, central and southern regions, respectively). As far as quantity of groundwater is concerned, the sustainable yield computed for each island indicates that the groundwater resources in all the islands are sufficient to meet the normal daily household water demand, especially for non-potable uses. However, when the water needs for gardening/backyard farming and agriculture sector are taken into account, the results demonstrate that the groundwater in some islands is not sustainable. For example, sustainable yield for S. Hithadhoo (208.9 lpcpd) is very close to the average water consumption pcpd for the southern region (195 lpcpd), suggesting that the groundwater resources on this island may not be sufficient to meet the normal daily household. Furthermore, for the case of HA. Baarah, the groundwater extracted (317 lpcpd) exceeds the sustainable yield of 291.8 lpcpd. On the other hand, if quality of groundwater is considered, the responses received from the island offices and households suggest that the groundwater in the islands is often polluted; 37.6, 33.7 and 40.8% of the households in northern, central and southern regions reported groundwater problems such as contamination, smells and colour. Furthermore, 24-32% of the households identified salinity in household groundwater. This demonstrates that the Maldives water resources and agricultural sector are vulnerable to drought and flood impacts and these impacts cannot be avoided. Since full assessment of mitigation and

adaptation options is beyond the scope of this study, mitigation and adaptation measures to combat damages due to droughts and floods, need to be identified, and have to be implemented from the individual household and farmer level to communities and to national government level, to reduce the impacts.

9.2 Conclusions

The main conclusions that can be drawn from this research include:

- There exists both spatial and temporal variability in the Maldives annual and monsoon rainfall pattern which is consistent with a regional monsoon.
- The monsoon rainfall over the Maldives is characterised by inter-decadal, inter-annual and intra-seasonal variability.
- The monsoon onset first occurs around southern Maldives in April and then propagates northward, covering the whole of Asia, and then starts to withdraw from north, completely withdrawing from the Maldives in November/December.
- Meteorological parameters influencing Maldives monsoon rainfall have been used to formulate a regression model to predict core-monsoon rainfall for the Maldives, which is important for the management of water resources for both household and agricultural use.
- ENSO influences monsoon rainfall, with the Maldives/India region experiencing deficiencies in monsoon rainfall about 71.4% of the time during strong/moderate El Niño events, while the Maldives/India region experiences excessive monsoon rainfall about 75% of the time during strong/moderate La Niña events.
- There appears to be a very weak connection between Eurasian snow cover and the Maldives monsoon rainfall.
- Variation in Maldives monsoon rainfall indicates a transition from a relatively strong/weak to a relatively weak/strong monsoon, demonstrating biennial variability (linked to the TBO).
- The households and farms of the Maldives heavily depend on monsoon rainfall, and domestic water resources and the agricultural sector of the Maldives are impacted by rainfall variability (droughts and flood events).

9.3 Limitations and future research

This study has explored many important aspects of local meteorology and climatology in the context of the Maldives, including global and regional factors that

influence the Maldives monsoon rainfall, using both in situ and satellite data. However, there are many areas which could have been explored further, but the present study was limited by available time and other resources. There is therefore scope for future studies.

Presence or absence of prolonged break periods during the core monsoon season can play a crucial role in the intra-seasonal and inter-annual variability of the monsoon. Long intense breaks are often associated with monsoon seasons with deficient rainfall, and breaks in critical growth periods of agricultural crops can lead to substantially reduced yields. In-depth analysis of active and break periods on the variability of Maldives monsoon rainfall on the intra-seasonal scale was limited due to the lack of high resolution daily gridded observational data (e.g. precipitation radar). The role of active and break periods on the intra-seasonal and interannual variability needs to be investigated once a sufficiently dense observational monitoring network and/or precipitation radar data are made available. A criterion for defining active and break monsoon conditions also needs to be identified for the Maldives.

Although the available rainfall time series indicate interdecadal variability of the Maldives monsoon, analysis of interdecadal variability of monsoon rainfall patterns over the area is hampered by the lack of long-term local observational data. Interdecadal changes in the distribution of rainy events as a function of the rain rate and assessment of their contribution to the monsoon rainfall needs to be investigated, together with the large-scale circulation patterns influencing monsoon rainfall on the interdecadal time scale. The model formulated in this study for the prediction of monsoon rainfall would enable prediction of monsoon rainfall before the season commences and would facilitate determination of whether the monsoon rainfall during the monsoon season is likely to be below or above mean seasonal rainfall, helping water resource managers to be prepared. However, it should be noted that the model prediction is based on statistical relations in the past and the statistical relationship may change in the future. Hence, the formulated model should be re-evaluated in the future as more data and new techniques become available. Furthermore, climate modelling techniques also need to be explored to assist in the prediction of Maldives monsoon rainfall.

Modelling studies are also needed to verify the links established in this study, between Maldives monsoon rainfall and the global scale (ENSO) and regional scale processes (snow cover and TBO), and the teleconnection mechanism through which the atmospheric circulation over the Maldives is affected. The fact that inconsistent results were obtained when compared to some previous studies, for example between Eurasian

snow cover and Maldives monsoon rainfall, suggests that further studies should be undertaken to investigate the relationship between rainfall and Eurasian snow cover using climate modelling and long-term data. It was pointed out earlier that during most of the non-ENSO events, monsoon rainfall over the Maldives and India are out of phase, indicating that monsoon rainfall over the Maldives during non-ENSO events is influenced by different factors, from those affecting India during the same events. This topic needs to be investigated in future studies. Given the complexity of the monsoon in the Asian region, modelling studies need to be carried out to determine the combined effect of interactions between different processes on the Maldives monsoon rainfall.

Due to the lack of dense observational and precipitation radar data, one important area that was untouched in this research includes mesoscale to local scale processes governing rainfall variability over the Maldives. Most significant weather systems or events in the monsoon regions are localised or mesoscale in nature and need to be studied in relation to the Maldives rainfall patterns.

Detailed household and agricultural water usage studies also need to be carried out to verify the quantity of water usage estimated in this research. Static water demand was assumed (assuming the same number of occupants living in a household throughout the year and the same quantity of water used by each of the occupants per day throughout the year) in estimating estimated household water demand. It is recommended that a proper water demand analysis study is carried out by incorporating changes in household water demand due to climate change (warming), population growth, changes in number of household occupants and changes in technology. The field survey component of this research was hampered by the lack of responses from the tourism sector of the Maldives, and tourism sector water resource impacts need to be investigated in future studies. Further research is also needed to determine best available mitigation and adaptation measures in the context of Maldives, to minimise impacts associated with flood and drought events, and hence water resource issues faced by the outer island communities.

The research findings presented in the thesis may have some limitations/weaknesses due to the use of multiple rainfall datasets. One of the major drawbacks in this study is the lack of dense observational data. Also all the findings in this study are based on statistical analysis and the results presented in the thesis may have some uncertainty due to the nature of the statistical methods used. Although this research has identified some important processes that influence monsoon rainfall over the Maldives, there are many other areas which could have been explored. The Pacific Decadal Oscillation (PDO), Quasi-Biennial

Oscillation (QBO), Indian Ocean Dipole (IOD) and Madden-Julian Oscillation (MJO) are some of the other potential drivers of monsoon variability that this research was not able to explore due to both time and data constrains, but which need to be studied in future research in relation to Maldives rainfall.

References

AAI. 2005: Flood in Mumbai and Maharashtra-2005. ActionAid International, Bangalore, India.

ADB. 2010: Every drop counts-learning from good practices in eight Asian cities. Asian Development Bank (ADB), Mandaluyong City, Philippines.

AG-DHA. 2004: Guidance on use of rainwater tanks. Australian Government-Department of Health and Ageing (DHA) Canberra.

Ahmed, A. O., Cherif , Yasuda, H., Hattori, K., and Nagasawa, R. 2008: Analysis of rainfall records (1923–2004) in Atar-Mauritania. *Geofizika*, **25**, 53-64.

Ahmed, D. A. A., Hundt, G. L., and Blackburn, C. 2010: Issues of gender, reflexivity and positionality in the field of disability: researching visual impairment in an Arab society. *Qualitative Social Work*, **0**.

Ahmed, R., and Karmakar, S. 1993: Arrival and withdrawal dates of the summer monsoon in Bangladesh. *International Journal of Climatology*, **13**, 727-740.

Al-Turki, A., I (2009). "Evaluation of well water quality in Hael region of central Saudi Arabia." In: *Thirteenth International Water Technology Conference*, Hurghada, Egypt, 1121-1132.

Amira, F. 2009: The role of local food in Maldives tourism: a focus on promotion and economic development, Master of Philosophy (MPhil) in Tourism, Auckland University of Technology, Auckland.

Ammentorp, H. C., Radaideh, M., and Host-Madsen, J. (2006). "Advances in flash flood forecasting and mitigation." In: *International Workshop on Flash Floods in Urban Areas and Risk Management*, Muscat, Sultanate of Oman.

Ananthakrishnan, R., and Soman, M. K. 1991: The onset of the southwest monsoon in 1990. *Current Science*, **61**, 447-453.

Anderson, S., E, and Gansender, B., M. 1995: Using electronic mail surveys and computer-monitored data for communication systems. *Social Science Computer Review*, **13**, 33-46.

Annamalai, H., Hamilton, K., and Sperber, K. R. 2007: South Asian summer monsoon and its relationship with ENSO in the IPCC AR4 simulations. *Journal of Climate*, **20**, 1071–1092.

Annamalai, H., Slingo, J. M., Sperber, K. R., and Hodges, K. 1999: The mean evolution and variability of the Asian summer monsoon: Comparison of ECMWF and NCEP-NCAR reanalyses. *Monthly Weather Review*, **127**, 1157-1186.

Antonopoulos, V. Z., Papamichail, D. M., and Mitsiou, K. A. 2001: Statistical and trend analysis of water quality and quantity data for the Strymon River in Greece. *Hydrology and Earth System Sciences*, **5**, 679-691.

Azad, S., Narasimha, R., and Sett, S. K. 2008: A wavelet based significance test for periodicities in Indian monsoon rainfall. *International Journal of Wavelets Multiresolution and Information Processing*, **6**, 291-304.

Bailey, R., T, Jenson, J., W , Rubinstein, D., and Olsen, A., E. 2008: Groundwater resources of atoll islands: observations, modeling, and management. University of Guam-Water and Environmental Research Institute of the Western Pacific, Mangilao, Guam.

Bamzai, A. S., and Shukla, J. 1999: Relation between Eurasian snow cover, snow depth, and the Indian summer monsoon: An observational study. *Journal of Climate*, **12**, 3117-3132.

Bernard, H. R. 2006: *Research methods in anthropology: Qualitative and quantitative approaches*, Fourth Ed., AltaMira Press, Oxford, UK.

Beswick, R. 2000: Water supply and sanitation, a strategy and plan for the Republic of Maldives, Parts 1 & 2. Ministry of Health, Male', Maldives.

Bhatla, R., Mohanty, U. C., and Raju, P. V. S. 2006: The variability of Indian Ocean surface meteorological fields during summer monsoon in El Niño/La Niña years. *Indian Journal of Marine Sciences*, **52**, 93-103.

Bindoff, N. L., Willebrand, J., Artale, V., Cazenave, A., Gregory, J., Gulev, S., Hanawa, K., Le Quéré, C., Levitus, S., Nojiri, Y., Shum, C. K., Talley, L. D., and Unnikrishnan, A. 2007: Observations: Oceanic climate change and sea level. In: *Climate Change 2007: The Physical Science Basis. Contribution of Working Group I to the Fourth Assessment Report of the Intergovernmental Panel on Climate Change* S. Solomon, D. Qin, M. Manning, Z. Chen, M. Marquis, K.B. Averyt, M. Tignor and H.L. Miller, ed., Cambridge University Press, Cambridge, United Kingdom and New York, NY, USA, 386-432.

Birchfield, D., and Easton, L. 2007: Demand management through water retrofit programmes. Beacon Pathway Limited, Auckland, New Zealand.

Bony, S., and Dufresne, J. L. 2005: Marine boundary layer clouds at the heart of tropical cloud feedback uncertainties in climate models. *Geophysical Research Letters*, **32**.

Bony, S., Dufresne, J. L., Le Treut, H., Morcrette, J. J., and Senior, C. 2004: On dynamic and thermodynamic components of cloud changes. *Climate Dynamics*, **22**, 71-86.

Bracco, A., Kucharski, F., Molteni, F., Hazeleger, W., and Severijns, C. 2007: A recipe for simulating the interannual variability of the Asian summer monsoon and its relation with ENSO. *Climate Dynamics*, **28**, 441-460.

Bretherton, C. S., Smith, C., and Wallace, J. M. 1992: An intercomparison of methods for finding coupled patterns in climate data. *Journal of Climate*, **5**, 541-560.

Burgers, G., and Stephenson, D. B. 1999: The "normality" of El Niño. *Geophysical Research Letters*, **26**, 1027-1030.

Cannon, A. J., and McKendry, I. G. 1999: Forecasting all-India summer monsoon rainfall using regional circulation principal components: A comparison between neural network and multiple regression models. *International Journal of Climatology*, **19**, 1561-1578.

CEHI. 2009: *Caribbean rainwater harvesting Handbook*, The Caribbean Environmental Health Institue (CEHI) for the United nations environment programme.

Chakraborty, A., Nanjundiah, R. S., and Srinivasan, J. 2006: Theoretical aspects of the onset of Indian summer monsoon from perturbed orography simulations in a GCM. *Annales Geophysicae*, **24**, 2075-2089.

Chang, C. P., and Li, T. 2000: A theory for the tropical tropospheric biennial oscillation. *Journal of the Atmospheric Sciences*, **57**, 2209-2224.

Chen, T. C., and Yen, M. C. 1994: Interannual variation of the Indian monsoon simulated by the NCAR Community Climate Model: Effect of the tropical Pacific SST. *Journal of Climate*, **7**, 1403–1415.

Chou, C., Tu, J. Y., and Yu, J. Y. 2003: Interannual variability of the western North Pacific summer monsoon: Differences between ENSO and non-ENSO years. *Journal of Climate*, **16**, 2275-2287.

Chowdhury, M. R. 2003: The El Niño-Southern Oscillation (ENSO) and seasonal flooding - Bangladesh. *Theoretical and Applied Climatology*, **76**, 105-124.

Christensen, J. H., B. Hewitson, A. Busuioc, A. Chen, X. Gao, I. Held, R. Jones, R.K. Kolli, W.-T. Kwon, R. Laprise, V. Magaña Rueda, L. Mearns, C.G. Menéndez, J. Räisänen, A. Rinke, Sarr, A., and P. Whetton. 2007: Regional climate projections.

In: Climate change 2007: The physical science basis. Contribution of working group I to the fourth assessment report of the intergovernmental panel on climate change, S. Solomon, D. Qin, M. Manning, Z. Chen, M. Marquis, K.B. Averyt, M. Tignor and H.L. Miller, ed., Cambridge University Press, Cambridge, United Kingdom and New York, NY, USA.

Clarke, C. O., Cole, J., E, and Webster, P., J. 2000: Indian Ocean SST and Indian summer rainfall: Predictive relationships and their decadal variability. *Journal of Climate*, **13**, 2503.

Clift, P. D., and Plumb, R. A. 2008: *The Asian Monsoon: Causes, history & effects*, Cambridge University Press, Cambridge.

Cohen, J. 1994: Snow cover and climate. *Weather*, **49**, 150-156.

Conrady, R., and Bakan, S. 2008: Climate change and its impact on the tourism industry. In: *Trends and issues in global tourism.* R. Conrad and M. Buck, eds., Springer, Berlin, Germany.

Cresti. 2007: Analysis and design of household rainwater catchment systems for rural Rwanda, Thesis, Massachusetts Institute of Technology, Italy.

D'Abreton, P. C., and Tyson, P. D. 1995: Divergent and non-divergent water-vapor transport over southern Africa during wet and dry conditions. *Meteorology and Atmospheric Physics*, **55**, 47-59.

Dahmen, E. R., and Hall, M. J. 1990: *Screening of hydrological data: tests for stationarity and relative consistency*, International Institute for Land Reclamation and Improvement, Publication 49. Wageningen, The Netherlands, 58.

De Luis, M., Raventos, J., Gonzalez-Hidalgo, J. C., Sanchez, J. R., and Cortina, J. 2000: Spatial analysis of rainfall trends in the region of Valencia (East Spain). *International Journal of Climatology*, **20**, 1451-1469.

DelSole, T., and Shukla, J. 2002: Linear prediction of Indian monsoon rainfall. *Journal of Climate*, **15**, 3645-3658.

Deser, C., and Timlin, M. S. 1997: Atmosphere-ocean interaction on weekly timescales in the North Atlantic and Pacific. *Journal of Climate*, **10**, 393-408.

Dickson, R. R. 1984: Eurasian snow cover versus Indian monsoon rainfall - An extension of the Hahn-Shukla results. *Journal of Climate and Applied Meteorology*, **23**, 171-173.

Dickson, R. R., 1983: Investigation of a possible feedback loop involving Eurasian snow cover, Indian monsoon rainfall and southern oscillation. *Proceeding of Seventh Annual Climate Diagnostics Workshop*, Washington, DC, NOAA, 437-443.

Ding, Y. 2007: The variability of the Asian summer monsoon. *Journal of the Meteorological Society of Japan*, **85B**, 21-54.

Ding, Y. H., and Chan, J. C. L. 2005: The East Asian summer monsoon: An overview. *Meteorology and Atmospheric Physics*, **89**, 117-142.

DNP. 2006: *Island level basic indicators-census 2006*. Retrieved 5 January 2009. 2009, from http://www.planning.gov.mv/publications/census/Census_2006-Island_level_Indicators.pdf

DNP. (2010). "Statistical yearbook of Maldives 2010." Department of National Planning (DNP), Male', Maldives.

Draper, N. R., and Smith, H. 1981: *Applied regression analysis*, Second Ed., John Wiley and Sons, New York.

Duchon, C. E. 1979: Lanczos filtering in one and two dimensions. *Journal of Applied Meteorology*, **18**, 1016-1022.

Falconer, A.-H., Karen, and Kawabata, H. 2002: Toward a more fully reflexive feminist geography. . In: *Feminist geography in practice: Research and methods*, P. Moss, ed., Blackwell, Oxford, 103-115.

Falkland, A. C. (1993). "Hydrology and water management on small tropical islands." In: *Hydrology of warm humid regions-proceedings of the Yokohama Symposium*, 42.

Falkland, A. C. (1994). "Climate, hydrology and water resources of the Cocos (Keeling) islands." Atoll Research Bulletin, Smithsonian Institute, Washington D.C, USA, 51.

Falkland, A. C. 2000: Report on groundwater investigations, Addu atoll-Southern development region. Prepared for MacAlister Elliott and Partners Ltd OPT International BFS Consulting Group, as part of the Asian Development Bank funded Regional Development Project, First Phase, December 2000

Falkland, A. C. 2001a: Report on groundwater investigations, Northern development region. Prepared for MacAlister Elliott and Partners Ltd OPT International BFS Consulting Group, as part of the Asian Development Bank funded Regional Development Project, First Phase, August 2001

Falkland, T. 2001b: Report on integrated water resources management and sustainable sanitation for 4 islands, Maldives. UNICEF & Maldives Water and Sanitation Authority, Male', Maldives.

Falloon, P., and Betts, R. 2010: Climate impacts on European agriculture and water management in the context of adaptation and mitigation-The importance of an integrated approach. *Science of the Total Environment*, **408**, 5667-5687.

Fasullo, J. 2005: Atmospheric hydrology of the anomalous 2002 Indian summer monsoon. *Monthly Weather Review*, **133**, 2996-3014.

Fasullo, J., and Webster, P. J. 2002: Hydrological signatures relating the Asian summer monsoon and ENSO. *Journal of Climate*, **15**, 3082-3095.

Fasullo, J., and Webster, P. J. 2003: A hydrological definition of Indian monsoon onset and withdrawal. *Journal of Climate*, **16**, 3200-3211.

FDMG. 2006: Audit report (floods in Maharashtra) for the year ended 31 March 2006. Finance Department of Maharashtra Government, India.

Fernandez, J., Saenz, J., and Zorita, E. 2003: Analysis of wintertime atmospheric moisture transport and its variability over southern Europe in the NCEP reanalyses. *Climate Research*, **23**, 195-215.

Fewkes, A. 2006: The technology, design and utility of rainwater catchment systems. In: *Water Demand Management*, D. Butler and F. A. Memon, eds., IWA Publishing, London, 27-61.

Field, A. P. 2005: *Discovering statistics using SPSS : (and sex, drugs and rock 'n' roll)*, Sage Publications, London, England.

Flatau, M. K., Flatau, P. J., and Rudnick, D. 2001: The dynamics of double monsoon onsets. *Journal of Climate*, **14**, 4130-4146.

Flatau, M. K., Flatau, P. J., Schmidt, J., and Kiladis, G. N. 2003: Delayed onset of the 2002 Indian monsoon. *Geophysical Research Letters*, **30**.

Frankfort-Nachmias, C., and Nachmias, D. 1996: *Research methods in the social sciences*, Arnold, London, UK.

Fu, C., Guan, Z., He, J., Jiang, Z., and Yang, X. 2008: *Regional climate of China*, Springer Berlin, Berlin.

Gadgil, S. 2008: The Indian monsoon: links to cloud systems over the tropical Oceans. *Resonance*, **13**, 218-235.

Gadgil, S., Rajeevan, M., and Nanjundiah, R. 2005: Monsoon prediction-Why yet another failure? *Current Science* **88**, 1389-1400.

Ghassemi, F., Molson, J. W., Falkland, A., and Alam, K. 1998: Three-dimensional simulation of the home island freshwater lens: Preliminary results. *Environmental Modelling and Software*, **14**, 181-190.

Gibson, P., and Abrams, L. 2003: Racial difference in engaging, recruiting, and interviewing African American women in qualitative research. *Qualitative Social Work*, **2**, 457–476.

Gilgun, J. F., and Abrams, L. S. 2002: The nature and usefulness of qualitative social work research: Some thoughts and an invitation to dialogue. *Qualitative Social Work* **1**, 39-55.

Godfred, S., C. R., and Reason, C. J. C. 2002: Interannual variability of lower-tropospheric moisture transport during the Australian monsoon. *International Journal of Climatology*, **22**, 509-532.

Goes, J. I., Thoppil, P. G., Gomes, H. D., and Fasullo, J. T. 2005: Warming of the Eurasian landmass is making the Arabian Sea more productive. *Science*, **308**, 545-547.

Goswami, B. N. 1998: Interannual variations of Indian summer monsoon in a GCM: External conditions versus internal feedbacks. *Journal of Climate*, **11**, 501-522.

Goswami, B. N. 2004: South Asian summer monsoon: An overview. *70*, World Meteorological Organization, Hangzhou, China.

Goswami, B. N. 2005: South Asian monsoon. In: *Intraseasonal variability of the Atmosphere-Ocean climate system*, K. Lau and D. Waliser, eds., Springer - Praxis, Chinchester, UK.

Goswami, B. N. 2006: The Asian Monsoon: Interdecadal variability. In: *The Asian monsoon*, B. Wang, ed., Springer and Praxis Publishing, Berlin Heidelberg, 296-327.

Goswami, B. N., and , and Mohan, A. R. S. 2001: Intraseasonal oscillations and interannual variability of the Indian summer monsoon. *Journal of Climate*, **14**, 1180-1198.

Goswami, P., and Gouda, K. C. 2007: Objective determination of the date of onset of monsoon rainfall over India based on duration of persistence. CSIR Centre for Mathematical Modelling and Computer Simulation, Bangalore, India.

Gould, J., and Nissen-Peterson, E. 1999: *Rainwater catchment systems for domestic supply: Design, construction and implementation*, Intermediate Technology Publications, London.

Grantz, K., Rajagopalan, B., Clark, M., and Zagona, E. 2007: Seasonal shifts in the North American monsoon. *Journal of Climate*, **20**, 1923-1935.

Guhathakurta, P., and Rajeevan, M. 2008: Trends in the rainfall pattern over India. *International Journal of Climatology*, **28**, 1453-1469.

Guilyardi, E., Wittenberg, A., Fedorov, A., Collins, M., Wang, C. Z., Capotondi, A., van Oldenborgh, G. J., and Stockdale, T. 2009: Understanding El-Niño in Ocean-Atmosphere general circulation models-Progress and challenges. *Bulletin of the American Meteorological Society*, **90**, 325-340.

Hahn, D. G., and Shukla, J. 1976: Apparent relationship between Eurasian snow cover and Indian monsoon rainfall. *Journal of the Atmospheric Sciences*, **33**, 2461-2462.

Hair, J. F., Black, B., Babin, B., Anderson, R. E., and Tatham, R. L. 2006: *Multivariate data analysis* Sixth Ed., Pearson Prentice Hall, Upper Saddle River, N.J.

Haleem, A. (2009). "Sixty islands without rainwater." In: *Haveeru*, Haveeru Daily News Paper, Male', Maldives.

Haque, M. A., and Lal, M. 1991a: Space and time variability analysis of the Indian monsoon rainfall as inferred from satellite-derived OLR data. *Climate Research*, **1**, 187-197.

Haque, M. A., and Lal, M. 1991b: Space and time variability analysis of the Indian monsoon rainfall as inferred from satellite-derived OLR data. *Climate Research*, **1**, 187-197.

Hartmann, D. L., and Michelsen, M. L. 1989: Intraseasonal periodicities in Indian rainfall. *Journal of Atmospheric Science*, **46**, 2838-2862.

Hay, J., E 2006: Climate risk profile for the Maldives. Ministry of Envrionment Energy and Water, Republic of the Maldives, Male'.

Haylock, M. R., Cawley, G. C., Harpham, C., Wilby, R. L., and Goodess, C. M. 2006: Downscaling heavy precipitation over the United Kingdom: A comparison of dynamical and statistical methods and their future scenarios. *International Journal of Climatology*, **26**, 1397-1415.

He, J. H., Sun, C. H., Liu, Y. Y., Matsumo, J., and Li, W. J. 2007: Seasonal transition features of large-scale moisture transport in the Asian-Australian monsoon region. *Advances in Atmospheric Sciences*, **24**, 1-14.

Heinrich, M. 2006: Residential water end use literature survey. *BRANZ study report 149*, Branz Ltd, Judgeford, New Zealand.

Heinrich, M. 2007: Water end use and efficiency project (WEEP)-final report. *159*, BRANZ Ltd, Judgeford, New Zealand.

Hendon, H. H., and Liebmann, B. 1990: A composite study of onset of the Australian summer monsoon. *Journal of the Atmospheric Sciences*, **47**, 2227-2240.

Higgins, R. W., Chen, Y., and Douglas, A. V. 1999: Interannual variability of the North American warm season precipitation regime. *Journal of Climate*, **12**, 653-680.

Ho, C. H., Lee, J. Y., Ahn, M. H., and Lee, H. S. 2003: A sudden change in summer rainfall characteristics in Korea during the late 1970s. *International Journal of Climatology*, **23**, 117-128.

Holton, J., R. 2004: *An introduction to dynamic meteorology*, fourth Ed., Elsevier Academic Press, California, USA.

Houghton, J. T., Ding, Y., Griggs, D. J., Noguer, M., Linden., v. d., P.J. Dai, X., Maskell, K., and Johnson, C. A. 2001: *Climate change 2001: The scientific basis*, Cambridge University Press, Cambridge.

Hoyos, C., D, and Webster, P., J. 2007: The role of intraseasonal variability in the nature of Asian monsoon precipitation. *Journal of Climate*, **20**, 4402-4424.

HRSA. 2010: *Calculating sample size. U.S. Department of Health and Human Services-Health Resources and Services Administration.*, Retrieved 24 November. 2010, from http://bphc.hrsa.gov/patientsurvey/samplesize.htm

Huth, R. 1996: Properties of the circulation classification scheme based on the rotated principal component analysis. *Meteorology and Atmoheric Physics*, **59**, 217-233.

Ibrahim, S. A. (2008). "Water supply and sanitation in the Maldives." In: *The Third South Asian Conference on Sanitation (SACOSAN III)*, Department of Drinking Water Supply, Ministry of Rural Development, Government of India., New Delhi, India.

IPCC. 2007: Climate change 2007: The physical science basis.

Izumo, T., Montegut, C. D., Luo, J. J., Behera, S. K., Masson, S., and Yamagata, T. 2008: The role of the western Arabian Sea upwelling in Indian monsoon rainfall variability. *Journal of Climate*, **21**, 5603-5623.

Jin, F. F., An, S. I., Timmermann, A., and Zhao, J. X. 2003: Strong El Niño events and nonlinear dynamical heating. *Geophysical Research Letters*, **30**.

Jones, J., Paul III, Nast, H., and Roberts, S. 1997: *Thresholds in feminist geography: Difference, methodology, representation*, Rowman and Littlefield, New York.

Jones, P. D., and Reid, P. A. 2001: Assessing future changes in extreme precipitation over Britain using regional climate model integrations. *International Journal of Climatology*, **21**, 1337-1356.

Ju, J. H., and Slingo, J. 1995: The Asian summer monsoon and ENSO. *Quarterly Journal of the Royal Meteorological Society*, **121**, 1133-1168.

Kalnay, E., Kanamitsu, M., Kistler, R., Collins, W., Deaven, D., Gandin, L., Iredell, M., Saha, S., White, G., Woollen, J., Zhu, Y., Chelliah, M., Ebisuzaki, W., Higgins, W., Janowiak, J., Mo, K. C., Ropelewski, C., Wang, J., Leetmaa, A., Reynolds, R., Jenne, R., and Joseph, D. 1996: The NCEP/NCAR 40-year reanalysis project. *Bulletin of the American Meteorological Society*, **77**, 437-471.

Kane, R. P. 1998: Extremes of the ENSO phenomenon and Indian summer monsoon rainfall. *International Journal of Climatology*, **18**, 775-791.

Kang, I. S., and Kug, J. S. 2002: El Niño and La Niña sea surface temperature anomalies: Asymmetry characteristics associated with their wind stress anomalies. *Journal of Geophysical Research-Atmospheres*, **107**.

Kay, A. L., Jones, R. G., and Reynard, N. S. 2006: RCM rainfall for UK flood frequency estimation. II. Climate change results. *Journal of Hydrology*, **318**, 163-172.

Khan, T. M. A., Quadir, D. A., Murty, T. S., Kabir, A., Aktar, F., and Sarker, M. A. 2002: Relative sea level changes in Maldives and vulnerability of land due to abnormal coastal inundation. *Marine Geodesy*, **25**, 133 - 143.

Khastagir, A., and Jayasuriya, N. (2007). "Parameters influencing the selection of an optimal rainwater tank size: a case study for Melbourne." In: *Rain Water and Urban Design Conference*, Sydney.

Khastagir, A., and Jayasuriya, N. 2010: Optimal sizing of rain water tanks for domestic water conservation. *Journal of Hydrology*, **381**, 181-188.

Kinter, J. L., Miyakoda, K., and Yang, S. 2002: Recent change in the connection from the Asian monsoon to ENSO. *Journal of Climate*, **15**, 1203-1215.

Kousky, V. E. 1988: Pentad outgoing longwave radiation climatology for the South American sector. *Rev. Bras. Meteor.*, **3**, 217-231.

Kripalani, R. H., and Kulkarni, A. 1999: Climatology and variability of historical Soviet snow depth data: some new perspectives in snow - Indian monsoon teleconnections. *Climate Dynamics*, **15**, 475-489.

Kripalani, R. H., and Kulkarni, A. 2001: Monsoon rainfall variations and teleconnections over south and east asia. *International Journal of Climatology*, **21**, 603-616.

Kripalani, R. H., Kulkarni, A., Sabade, S. S., Revadekar, J. V., Patwardhan, S. K., and Kulkarni, J. R. 2004: Intra-seasonal oscillations during monsoon 2002 and 2003. *Current Science*, **87**.

Krishnamurthy, V., and Goswami, B. N. 2000: Indian monsoon-ENSO relationship on interdecadal timescale. *Journal of Climate*, **13**, 579-595.

Krishnamurthy, V., and Kinter, J., L. . 2003: The Indian monsoon and its relation to global climate variability. In: *Global Climate*, X. Rodo, and Comin, F.A., , ed., Springer, Berlin.

Krishnamurthy, V., and Shukla, J. 2000: Intraseasonal and interannual variability of rainfall over India. *Journal of Climate*, **13**, 4366-4377.

Krishnamurti, T. N. 1971: Tropical East-West circulations during the Northern summer. *Journal of the Atmospheric Sciences*, **28**, 1342-1347.

Krishnamurti, T. N., and Ardanuy, P. 1980: The 10-20-day westward propagating mode and breaks in the monsoon, . *Tellus*, **32**, 15-26.

Krishnamurti, T. N., Bedi, H. S., and Subramaniam, M. 1990: The summer monsoon of 1988. *Meteorology and Atmospheric Physics*, **42**, 19-37.

Krishnamurti, T. N., and Bhalme, H. N. 1976: Oscillations of a monsoon system. Part I. Observational aspects. *Journal of Atmospheric Science*, **33**, 1937-1954.

Krishnamurti, T. N., Kanamitsu, M., Koss, W. J., and Lee, J. D. 1973: Tropical East-West circulations during the Northern winter. *Journal of the Atmospheric Sciences*, **30**, 780-787.

Kucharski, F., Molteni, F., and Yoo, J. H. 2006: SST forcing of decadal Indian monsoon rainfall variability. *Geophysical Research Letters*, **33**.

Kumar, K. 1997: Seasonal forecasting of Indian summer monsoon rainfall: diagnostics and synthesis of regional and global signals, University of Pune, Pune.

Kumar, K., Soman, M. K., and Kumar, R. K. 1995: Seasonal forecasting of Indian summer monsoon rainfall: A review. *Weather*, **50**, 449-467.

Kumar, K. K., Kumar, K. R., and Pant, G. B. 1997: Pre-monsoon maximum and minimum temperatures over India in relation to the summer monsoon rainfall. *International Journal of Climatology*, **17**, 1115-1127.

Kumar, M., and Prasad, T. G. 1997: Annual and interannual variation of precipitation over the tropical Indian Ocean. *Journal of Geophysical Research*, **102**, 18519-18527.

Kundzewicz, Z. W., Mata, L. J., Arnell, N. W., Döll, P., Kabat, P., Jiménez, B., Miller, K. A., Oki, T., Sen, Z., and Shiklomanov, I. A. 2007: Freshwater resources and their management. In: *Climate change 2007: Impacts, adaptation and vulnerability. Contribution of working group II to the fourth assessment report of the intergovernmental panel on climate change*, M. L. Parry, O. F. Canziani, J. P. Palutikof, v. d. L. P.J, and C. E. Hanson, eds., Cambridge University Press, Cambridge, United Kingdom, 173-210.

Labaree, R. V. 2002: The risk of "going observationalist": Negotiating the hidden dilemmas of being an insider participant observer. *Qualitative Research*, **2**, 97–122.

Lal, M., Bengtsson, L., Cubasch, U., Esch, M., and Schlese, U. 1995: Synoptic scale disturbances of the Indian summer monsoon as simulated in a high resolution climate model. *Climate Research*, **5**, 243-258.

Lal, M., Nozawa, T., Emori, S., Harasawa, H., Takahashi, K., Kimoto, M., Abe-Ouchi, A., Nakajima, T., Takemura, T., and Numaguti, A. 2001: Future climate change: Implications for Indian summer monsoon and its variability. *Current Science*, **81**, 1196-1207.

Lau, K., M, Lau, N., C, and Yang, S., 2004: Current topics on interannual variability of the Asian monsoon. *The global monsoon system: Research and forecast*, World Meteorological Organization, Hangzhou, China, 440-454.

Lau, K. M., Kim, K. M., and Yang, S. 2000: Dynamical and boundary forcing characteriustics of regional components of the Asian summer monsoon. *Journal of Climate*, **13**, 2461-2482.

Lau, K. M., and Sheu, P. J. 1988: Annual cycle, quasi-biennial oscillation, and Southern oscillation in global precipitation. *Journal of Geophysical Research-Atmospheres*, **93**, 10975-10988.

Lau, K. M., and Wu, H. T. 1999: Assessment of the impacts of the 1997-98 El Niño on the Asian-Australia monsoon. *Geophysical Research Letters*, **26**, 1747-1750.

Lau, K. M., and Yang, S. 1997: Climatology and interannual variability of the southeast Asian summer monsoon. *Advances In Atmospheric Sciences*, **14**, 141-162.

Lau, N. C., and Nath, M. J. 2000: Impact of ENSO on the variability of the Asian-Australian monsoons as simulated in GCM experiments. *Journal of Climate*, **13**, 4287-4309.

Lau, N. C., and Wang, B. 2005: Interactions between the Asian monsoon and the El Niño - Southern Oscillation. In: *The Asian monsoon*, B. Wang, ed., Springer ; Published in association with Praxis Publishing, Berlin; New York; Chichester, 787.

Lawrence, D. M., and Webster, P. J. 2000: Interannual variations of the intraseasonal oscillation in the South Asian summer monsoon region. *Journal of Climate*, **14**, 2910-2922.

Lawrence, D. M., and Webster, P. J. 2001: Interannual variability of intraseasonal convection and the Asian monsoon. *Journal of Climate*, **14**, 2910-2922.

Li, C. F., and Yanai, M. 1996: The onset and interannual variability of the Asian summer monsoon in relation to land sea thermal contrast. *Journal of Climate*, **9**, 358-375.

Li, T., Wang, B., Chang, C. P., and Zhang, Y. S. 2003: A theory for the Indian Ocean dipole-zonal mode. *Journal of the Atmospheric Sciences*, **60**, 2119-2135.

Li, T., and Zhang, Y. S. 2002: Processes that determine the quasi-biennial and lower-frequency variability of the South Asian monsoon. *Journal of the Meteorological Society of Japan*, **80**, 1149-1163.

Li, T., Zhang, Y. S., Chang, C. P., and Wang, B. 2001: On the relationship between Indian Ocean sea surface temperature and Asian summer monsoon. *Geophysical Research Letters*, **28**, 2843-2846.

Liebmann, B., Camargo, S. J., Seth, A., Marengo, J., A, Carvalho, L. M. V., Allured, D., Fu, R., and Vera, C. S. 2007: Onset and end of the rainy season in South America in observations and the ECHAM 4.5 atmospheric general circulation model. *Journal of Climate*, **20**, 2037-2050.

Liebmann, B., and Smith, C. A. 1996: Description of a complete (interpolated) outgoing longwave radiation dataset. *Bulletin of the American Meteorological Society*, **77**, 1275-1277.

Lindsey, R., and Simmon, R. 2006: *Winds connect snow to sea*. Retrieved 18 September. 2009, from http://earthobservatory.nasa.gov/Features/Monsoon/

Liu, W. T., and Tang, W. Q. 2005: Estimating moisture transport over oceans using space-based observations. *Journal of Geophysical Research-Atmospheres*, **110**.

Liu, X., and Yanai, M. 2002: Influence of Eurasian spring snow cover on Asian summer rainfall. *International Journal of Climatology*, **22**, 1075-1089.

Loschnigg, J., Meehl, G. A., Webster, P. J., Arblaster, J. M., and Compo, G. P. 2003: The Asian monsoon, the tropospheric biennial oscillation, and the Indian Ocean zonal mode in the NCAR CSM. *Journal of Climate*, **16**, 1617-1642.

Madge, C. 1993: Boundary disputes: comments on Sidaway. *Area*, **25**, 294-299.

Manabe, S., Milly, P. C. D., and Wetherald, R. 2004: Simulated long-term changes in river discharge and soil moisture due to global warming. *Hydrological Sciences Journal-Journal Des Sciences Hydrologiques*, **49**, 625-642.

Mancuso, R. L. 1967: A numerical procedure for computing fields of stream function and velocity potential. *Journal of Applied Meteorology*, **6**, 994-1001.

Mao, J., and Wu, G. 2007: Interannual variability in the onset of the summer monsoon over the Eastern Bay of Bengal. *Theoretical and Applied Climatology*, **89**, 155-170.

Marengo, J. A., Liebmann, B., Kousky, V. E., Filizola, N. P., and Wainer, I. C. 2001: Onset and end of the rainy season in the Brazilian Amazon Basin. *Journal of Climate*, **14**, 833-852.

Mason, S. J. 1998: Seasonal forecasting of South African rainfall using a non-linear discriminant analysis model. *International Journal of Climatology*, **18**, 147-164.

Mayer, P., DeOreo, W., and Lewis, D. 2000: Seattle home water conservation study, The impacts of high efficiency plumbing fixture retrofits in single-family homes.

Aquacraft, Inc. Water Engineering and Management for Seattle Public Utilities and the U.S. Environmental Protection Agency, Colorado, USA.

McCarthy, J. J., Canziani, O. F., Leary, N. A., Dokken, D. J., and White, K. S. 2001: *Climate change 2001: Impacts, adaptation, and vulnerability*, Cambridge University Press Cambridge, UK.

McGregor, G. R., and Nieuwolt, S. 1998: *Tropical climatology : An introduction to the climates of the low latitudes*, Second Ed., Wiley, New York.

McGuffie, K. A., Henderson-Sellers, N., Holbrook, Z., Kothavala, O., Balachova, J., and Hoekstra. 1999: Assessing simulations of daily temperature and precipitation variability with

global climate models for present and enhanced greenhouse climates. *International Journal of Climatology*, **19**, 1-26.

MEC. 2004: State of the environment, 2004. Ministry of Environment & Construction, Male', Maldives.

Meehl, G. A. 1987: The annual cycle and interannual variability in the tropical Pacific and Indian-Ocean regions. *Monthly Weather Review*, **115**, 27-50.

Meehl, G. A. 1993: A Coupled Air-Sea Biennial Mechanism in the Tropical Indian and Pacific Regions - Role of the Ocean. *Journal of Climate*, **6**, 31-41.

Meehl, G. A. 1997: The south Asian monsoon and the tropospheric biennial oscillation. *Journal of Climate*, **10**, 1921-1943.

Meehl, G. A., and Arblaster, J. M. 2001: The tropospheric biennial oscillation and Indian monsoon rainfall. *Geophysical Research Letters*, **28**, 1731-1734.

Meehl, G. A., and Arblaster, J. M. 2002a: Indian monsoon GCM sensitivity experiments testing tropospheric biennial oscillation transition conditions. *Journal of Climate*, **15**, 923-944.

Meehl, G. A., and Arblaster, J. M. 2002b: The tropospheric biennial oscillation and Asian-Australian monsoon rainfall. *Journal of Climate*, **15**, 722-744.

Meehl, G. A., and Arblaster, J. M. 2003: Mechanisms for projected future changes in south Asian monsoon precipitation. *Climate Dynamics*, **21**, 659–675.

MEEW. 2007: National adaptation of programme of action (NAPA). Ministry of Environment, Energy and Water (MEEW), Male', Maldives.

Meho, L., I. 2006: E-mail interviewing in qualitative research: A methodological discussion. *Journal of the American society for information science and technology*, **57**, 1284-1295.

MFA. 1996: Maldives: Country report to the FAO international technical conference on plant genetic resources. Ministry of Fisheries and Agriculture, Male', Maldives.

MFAMR. 2006: Agricultural development master plan Maldives (2006 - 2020). Food and Agriculture Organization of United Nations, Ministry of Fisheries, Agriculture and Marine Resources-Maldives, Male'.

MHAHE. 1999: Second national environment action plan (NEAP II). Ministry of Home Affairs Housing and Environment, Male', Maldives.

MHAHE. 2001: First national communication of the republic of Maldives to the United Nations framework convention on climate change., Ministry of Home Affairs, Housing and Environment, Male', Maldives.

MHAHE. 2002: State of the environment, 2002. Ministry of Home Affairs, Housing and Environment, Male', Maldives.

MHTE. (2009). "National adaptation to climate change." In: *Maldives partnership forum*, Ministry of Housing, Transport and Environment (MHTE) Male', Maldives.

Millar, J. 2002: The ability of the Maldives to cope with freshwater scarcity via the adaptive capacity of its political economy, Occasional Paper No 44, University of London, London.

Minoura, D., Kawamura, R., and Matsuura, T. 2003: A mechanism of the onset of the south Asian summer monsoon. *Journal of the Meteorological Society of Japan*, **81**, 563-580.

Mohanty, U. C., and Ramesh, K. J. 1993: Characteristics of certain surface meteorological parameters in relation to the interannual variability of Indian-summer monsoon. *Proceedings of the Indian Academy of Sciences-Earth and Planetary Sciences*, **102**, 73-87.

Mooley, D. A., and Parthasarathy, B. 1984: Fluctuations in all-India summer monsoon rainfall during 1871-1978. *Climatic Change*, **6**, 287-301.

Moosa, S. 2006: Climate change vulnerability and adaptation assessment of human health in Maldives. *Maldives climate change policy research working papers*, Ministry of Environment, Energy and Water, Male‟, Maldives.

MPND. 2000: Statistical yearbook of Maldives 2000. Ministry of Planning and National Development, Male', Maldives.

MPND. 2005: Maldives' strategic economic plan. Ministry of Planning and National Development, Male', Maldives.

MPND. 2007a: Seventh national development plan 2006-2010. Ministry of Planning and National Development (MPND), Male', Maldives.

MPND. 2007b: Statistical yearbook of Maldives 2007 Ministry of Planning and National Development, Male', Maldives.

MPND. 2008: Analytical report 2006-Population and housing census 2006. Ministry of Planning and National Development (MPND), Male', Maldives.

MTAC. (2009). "Regulation on the protection and conservation of environment in the tourism industry." Ministy of Tourism, Arts and Culture, Male', Maldives.

MTAC. 2010: *Tourism yearbook 2010*, Novelty Printers and Publishers, Male', Maldives.

Munot, A. A., and Kothawale, D. R. 2000: Intra-seasonal, inter-annual and decadal scale variability in summer monsoon rainfall over India. *International Journal of Climatology*, **20**, 1387-1400.

Munot, A. A., and Kumar, K. K. 2007: Long range prediction of Indian summer monsoon rainfall. *Journal of Earth System Science*, **116**, 73–79.

Munoz, D. D., and Rodrigo, F. S. 2004: Spatio-temporal patterns of seasonal rainfall in Spain (1912–2000) using cluster and principal component analysis: comparison. *Annales Geophysicae*, **22**, 1435–1448.

Murakami, M. 1979: Large-scale aspects of deep convective activity over the GATE data. *Monthly Weather Review*, **107**, 994–1013.

MWSA. 2005: Water resources tsunami impact assessment and sustainable water sector recovery strategies. Maldives water and sanitation authodity (MWSA), Male', Maldives.

Naidu, C. V., Rao, B. R. S., and Rao, D. V. B. 1999: Climatic trends and periodicities of annual rainfall over India. *Meteorological Applications*, **6**, 395-404.

Nayagam, L. R., Janardanan, R., and Mohan, H. S. R. 2008: An empirical model for the seasonal prediction of southwest monsoon rainfall over Kerala, a meteorological subdivision of India. *International Journal of Climatology*, **28**, 823-831.

Nicholls, R. J., and Cazenave, A. 2010: Sea-level rise and its impact on coastal zones. *Science*, **328**, 1517-1520.

Nigam, S. 1994: On the dynamical basis for the Asian summer monsoon rainfall El-Niño relationship. *Journal of Climate*, **7**, 1750-1771.

NOAA. 2010: *El Niño theme page*. Retrieved 21 April. 2010, from http://www.pmel.noaa.gov/tao/elnino/nino-home.html

O'Connor, P. 2004: The conditionality of status: experience-based reflections on the insider/outsider issue. *Australian Geographer*, **35**, 169-176.

Oberdorfer, J. A., and Buddemeier, R. W. 1988: Climate change: Effects on reef island resources. *Proceedings of 6th International Coral Reef Congress*, 523-527.

Okumura, Y., M, and Deser, C. (2009). "Asymmetry in the duration of El Niño and La Niña." In: *Journal of Climate*, Climate and Global Dynamics Division, National Center for Atmospheric Research, 45.

Otaki, Y., Otaki, M., Pengchai, P., Ohta, Y., and Aramaki, T. 2008: Micro-components survey of residential indoor water consumption in Chiang Mai. *Drinking Water Engineering and Sciences*, **1**, 17-25.

Oyegun, R. O. 1985: The use and waste of water in a third world city. *GeoJournal*, **10**, 205-210.

Pai, D. S., and Rajeevan, M. 2006: Empirical prediction of Indian summer monsoon rainfall with different lead periods based on global SST anomalies. *Meteorology and Atmospheric Physics*, **92**, 33-43.

Pallant, J. 2007: *SPSS survival manual : A step by step guide to data analysis using SPSS for Windows (Version 15)*, Open University Press, Crows Nest, N.S.W. : Allen & Unwin ; Maidenhead

Palmer, T. N., and Sun, Z. 1985: A modelling and observational study of the relationship between sea surface temperature in the north-west Atlantic and atmospheric general circulation. *Quarterly Journal of the Royal Meteorological Society*, **111**, 947-975.

Pang, H. X., He, Y. Q., Lu, A. G., Zhao, J. D., Song, B., Ning, B. Y., and Yuan, L. L. 2005: Influence of Eurasian snow cover in spring on the Indian Ocean Dipole. *Climate Research*, **30**, 13-19.

Parthasarathy, A., Munot, A., and Kothawale, D. R. 1994: All-India monthly and seasonal rainfall series: 1871–1993. *Theoretical and Applied Climatology*, **49**, 217-224.

Pattanaik, D. R. 2007: Variability of convective activity over the north indian ocean and its associations with monsoon rainfall over india. *Pure and Applied Geophysics*, **164**, 1527-1545.

Pattanaik, D. R., Kalsi, S. R., and Hatwar, H. R. 2005: Evolution of convection anomalies over the Indo-Pacific region in relation to Indian monsoon rainfall. *Mausam*, **56**, 811-824.

PDHO. 2010: *Hot water plumbing systems*. Retrieved 2 December. 2010, from http://www.pdhonline.org

Peixoto, J. P., and Oort, A. H. 1983: The atmospheric branch of the hydrological cycle and climate. In: *Variations in the global water budget*, A. Street-Perrott, M. Beran, and R. Ratcliffe, eds., Reidel, London, pp 5–65.

Peng, S. L., and Fyfe, J. 1996: The coupled patterns between sea level pressure and sea surface temperature in the midlatitude North Atlantic. *Journal of Climate*, **9**, 1824-1839.

Peters, E. (2003). "Sizing of rainwater cisterns for domestic water supply in the Grenadines." In: *St Vincent and the Grenadines Country Conference*, The University of the West Indies, Cave Hill, Barbados.

Philander, S., G. 1999: El Niño and La Niña predictable climate fluctuations. *Reports on Progress in Physics*, **62**, 123-142.

Pillai, P. A., and Mohankumar, K. 2007: Tropospheric biennial oscillation of the Indian summer monsoon with and without the El Niño-Southern Oscillation. *International Journal of Climatology*, **27**, 2095-2101.

Pillai, P. A., and Mohankumar, K. 2008: Local Hadley circulation over the Asian monsoon region associated with the tropospheric biennial oscillation. . *Theoretical and Applied Climatology*, **91**, 171-179.

Pillai, P. A., and Mohankumar, K. 2009: Role of TBO and ENSO scale ocean-atmosphere interaction in the Indo-Pacific region on Asian summer monsoon variability. *Theoretical and Applied Climatology*, **97**, 99-108.

Prasad, K. D., Bansod, S. D., and Sabade, S. S. 2000: Forecasting Indian summer monsoon rainfall by outgoing longwave radiation over the Indian Ocean. *International Journal of Climatology*, **20**, 105-114.

Prasad, V. S., and Hayashi, T. 2005: Onset and withdrawal of Indian summer monsoon. *Geophysical Research Letters*, **32**.

Qi, Y. J., Zhang, R. H., Li, T., and Wen, M. 2008: Interactions between the summer mean monsoon and the intraseasonal oscillation in the Indian monsoon region. *Geophysical Research Letters*, **35**.

Qian, B. D., and Saunders, M. A. 2003: Summer UK temperature and its links to preceding Eurasian snow cover, North Atlantic SSTs, and the NAO. *Journal of Climate*, **16**, 4108-4120.

Raheem, E., and Khan, S. H. 2006: Combining probability of emptiness and mean first overflow time of dam to determine its capacity. *Journal of Spatial Hydrology*, **2**, 1-7.

Rahman, M. M., and Yusuf, F.-U.-A., M.S. (2000). "Rainwater harvesting and the reliability concept." In: *8th ASCE Specialty Conference on Probabilistic Mechanics and Structural Reliability*, University of Notre Dame, Notre Dame, Indiana.

Rajeevan, M., and Pai, D. S. 2006: On El Niño-Indian monsoon predictive relationships. *4/2006*, National Climate Centre, India Meteorological Department.

Rajeevan, M., Pai, D. S., Dikshit, S. K., and Kelkar, R. R. 2004: IMD's new operational models for long-range forecast of southwest monsoon rainfall over India and their verification for 2003. *Current Science*, **86**, 422-431.

Rajeevan, M., Pai, D. S., Kumar, R. A., and Lal, B. 2007: New statistical models for long-range forecasting of southwest monsoon rainfall over India. *Climate Dynamics*, **28**, 813-828.

Raju, P. V. S., Mohanty, U. C., and Bhatla, R. 2005: Onset characteristics of the southwest monsoon over India *International Journal of Climatology*, **25**, 167-182.

Ramage, C. S. 1971: *Monsoon meteorology*, Academic Press, New York.

Ramiz, A. M. 2007: Monsoons in the central Maldives. *Rain O Shine*, **2**, 42-46.

Rao, K. G., and Goswami, B. N. 1988: Interannual variations of sea surface temperature over the Arabian Sea and the Indian monsoon: A new perspective. *Monthly Weather Review*, **116**, 558-568.

Reddy, P. R. C., and Salvekar, P. S. 2003: Equatorial East Indian Ocean sea surface temperature: A new predictor for seasonal and annual rainfall. *Current Science*, **85**, 1600-1604.

Rijal, M., Idrus. 2009: Investigating coastal resource utilisations and management systems in Sulawesi, Indonesia, University of Canterbury, Chirstchurch.

Rippl, W., 1983: The capacity of storage reservoirs for water supply. *Proceedings of the Institute of Civil Engineers*, 270-278.

Robinson, D. A., Dewey, K. F., and Heim, R. R. 1993: Global snow cover monitoring - An update. *Bulletin of the American Meteorological Society*, **74**, 1689-1696.

Robinson, D. A., and Frei, A. 2000: Seasonal variability of Northern Hemisphere snow extent using visible satellite data. *Professional Geographer*, **52**, 307-315.

Robock, A., Mu, M., Vinnikov, K., and Robinson, D. 2003: Land surface conditions over Eurasia and Indian summer monsoon rainfal. *Journal of Geophysical Research*, **108**.

Rose, G. 1997: Situating knowledges: positionality, reflexivities and other tactics. *Progress in Human Geography*, **21**, 305-320.

Rossi, G., Castiglione, L., and Bonaccorso, B. 2007: Guidelines for planning and implementing drought mitigation measures. In: *Methods and Tools for Drought Analysis and Management*, G. Rossi, T. Vega, and B. Bonaccorso, eds., Springer Netherlands, 325-347.

Roxy, M., and Tanimoto, Y. 2007: Notes and correspondence - Role of SST over the Indian ocean in influencing the intraseasonal variability of the Indian summer monsoon. *Journal of the Meteorological Society of Japan*, **85**, 349-358.

Sadhuram, Y., and Murthy, T. V. R. 2008: Simple multiple regression model for long range forecasting of Indian summer monsoon rainfall. *Meteorology and Atmospheric Physics*, **99**, 17-24.

Saji, N. H., Goswami, B. N., Vinayachandran, P. N., and Yamagata, T. 1999: A dipole mode in the tropical Indian Ocean. *Nature*, **401**, 360-363.

SankarRao, M., Lau, K. M., and Yang, S. 1996: On the relationship between Eurasian snow cover and the Asian summer monsoon. *International Journal of Climatology*, **16**, 605-616.

Semenov, E. K., Sokolikhina, E. V., and Sokolikhina, N. N. 2008: Vertical circulation in the tropical atmosphere during extreme El Niño-Southern Oscillation events. *Russian Meteorology and Hydrology*, **33**, 416-423.

Senan, R., Sengupta, D., and Goswami, B. N. 2003: Intraseasonal "monsoon jets" in the equatorial Indian Ocean. *Geophysical Research Letters*, **30**.

Seo, H., Murtugudde, R., Jochum, M., and Miller, A. J. 2008: Modeling of mesoscale coupled ocean-atmosphere interaction and its feedback to ocean in the western Arabian Sea. *Ocean Modelling*, **25**, 120-131.

Shaig, A. 2006: Population and development consolidation as a strategy to reduce risk from natural disasters and global climate change in Maldives, James Cook University, Townsville.

Shaman, J., Cane, M., and Kaplan, A. 2005: The relationship between tibetan snow depth, ENSO, river discharge and the monsoons of Bangladesh. *International Journal of Remote Sensing*, **26**, 3735 - 3748.

Sharma, K. D., and Singh, P. 2007: Impacts of climate change on hydrological extremes: floods and droughts. *Hydrology Journal*, **30**, 129-145.

Sharma, S. 1996: *Applied multivariate techniques / Subhash Sharma.*, John Wiley & Sons, Inc, New York.

Simsek, Z. 1999: Sample surveys via electronic mail: A comprehensive perspective. *Revista de Administração de Empresas (RAE)*, **39**, 77-83.

Singh, C. V. 2006: Pattern characteristics of Indian monsoon rainfall using principal component analysis (PCA). *Atmospheric Research*, **79**, 317-326.

Singh, G. P., and Oh, J. H. 2007: Impact of Indian Ocean sea-surface temperature anomaly on Indian summer monsoon precipitation using a regional climate model. *International Journal of Climatology*, **27**, 1455-1465.

Sivakumaran, S., and Aramaki, T. 2010: Estimation of household water end use in Trincomalee, Sri Lanka. *Water International*, **35**, 94 - 99.

Slingo, J. M., and Annamalai, H. 2000: 1997: The El Niño of the century and the response of the Indian summer monsoon. *Monthly Weather Review*, **128**, 1778-1797.

Smith, T. M., Reynolds, R. W., Peterson, T. C., and Lawrimore, J. 2008: Improvements to NOAA's historical merged land-ocean surface temperature analysis (1880-2006). *Journal of Climate*, **21**, 2283-2296.

Soman, M. K., and Slingo, J. 1997: Sensitivity of the Asian summer monsoon to aspects of sea-surface-temperature anomalies in the tropical Pacific Ocean. *Quarterly Journal of the Royal Meteorological Society*, **123**, 309-336.

Sousa, S. I. V., Martins, F. G., Alvim-Ferraz, M. C. M., and Pereira, M. C. 2007: Multiple linear regression and artificial neural networks based on principal components to predict ozone concentrations. *Environmental Modelling & Software*, **22**, 97-103.

Stern, N. H. 2007: *The economics of climate change : the Stern review*, Cambridge University Press, Cambridge, UK.

Sterr, H. 2008: Assessment of vulnerability and adaptation to sea-level rise for the coastal zone of Germany. *Journal of Coastal Research*, **24**, 380-393.

Stewart, J., Gardner, T., and McMaster, J. 2005: *Draft urban water use study of South East Queensland*. Retrieved 2 December. 2010, from

http://www.dip.qld.gov.au/resources/senate/Doc_26_Draft_Urban_Water_Use_Study_of_SEQ.pdf

Stidd, C. K. 1953: Cube-root-normal precipitation distributions. *Transactions of the American Geophysical Union*, **34**, 31-35.

Stocker, T. F., Clarke, G. K. C., Le Treut, H., Lindzen, R. S., Meleshko, V. P., Mugara, R. K., Palmer, T. N., Pierrehumbert, R. T., Sellers, P. J., Trenberth, K. E., and Willebrand, J. 2001: Physical climate processes and feedbacks. In: *Climate change 2001: The scientific basis. Contribution of working group I to the third assessment report of the intergovernmental panel on climate change*, J. T. Houghton, Y. Ding, D. J. Griggs, M. Noguer, P. J. van der Linden, X. Dai, K. Maskell, and C. A. Johnson, eds., Cambridge University Press, Cambridge, United Kingdom and New York, NY, USA, 881pp.

Sultana, F. 2007: Reflexivity, positionality and participatory ethics: Negotiating fieldwork dilemmas in international research. *Journal compilation ACME Editorial Collective, An International E-Journal for Critical Geographies*, **6**, 374-385.

Sumi, A., Lau, N. C., and Wang, W. C. 2005: Present status of Asian monsoon simulation. In: *The Global Monsoon System: Research and Forecast*, WMO/TD No. 1266 and TMRP Report No. 70, Hangzhou, China, 376-385.

Suppiah, R. 1997: Extremes of the Southern Oscillation phenomenon and the rainfall of Sri Lanka. *International Journal of Climatology*, **17**, 87-101.

Syroka, J., and Toumi, R. 2004: On the withdrawal of the Indian summer monsoon. *Querterly Jounal of Royal Meteorological Society*, **130**, 989-1008.

Tabachnick, B. G., and Fidell, L. S. 2007: *Using multivariate statistics*, 5th Ed., Pearson/Allyn & Bacon, Boston

Taleb, H. M., and Sharples, S. 2010: Developing sustainable residential buildings in Saudi Arabia: A case study. *Applied Energy*, **88**, 383-391.

Tekken, V., Costa, L., and Kropp, J. P. 2009: Assessing the regional impacts of climate change on economic sectors in the low-lying coastal zone of Mediterranean East Morocco. *Journal of Coastal Research*, 272-276.

Thomas, B., Kasture, S. V., and Satyan, V. 2000: Sensitivity of Asian summer monsoon and tropical circulations to 1987 and 1988 sea surface temperature anomalies. *Atmosfera*, **13**, 147-166.

Torrence, C., and Webster, P. J. 1999: Interdecadal changes in the ENSO-monsoon system. *Journal of Climate*, **12**, 2679-2690.

Trenberth, K. E. 1997: The definition of El Niño. *Bulletin of the American Meteorological Society*, **78**, 2771-2777.

Trenberth, K. E., Stepaniak, D. P., and Caron, J. M. 2000: The global monsoon as seen through the divergent atmospheric circulation. *Journal of Climate*, **13**, 3969-3993.

Turalioglu, F. S., Nuhoglu, A., and Bayraktar, H. 2005: Impacts of some meteorological parameters on SO2 and TSP concentrations in Erzurum, Turkey. *Chemosphere*, **59**, 1633-1642.

Turner, A. G., Inness, P. M., and Slingo, J. M. 2005: The role of the basic state in the ENSO-monsoon relationship and implications for predictability. *Quarterly Journal of the Royal Meteorological Society*, **131**, 781-804.

Turner, A. G., Inness, P. M., and Slingo, J. M. 2007a: The effect of doubled CO2 and model basic state biases on the monsoon-ENSO system. I: Mean response and interannual variability. *Quarterly Journal of the Royal Meteorological Society*, **133**, 1143-1157.

Turner, A. G., Inness, P. M., and Slingo, J. M. 2007b: The effect of doubled CO2 and model basic state biases on the monsoon-ENSO system. II: Changing ENSO regimes. *Quarterly Journal of the Royal Meteorological Society*, **133**, 1159-1173.

UKIERI. 2007: *The Indian monsoon and climate change*. *UK-India Education and Research Initiative*, Retrieved 25 November. 2010, from http://www.walker-institute.ac.uk/publications/factsheets/walker%20factsheet_India.pdf

UN-OHRLLS. 2009a: The impacts of climate change on the development prospects of the least developed countries and small island developing states. United Nations-Office of the High Representative for the Least Developed Countries, Landlocked Developing Countries and Small Island Developing States, New York, USA.

UN-OHRLLS. 2009b: *The impacts of climate change on the development prospects of the least developed countries and small island developing states*. Retrieved 30 November. 2010, from http://www.unohrlls.org/UserFiles/File/LDC%20Documents/The%20impact%20of%20CC%20on%20LDCs%20and%20SIDS%20for%20web.pdf

UNDP. 2007a: Detailed island risk assessment in Maldives: Detailed island reports, L. Gan – Part 1. UNDP Maldives-Disaster Risk Management Programme, Male'.

UNDP. 2007b: Detailed island risk assessment in Maldives: Detailed island reports, Sh. Funadhoo - Part 1. UNDP Maldives-Disaster Risk Management Programme, Male'.

UNEP. 2005: Maldives post-tsunami environmental assessment. United Nations Environment Programme.

UNESCO. 2006: Watching the oceans for signs of climate change. *A world of science*, **4**.

UNSM. 2007: United nations-common country assessment republic of Maldives. United Nations system in the Maldives, Male', Maldives.

Vecchi, G. A., Xie, S. P., and Fischer, A. S. 2004: Ocean-atmosphere covariability in the western Arabian Sea. *Journal of Climate*, **17**, 1213-1224.

Veiga, J. A. P., Rao, V. B., and Franchito, S. H. 2005: Heat and moisture budgets of the Walker circulation and associated rainfall anomalies during El Niño events. *International Journal of Climatology*, **25**, 193-213.

Venegas, S. A., Mysak, L. A., and Straub, D. N. 1997: Atmosphere-ocean coupled variability in the South Atlantic. *Journal of Climate*, **10**, 2904-2920.

Verma, R. K., Subrmaniam, K., and Dugam, S. S. 1985: Interannual and long-term variability of the summer monsoon and its possible link with northern hemispheric surface air temperature. *Proceedings of the Indian Academy of Sciences (Earth and Planetary Sciences)*, **94**, 187-198.

Vernekar, A. D., Zhou, J., and Shukla, J. 1995: The effect of Eurasian snow cover on the Indian monsoon. *Journal of Climate*, **8**, 248-266.

Wallace, J. M., and Bretherton, C. S. 1992: Singular value decomposition of wintertime sea surface temperature and 500-mb height anomalies. *Journal of Climate*, **5**, 561–576.

Wallace, J. M., Rasmusson, E. M., Mitchell, T. P., Kousky, V. E., Sarachik, E. S., and von Storch, H. 1998: The structure and evolution of ENSO-related climate variability in the tropical Pacific: Lessons from TOGA. *Journal of Geophysical Research-Oceans*, **103**, 14241-14259.

Wang, B. 2006: *The Asian monsoon*, Springer ; Published in association with Praxis Publishing, Berlin; New York; Chichester.

Wang, B., and Fan, Z. 1999: Choice of South Asian summer monsoon indices. *Bulletin of the American Meteorological Society*, **80**, 629-638.

Wang, B., and LinHo. 2002: Rainy season of the Asian-Pacific summer monsoon. *Journal of Climate*, **15**, 386–398.

Wang, B., Wu, R., and Lau, K., M. 2001: Interannual variability of the Asian summer monsoon: Contrasts between the Indian and the Western North Pacific-East Asian monsoons. *Journal of Climate*, **14**, 4073-4090.

Wang, B., Wu, R. G., and Li, T. 2003: Atmosphere-warm ocean interaction and its impacts on Asian-Australian monsoon variation. *Journal of Climate*, **16**, 1195-1211.

Wang, C. Z. 2002: Atmospheric circulation cells associated with the El Niño-Southern Oscillation. *Journal of Climate*, **15**, 399-419.

Wang, G., and Hendon, H. H. 2007: Sensitivity of Australian rainfall to inter-El Niño variations. *Journal of Climate*, **20**, 4211-4226.

Wang, P. X., Clemens, S., Beaufort, L., Braconnot, P., Ganssen, G., Jian, Z. M., Kershaw, P., and Sarnthein, M. 2005: Evolution and variability of the Asian monsoon system: State of the art and outstanding issues. *Quaternary Science Reviews*, **24**, 595-629.

Webster, P. J. 1987: *The elementary monsoon*, Wiley, New York.

Webster, P. J., Magana, V. O., Palmer, T. N., Shukla, J., Tomas, R. A., Yanai, M., and Yasunari, T. 1998: Monsoons: Processes, predictability, and the prospects for prediction. *Journal of Geophysical Research-Oceans*, **103**, 14451-14510.

Webster, P. J., and Yang, S. 1992: Monsoon and ENSO: Selectively interactive systems. *Quarterly Jopurnal of the Royal Meteorological Society*, **118**, 877–926.

Weng, C., N, and Nittivatananon, V. (2006). "Women‟s role in water conservation in Malaysia." In: *Regional conference on urban water and sanitation in Southeast Asian cities*, Asian Institute of Technology, Vientiane, Lao PDR.

West, M. J. H., and Arnell, D. J. 1976: Assessment and proposals for the development of the water resources of Male - A small tropical island. *Proceedings of the second world congress, international water resources association*, New Delhi, India, 409-427.

WHO. 1993: Guidelines for drinking-water quality. World Health Organisation, Volume 1, Recommendations, Geneva, Switzaland.

Wilks, D. S. 1995: *Statistical methods in the atmospheric sciences*, Academic Press, San Diego.

Woodroffe, C. D. (1989). "Salt water intrusion into groundwater-an assessment of effects on small island states due to rising sea level." In: *Small state conference on sea level rise*, Ministry of Planning and Environment, Male', Maldives.

Wu, B., Zhou, T. J., and Li, T. 2009: Contrast of rainfall-SST relationships in the Western North Pacific between the ENSO-developing and ENSO-decaying summers. *Journal of Climate*, **22**, 4398-4405.

Wu, R., and Kirtman, B. P. 2007: Role of Indian Ocean in biennial transition of the Indian summer monsoon. *Journal of Climate*, **20**, 2147–2164.

Wu, R., and Wang, B. 2000: Interannual variability of summer monsoon onset over the Western North Pacific and the underlying processes. *Journal of Climate*, **13**, 2483-2501.

Wu, R. G. 2008: Possible role of the Indian Ocean in the in-phase transition of the Indian-to-Australian summer monsoon. *Journal of Climate*, **21**, 5727-5741.

Wu, T.-W., and Qian, Z.-A. 2003: The relation between the Tibetan Winter snow and the Asian summer monsoon and rainfall: An observational investigation. *Journal of Climate*, **16**, 2038-2051.

Wu, Z., and Li, J. 2008: Prediction of the Asian-Australian monsoon interannual variations with the Grid-Point atmospheric model of IAP LASG (GAMIL). *Advances in Atmospheric Sciences*, **25**, 387-394.

Xavier, P. K., Marzin, C., and Goswami, B. N. 2007: An objective definition of the Indian summer monsoon season and a new perspective on the ENSO-monsoon relationship. *Quarterly Journal of the Royal Meteorological Society*, **133**, 749-764.

Yanai, M., and Li, C. 1994: Mechanism of heating and the boundary layer over the Tibetan Plateau. *Monthly Weather Review*, **122**, 305-323.

Yang, S., and Lau, W. K. L. 2006: Interannual variability of the Asian monsoon. In: *The Asian monsoon*, B. Wang, ed., Springer and Praxis Publishing, Berlin Heidelberg, 259-293.

Yasunari, T. 1980: A quasi-stationary appearance of 30-40-day period in the cloudiness fluctuations during the summer monsoon over India. *Journal of Meteorological Scociety of Japan*, **58**, 225-229.

Yasunari, T. 1990: Impact of Indian monsoon on the coupled atmosphere–ocean system in the tropical Pacific. *Meteorology and Atmospheric Physics*, **44**, 29–41.

Yaziz, M., Gunting, H., Sapari, N., and Ghazali, W. 1989: Variations in rainwater quality from roof catchments. *Water Resources*, **23, 6**, 761-765.

Ye, H. C., and Bao, Z. H. 2001: Lagged teleconnections between snow depth in northern Eurasia, rainfall in Southeast Asia and sea-surface temperatures over the tropical Pacific Ocean. *International Journal of Climatology*, **21**, 1607-1621.

Yokoi, S. (2007). "pers. comm." Tokyo, Japan.

Yokoi, S., Satomura, T., and Matsumoto, J. 2007: Climatological characteristics of the intraseasonal variation of precipitation over the Indochina Peninsula. *Journal of Climate*, **20**, 5301-5315.

Zeng, X., and Lu, E. 2004: Globally unified monsoon onset and retreat indexes. *Journal of Climate*, **17**, 2241-2248.

Zhang, S., and Wanga, B. 2008: Global summer monsoon rainy seasons. *International Journal of Climatology*, **28**, 1563-1578.

Zhang, Y., Li, T., and Wang, B. 2004a: Decadal change of the spring snow depth over the Tibetan Plateau: The associated circulation and influence on the East Asian summer monsoon. *Journal of Climate*, **17**, 2780-2793.

Zhang, Y., Li, T., Wang, B., and Wu, G. 2002: Onset of the summer monsoon over the Indochina Peninsula: Climatology and interannual variations. *Journal of Climate*, **15**, 3206-3221.

Zhang, Z. Q., Chan, J. C. L., and Ding, Y. H. 2004b: Characteristics, evolution and mechanisms of the summer monsoon onset over Southeast Asia. *International Journal of Climatology*, **24**, 1461-1482.

Appendices

Appendix 1: Questionnaire for the Island office

My name is Zahid and I am a PhD student at the University of Canterbury, New Zealand. I am working on a research project that looks at the impacts on water resources associated with monsoon rainfall variability for the case of Maldives. I am trying to get information on salinity, drought and flood events experienced by the islands of the Maldives. Your island is among the islands chosen as a study location for this research. Therefore, you are invited to participate in this research project by completing the following questionnaire.

Island Name: _____

A1. What is your island's primary source of water for daily needs (e.g; drinking, cooking, bathing, etc.)? (tick one box only)

Ground water ☐

Rain water ☐

Desalinated water ☐

Bottled water

Others (please specify): _____

A2. Does your island experience groundwater salinity problems? Yes/No

(If the answer is yes, then complete the following questions. Otherwise skip to Question A3)

i. *In which years since 1992? _____*

ii. *During which months?*

May-November ☐

December-April ☐

A3. Does your island experience shortage of groundwater? Yes/No

(If the answer is yes, then complete the following questions. Otherwise skip to Question A4)

i. *In which years since 1992? _____*

ii. *During which months?*

May-November ☐

☐

December-April

iii. *During such situations, the island community depends mainly on which water resource? (tick one box only)*

Rain water ☐

Desalinated water ☐

Bottled water ☐

Other sources (please specify): _____

A4. Does your island experience rainwater (harvested rainwater) shortage? Yes/No

(If the answer is yes, then complete the following questions. Otherwise skip to Question A5)

i. *In which years since 1992? _____*

ii. *During which period of the year?*

May-November ☐

December-April ☐

iii. *During such situations, the island community depends mainly on which water resource? (tick one box only)*

Ground water ☐

Desalinated water ☐

Bottled water ☐

Other sources (please specify): _____

A5. How many public rainwater tanks and desalination plants does your island have?

No of public rainwater tanks: _____

Capacity of each tank (L): _____

No of desalination plants: _____

Capacity of each plant (L): _____

i. Who manage the tanks and plants?

ii. How many household rain water tanks in the Island (if known)?

iii. During which period of the year, does your island harvest rainwater?

May-November ☐

December-April ☐

A6. On average how much it costs to install a 2500L tank (including cost of tank) in your island?

_____

A7. Does your island experience flooding (e.g. damage and blocked roads) due to rain? Yes/No

(If the answer is yes, then complete the following questions. Otherwise skip to Question A7)

i. *In which years since 1992?* _____

ii. *During which period of the year?*

May-November ☐

December-April ☐

A8. What are the major problems regarding the water supplies of your island community?
_____
_____
_____

A9. Would you like to add anything else regarding the groundwater salinity problems, or drought or flood events experienced by your island?
_____
_____

Thank you for your time and participating in this survey!

Island office response summary

Island Name	Rainwater as a primary source of potable water?	Groundwater as a primary source Non-potable of water?	Groundwater salinity problems?	Salinity problems in which years since 1992?	Salinity problems during December to April?	Shortage of groundwater?	Shortage of rainwater?	Shortage of rainwater in which years since 1992?	Shortage of rainwater during December to April?	Groundwater used during shortage of rain as an alternative?
Gn.Fuvahmulah	Yes	Yes	Yes	2007 and 2008	Yes	No	y	1992 onwards	Yes	Yes
S.Hithadhoo	Yes	Yes	Yes	all the years	Yes	No	Yes	2009	Yes	Yes
S.Meedhoo	Yes	Yes	No	-	-	No	Yes	2009-only	Yes	-
Gdh.Vaadhoo	Yes	Yes	No	-	-	No	Yes	all the years	Yes	Yes
L.Gan	Yes	Yes	No	-	-	No	Yes	all the years	Yes	-
L.Hithadhoo	Yes	Yes	No	-	-	No	Yes	2007 and 2009	Yes	-
HA.Baarah	Yes	Yes	No	-	-	No	Yes	all the years	Yes	Yes
HA.Kelaa	Yes	Yes	No	-	-	No	Yes	2009	Yes	Yes
Hdh.Finey	Yes	Yes	No	-	-	No	Yes	2007 and 2009	Yes	Yes
Sh.Feevah	Yes	Yes	No	-	-	No	Yes	2009 and 2007	Yes	-
K.Kaashidhoo	Yes	Yes	No	-	-	No	Yes	All the years since 2005	Yes	Yes
AA.Thoddu	Yes	Yes	No	-	-	No	No	-	-	-
Percentage (Yes)	**100**		**17**	**-**	**100**	**0**			**100**	**64**

Continuation from previous page

Island Name	Desalinated water used during shortage of rain?	Total public rainwater tank capacity (L)	No of desalination plants	Who manages the public rainwater tanks and desalination plants?	No of household rainwater tanks	Household rainwater tank size	2500 L rainwater tank installation cost (US$)	Rainwater harvested only during May-November?	Flood due to rain?	Food only during May-November?
Gn.Fuvahmulah	-	287500	0	Island office	2110	2500	322	Yes	Yes	Yes
S.Hithadhoo	-	160000	0	Island office	2263	2500	260	Yes	No	-
S.Meedhoo	Yes	150000	0	Island office	200	2500	510	Yes	Yes	Yes
Gdh.Vaadhoo	-	95000	0	Island office	136	2500	431	Yes	Yes	Yes
L.Gan	Yes	40500	1	Atoll and Island committee	115	2500	627	Yes	Yes	Yes
L.Hithadhoo	Yes	22500	0	Island office	170	2500	784	Yes	Yes	Yes
HA.Baarah	-	97500	0	Island office	310	2500	588	Yes	Yes	Yes
HA.Kelaa	-	100000	0	Island office	500	2500	439	Yes	Yes	Yes
Hdh.Finey	-	52500	0	Island office	124	2500	392	Yes	No	-
Sh.Feevah	Yes	80000	0	Island office	151	2500	494	Yes	Yes	Yes
K.Kaashidhoo	-	105000	0	Island office	350	2500	627	Yes	No	-
AA.Thoddu	-	40000	0	Island office	239	2500	573	Yes	No	-
Percentage (Yes)	36							**100**	**67**	100

Continuation from previous page

Island Name	In which years since 1992?	Centralized sewerage system?	Major problems regarding the water supplies
Gn.Fuvahmulah	2000 (some areas) and all the years (wetland area)	No	Shortage of water due to contamination
S.Hithadhoo		No	Contamination
S.Meedhoo	2007- damages to the household items	No	Contamination is an issue-it is necessary to have desalination plants
Gdh.Vaadhoo	2005,2006,2007,2008-sometimes two times	No	Most of the houses experiencing groundwater contamination
L.Gan	2007 and 2008	No	Groundwater not suitable for use due to septic tanks
L.Hithadhoo	2007	No	Smells-not suitable for any use-alternative water source is needed
HA.Baarah	2007 & 2008	No	Groundwater in some homes are contaminated
HA.Kelaa	1994 and 2008	No	Contamination due to lack of proper sewerage system
Hdh.Finey		No	Contamination due to lack of proper sewerage system
Sh.Feevah	all the years since 2004 tsunami	No	Groundwater contamination
K.Kaashidhoo		No	Not enough rain water for potable use
AA.Thoddu		No	Contamination due to lack of proper sewerage system
Percentage (Yes)		0	

Continuation from previous page

Island Name	Factors which may influence water consumption now and in the future
Gn.Fuvahmulah	Increase due to agriculture and population
S.Hithadhoo	It is planned to install plants and use kulhi (pond) for water supply and improved water situation due to sewerage system
S.Meedhoo	Agriculture sector will expand
Gdh.Vaadhoo	Will increase due to agriculture
L.Gan	Will increase due to increase in population, migration and water use for washing cars
L.Hithadhoo	Will increase due to increase in population -now also it is not enough
HA.Baarah	Will increase due to increase in population and more buildings
HA.Kelaa	Will increase due to increase in population
Hdh.Finey	Will increase due to agriculture, population, infrastructure and increase in coconut plants
Sh.Feevah	Will increase due to population, agriculture, cleaning or washing boats
K.Kaashidhoo	Will increase due to population, industrial activities, and agricultural(widen)
AA.Thoddu	Will increase due to population, agriculture and construction
Percentage (Yes)	

Continuation from previous page

Island Name	Other comments regarding groundwater salinity problems, or drought or flood events
Gn.Fuvahmulah	Water from two kulhis (ponds) are cleaned, island might not face water shortage problems
S.Hithadhoo	Drying out wetland areas-one side of the island is higher-so a gradient is created-which cause shortage of water in some areas
S.Meedhoo	Groundwater test shows it is not suitable for human consumption -this issue was raised and informed to the concerning authorities
Gdh.Vaadhoo	If the current trend continues in ten years time, the island groundwater cannot be used due to contamination
L.Gan	Contamination- sewage system is required urgently
L.Hithadhoo	Desalination plant is needed-ground water in some parts of the island are not suitable for human use
HA.Baarah	Use water wisely-it is important to consider to install sewerage system
HA.Kelaa	Desalination plant is needed and sewerage system also needed for effective use of groundwater
Hdh.Finey	If the current consumption rate continues, the groundwater will become saline
Sh.Feevah	Contamination problem: Alternative drinking water is needed to reduce health problems and sewerage system is needed
K.Kaashidhoo	Groundwater is a limited resource and people needed to be educated. Desalinated water is needed to reduce groundwater consumption
AA.Thoddu	Water has to be used sustainably
Percentage (Yes)	

Appendix 2: Questionnaire for the households

My name is Zahid and I am a PhD student at the University of Canterbury, New Zealand. I am working on a research project that looks at the impacts on water resources associated with monsoon rainfall variability for the case of the Maldives. I am trying to get information on the use of different water resources and their use by the households. You are invited to participate in this research project by completing the following questionnaire. You may withdraw your participation, including withdrawal of any information you have provided, until your questionnaire has been analyzed and included in the research. All the information provided by you will be kept confidential. Results of the survey will be included in my thesis or journals, in the form of grouped results only. Individual household information will not be made available to anyone other than me and my supervisors. To ensure the survey is anonymous, the questionnaire does not ask for house or your name or any other form of identification.

Island name: _____

Serial No: _____

Gender of respondent: ***Male*** ☐ ***Female*** ☐

B1. How many people (> 5 years of age) live in your household? _____

B2. What kind of toilet facility do members of your household usually use?

Pour flush toilet ☐

Cistern flush toilet ☐

No facilities or Bush or field ☐

Others (please specify): _____

B3. Do you use ground water for household purposes (e.g. drinking, cooking, dish washing, bathing etc.)? Yes/No

(If the answer is yes, then complete the following questions. Otherwise skip to Question B4)

a. *Is ground water, the only source of water for your household? Yes/No*

b. *How do you obtain groundwater?*

Pumped from Household well ☐

Manually from house well ☐

Neighbours' well ☐

Public well ☐

No of wells: _____

c. *Does your household use groundwater for toilet flushing? Yes/No*

d. *If yes, how many times do you flush toilet using groundwater per day?*

If more than one type of toilet facility used, please specify the types and number of times each toilet facility used: _____

e. *Does your household use groundwater for gardening and backyard farming? Yes/No*

If yes, on average approximately how many litres of groundwater are used for gardening and backyard farming per day over a year? _____

f. *Does your household use groundwater for washing clothes? Yes/No*

If Yes, on average approximately how many litres of groundwater are used for washing clothes in your household per day over a year?

g. *Does your household use groundwater for dish washing? Yes/No*

If Yes, on average approximately how many litres of groundwater are used for dish washing in your household per day over a year?_____

h. *On average, approximately how many litres of groundwater are used per day/person in your household for the following purpose?*

Purpose Litres/person/ day

Drinking and cooking: _____

Bathing and hygiene: _____

Others: _____

i. *Have you experienced shortage of groundwater? Yes/No*

   i. *If Yes, in which years since 1992? _____*

   ii. *During which period of the year?*

May-November ☐

December-April ☐

   iii. *Usually how long does the shortage of ground water last for?*

1-2 months ☐

2-3 months ☐

3-4 months ☐

4-5 months ☐

5-6 months ☐

6 months or more ☐

j. During such situations, your household depends mainly on which water resource? (tick one box only)

Rain water ☐

Desalinated water ☐

Bottled water ☐

Other sources (please specify): _____

k. Is there any difference in ground water usage in your household between May-November/December-April? Yes/No

i. If Yes, during which period of the year (May-November/December-April), does your household use ground water most frequently?

May-November ☐

December-April ☐

ii. What is the reason for using ground water during this period?_____
_____

l. Does your household experience salinity problems in groundwater? Yes/No

i. If Yes, in which years since 1992? _____

ii. During which period of the year?

May-November ☐

December-April ☐

m. Do you mind if I take a measurement of salinity and depth of your groundwater source/well? Yes/No

i. Salinity measurement (mg/L or ppm): _____

ii. Depth (m): _____

B4. Do you use rainwater for household purposes (e.g. drinking, cooking, dish washing, bathing etc.)? Yes/No

(If the answer is yes, then complete the following questions. Otherwise skip to Question B5)

a. Is rainwater, the only source of water for your household? Yes/No

b. How do you obtain rainwater?

Own rainwater tank ☐

Public water tank ☐

☐

Private rainwater tank

Others (please specify): _____

Size of the tank (L): _____

c. *If you harvest your own rainwater, then during which period(s) of the year, do you mostly harvest rainwater?*

May-November ☐

December-April ☐

Size of roof used for rainwater collection (m2) :_____

d. *Does your household use rainwater for toilet flushing? Yes/No*

If yes, on average how many times do you flush toilet using rain water per day?_____

If more than one type of toilet facility used, please specify the types and number of times each toilet facility used: _____

e. *Does your household use rainwater for gardening and backyard farming?*

If Yes, on average approximately how many litres of rainwater are used for gardening and backyard farming per day over a year?_____

f. *Does your household use rainwater for washing clothes? Yes/No*

If Yes, on average approximately how many litres of rainwater are used for washing clothes in your household per day over a year?_____

g. *Does your household use rainwater for dish washing? Yes/No*

If Yes, on average approximately how many liters of rainwater are used for dish washing in your household per day over a year?_____

h. *On average, approximately how many litres of rainwater are used per day/person in your household for the following purpose?*

Purpose Liters/person/day:

Drinking and cooking: _____

Bathing and hygiene: _____

Others: _____

i. *Is there any difference in rainwater usage in your household between May-November/December-April? Yes/No*

   i. *If yes, during which period of the year, your household uses rainwater most frequently?*

May-November ☐

December-April ☐

ii. *What is the reason for using rain water during this period?*_____
_____

j. *Have you experienced shortage of rainwater? Yes/No*

i. *In which years since 1992?* _____

ii. *During which season?*

May-November ☐

December-April ☐

k. *What is the reason for the shortage of rainwater?*

a. *Tank size* ☐

b. *Prolonged dry period* ☐

c. *Others(specify):* ☐

l. *During shortage of rainwater, on which alternative water resource does your household mostly depend on? (tick one box only)*

Ground water ☐

Desalinated water ☐

Bottled water ☐

Other sources (please specify): _____

m. *Usually how long does the shortage of rain water last for?*

1-2 months ☐

2-3 months ☐

3-4 months ☐

4-5 months ☐

5-6 months ☐

More than 6 months ☐

B5. Does your household use desalinated water for household purposes (e.g. drinking, cooking, dish washing, bathing etc.)? Yes/No

(If the answer is yes, then complete the following questions. Otherwise skip to Question B6)

a. *Is desalinated water, the only source of water for your household? Yes/No*

b. Does your household use desalinated water for gardening and backyard farming?

If yes, on average approximately how many liters of desalinated water are used for gardening and backyard farming per day over a year? _____

c. Does your household use desalinated water for washing clothes? Yes/No

If Yes, on average approximately how many liters of desalinated water are used for washing clothes in your household per day over a year?_____

d. Does your household use desalinated water for dish washing? Yes/No

If Yes, on average approximately how many litres of desalinated water are used for dish washing in your household per day over a year?_____

e. Does your household use desalinated water for toilet flushing? Yes/No

If yes, on average how many times do you flush toilet using desalinated water per day? _____

If more than one type of toilet facility used, please specify the types and number of times each toilet facility used: _____

f. On average, approximately how many liters of desalinated water are used per day/person in your household for the following purpose?

Purpose Liters/person/ day

Drinking and cooking: _____

Bathing and hygiene: _____

Others: _____

g. Is there any difference in desalinated water use in your household between May-November/December-April? Yes/No

i. If yes, during which period of the year (May-November/December-April), your household use desalinated water most frequently?

May-November ☐

December-April ☐

ii. What is the reason for using desalinated water during this period?_____
_____

B6. Does your household use bottled water? Yes/No

(If the answer is yes, then complete the following questions. Otherwise skip to Question B7).

a. Is bottled water, the only source of water for your household? Yes/No

On average, approximately how many litres of bottled water are used per day in your household for the following?

Purpose ***Litres/person/ day***

Drinking and cooking: _____

Others: _____

b. Is there any difference in bottled water use in your household between May-November/December-April? Yes/No

i. If Yes, during which period of the year (May-November/December-April), your household use bottled water most frequently?

May-November ☐

December-April ☐

*iii. What is the reason for using bottled water during this period?*_____
_____

B7. Does your household use any other sources of water, other than ground water, rainwater, desalinated water and bottled water? Yes/No

i. If Yes, what other sources of water are used by your household? _____

B8. Have you experienced flood damage due to rain in your household? Yes/No

i. During which period of the year?

May-November ☐

December-April ☐

ii. In which years since 1992? _____

B9. Has anyone in your household experienced water quality related illness? Yes/No

B10. What factors may reduce/increase water consumption of your household in the future?
_____

B11. Would you like to add anything else regarding the water resources in your household?
_____

B12. If I leave a water use log sheet (see below) with you, do you mind filling the sheet for five days? Yes/No

Note: If yes, the log sheet was given to the participant and sheet will be collected at the end of 5 day period.

Thank you for your time and participating in this survey!

Household water use log sheet

Serial no:	*Number of people in your household (>5 years):*				
Type of toilet facility used by the household: Pour flush toilet ☐	*Cistern flush toilet:* ☐			*Beach or bush* ☐	
Ground water usage	***Day1***	***Day2***	***Day3***	***Day4***	***Day5***
*Number of times you have flushed toilet using groundwater**					
Amount of groundwater used by you for drinking(in liters)					
Amount of ground water used by you for bathing and hygiene (in liters)					
Amount of groundwater used for washing clothes in your household(in liters)					
Amount of groundwater used for dish washing in your household(in liters)					
Amount of groundwater used for cooking in your household (in liters)					
Amount of groundwater used for gardening and backyard farming in your household (in liters)					
Amount of groundwater used for other purposes in your household (in liters)					
Rain water usage	***Day1***	***Day2***	***Day3***	***Day4***	***Day5***
*Number of times you have flushed toilet using rainwater**					
Amount of rain water used by you for drinking(in liters)					
Amount of rain water used by you for bathing and hygiene (in liters)					
Amount of rainwater used for washing clothes in your household(in liters)					
Amount of rainwater used for dish washing in your household(in liters)					
Amount of rainwater used for cooking in your household (in liters)					
Amount of rainwater used for gardening and backyard farming in your household (in liters)					
Amount of rainwater used for other purposes in your household (in liters)					
Desalinated water usage	***Day1***	***Day2***	***Day3***	***Day4***	***Day5***
Amount of desalinated water used by you for drinking					
Amount of desalinated water used by you for bathing and hygiene (in liters)					
Amount of desalinated water used for washing clothes in your household(in liters)					
Amount of desalinated water used for dish washing in your household(in liters)					
Amount of desalinated water used for cooking in your household (in liters)					
Amount of desalinated water used for gardening and backyard farming in your household (in liters)					
Amount of desalinated water used for other purposes in your household (in liters)					
Bottled water usage	***Day1***	***Day2***	***Day3***	***Day4***	***Day5***
Amount of bottled water used by you for drinking(in liters)					
Amount of bottled water used for cooking in your household (in liters)					
Amount of bottled water used for other purposes in your household (in liters)					

If you use more than one type of toilet facility, please specify the type of toilet (P=Pour, C = Cistern and B = Beach or bush) you used every time

Appendix 3: Questionnaire for the farmers

My name is Zahid and I am a PhD student at the University of Canterbury, New Zealand. I am working on a research project that looks at the impacts on water resources associated with monsoon rainfall variability for the case of Maldives. I am trying to get information on the use of different water resources and their use by the Agricultural sector. You are invited to participate in this research project by completing the following questionnaire. You may withdraw your participation, including withdrawal of any information you have provided, until your questionnaire has been analyzed and included in the research. All the information provided by you will be kept confidential Results of the survey will be included in my thesis or articles, in the form of grouped results only. Individual farm information will not be made available to anyone other than me and my supervisors. To ensure the survey is anonymous, the questionnaire does not ask for your name or any other form of identification.

Island name: _____

Area of farm (m2):_____

C1. What are the main types of crops grown in your farm and growing season(s) for different crops in your farm?

Main crops	***growing season(s)***
1. _____	_____
2. _____	_____
3. _____	_____
4. _____	_____
5. _____	_____

C2. Do you use ground water for watering your crops? Yes/No

(If the answer is yes, complete the following questions. Otherwise skip to Question C3)

a. *How do you extract or obtain groundwater?*

Manual extraction from a well within farm ☐

Pumped supply from a well within farm ☐

From public well(s) ☐

Government supply ☐

Others (please specify): _____

b. *On average, approximately how many liters of ground water are used by your farm per day over a year?* _____

c. *Is there any difference in ground water usage in your farm between May-November/December-April? Yes/No*

i. *If Yes, during which period of the year (May-November /December-April), does your farm use ground water most frequently for watering the crops?*

May-November ☐

December-April ☐

d. *Have you experienced shortage of groundwater in your farm? Yes/No*

i. *In which years since 1992? _____*

ii. *During which period of the year?*

May-November ☐

December-April ☐

iii. *What is the estimated cost of damage (MRF)? _____*

e. *During shortage of groundwater, on which water resource does your farm mostly depend? (tick one box only)*

Rainwater ☐

Desalinated water ☐

Other sources (please specify): _____

f. *How long does the shortage of groundwater last for?*

1-2 months ☐

2-3 months ☐

3-4 months ☐

4-5 months ☐

5-6 months ☐

More than 6 months ☐

C3. Do you use groundwater for watering your crops if it rains? Yes/No

C4. Do you use rainwater for watering your crops? Yes/No

(If the answer is yes, then complete the following questions. Otherwise skip to Question C4)

a. *How do you obtain or harvest rainwater?*

Rainwater tank within the farm ☐

Public rainwater tank ☐

From a private rainwater tank ☐

Tank size (L):_____

b. *On average, approximately how many liters of rain water are used by your farm per day over a year? _____*

c. *Is there any difference in rainwater usage in your farm between May-November/December-April? Yes/No*

i. *If yes, during which period of the year (May-November /December-April) does your farm use rainwater most frequently?*

May-November ☐

December-April ☐

ii. *What is the main reason for using rainwater during this period?* _____

C5. Do you use desalinated water for your crops? Yes/No

(If the answer is yes, then complete the following questions. Otherwise skip to Question C5)

a. *On average, approximately how many liters of desalinated water are used by your farm per day?*

b. *Is there any difference in desalinated water use in your farm between May-November / December-April? Yes/No*

c. *If Yes, during which period of the year May-November /December-April) does your farm use desalinated water most frequently?*

May-November ☐

December-April ☐

C6. Do you use any other source of water for your crops, other than ground water, rainwater and desalinated water? Yes/No

(If the answer is yes, then complete the following question. Otherwise skip to Question C6)

a. *What other sources of water used by your farm?* _____ _____

b. *On average, approximately how many liters of water from these sources are used by your farm per day over a year?*

C7. Have you experienced flood related damage to your farm? Yes/No

(If yes - continue this section. Otherwise skip to Question C7)

i. *In which years since 1992? _____*

ii. *During which season?*

May-November ☐

December-April ☐

iii. *What kind of damage?*

Erosion ☐

Plants damage ☐

Unable to cultivate ☐

Others (please specify): _____

C8. Have you experienced drought or prolong dry period or shortage of rain for your farm? Yes/No

(If yes - continue this section. Otherwise skip to Question C8)

i. *In which years since 1992? _____*

ii. *During which period of the year?*

May-November ☐

December-April ☐

iii. *What is the estimated cost of damage (MRF)? _____*

i. *During shortage of rainwater, on which water resource does your farm mostly depend on? (tick one box only)*

Ground water ☐

Desalinated water ☐

Other sources (please specify): _____

ii. *How long does the shortage of rainwater last for?*

1-2 months ☐

2-3 months ☐

3-4 months ☐

4-5 months ☐

5-6 months ☐

More than 6 months ☐

C9. Have you experienced salinity problems in your farm? Yes/No

(If yes - continue this section. Otherwise skip to Question C9)

i. *In which years since 1992? _____*

ii. *During which season?*

May-November ☐

December-April ☐

C10. Do you mind if I take a measurement of salinity and depth of your groundwater source? Yes/No

i. *Salinity measurement (mg/L or ppm): _____*

ii. *Depth (m): _____*

C11. What factors may increase or decrease water consumption of your farm Now and in the future?

_____
_____
_____

C12. Would you like to add anything else regarding the water resources in your farm?
_____
_____
_____

C13. If I leave a water use log sheet with you, do you mind filling the sheet for five days? Yes/No

Note: If yes, the log sheet will be given to the participant and sheet will be collected at the end of 5 day period.

Thank you for your time and participating in this survey!

Farm water usage log sheet

Serial no:

Types of water	*Amount of water used (in liters)*				
	Day1	*Day2*	*Day3*	*Day4*	*Day5*
Groundwater: *Amount of groundwater used for watering crops in your farm*					
Rainwater: *Amount of rain water used for watering crops in your farm*					
Desalinated water: *Amount of desalinated water used for watering crops in your farm*					
Other sources: *Amount of other sources of water used for watering crops in your farm*					

Appendix 4: Questionnaire for the tourism sector

My name is Zahid and I am a PhD student at the University of Canterbury, New Zealand. I am working on a research project that looks at the impacts on water resources associated with monsoon rainfall variability for the case of Maldives. I am trying to get information on the use of different water resources by the tourism sector. Your resort is among the resorts chosen as a study location for this research. Therefore, you are invited to participate in this research project by completing the following questionnaire. All the information provided by your resort will be kept confidential. Individual resort information will not be made available to anyone other than me and my supervisors.

Resort Name: _____

D1. Does your resort use ground water for any purpose? Yes/No

(If the answer is yes, then complete the following questions. Otherwise skip to Question D2)

a. For what purpose(s) is ground water used?

Cooking ☐

Drinking ☐

Bathing and hygiene ☐

Dish washing ☐

Clothes washing ☐

Watering the garden ☐

Watering crops ☐

Others (please specify): _____

b. Does your resort use groundwater for toilet flushing? Yes/No

c. Does your resort experience groundwater salinity problems? Yes/No

d. Is there any difference in ground water usage in your resort between May-November/December-April? Yes/No

e. If Yes, during which period of the year (May-November/ December-April), does your resort use ground water most frequently?

May-November ☐

December-April ☐

f. Does your resort experience shortage of groundwater? Yes/No

i. In which years since 1992? _____

ii. *During which period of the year?*

May-November ☐

December-April ☐

g. *During shortage of groundwater, on which water resource does your resort mostly depend? (tick one box only)*

Rainwater ☐

Desalinated water ☐

Bottled water ☐

Other sources (please specify): _____

h. *How long does the shortage of groundwater last for?*

1-2 months ☐

2-3 months ☐

3-4 months ☐

4-5 months ☐

5-6 months ☐

> 6 months ☐

i. *If your resort uses groundwater, approximately how many liters of groundwater are used by your resort per day in total?*

Daily total (Liters): _____

D2. Does your resort use rainwater? Yes/No

(If the answer is yes, then complete the following questions. Otherwise skip to Question D3)

a. *For what purpose(s) is rainwater used?*

Cooking ☐

Drinking ☐

Bathing and hygiene ☐

Dish washing ☐

Clothes washing ☐

Watering the garden ☐

Watering crops ☐

Others (please specify): _____

b. *Does your resort use rainwater for toilet flushing? Yes/No*

c. *Is there any difference in rain water usage in your resort between May-November/ December-April? Yes/No*

d. *If Yes, during which period of the year (May-November/ December-April), does your resort use rainwater most frequently?*

May-November ☐

December-April ☐

e. *Does your resort experience shortage of rainwater? Yes/No*

i. *If Yes, in which years since 1992? _____*

ii. *During which period of the year?*

May-November ☐

December-April ☐

f. *During shortage of rainwater, on which water resource does your resort mostly depend on? (tick one box only)*

Ground water ☐

Desalinated water ☐

Bottled water ☐

Other sources (please specify): _____

g. *How long does the shortage of rain water lasts for?*

1-2 months ☐

2-3 months ☐

3-4 months ☐

4-5 months ☐

5-6 months ☐

> 6 months ☐

h. *If your resort uses rainwater, approximately how many liters of rainwater are used by your resort per day in total?*

Daily total (Liters): _____

D3. Does your resort use desalinated water? Yes/No

(If the answer is yes, then complete the following questions. Otherwise skip to Question D4)

a. For what purpose(s) is desalinated water used?

Cooking ☐

Drinking ☐

Bathing and hygiene ☐

Dish washing ☐

Clothes washing ☐

Watering the garden ☐

Watering crops ☐

Others (please specify): _____

b. Does your resort use desalinated water for toilet flushing? Yes/No

c. Is there any difference in desalinated water usage in your resort between May-November/December-April? Yes/No

d. If yes, during which period of the year (May-November/December-April) does your resort use desalinated water most frequently?

May-November ☐

December-April ☐

e. If your resort uses desalinated water, approximately how many liters of desalinated water are used per day in total?

Daily total (Liters): _____

D4. Does your resort use bottled water? Yes/No

(If the answer is yes, then complete the following questions. Otherwise skip to Question D5).

a. For what purpose(s) is bottled water used?

Cooking ☐

Drinking ☐

Bathing and hygiene ☐

Dish washing ☐

Clothes washing ☐

Watering the garden ☐

Watering crops ☐

Others (please specify): _____

b. *Is there any difference in bottled water usage in your resort between May-November/December-April? Yes/No*

c. *If yes, during which period of the year (May-November/December-April) does your resort use bottled water most frequently?*

May-November ☐

December-April ☐

d. *If your resort uses bottled water, approximately how many liters of bottled water are used by your resort per day in total?*

Daily total (Liters): _____

D5. Does your resort use any other source of water (e.g. treated waste water), other than ground water, rainwater, desalinated water and bottled water? Yes/No

(If the answer is yes, then complete the following question. Otherwise skip to Question D6)

i. *What other sources of water are used by your resort (please specify)? Water source 1: _____*

Water source 2: _____

ii. *For what purpose water source 1 is used?*

Cooking ☐

Drinking ☐

Bathing and hygiene ☐

Dish washing ☐

Clothes washing ☐

Watering the garden ☐

Watering crops ☐

Others (please specify): _____

iii. *For what purpose water source 2 is used?*

Cooking ☐

Drinking ☐

Bathing and hygiene ☐

Dish washing ☐

Clothes washing ☐

Watering the garden ☐

Watering crops ☐

Others (please specify): _____

D6. Does your resort experience flood due to rain? Yes/No

i. If Yes, in which years since 1992? _____

ii. During which period of the year?

May-November ☐

December-April ☐

iii. If yes, what is the estimated cost of damage (MRF)? _____

D7. What factors may increase or decrease water consumption of your resort Now and in the future? _____

D8. Would you like to add anything else regarding the water resources, drought (prolonged dry periods or shortage of water) and flood situation in your resort? _____

D9. Do you mind filling the water use log sheet (see below) for five days? Yes/No

Note: A log sheet was e-mailed together with the questionnaire.

Thank you for your time and participating in this survey!

Resort water usage log sheet

Serial no:

Types of water	*Amount of water used (in liters)*				
	Day1	*Day2*	*Day3*	*Day4*	*Day5*
***Groundwater:** Amount of groundwater used by your resort*					
***Rainwater:** Amount of rain water used by your resort*					
***Desalinated water:** Amount of desalinated water used by your resort*					
***Bottled water:** Amount of bottled water used by your resort*					
***Other sources:** Amount of other sources of water used by your resort*					

Appendix 5 - Human Ethics Committee Approval letter

Human Ethics Committee
Secretary
Tel: +64 3 364 2241, Fax: +64 3 364 2856, Email: human-ethics@canterbury.ac.nz

UNIVERSITY OF CANTERBURY
Te Whare Wānanga o Waitaha
CHRISTCHURCH NEW ZEALAND

Ref: HEC 2008/148

4 February 2009

Mr Zahid
Department of Geography
UNIVERSITY OF CANTERBURY

Dear Zahid

The Human Ethics Committee advises that your research proposal "Variability of the Asian monsoon and its influence on precipitation patterns over the Maldives" has been considered and approved.

Please note that this approval is subject to the incorporation of the amendments you have provided in your email of 22 January 2009.

Best wishes for your project.

Yours sincerely

Dr Michael Grimshaw
Chair, Human Ethics Committee

Appendix 6 – Department of National Planning Approval letter

بسم الله الرحمن الرحيم

Department of National Planning

Ministry of Finance and Treasury

Ghazee Building 4th Floor, Ameer Ahmed Magu, Male' 20125, Rep. of Maldives

ދިވެހިރާއްޖެ ގެ ނޭޝަނަލް ފްލޭނިންގ ދިވެހިރާއްޖެ ގެ ފައިނޭންސް ޓްރެޜަރީ

ޣާޒީ ބިލްޑިން 4 ވަނަ ފަންގިފިލާ، އަމީރ އަހުމަދު މަގު، މާލެ 20125، ދިވެހިރާއްޖެ

SOCIAL HARMONY - OUR NATION'S STRENGTH

ދިވެހިންގެ ހަމަހަމަކަން - ދިވެހި ގައުމުގެ ބާރު

No: 100-ST 3/ 2009/١١

Mr. Zahid

3/48 Starven Road, Ricccarton,

New Zealand

08th January 2009

Dear Mr. Zahid

Subject: Variability of the Asian monsoon and its influence on precipitation patterns over the Maldives

With reference to your application form, we hereby approve conducting of the above mentioned survey from 05th March 2009 to 20th May 2009.

Attached please find the official form "Permission to Conduct Survey". We would appreciate it if you could inform us if there is any change in the survey period and the final questionnaire.

Yours sincerely,

Mariyam Niyaf

Assistant Director General

Email:info@planning.gov.mv :ޕ.ޢ Website:www.planning.gov.mv :ވެބްސައިޓް Fax: (960) 3327351 :ފެކްސް Operator: (960) 3348383 :ޓެލިފޯން

Department of National Planning,
Ministry of Finance and Treasury
Ghaazee Building, 20125
Male', Republic of Maldives

PERMISSION TO CONDUCT SURVEY

1. Name of Organisation/ Individual : Zahid/ University of Canterbury
2. Survey title : Variability of the Asian monsoon and its influence on percipitation patterns over the Maldives
3. Survey objectives : 1.To determine island community dependence on rainfall for daily need and water usage by households for different purpose. 2.To determine water usage by the agriclutural sector. 3. To determine the main water resources in the tourism sector.
4. Period of data collection : 5th March - 20th May 2009
5. Survey areas (Atoll/Island) :

6. Government authorities consulted:
   1) .....
   2) .....
   3) .....
   4) .....

Under the Statistical Regulation of the Republic of Maldives, we hereby give permission to undertake the above mentioned survey.

Name: Mariyam Niyaf Signature:

Designation: Assistant Director General

Date: 08/.01../2009

Seal

FOR THE ATTENTION OF RESPONDENTS

Under the Statistical Regulation of Republic of Maldives :-

Any person, who is authorised by the Department of National Planning, Ministry of Finance and Treasury to conduct a survey, shall be provided with true information, within the permitted time.

The work of any person permitted to carry out a survey under this regulation shall not be hindered or obstructed

Confidentiality will be accorded to any information that is obtained from permitted data collection operations, which would disclose the identity of the provider.

Statistics Division-Department of National Planning Phone: 3348383,3348309 Fax: 3327351 email: stats@planning.gov.mv

Acronyms

ABSE	Absolute Error
AIMR	All-Indian Monsoon Rainfall
AIR	All-Indian Rainfall
AIRI	All-India Rainfall Index
AISMR	All-Indian Summer Monsoon Rainfall
AM	Asian Monsoon
AMR	All-Maldives Rainfall
ANOVA	Analysis of Variance
ASMR	All-India Summer Monsoon Rainfall
BIAS	Bias in the Model Forecast
BOB	Bay Of Bengal
C.V	Coefficient Of Variation
CC	Correlation Coefficient
CC	Correlation Coefficient
CI	Central India
CMAP	Climate Merged Analysis of precipitation
CPC	Climate Prediction Centre
DISC	Data and Information Services Centre
DJF	December January February
DJF	December January February
DJFM	December January February March
DV	Dependent Variable
DW	Durbin Watson
EA	East Asia
EI	Equatorial Indian
ENSO	EI Nino- Southern Oscillation
ENSO-SST	El Niño-Southern Oscillation
EOF	Empirical Orthogonal Function
ERA	Effective roof area
ERSST	Extended Reconstructed Sea Surface Temperature
ESC	Eurasian Snow Cover
GB	Ganges-Mahanadi Basin
GCMs	General Circulation Models
GDP	Gross Domestic Product
GES	Goddard Earth Sciences
GIOVANNI	Interactive-online Visualization and Analysis Infrastructure
GWD	Groundwater depth
HHs	Households
IAV	Inter-annual variability
ICOADS	International Comprehensive Ocean-Atmosphere Data Set
IMD	Indian Meteorological Department

IMR	Indian Monsoon Rainfall
IMR	Indian Monsoon Rainfall
IO	Indian Ocean
IOD	Indian Ocean Dipole
ISM	Indian Summer Monsoon
ISMR	Indian Summer Monsoon Rainfall
ITCZ	inter-tropical Convergence Zone
IV	Independent Variable
JJA	June July August
JJAS	June July August September
Lpcpd	Litre per capita per day
LRS	Length of Rain Season
MA	March April
MAC	Mean Annual Cycle
MAM	March April May
MI	Maldives Island
MJJASON	May-June-July-August-September-October-November
MJO	Madden-Julian Oscillation
MMR	Maldives Monsoon Rainfall
MMRI	Maldives Monsoon Rainfall Index
MSL	Mean sea level
MSLP	Mean Sea Level Pressure
NAO	North Atlantic Oscillation
NCEP-NCAR	National Center for Environmental Perdition-National Center for Atmospheric Research
NESDIS	National Environmental Satellite Data and Information Services
NH	Northern Hemisphere
NOAA	National Oceanic and Atmospheric Administration
OLR	Outgoing longwave radiation
PC	Principal Components
PCA	Principal Component Analysis
pcpd	Per capita per day
ppm	parts per million
QBO	Quasi-biennial Oscillation
RMSE	Root Mean Square Error
SAM	South Asian Summer Monsoon
SLP	Sea Level Pressure
SMAC	Smoothed Mean Annual Cycle
SOI	Southern Oscillation Index
SRHAPR	Surface Relative Humidity during April
SST	Sea Surface Temperature
SSTA	Sea Surface Temperature Anomaly
SVD	Singular Value Decomposition

TBO	Tropospheric Biennial Oscillation
TMPA	TRMM Multi-Satellite Precipitation Analysis
TRMM	Tropical Rainfall Measuring Mission
VIF	Variance Inflation Factor
VIMT	Vertically Integrated Moisture Transport
WC	Walker Circulation
WG	Western Ghats
850RHMAY	850 hPa Relative Humidity during May